ENVIRONMENT AND SKIN CANCER

EDITED BY: Nabiha Yusuf, Thomas Haarmann-Stemmann and Motoki Nakamura

PUBLISHED IN: Frontiers in Oncology

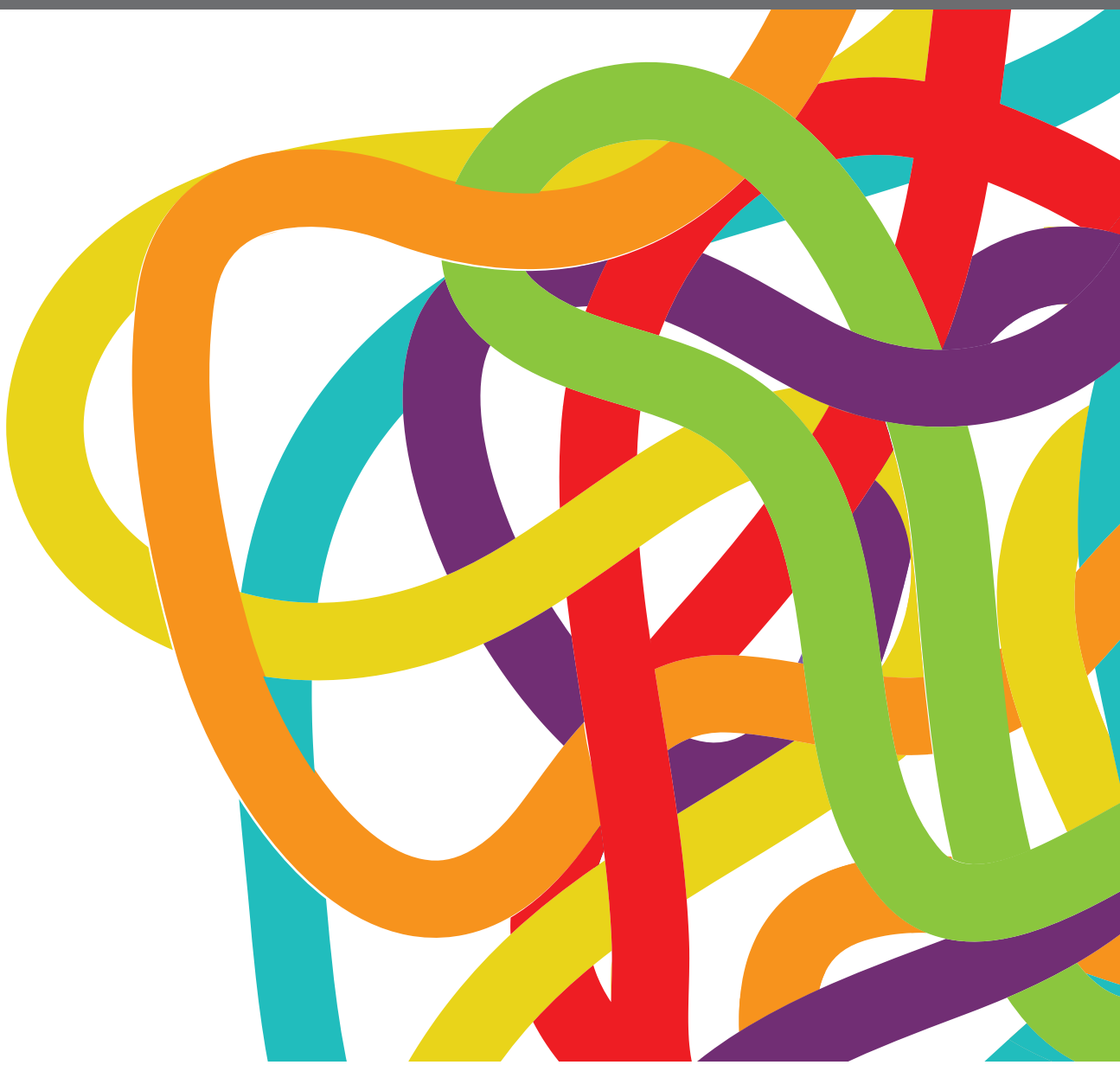

frontiers Research Topics

ISSN 1664-8714
ISBN 978-2-88976-396-2
DOI 10.3389/978-2-88976-396-2

About Frontiers

Frontiers is more than just an open-access publisher of scholarly articles: it is a pioneering approach to the world of academia, radically improving the way scholarly research is managed. The grand vision of Frontiers is a world where all people have an equal opportunity to seek, share and generate knowledge. Frontiers provides immediate and permanent online open access to all its publications, but this alone is not enough to realize our grand goals.

Frontiers Journal Series

The Frontiers Journal Series is a multi-tier and interdisciplinary set of open-access, online journals, promising a paradigm shift from the current review, selection and dissemination processes in academic publishing. All Frontiers journals are driven by researchers for researchers; therefore, they constitute a service to the scholarly community. At the same time, the Frontiers Journal Series operates on a revolutionary invention, the tiered publishing system, initially addressing specific communities of scholars, and gradually climbing up to broader public understanding, thus serving the interests of the lay society, too.

Dedication to Quality

Each Frontiers article is a landmark of the highest quality, thanks to genuinely collaborative interactions between authors and review editors, who include some of the world's best academicians. Research must be certified by peers before entering a stream of knowledge that may eventually reach the public - and shape society; therefore, Frontiers only applies the most rigorous and unbiased reviews.
Frontiers revolutionizes research publishing by freely delivering the most outstanding research, evaluated with no bias from both the academic and social point of view. By applying the most advanced information technologies, Frontiers is catapulting scholarly publishing into a new generation.

What are Frontiers Research Topics?

Frontiers Research Topics are very popular trademarks of the Frontiers Journals Series: they are collections of at least ten articles, all centered on a particular subject. With their unique mix of varied contributions from Original Research to Review Articles, Frontiers Research Topics unify the most influential researchers, the latest key findings and historical advances in a hot research area! Find out more on how to host your own Frontiers Research Topic or contribute to one as an author by contacting the Frontiers Editorial Office: frontiersin.org/about/contact

ENVIRONMENT AND SKIN CANCER

Topic Editors:
Nabiha Yusuf, University of Alabama at Birmingham, United States
Thomas Haarmann-Stemmann, Leibniz-Institut für Umweltmedizinische Forschung (IUF), Germany
Motoki Nakamura, Nagoya City University, Japan

Citation: Yusuf, N., Haarmann-Stemmann, T., Nakamura, M., eds. (2022). Environment and Skin Cancer. Lausanne: Frontiers Media SA.
doi: 10.3389/978-2-88976-396-2

Table of Contents

frontiers | Frontiers in Oncology

EDITORIAL
published: 27 May 2022
doi: 10.3389/fonc.2022.924225

Editorial: Environment and Skin Cancer

Nabiha Yusuf[1]*, *Thomas Haarmann-Stemmann*[2] *and Motoki Nakamura*[3]

[1] Department of Dermatology, University of Alabama at Birmingham, Birmingham, AL, United States, [2] Department of Dermatology, IUF – Leibniz-Research Institute for Environmental Medicine, Düsseldorf, Germany, [3] Department of Environmental and Geriatric Dermatology, Graduate School of Medical Sciences, Nagoya City University, Nagoya, Japan

Keywords: ultraviolet radiation, non-melanoma skin cancer, melanoma, exposome, merkel cell carcinoma

Editorial on the Research Topic

Environment and Skin Cancer

The incidence of melanoma and non-melanoma skin cancer (NMSC) has been steadily increasing over the past decades (1). With millions of people affected worldwide, skin cancer poses a global threat for the health of the general population and a tremendous economic burden to health care systems (2). The major risk factor for the development of the vast majority of skin cancers, including basal cell carcinoma (BCC), squamous cell carcinoma (SCC), and melanoma, is a repetitive exposure to ultraviolet (UV) radiation. Second to polyomavirus infection, UV exposure is also major risk factor for the development of Merkel cell carcinoma (MCC), a rare but highly aggressive type of skin cancer (3). Whereas UVB radiation is absorbed by the DNA resulting in the formation of mutagenic DNA photoproducts, UVA rays interact with endogenous photosensitizers to induce oxidative stress and oxidative damage of DNA, proteins, and lipids (4). DNA damage-dependent and -independent responses stimulate pro-inflammatory, anti-apoptotic and immunosuppressive effects thereby facilitating the accumulation of damaged cells which may give rise to skin cancer. Accordingly, parameters such as the depletion of the ozone layer, the demographic development, and recreational behavior (sun bathing, tanning beds) sign responsible for the increasing numbers of skin cancers. However, next to UV radiation, exposure to various environmental chemicals, including arsenic compounds and combustion-derived polycyclic aromatic hydrocarbons (PAH), and even to therapeutic agents, such as sulfonamide-based protein kinase inhibitors, may induce skin carcinogenesis, by either directly damaging the DNA, causing oxidative stress, or interacting with signal transduction networks and transcription factors (5).

The identification of risk factors across the skin exposome and their mutual interaction, the elucidation of pathomechanisms and the identification of biomarkers is key to the development of novel preventive and therapeutic strategies for skin cancer. In this Research Topic of *Frontiers in Oncology* the authors shed light on different levels and facets of skin cancer development and biology which hopefully stimulates the field to enforce and improve the fight against this devastating disease.

Starting in the stratosphere, Umar and Tasduq focus on the depletion of the ozone layer, its impact on the UV index and the resulting consequences for human health. The authors also address potential adverse health effects of skin photoprotection, i.e. a vitamin D deficiency and associated disorders. The authors also contributed to another work emphasizing that autophagy positively regulates skin homeostasis by enhancing DNA damage recognition. Specifically, exposure of human dermal fibroblasts to UVB radiation impaired the autophagy response in a time- and intensity-independent manner, which was reversed after treatment with pharmacological activators, thus protecting against UVB radiation-induced photodamage [Umar et al.].

OPEN ACCESS

Edited and reviewed by:
Vladimir Spiegelman, Penn State Milton S. Hershey Medical Center, United States

***Correspondence:**
Nabiha Yusuf
nabihayusuf@uabmc.edu

Specialty section:
This article was submitted to Skin Cancer, a section of the journal Frontiers in Oncology

Received: *20 April 2022*
Accepted: *04 May 2022*
Published: *27 May 2022*

Citation:
Yusuf N, Haarmann-Stemmann T and Nakamura M (2022) Editorial: Environment and Skin Cancer. Front. Oncol. 12:924225. doi: 10.3389/fonc.2022.924225

The occurrence of NMSC with advanced age and UVB exposure is specifically linked to diminished insulin-like growth factor-1 (IGF-1) signaling from senescent dermal fibroblasts in geriatric skin. Frommeyer et al. found that wounding therapies, such as dermabrasion, microneedling, chemical peeling, and fractionated laser resurfacing, restore IGF-1/IGF-1R signaling in geriatric skin. Wondrak and co-workers report about another potential therapeutic approach involving hypochlorous acid (HOCl), an agent that has emerged as an important component of the skin exposome. While exploring the interaction between solar UV exposure and environmental HOCl exposure, they identified an unrecognized photo-chemopreventive activity of topical HOCl and associated chlorination stress that blocked tumorigenic inflammatory progression in UV-induced high-risk mouse skin [Snell et al.].

Nurzat et al. investigate the functional role of different integrin alpha/beta (ITGA/ITGB) subunits in cutaneous melanoma. Bioinformatic analysis tools were used to identify abnormally-expressed genes and gene regulatory networks associated with melanoma, which may improve our understanding of the melanoma pathogenesis. Specifically, they found that the expression level of various ITGA and ITGB subunits was associated with immune cell infiltration, metastasis, and disease-free and overall survival. Vogeley et al. focus on environmental and occupational risk factors, in particular UV radiation and PAHs, which initiate the development of cutaneous SCC, at least in part, by activating the aryl hydrocarbon receptor and impairing defense mechanisms, such as DNA repair, apoptosis and anti-tumor immune responses. Apart from environmental and occupational stressors, certain therapeutic drugs induce the development of cutaneous SCC as an off-target effect. The BRAF inhibitor vemurafenib, approved for treating patients with BRAF V600E-mutant melanomas, for instance, causes various cutaneous adverse events, including hyperkeratotic skin lesions and cutaneous SCCs. Tham et al. report that both cutaneous adverse events are under direct control of vemurafenib-dependent MEK-ERK hyperactivation and confirm the dependence on preexisting genetic alterations in epidermal keratinocytes that predispose to carcinogenesis.

Another protein involved in carcinogenesis, in particular in the pathogenesis of melanoma, is the plasminogen activating inhibitor-1 (PAI-1). Several reports indicate pro-tumorigenic functions of PAI-1 in cancer progression and metastasis, for instance controlling PD-L1 expression. Moreover, baseline serum levels of PAI-1 were significantly decreased in therapy responders compared to non-responders. These results suggest that baseline serum levels of PAI-1 may be useful as a biomarker for identifying patients who would respond to anti-melanoma immunotherapy [Ohuchi et al.]. Irrespective of molecular pathomechanisms, Chang et al. assess whether and to which extent comorbidities and stages may influence the prognosis of melanoma patients. In a retrospective cohort study by using the national health insurance research database in Taiwan, a higher risk of mortality was found in patients who had localized tumors, regional metastases, or distant metastases with more comorbidity scores.

Wijaya et al. conducted a systematic review and meta-analysis to assess the association between MCC polyoma virus (MCPyV) infection and MCC, non-MCC skin lesions, and healthy skin. MCPyV infection significantly increased the risk for MCC. However, the low prevalence of MCPyV in non-MCC skin lesions did not exclude a pathogenic association of this virus with the development of non-MCC skin lesions. Staying in the MCC context, Nakamura et al. investigated the prognostic value of tertiary lymphoid structures (TLSs) in patients suffering from MCPyV-positive and MCPyV-negative MCC. They found that TLSs can indeed serve as prognostic biomarker for MCC patients, even in cohorts encompassing MCPyV-negative, thus UV-induced cases. Furthermore, the assessment of TLS-associated chemokine profiles may enable a better understanding of the tumor microenvironment in patients with MCPyV-positive or MCPyV-negative MCC.

AUTHOR CONTRIBUTIONS

NY wrote the draft. TH and MN edited the draft and finalized the current version. All the authors made substantial intellectual contribution and approved the article for publication.

FUNDING

This work was supported by 1R01AR071157-01A1 (Nabiha Yusuf) from the National Institute of Arthritis and Musculoskeletal and Skin Diseases.

REFERENCES

1. Aggarwal P, Knabel P, Fleischer ABJr. United States Burden of Melanoma and non-Melanoma Skin Cancer From 1990 to 2019. *J Am Acad Dermatol* (2021) 85:388–95. doi: 10.1016/j.jaad.2021.03.109
2. Guy GPJr., Machlin SR, Ekwueme DU, Yabroff KR. Prevalence and Costs of Skin Cancer Treatment in the U.S., 2002-2006 and 2007-2011. *Am J Prev Med* (2015) 48:183–7. doi: 10.1016/j.amepre.2014.08.036
3. Wong SQ, Waldeck K, Vergara IA, Schroder J, Madore J, Wilmott JS, et al. UV-Associated Mutations Underlie the Etiology of MCV-Negative Merkel Cell Carcinomas. *Cancer Res* (2015) 75:5228–34. doi: 10.1158/0008-5472.CAN-15-1877
4. Cadet J, Douki T. Formation of UV-Induced DNA Damage Contributing to Skin Cancer Development. *Photochem Photobiol Sci* (2018) 17:1816–41. doi: 10.1039/C7PP00395A
5. Schwarz M, Munzel PA, Braeuning A. Non-Melanoma Skin Cancer in Mouse and Man. *Arch Toxicol* (2013) 87:783–98. doi: 10.1007/s00204-012-0998-9

Conflict of Interest: The authors declare that the research was conducted in the absence of any commercial or financial relationships that could be construed as a potential conflict of interest.

this article, or claim that may be made by its manufacturer, is not guaranteed or endorsed by the publisher.

frontiers in Oncology

ORIGINAL RESEARCH
published: 02 August 2021
doi: 10.3389/fonc.2021.726066

Pharmacological Activation of Autophagy Restores Cellular Homeostasis in Ultraviolet-(B)-Induced Skin Photodamage

Sheikh Ahmad Umar[1,2], *Naikoo Hussain Shahid*[1,2], *Lone Ahmad Nazir*[1,2], *Malik Ahmad Tanveer*[1,2], *Gupta Divya*[1,2], *Sajida Archoo*[1,2], *Sharma Rai Raghu*[1,2] *and Sheikh Abdullah Tasduq*[1,2*]

[1] *Biological Sciences, Academy of Scientific & Innovative Research (AcSIR), Ghaziabad, India,* [2] *Pharmacokinetics-Pharmacodynamics (PK-PD) and Toxicology Division, Council of Scientific & Industrial Research (CSIR)-Indian Institute of Integrative Medicine, Jammu Tawi, India*

OPEN ACCESS

Edited by:
Nabiha Yusuf, University of Alabama at Birmingham, United States

Reviewed by:
Tahseen H. Nasti, Emory University, United States
Mohammad Asif Sherwani, University of Alabama at Birmingham, United States

***Correspondence:**
Sheikh Abdullah Tasduq
stabdullah@iiim.res.in; tasduq11@gmail.com

Specialty section:
This article was submitted to Skin Cancer, a section of the journal Frontiers in Oncology

Received: *16 June 2021*
Accepted: *15 July 2021*
Published: *02 August 2021*

Citation:
Umar SA, Shahid NH, Nazir LA, Tanveer MA, Divya G, Archoo S, Raghu SR and Tasduq SA (2021) Pharmacological Activation of Autophagy Restores Cellular Homeostasis in Ultraviolet-(B)-Induced Skin Photodamage. Front. Oncol. 11:726066. doi: 10.3389/fonc.2021.726066

Ultraviolet (UV) exposure to the skin causes photo-damage and acts as the primary etiological agent in photo-carcinogenesis. UV-B exposure induces cellular damage and is the major factor challenging skin homeostasis. Autophagy allows the fundamental adaptation of cells to metabolic and oxidative stress. Cellular dysfunction has been observed in aged tissues and in toxic insults to cells undergoing stress. Conversely, promising anti-aging strategies aimed at inhibiting the mTOR pathway have been found to significantly improve the aging-related disorders. Recently, autophagy has been found to positively regulate skin homeostasis by enhancing DNA damage recognition. Here, we investigated the geno-protective roles of autophagy in UV-B-exposed primary human dermal fibroblasts (HDFs). We found that UV-B irradiation to HDFs impairs the autophagy response in a time- and intensity-independent manner. However, improving autophagy levels in HDFs with pharmacological activators regulates the UV-B-induced cellular stress by decreasing the induction of DNA photo-adducts, promoting the DNA repair process, alleviating oxidative and ER stress responses, and regulating the expression levels of key cell cycle regulatory proteins. Autophagy also prevents HDFs from UV-B-induced nuclear damage as is evident in TUNEL assay and Acridine Orange/Ethidium Bromide co-staining. Salubrinal (an $eIF_2\alpha$ phosphatase inhibitor) relieves ER stress response in cells and also significantly alleviates DNA damage and promotes the repair process in UV-B-exposed HDFs. P62-silenced HDFs show enhanced DNA damage response and also disturb the tumor suppressor PTEN/pAKT signaling axis in UV-B-exposed HDFs whereas *Atg7*-silenced HDFs reveal an unexpected consequence by decreasing the UV-B-induced DNA damage. Taken together, these results suggest that interventional autophagy offers significant protection against UV-B radiation-induced photo-damage and holds great promise in devising it as a suitable therapeutic strategy against skin pathological disorders.

Keywords: ultraviolet radiation (UV-B), oxidative stress, endoplasmic reticulum stress, autophagy, DNA damage response, genotoxicity

INTRODUCTION

Skin being the external covering of the body protects internal organs from outside environmental insults including the adverse effects of ultraviolet (UV) irradiation (1). Solar radiation is essential for survival to different life forms on earth, but excessive exposure leads to skin photoaging and malignancies constituting photo-damage and photo-carcinogenesis (2). Macro-autophagy (hereafter referred to as autophagy) at basal levels protects cells from stress and nutrient deprivation during starvation conditions and thereby maintains tissue homeostasis (3). Cellular autophagy levels can be improved chemically in order to restore tissue homeostasis in response to diverse physiological and pathological stresses, including from solar UV-B irradiation (4–6). Dysfunctional autophagy has been associated to multiple human pathologies, such as metabolic diseases, cardiovascular diseases, aging, neuro-degeneration, infectious diseases, and cancer, and attempts are being made to use autophagy as a selective therapeutic intervention in different disease conditions based on the differential roles it performs in maintaining tissue homeostasis (7, 8). The role of autophagy is context dependent and performs both oncogenic and tumor-suppressive functions (9), promoting or suppressing tumorigenesis and thereby regulates inflammation, cell proliferation, and migration (10, 11). Autophagy removes cellular debris to prevent genomic damage or promotes DNA repair in response to ionizing radiation-induced DNA double-strand breaks in mammalian cells (11, 12). In either way, the role of autophagy is to protect cells from external insults that disturb the integrity of cells. Recently, it has been observed that autophagy regulates nucleotide excision repair (NER) and eliminates DNA base lesions, including cyclobutane pyrimidine dimers (CPD) and pyrimidine-(6-4)-pyrimidone photoproducts (6-4PP) induced by solar UV-B radiation (13–15). It has also been found that recruitment of DDB2 to UV-induced CPD sites is significantly impaired in autophagy-deficient cells. In mice, Rapamycin has been found to decrease the UV-B-induced tumorigenesis while the inhibitor Spautin-1 augments it (16, 17). These findings cite the critical role of autophagy in maintaining proper NER activity and suggest a new tumor-suppressive mechanism of autophagy in tumor initiation and regulation. Previously, we have reported from our own lab that UV-B-induced Ca^{2+} deficit within ER lumen is mediated by immediate oxidative stress induced upon UV-B irradiation to skin cells. Insufficient Ca^{2+} reserves within ER lumen develops ER stress leading to Unfolded Protein Response (UPR) in skin cells that ultimately disturb the cellular homeostasis (18). We have also reported in another study that the natural anti-oxidant bio-active molecule Glycyrrhizic acid (GA) alleviates oxidative stress-induced DNA damage response (DDR) by improving cellular autophagy signaling in UV-B-irradiated primary HDFs (19). Despite these preliminary findings, the role of autophagy in UV-B-induced photo-damage response is unclear and warrants further studies to unravel the facts. In line with these previous findings, we hypothesized the possible integration of DDR and autophagy signaling axis as a positive association in protecting skin cells against genotoxic stress response (20). Here, in this study, we attempted to investigate the roles of autophagy in regulating skin homeostasis notably under genotoxic stress on UV-B radiation exposure to HDFs. We found that UV-B irradiation to HDFs induce impaired autophagic flux at a lethal dose of UV-B irradiation (30 mJ/cm^2). However, improving autophagy response with pharmacological activator Rapamycin significantly alleviates the induction of oxidatively induced DNA photo-adducts and enhances the DNA repair mechanism, alleviates the TUNEL-positive cells, and reduces early and late apoptotic cells and prevents ER calcium leakage in HDFs in 6 h UV-B post-irradiation. Furthermore, we found that relieving ER stress response with Salubrinal prevents oxidative DNA damage by improving autophagy response in UV-B-exposed HDFs. The GFP-RFP-LC3B puncta assay depicts appreciable red puncta dots in Rapamycin- and Salubrinal-treated cells showing enhanced autophagic flux upon UV-B exposure to HDFs compared to those exposed only to UV-B. Rapamycin treatment also significantly decreases the expression profile of key cell cycle regulatory proteins P21 and P27 and DDR pathway proteins DDB2 and p-P53, indicating that autophagy has cell protective roles in UV-B-induced photo-damage. Decreasing autophagic flux by silencing P62 confirmed our preliminary findings as the p-χH_2AX foci are significantly augmented in P62-silenced cells but not in *Atg7*-silenced HDFs citing differential roles of autophagy-related genes in regulating UV-B-induced genotoxic stress response. Together, the above findings suggest that pharmacological activation of autophagy significantly alleviates the DNA damage and promotes the DNA repair process in UV-B-exposed HDFs and is critical in restoring cellular homeostasis. Furthermore, these results suggest that interventional autophagy holds great promise to be devised as a suitable therapeutic strategy against radiation-induced skin photo-damage disorders.

MATERIALS AND METHODS

Chemicals

Human primary dermal fibroblast cell line from juvenile foreskin (HDF) and primary fibroblast expansion media was obtained from HiMedia, Mumbai, India. Fetal bovine serum (FBS), penicillin–streptomycin, trypsin–EDTA, 3-(4, 5-dimetylthiazol-yl)-diphenyl tetrazolium bromide (MTT), phosphatase-protease cocktail, RIPA buffer, and H_2DCFDA dye were purchased from Sigma–Aldrich Chemicals (St. Louis, MO). Antibodies against P62, BECN1, phospho-ATM, phospho-ATR, phospho-mTOR, phospho-p53, phospho-Chk1, phospho-Chk2, Bcl-2, phospho-e$IF_2\alpha$, e$IF_2\alpha$, LC3B, phospho-AMPKα, AMPK, and phospho-χH_2AX were purchased from Cell Signaling Technology, Danvers, MA. Antibodies against GRP78, PTEN, CHOP/GAD153, DDB2, phospho-AKT, and siRNA P62/*Atg7* and secondary antibodies were purchased from Santa Cruz Biotechnologies (Santa Cruz, CA, USA). Fura 3 AM, DAPI, ER tracker, Acridine Orange, Ethidium Bromide, Salubrinal, Rapamycin, Chloroquine, Bafilomycin A1, Everolimus, and GFP-RFP-LC3B puncta assay kit were purchased from Thermo Scientific. Antibodies against P21 and P27, TUNEL assay, and CPD ELISA kits were procured from Abcam. Bradford reagent was obtained from Sigma-Aldrich. PVDF membrane was purchased from Bio-Rad, Hercules, CA. Antibody against β-actin was purchased from Sigma-Aldrich.

Cell Culture and UV-B Exposure to HDFs

HDFs were maintained in primary fibroblast expansion media from HiMedia supplemented with all the essentials including antibiotics, L-Glutamine, glucose (3.5 g/L), Hepes (15 mM), Penicillin (120 mg/L), Streptomycin (270 mg/L), and FBS (10% v/v) at 37°C in a humidified atmosphere of 5% CO_2. Cells were exposed to UV-B using DAAVLIN UVA/UVB Research Irradiation Unit (Bryan, OH, USA) having digital control. The lamps were maintained at a fixed distance of 24 cm from the surface of cell culture dishes. Majority of the resulting wavelengths (>90%) were in the UV-B range (280–320 nm). UV-B irradiation of 10, 20, and 30 mJ/cm^2 was used for initial standardization and dose optimization and 30 mJ/cm^2 dose was then selected and used for further experiments for mechanistic studies based on the analysis of cell toxicity induced by UV-B exposure to HDFs. Though 10 mJ/cm^2 is considered as the physiological dose mimicking the environmental dosage of UV-B in the solar radiation spectrum (21), it induces less cytotoxicity (10%–20%) and shows least molecular changes to be selected for mechanistic studies. Before UV-B exposure, cells were first sensitized with chemical mediators like Rapamycin, Chloroquine, Salubrinal, Bafilomycin, and siRNA P62/*Atg7* for a specified time period as per the particular experimental requirements to induce or inhibit autophagy. Cell monolayers were then first washed with Dulbecco's phosphate buffered saline (DPBS) and then UV-B-irradiated under a thin layer of pre-warmed DPBS. After irradiation, cells were again washed with DPBS twice and incubated in fresh medium with or without chemical mediators as per the experimental protocol requirements for 1, 3, 6, or 24 h UV-B post-irradiation.

Cell Viability Analysis

Colorimetric-based MTT assay was employed for cell viability analysis as described earlier (22). Briefly, cells were seeded and incubated overnight in a humidified chamber. After treatment with autophagy modulators or UV-B or both, the cells were further incubated for 24 h. Cell viability was evaluated by assaying for the ability of functional mitochondria to catalyze the reduction of MTT to formazan salt by an enzyme mitochondrial dehydrogenase that appears as crystals at the bottom of culture wells/dishes and was quantified by a MULTISKAN SPECTRUM plate reader (Thermo Electron Corporation) at 570 nm using DMSO as solvent. The mean of three independent readings was taken for final quantification of data for result analysis.

Determination of Reactive Oxygen Species

Dichlorofluorescin Diacetate (H_2DCF-DA) staining was employed for the measurement of immediate ROS generated upon UV-B exposure to HDFs (1 h) post-UV-B irradiation, as described previously (21). Briefly, HDFs were seeded in six-well plates and allowed to attach overnight. Cell monolayers were pre-treated with Salubrinal (25 μM) and Everolimus (200 nM) for 2 h. Cells were washed three times with DPBS and then exposed to UV-B 30 mJ/cm^2. After UV-B irradiation, cells were then again washed with DPBS twice and incubated with fresh media with Salubrinal (25 μM) and Everolimus (200 nM) for 1 h UV-B post-irradiation. After treatment, the cells were stained with 5 μM H_2DCF-DA for 30 min at 37°C. The cells were then washed with DPBS thrice and observed immediately under a fluorescent microscope (EVOS FL Color Imaging System from Life Technologies, B2014-155G-054). Five random microscopic fields were selected and the intensity of fluorescence was quantified using the ImageJ software, as mentioned previously (23).

Confocal Microscopy Imaging Of Intracellular Ca^{2+} Release

Ca^{2+} levels were determined by the Ca^{2+} indicator Fura 3 AM (Thermo Scientific) using confocal microscopy imaging as described previously. Briefly, the cells were seeded to sterile coverslips and incubated overnight in a humidified chamber to adhere. Cells were or were not treated with Salubrinal (25 μM), Rapamycin (100 nM), and Bafilomycin A1 (100 nM) for 2 h. Cells were then thrice washed with DPBS and exposed to UV-B treatment at 30 mJ/cm^2 as described earlier and supplemented with fresh DMEM media with indicated concentrations of Salubrinal, Rapamycin, and Bafilomycin as required and incubated further for 6 h post-UV-B irradiation. HDFs were loaded with fluorescent Ca^{2+} indicator dye Fura 3 AM at 5 μM for 45 min before imaging post 6 h UV-B irradiation. Cells were washed three times with live cell imaging solution for imaging using a laser scanning confocal microscope (OLYMPUS FUOVIEW FV1000) by using a 40× objective lens. Five random microscopic fields were selected, and the intensity of fluorescence was quantified using the ImageJ software.

siRNA-Mediated Knockdown of P62/*Atg7*

Validated siRNA P62/*Atg7* were purchased from Santa Cruz Biotechnology. siRNA and Lipofectamine (Invitrogen) were diluted in Opti-MEM I reduced serum medium (Invitrogen) per the manufacturer's instructions. HDFs were incubated for 16 h with transfection mixture at a final siRNA concentration of 50 pmol as described previously (24) and then exposed to UV-B (30 mJ/cm^2) and were finally supplemented with fresh medium for further 6 h UV-B post-irradiation.

Protein Isolation and Western Blotting

Cells were trypsinized, harvested in PBS (pH 7.4), centrifuged, and resuspended in RIPA buffer (Sigma-Aldrich). After incubation for 45 min at 4°C, cell lysates were centrifuged at 17,530*g* for 30 min at 4°C to remove cellular debris. Protein concentrations were determined by Bradford reagent. For Western blotting, 30–80 μg protein loads were denatured at 100°C for 3 min in Laemmli buffer. Protein samples were resolved on 4%–15% SDS gels at 70–80 V. Proteins were electro-transferred to PVDF membrane using a *BIO-RAD* Mini Transblot Electrophoretic Transfer unit. Membranes were blocked in 5% fat-free dry milk/3% BSA in 50 mM Tris, pH 8.0, with 150 mM sodium chloride, 2.6 mM KCl, and 0.05% Tween20 for 2 h. Primary antibodies were used either in fat-free milk or BSA and incubated overnight at 4°C. Anti-GRP78, anti-SQSTM1/p62, anti-Bcl_2, anti-p-mTOR, anti-mTOR, anti-CHOP/GAD153, anti-p-$elf_2\alpha$, anti-$elf_2\alpha$, anti-BECN1, anti-p-ATM, anti-p-ATR, anti-p-P53, anti-p-Chk1, anti-LC3B, anti-p-AMPKα, anti-AMPKα, anti-p-χH_2AX, anti-PTEN, anti-p-AKT, and anti-*Atg7* were from Cell Signaling Technology, Danvers, MA, and mouse and anti-actin were from Sigma-Aldrich. Goat anti-rabbit and goat anti-mouse

immunoglobulin G antibodies conjugated with HRP (Santa Cruz Biotechnologies) were used as secondary antibodies. Chemiluminescence was detected by Immobilon chemiluminescent HRP substrate (EMD-Millipore, Billerica, MA) and visualized by Molecular Image ChemiDocTM XRS+ (BIO-RAD), Universal Hood II, Serial No 721BR04356. Densitometric measurement of the bands was performed using Image LabTM software (version 3.0; Bio-Rad).

TUNEL Assay

TUNEL assay was performed with an In Situ Direct DNA Fragmentation (TUNEL) Assay Kit (ab66108) from (Abcam) according to the manufacturer's instructions as described previously (19). Briefly, the cells were seeded in dishes and incubated overnight in a humidified chamber to adhere. Cells were or were not treated with Salubrinal (25 μM), Rapamycin (100 nM), and Chloroquine (50 μM) for 2 h. Cell monolayers were then washed thrice with DPBS and exposed to UV-B (20 and 30 mJ/cm^2). Again, the cells were washed thrice with DPBS and supplemented with fresh DMEM media with or without the indicated concentrations of Salubrinal, Rapamycin, and Chloroquine as required and incubated further for 6 h post-UV-B irradiation. Cell smears after fixation, blocking, and permeabilization were incubated with TUNEL reaction mixture for 1 h and wrapped in aluminum foil to avoid light exposure at 37°C and counterstained with RNase/PI solution for an additional 20 min. Substrate solution was added, and cells were imaged by a fluorescent microscope (EVOS FL Colour Imaging System) for the detection of TUNEL-positive cells, and the intensity of fluorescence was quantified using the ImageJ software.

ELISA-Based Detection of DNA Photo-Adducts

UV-B-induced CPD/6,4 PP photo-adducts were quantified with an *in situ* OxiSelect UV-Induced DNA Damage staining kit (CPD/6,4PP quantification kit from Cell Bio Labs, Inc., San Diego, CA, USA) according to the manufacturer's instruction. Briefly, the cells were seeded and allowed to adhere overnight. Cells were or were not treated with Salubrinal (25 μM), Rapamycin (100 nM), and Chloroquine (50 μM) for 2 h or were silenced for P62 using siRNA. After the corresponding treatments to HDFs, cell monolayers were exposed to UV-B at (10, 20 and 30 mJ/cm^2) and supplemented with fresh DMEM media with or without the indicated concentrations of Salubrinal, Rapamycin, and Chloroquine for further 6 h post-UV-B irradiation. DNA was isolated and incubated with the anti-CPD antibody overnight on an orbital shaker at room temperature. Then, the cells were washed and incubated with Secondary Antibody-HRP Conjugate for 2 h. The absorbance was measured at 450 nM using the MULTISKAN SPECTRUM plate reader (Thermo Electron Corporation). A mean of three independent readings was used to quantify the data for final result analysis.

Dual Acridine Orange/Ethidium Bromide Fluorescent Staining for Detection of Apoptotic Cells

Briefly, the cells were seeded in six-well plates and allowed to adhere overnight in an incubator. Cells were left untreated or treated with Salubrinal (25 μM), Rapamycin (100 nM), and Chloroquine (50 μM) for 2 h and washed thrice with DPBS. Cells were then exposed to UV-B at 30 mJ/cm^2 and again washed thrice with DPBS. Cells were then supplemented with fresh DMEM media with or without indicated concentrations of Salubrinal, Rapamycin, and Chloroquine as explained for an additional 6 h post-UV-B irradiation. Dual fluorescent staining solution (1 μl) containing 100 μg/ml AO and 100 μg/ml EtBr was added to cell monolayers for 5 min at RT and then covered with coverslip and were fixed as described previously (25). The morphology of HDFs into early and late apoptotic cells was examined within 20 min using a fluorescent microscope (EVOS FL Colour Imaging System). AO/EtBr staining method was repeated at least three times for quantification and the data are presented by the classification of cells to live cells, early apoptotic, late apoptotic, and necrotic cells as reported previously (26).

Immunostaining

Cultured cells were seeded on coverslips in six-well plates and incubated in the presence or absence of indicated concentrations of Salubrinal (25 μM), Rapamycin (100 nM), and Chloroquine (50 μM) for 2 h. Cells were then exposed to UV-B (30 mJ/cm^2) and again washed thrice with DPBS and supplemented with fresh DMEM media with indicated concentrations of Salubrinal, Rapamycin, and Chloroquine for required post UV-B time intervals of 1, 6, and 24 h and were fixed in 4% paraformaldehyde for 15 min at room temperature. Cells were permeabilized in PBS containing 0.1%Triton X-100 at room temperature for 10 min. Non-specific binding sites were blocked by incubating the cells with 1% BSA and 22.52 mg/ml Glycine in PBST (PBS+0.1% Tween 20) at room temperature for 30 min. Cells were incubated with P62, LC3B, p-P53, p-χH_2AX, PTEN, p-AKT, DDB2, *Atg7*, p-AMPKα, P21, and P27 antibodies at a dilution of 1:100 in 1% BSA and 22.52 mg/ml Glycine in PBST (PBS+0.1% Tween 20) overnight at 4°C. Cells were later on washed and incubated with Alexa Fluor 488/594-conjugated antimouse/antirabbit secondary antibody as required at a dilution of 1:500 in 1% BSA and 22.52 mg/ml Glycine in PBST (PBS+0.1% Tween 20) for 2 h at room temperature in dark conditions. Cells were then washed three times with PBS and stained with DAPI 1 μg/ml in PBS. The coverslips were mounted on glass slides, and cells were imaged by a laser scanning confocal microscope (OLYMPUS FUOVIEW FV1000) by using a ×40 objective lens. Five random microscopic fields were selected, and the intensity of fluorescence was quantified using the ImageJ software.

GFP-RFP-LC3B Puncta Assay for the Detection of Autophagic Flux

For analysis of autophagosomes, the cells were seeded in dishes and allowed to adhere overnight in an incubator. BacMam 2.0 RFP-GFP-LC3B reagent was added to HDFs and incubated overnight to ensure maximum protein expression. The cells were thrice washed with DPBS. Then, the cells were or were not treated with Rapamycin (100 nM), Salubrinal (25 μM), and Bafilomycin (100 nM) for 2 h. The cells were then exposed to UV-B (30 mJ/cm^2) and again washed thrice with DPBS and supplemented with fresh DMEM media with indicated

concentrations of Rapamycin, Salubrinal, and Bafilomycin for an additional 6 h post UV-B irradiation. Cells were then again washed with DPBS thrice and visualized using standard GFP (green fluorescent protein) and RFP (red fluorescent protein) settings. The punctae dots were imaged by a laser scanning confocal microscope (OLYMPUS FUOVIEW FV1000) by using a ×40 objective lens. Five random microscopic fields were selected, and quantification of punctae dots was done as reported previously (27).

Statistical Analysis

Data are expressed as the mean ± standard deviation (SD). INSTAT statistical software was used to perform statistical analysis. Data are presented as mean ± SE from three independent experiments. Comparison between two groups was performed by Student's *t*-test and that among groups was carried out by one-way ANOVA for statistical significance. $p \leq 0.05$, $p < 0.01$, and $p < 0.001$ were considered as statistically significant.

RESULTS

UV-B Exposure to HDFs Induce Impaired Autophagy Response

UV-B irradiation induces impaired autophagy response in a dose-independent manner as is evident from the Western blotting analysis of key autophagy marker proteins. UV-B exposure to HDFs increases the expression levels of LC3BII at 24 h but not at 3 and 6 h, downregulates P62 expression initially in an insignificant manner but not at 24 h, and increases the expression of BECN1 in an altered fashion, which increases immediately after UV-B exposure, but the expression is blocked in delayed post-exposure, which does not correspond to induction of autophagy response. Similarly, the expression levels of p-AMPKα increases in 3 and 6 h UV-B exposure but starts decreasing in 24 h post-UV-B irradiation. The expression of p-mTOR also increases dose dependently at 3 and 6 h UV-B post-irradiation but not at 24 h, indicating induction of impaired autophagy response upon UV-B exposure to HDFs, because the expression status of different autophagy proteins is modulated in an altered fashion not corresponding to normal autophagy response (**Figures 1A–E**). We confirmed the induction of impaired autophagic flux response upon UV-B 30 mJ/cm^2 exposure to HDFs through GFP-RFP-LC3B puncta assay in confocal microscopy depicting appreciable red puncta dots, indicative of autolysosomes compared to yellow puncta dots indicative of autophagosomes in Rapamycin- and Salubrinal-treated cells showing enhanced autophagy flux upon UV-B exposure to HDFs compared to those exposed only to UV-B. Bafilomycin A1 treatment to UV-B-exposed HDFs was used as a positive control (**Figures 1F, G**).

Improving Autophagy and Relieving ER Stress Response Alleviates DNA Photo-Adducts (CPD and 6,4PP) in UV-B-Exposed HDFs

UV-B irradiation to HDFs leads to induction of DNA photo-adducts (CPD and 6, 4PP) in an intensity-dependent manner in 6 h UV-B post-irradiation. Improving autophagy in HDFs with Rapamycin (100 nM) and upon relieving ER stress response with Salubrinal (25 μM) in UV-B-irradiated HDFs significantly alleviates the induction of both CPD and 6,4PP photo-adducts by 0.65- and 0.5-fold, respectively. Inhibition of autophagy response with Chloroquine (50 μM) increases the formation of CPD by 0.2-fold, whereas it increases the formation of 6,4PP by about 0.35-fold compared to UV-B-treated HDFs (**Figure 2A**). To confirm our findings whether pharmacological activation of autophagy improves the UV-B-induced photo-damage response in HDFs, we silenced key autophagy cargo protein P62 and found that it significantly impacts the induction of photo-adducts, CPD, compared to that of 6,4PP and augments the induction of CPD by 0.5-fold and 6,4PP by 0.22-fold. siRNA P62 only treated cells had negligible effect on the induction of DNA photo-adducts compared to both control and UV-B-treated cells (**Figure 2B**). We confirmed ELISA-based findings through immunofluorescence and found that the expression levels of CPD are significantly increased in UV-B-exposed HDFs in an intensity-dependent manner in 6 h UV-B post-irradiation. Inhibiting autophagy response with Chloroquine increases the expression of CPD in immunofluorescence (**Figures 2D, E**). To check whether increasing the autophagy level in HDFs has any effect on the cellular viability in UV-B-irradiated HDFs, we found that UV-B 30 mJ/cm^2 decreases the cell viability by 25% compared to control. Rapamycin treatment has no significant effect on restoring the cellular viability in UV-B-irradiated HDFs at UV-B 30 mJ/cm^2 acute dose whereas Chloroquine treatment significantly reduces the cell viability by 0.8-fold compared to those exposed only to UV-B (**Figure 2C**).

Pharmacological Activation of Autophagy Alleviates Apoptosis and Nuclear Damage in UV-B-Exposed HDFs

Oxidatively induced DDR is the hallmark of UV-B-induced skin pathologies. To check whether improving autophagy levels in UV-B-irradiated HDFs could alleviate the nuclear alterations by alleviating apoptotic like events in cells, we performed TUNEL assay and Acridine Orange/Ethidium Bromide co-staining. We found that UV-B treatment of HDFs induces TUNEL-positive cells in an intensity-dependent manner in 6 h UV-B post-irradiation. Rapamycin treatment (100 nM) significantly alleviates the fluorescence of TUNEL-positive cells in UV-B 30 mJ exposed HDFs by threefold, whereas Chloroquine treatment (50 μM) of HDFs increases the fluorescence of TUNEL-positive cells by 0.2-fold compared to those exposed only to UV-B 30 mJ (**Figures 3A, B**). In AO/EtBr co-staining, we found that UV-B 30 mJ/cm^2 irradiation increases early as well as late apoptotic cells in microscopic studies, indicating induction of nuclear damage. Salubrinal 25 μM treatment significantly increases live cells and decreases apoptotic cells by 0.4-fold compared to those irradiated only to UV-B. Similarly, Rapamycin treatment also significantly decreases apoptotic cells in fluorescent microscopy by half compared to those exposed only to UV-B. On the other hand, Chloroquine treatment of HDFs significantly increases early apoptotic and late apoptotic cells by twofold but not necrotic cells compared to those irradiated only to UV-B (**Figures 3C, D**).

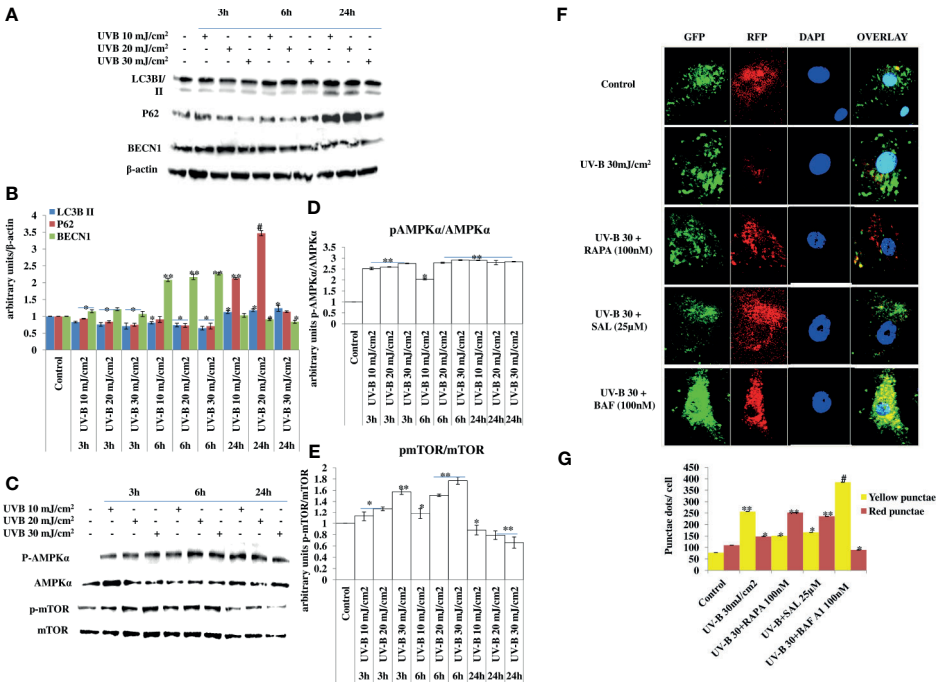

FIGURE 1 | UV-B exposure to HDFs induce impaired autophagy response. **(A–E)** Western blotting analysis of key autophagy marker proteins showing impaired autophagy response in a time- and intensity-independent manner in UV-B 10, 20, and 30 mJ/cm^2 exposed HDFs. **(F, G)** GFP-RFP-LC3B puncta assay depicting yellow and red punctae dots representative of autophagosomes and autolysosomes in UV-B 30 mJ/cm^2 exposed HDFs and effect of Rapamycin (100 nM), Salubrinal (25 μM), and Bafilomycin A1 (100 nM) on autophagic flux in 6 h UV-B post-irradiation to HDFs (*$p \leq 0.05$, **$p \leq 0.01$, $^{\#}p \leq 0.001$ were considered as statistically significant). Western blots were analyzed using Image Lab.exe 3.0.0.39529 and micrographs with ImageJ.exe 1.8.0_172 software.

ROS is the main oxidative damage-causing agent in UV-B-exposed HDFs. To check the effect of autophagy inducer Everolimus (200 nM) and Salubrinal (25 μM) on generation of primary ROS species in 1 h UV-B post-irradiation to HDFs, we found that oxidative stress is the immediate event following UV-B 30 mJ/cm^2 exposure to HDFs (1 h) by increasing ROS species. Salubrinal and Everolimus treatment to UV-B-exposed HDFs significantly alleviate the production of ROS species by half compared to those exposed only to UV-B and offers significant photo-protection to HDFs by regulating oxidative stress-mediated ER stress response (**Figures 3E, F**).

Improving Cellular Autophagy Response in UV-B-Exposed HDFs Alleviates DNA Damage Whereas Blockage of Autophagy Augments It

DDR is the natural defense response system activated in cells against any genotoxic stimulus and is attributed at repairing the damaged state to prevent tumorigenesis. Here, we found that UV-B exposure at 10, 20, and 30 mJ/cm^2 induces DDR in HDFs in an intensity- and time-dependent manner, which is more aberrant in 30 mJ/cm^2 exposed HDFs as is evident from the Western blotting analysis of key DDR proteins (**Figures 4A, B**). The expression profile of key damage responsive proteins in DNA damage pathway p-χH_2AX, p-ATM, and p-ATR is significantly modulated in UV-B-exposed HDFs, indicating induction of damage response upon UV-B exposure to HDFs. Moreover, the expression level of p-AKT, which has a crucial role in pro-survival signaling and also inhibits apoptosis in UV-B response is also significantly increased, and the increase is more profound in UV-B 30 mJ/cm^2 exposed HDFs (**Figures 4A, C**). We confirmed our Western blotting results through immunofluorescence in 6 h UV-B post-irradiation to HDFs in confocal microscopy by imaging for the UV-B-induced p-χH_2AX foci, which directly reflect the intensity of damage response. In microscopic analysis, we found that UV-B 30 mJ exposure to HDFs induces the expression of p-χH_2AX foci. Treatment of Rapamycin (100 nM) and Salubrinal (25 μM) to UV-B-exposed HDFs significantly rescue damage response in HDFs as is evident from the decreased expression of p-χH_2AX in confocal microscopy. Bafilomycin A1 (100 nM) treatment significantly potentiates the expression levels of p-χH_2AX nuclei in UV-B-exposed HDFs (**Figures 4D, E**). We further carried out the immunofluorescence of DNA damage pathway protein DDB2 in confocal microscopy and found that DDB2 protein expression levels are also significantly upregulated by threefold in UV-B-exposed HDFs compared to control levels. Rapamycin (100 nM) significantly brings the DDB2 level to half whereas Chloroquine (50 μM) treatment drastically increases the expression level of DDB2 protein by 0.2-fold compared to those exposed only to UV-B (**Figures 4F, G**).

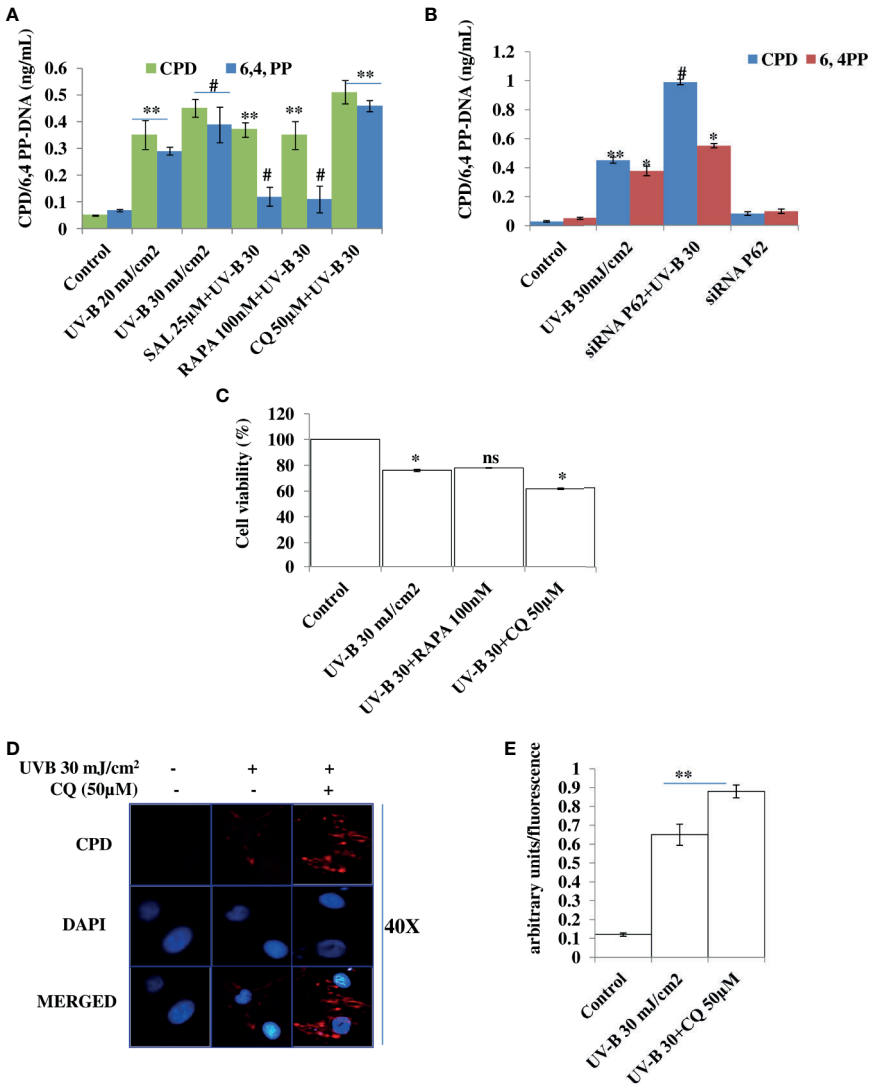

FIGURE 2 | Improving autophagy and relieving ER stress response alleviates DNA photo-adducts in UV-B-exposed HDFs. **(A)** ELISA based quantification of CPD and 6,4PP in UV-B 20–30 mJ/cm^2 exposed HDFs in 6 h UV-B post-irradiation and effect of Salubrinal (25 μM), Rapamycin (100 nM), and Chloroquine (50 μM) on UV-B-induced CPD and 6,4PP levels. **(B)** ELISA-based quantification of CPD and 6,4PP in siRNA P62-treated HDFs. **(C)** Cell viability analysis of UV-B 30 mJ/cm^2 exposed HDFs treated with Rapamycin (100 nM) and Chloroquine (50 μM). **(D, E)** Immunofluorescence analysis of CPD protein levels in microscopy in UV-B 30 mJ/cm^2 exposed HDFs treated with Chloroquine (50 μM) (*$p \leq 0.05$, **$p \leq 0.01$, $^{\#}p \leq 0.001$ were considered as statistically significant). Western blots were analyzed using Image Lab.exe 3.0.0.39529 and micrographs with ImageJ.exe 1.8.0_172 software. ns. non-significant.

Salubrinal Alleviates DNA Damage and Prevents Immediate ER Calcium Leakage by Improving Cellular Autophagy Levels in UV-B-Exposed HDFs

ER stress response is the immediate manifestation of oxidative stress in UV-B exposure to HDFs. Here, we used Salubrinal, an eIF$_2\alpha$ phosphatase inhibitor that relieves ER stress response upon UV-B exposure to cells. We first performed the cell viability assay of Salubrinal in UV-B-exposed HDFs and found it cytoprotective in nature. UV-B exposure decreases the cellular viability in HDFs in an intensity-dependent manner in 24 h MTT assay by 20%, 27%, and 35% at 10, 20, and 30 mJ/cm^2 exposure, respectively (**Figure 5A**). Salubrinal treatment at 10, 20, and 30 μM improves the cellular viability by 1-fold, 0.5-fold, and 0.5-fold in UVB 10 mJ+SAL 10 μM-, 20 mJ+SAL 20 μM-, and UVB 30 mJ+SAL 30 μM-treated HDFs respectively. Furthermore, we checked the expression of autophagy, ER stress, and DDR p-χH$_2$AX protein levels in UV-B-exposed HDFs in Western blotting in 24 h upon Salubrinal treatment. UV-B exposure to HDFs induces ER stress response as evident from the expression levels of p-eIF$_2\alpha$ and upregulates expression of DNA damage sensor protein p-χH$_2$AX in Western blotting, but Salubrinal (20 μM) fails to significantly improve the ER stress and damage response events in UV-B-exposed HDFs in 24 h

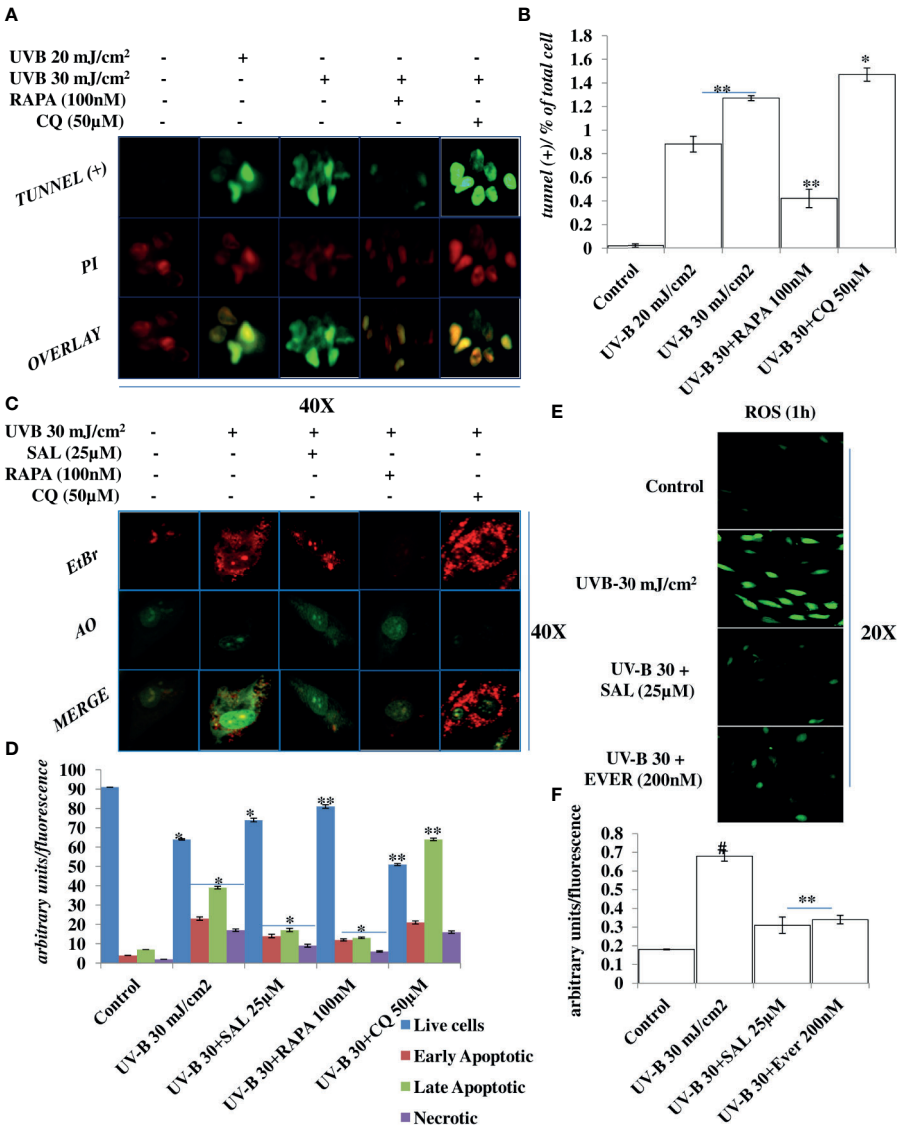

FIGURE 3 | Improving autophagy alleviates apoptotic cells in UV-B-exposed HDFs in fluorescent microscopy. **(A, B)** Fluorescent microscopic analysis of TUNEL (+) cells in UV-B 30 mJ/cm^2 exposed HDFs showing nuclear damage in 6 h UV-B post-irradiation and effect of Rapamycin (100 nM) and Chloroquine (50 μM) on UV-B-induced TUNEL (+) cells. **(C, D)** Acridine orange and Ethidium Bromide (AO-EtBr) co-staining depicting early and late apoptotic (+) cells in UV-B 30 mJ/cm^2 exposed HDFs in 6 h UV-B post-irradiation and effect of Salubrinal (25 μM), Rapamycin (100 nM), and Chloroquine (50 μM) on UV-B-induced apoptosis. **(E, F)** Reactive Oxygen Species (ROS) estimation in UV-B 30 mJ/cm^2 exposed HDFs treated with Salubrinal (25 μM) and Everolimus (200 nM) in 1 h UV-B post-irradiation (*$p \leq 0.05$, **$p \leq 0.01$, $^{\#}p \leq 0.001$ were considered as statistically significant). Micrographs were analyzed using ImageJ.exe 1.8.0_172 software.

UV-B post-irradiation (**Supplementary Figure S1**). We reduced the UV-B post-exposure time interval to 6 h, because both autophagy and ER stress responses are the initial molecular events following UV-B exposure to HDFs as already reported in our previous study (19). We found that Salubrinal 25 μM improves autophagy response in UV-B-exposed HDFs in 6 h UV-B post-irradiation as is evident from expression levels of LC3B II, P62, and BECN1 in Western blotting (**Figures 5B, C**) as well as augments the punctae dots in GFP-RFP-LC3B puncta assay in confocal microscopy (**Figures 1F, G**). We further found that ER stress is induced upon UV-B exposure to HDFs in an intensity-dependent manner in 6 h UV-B post-irradiation and is significantly alleviated by treatment with Salubrinal 25 μM as evident from the expression of key ER stress response proteins, p-eIF$_2\alpha$, GRP78, and CHOP/GAD153. Rapamycin (100 nM) treatment also significantly relieves the UV-B-induced ER stress response whereas Chloroquine (50 μM) fails to rescue the cells from ER stress response in UV-B-exposed HDFs (**Figures 5D, E**). Furthermore, to check whether relieving ER stress response with Salubrinal and improving cellular autophagy response with Rapamycin have any impact on rescuing the UV-B-exposed HDFs from aberrant DDR, we looked for the expression of DNA

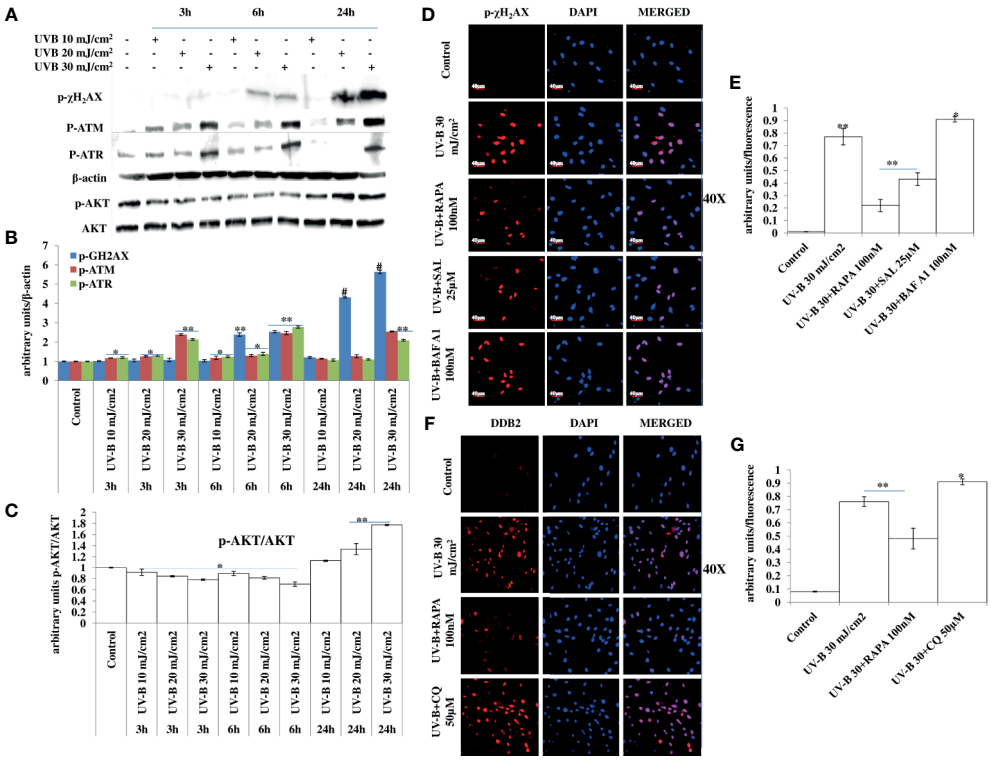

FIGURE 4 | Improving autophagy response alleviates DNA damage in UV-B-exposed HDFs. **(A, B)** Western blotting analysis of DNA damage response proteins showing time- and intensity-dependent effect of UV-B irradiation on DNA damage response proteins in UV-B 10, 20, and 30 mJ/cm^2 exposed HDFs. **(A, C)** Western blotting analysis of p-AKT protein levels showing the effect of UV-B irradiation on the expression levels of p-AKT decreasing in 3 and 6 h but again augments in 24 h UV-B 10, 20, and 30 mJ/cm^2 exposed HDFs. **(D, E)** Immunofluorescence analysis of damage sensor protein p-χH_2AX foci in UV-B 30 mJ/cm^2 exposed HDFs in 6 h UV-B post-irradiation and effect of Salubrinal (25 μM), Rapamycin (100 nM), and Bafilomycin A1 (100 nM) on p-χH_2AX expression levels under UV-B exposure to HDFs. **(F, G)** Immunofluorescence analysis of DDB2 protein expression levels in UV-B 30 mJ/cm^2 exposed HDFs and effect of Rapamycin (100 nM) and Chloroquine (50 μM) on the expression levels of DDB2 (*$p \leq 0.05$, **$p \leq 0.01$, $^{\#}p \leq 0.001$ were considered as statistically significant). Western blots were analyzed using Image Lab.exe 3.0.0.39529 and micrographs with ImageJ.exe 1.8.0_172 software.

damage sensor protein p-χH_2AX and p-Chk1 and found that Salubrinal (25 μM) and Rapamycin (100 nM) significantly alleviate the expression of both p-χH_2AX and p-Chk1 in Western blotting (**Figures 5D, E**). Salubrinal (25 μM) and Rapamycin (100 nM) treatment also significantly restores the expression levels of anti-apoptotic protein Bcl_2, whose expression is dwindled upon UV-B 30 mJ/cm^2 exposure to HDFs, whereas Chloroquine (50 μM) augments the expression of Bcl2 compared to those exposed only to UV-B (**Figures 5D, E**). ER calcium depletion is the immediate molecular event following UV-B exposure to HDFs. Rapamycin (100 nM) and Salubrinal (25 μM) treatment significantly prevents the ER Calcium leakage in UV-B-exposed HDFs; Bafilomycin A1 (100 nM) potentiates the ER calcium depletion from UV-B-exposed HDFs as is evident from confocal microcopy analysis in calcium staining (**Figures 5F, G**).

Autophagy Blockage *via* P62 Silencing Augments the DDR in UV-B-Exposed HDFs

Autophagy is the main cellular pathway that is activated during stress response in order to restore the normal homeostasis in cells subjected to genotoxic stress. We blocked autophagy response in UV-B-exposed HDFs through silencing autophagy cargo protein P62 to find the impact of autophagy blockage on DDR in 6 h UV-B post-irradiation to HDFs. Western blotting analysis confirmed the silencing of P62 and depicts 95% silencing efficiency. UVB 30 mJ exposure to HDFs shows mild autophagy induction as evident from the downregulation of P62 protein levels by 0.25-fold in Western blotting analysis (**Figures 6A, B**). Furthermore, we found that P62-silenced HDFs reveal enhanced DDR upon UV-B 30 mJ exposure in 6 h post-irradiation as is clear from augmented expression levels of DDR proteins p-χH_2AX, p-ATR, p-Chk2, and p-P53 in Western blotting analysis (**Figures 6A, B**). P62 siRNA-only-treated cells show negligible effect on the change in expression of DDR proteins in Western blotting analysis compared to control levels. We confirmed our Western blotting results through immunofluorescence in confocal microscopy by looking for the p-χH_2AX foci and found that UV-B 30 mJ exposure significantly induces the expression of p-χH_2AX foci in P62-silenced cells compared to those exposed only to UV-B. Rapamycin (100 nM) treatment to P62-silenced HDFs upon UV-B

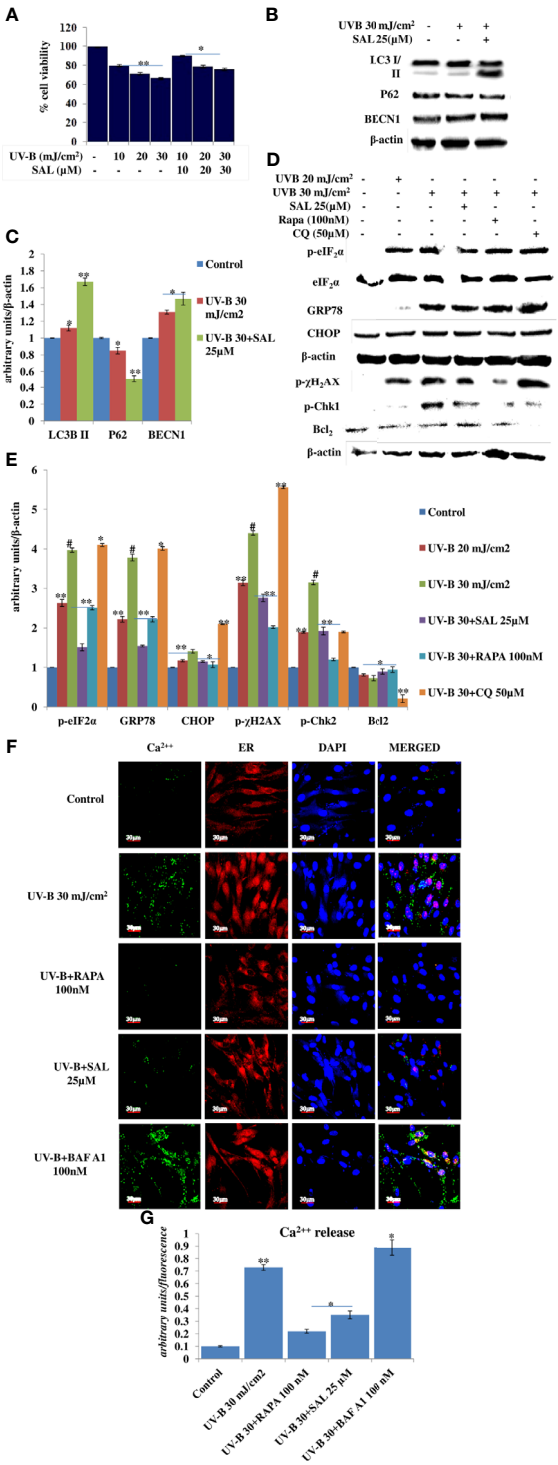

FIGURE 5 | Salubrinal alleviates DNA damage and prevents immediate ER calcium leakage in UV-B-exposed HDFs. **(A)** Cell viability analysis of UV-B 10, 20, and 30 mJ/cm^2 exposed HDFs in the presence of Salubrinal (10, 20, and 30 μM) in 24 h UV-B post-irradiation. **(B, C)** Western blotting analysis of autophagy marker proteins in Salubrinal (25 μM)-treated HDFs exposed to UV-B. **(D, E)** Western blotting analysis of ER stress and DNA damage response proteins in 20 and 30 mJ/cm^2 exposed HDFs in the presence of Salubrinal (25 μM), Rapamycin (100 nM), and Chloroquine (50 μM) in 6 h UV-B post-irradiation. **(F, G)** Confocal microscopy analysis of ER calcium depletion in 30 mJ/cm^2 exposed HDFs in 6 h UV-B post-irradiation in the presence of Rapamycin (100 nM), Salubrinal (25 μM), and Bafilomycin A1 (100 nM) (*$p \leq 0.05$, **$p \leq 0.01$, $^{\#}p \leq 0.001$ were considered as statistically significant). Western blots were analyzed using Image Lab.exe 3.0.0.39529 and micrographs with ImageJ.exe 1.8.0_172 software.

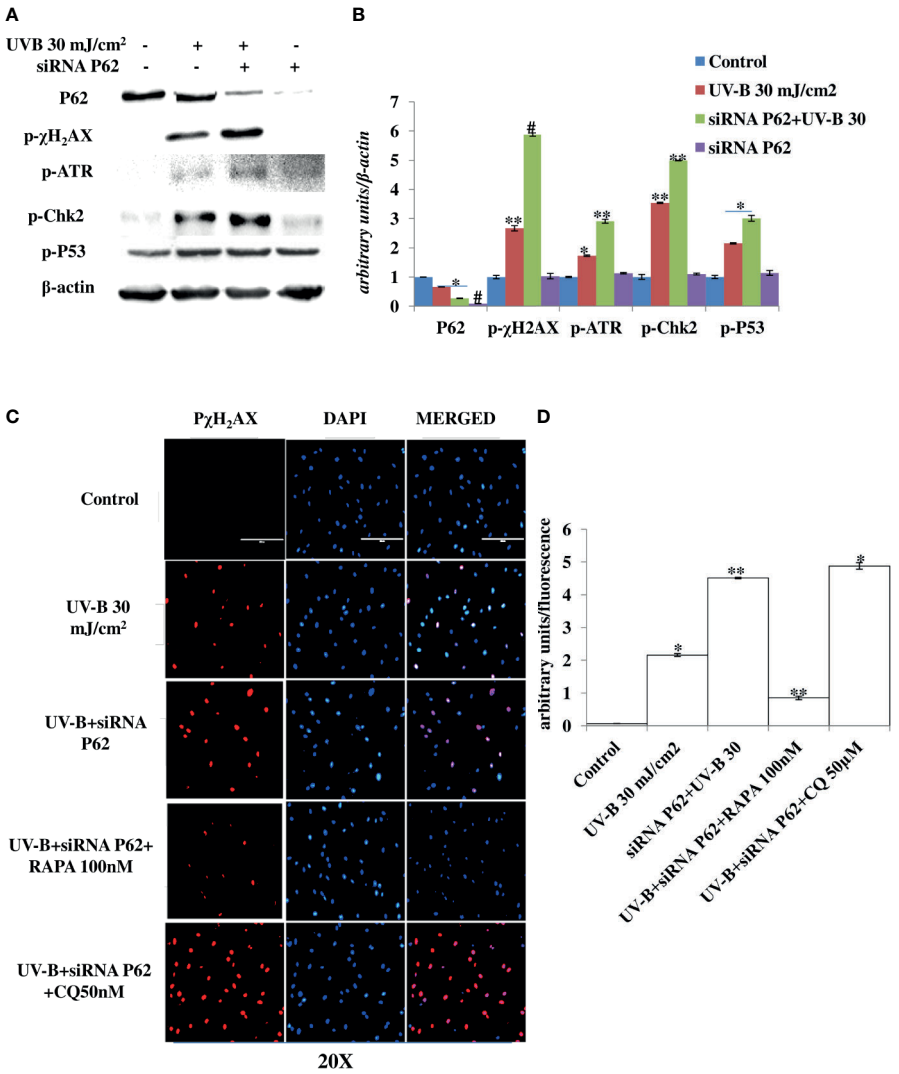

FIGURE 6 | P62 silencing enhances the DNA damage response in UV-B-exposed HDFs. **(A, B)** Western blotting analysis of DNA damage response proteins in siRNA P62-treated HDFs in 6 h UV-B 30 mJ/cm^2 post-irradiation. **(C, D)** Immunofluorescence analysis of DNA damage sensor protein p-χH$_2$AX in siRNA P62-treated HDFs in 6 h UV-B post-irradiation in the presence of Rapamycin (100 nM) and Chloroquine (50 μM) (*$p \leq 0.05$, **$p \leq 0.01$, $^{\#}p \leq 0.001$ were considered as statistically significant). Western blots were analyzed using Image Lab.exe 3.0.0.39529 and micrographs with ImageJ.exe 1.8.0_172 software.

exposure decreases the p-χH$_2$AX foci by twofold in immunofluorescence. Chloroquine (50 μM) treatment to P62-silenced cells upon UV-B exposure fails to alleviate the DDR in HDFs as is evident in immunofluorescence (**Figures 6C, D**).

Autophagy Blockage *via* P62 Silencing Dwindles the Tumor Suppressor PTEN/AKT Pathway in UV-B-Exposed HDFs

The PTEN/AKT pathway is the main tumor suppressor pathway that promotes cell survival and reduces tumorigenesis in UV-B-induced photo-damage. Here we checked whether blockage of autophagy has any substantial impact on the PTEN/AKT pathway in UV-B 30 mJ exposed HDFs in 6 h UV-B post-irradiation. We found that UV-B irradiation to HDFs significantly downregulates the expression level of PTEN by 0.2-fold and increases the expression of p-AKT protein by 0.25-fold in Western blotting analysis (**Figures 7A, B**). Autophagy blockage *via* P62 silencing significantly downregulates the expression of PTEN by twofold in UV-B +P62-treated HDFs compared to those exposed only to UV-B. We got very interesting results for p-AKT, and the protein expression level of p-AKT is upregulated by 0.4-fold in P62-silenced HDFs compared to those exposed only to UV-B. Similar results were obtained for PTEN and p-AKT in immunofluorescence in confocal microscopy analysis. PTEN protein expression levels are significantly downregulated upon UV-B exposure to HDFs in immunofluorescence. Autophagy activator Rapamycin (100 nM) significantly restores the PTEN

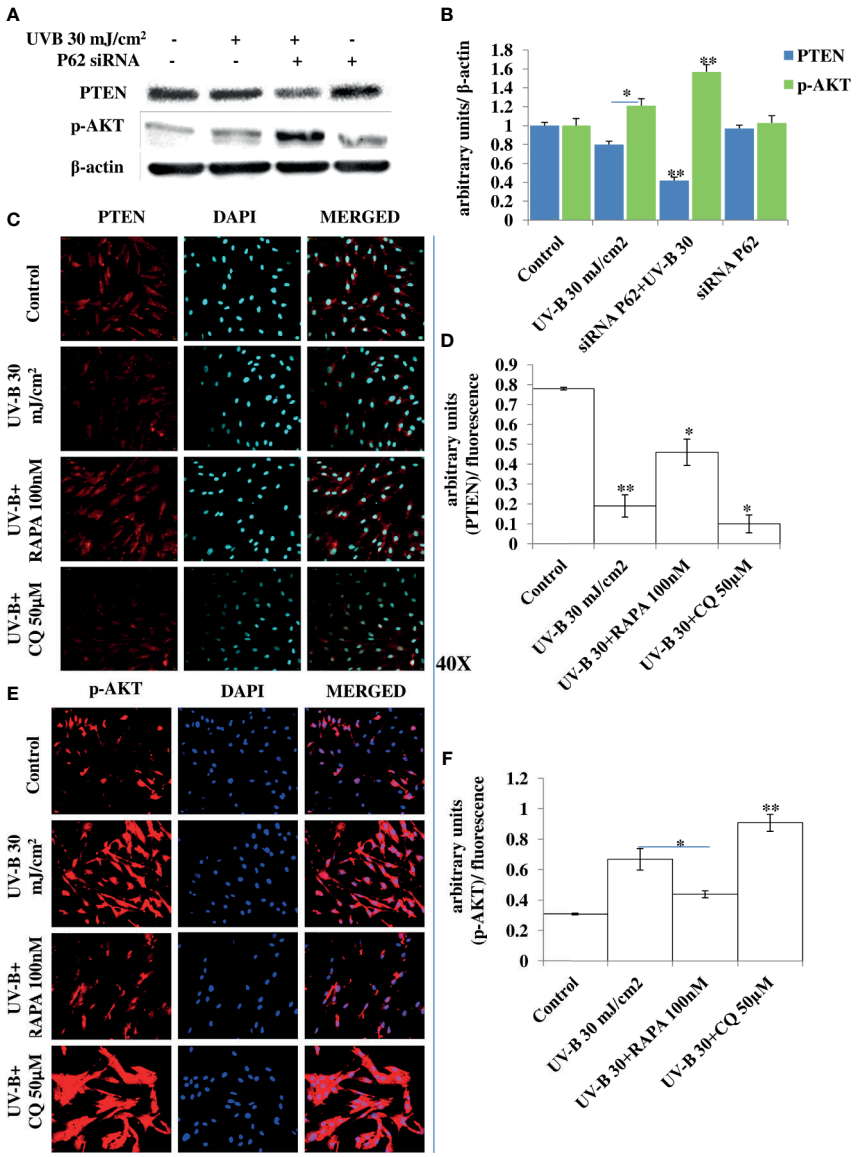

FIGURE 7 | P62 silencing dwindles the PTEN/AKT tumor suppressor signaling axis in UV-B-exposed HDFs. **(A, B)** Western blotting analysis of PTEN/p-AKT protein expression levels in siRNA P62-treated HDFs in 6 h UV-B 30 mJ/cm^2 post-irradiation. **(C, D)** Immunofluorescence analysis of PTEN protein expression levels in UV-B 30 mJ/cm^2 exposed HDFs in 6 h UV-B post-irradiation in the presence of Rapamycin (100 nM) and Chloroquine (50 μM). **(E, F)** Immunofluorescence analysis of p-AKT protein expression levels in UV-B 30 mJ/cm^2 exposed HDFs in 6 h UV-B post-irradiation in the presence of Rapamycin (100 nM) and Chloroquine (50 μM) (*$p \leq 0.05$, **$p \leq 0.01$ were considered as statistically significant). Western blots were analyzed using Image Lab.exe 3.0.0.39529 and micrographs with ImageJ.exe 1.8.0_172 software.

expression level by twofold whereas inhibitor of autophagy, Chloroquine (50 μM), could not restore the PTEN expression but adversely augments the expression level of PTEN by onefold compared to those exposed only to UV-B as is evident from immunofluorescence (**Figures 7C, D**). p-AKT expression level in UV-B-exposed HDFs on the other hand is upregulated by twofold in immunofluorescence compared to control levels. Rapamycin (100 nM) treatment significantly brings the expression of p-AKT close to control levels whereas Chloroquine (50 μM) drastically increases the expression of p-AKT in UV-B-exposed HDFs by 0.35-fold compared to those exposed only to UV-B (**Figures 7E, F**).

Pharmacological Activation of Autophagy Improves the Expression of Cell Cycle Regulatory Proteins in UV-B-Exposed HDFs

Cell cycle regulatory proteins play an important role in quality control mechanism and respond to any genotoxic insult and prevent cancer development in cells. In line with this, we checked

the effect of pharmacologically stimulated autophagy response on main cell cycle regulator proteins in immunofluorescence through confocal microscopy in 24 h UV-B post-irradiation to HDFs. We found that the expression of P21 protein upregulates in UV-B-exposed HDFs by threefold compared to control levels. Rapamycin (100 nM) treatment significantly improves the expression level of P21 compared to those exposed only to UV-B. Chloroquine (50 μM) on the other hand, drastically increases the expression of P21 in immunofluorescence by 1.5-fold compared to those exposed only to UV-B (**Figures 8A, B**). Similarly, we got augmented expression in the protein levels of P27 in UV-B 30 mJ exposed HDFs by threefold compared to control levels. Salubrinal (25 μM) and Rapamycin (100 nM) treatment brought the expression of P27 to that of control levels, whereas Chloroquine (50 μM) significantly increased the expression of p27 by 0.2-fold compared to UV-B levels in immunofluorescence (**Figures 8C, D**). Similar results were obtained in Western blotting as well wherein UV-B exposure to HDFs increases the expression of P21 and P27 whereas Salubrinal (25 μM) and Rapamycin (100 nM) alleviate the expression of both P21 and P27 whereas Chloroquine (50 μM) augments the UV-B-induced expression of P21 and P27 in Western blotting analysis (**Figures 8E, F**).

Atg7 Silencing in an Unexpected Consequence Alleviates the DDR in UV-B-Exposed HDFs

Autophagy-related genes play an important role in the initiation and execution process of autophagy response. Recently, autophagy-related *Atg7* gene deletion has been found to be involved in the suppression of UV-B-induced inflammation and tumorigenesis. To check the specific role of autophagy-related proteins particularly the role of *Atg7* in UV-B-induced photodamage, we subjected HDFs to *Atg7* silencing in 6 h UV-B post-irradiation. Western blotting analysis confirmed the silencing of *Atg7* with 95% efficiency compared to control levels. UV-B 30 mJ exposure to HDFs increases the protein expression of *Atg7* and BECN1 by 1- and 1.25-fold, respectively, and decreases the protein expression of P62 by 0.5-fold compared to control levels. UV-B exposure to HDFs also induces the expression of key DDR proteins p-χH_2AX and p-P53 by 5- and 4.5-fold, respectively. *Atg7* silencing in UV-B-exposed HDFs significantly alleviates the DDR as is evident from decrease in the protein expression levels of DDR proteins p-χH_2AX and p-P53 in Western blotting by 2.5- and 2-fold, respectively. *Atg7*-only silenced HDFs show negligible effect on the modulation in expression level of autophagy and DNA damage marker proteins in Western blotting analysis. Everolimus (200 nM) treatment to *Atg7*-silenced HDFs upon UV-B exposure also decreases the expression levels of DDR proteins compared to those exposed only to UV-B but not compared to *Atg7*+UV-B-exposed cells (**Figures 9A, B**). We confirmed our Western blotting results through immunofluorescence by looking out for p-χH_2AX foci and found that UV-B exposure to HDFs significantly induces the p-χH_2AX damage foci by 3-fold compared to control levels but are significantly alleviated in *Atg7*-silenced UV-B-exposed HDFs by 0.35-fold compared to that of those exposed only to UV-B (**Figures 9C, D**). Furthermore, confocal microscopy analysis of p-AMPKα protein expression levels in 6 h UV-B post–irradiation to HDFs show that autophagy protein *Atg7* silencing significantly enhances the p-AMPKα expression levels in UV-B-irradiated HDFs compared to those exposed only to UV-B (**Figures 9E, F**).

DISCUSSION

Skin aging is a dynamic process and depends on both intrinsic factors such as genetics and hormones, as well as extrinsic factors including UV radiation and environmental pollutants (28). UV radiation in particular is considered the most crucial factor for skin aging due to the process known as photoaging (29). Incidences of skin cancer have increased in recent years, possibly due to increased exposure to solar UV radiation because of the depletion of ozone layer in the stratosphere (30). UV-B irradiation to skin stimulates diverse cellular and molecular responses like inflammation, reactive oxygen species (ROS) formation, and endoplasmic reticulum (ER) stress response that ultimately leads to autophagy induction in skin cells aimed at restoring the cellular homeostasis upon encountering insult. Acute and chronic exposure of UV-B to skin lead to various perturbations that leads to aging-related signal transduction amplification, ultimately resulting in skin damage and photoaging (31). UV-B radiation is considered as the most mutagenic component of UV spectrum reaching the earth's surface and causes DNA damage in the form of cyclobutane pyrimidine dimers (CPD) and pyrimidine-(6-4)-pyrimidone photoproducts (6,4PP) affecting DNA integrity and tissue homeostasis, and causes mutations in oncogenes and in tumor suppressor genes (32). Cells have, in defense, a natural, inbuilt, and well-established molecular response system known as DDR that checks any mutagenic insult to genome and repairs it immediately through the Nucleotide Excision Repair system, to prevent tumor development and cancer progression in cells. Any unrepaired part can lead to abnormal cell growth, increasing the risk of cancer (33). Autophagy is a cellular catabolic process that has roles in sensing nutrient stress during starvation conditions and cleanses cellular debris generated as a metabolic by-product (34). Dysfunction of the autophagic process is known to have a role in the development of human chronic pathologies, such as metabolic, cardiovascular, and neurodegenerative diseases, and in cancer as well. Comprehensive research is ongoing to discover new therapeutic strategies and agents able to modulate the autophagic process. Special attention is given in particular to understand the complex role of autophagy in disease pathogenesis. Research efforts are now focused on understanding the context-dependent roles of autophagy and on the evaluation of the pharmacological effects of autophagy signaling in a more in-depth and mechanistic way (35). Furthermore, the development of skin aging is associated with several molecular changes including the accumulation of DNA damage, genome instability, epigenetic dysregulation, mitochondrial dysfunction, inflammation, extracellular matrix degradation, loss of proteostasis, ER stress,

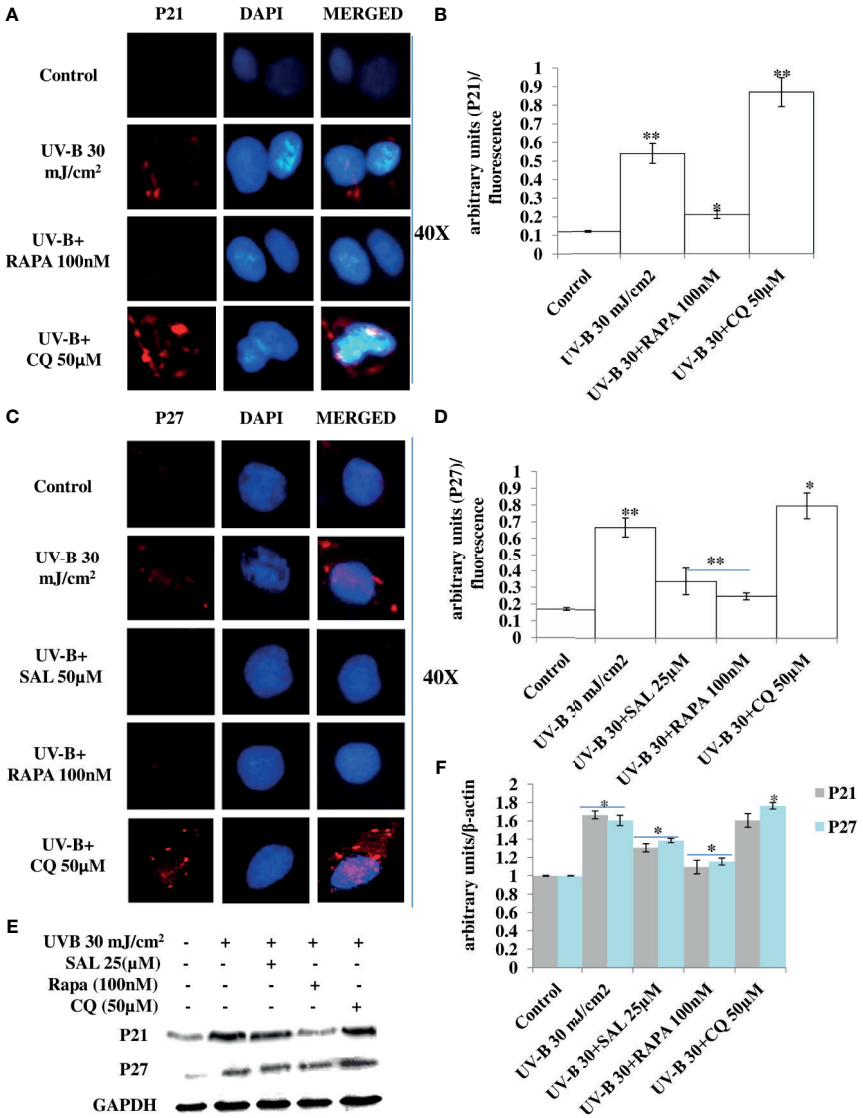

FIGURE 8 | Pharmacological activation of autophagy regulates the expression of cell cycle regulatory proteins in UV-B-exposed HDFs. **(A, B)** Immunofluorescence analysis of P21 protein expression levels in UV-B 30 mJ/cm^2 exposed HDFs in 24 h UV-B post-irradiation in the presence of Rapamycin (100 nM) and Chloroquine (50 µM). **(C, D)** Immunofluorescence analysis of P27 protein expression levels in UV-B 30 mJ/cm^2 exposed HDFs in 24 h UV-B post-irradiation in the presence of Salubrinal (25 µM), Rapamycin (100 nM), and Chloroquine (50 µM). **(E, F)** Western blotting analysis of P21 and P27 protein expression levels in UV-B 30 mJ/cm^2 exposed HDFs in 24 h UV-B post-irradiation in the presence of Salubrinal (25 µM), Rapamycin (100 nM), and Chloroquine (50 µM) (*$p \leq 0.05$, **$p \leq 0.01$ were considered as statistically significant). Western blots were analyzed using Image Lab.exe 3.0.0.39529 and micrographs with ImageJ.exe 1.8.0_172 software.

and autophagy dysfunction (36). Many of these genome alterations are directly associated with cellular damage and senescence, which is one of the hallmarks of skin aging. Recent evidence from autophagy research in UV-B-induced skin DNA damage has provided novel insights and has been found to play a positive and pivotal role in DNA damage recognition by nucleotide excision repair and also controls p38 activation to promote cell survival under genotoxic stress conditions (5, 37). In another similar study, it has been found that autophagic UVRAG promotes UV-induced photolesion repair by activation of the CRL4 (DDB2) E3 Ligase (38) citing the positive role of autophagy in regulating UV-B-induced damage response in skin. We have recently reported that a natural product-based anti-oxidant molecule, Glycyrrhizic acid, alleviates oxidatively induced DNA damage through improving cellular autophagy levels in primary human dermal fibroblasts (19). Furthermore, recent works have revealed that genotoxic stress is a trigger for autophagy and autophagy regulates repair of UV-induced DNA damage. Previously, it has been revealed that knockdown of autophagy genes such as AMPK, *Atg5*, *Atg7*, *Atg12*, and *Atg14* impairs the repair of UVB-induced DNA damage (39). Despite these preliminary studies conducted so far in demystifying the role of autophagy in UV-B-induced DDR, the

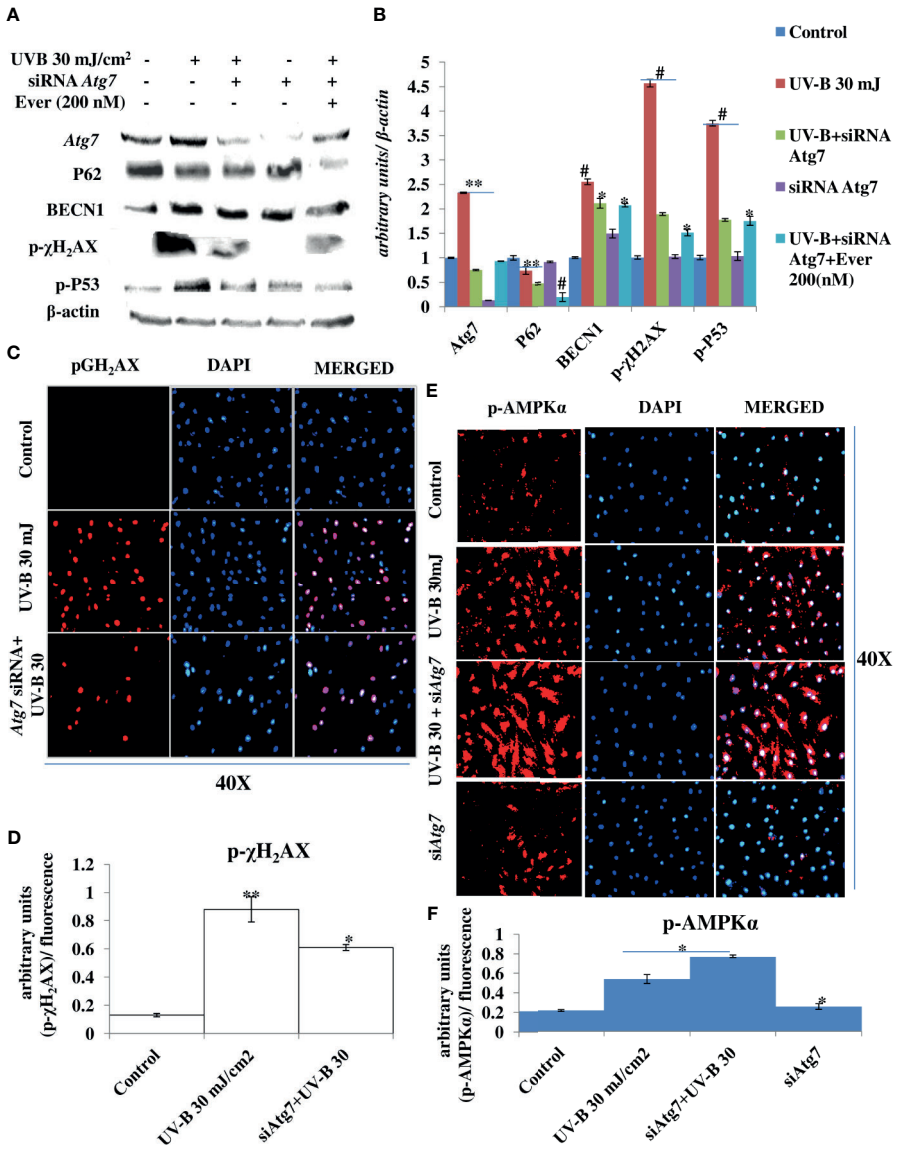

FIGURE 9 | *Atg7* silencing in an unexpected consequence alleviates the DNA damage response in UV-B-exposed HDFs. **(A, B)** Western blotting analysis of autophagy and DNA damage response proteins in siRNA *Atg7*-treated HDFs in 6 h UV-B post-irradiation in the presence of Everolimus (200 nM). **(C, D)** Immunofluorescence analysis of DNA damage sensor protein p-χH_2AX in siRNA *Atg7*-treated HDFs in 6 h UV-B post-irradiation. **(E, F)** Immunofluorescence analysis of p-AMPKα expression levels in siRNA *Atg7*-treated HDFs in 6 h UV-B post-irradiation ($^*p \leq 0.05$, $^{**}p \leq 0.01$, $^{\#}p \leq 0.001$ were considered as statistically significant). Western blots were analyzed using Image Lab.exe 3.0.0.39529 and micrographs with ImageJ.exe 1.8.0_172 software.

precise role of autophagy in regulating UV-B-induced genotoxic stress is yet to be ascertained and warrants further studies to unravel the facts. In line with these findings, we planned the current study and hypothesized that autophagy might be playing a very crucial role in regulating UV-B-induced DDR. Our results suggest that UV-B irradiation induces impaired autophagy response in a dose-independent manner as is evident from the Western blotting analysis of key autophagy marker proteins not corresponding to induction of healthy autophagy response in cells (**Figures 1A–E**). Induction of impaired autophagic flux response upon UV-B 30 mJ/cm^2 exposure to HDFs was confirmed through GFP-RFP-LC3B puncta assay in confocal microscopy where we obtained appreciable red puncta dots, indicative of autolysosomes compared to yellow puncta dots indicative of autophagosomes in Rapamycin- and Salubrinal-treated cells showing enhanced autophagy flux upon UV-B exposure to HDFs compared to those exposed only to UV-B (**Figures 1F, G**). ELISA-based results reveal that DNA photo-adducts (CPD and 6,4PP) are the immediate by-products of oxidative damage in UV-B-exposed HDFs in 6 h UV-B post-irradiation. Improving autophagic flux with Rapamycin (100 nM) and relieving UV-B-induced ER stress response with Salubrinal (25 μM) significantly alleviate the induction of both CPD and 6,4PP in

UV-B-exposed HDFs. Autophagy inhibitor [Chloroquine (25 μM)] treatment of HDFs on the other hand augments the induction of both CPD and 6,4PP in UV-B-treated HDFs (**Figure 2A**), indicating that autophagy induction positively regulates the formation of DNA photo-adducts in UV-B-induced photo-damage. We confirmed these findings by silencing the autophagy cargo protein P62 and found that it significantly increases the induction of photo-adducts, indicating that autophagy plays a very critical role in regulating the UV-B-induced photo-damage response (**Figure 2B**). Similar effects were obtained in immunofluorescence on checking the effect of improving cellular autophagy levels on CPD induction, further revealing that pharmacological activation of autophagy positively regulates the DDR in UV-B exposure to HDFs (**Figures 2D, E**). Our results further reveal that Rapamycin (100 nM) treatment of HDFs has no significant effect on improving the cellular viability in acute dose (UV-B 30 mJ/cm^2) exposed HDFs whereas Chloroquine 50 μM treatment significantly reduces the cell viability from 65% in UV-B 30 mJ/cm^2 only exposed to 60% in UV-B 30+CQ (50 μM) treated, indicating that inhibition of autophagy potentiates the cell death effect in UV-B-exposed HDFs (**Figure 2C**). It is a fact that UV-induced skin damage triggers cascade of response signaling pathways, including cell cycle arrest, DNA repair, and, if left unrepaired, can lead to apoptotic events (40). Oxidatively induced DDR is the hallmark of UV-B-induced skin photo damage that ultimately leads to genotoxic stress response in skin (41). We found that UV-B treatment of HDFs induces TUNEL-positive cells in an intensity-dependent manner in 6 h UV-B post-irradiation. Rapamycin treatment (100 nM) significantly alleviates TUNEL-positive cells in UV-B 30 mJ/cm^2 exposed HDFs whereas Chloroquine treatment (50 μM) of HDFs increases TUNEL-positive cells compared to those exposed only to UV-B (**Figures 3A, B**). AO/EtBr co-staining also reveals increased ratio in early to late apoptotic nuclei in UV-B-exposed HDFs indicating nuclear damage upon UV-B exposure. Salubrinal (25 μM) and Rapamycin (100 nM) treatment significantly alleviates the fluorescence of apoptotic nuclei to that of control levels whereas Chloroquine (50 μM) treatment increases the apoptotic nuclei compared to UV-B levels, indicating that Salubrinal and Rapamycin have a positive role in regulating the UV-B-induced apoptosis whereas Chloroquine potentiates the damage by increasing the late apoptotic cells, but not necrotic cells. These results clearly indicate that oxidative stress, ER stress, and autophagy are intricately interconnected and autophagy has a very critical role in alleviating stress response in UV-B-exposed HDFs (**Figures 3C, D**). Moreover, oxidative stress induced upon UV-B exposure to skin cells also induces autophagy and ROS is the main oxidative damage-causing agent in UV-B-exposed cells (42). We found that treatment with Salubrinal and Everolimus significantly alleviates the ROS levels produced in response to UV-B exposure to skin cells, indicating that improving autophagy has a role to play in regulating oxidative stress response and that ER stress and oxidative stress are mutually related to each other, disturbing the cellular homeostasis (**Figures 3E, F**). Intense UV-B exposure to HDFs induces genomic damage and cell cycle arrest, which is critical at providing ample time gap for DNA damage recognition and subsequent execution of repair process. UV-induced DNA damage activates the sensors ataxia telangiectasia mutated (ATM) and ataxia telangiectasia and Rad3-related (ATR) to trigger cell cycle arrest *via* p53 stabilization (43) and also phosphorylates checkpoint kinase 1 (Chk1) to activate checkpoints at the G1, S, and G2/M phases. Damage-related protein DDB2 has been shown to facilitate the recruitment of ATM and ATR to sites of DNA damage and promote the activation of cell cycle arrest pathways (44–46). We found that UV-B exposure to skin cells induces DDR and is both a time- and intensity-dependent event as is evident from the Western blotting analysis of DDR proteins (**Figures 4A, B**). The expression levels of p-AKT, which has a crucial role in pro-survival signaling and also inhibits apoptosis in UV-B response, are significantly downregulated initially at low UV-B intensity but increase in 24 h UV-B post-irradiation exposure to HDFs (**Figures 4A, C**). p-χH_2AX foci are immediately induced upon DNA damage in cells, sensing damage and facilitating repair process. Here, we found that UV-B 30 mJ/cm^2 exposure to HDFs induces the expression of p-χH_2AX foci in immunofluorescence. Rapamycin (100 nM) and Salubrinal (25 μM) treatment rescues the DNA damage and accelerates the repair process in UV-B-exposed HDFs as is evident from the decreased expression of p-χH_2AX, whereas Bafilomycin A1 (100 nM) treatment shows enhanced expression levels of p-χH_2AX nuclei in UV-B 30 mJ/cm^2 exposed HDFs, indicating that autophagy positively regulates the damage response and repair process in UV-B exposure to skin (**Figures 4D, E**). Immunofluorescence of DDB2 also reveals upregulated levels of expression in UV-B 30 mJ exposed HDFs. Here, Rapamycin (100 nM) also significantly brings the DDB2 level to that of control levels whereas Chloroquine (50 μM) treatment drastically increases the expression level of DDB2 protein compared to UV-B-exposed HDFs (**Figures 4F, G**), indicating that DDR dwindles and subsequent repair processes are accelerated if autophagy levels are improved in UV-B-exposed HDFs and the pro-survival capacity of cells is enhanced due to clearing of damage incurred due to UV-B exposure to HDFs.

Previously, we have reported that oxidative stress-mediated Ca^{2+} release manifests ER stress leading to unfolded protein response in UV-B-irradiated human skin cells (18). In another study, it was reported that Salubrinal, an $eIF_2\alpha$ phosphatase inhibitor, protects human skin fibroblasts against UVB-induced cell death by blocking ER stress and regulating calcium homeostasis (47). Many other studies reported the diverse roles of Salubrinal on autophagy in different pathological conditions (48, 49) but not in skin photo-damage response. Here, we found that Salubrinal (10–30 μM) significantly improves the cellular viability in MTT assay in UV-B 10–30 mJ/cm^2 exposed HDFs (**Figure 5A**). Salubrinal (25 μM) also improves cellular autophagy levels in 6 h UV-B post-irradiation to HDFs (**Figures 5B, C**, **Figures 1F, G**). Furthermore, Salubrinal significantly alleviates ER stress response as well as DNA damage and accelerates repair process in 6 h UV-B post exposure to HDFs (**Figures 5D, E**) but not in 24 h UV-B post-irradiation (**Supplementary Figure S1**). ER calcium leakage is the immediate post-event following UV-B exposure to HDFs as reported earlier (18). We found that UV-B-mediated ER calcium

leakage is significantly prevented by Rapamycin (100 nM) and Salubrinal (25 μM) treatment to UV-B-exposed HDFs in 6 h UV-B post-irradiation, whereas Bafilomycin A1 (100 nM) fails to prevent the ER calcium depletion in calcium staining in microscopic analysis (**Figures 5F, G**).

Previous studies have reported that P62 modulates the intrinsic signaling in UVB-induced apoptosis (50) and that autophagy performs a crucial role in promoting cell survival under genototoxic stress and helps in preventing tumorigenesis. Degradation of P62 has been found to mediate an important tumor-suppressive function of autophagy, and autophagy-deficient conditions have shown enhanced P62 accumulation and act as a signaling hub by forming interactions with a number of pro-tumorigenic proteins, thereby promoting tumorigenesis (51). Here, we found that autophagy blockage *via* P62 silencing shows enhanced DNA damage and defective repair in 6 h UV-B 30 mJ post-irradiation as is clear in Western blotting analysis of DDR proteins (**Figures 6A, B**) and similar results were obtained in immunofluorescence of p-χH_2AX foci in confocal microscopy, which significantly increase in P62-silenced cells compared to those exposed only to UV-B. Rapamycin (100 nM) decreases the expression of damage sensor p-χH_2AX to that of control levels whereas Chloroquine (50 μM) significantly increases the expression of p-χH_2AX in immunofluorescence than in UV-B alone and P62-silenced HDFs irradiated with UV-B, indicating that autophagy induction regulates the UV-B-induced damage and also impacts upon repair process and imparts pro-survival capability to UV-B-exposed HDFs, thereby reducing chances of cancer development (**Figures 6C, D**). Earlier, it has been reported that PTEN, which otherwise activates autophagy, is inhibited by Sestrin 287 and, in response to UV-B exposure, impairs the GG-NER by downregulating XPC transcription. However, it is still elusive to conclude whether downregulation of autophagy has a significant role in PTEN-regulated DNA damage repair in response to UV-B exposure to skin cells (52, 53). The PTEN/AKT pathway is the crucial tumor suppressor pathway that promotes cell survival under genotoxic stress, and earlier studies have found that ERK/AKT-dependent PTEN suppression promotes survival of epidermal keratinocytes under UV-B exposure. Our results are in complete agreement with these initial findings as P62 silencing disturbs the PTEN/p-AKT pathway in UV-B-exposed HDFs in 6 h UV-B post-irradiation by decreasing the PTEN protein expression level but increases the p-AKT levels compared to UV-B (**Figures 7A, B**). Similar results were obtained in immunofluorescence of PTEN and p-AKT (**Figures 7C–F**, respectively), which indicate that autophagy also regulates tumor suppressor pathway under UV-B-induced genotoxic stress. Furthermore, Rapamycin (100 nM) improves the PTEN/p-AKT-mediated tumor suppressor pathway whereas Chloroquine (50 μM) potentiates the UV-B response to the PTEN/p-AKT pathway in UV-B-exposed HDFs in microscopy backing our silencing results. Furthermore, the massive accumulation of DNA lesions within the cells under different genotoxic stimuli interferes with the replication process, prompting cells to stop division and to repair damaged DNA (54). Cell cycle regulator proteins play a very important part in the quality control of cells and in sensing any external insult and preventing mutations. We found that Salubrinal (25 μM) and Rapamycin (100 nM) improve the fate of cell cycle regulator proteins P21 (**Figures 8A, B**) and P27 (**Figures 8C, D**) in immunofluorescence as well as in Western blotting (**Figures 8E, F**) in 24 h UV-B post-irradiation by regulating autophagy response whereas Chloroquine (50 μM) further worsens the damage regulation by increasing the expression of P21 and P27, which indicates that autophagy also plays its part in regulating cell cycle under genotoxic stress conditions.

Earlier studies have revealed an unexpected consequence of *Atg7* gene deletion in the suppression of UVB-induced inflammation, and tumorigenesis and epidermis-specific deletion of *Atg7* have been found to protect against UVB-induced sunburn, vascular permeability, and skin tumorigenesis. Moreover, *Atg7* deletion has been found to regulate UVB-induced skin tumorigenesis by regulating the AMPK and ER pathways (55). Our results are in complete agreement with these previous findings because *Atg7* silencing in UV-B-exposed HDFs alleviates the DDR and accelerates the repair process induced in 6 h UV-B post-irradiation to HDFs as is evident from the Western blotting analysis of key DNA damage marker proteins. Everolimus (200 nM) also rescues the HDFs from UV-B-induced DNA damage under *Atg7* silencing conditions but not as in *UV-B+Atg7*-silenced cells exposed to UV-B (**Figures 9A, B**). Similar results were obtained in immunofluorescence by looking for p-χH_2AX expression levels that are significantly alleviated in *Atg7*-silenced HDFs compared to those exposed only to UV-B (**Figures 9C, D**) demonstrating an unexpected consequence of *Atg7* silencing and its role in the suppression of UVB-induced DNA damage and in augmenting the repair process. Furthermore, the expression levels of p-AMPKα in *Atg7*-silenced HDFs irradiated with UV-B also increase significantly (**Figures 9E, F**), which is in complete agreement to what the role of *Atg7* has been stated previously, and this activation of p-AMPKα is likely an adaptive response to multiple stresses caused by autophagy deficiency mediated by *Atg7* silencing leading to ER accumulation and subsequent reduction in ER stress, but warrants further studies to clearly understand the role of the autophagy process, particularly the contrasting role of *Atg7* in the regulation of UV-B-induced genotoxic stress response in skin.

CONCLUSION

The above findings provide critical insights that indicate the regulatory and functional role of pharmacological activation of autophagy in the regulation of UV-B-induced skin photo-damage and subsequent repair process. These findings further reveal that cellular autophagy levels are critical in sensing and repairing UV-B-induced DNA damage and are crucially involved in DDR under UV-B-induced photo-damage conditions. Oxidative stress–ER stress and DDR mechanisms are tightly regulated, and autophagy is involved in the regulation of all the three pathways and promotes pro-survival capacity of cells under genotoxic stress conditions notably under UV-B-induced DNA damage. Moreover, our findings support the potential role of the autophagy pathway to be explored as a promising therapeutic strategy against UV-B-mediated photo-

damage disorders but warrant further studies to clearly demystify the molecular association existing between autophagy and DDR and repair process under genotoxic stress conditions.

DATA AVAILABILITY STATEMENT

The original contributions presented in the study are included in the article/**Supplementary Material**. Further inquiries can be directed to the corresponding author.

AUTHOR CONTRIBUTIONS

SU performed the major experiments. NS and LN performed the high-throughput experiments. MT and GD performed the TUNEL assay experiment. ST conceived and developed the hypothesis, supervised the research work, and arranged the research funding for the work. SU and ST planned the experiments and analyzed the data. SU and ST wrote the manuscript. SA and SR helped in manuscript editing. All authors contributed to the article and approved the submitted version.

FUNDING

Authors acknowledge the financial assistance by Director CSIR-Indian Institute of Integrative Medicine, Jammu vide project No. MLP-1003 and by Department of Biotechnology (DBT), Ministry of Science and Technology, New Delhi, India vide project No. GAP-2166. Senior Research Fellowship (SRF) to author SA by the Department of Science and Technology (DST), Ministry of Science and Technology, New Delhi, India Vide Letter No. IF-160982 is acknowledged. Senior Research Fellowship (SRF) to authors LN, MT, and GD by University Grants Commission (UGC) New Delhi, India and to NS by CSIR, New Delhi, India is acknowledged. Junior Research Fellowship to authors SR by Department of Science and Technology (DST), Ministry of Science and Technology, New Delhi, India and to SA by University Grants Commission (UGC) New Delhi is acknowledged.

ACKNOWLEDGMENTS

The authors also thank all the members of PK-PD and the Toxicology Division for their logistic support and help throughout the study.

SUPPLEMENTARY MATERIAL

The Supplementary Material for this article can be found online at: https://www.frontiersin.org/articles/10.3389/fonc.2021.726066/full#supplementary-material

REFERENCES

1. Kligman AM. What is the 'True'function of Skin? *Exp Dermatol* (2002) 11 (2):159. doi: 10.1034/j.1600-0625.2002.00112.x
2. Biniek K, Levi K, Dauskardt RH. Solar UV Radiation Reduces the Barrier Function of Human Skin. *Proc Natl Acad Sci* (2012) 109(42):17111–6. doi: 10.1073/pnas.1206851109
3. Chun Y, Kim J. Autophagy: An Essential Degradation Program for Cellular Homeostasis and Life. *Cells* (2018) 7(12):278. doi: 10.3390/cells7120278
4. Kroemer G, Mariño G, Levine B. Autophagy and the Integrated Stress Response. *Mol Cell* (2010) 40(2):280–93. doi: 10.1016/j.molcel.2010.09.023
5. Qiang L, Wu C, Ming M, Viollet B, He YY. Autophagy Controls P38 Activation to Promote Cell Survival Under Genotoxic Stress. *J Biol Chem* (2013) 288(3):1603–11. doi: 10.1074/jbc.M112.415224
6. Chen L-H, Chu PM, Lee YJ, Tu PH, Chi CW, Lee HC, et al. Targeting Protective Autophagy Exacerbates UV-Triggered Apoptotic Cell Death. *Int J Mol Sci* (2012) 13(1):1209–24. doi: 10.3390/ijms13011209
7. Mizushima N, Levine B, Cuervo AM, Klionsky DJ. Autophagy Fights Disease Through Cellular Self-Digestion. *Nature* (2008) 451(7182):1069–75. doi: 10.1038/nature06639
8. Choi AM, Ryter SW, Levine B. Autophagy in Human Health and Disease. *N Engl J Med* (2013) 368(7):651–62. doi: 10.1056/NEJMra1205406
9. Zhi X, Zhong Q. Autophagy in Cancer. *F1000prime Rep* (2015) 7. doi: 10.12703/P7-18
10. Bj0rk0y G, Lamark T, Brech A, Outzen H, Perander M, 0verath A, et al. P62/SQSTM1 Forms Protein Aggregates Degraded by Autophagy and has a Protective Effect on Huntingtin-Induced Cell Death. *J Cell Biol* (2005) 171 (4):603–14. doi: 10.1083/jcb.200507002
11. Karantza-Wadsworth V, Patel S, Kravchuk O, Chen G, Mathew R, Jin S, et al. Autophagy Mitigates Metabolic Stress and Genome Damage in Mammary Tumorigenesis. *Genes Dev* (2007) 21(13):1621–35. doi: 10.1101/gad.1565707
12. Vessoni A, Filippi-Chiela EC, Menck CF, Lenz G. Autophagy and Genomic Integrity. *Cell Death Differ* (2013) 20(11):1444–54. doi: 10.1038/cdd.2013.103
13. Sancar A, Lindsey-Boltz LA, Ünsal-Kaçmaz K, Linn S. Molecular Mechanisms of Mammalian DNA Repair and the DNA Damage Checkpoints. *Annu Rev Biochem* (2004) 73(1):39–85. doi: 10.1146/annurev.biochem.73.011303.073723
14. Niggli HJ, Röthlisberger R. Cyclobutane-Type Pyrimidine Photodimer Formation and Induction of Ornithine Decarboxylase in Human Skin Fibroblasts After UV Irradiation. *J Invest Dermatol* (1988) 91(6):579–84. doi: 10.1111/1523-1747.ep12477095
15. Vink AA, Berg RJ, Gruijl FR, Roza L, Baan RA. Induction, Repair and Accumulation of Thymin Dimers in the Skin of UV-B-Irradiated Hairless Mice. *Carcinogenesis* (1991) 12(5):861–4. doi: 10.1093/carcin/12.5.861
16. Kim I, He Y-Y. Ultraviolet Radiation-Induced non-Melanoma Skin Cancer: Regulation of DNA Damage Repair and Inflammation. *Genes Dis* (2014) 1 (2):188–98. doi: 10.1016/j.gendis.2014.08.005
17. Shah P, He YY. Molecular Regulation of UV-Induced DNA Repair. *Photochem Photobiol* (2015) 91(2):254–64. doi: 10.1111/php.12406
18. Farrukh MR, Nissar UA, Afnan Q, Rafiq RA, Sharma L, Amin S, et al. Oxidative Stress Mediated Ca2+ Release Manifests Endoplasmic Reticulum Stress Leading to Unfolded Protein Response in UV-B Irradiated Human Skin Cells. *J Dermatol Sci* (2014) 75(1):24–35. doi: 10.1016/j.jdermsci.2014.03.005
19. Umar SA, Tanveer MA, Nazir LA, Divya G, Vishwakarma RA, Tasduq SA. Glycyrrhizic Acid Prevents Oxidative Stress Mediated DNA Damage Response Through Modulation of Autophagy in Ultraviolet-B-Irradiated Human Primary Dermal Fibroblasts. *Cell Physiol Biochem* (2019) 53 (1):242–57. doi: 10.33594/000000133
20. Umar SA, Tasduq SA. Integrating DNA Damage Response and Autophagy Signalling Axis in Ultraviolet-B Induced Skin Photo-Damage: A Positive Association in Protecting Cells Against Genotoxic Stress. *RSC Adv* (2020) 10(60):36317–36. doi: 10.1039/D0RA05819J
21. Adil MD, Kaiser P, Satti NK, Zargar AM, Vishwakarma RA, Tasduq SA. Effect of Emblica Officinalis (Fruit) Against UVB-Induced Photo-Aging in Human Skin

Fibroblasts. *J Ethnopharmacol* (2010) 132(1):109–14. doi: 10.1016/j.jep.2010.07.047
22. Afnan Q, Adil MD, Nissar-Ul A, Rafiq AR, Amir HF, Kaiser P. Glycyrrhizic Acid (GA), a Triterpenoid Saponin Glycoside Alleviates Ultraviolet-B Irradiation-Induced Photoaging in Human Dermal Fibroblasts. *Phytomedicine* (2012) 19 (7):658–64. doi: 10.1016/j.phymed.2012.03.007
23. Love S, Mudasir MA, Bhardwaj SC, Singh G, Tasduq SA. Long-Term Administration of Tacrolimus and Everolimus Prevents High Cholesterol-High Fructose-Induced Steatosis in C57BL/6J Mice by Inhibiting De-Novo Lipogenesis. *Oncotarget* (2017) 8(69):113403. doi: 10.18632/oncotarget.15194
24. Nissar AU, Sharma L, Mudasir MA, Nazir LA, Umar SA, Sharma PR, et al. Chemical Chaperone 4-Phenyl Butyric Acid (4-PBA) Reduces Hepatocellular Lipid Accumulation and Lipotoxicity Through Induction of Autophagy. *J Lipid Res* (2017) 58(9):1855–68. doi: 10.1194/jlr.M077537
25. Liu K, Liu PC, Liu R, Wu X. Dual AO/EB Staining to Detect Apoptosis in Osteosarcoma Cells Compared With Flow Cytometry. *Med Sci Monit Basic Res* (2015) 21:15. doi: 10.12659/MSMBR.893327
26. Kasibhatla S, Amarante-Mendes GP, Finucane D, Brunner T, Bossy-Wetzel E, Green DR. Acridine Orange/Ethidium Bromide (AO/EB) Staining to Detect Apoptosis. *Cold Spring Harb Protoc* (2006) 2006(3):pdb. prot4493. doi: 10.1080/15548627.2020.1797280
27. Klionsky DJ, Abdel-Aziz AK, Abdelfatah S, Abdellatif M, Abdoli A, Abel S, et al. Guidelines for the Use and Interpretation of Assays for Monitoring Autophagy. *Autophagy* (2021) 17(1):1–382. doi: 10.1080/15548627.2020.1797280
28. Rittié L, Fisher GJ. UV-Light-Induced Signal Cascades and Skin Aging. *Ageing Res Rev* (2002) 1(4):705–20. doi: 10.1016/S1568-1637(02)00024-7
29. Silveira JEPS, Pedroso DMM. UV Light and Skin Aging. *Rev Environ Health* (2014) 29(3):243–54. doi: 10.1515/reveh-2014-0058
30. Kerzendorfer C, O'Driscoll M. UVB and Caffeine: Inhibiting the DNA Damage Response to Protect Against the Adverse Effects of UVB. *J Invest Dermatol* (2009) 129(7):1611–3. doi: 10.1038/jid.2009.99
31. D'Orazio J, Jarrett S, Amaro-Ortiz A, Scott T. UV Radiation and the Skin. *Int J Mol Sci* (2013) 14(6):12222–48. doi: 10.3390/ijms140612222
32. Ravanat J-L, Douki T, Cadet J. Direct and Indirect Effects of UV Radiation on DNA and its Components. *J Photochem Photobiol B Biol* (2001) 63(1-3):88–102. doi: 10.1016/S1011-1344(01)00206-8
33. Marrot L, Meunier J-R. Skin DNA Photodamage and its Biological Consequences. *J Am Acad Dermatol* (2008) 58(5):S139–48. doi: 10.1016/j.jaad.2007.12.007
34. Kuma A, Mizushima N. Physiological Role of Autophagy as an Intracellular Recycling System: With an Emphasis on Nutrient Metabolism. *Semin Cell Dev Biol* (2010) 21(7):683–90. doi: 10.1016/j.semcdb.2010.03.002
35. Giampieri F, Afrin S, Forbes-Hernandez TY, Gasparrini M, Cianciosi D, Reboredo-Rodriguez P, et al. Autophagy in Human Health and Disease: Novel Therapeutic Opportunities. *Antioxid Redox Signal* (2019) 30(4):577–634. doi: 10.1089/ars.2017.7234
36. Martínez-Gutiérrez A, Fernández-Duran I, Marazuela-Duque A, Simonet NG, Yousef I, Martínez-Rovira I, et al. Shikimic Acid Protects Skin Cells From UV-Induced Senescence Through Activation of the NAD+-Dependent Deacetylase SIRT1. *Aging* (2021) 13(9):12308. doi: 10.18632/aging.203010
37. Qiang L, Zhao B, Shah P, Sample A, Yang S, He YY. Autophagy Positively Regulates DNA Damage Recognition by Nucleotide Excision Repair. *Autophagy* (2016) 12(2):357–68. doi: 10.1080/15548627.2015.1110667
38. Yang Y, He S, Wang Q, Li F, Kwak MJ, Chen S, et al. Autophagic UVRAG Promotes UV-Induced Photolesion Repair by Activation of the CRL4DDB2 E3 Ligase. *Mol Cell* (2016) 62(4):507–19. doi: 10.1016/j.molcel.2016.04.014
39. Wu C, Qiang L, Han W, Ming M, Viollet B, He YY. Role of AMPK in UVB-Induced DNA Damage Repair and Growth Control. *Oncogene* (2013) 32 (21):2682–9. doi: 10.1038/onc.2012.279
40. Sample A, He YY. Autophagy in UV Damage Response. *Photochem Photobiol* (2017) 93(4):943–55. doi: 10.1111/php.12691
41. Panich U, Sittithumcharee G, Rathviboon N, Jirawatnotai S. Ultraviolet Radiation-Induced Skin Aging: The Role of DNA Damage and Oxidative Stress in Epidermal Stem Cell Damage Mediated Skin Aging. *Stem Cells Int* (2016) 2016. doi: 10.1155/2016/7370642
42. Filomeni G, De Zio D, Cecconi F. Oxidative Stress and Autophagy: The Clash Between Damage and Metabolic Needs. *Cell Death Differ* (2015) 22(3):377–88. doi: 10.1038/cdd.2014.150
43. Latonen L, Laiho M. Cellular UV Damage Responses—Functions of Tumor Suppressor P53. *Biochim Biophys Acta (BBA)-Rev Cancer* (2005) 1755(2):71–89. doi: 10.1016/j.bbcan.2005.04.003
44. Smith J, Tho LM, Xu N, Gillespie DA. The ATM–Chk2 and ATR–Chk1 Pathways in DNA Damage Signaling and Cancer. *Adv Cancer Res* (2010) 108:73–112. doi: 10.1016/B978-0-12-380888-2.00003-0
45. Bartek J, Falck J, Lukas J. CHK2 Kinase—a Busy Messenger. *Nat Rev Mol Cell Biol* (2001) 2(12):877–86. doi: 10.1038/35103059
46. Ray A, Milum K, Battu A, Wani G, Wani AA. NER Initiation Factors, DDB2 and XPC, Regulate UV Radiation Response by Recruiting ATR and ATM Kinases to DNA Damage Sites. *DNA Repair* (2013) 12(4):273–83. doi: 10.1016/j.dnarep.2013.01.003
47. Ji C, Yang B, Huang SY, Huang JW, Cheng B. Salubrinal Protects Human Skin Fibroblasts Against UVB-Induced Cell Death by Blocking Endoplasmic Reticulum (ER) Stress and Regulating Calcium Homeostasis. *Biochem Biophys Res Commun* (2017) 493(4):1371–6. doi: 10.1016/j.bbrc.2017.10.012
48. Wang ZF, Gao C, Chen W, Gao Y, Wang HC, Meng Y, et al. Salubrinal Offers Neuroprotection Through Suppressing Endoplasmic Reticulum Stress, Autophagy and Apoptosis in a Mouse Traumatic Brain Injury Model. *Neurobiol Learn Mem* (2019) 161:12–25. doi: 10.1016/j.nlm.2019.03.002
49. Li J, Li X, Liu D, Hamamura K, Wan Q, Na S, et al. eIF2α Signaling Regulates Autophagy of Osteoblasts and the Development of Osteoclasts in OVX Mice. *Cell Death Dis* (2019) 10(12):1–15. doi: 10.1038/s41419-019-2159-z
50. Ito S, Kimura S, Warabi E, Kawachi Y, Yamatoji M, Uchida F, et al. P62 Modulates the Intrinsic Signaling of UVB-Induced Apoptosis. *J Dermatol Sci* (2016) 83(3):226–33. doi: 10.1016/j.jdermsci.2016.05.005
51. Mathew R, Karp CM, Beaudoin B, Vuong N, Chen G, Chen HY, et al. Autophagy Suppresses Tumorigenesis Through Elimination of P62. *Cell* (2009) 137(6):1062–75. doi: 10.1016/j.cell.2009.03.048
52. Ming M, Han W, Maddox J, Soltani K, Shea CR, Freeman DM, et al. UVB-Induced ERK/AKT-Dependent PTEN Suppression Promotes Survival of Epidermal Keratinocytes. *Oncogene* (2010) 29(4):492–502. doi: 10.1038/onc.2009.357
53. Ming M, Feng L, Shea CR, Soltani K, Zhao B, Han W, et al. PTEN Positively Regulates UVB-Induced DNA Damage Repair. *Cancer Res* (2011) 71 (15):5287–95. doi: 10.1158/0008-5472.CAN-10-4614
54. Majchrzak M, Bowater RP, Staczek P, Parniewski P. SOS Repair and DNA Supercoiling Influence the Genetic Stability of DNA Triplet Repeats in Escherichia Coli. *J Mol Biol* (2006) 364(4):612–24. doi: 10.1016/j.jmb.2006.08.093
55. Qiang L, Sample A, Shea CR, Soltani K, Macleod KF, He YY. Autophagy Gene ATG7 Regulates Ultraviolet Radiation-Induced Inflammation and Skin Tumorigenesis. *Autophagy* (2017) 13(12):2086–103. doi: 10.1080/15548627.2017.1380757

Conflict of Interest: The authors declare that the research was conducted in the absence of any commercial or financial relationships that could be construed as a potential conflict of interest.

Publisher's Note: All claims expressed in this article are solely those of the authors and do not necessarily represent those of their affiliated organizations, or those of the publisher, the editors and the reviewers. Any product that may be evaluated in this article, or claim that may be made by its manufacturer, is not guaranteed or endorsed by the publisher.

frontiers in Oncology

ORIGINAL RESEARCH
published: 30 September 2021
doi: 10.3389/fonc.2021.751875

Identification of Therapeutic Targets and Prognostic Biomarkers Among Integrin Subunits in the Skin Cutaneous Melanoma Microenvironment

Yeltai Nurzat[†], *Weijie Su*[†], *Peiru Min*, *Ke Li*, *Heng Xu*[*] *and Yixin Zhang*[*]

Department of Plastic and Reconstructive Surgery, Shanghai Ninth People's Hospital, Shanghai JiaoTong University School of Medicine, Shanghai, China

OPEN ACCESS

Edited by:
Motoki Nakamura,
Nagoya City University, Japan

Reviewed by:
Tetsuya Magara,
Nagoya City University, Japan
Tadahiro Kobayashi,
Kanazawa University, Japan

***Correspondence:**
Heng Xu
xuh1990@gmail.com
Yixin Zhang
zhangyixin6688@hotmail.com

[†]*These authors have contributed equally to this work and share first authorship*

Specialty section:
This article was submitted to Skin Cancer, a section of the journal Frontiers in Oncology

Received: *02 August 2021*
Accepted: *09 September 2021*
Published: *30 September 2021*

Citation:
Nurzat Y, Su W, Min P, Li K, Xu H and Zhang Y (2021) Identification of Therapeutic Targets and Prognostic Biomarkers Among Integrin Subunits in the Skin Cutaneous Melanoma Microenvironment. Front. Oncol. 11:751875. doi: 10.3389/fonc.2021.751875

The roles of different integrin alpha/beta (ITGA/ITGB) subunits in skin cutaneous melanoma (SKCM) and their underlying mechanisms of action remain unclear. Oncomine, UALCAN, GEPIA, STRING, GeneMANIA, cBioPortal, TIMER, TRRUST, and Webgestalt analysis tools were used. The expression levels of ITGA3, ITGA4, ITGA6, ITGA10, ITGB1, ITGB2, ITGB3, ITGB4, and ITGB7 were significantly increased in SKCM tissues. The expression levels of ITGA1, ITGA4, ITGA5, ITGA8, ITGA9, ITGA10, ITGB1, ITGB2, ITGB3, ITGB5, ITGB6 and ITGB7 were closely associated with SKCM metastasis. The expression levels of ITGA1, ITGA4, ITGB1, ITGB2, ITGB6, and ITGB7 were closely associated with the pathological stage of SKCM. The expression levels of ITGA6 and ITGB7 were closely associated with disease-free survival time in SKCM, and the expression levels of ITGA6, ITGA10, ITGB2, ITGB3, ITGB6, ITGB7, and ITGB8 were markedly associated with overall survival in SKCM. We also found significant correlations between the expression of integrin subunits and the infiltration of six types of immune cells (B cells, CD8+ T cells, CD4+T cells, macrophages, neutrophils, and dendritic cells). Finally, Gene Ontology (GO) enrichment analysis and Kyoto Encyclopedia of Genes and Genomes (KEGG) pathway analysis were performed, and protein-protein interaction (PPI) networks were constructed. We have identified abnormally-expressed genes and gene regulatory networks associated with SKCM, improving understanding of the underlying pathogenesis of SKCM.

Keywords: biomarkers, integrin subunit family, melanoma, skin cutaneous melanoma, cancer genome atlas

INTRODUCTION

Skin cutaneous melanoma (SKCM) is one of the most aggressive and lethal skin cancers (1). In the past decade, incidence of SKCM has increased rapidly worldwide (1). Hence, SKCM poses a major global threat to human health. Recently, associations between molecular biological biomarkers and tumor prognosis during the development of SKCM have elicited great interest. However, our understanding of the etiology and pathogenesis of SKCM could be improved, and more effective prognostic biomarkers are required.

Integrins are glycosylated heterodimers composed of non-covalently bound α and β subunits (2). Specific integrin subunits are known to be closely associated with various tumors, including gallbladder cancer and breast cancer, etc. (3–5). The diversity of integrin function in tumors may be related to differences in the integrin domains. Therefore, we speculate that different integrin subunits may play a role in several biological processes underlying SKCM.

Several comprehensive scientific reviews of the molecular factors underlying SKCM biology, SKCM drug target mechanisms (6), and SKCM prognosis have been published. However, studies clarifying the role of integrins in SKCM are relatively scarce. In the present study, we evaluate the utility of abnormally-expressed integrin subunits as biomarkers in SKCM. In addition, we employ bioinformatics tools for analyzing the underlying mechanisms by which different integrin subunits affect SKCM. Our overall aim is to identify potential biological targets in the integrin subunit family which can be used as biomarkers in SKCM.

MATERIALS AND METHODS

ONCOMINE

The ONCOMINE Database is a multi-functional website based on the Cancer Genome Atlas (TCGA) tumor database (7). Here, we used ONCOMINE to analyze the differentially expressed integrins subunits using a threshold limited by P value<0.05, Fold change ≥2. The specific referencing steps are as follows: the filter of Analysis Type: Cancer *vs.* Normal Analysis; the filter of Cancer Type: Cutaneous Melanoma; the filter of Data Type: mRNA. The data was order by: over-expression: Gene Rank.

UALCAN

UALCAN (http://ualcan.path.uab.edu/index.html) is an integrated data-mining platform facilitating comprehensive analyses of the cancer transcriptome (8). The functionalities of UALCAN including identifying biomarkers, analyzing expression profile, analyzing gene correlation, and survival analysis (9). In this study, UALCAN database was used to analyze the expression of target genes in primary SKCM, metastasis SKCM and normal samples. The sample information of UALCAN was derived from the TCGA database, and it used the TCGA-Assembler (10) to download the RNA-Seq data of 31 tumors in the TCGA database. RNA-Seq data were obtained for 'Primary Solid Tumor' and 'Solid Tissue Normal' for each cancer, and the tumor staging in UALCAN was based on the pathological tumor staging data of the American Joint Committee on Cancer (AJCC), which divided the samples into different stages (8). Data visualization was conducted by Highcharts (Highsoft AS Highcharts, http://www.highcharts.com/), a JavaScript library from Highsoft AS (8).

GEPIA

Developed by Gepia Zefang Tang, is a website that analyzes RNA sequence expression databases based on the TCGA and GTEX projects. Using a deconvolution strategy, it can present cell type information combined with clinical data to help us explore the relationship between cell proportion and prognosis (11). The cancer data of GEPIA was collected from TCGA or GTEx, and the tumor staging definition in GEPIA was based on the pathological tumor staging data of the American Joint Committee on Cancer (AJCC) (12, 13). For the calculation methods of survival analysis, the python package lifeline (https://github.com/CamDavidsonPilon/lifelines) was used for the survival analysis (11). Here, we mainly used the Multiple Gene Analysis module for analyzing the expression of integrins in SKCM at different pathological stages, and correlations between integrin subunit expression and overall survival and disease-free survival.

STRING

String is a website that can analyze the interaction relationship between genes. In order to understand the interaction relationship between integrin genes in this study, we used STRING website to build a PPI network. Each gene is represented by nodes in the network, and the strength and connections in the network are represented by the color and thickness of the lines.

GeneMANIA

GeneMANIA is a website for reprocessing PPI network maps (14). GeneMANIA can perform cluster analysis on nodes in the PPI network graph by collecting hundreds of data sets from GEO, Biogrid, Pathway Commons and I2D, so as to provide biological function analysis of each gene in the PPI network graph (14).

CBioPortal

CBioPortal (http://www.cbioportal.org) is a website used to analyze and visualize cancer genomics data (15). Cbioportal collected the data of 126 tumor genomic studies from TCGA data, based on which cBioPortal can detect the genetic variation, gene network and co-expression of target genes in SKCM (9). Here, we analyzed the gene variation of integrins in SKCM using cBioPortal.

TIMER

TIMER is a website that analyzes the relationship between tumor purity and immune cell infiltration. Specifically, TIMER can

Abbreviations: SKCM, skin cutaneous melanoma; AJCC, American Joint Committee on Cancer.

explore the correlation between the degree of infiltration of immune cells in tumor microenvironment and clinical results, somatic mutations, gene expression and somatic copy number changes (16). By collecting the gene expression information of different tumors in the TCGA database, TIMER inferred the abundance of tumor-infiltrated immune cells in the gene expression profile using deconvolution method (17). In this study, the relationship between immune cell infiltration and integrin subunit in SKCM was investigated by using the "gene" module in TIMER.

Trrust

TRRUST (https://www.grnpedia.org/trrust/) is a curated database of human and mouse transcriptional regulatory networks. TRRUST is useful as a tool in predicting these transcriptional regulatory networks (18). Here, TRRUST was used to identify the relationships between selected integrin subunit genes and other target genes.

Webgestalt

WebGestalt is a website for gene enrichment analysis based on David database. Through the use of WebGestalt, we can quickly visualize the results of the enrichment analysis of DAVID, and at the same time, we can also visualize the results of KEGG pathway (19, 20).

RESULTS

1. Aberrant Expression of Integrin Subunits in SKCM Patients

Firstly, we used the ONCOMINE database to compare the expression profiles of integrin subunits in cutaneous melanoma patients and control groups (**Figure 1** and **Table 1**). The results reveal that the transcription levels of ITGA3, ITGA4, ITGA6, ITGA10, ITGB1, ITGB2, ITGB3, ITGB4, and ITGB7 in Cutaneous Melanoma samples were significantly increased (compared with normal control samples). These results were compiled from several sources. According to Riker et al., the transcription levels of ITGA4, ITGA10, ITGB1, ITGB2, and ITGB7 in SKCM patients were significantly increased (compared with normal skin tissue), with fold changes of 3.224, 2.074, 3.525, 3.968, and 2.84 respectively (21). Haqq et al. reported that the transcription level of ITGB3 in melanoma patients was significantly increased (compared with normal skin tissue), with a fold change of 3.147 (22). Talatov et al. reported that the transcription levels of ITGA3, ITGA6, and ITGB4 in cutaneous melanoma were significantly increased (compared with normal tissue), with fold changes of 14.807, 16.226, and 10.644 (23). The significant differences in the expression levels of other integrin subunits were not observed between SKCM patients and normal patients. For specific sample information, please refer to the references mentioned in **Table 1**.

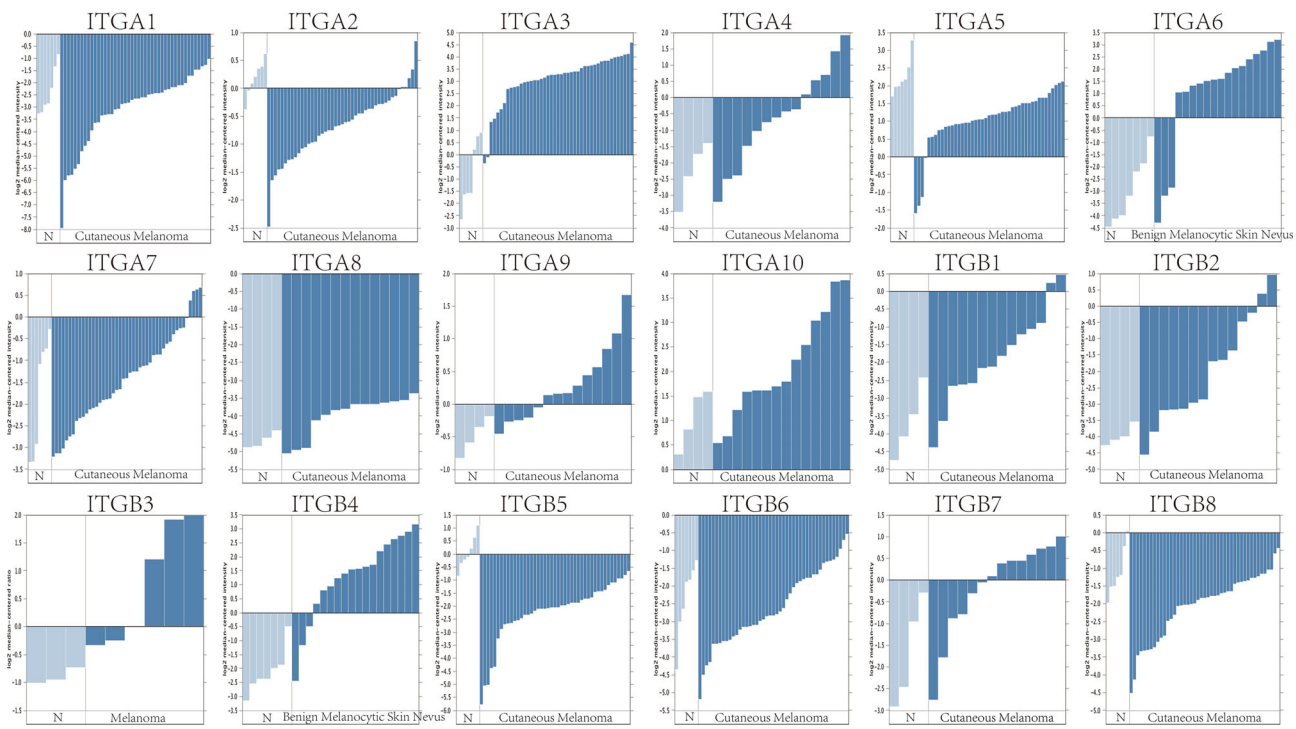

FIGURE 1 | The mRNA expression levels of different integrin subunits in cutaneous melanoma/melanoma/benign melanocytic skin nevus and normal skin tissue (N). The t-test statistic provided in ONCOMINE reflects the magnitude of the difference between the groups. Each bar represents the gene expression of one sample. The p value was set at 0.05.

TABLE 1 | Aberrant expression of integrin subunits in SKCM patients.

GENE	CANCER TYPE	FOLD CHANGE	p-value	t-test	Reference	PMID
ITGA3	Cutaneous Melanoma *vs.* Normal	14.807	9.58E-05	7.105	Talantov Melanoma	PMID: 16243793
ITGA4	Cutaneous Melanoma *vs.* Normal	3.224	0.013	2.75	Riker Melanoma	PMID: 18442402
ITGA6	Benign Melanocytic Skin Nevus *vs.* Normal	16.226	1.71E-05	5.491	Talantov Melanoma	PMID: 16243793
ITGA10	Cutaneous Melanoma *vs.* Normal	2.074	0.015	2.55	Riker Melanoma	PMID: 18442402
ITGB1	Cutaneous Melanoma *vs.* Normal	3.525	0.011	2.983	Riker Melanoma	PMID: 18442402
ITGB2	Cutaneous Melanoma *vs.* Normal	3.968	3.61E-04	4.213	Riker Melanoma	PMID: 18442402
ITGB3	Melanoma *vs.* Normal	3.147	0.006	3.681	Haqq Melanoma	PMID: 15833814
ITGB4	Benign Melanocytic Skin Nevus *vs.* Normal	10.644	2.76E-03	7.278	Talantov Melanoma	PMID: 16243793
ITGB7	Cutaneous Melanoma *vs.* Normal	2.84	0.043	2.21	Riker Melanoma	PMID: 18442402

To further validate the above results, we assessed the expression levels of different integrin subunits in primary SKCM samples and metastatic SKCM samples with UALCAN. Our analysis revealed that the transcriptional levels of ITGA1 ($p = 6.89\times10^{-7}$), ITGA4 ($p = 6.27\times10^{-8}$), ITGA5 ($p = 6.30\times10^{-5}$), ITGA8 ($p = 6.40\times10^{-4}$), ITGA9 ($p = 3.24\times10^{-3}$), ITGA10 ($p = 1.06\times10^{-3}$), ITGB1 ($p = 1.22\times10^{-6}$), ITGB2 ($p < 1\times10^{-12}$), ITGB3 ($p = 5.61\times10^{-4}$), ITGB5 ($p = 1.74\times10^{-3}$), and ITGB7 ($p = 3.15\times10^{-11}$) in metastatic SKCM tissues were significantly increased compared with primary SKCM tissues (**Figure 2**). Whereas, the expression level of ITGB6 ($p = 1.18\times10^{-2}$) in metastatic SKCM tissue was decreased compared with primary SKCM tissue (**Figure 2**). All other comparisons do not meet our threshold by p value<0.05 and fold change ≥ 2.

Lastly, to clarify the clinical significance of the observed changes in integrin subunit expression, we analyzed the correlations between integrin subunit expression and the pathological stage of SKCM using GEPIA. The analysis revealed that ITGA1 ($p = 0.000326$), ITGA4 ($p = 1.1\times10^{-5}$), ITGB1 ($p = 0.0213$), ITGB2 ($p = 5.78\times10^{-5}$), ITGB6 ($p = 0.00257$), and ITGB7 ($p = 0.00017$) were notably associated with the pathological stage of SKCM (**Figure 3**). To clarify the gene expression rank of integrin subunit gene expression, we analyzed the expression levels of these genes in SKCM tissue using the GEPIA website (**Figure 4**). The results reveal that the expression level of ITGB1 in SKCM patients was highest among the integrin genes of interest.

2. The Prognostic Value of Integrin Subunits in SKCM Patients

We next investigated correlations between integrin subunit expression levels and patient prognosis using GEPIA. The results of this analysis reveal that integrin subunit expression and disease-free survival time in SKCM patients are related. Two of these correlations — those involving ITGA6 and ITGB7 — were statistically significant (**Figure 5**). We next analyzed the associations between integrin subunit expression levels and overall survival in SKCM patients. The results reveal that the expression levels of ITGA6, ITGA10, ITGB2, ITGB3, ITGB6, ITGB7, and ITGB8 were remarkably correlated with overall survival in SKCM patients (**Figure 6**).

3. Relationship Between Integrin Subunit Expression and Immune Cell Infiltration

Tumor immune microenvironment (TIME) refers to the mutual environment composed of tumor cells and their surrounding immune cells. Evidence is accumulating to suggest that immune cell infiltration is closely related with cancer occurrence and resistance, and the degree of immune cell infiltration can evaluate the effectiveness of clinical tumor immunotherapy (16, 24). If the expression of the gene in SKCM TIME is related to the infiltration of immune cells and tumor purity, it is suggested that the gene may become a target of tumor immunotherapy. To further explore the function of integrin subunits in SKCM, the immune effects of integrin subunits were analyzed using the TIMER website (**Figures 7** and **8**).

The expression of *ITGA4, ITGA8, ITGB2*, *ITGB7* and *ITGB8* was correlated with the infiltration of all types immune cell and tumor purity in the SKCM TIME. *ITGA5* was related with tumor purity, B cell, Macrophage cell, Neutrophil cell, and Dendritic cell invasion in SKCM TIME. The expression of *ITGA1* and *ITGA9* was correlated with the infiltration of all types immune cell in the SKCM TIME, but not tumor purity. The expression of *ITGA2* was correlated with the infiltration of CD8+/CD4+ T cell, Macrophage cell, Neutrophil cell and Dendritic cell in SKCM patients. *ITGA6*, *ITGB1* and *ITGB3* was correlated with B cell, CD8+ T cell, Macrophage cell, Neutrophil cell and Dendritic cell infiltration. *ITGA10* was associated with CD4+/CD8+ T cell, Macrophage cell and Neutrophil cell infiltration. *ITGB5* was related with the invasion of CD4+ T cell, Macrophage cell, Neutrophil cell and Dendritic cell. *ITGB8* was correlated with CD8+ T cell, B cell and Neutrophil cell invasion.

4. Integrin Subunit Genetic Alteration and Protein Interaction Network in 1SKCM Patients

Firstly, we explored genetic alterations in the integrin subunit family in SKCM using the cBioportal website. The results of this analysis reveal that *ITGA1, ITGA2, ITGA3, ITGA4, ITGA5, ITGA6, ITGA7, ITGA8, ITGA9, ITGA10, ITGB1, ITGB2, ITGB3, ITGB4, ITGB5, ITGB6, ITGB7*, and *ITGB8* were changed in 6%, 3%, 3%, 8%, 5%, 3%, 5%, 7%, 4%, 7%, 1.6%, 3%, 4%, 8%, 2.1%, 4%, 1.9%, and 6% of the queried SKCM samples, respectively (**Figure 9A**). Next a PPI network of the integrin subunit family was constructed to explore possible interactions. A PPI network with 18 nodes and 152 edges was constructed using STRING (**Figure 9B**). According to the statistical results reported by the String website, the P-value of PPI enrichment was <1.0e-16. Further analysis using GeneMANIA revealed that the above-mentioned integrin subunits were mainly involved in extracellular matrix

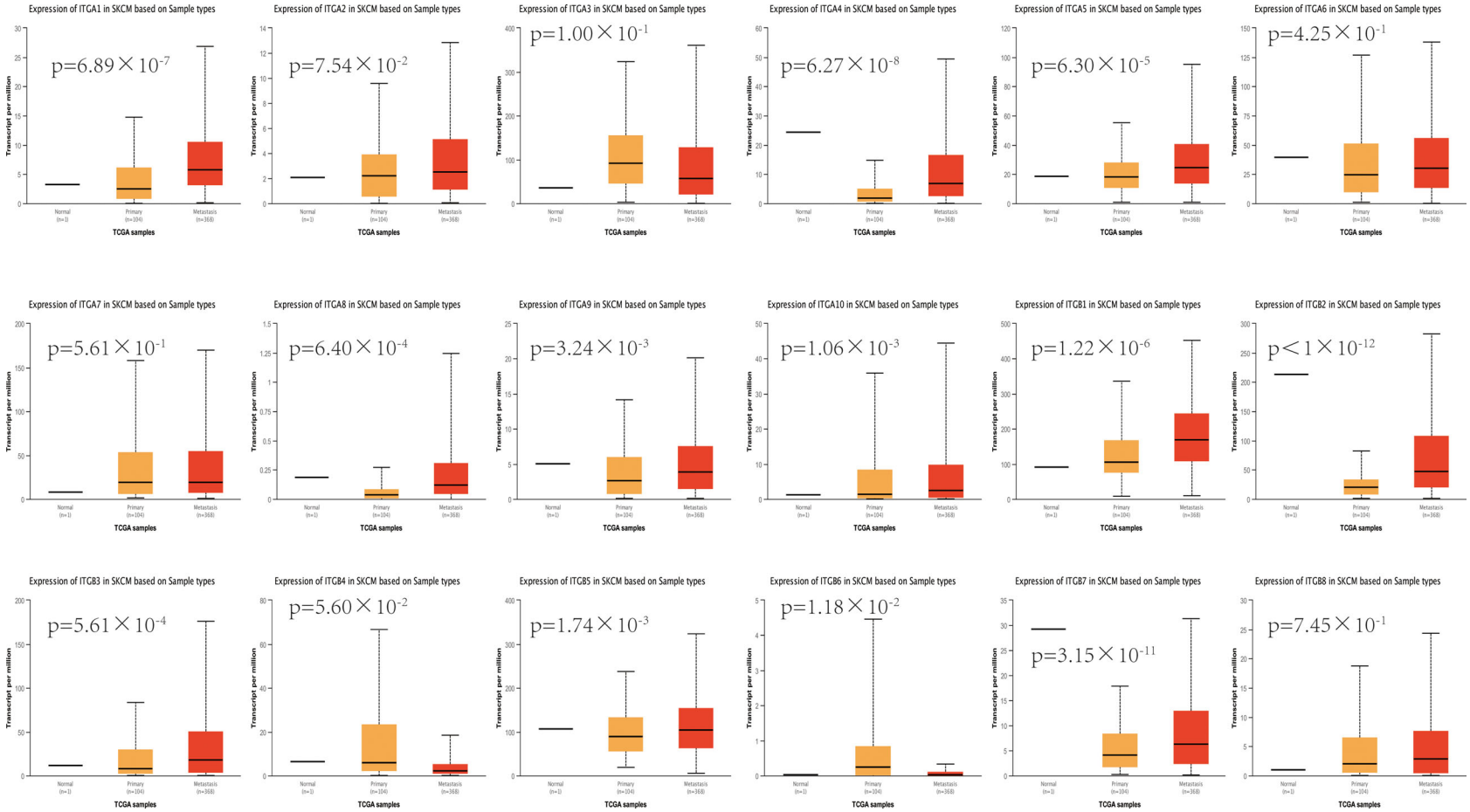

FIGURE 2 | The expression levels of different integrin subunits in primary SKCM samples and metastatic SKCM samples (UALCAN). Student's t test was used to generate a p value. The p value was set at 0.05.

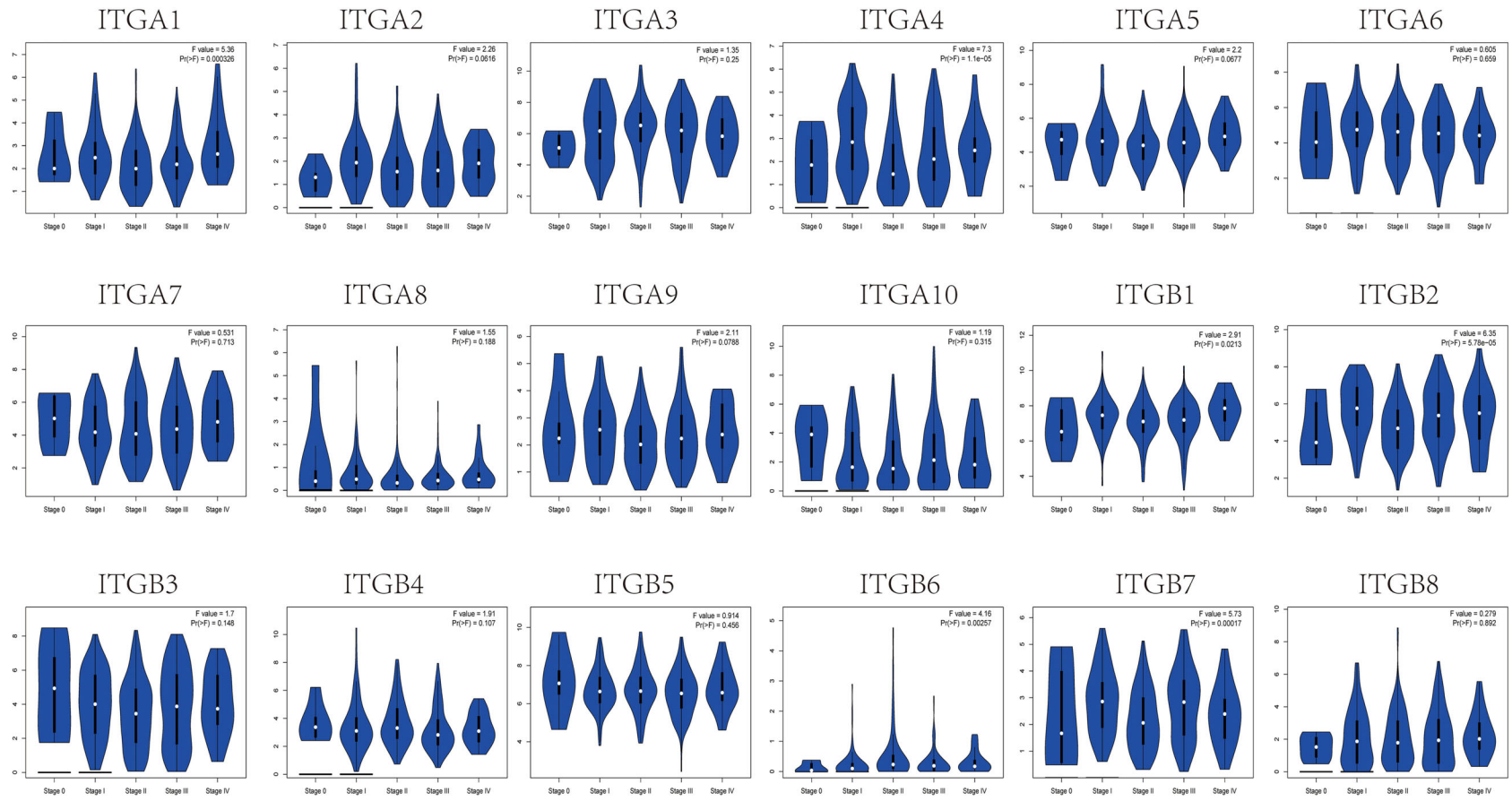

FIGURE 3 | Correlation between different expressed integrin subunits and the pathological stage of SKCM patients (GEPIA). A P value less than 0.05 was used to determine statistical difference. Student's t test was used to generate a p value for expression or pathological stage analysis.

FIGURE 4 | The relative expression levels of integrin subunits in SKCM.

organization, extracellular structure organization, integrin complex, receptor complex, and leukocyte migration (**Figure 9C**). To further corroborate these observations, we used STRING to analyze the top 48 most interacting neighboring genes associated with 18 integrin subunits. The results demonstrate that ALB, CBL, CBY1, CD247, CDC25C, CTGF, EGF, EGFR, ERBB2, ERBB3, ERBB4, FBN1, FLNA, FN1, GRB2, ICAM1, ICAM3, ICAM5, ILK,IRS1, ITGA1, ITGA10, ITGA2, ITGA2B, ITGA3, ITGA4, ITGA5, ITGA6, ITGA7, ITGA8, ITGA9, ITGAL, ITGAM, ITGAV, ITGAX, ITGB1, ITGB1BP1, ITGB2, ITGB3, ITGB4, ITGB5, ITGB6, ITGB7, ITGB8, NPNT, NTRK1, NTRK2, PCSK9, PIK3R1, PIK3R2, PLEC, PXN, RAF1, SHC1, SMAD2, SOS1, SRC, TGFB1, TGFBR1, TGFBR2, TLN1, VEGFA, VTN, VWF, YWHAB, YWHAG, YWHAH, and YWHAZ are all involved in either the regulation or function of integrin subunit family members in SKCM patients (**Figure 9D**).

5. Gene Ontology and KEGG Pathway Analysis of Integrin Subunits in SKCM Patients

Go and KEGG pathway analysis for 18 integrin subunits and top 48 most interacting neighboring genes was performed using the Webgestalt website (**Figures 9E, F**). In the KEGG pathway analysis, the top 5 pathways identified were ECM-receptor interaction, arrhythmogenic right ventricular cardiomyopathy, hypertrophic cardiomyopathy, dilated cardiomyopathy, and focal adhesion. In the GO enrichment analysis, the results pertaining to biological processes were response to stimulus, biological regulation, and cell communication. For the results pertaining to the analysis of cellular components, the top five cellular components were membrane, protein-containing complex, vesicle, extracellular space, and endomembrane system. For the results pertaining to the analysis of molecular function, the top 5 molecular functions were protein binding, ion binding, molecular transducer activity, transferase activity, and nucleic acid binding.

DISCUSSION

Recent studies indicate that ITGA1 is associated with melanoma proliferation *via* the regulation of miR-3065-5p (25). In addition, as a mediator of cell-cell and cell-matrix adhesion, ITGA1 was differentially expressed in melanoma samples (26). In the present study, we found that ITGA1 expression levels in SKCM tissues are correlated with different stages of SKCM and with migration in SKCM. ITGA1 protein mediate the adhesion of extracellular matrix proteins (27). We hypothesized that ITGA1 protein in SKCM promote the adhesion of melanocytes to the epidermal basement membrane (28), thus affecting the metastasis of SKCM. Besides, we found a positive correlation between the expression of *ITGA1* and infiltration of all types of immune cell, but not tumor purity (**Figure 7**). Therefore, the effect of ITGA1 in tumor immune therapy may need further verification.

ITGA2 plays a role in melanoma by regulating the expression GTSE1, thereby restoring the epithelial-to-mesenchymal transition in SKCM (29). However, according to our results, the increased expression of ITGA2 may only be related to the infiltration of some immune cells, and this infiltration of immune cells does not lead to the reduction of tumor purity in SKCM TIME, suggesting that the infiltration of immune cells may not play a decisive role in SKCM.

Schumacher et al. reported that flocculating material observed around melanoma cells or nests contains basal membrane protein components, particularly ITGA3 (30). In line with previous research, we found that ITGA3 expression in SKCM tissues was significantly increased (in comparison with non-tumor tissue). Moreover, it is worth mentioning that ITGA3 has most biological functions compared with other integrin subunits, suggesting that it may play a central role in integrin subunits gene clusters (**Figure 9C**).

ITGA4 is closely related to the occurrence and development of melanoma, and ITGA4 can promote the metastasis of melanoma by promoting the aggregation of melanoma cells in the lymphatic system (31). J. Zhao et al. reported that ITGA4 down-regulation inhibits the adhesion and migration of melanoma cells *in vitro* and *in vivo* (32). The immunomodulatory mechanism of ITGA4 in melanoma has also been reported in previous studies. Geherin et al. reported that IL-10+ B1 cells are part of the skin immune system and require $\alpha4\beta1$ integrin for homing into the skin (33). In addition, Kobayashi et al. reported that IL-10+ B1a B cells suppress melanoma tumor immunity by inhibiting Th1 cytokine production in tumor-infiltrating CD8+ T cells (34). According to

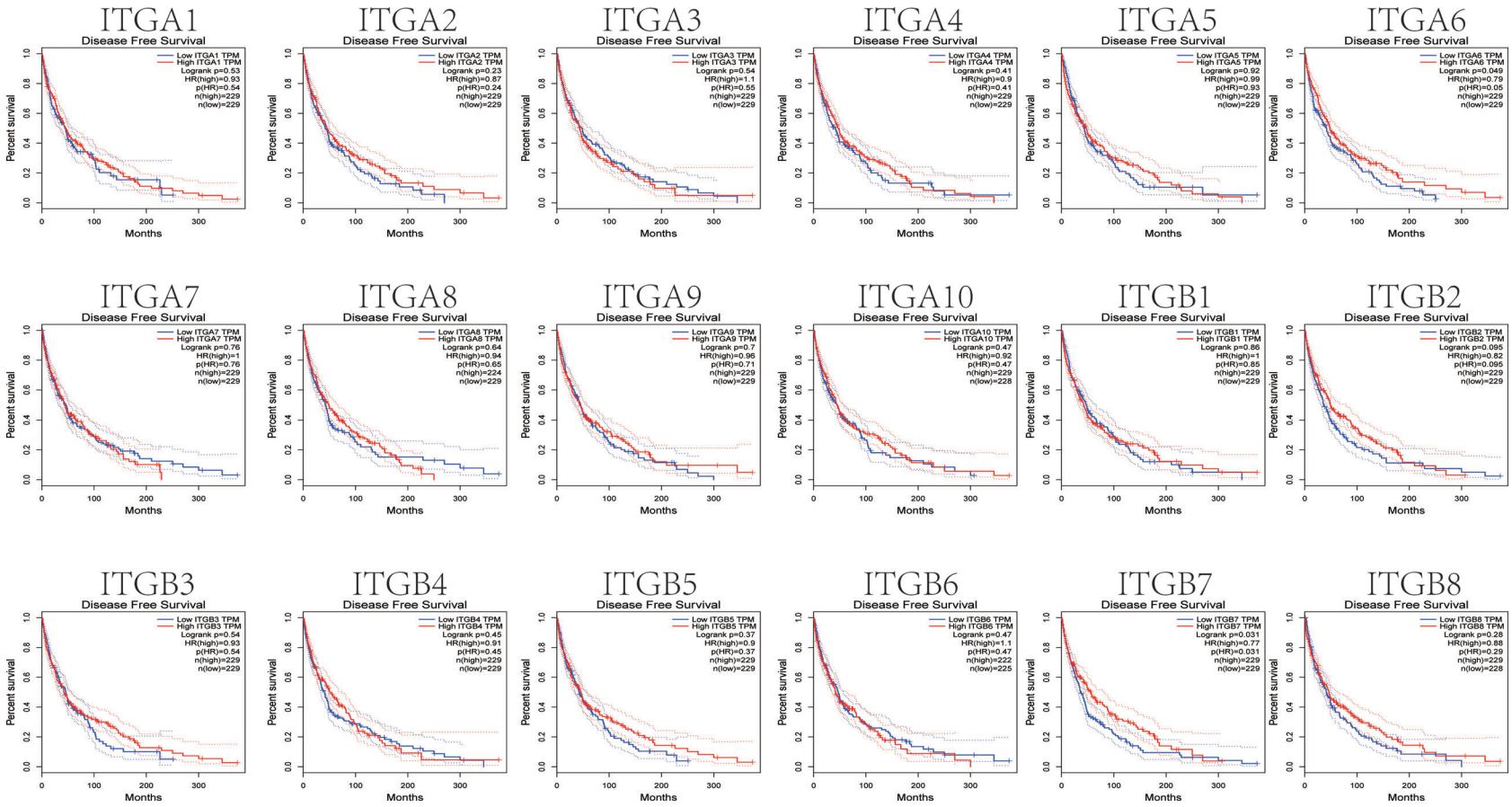

FIGURE 5 | The prognostic value of differentially-expressed integrin subunits in the disease-free survival curve (GEPIA) for SKCM patients. Prognostic analysis was performed using a Kaplan–Meier curve. The p value was set at 0.05.

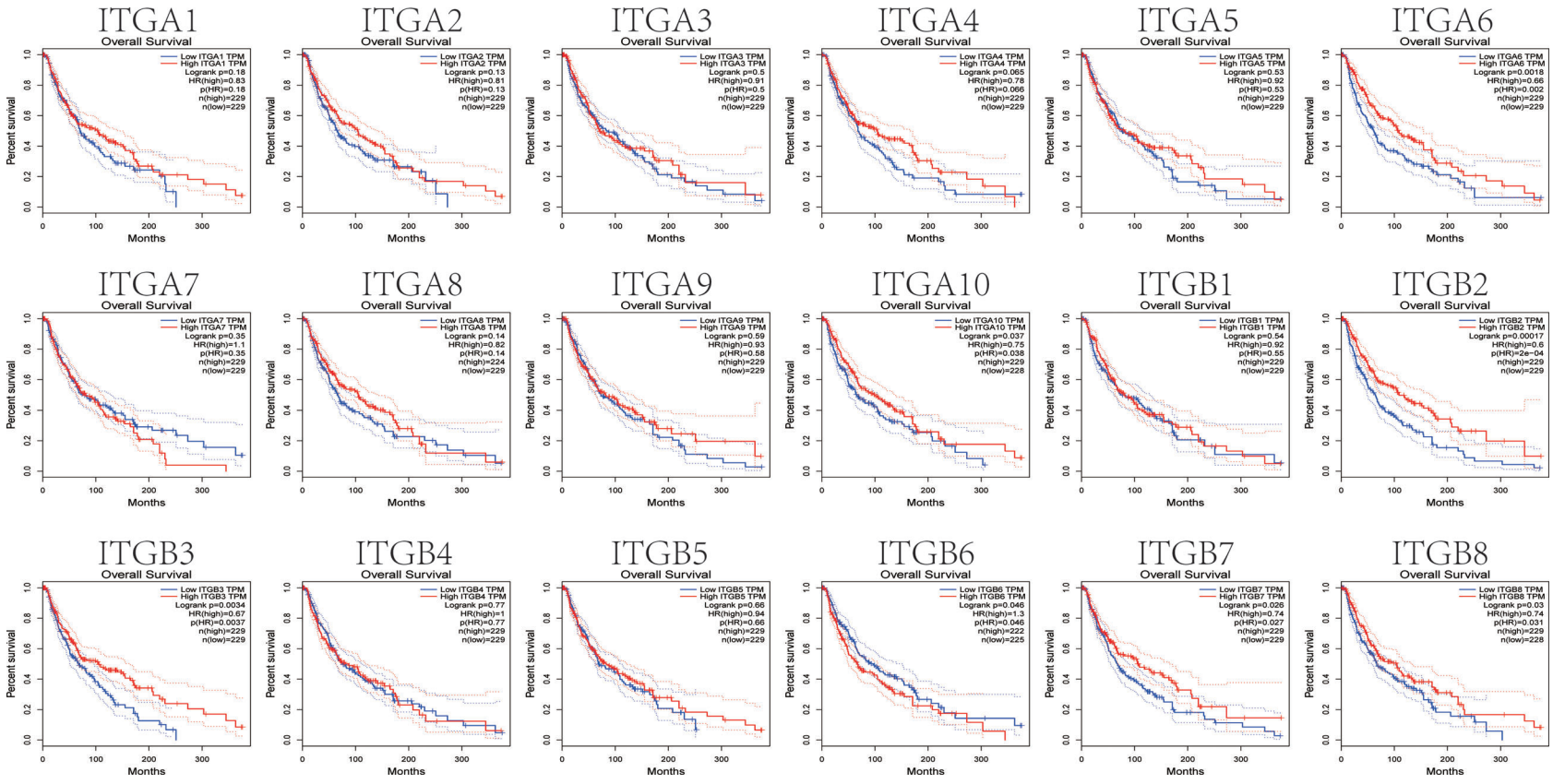

FIGURE 6 | The prognostic value of differentially-expressed integrin subunits in the overall survival curve (GEPIA) for SKCM patients. Prognostic analysis was performed using a Kaplan–Meier curve. The p value was set at 0.05.

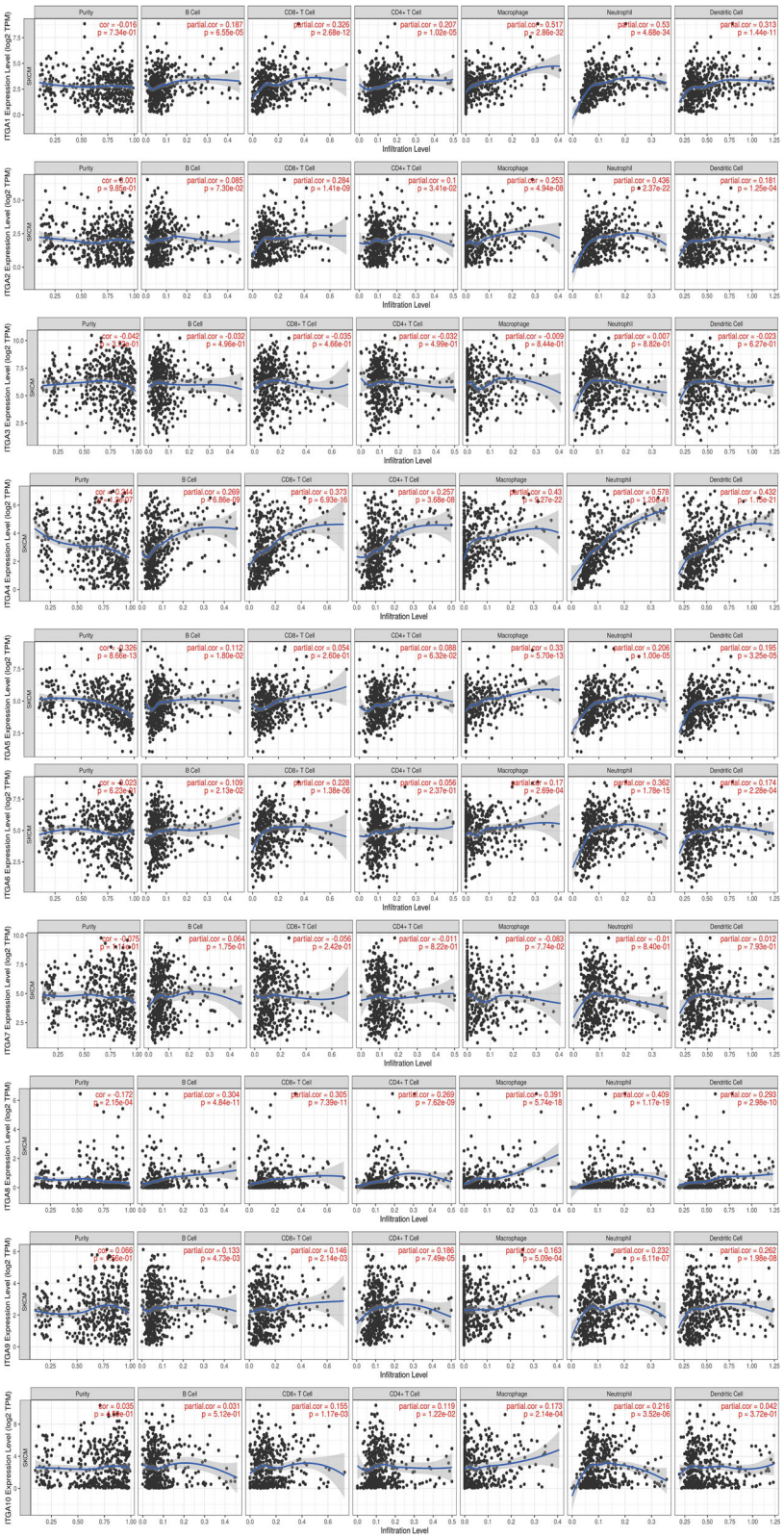

FIGURE 7 | Immune infiltration associated with ITGA1 – ITGA10 in SKCM patients (TIMER). Spearman correlation coefficient was used for statistical analysis. A P value less than 0.05 was used to determine statistical difference.

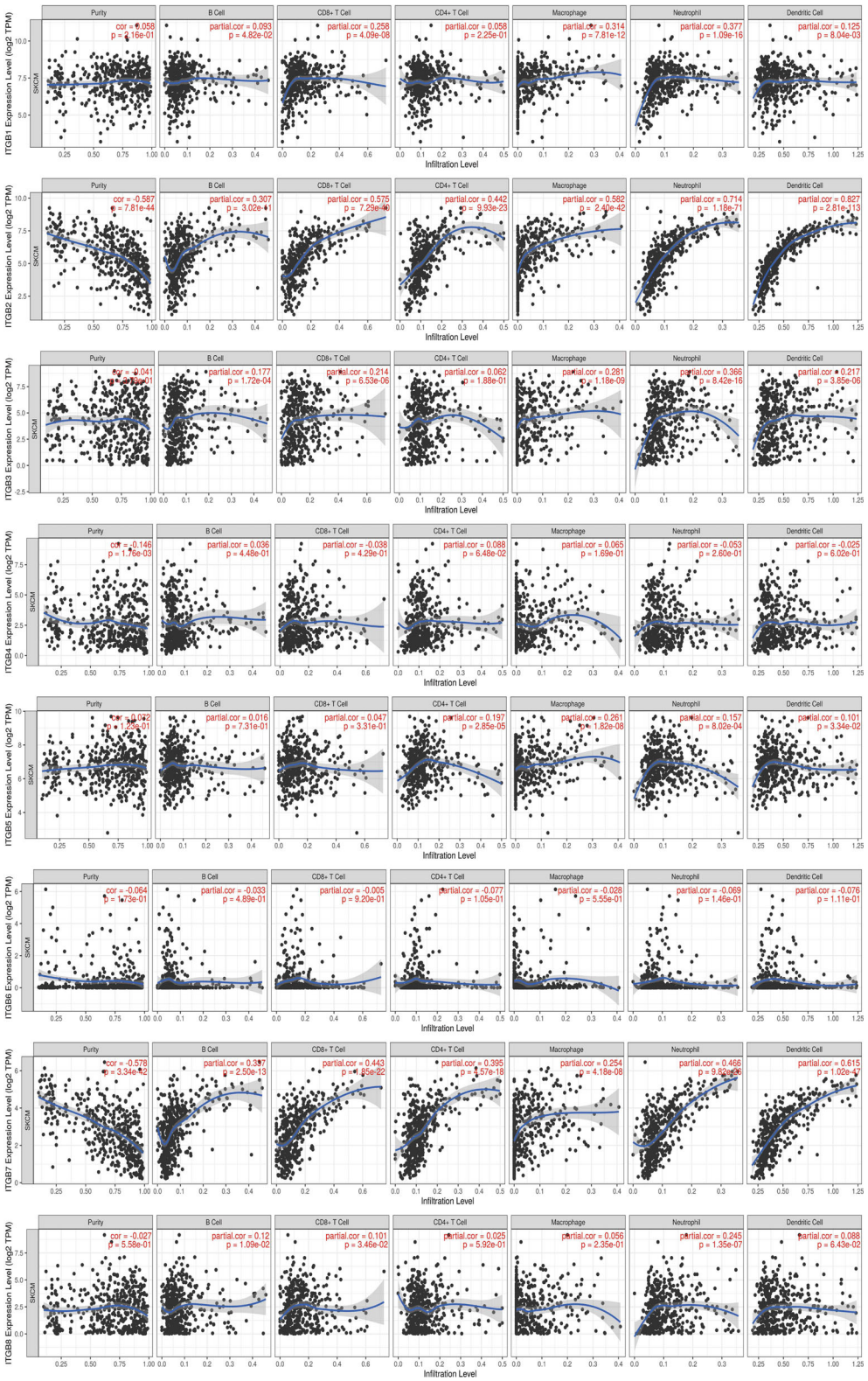

FIGURE 8 | Immune infiltration associated with ITGB1 – ITGB8 in SKCM patients (TIMER). Spearman correlation coefficient was used for statistical analysis. A P value less than 0.05 was used to determine statistical difference.

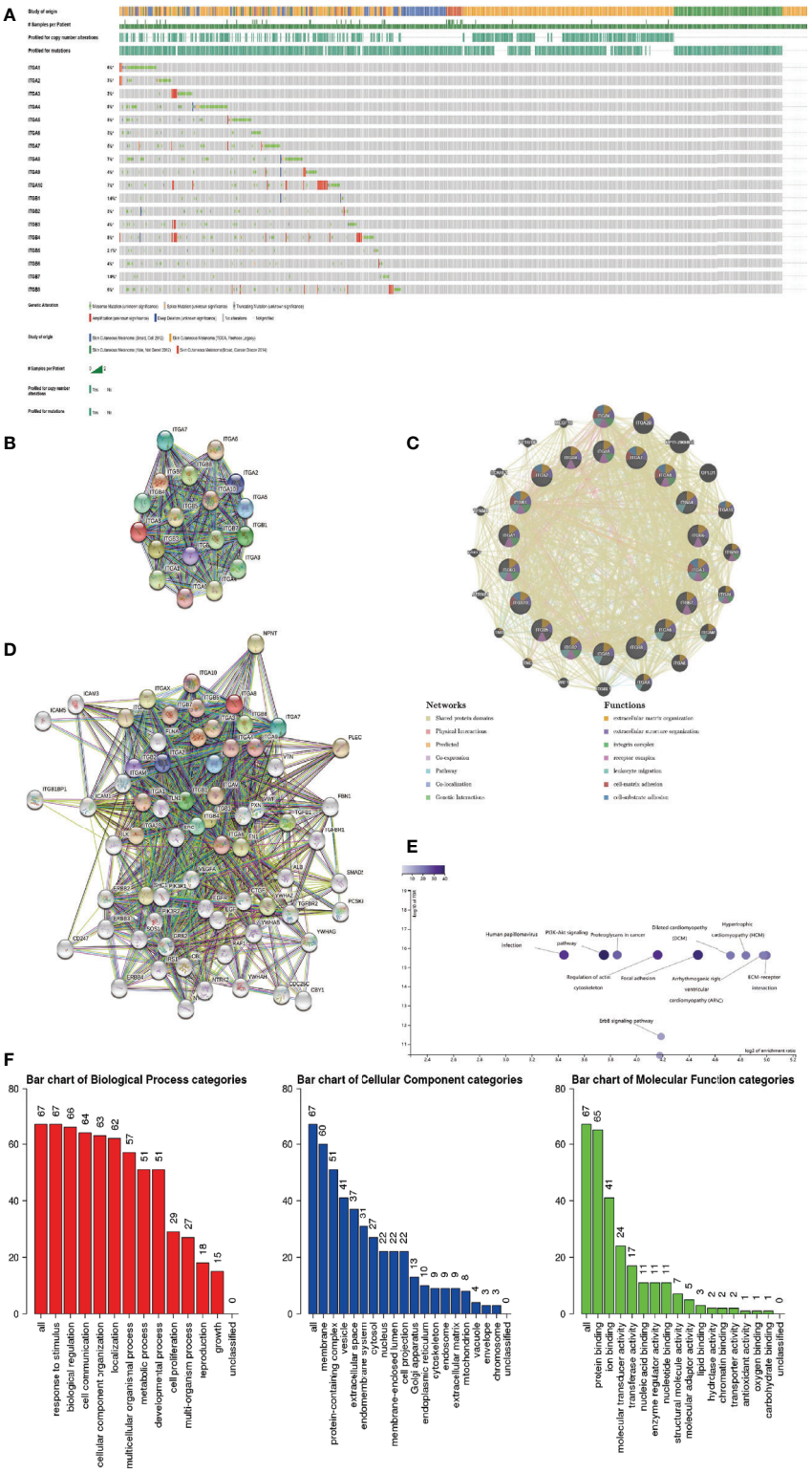

FIGURE 9 | **(A)** Summary of genetic alterations in different integrin subunits in SKCM. **(B, C)** Protein-protein interaction network of different integrin subunits. **(D)** Gene-gene interaction network of different integrin subunits and 48 most frequently altered neighboring genes. **(E, F)** Enrichment analysis of different integrin subunits and 48 most frequently altered neighboring genes in SKCM (Webgestalt). **(E)** Bar plot of KEGG enriched terms. **(F)** Bar plot of GO enrichment in biological process terms, cellular component terms, and molecular function terms.

our results, we speculated that the differentially expressed ITGA4 may recruit immune cells by effecting leukocyte migration, reduce the percentage of melanoma cells in SKCM TIME by affecting cell matrix adhesion in SKCM TIME, and ultimately affect the metastasis and tumor stage of SKCM (**Figures 7** and **9C**).

ITGA5 forms a receptor for extracellular fibronectin, which known to be involved in the formation of malignant tumor cells and tumor vascular systems (35). ITGA5 is known to play a role in melanoma by regulating miR-148b (36). Combined with our results, we hypothesized that ITGA5 may affect the infiltration of immune cells and tumor purity in SKCM TIME by regulating leukocyte migration (**Figures 7** and **9C**).

Specific ITGA6 variants were reported to be associated with a decreased risk of melanoma, and Luo et al. reported that ITGA6 can be considered a prognostic gene for uveal melanoma (37, 38). We also found that abnormally expressed ITGA6 is a potential prognostic biomarker in SKCM, and we speculate that missense mutation is one of the main reasons for the abnormal expression of ITGA6 (**Figure 9A**).

ITGA8 is a transmembrane cell surface receptor belonging to the alpha integrin family (39). To date, several studies have linked ITGA8 and tumorigenesis (40, 41). In addition, anti-ITGA8 therapies have been reported to play a role in the treatment of lupus and other glomerular diseases (42). Tumor cells express antigens that mediate recognition by CD8+ T cells and the infiltration of CD8+ T cells in SKCM TIME is a very important part of immunotherapy (43). Combined with our results, we speculated that interference against ITGA8 expression could effectively increase the infiltration of CD8+ T cells in SKCM TIME and reduce the percentage of tumor cells in SKCM, which is a potential target of SKCM targeted therapy (**Figure 7**).

Several studies have reported a close association between ITGA9 and cell adhesion, proliferation, and migration (44). Changes in ITGA9 expression levels affect the interaction between tumor cells and the extracellular matrix (45). *ITGA9* is a host gene for various long non-coding RNAs, including LncCCAT1 and HOXA11-AS. Therefore, proliferation, apoptosis, metastasis of melanoma cells may be modulated *via* regulation of *ITGA9*-related non-coding RNAs (46, 47). In the present study *ITGA9* was positively correlated with the invasion of several immune cells in SKCM TIME, but not tumor purity (**Figure 7**). Combined with our results and previous reports, we suggest that ITGA9 in SKCM may mediate cell-cell communication between cancer cells and their microenvironment by influencing the formation of integrin and receptor complexes, and ultimately effect SKCM metastasis and progression (**Figure 9C**) (48).

ITGA10 is a transmembrane glycoprotein involved in cell adhesion and integrin-mediated signaling pathways (49). ITGA10 is associated with various cancers development and metastasis, and variants in *ITGA10* are associated with changes of melanoma risks (50). In the present study, we found that ITGA10 expression was up-regulated in SKCM tissues (in comparison with control tissues), and this abnormal expression of ITGA10 may be the results of amplification mutations or the missense mutations (**Figure 9A**).

Previous studies have confirmed the correlation between ITGB1 expression and SKCM metastasis (51). In line with previous studies, we report aberrant ITGB1 expression in SKCM, and we reveal that ITGB1 expression is closely associated with SKCM metastasis by effecting cell migration (**Figure 2**) (52).

According to a bioanalysis conducted by Jun Zhu et al., ITGB2 was one of the top hub genes in malignant melanoma, and its expression was related to overall survival and disease-free survival (53). Combined with our results, we believe that ITGB2 is one of the integrin subunits most closely related to SKCM. ITGB2 plays a variety of roles in integrin complex, including extracellular matrix formation, Integrin complex formation, leukocyte migration, etc. Through the above functions, the highly expressed ITGB2 can effectively recruit T cells in SKCM TIME and reduce the purity of tumor cells in SKCM, so the overexpression of ITGB2 may effectively improve the effectiveness of immunotherapy against SKCM and improve the overall survival rate.

ITGB3 may play a vital role in the treatment of melanoma. Inhibition of ITGB3-SRC-STAT3 pathway activation can sensitize tumor-repopulating cells to the effects of IFN-α, and enhance the overall efficacy of melanoma treatment (54). In addition, the ADAR1-ITGB3 network may also play a central role in acquisition of an invasive phenotype in metastatic melanoma (55, 56). Transcription of ITGB3 gene induces the expression of NME1, a metastatic suppressor, in melanoma (57). According to our results, we hypothesized that the abnormal expression of ITGB3 in SKCM suggesting its value as a prognostic marker.

ITGB4 and ITGA6 are heterodimeric cambium adhesin receptors. ITGB4 has a long cytoplasmic domain and has unique cytoskeleton and signaling functions (58, 59). In addition, a mutation in ITGB4 has been identified in a metastasis sample taken from acral melanoma patients (60). The findings presented here are consistent with this previous research. In particular, ITGB4 expression was significantly increased in SKCM tissues compared with non-tumor tissues (**Figure 1**).

ITGB5, which is located between 13:133161078 and 13:139609422 in the SSC13Q41 region, encodes the integrin β5 subunit, and this coordinates with the αV subunit to produce the integrin αVβ5 (61). Reports concerning the role of ITGB5 in melanoma are scarce.

ITGB6 is extensively involved in wound healing and the pathogenesis of a variety of diseases, including fibrosis and cancer (62). Previous studies have identified abnormal expression of ITGB6 in SK-Mel-28 human melanoma cells (63). In line with previous findings, we demonstrate here that ITGB6 expression was positively associated with SKCM tumor stage (**Figure 3**).

There are only a few reports concerning ITGB7 expression in melanoma and its potential role. However, we found that ITGB7 was not only abnormally expressed in SKCM, but also correlated with the prognosis of SKCM. The expression of ITGB7 in SKCM TIME was positively correlated with immune cell infiltration and negatively correlated with tumor purity. integrin subunits target therapy such as etrolizumab may play a role in the treatment of SKCM by mediated the infiltration of immune cells, of course, this needs further trial verification.

As for ITGA7 and ITGB8, there have been few reports confirming their connection to SKCM, and we did not find

meaningful results in our study, we prefer to leave this question open.

Integrins form a heterodimer with α subunit and β subunit, and there is an intimate connection between integrin α subunits and β subunits (**Figure 9B**). Considering the biological functions of integrin subunits family and the results of our gene enrichment analysis (**Figures 9E, F**), we believe that integrin subunits family, which are mainly distributed in cell membrane and protein-containing complex, may affect protein-binding in SKCM by participating in biological processes such as cell communication, cellular component organization and response to stimulus and other biological processes. Further, these biological functions of the integrin family may also be inseparable from 48 genes (**Figure 9D**) that interact with them.

CONCLUSION

In conclusion, ITGA4, ITGB2 and ITGB7 was identified as novel biomarkers which may assist in the design of new immunotherapeutic drugs and server as diagnostic biomarkers. However, there are several limitations with our research. Firstly, *in vivo* and *in vitro* research should be conducted to verify our results. Secondly, this research was conducted mainly based on public databases. As we have not explained all the statistics and code information used in these databases in detail, this may cause some confusion in non-specialist readers.

DATA AVAILABILITY STATEMENT

The datasets presented in this study can be found in online repositories. The names of the repository/repositories and accession number(s) can be found in the article/supplementary material.

AUTHOR CONTRIBUTIONS

YN and WS carried out the experiment and wrote the manuscript with support from PM and KL, HX, and YZ helped supervise the project and conceived the original idea. All authors contributed to the article and approved the submitted version.

REFERENCES

1. Bertolotto C. Melanoma: From Melanocyte to Genetic Alterations and Clinical Options. *Scientifica* (2013) 2013:635203. doi: 10.1155/2013/635203
2. Valero MC, Huntsman HD, Liu J, Zou K, Boppart MD. Eccentric Exercise Facilitates Mesenchymal Stem Cell Appearance in Skeletal Muscle. *Plos one* (2012) 7:e29760. doi: 10.1371/journal.pone.0029760
3. Zhang H, Cui X, Cao A, Li X, Li L. ITGA3 Interacts With VASP to Regulate Stemness and Epithelial-Mesenchymal Transition of Breast Cancer Cells. *Gene* (2020) 734:144396. doi: 10.1016/j.gene.2020.144396
4. Brooks DL, Schwab LP, Krutilina R, Parke DN, Sethuraman A, Hoogewijs D, et al. ITGA6 Is Directly Regulated by Hypoxia-Inducible Factors and Enriches for Cancer Stem Cell Activity and Invasion in Metastatic Breast Cancer Models. *Mol Cancer* (2016) 15:26. doi: 10.1186/s12943-016-0510-x
5. Bhandari A, Xia E, Zhou Y, Guan Y, Xiang J, Kong L, et al. ITGA7 Functions as a Tumor Suppressor and Regulates Migration and Invasion in Breast Cancer. *Cancer Manag Res* (2018) 10:969–76. doi: 10.2147/cmar.S160379
6. Kobayashi T, Matsumoto S, Shimizu K, Miyake M, Maeda S, Hamaguchi Y, et al. Discrepancy in Responses to Dabrafenib Plus Trametinib Combination Therapy in Intracranial and Extracranial Metastases in Melanoma Patients. *J Dermatol* (2021) 48:e82–82e83. doi: 10.1111/1346-8138.15677
7. Rhodes DR, Yu J, Shanker K, Deshpande N, Varambally R, Ghosh D, et al. ONCOMINE: A Cancer Microarray Database and Integrated Data-Mining Platform. *Neoplasia* (2004) 6:1–6. doi: 10.1016/s1476-5586(04)80047-2
8. Chandrashekar DS, Bashel B, Balasubramanya SAH, Creighton CJ, Ponce-Rodriguez I, Chakravarthi B, et al. UALCAN: A Portal for Facilitating Tumor Subgroup Gene Expression and Survival Analyses. *Neoplasia* (2017) 19:649–58. doi: 10.1016/j.neo.2017.05.002
9. Zhou X, Peng M, He Y, Peng J, Zhang X, Wang C, et al. CXC Chemokines as Therapeutic Targets and Prognostic Biomarkers in Skin Cutaneous Melanoma Microenvironment. *Front Oncol* (2021) 11:619003. doi: 10.3389/fonc.2021.619003
10. Zhu Y, Qiu P, Ji Y. TCGA-Assembler: Open-Source Software for Retrieving and Processing TCGA Data. *Nat Methods* (2014) 11:599–600. doi: 10.1038/nmeth.2956
11. Tang Z, Kang B, Li C, Chen T, Zhang Z. GEPIA2: An Enhanced Web Server for Large-Scale Expression Profiling and Interactive Analysis. *Nucleic Acids Res* (2019) 47:W556–60. doi: 10.1093/nar/gkz430
12. Human genomics. The Genotype-Tissue Expression (GTEx) Pilot Analysis: Multitissue Gene Regulation in Humans. *Science* (2015) 348:648–60. doi: 10.1126/science.1262110
13. Weinstein JN, Collisson EA, Mills GB, Shaw KR, Ozenberger BA, Ellrott K, et al. The Cancer Genome Atlas Pan-Cancer Analysis Project. *Nat Genet* (2013) 45:1113–20. doi: 10.1038/ng.2764
14. Warde-Farley D, Donaldson SL, Comes O, Zuberi K, Badrawi R, Chao P, et al. The GeneMANIA Prediction Server: Biological Network Integration for Gene Prioritization and Predicting Gene Function. *Nucleic Acids Res* (2010) 38:W214–20. doi: 10.1093/nar/gkq537
15. Cerami E, Gao J, Dogrusoz U, Gross BE, Sumer SO, Aksoy BA, et al. The Cbio Cancer Genomics Portal: An Open Platform for Exploring Multidimensional Cancer Genomics Data. *Cancer Discov* (2012) 2:401–4. doi: 10.1158/2159-8290.Cd-12-0095
16. Li T, Fan J, Wang B, Traugh N, Chen Q, Liu JS, et al. TIMER: A Web Server for Comprehensive Analysis of Tumor-Infiltrating Immune Cells. *Cancer Res* (2017) 77(21):e108–10. doi: 10.1158/0008-5472.Can-17-0307
17. Li T, Fu J, Zeng Z, Cohen D, Li J, Chen Q, et al. TIMER2.0 for Analysis of Tumor-Infiltrating Immune Cells. *Nucleic Acids Res* (2020) 48:W509–509W514. doi: 10.1093/nar/gkaa407
18. Han H, Cho JW, Lee S, Yun A, Kim H, Bae D, et al. TRRUST V2: An Expanded Reference Database of Human and Mouse Transcriptional Regulatory Interactions. *Nucleic Acids Res* (2018) 46:D380–6. doi: 10.1093/nar/gkx1013
19. Zhang B, Kirov S, Snoddy J. WebGestalt: An Integrated System for Exploring Gene Sets in Various Biological Contexts. *Nucleic Acids Res* (2005) 33:W741–8. doi: 10.1093/nar/gki475
20. Wang J, Vasaikar S, Shi Z, Greer M, Zhang B. WebGestalt 2017: A More Comprehensive, Powerful, Flexible and Interactive Gene Set Enrichment Analysis Toolkit. *Nucleic Acids Res* (2017) 45:W130–7. doi: 10.1093/nar/gkx356
21. Riker AI, Enkemann SA, Fodstad O, Liu S, Ren S, Morris C, et al. The Gene Expression Profiles of Primary and Metastatic Melanoma Yields a Transition Point of Tumor Progression and Metastasis. *BMC Med Genomics* (2008) 1:13. doi: 10.1186/1755-8794-1-13
22. Haqq C, Nosrati M, Sudilovsky D, Crothers J, Khodabakhsh D, Pulliam BL, et al. The Gene Expression Signatures of Melanoma Progression. *Proc Natl Acad Sci USA* (2005) 102:6092–7. doi: 10.1073/pnas.0501564102

23. Talantov D, Mazumder A, Yu JX, Briggs T, Jiang Y, Backus J, et al. Novel Genes Associated With Malignant Melanoma But Not Benign Melanocytic Lesions. *Clin Cancer Res* (2005) 11:7234–42. doi: 10.1158/1078-0432.CCR-05-0683
24. Kobayashi T, Hamaguchi Y, Hasegawa M, Fujimoto M, Takehara K, Matsushita T. B Cells Promote Tumor Immunity Against B16F10 Melanoma. *Am J Pathol* (2014) 184:3120–9. doi: 10.1016/j.ajpath.2014.07.003
25. Palkina N, Komina A, Aksenenko M, Moshev A, Savchenko A, Ruksha T. miR-204-5p and miR-3065-5p Exert Antitumor Effects on Melanoma Cells. *Oncol Lett* (2018) 15:8269–80. doi: 10.3892/ol.2018.8443
26. Cioanca AV, Wu CS, Natoli R, Conway RM, McCluskey PJ, Jager MJ, et al. The Role of Melanocytes in the Human Choroidal Microenvironment and Inflammation: Insights From the Transcriptome. *Pigment Cell Melanoma Res* (2021). doi: 10.1111/pcmr.12972
27. Hynes RO. Integrins: Bidirectional, Allosteric Signaling Machines. *Cell* (2002) 110:673–87. doi: 10.1016/s0092-8674(02)00971-6
28. Pinon P, Wehrle-Haller B. Integrins: Versatile Receptors Controlling Melanocyte Adhesion, Migration and Proliferation. *Pigment Cell Melanoma Res* (2011) 24:282–94. doi: 10.1111/j.1755-148X.2010.00806.x
29. Xu T, Ma M, Chi Z, Si L, Sheng X, Cui C, et al. High G2 and S-Phase Expressed 1 Expression Promotes Acral Melanoma Progression and Correlates With Poor Clinical Prognosis. *Cancer Sci* (2018) 109:1787–98. doi: 10.1111/cas.13607
30. Schumacher D, Schaumburg-Lever G. Ultrastructural Localization of Alpha-3 Integrin Subunit in Malignant Melanoma and Adjacent Epidermis. *J Cutan Pathol* (1999) 26:321–6. doi: 10.1111/j.1600-0560.1999.tb01853.x
31. Rebhun RB, Cheng H, Gershenwald JE, Fan D, Fidler IJ, Langley RR. Constitutive Expression of the Alpha4 Integrin Correlates With Tumorigenicity and Lymph Node Metastasis of the B16 Murine Melanoma. *Neoplasia* (2010) 12:173–82. doi: 10.1593/neo.91604
32. Zhao J, Qi Q, Yang Y, Gu HY, Lu N, Liu W, et al. Inhibition of Alpha(4) Integrin Mediated Adhesion was Involved in the Reduction of B16-F10 Melanoma Cells Lung Colonization in C57BL/6 Mice Treated With Gambogic Acid. *Eur J Pharmacol* (2008) 589:127–31. doi: 10.1016/j.ejphar.2008.04.063
33. Geherin SA, Gómez D, Glabman RA, Ruthel G, Hamann A, Debes GF. IL-10+ Innate-Like B Cells Are Part of the Skin Immune System and Require α4β1 Integrin To Migrate Between the Peritoneum and Inflamed Skin. *J Immunol* (2016) 196:2514–25. doi: 10.4049/jimmunol.1403246
34. Kobayashi T, Oishi K, Okamura A, Maeda S, Komuro A, Hamaguchi Y, et al. Regulatory B1a Cells Suppress Melanoma Tumor Immunity *via* IL-10 Production and Inhibiting T Helper Type 1 Cytokine Production in Tumor-Infiltrating CD8(+) T Cells. *J Invest Dermatol* (2019) 139:1535–44.e1. doi: 10.1016/j.jid.2019.02.016
35. Feng C, Jin X, Han Y, Guo R, Zou J, Li Y, et al. Expression and Prognostic Analyses of ITGA3, ITGA5, and ITGA6 in Head and Neck Squamous Cell Carcinoma. *Med Sci Monit* (2020) 26:e926800. doi: 10.12659/msm.926800
36. Quirico L, Orso F, Esposito CL, Bertone S, Coppo R, Conti L, et al. Axl-148b Chimeric Aptamers Inhibit Breast Cancer and Melanoma Progression. *Int J Biol Sci* (2020) 16:1238–51. doi: 10.7150/ijbs.39768
37. Lenci RE, Rachakonda PS, Kubarenko AV, Weber AN, Brandt A, Gast A, et al. Integrin Genes and Susceptibility to Human Melanoma. *Mutagenesis* (2012) 27:367–73. doi: 10.1093/mutage/ger090
38. Karhemo PR, Ravela S, Laakso M, Ritamo I, Tatti O, Mäkinen S, et al. An Optimized Isolation of Biotinylated Cell Surface Proteins Reveals Novel Players in Cancer Metastasis. *J Proteomics* (2012) 77:87–100. doi: 10.1016/j.jprot.2012.07.009
39. Wu J, Cheng J, Zhang F, Luo X, Zhang Z, Chen S. Estrogen Receptor α Is Involved in the Regulation of ITGA8 Methylation in Estrogen Receptor-Positive Breast Cancer. *Ann Transl Med* (2020) 8:993. doi: 10.21037/atm-20-5220
40. Matsushima S, Aoshima Y, Akamatsu T, Enomoto Y, Meguro S, Kosugi I, et al. CD248 and Integrin Alpha-8 Are Candidate Markers for Differentiating Lung Fibroblast Subtypes. *BMC Pulm Med* (2020) 20:21. doi: 10.1186/s12890-020-1054-9
41. Talbot JC, Nichols JT, Yan YL, Leonard IF, BreMiller RA, Amacher SL, et al. Pharyngeal Morphogenesis Requires Fras1-Itga8-Dependent Epithelial-Mesenchymal Interaction. *Dev Biol* (2016) 416:136–48. doi: 10.1016/j.ydbio.2016.05.035
42. Scindia Y, Deshmukh U, Thimmalapura PR, Bagavant H. Anti-Alpha8 Integrin Immunoliposomes in Glomeruli of Lupus-Susceptible Mice: A Novel System for Delivery of Therapeutic Agents to the Renal Glomerulus in Systemic Lupus Erythematosus. *Arthritis Rheum* (2008) 58:3884–91. doi: 10.1002/art.24026
43. Yan K, Lu Y, Yan Z, Wang Y. 9-Gene Signature Correlated With CD8(+) T Cell Infiltration Activated by IFN-Gamma: A Biomarker of Immune Checkpoint Therapy Response in Melanoma. *Front Immunol* (2021) 12:622563. doi: 10.3389/fimmu.2021.622563
44. Zhang J, Na S, Liu C, Pan S, Cai J, Qiu J. MicroRNA-125b Suppresses the Epithelial-Mesenchymal Transition and Cell Invasion by Targeting ITGA9 in Melanoma. *Tumour Biol* (2016) 37:5941–9. doi: 10.1007/s13277-015-4409-8
45. Xu TJ, Qiu P, Zhang YB, Yu SY, Xu GM, Yang W. MiR-148a Inhibits the Proliferation and Migration of Glioblastoma by Targeting ITGA9. *Hum Cell* (2019) 32:548–56. doi: 10.1007/s13577-019-00279-9
46. Fan J, Kang X, Zhao L, Zheng Y, Yang J, Li D. Long Noncoding RNA CCAT1 Functions as a Competing Endogenous RNA to Upregulate ITGA9 by Sponging MiR-296-3p in Melanoma. *Cancer Manag Res* (2020) 12:4699–714. doi: 10.2147/cmar.S252635
47. Xu Y, Zhang J, Zhang Q, Xu H, Liu L. Long Non-Coding RNA HOXA11-AS Modulates Proliferation. Apoptosis Metastasis EMT Cutaneous Melanoma Cells Partly *via* miR-152-3p/ITGA9 Axis. *Cancer Manag Res* (2021) 13:925–39. doi: 10.2147/cmar.S281920
48. Peng Y, Wu D, Li F, Zhang P, Feng Y, He A. Identification of Key Biomarkers Associated With Cell Adhesion in Multiple Myeloma by Integrated Bioinformatics Analysis, Apoptosis, Metastasis and EMT in Cutaneous Melanoma Cells Partly *via* miR-152-3p/ITGA9 Axis. *Cancer Cell Int* (2020) 20:262. doi: 10.1186/s12935-020-01355-z
49. Hamaia SW, Luff D, Hunter EJ, Malcor JD, Bihan D, Gullberg D, et al. Unique Charge-Dependent Constraint on Collagen Recognition by Integrin Alpha10beta1. *Matrix Biol* (2017) 59:80–94. doi: 10.1016/j.matbio.2016.08.010
50. Lasić V, Kosović I, Jurić M, Racetin A, Čurčić J, Šolić I, et al. GREB1L, CRELD2 and ITGA10 Expression in the Human Developmental and Postnatal Kidneys: An Immunohistochemical Study. *Acta Histochem* (2021) 123:151679. doi: 10.1016/j.acthis.2021.151679
51. Menefee DS, McMasters A, Pan J, Li X, Xiao D, Waigel S, et al. Age-Related Transcriptome Changes in Melanoma Patients With Tumor-Positive Sentinel Lymph Nodes. *Aging (Albany NY)* (2020) 12:24914–39. doi: 10.18632/aging.202435
52. El-Hachem N, Habel N, Naiken T, Bzioueche H, Cheli Y, Beranger GE, et al. Uncovering and Deciphering the Pro-Invasive Role of HACE1 in Melanoma Cells. *Cell Death Differ* (2018) 25:2010–22. doi: 10.1038/s41418-018-0090-y
53. Zhu J, Hao S, Zhang X, Qiu J, Xuan Q, Ye L. Integrated Bioinformatics Analysis Exhibits Pivotal Exercise-Induced Genes and Corresponding Pathways in Malignant Melanoma. *Front Genet* (2020) 11:637320. doi: 10.3389/fgene.2020.637320
54. Li Y, Song Y, Li P, Li M, Wang H, Xu T, et al. Downregulation of RIG-I Mediated by ITGB3/c-SRC/STAT3 Signaling Confers Resistance to Interferon-α-Induced Apoptosis in Tumor-Repopulating Cells of Melanoma. (2020) 8:e000111. doi: 10.1136/jitc-2019-000111
55. Nemlich Y, Baruch EN, Besser MJ, Shoshan E, Bar-Eli M, Anafi L, et al. ADAR1-Mediated Regulation of Melanoma Invasion. *Nat Commun* (2018) 9:2154. doi: 10.1038/s41467-018-04600-2
56. Nemlich Y, Besser MJ, Schachter J, Markel G. ADAR1 Regulates Melanoma Cell Invasiveness by Controlling Beta3-Integrin *via* microRNA-30 Family Members. *Am J Cancer Res* (2020) 10:2677–86.
57. Leonard MK, Novak M, Snyder D, Snow G, Pamidimukkala N, McCorkle JR, et al. The Metastasis Suppressor NME1 Inhibits Melanoma Cell Motility *via* Direct Transcriptional Induction of the Integrin Beta-3 Gene. *Exp Cell Res* (2019) 374:85–93. doi: 10.1016/j.yexcr.2018.11.010
58. Sung JS, Kang CW, Kang S, Jang Y, Chae YC, Kim BG, et al. ITGB4-Mediated Metabolic Reprogramming of Cancer-Associated Fibroblasts. *Oncogene* (2020) 39:664–76. doi: 10.1038/s41388-019-1014-0
59. Li M, Jiang X, Wang G, Zhai C, Liu Y, Li H, et al. ITGB4 Is a Novel Prognostic Factor in Colon Cancer. *J Cancer* (2019) 10:5223–33. doi: 10.7150/jca.29269
60. Abramov IS, Emelyanova MA, Ryabaya OO, Krasnov GS, Zasedatelev AS, Nasedkina TV. Somatic Mutations Associated With Metastasis in Acral Melanoma. *Mol Biol (Mosk)* (2019) 53:648–53. doi: 10.1134/S0026898419040025

61. Zhang LY, Guo Q, Guan GF, Cheng W, Cheng P, Wu AH. Integrin Beta 5 Is a Prognostic Biomarker and Potential Therapeutic Target in Glioblastoma. *Front Oncol* (2019) 9:904. doi: 10.3389/fonc.2019.00904
62. Meecham A, Marshall JF. The ITGB6 Gene: Its Role in Experimental and Clinical Biology. *Gene* (2020) 5:100023. doi: 10.1016/j.gene.2019.100023
63. Klein A, Capitanio JS, Maria DA, Ruiz IR. Gene Expression in SK-Mel-28 Human Melanoma Cells Treated With the Snake Venom Jararhagin. *Toxicon* (2011) 57:1–8. doi: 10.1016/j.toxicon.2010.09.001

Conflict of Interest: The authors declare that the research was conducted in the absence of any commercial or financial relationships that could be construed as a potential conflict of interest.

Publisher's Note: All claims expressed in this article are solely those of the authors and do not necessarily represent those of their affiliated organizations, or those of the publisher, the editors and the reviewers. Any product that may be evaluated in this article, or claim that may be made by its manufacturer, is not guaranteed or endorsed by the publisher.

frontiers in Oncology

ORIGINAL RESEARCH
published: 29 November 2021
doi: 10.3389/fonc.2021.798385

Plasminogen Activating Inhibitor-1 Might Predict the Efficacy of Anti-PD1 Antibody in Advanced Melanoma Patients

Kentaro Ohuchi, Yumi Kambayashi, Takanori Hidaka and Taku Fujimura *

Department of Dermatology, Tohoku University Graduate School of Medicine, Sendai, Japan

Plasminogen activating inhibitor-1 (PAI-1) plays crucial roles in the development of various cancers, including melanomas. Indeed, various pro-tumorigenic functions of PAI-1 in cancer progression and metastasis have been widely reported. Among them, PAI-1 is also reported as a key regulator of PD-L1 expression on melanoma cells through endocytosis, leading to abrogating the efficacy of anti-PD1 antibodies (Abs). These findings suggested that PAI-1 expression might predict the efficacy of anti-PD1 Abs. In this report, the expression and production of PAI-1 in melanoma patients were evaluated, and the immunomodulatory effects of PAI-1 on tumor-associated macrophages were investigated *in vitro*. Immunohistochemical staining of PAI-1 showed that PAI-1 expression on melanoma cells was significantly decreased in responders compared to non-responders. Moreover, baseline serum levels of PAI-1 were significantly decreased in responders compared to non-responders. Notably, PAI-1 decreased the production of various chemokines from monocyte-derived M2 macrophages *in vitro*, suggesting that PAI-1 might decrease tumor-infiltrating lymphocytes to hamper the anti-tumor effects of anti-PD1 Abs. These results suggest that baseline serum levels of PAI-1 may be useful as a biomarker for identifying patients with advanced cutaneous melanoma most likely to benefit from anti-melanoma immunotherapy.

Keywords: melanoma, PAI-1, TAMs, Anti-PD1 Abs, efficacy

OPEN ACCESS

Edited by:
Motoki Nakamura,
Nagoya City University, Japan

Reviewed by:
Tetsuya Magara,
Nagoya City University, Japan
Tadahiro Kobayashi,
Kanazawa University, Japan

***Correspondence:**
Taku Fujimura
tfujimura1@mac.com

Specialty section:
This article was submitted to Skin Cancer, a section of the journal Frontiers in Oncology

Received: *20 October 2021*
Accepted: *05 November 2021*
Published: *29 November 2021*

Citation:
Ohuchi K, Kambayashi Y, Hidaka T and Fujimura T (2021) Plasminogen Activating Inhibitor-1 Might Predict the Efficacy of Anti-PD1 Antibody in Advanced Melanoma Patients. Front. Oncol. 11:798385. doi: 10.3389/fonc.2021.798385

INTRODUCTION

Plasminogen activating inhibitor-1 (PAI-1) is a serine protease that plays crucial roles in the development of various cancers, including melanomas (1–3). PAI-1 inhibits urokinase-type plasminogen activator and tissue type plasminogen activator, leading to attenuation of plasminogen activation and the development of thrombosis formation at tumor sites. PAI-1 increases the expression of focal adhesion kinase on tumor-associated macrophages (TAMs) to facilitate the migration of macrophages into tumor sites in a melanoma model (1). More recently, PAI-1 was found to facilitate PD-L1 endocytosis of melanoma cells to abrogate the efficacy of anti-PD-L1 antibodies

(Abs) in mouse melanoma models (2). In addition, PAI-1 was found to induce resistance to chemotherapy in mouse B16F10 melanoma (3). These reports suggested that PAI-1 could play a significant role in maintaining the immunosuppressive microenvironment in melanoma through TAMs. In this study, the expression and production of PAI-1 were evaluated in melanoma patients, and the immunomodulatory effects of PAI-1 on TAMs were investigated *in vitro*.

PATIENTS AND METHODS

Ethics Statement for Human Experiments

The protocol for this human study was approved by the ethics committee of Tohoku University Graduate School of Medicine, Sendai, Japan (permit no. 2020-1-759). All methods were performed in accordance with the relevant guidelines and regulations. All patients provided written, informed consent prior to enrolment in the study.

Patients

Patients were eligible if they had unresectable stage III melanoma or if they had stage IV melanoma with accessible cutaneous, subcutaneous, and/or nodal lesions (staging was performed according to the AJCC Staging Manual, 8th edition, 2018). All patients received 2 mg/kg of nivolumab every three weeks, 3 mg/kg of nivolumab every two weeks, 240 mg of nivolumab every two weeks, 480 mg of nivolumab every four weeks, or 200 mg of pembrolizumab every three weeks. Serum was obtained from patients before the administration of anti-PD1 Abs. The response to anti-PD1 Abs was assessed according to the Response Evaluation Criteria In Solid Tumors.

Tissue Samples and Immunohistochemical Staining

Polyclonal rabbit Abs for human PAI-1 (Abcam, Tokyo, Japan) were used for immunohistochemical (IHC) staining. Archival formalin-fixed paraffin-embedded skin specimens were collected at the initial visit from 30 advanced melanoma patients who were treated with anti-PD1 Abs in the Department of Dermatology at Tohoku University Graduate School of Medicine. The patients' characteristics are summarized in **Table 1**.

Quantitative and Semiquantitative Analyses of Immunohistochemical (IHC) Staining

For semiquantitative analysis of IHC staining, PAI-1 expression on tumor cells was examined in more than 3 random, representative fields from each section. The expression levels were determined independently by two dermatologists. The expression level of PAI-1 was determined as follows: - (negative: **Figure 1A**), 1+ (weakly positive: **Figure 1B**), and 2+ (intensely positive): **Figure 1C**.

To quantify the IHC staining of each sample, the positive cells were counted using a BZ-X800 (KEYENCE, Tokyo, Japan). The percentage of IHC-positive cells per all tumor-infiltrating cells or melanoma cells was automatically counted.

Serum PAI-1 Levels

The baseline serum PAI levels were evaluated in 49 patients with advanced melanoma. The serum PAI-1 levels were determined by an enzyme-linked immunosorbent assay (ELISA) according to the manufacturer's protocol (R&D Systems, Minneapolis, MN). Data from each donor were obtained as the mean of duplicate assays. The protocol for this human study was approved by the ethics committee of Tohoku University Graduate School of Medicine, Sendai, Japan (approval no. 2020-1-759).

Culturing of M2 Macrophages From Human Peripheral Blood Monocytes

CD14+ monocytes were isolated from the peripheral blood mononuclear cells of healthy donors using MACS beads (CD14 microbeads, Miltenyi Biotec Inc., Sunnyvale, CA) according to the manufacturer's protocol. The CD14+ monocytes (2×10^5 cells/ml) were cultured in complete medium containing 100 ng/ml of recombinant human macrophage colony-stimulating factor for 5 days, as previously reported (4). On the fifth day, monocyte-derived macrophages were treated with or without PAI-1 (0.1 μg/ml) (5) for 48 hours, and the culture supernatant was harvested. Each chemokine level was determined by an ELISA. This study was approved by the ethics committee of Tohoku University Graduate School of Medicine, Sendai, Japan (2019–1–925).

Statistical Methods

Pearson's correlation coefficient was used to investigate the correlation between the therapeutic effect and PAI-1 expression levels. Receiver operating characteristic (ROC) curves were used to calculate cut-off values for serum levels of PAI-1 and areas under the curve (AUCs). Cut-offs were determined using Youden's index (sensitivity + specificity -1) to determine the maximum index value. ROC curves were established to evaluate serum levels of PAI-1 in patients administered nivolumab. For a single comparison between two groups, the Mann-Whitney U-test was used. All statistical analyses were performed using JMP version 16.1 software (SAS Institute, Tokyo, Japan). The level of significance was set at $p<0.05$.

RESULTS

Demographic Data

Patients' demographic data of cohort 1 (IHC staining) and cohort 2 (serum PAI-1) are shown in **Tables 1**, **2**, respectively.

PAI-1 Expression on Melanoma Correlated With the Efficacies of Anti-PD1 Abs

Since PAI-1 is associated with a poor prognosis in various cancers, and since PAI-1 possesses immunomodulatory effects to polarize TAMs toward proinflammatory and immunosuppressive M2 phenotypes (6, 7), we hypothesized that PAI-1 expression correlates with the efficacies of anti-PD1 Abs for advanced

TABLE 1 | Characteristics and PAI-1 expression levels of 31 patients with advanced melanomas.

	Age (y)	Sex	Location	Clark's classification	Bastian's classification	Efficacy	PAI-1
1	81-90	F	cheek	NM	CSD	PR	2+
2	71-80	F	toe	ALM	Acral	CR	2+
3	71-80	M	shoulder	NM	non-CSD	PD	–
4	71-80	M	heel	ALM	Acral	PD	–
5	81-90	F	toe	ALM	Acral	PR	2+
6	81-90	M	sole	ALM	Acral	PD	–
7	51-60	M	back	NM	non-CSD	PD	1+
8	71-80	M	toe	ALM	Acral	PD	–
9	81-90	F	sole	ALM	Acral	PD	2+
10	71-80	F	femor	SSM	non-CSD	PD	–
11	71-80	F	toe	ALM	Acral	PD	2+
12	81-90	F	back	SSM	non-CSD	PD	–
13	61-70	M	toe	ALM	Acral	PR	2+
14	71-80	M	sole	ALM	Acral	PR	2+
15	91-100	M	sole	ALM	Acral	PD	2+
16	81-90	M	lower leg	NM	non-CSD	SD	2+
17	51-60	F	lip	LMM	CSD	PD	–
18	31-40	M	cervical	NM	CSD	PD	2+
19	31-40	F	lower leg	SSM	non-CSD	PR	1+
20	31-40	M	lower leg	NM	non-CSD	PD	–
21	71-80	F	sole	ALM	Acral	PD	2+
22	61-70	F	head	NM	CSD	CR	2+
23	61-70	M	back	NM	non-CSD	PR	2+
24	71-80	M	ear	NM	CSD	PD	–
25	71-80	F	toe	ALM	Acral	PR	2+
26	41-50	M	head	NM	CSD	PD	1+
27	71-80	F	heel	ALM	Acral	PD	–
28	61-70	M	sole	ALM	Acral	PR	1+
29	61-70	F	back	NM	non-CSD	PR	2+
30	31-40	M	cheek	NM	CSD	PD	–
31	41-50	M	lower leg	NM	non-CSD	PD	–

ALM, acral lentiginous melanoma; NM, nodular melanoma; SSM, superficial spreading melanoma; LMM, lentigo maligna melanoma; CSD, cumulative sun damage.

melanoma patients. To test this hypothesis, IHC staining for PAI-1 and semiquantitative analysis of IHC staining of PAI-1 were used. The expression levels of PAI-1 and the best response to anti-PD1 Abs in each patient in cohort 1 are presented in **Table 1**. Pearson's correlation coefficient showed a significant correlation between the PAI-1 expression level on tumor cells and the best response to anti-PD1 Abs (p=0.0029) (**Figure 1**).

PD-L1 Expression on Melanoma Correlated With the PAI-1 Expression

As previous report suggested, PAI-1 facilitates PD-L1 endocytosis of melanoma cells to abrogate the efficacy of anti-PD-L1Abs (2), next we evaluated the PD-L1 expression on melanoma cells in each patient in cohort 1. IHC staining for PD-L1 was performed, and the percentage of PD-L1+ cells per all melanoma cells was automatically counted and quantitatively analyzed by BZ-X800. Percentage of PD-L1 expression on melanoma cells was significantly higher in the low PAI-1 expression group (**Figure 1E**) compared to that of the high PAI-1 expression group (**Figure 1F**) (p=0.0168) (**Figure 1**).

Serum PAI-1 Levels in Melanoma Patients Treated With Anti-PD1 Abs

Next, to determine whether baseline serum levels of PAI-1 might be associated with early response in melanoma patients treated with anti-PD1 Abs, PAI-1 levels were evaluated in 49 patients (cohort 2) with advanced melanoma treated with anti-PD1 Abs. The baseline serum levels of PAI-1 and the best response to anti-PD1 Abs in each patient in cohort 2 are presented in **Table 2**. The threshold value of PAI-1 at baseline to distinguish responders from non-responders was 2.860 ng/ml. The sensitivity and specificity of the baseline serum PAI-1 in advanced melanoma were 71.4% and 76.5%, respectively (p=0.0016; **Figure 2**). High baseline serum levels of PAI-1 were significantly correlated with resistance to nivolumab in patients with advanced melanoma (p=0.0020) (**Figure 2**).

CD163+ Tumor-Associated Macrophages (TAMs) and the Efficacies of Anti-PD1 Abs in Melanoma

Since PAI-1 polarized TAMs toward proinflammatory and M2 phenotypes (6), the correlation between the ratio of TAMs among tumor-infiltrating lymphocytes (TILs) and the efficacies of anti-PD1 Abs were evaluated in melanoma patients. IHC staining for CD163, which is a commonly used marker for M2 macrophages (8), was performed, and the percentage of CD163+ TAMs in melanoma was quantitatively analyzed (**Supplementary Figure 1**). There was no significant correlation between the ratio of CD163+ macrophages among tumour-infiltrating cells and the efficacy of anti-PD1 Abs for melanoma (p=0.4288).

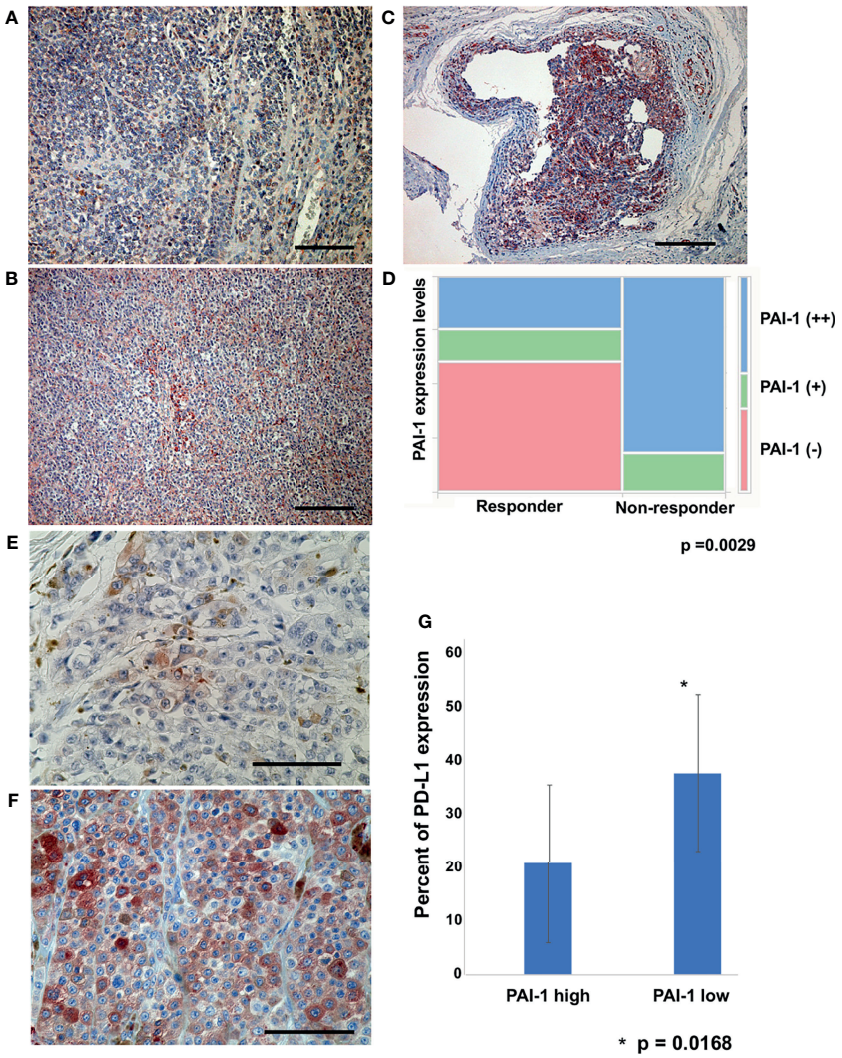

FIGURE 1 | PAI-1-expressing cells in melanoma patients. Representative paraffin-embedded tissue samples from lesional skin of patients with melanoma. Sections were deparaffinized and stained with anti-PAI-1, then developed with liquid permanent red. PAI-1 negative (-) **(A)**, weakly positive (+) **(B)**, and intensely positive (++) **(C)**. Scale bar, 100 μm. Pearson's correlation coefficient was used to investigate the correlation between therapeutic effect and PAI-1 expression level **(D)**. Sections of melanoma from an anti-PD1 Abs in a high PAI-1 expression patient **(E)** and a low PAI-1 expression patient **(F)** were deparaffinized and stained using anti-PD-L1 antibodies. Sections were developed with liquid permanent red. The percentages of PD-L1+ cells per all melanoma cells were automatically counted by BZ-X800 **(G)**. Scale bar, 100 μm.

Immunomodulatory Effects of PAI-1 on CD163+ Macrophages *In Vitro*

Since the ratio of CD163+ TAMs was not different between the responder group and the non-responder group, to further examine the immunomodulatory roles of PAI-1 on TAMs in the tumor microenvironment, CD163+ M2 macrophages were generated from CD14+ monocytes and stimulated by recombinant PAI-1 *in vitro* (4). PAI-1 decreased the production of CXCL10 and CCL22 (**Figure 3**), suggesting that PAI-1 might decrease the TILs in melanoma. In contrast, PAI-1 increased the production of CXCL5, suggesting that PAI-1 might increase the tumor infiltrating CXCR2+ myeloid-derived suppressor cells (MDSCs) and tumor-associated neutrophils (TANs) (**Figure 3**), both of which are known to be immunosuppressive cells [12]. There was no significant difference of the production of CCL20, suggesting that PAI-1 might not effect on the production of CCL20 from TAMs (**Figure 3**).

TILs Were Decreased in PAI-1 Highly Expressing Melanoma

To further confirm immunomodulatory effects of PAI-1 on TAMs in melanoma patients, we employed IHC staining for CD8 in each patient in cohort 1. The percentage of CD8+ cells per all tumor-infiltrating leukocytes was automatically counted and quantitatively analyzed by BZ-X800. The absolute number of CD8+ cells per mm^2 was automatically counted by BZ-X800.

TABLE 2 | Characteristics and serum levels of PAI-1 in 49 patients with advanced melanomas.

	Age (y)	Sex	Location	Clark's classification	Bastian's classification	Efficacy	Serum PAI-1 (pg/ml)
1	81-90	F	cheek	NM	CSD	PD	2.506
2	61-70	M	sole	ALM	Acral	PR	6.285
3	81-90	F	toe	ALM	Acral	PD	4.892
4	71-80	M	lower leg	SSM	non-CSD	SD	3.159
5	81-90	M	head	NM	CSD	PR	2.178
6	51-60	F	upper lip	NM	CSD	PD	2.534
7	31-40	F	lower leg	SSM	non-CSD	SD	6.372
8	71-80	M	groin	NM	non-CSD	PR	2.86
9	71-80	F	vulva	mucosal	mucosal	PD	3.101
10	31-40	M	cheek	LMM	CSD	PD	8.999
11	71-80	F	sole	ALM	Acral	PD	5.034
12	51-60	F	chest	NM	non-CSD	PD	3.781
13	61-70	M	auricle	SSM	CSD	PD	3.288
14	41-50	M	lower leg	SSM	non-CSD	PD	6.657
15	31-40	M	lower leg	NM	non-CSD	PD	2.676
16	71-80	F	toe	ALM	Acral	PR	0.1261
17	59-60	M	femur	NM	non-CSD	PR	2.395
18	41-50	M	sole	ALM	Acral	PD	1.041
19	71-80	F	lower leg	SSM	non-CSD	PR	3.825
20	81-90	M	sole	ALM	Acral	PR	2.486
21	81-90	F	vagina	mucosal	mucosal	PD	2.887
22	61-70	F	back	SSM	non-CSD	PR	2.142
23	41-50	F	vulva	mucosal	mucosal	PR	1.546
24	51-60	F	vagina	mucosal	mucosal	PD	7.166
25	71-80	F	sole	ALM	Acral	PD	3.812
26	71-80	M	sole	ALM	Acral	PR	5.854
27	61-70	F	upper arm	SSM	non-CSD	SD	4.015
28	71-80	M	sole	ALM	Acral	PD	4.402
29	51-60	F	anus	mucosal	mucosal	PD	2.957
30	61-70	M	back	NM	non-CSD	PD	4.647
31	81-90	F	cheek	LMM	CSD	PD	2.8
32	81-90	M	nasal cavity	mucosal	mucosal	PR	2.332
33	41-50	M	cheek	LMM	CSD	PD	3.586
34	71-80	M	sole	ALM	Acral	PD	2.715
35	71-80	M	sole	ALM	Acral	PD	7.636
36	71-80	F	toe	ALM	Acral	PR	3.124
37	61-70	M	penis	NM	non-CSD	PD	4.981
38	81-90	M	sole	ALM	Acral	PD	2.598
39	61-70	M	sole	ALM	Acral	PD	8.59
40	71-80	M	sole	ALM	Acral	PD	5.313
41	41-50	F	sole	ALM	Acral	PD	3.706
42	61-70	F	femur	SSM	non-CSD	SD	5.647
43	41-50	M	shoulder	NM	non-CSD	SD	14.77
44	81-90	F	lower leg	SSM	non-CSD	PR	1.207
45	71-80	M	abdomen	SSM	non-CSD	PD	2.222
46	31-40	F	back	NM	non-CSD	PD	3.938
47	81-90	M	eyelid	NM	CSD	PR	1.539
48	41-50	M	abdomen	SSM	non-CSD	PD	13.97
49	61-70	M	palm	ALM	Acral	PD	2.628

The absolute number of CD8+ cells per mm^2 was significantly increased in a low PAI-1 expression group than that of a high PAI-1 expression group (**Figure 4**).

DISCUSSION

Plasminogen activator inhibitor-1 (PAI-1) is highly expressed in various types of tumors including melanoma (9), and various pro-tumorigenic functions of PAI-1 in cancer progression and metastasis have been widely reported (9). Among them, tumor-associated inflammation is one of the key pro-tumorigenic functions of PAI-1 (10). Indeed, PAI-1 stimulates the recruitment of fibrosis-inducing cells and macrophages. For example, tumor-derived PAI-1 promotes the migration of monocytes and polarizes tumor-associated macrophages (TAMs) towards proinflammatory phenotypes (7), leading to the production of proinflammatory and angiogenesis-promoting factors such as IL-1, IL-8, CCL2, CCL3, CCL5, and VEGF (11). *Via* an autocrine loop, IL-6 activates signal transduction and activator of transcription (STAT) 3 in monocytes, leading to an increase in the expression of arginase, IL-10, and CD163. Moreover, the expression of these M2-associated markers increases in parallel with immune checkpoints such as B7-

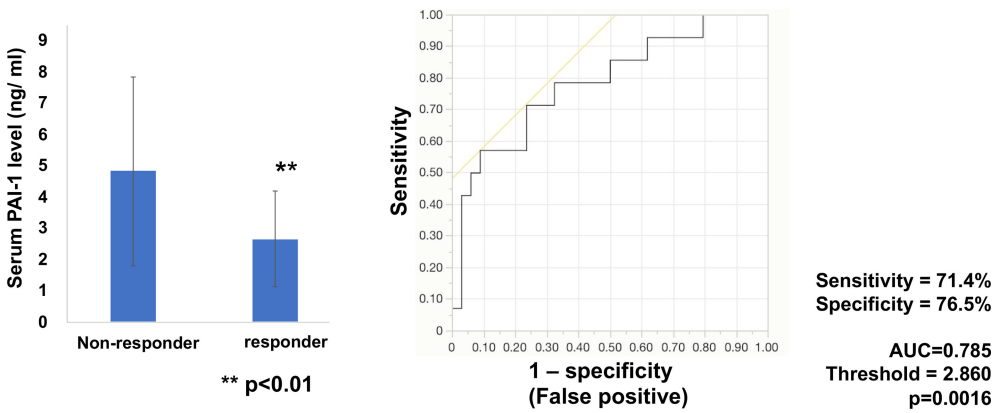

FIGURE 2 | Serum levels of PAI-1 and the ROC curve in melanoma. Mean serum levels of PAI-1 in non-responders (n=34) and responders (n=14) at day 0. The ROC curve was used to calculate cut-offs for PAI-1 serum levels and the AUC. Cut-offs were determined to distinguish responders from non-responders using Youden's index.

homolog superfamily, including B7-H1 (PD-L1) (8). These reports suggested that PAI-1 promotes pro-tumorigenic, immunosuppressive functions through TAMs.

TAMs play various immunosuppressive roles in melanoma (8). For example, TAMs express immune checkpoint modulators that directly suppress activated T cells (12). In addition, TAMs produce various chemokines that attract other immunosuppressive cells such as Tregs and precursors of TAMs to maintain the immunosuppressive tumor microenvironment (8, 13, 14). Notably, TAM-related chemokines, such as CXCL5, CXCL10, and CCL22, as well as a TAM-activation marker, soluble (s)CD163, could be predictive markers for efficacy and immune-related adverse events (irAEs) in anti-PD1 Abs-treated advanced melanoma patients (15–17). In aggregate, TAMs and TAM-related factors could be important biomarkers to predict the efficacies of anti-PD1 Abs in advanced melanoma patients.

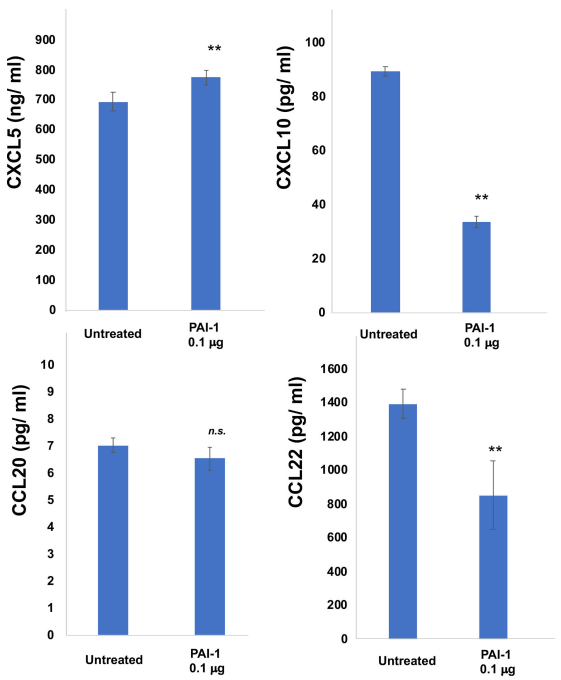

FIGURE 3 | Production of CXCL5, CXCL10, CCL20, and CCL22 by M2 macrophages treated with PAI-1. Culture supernatant from M2 macrophages was harvested as described in Materials and Methods and measured by ELISA (n=3). Data from each donor were obtained from triplicate assays, and mean ± SD values were calculated. Representative data from at least three independent experiments are shown. $^{**}p < 0.01$, Mann-Whitney U-test; *n.s.*, not significant.

From the above findings, we hypothesized that PAI-1 expression on melanoma cells is correlated with the efficacy of anti-PD1 Abs for unresectable melanoma patients. Indeed, the present data suggested that both the expression levels of PAI-1 on melanoma cells and serum PAI-1 levels were significantly correlated with the efficacy of anti-PD1 Abs in advanced melanoma patients. Since the efficacy of anti-PD1 Abs correlates with the number of TILs at the tumor site in various cancers (5), the decreased chemokine production from TAMs might abrogate the anti-tumor immune response against melanoma. In addition, PAI-1 also increased CXCL5 production, suggesting that PAI-1 might increase the immunosuppressive CXCR2+ MDSCs and TANs. Moreover, as a previous report suggested, PAI-1 decreases PD-L1 expression on melanoma cells to abrogate the efficacy of anti-PD-L1 Abs in mouse melanoma models, suggesting another mechanism of inducing tolerance to anti-PD1 Abs (2). Indeed, The PD-L1 expression in a low PAI-1 expression group is significantly higher than that in a high PAI-1 expression group. Furthermore, the number of CD8+ cells in a low PAI-1 expression group was significantly increased than that in a high PAI-1 expression group. In aggregate, PAI-1 induces resistance to anti-PD1 Abs in melanoma, and co-administration of PAI-1 inhibitors might improve the anti-melanoma effects of anti-PD1 Abs. To prove

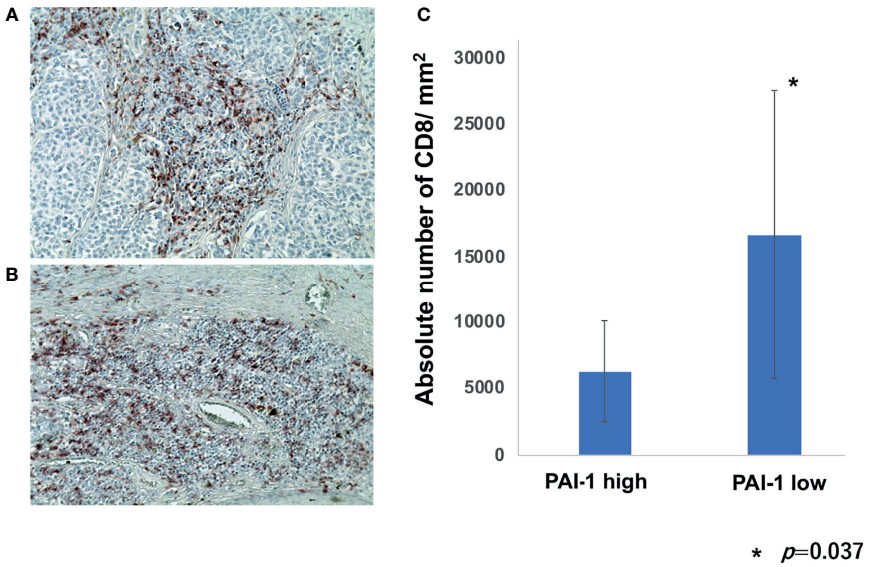

FIGURE 4 | Percentage of CD8+ cells per TILs in melanoma patients. Sections of melanoma from an anti-PD1 Abs in a high PAI-1 expression patient **(A)** and a low PAI-1 expression patient **(B)** were deparaffinized and stained using anti-CD8 antibodies. Sections were developed with liquid permanent red. The percentages of CD8+ cells per TILs were automatically counted by BZ-X800 **(C)**.

this hypothesis, from September 2021, we have started a phase II study investigating the safety and efficacy of TM5614, a novel PAI-1 inhibitor with better oral bioavailability that selectively inhibits PAI-1 activity (18), in combination with nivolumab in the treatment of unresectable malignant melanoma (jRCT2021210029).

DATA AVAILABILITY STATEMENT

The original contributions presented in the study are included in the article/**Supplementary Material**. Further inquiries can be directed to the corresponding author.

ETHICS STATEMENT

The protocol was approved by the institutional review board of Tohoku University Hospital. This study was approved by the ethics committee of Tohoku University Graduate School of Medicine, Sendai, Japan (2020-1-759). The patients/participants provided their written informed consent to participate in this study.

AUTHOR CONTRIBUTIONS

TH and TF designed the research study. KO and TF collected and analyzed the data. KO, YK, and TF treated the patients and collected the clinical data and samples. TF wrote the manuscript. TF supervised the study. All authors contributed to the article and approved the submitted version.

FUNDING

This study was supported in part by the Japan Agency for Medical Research and Development (21ym0126041h0001).

SUPPLEMENTARY MATERIAL

The Supplementary Material for this article can be found online at: https://www.frontiersin.org/articles/10.3389/fonc.2021.798385/full#supplementary-material

Supplementary Figure 1 | Sections of melanoma from an anti-PD1 Abs non-responding patient **(A)** and a responding patient **(B)** were deparaffinized and stained using anti-PAI-1 antibodies. Sections were developed with liquid permanent red. The percentages of IHC-positive cells per all tumor-infiltrating cells were automatically counted by BZ-X800 **(C)**. Scale bar, 100 μm.

REFERENCES

1. Thapa B, Koo BH, Kim YH, Kwon HJ, Kim DS. Plasminogen Activator Inhibitor-1 Regulates Infiltration of Macrophages Into Melanoma *via* Phosphorylation of FAK-Tyr925. *Biochem Biophys Res Commun* (2014) 450 (4):1696–701. doi: 10.1016/j.bbrc.2014.07.070
2. Tseng YJ, Lee CH, Chen WY, Yang JL, Tzeng HT. Inhibition of PAI-1 Blocks PD-L1 Endocytosis and Improves the Response of Melanoma Cells to Immune Checkpoint Blockade. *J Invest Dermatol* (2021) 141(11):2690–98. doi: 10.1016/j.jid.2021.03.030
3. Tzeng HT, Yang JL, Tseng YJ, Lee CH, Chen WJ, Chyuan IT. Plasminogen Activator Inhibitor-1 Secretion by Autophagy Contributes to Melanoma

Resistance to Chemotherapy Through Tumor Microenvironment Modulation. *Cancers (Basel)* (2021) 13(6):1253. doi: 10.3390/cancers13061253
4. Fujimura T, Kambayashi Y, Furudate S, Asano M, Kakizaki A, Aiba S. Receptor Activator of Nuclear Factor Kappa-B Ligand (RANKL) Promotes the Production of CCL17 From RANK+ M2 Macrophages. *J Invest Dermatol* (2015) 135(11):2884–7. doi: 10.1038/jid.2015.209
5. Taube JM, Klein A, Brahmer JR, Xu H, Pan X, Kim JH, et al. Association of PD-1, PD-1 Ligands, and Other Features of the Tumor Immune Microenvironment With Response to Anti-PD-1 Therapy. *Clin Cancer Res* (2014) 20(19):5064–74. doi: 10.1158/1078-0432
6. Chen S, Morine Y, Tokuda K, Yamada S, Saito Y, Nishi M, et al. Cancer-Associated Fibroblast-Induced M2-Polarized Macrophages Promote Hepatocellular Carcinoma Progression *via* the Plasminogen Activator Inhibitor-1 Pathway. *Int J Oncol* (2021) 59(2):59. doi: 10.3892/ijo.2021.5239
7. Kubala MH, Punj V, Placencio-Hickok VR, Fang H, Fernandez GE, Sposto R, et al. Plasminogen Activator Inhibitor-1 Promotes the Recruitment and Polarization of Macrophages in Cancer. *Cell Rep* (2018) 25(8):2177–2191.e7. doi: 10.1007/s10555-019-09806-4
8. Fujimura T, Kambayashi Y, Fujisawa Y, Hidaka T, Aiba S. Tumor-Associated Macrophages: Therapeutic Targets for Skin Cancer. *Front Oncol* (2018) 8:3. doi: 10.3389/fonc.2018.00003
9. Li S, Wei X, He J, Tian X, Yuan S, Sun L. Plasminogen Activator Inhibitor-1 in Cancer Research. *BioMed Pharmacother* (2018) 105:83–94. doi: 10.1016/j.biopha.2018.05.119
10. Kubala MH, DeClerck YA. The Plasminogen Activator Inhibitor-1 Paradox in Cancer: A Mechanistic Understanding. *Cancer Metastasis Rev* (2019) 38(3):483–92. doi: 10.1007/s10555-019-09806-4
11. Johnson DE, O'Keefe RA, Grandis JR. Targeting the IL-6/JAK/STAT3 Signalling Axis in Cancer. *Nat Rev Clin Oncol* (2018) 15(4):234–48. doi: 10.1038/nrclinonc.2018.8
12. Fujimura T, Ring S, Umansky V, Mahnke K, Enk AH. Regulatory T Cells Stimulate B7-H1 Expression in Myeloid-Derived Suppressor Cells in Ret Melanomas. *J Invest Dermatol* (2012) 132(4):1239–46. doi: 10.1038/jid.2011.416
13. Noy R, Pollard JW. Tumor-Associated Macrophages: From Mechanisms to Therapy. *Immunity* (2014) 41(1):49–61. doi: 10.1016/j.immuni.2014.06.010
14. Fujimura T, Aiba S. Significance of Immunosuppressive Cells as a Target for Immunotherapies in Melanoma and Non-Melanoma Skin Cancers. *Biomolecules* (2020) 10:E1087. doi: 10.3390/biom10081087
15. Fujimura T, Sato Y, Tanita K, Lyu C, Kambayash Y, Amagai R, et al. Association of Baseline Serum Levels of CXCL5 With the Efficacy of Nivolumab in Advanced Melanoma. *Front Med (Lausanne)* (2019) 6:86. doi: 10.3389/fmed.2019.00086
16. Fujimura T, Sato Y, Tanita K, Kambayashi Y, Otsuka A, Fujisawa Y, et al. Serum Soluble CD163 and CXCL5 Could be Predictive Markers for Immune Related Adverse Event in Patients With Advanced Melanoma Treated With Nivolumab. *Oncotarget* (2018) 9(21):15542–51. doi: 10.18632/oncotarget.24509
17. Fujimura T, Sato Y, Tanita K, Kambayash Y, Otsuka A, Fujisawa Y, et al. Serum Level of Soluble CD163 may be a Predictive Marker of the Effectiveness of Nivolumab in Patients With Advanced Cutaneous Melanoma. *Front Oncol* (2018) 8:530. doi: 10.3389/fonc.2018.00530
18. Yahata T, Ibrahim AA, Hirano KI, Muguruma Y, Naka K, Hozumi K, et al. Targeting of Plasminogen Activator Inhibitor-1 Activity Promotes Elimination of Chronic Myeloid Leukemia Stem Cells. *Haematologica* (2021) 106(2):483–94. doi: 10.3324/haematol.2019.230227

Conflict of Interest: The authors declare that the research was conducted in the absence of any commercial or financial relationships that could be construed as a potential conflict of interest.

Publisher's Note: All claims expressed in this article are solely those of the authors and do not necessarily represent those of their affiliated organizations, or those of the publisher, the editors and the reviewers. Any product that may be evaluated in this article, or claim that may be made by its manufacturer, is not guaranteed or endorsed by the publisher.

frontiers in Oncology

REVIEW
published: 07 January 2022
doi: 10.3389/fonc.2021.813132

Wounding Therapies for Prevention of Photocarcinogenesis

*Timothy C. Frommeyer[1], Craig A. Rohan[1,2,3], Dan F. Spandau[4,5], Michael G. Kemp[1,3], Molly A. Wanner[6], Elizabeth Tanzi[7] and Jeffrey B. Travers[1,2,3]**

[1] Department of Pharmacology & Toxicology, Boonshoft School of Medicine at Wright State University, Dayton, OH, United States, [2] Department of Dermatology, Boonshoft School of Medicine at Wright State University, Dayton, OH, United States, [3] Dayton Veterans Administration Medical Center, Dayton, OH, United States, [4] Departments of Dermatology and Biochemistry and Molecular Biology, Indiana University School of Medicine, Indianapolis, IN, United States, [5] Richard A. Roudebush Veterans Administration (VA) Medical Center, Indianapolis, IN, United States, [6] Department of Dermatology, Massachusetts General Hospital, Boston, MA, United States, [7] Capital Laser & Skin Care, Chevy Chase, MD, United States

The occurrence of non-melanoma skin cancer (NMSC) is closely linked with advanced age and ultraviolet-B (UVB) exposure. More specifically, the development of NMSC is linked to diminished insulin-like growth factor-1 (IGF-1) signaling from senescent dermal fibroblasts in geriatric skin. Consequently, keratinocyte IGF-1 receptor (IGF-1R) remains inactive, resulting in failure to induce appropriate protective responses including DNA repair and cell cycle checkpoint signaling. This allows UVB-induced DNA damage to proliferate unchecked, which increases the likelihood of malignant transformation. NMSC is estimated to occur in 3.3 million individuals annually. The rising incidence results in increased morbidity and significant healthcare costs, which necessitate identification of effective treatment modalities. In this review, we highlight the pathogenesis of NMSC and discuss the potential of novel preventative therapies. In particular, wounding therapies such as dermabrasion, microneedling, chemical peeling, and fractionated laser resurfacing have been shown to restore IGF-1/IGF-1R signaling in geriatric skin and suppress the propagation of UVB-damaged keratinocytes. This wounding response effectively rejuvenates geriatric skin and decreases the incidence of age-associated NMSC.

Keywords: non-melanoma skin cancer (NMSC), squamous cell carcinoma, ultraviolet light (UVB), insulin-like growth factor-1 (IGF- I), actinic keratosis (AK), laser resurfacing, chemical peel

OPEN ACCESS

Edited by:
Nabiha Yusuf, University of Alabama at Birmingham, United States

Reviewed by:
Georg Wondrak, University of Arizona, United States
Brian C. Capell, University of Pennsylvania, United States

***Correspondence:**
Jeffrey B. Travers
jeffrey.travers@wright.edu

Specialty section:
This article was submitted to Skin Cancer, a section of the journal Frontiers in Oncology

Received: *11 November 2021*
Accepted: *14 December 2021*
Published: *07 January 2022*

Citation:
Frommeyer TC, Rohan CA, Spandau DF, Kemp MG, Wanner MA, Tanzi E and Travers JB (2022) Wounding Therapies for Prevention of Photocarcinogenesis. Front. Oncol. 11:813132. doi: 10.3389/fonc.2021.813132

INTRODUCTION

Skin is the largest and most-exposed organ of the body. It functions as a barrier against environmental pressures, such as ultraviolet (UV) radiation (1). Prolonged and extensive exposure may result in major transformations in skin structure and function, leading to the development of cutaneous pathology (2–4). The American Cancer Society reports that skin cancer is the most commonly diagnosed cancer in the United States (5, 6). Comprised primarily of basal cell

Abbreviations: NMSC, Non-melanoma skin cancer; SCC, squamous cell carcinoma; BCC, basal cell carcinoma; AK, actinic keratosis; IGF-1, insulin-like growth factor-1; IGF-1R, insulin-like growth factor-1 receptor; FLR, fractionated laser resurfacing; UV, ultraviolet; NER, nucleotide excision repair; TLS, translesion synthesis.

carcinoma (BCC) and squamous cell carcinoma (SCC), the exact rates of non-melanoma skin cancer (NMSC) are unknown because most cancer registries do not collect their incidence and mortality data (5). However, it is estimated that 3.3 million are diagnosed each year, resulting in increased healthcare costs for disease management as well as significant morbidity, and rarely, mortality (5, 7). This necessitates exhaustive translational research for innovative treatments and preventative dermo-oncological therapies (8).

The epidemiological link between NMSC, sunlight, and advanced age is well-established, given that at least one in five Americans will develop skin cancer by the age of 70 (9). Moreover, over 80% of individuals with NMSC are older than 60 years of age (10). For some time, the direct causal link between the three observations was unknown, which spurred basic science exploration into photocarcinogenesis. Recent novel findings from our group has implicated the significance of the insulin-like growth factor-1/insulin-like growth factor-1 receptor (IGF-1/IGF-1R) pathway in the development of NMSC (11–13). It has been found that the intensity of UVB exposure directly correlates with the extent of DNA damage. Additionally the regulation between IGF-1/IGF-1R is vital in the protective response and indicative of the tendency for photocarcinogenesis (12, 14–18). Adequate IGF-1 production in dermal fibroblasts is necessary for the appropriate epidermal keratinocyte response to UVB-damaged DNA (11, 12, 19). Geriatric skin exhibits suppressed IGF-1 signaling due to an increased cellular senescence profile of fibroblasts (11, 12, 19). This has severe consequences in the protective response to UVB radiation whereby keratinocytes may have different destinies depending on the extent of DNA damage and state of IGF-1/IGF-1R signaling (11, 12, 19). Activation of keratinocyte IGF-1R induces favorable stress-induced cellular senescence or DNA damage repair such that malignancy prone mutations are arrested without compromising epidermal barrier function (11, 12, 19). However, if IGF-1R is inactive due to diminished IGF-1, keratinocytes may continue to propagate its procarcinogenic DNA damage to its daughter cells (11, 12, 19). This increases the likelihood for development of NMSC (20).

The IGF-1/IGF-1R signaling pathway may be exploited for therapy. In recent years, novel treatments aimed for geriatric patients both predisposed and exposed to NMSC have been developed. One such modality is wounding therapy, which attempts to reverse the geriatric fibroblast senescence phenotype by inducing a "wounding response" (19–23). This effectively serves to rejuvenate geriatric skin to a more youthful phenotypic and constitutive expression. In this review, the therapies of dermabrasion, microneedling, chemical peeling, and fractionated laser resurfacing will be discussed in the context of prevention of photocarcinogenesis.

BACKGROUND OF NON-MELANOMA SKIN CANCER

It is estimated that more people are diagnosed with skin cancer than all other types of cancer combined (5). In addition, between 1976-1984 and 2000-2010, epidemiologic research reveals an increasing overall incidence of 145% and 263% for BCC and SCC, respectively (24). Consequently, skin cancer is a major public health concern as the associative healthcare costs are extensive and rising (25). The increasing prevalence and economic burden underscore the need to understand the risks factors and etiology of NMSC.

As with other neoplastic pathologies, NMSC is of multifactorial origin. The exact mechanism of development is not well defined, but is likely due to the interplay of environmental, genetic, and phenotypical factors (26). NMSC is characterized by multiple risk factors that are both endogenous and exogenous in nature. The endogenous risk factors include patients with light-colored skin and blue eyes, Fitzpatrick Skin Phototypes I-III, presence of dysplastic nevi, evidence of family history, and genetic conditions such as oculocutaneous albinism and xeroderma pigmentosum (27). Furthermore, exogenous factors include infection by human papilloma viruses (HPV), sun protection behavior, history of sunburns, and magnitude of UV exposure (27). Lastly, individuals who are of advanced age, immunosuppressed, and demonstrate a chronic inflammatory state are also at risk for development of NMSC. Among the aforementioned risk factors, environmental exposure to UV light as well as advanced age are the most commonly acquired and will be the focus of this review.

Sunlight and Advanced Age

There is considerable evidence that substantiates sunlight and advanced aging as a likely cause of NMSC (16, 28–30). These studies include increased incidence in sunnier cities and those exhibiting a lifestyle of prolonged sunlight exposure, lower prevalence in darker skin phototypes, and a majority of cases occurring over sun-exposed skin and in those older than 60 (10, 31–33). In addition, skin cancer exhibits a strong correlation with age, such that nearly 80% of cases occurs in patients over the age of 60 (10). For a while, the epidemiological link between NMSC, sunlight exposure, and advanced age lacked direct causality, prompting basic science research to discover viable connections. UV exposure is known to induce the formation of reactive oxygen species (ROS) and cyclobutane pyrimidine dimers, often resulting in DNA mutations (34). Epidemiological evidence suggests that excessive sun exposure in the first two decades of life can lead to UVB-induced mutations in keratinocytes (35–38). It was thought that this DNA damage persists in the epidermis, eventually obtaining a growth advantage supporting skin carcinogenesis over many decades. However, recent literature suggests that almost 80% of lifetime exposure to sunlight occurs after the age of 18 (10). In addition, it is well-known that sunscreen use is protective against photocarcinogenesis, which suggests that the acquisition of skin cancer is an ongoing process (39–41). Since aging is also associated with a diminished ability to repair DNA, it is reasonable to assume that this component of aging contributes to skin carcinogenesis (11, 42, 43). Overall, studies ultimately support the association between UVB injury, advanced age, and NMSC.

Dermal Microenvironment

Human skin consists of an outer epidermal layer and inner dermal layer connected by a basement membrane as well as underlying subcutaneous fat (27, 44). Keratinocytes are the predominant cell in the epidermis, which is made up of four sub-layers (27, 44, 45). These cells proliferate in the basal layer while attached to the basement membrane. Once detached, keratinocytes stop dividing and undergo a final differentiation known as cornification (44, 45). Each epidermal sub-layer represents a different stage of keratinocyte maturity, whereby they function to strengthen the cytoskeleton as well as establish an epidermal protective barrier (27, 44, 45). The underlying dermis provides support and nutrients for the epidermis (27, 44). It is characterized by a lower cellular density and extensive extracellular matrix. In addition, the dermis is divided into two layers: the more superficial papillary layer and the deeper reticular layer (44). The papillary layer is densely populated by fibroblasts, which are the dominant dermal cell (44). The fibroblast cells of the adult dermis are specialized, post-mitotic, and non-proliferative, while epidermal keratinocytes are highly active and continuously dividing to renew the outer skin barrier (44–46). Since dermal fibroblasts are a long-lived cell population, they experience unceasing damage accumulation and adaptation processes that are associated with aging (44–46). Conversely, the epidermis experiences the direct effects of environmental exposure, which adds to senescent processes (44–46). Thus, cell aging and senescence of epidermal keratinocytes and dermal fibroblasts are largely implicated in skin aging.

Multiple studies have shown that the pathogenesis of photoaging is also associated with supportive tissue stroma, effectors of the immune system, diminished melanogenesis, inappropriate fibroblast deposition, and cytokines and growth factors (47, 48). Tumor growth and progression is dependent on its permissive microenvironment (49). One factor lending to the development of photocarcinogenesis is the senescence-associated secretory phenotype (SASP) (49–51). Senescent cells demonstrate not only an arrest of cell proliferation, but also high metabolic activity marked by widespread changes in protein expression and secretion (49, 50). This can lead to increased transcription of cytokines such as IL-1, IL-6, IL-8, MMP-1, and MMP-3, resulting in chronic low-level inflammation and disruption of normal physiologic processes (19, 49–51). Thus, the molecular profile of the senescent dermal microenvironment plays a major role in skin carcinogenesis. Importantly, the IGF-1/IGF-1R signal transduction pathway has been recently established as a major mechanism in the development of NMSC in the elderly (11, 12, 18). These findings highlight the complexity of NMSC and suggest its development is a gradual and sun-induced process (39–41).

PATHOGENESIS OF NON-MELANOMA SKIN CANCER

Aging and excessive UV exposure are two of the main drivers in the development of NMSC. For a while, the exact mechanisms underpinning how a lifetime of excessive sunlight exposure and advanced age lead to the development of skin cancer were not well understood. However, data from our laboratory suggested a new paradigm for the role of aging in photocarcinogenesis involving the IGF-1/IGF-1R signaling pathway, which regulates the cellular response of keratinocytes to UVB exposure (52). These studies propose a mechanism where geriatric skin deficient in IGF-1 expression is unable to activate the IGF-1R in keratinocytes, resulting in an aberrant response to UVB irradiation (11, 12). This leads to epidermal keratinocytes passing its UVB-induced DNA damage onto daughter cells, likening the formation of NMSC (11, 12, 18, 52).

UVB-Exposure and the Epidermis

Sunlight is composed of multiple types of light including infrared, visible, and ultraviolet (UV) (14). UV light is further classified into UV-A, UV-B, and UV-C. Wavelengths of light within the UV-A range are known to penetrate the atmosphere; although, its impact is indirect and facilitated by free radical formation (38, 53, 54). Conversely, most light in the UV-C range is absorbed in the atmosphere, limiting its dissemination to the earth's surface (14). UV-B comprises only 0.3% of the total light that reaches the surface of the earth; however, its wavelengths penetrate the outermost layer of the skin (15). Though limited to the epidermis, UV-B can directly damage keratinocyte DNA through induction of pyrimidine dimers and other DNA photoproducts that are potentially mutagenic (14, 53, 55–57). These mutagenic changes have the potential to be propagated to subsequent cellular populations, raising the possibility of pro-carcinogenic changes (58–60). The human body has repair mechanisms that respond to UV-B radiation; however, the extent of the epidermal response is largely dependent on the dose and duration of UV-B (53, 61, 62). Short-lived and low dose exposures spur DNA repair by temporarily halting the cell cycle of keratinocytes (11, 56). High doses of UVB cause extensive DNA damage, which results in apoptosis of keratinocytes (11, 56). In contrast, prolonged and intermediate doses of UV-B radiation results in enhanced DNA damage that may escape DNA repair and lead to pro-carcinogenic cellular proliferation (11, 56).

Humans possess a system for removing UV photoproducts from mutated DNA known as nucleotide excision repair (NER) (63). This repair system functions through removal of damaged DNA bases and repair of the gaps by the actions of DNA polymerase and ligase (63). Supplementary to NER, cells possess additional systems such as DNA damage checkpoints that detect the presence of UV photoproducts and control DNA replication and cell cycle progression (63). In particular, the ATR-CHK1 signaling network acts to transiently suppress DNA synthesis in UVB-damaged cells through the suppression of DNA synthesis and cell cycle progression by the G1-S DNA damage checkpoint (63). However, keratinocytes can sometimes escape the appropriate DNA repair. For those basal keratinocytes that experience intermediate doses of UVB-damage, several outcomes can occur: (1) apoptosis of the damaged cell, (2) pro-carcinogenic cellular proliferation, or (3) keratinocyte senescence as a tumor evasion mechanism (11, 12, 18, 19).

The first outcome has the benefit of removing the potential pro-carcinogenic agent, though at the expense of damaging the epidermal barrier function. It should be noted that all three outcomes can be modulated by the activation status of the IGF-1/IGF-1R signaling pathway. The keratinocyte response serves as a protective mechanism.

Aging, Fibroblast Senescence, and Photocarcinogenesis

The IGF-1/IGF-IR mechanism is compartmentalized within dermal-epidermal interactions, wherein dermal fibroblasts regulate basal keratinocyte differentiation (11, 12, 19). IGF-1R is a tyrosine kinase receptor expressed on epidermal keratinocytes that is activated by IGF-1, which is produced and secreted by papillary dermal fibroblasts (64). This signaling pathway is maintained throughout one's lifetime to allow the maintenance and growth of healthy skin (11, 12, 19). Among normal cellular upkeep, IGF-1R activation by IGF-1 plays an integral role in DNA replication and repair, checkpoint control, and induction of keratinocyte senescence (11, 63, 65, 66). Yet, stromal changes in aging skin can impair these processes. Aging causes a number of changes to skin morphology and physiology, including a decrease in epidermal thickness and cell turnover (63). More importantly, the aging process considerably alters IGF-1 synthesis and secretion from dermal fibroblasts (11, 12, 19). Consequently, the paucity of IGF-1 ligand in aged skin results in diminished activation of IGF-1R on keratinocytes (11, 12, 19). Outlined in **Figure 1**, four important components of the cellular DNA damage response are debilitated by the aging process in keratinocytes, including UV photoproduct removal by NER, checkpoint signaling through ATR-CHK1, the replication of damaged DNA by translesion synthesis (TLS), and the induction of gene products regulated by the tumor suppressor protein p53 (**Figure 1**) (18, 52, 65–68). Together, this altered DNA damage response results in keratinocytes that fail to undergo senescence and instead continue to proliferate (11, 12, 65, 66).

The ATR-CHK1 kinase signaling pathway acts to transiently suppress DNA synthesis and cell cycle progression when UVB-irradiation damages cellular DNA (63, 65). This signaling cascade works through various mechanisms including halting the progression from G1 to S phase of the cell cycle, decelerating the rate of ongoing replication fork progression, and hindering the initiation of DNA replication at new origins (63, 65). Our group studied that IGF-1R activation affects ATR-CHK1 signaling through introduction of small-molecule inhibitors or IGF-1 withdrawal (65). We found that disturbing the IGF-1/IGF-1R signaling pathway resulted in redaction of the ATR-CHK1 activation cascade and consequent failure to inhibit chromosomal DNA synthesis in UVB-damaged keratinocytes (65). This indicates that geriatric skin carcinogenesis in lieu of deficient IGF-1 signaling may be caused by defects in cellular responses to UVB-damaged DNA such as suppression of DNA synthesis and cell-cycle progression (65). Similarly, our group studied whether DNA damage tolerance systems including TLS are altered in geriatric individuals (66). The TLS pathway is known to recruit specialized DNA polymerases to damaged DNA, which can introduce nucleotides opposite to damaged template DNA in an error-prone manner (63, 65). Monoubiquitination of the replicative DNA polymerase clamp protein PCNA (proliferating cell nuclear antigen) was used as a biomarker of TLS pathway activation (66). UVB-exposure on geriatric (age >65) skin resulted in a higher level of PCNA monoubiquitination than that found in younger skin (66). Notably, both pharmacological inhibition of IGF-1R as well as IGF-1 deprivation potentiated UVB-induced PCNA monoubiquitination (66). Though the TLS polymerase pol eta can accurately replicate UV photoproducts, we found that its induction by UVB exposure is partially abrogated by the loss of IGF-1 signaling in keratinocytes and human skin explants (68). This suggests that altered IGF-1/IGF-1R signaling in aged skin may predispose keratinocytes to undergo a more mutagenic form of DNA synthesis after UVB-exposure (66).

Appropriate IGF-1/IGF-1R signaling is critical in the dermal response to sun-damaged skin (8). As mentioned before, intermediate doses of UVB can result in keratinocytes escaping effective DNA repair (11, 56). Keratinocytes in this scenario can either undergo apoptosis, cell proliferation with UVB-damaged DNA, or survive through cellular senescence (11). The last option yields the best outcome such that the epidermal skin barrier maintains its function and potentially mutagenic cellular

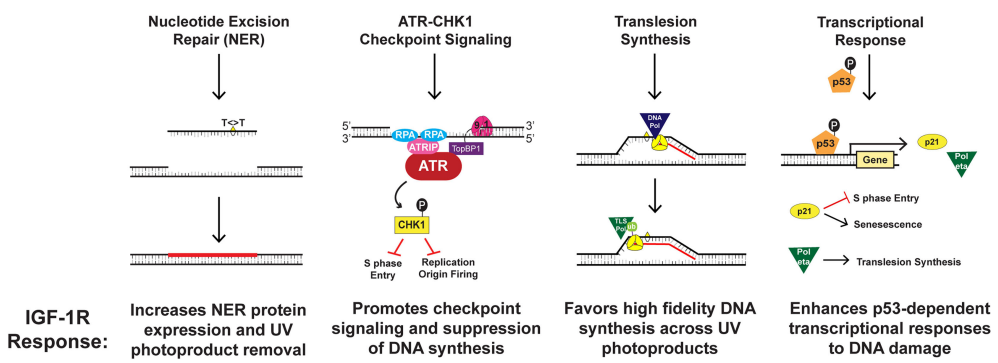

FIGURE 1 | Mechanisms by which IGF-1R activation results in keratinocyte protection from UVB-irradiation.

proliferation is halted. However, this signaling pathway loses its viability in geriatric skin, so that the reduced IGF-1 expression results in an inappropriate response to UVB-damage (11, 12). Since keratinocyte IGF-1R activation is dependent on its ligand, the paucity of IGF-1 in aged dermis results in pro-carcinogenic replication of UVB-damaged DNA (11, 12). In younger skin, IGF-1 synthesis and secretion is sufficient to uphold normal physiological activity of IGF-1R (11, 12). Thus, if UVB-damaged DNA of young keratinocytes is not fully repaired, then keratinocyte senescence stands as a tumor evasion mechanism (8, 11, 12). Unfortunately, when geriatric skin experiences UVB-irradiation, a portion of the epidermal keratinocytes respond inappropriately by allowing mutagenic DNA to replicate and potentially initiate neoplastic cells (8, 19). Consistent with this notion, recent studies by our group xenografted human skin onto immunodeficient mice, and the human skin grafts underwent a chronic UVB carcinogenesis protocol with/without treatment with a topical IGF-1R inhibitor. A 20 week UVB treatment of the skin treated with IGF-1R inhibitor, which would mimic geriatric skin, resulted in formation of actinic neoplastic (AKs/early SCC) lesions, findings not seen in vehicle irradiated skin (20). The data from these studies suggests that defective IGF-1/IGF-1R signaling due to senescent dermal fibroblasts is an important cause of geriatric NMSC.

CURRENT TREATMENT MODALITIES

Treatment options for NMSC depends on risk stratification of the tumor and its characteristics, availability of services, and patient preference and suitability (26, 69). There is a lack of high-quality and evidence-based studies with a 5-year follow-up for NMSC management (26). Additionally, the risk of recurrence after treatment is high, though these cancers seldom metastasize (26, 70). Thus, systemic treatments are not regularly of importance (70). Surgery has traditionally been the "gold standard" treatment due to its excellent cure rates and desirable cosmetic results (70, 71). Specifically, Mohs micrographic surgery (MMS) is the benchmark for high-risk lesions and locations (69). There are other non-surgical treatment modalities such as physical destruction (cryotherapy, radiotherapy, and curettage and cautery), chemical destruction (photodynamic therapy), local therapies (topical 5-fluorouracil, imiquimod, ingenol mebutate, and diclofenac), and novel hedgehog pathway inhibitors (HPI) (vismodegib and sonidegib) (71, 72). The recent development of HPI may antecede a shift towards medical management of NMSC (71).

The annual healthcare cost of treating NMSC in the United States is estimated at nearly $5 billion, which has encouraged exploration to identify and develop effective therapies (25). Most of the current therapies are appropriate only after tumors are clinically manifested and fail to attenuate the rising economic burden (8). However, therapies focused on prevention are successful in preventing pre-malignant transformation. Such is the case in treatments for actinic keratoses (AK), which are pre-cancerous lesions that may evolve into SCC (73). Successful therapies include cryotherapy, photodynamic therapy, 5-fluorouracil with or without topical calcipotriol, topical imiquimod, electrosurgery, and curettage (74–76). These modalities have revealed that early treatment of AK prevents the progression to SCC (74–76). More recently, the combination therapy of calcipotriol and 5-fluorouracil was effective in preventing SCC development within 3 years after treatment (76). Despite the success of AK treatment modalities, these therapies only focus on averting transformation of already established pre-cancerous lesions. Early treatment of AK is essential in preventing progression to SCC (77). As a result, untreated and histologically unaffected skin remains vulnerable to malignant transformation in at-risk individuals (8). This has oriented novel treatments towards skin rejuvenation and dermal IGF-1 restoration strategies, such as wounding therapy (8).

WOUNDING THERAPIES FOR REJUVENATION

The critical observations implicating deficient IGF-1/IGF-1R signaling in NMSC have led to the development of new potential targeted therapies. These treatments act by wounding the skin, which effectively restores IGF-1/IGF-1R signaling by reversing geriatric fibroblast senescence (21–23, 52, 77). Thus, wounding therapy has the potential to achieve an efficacious and long-term chemo-preventative effect, which allays the rising healthcare burden and morbidity associated with NMSC (21–23, 52, 77). In addition, these skin rejuvenation modalities are able to attain both cosmetic and cancer prophylactic effects (8, 78). Our group has identified four viable wounding therapies: dermabrasion, fractionated laser resurfacing (FLR), microneedling, and chemical peeling (19, 21–23, 63). However, the exact mechanism as to how wounding strategies are able to rejuvenate geriatric skin and prevent malignant transformation is unknown (77). Further translational research is needed to explicate the direct pathways.

Dermabrasion

Dermabrasion is a resurfacing technique that has been in use for over 100 years to treat a variety of dermatological conditions, such as scar revision, facial skin resurfacing, wound healing, and correction of pigmentary abnormalities (79–81). The technique is performed using a portable hand-held dermabrader with either wire brushes, diamond fraises, or serrated wheels attached for precise treatment (80). Additionally, sterilized sandpaper or sterile electrocautery scratch pads have been used to manually abrade the skin (79). Dermabrasion intentionally and selectively damages skin to promote reepithelialization and the production of dermal collagen fibrils (8, 19, 79, 81).

Accordingly, our group assessed if dermabrasion was a viable modality to upregulate IGF-1 expression and restore the appropriate UVB response (19). We recruited geriatric volunteers (age > 65 years) and dermabraded discrete areas of their skin, with complete removal of all epidermis and superficial dermis (2, 19). Three months later, the treated loci were

irradiated with UVB; and a punch biopsy was performed on the irradiated site as well as adjacent unirradiated skin for histological and biochemical analysis (19). Our group discovered that dermabrasion produced scarce senescent fibroblasts and fully restored levels of dermal IGF-1 mRNA in geriatric skin (19). Moreover, we found histological features characteristic of younger skin including elliptical fibroblast-replicating nuclei, denser distribution of fibroblasts, restoration of dermal collagen, recovery of the undulating dermal-epidermal basal membrane, and increased number of proliferative keratinocytes (19). Significantly, IGF-1 levels were restored to a profile comparable to skin found in young adults (age < 30) and there was no evidence of UVB-damaged basal keratinocytes (19). As a result, our group was first to demonstrate that dermabrasion restores a more youthful phenotype and induces a reversible molecular signature that can suppress the typical geriatric pro-carcinogenic UVB response (19). Although a promising therapy, the outcomes of dermabrasion are largely dependent on the appropriate technique and skill of the operator; and may produce potentially unfavorable cosmetic outcomes (79–82). For this reason, our group investigated whether other effective but less aggressive wounding modalities, such as FLR and microneedling, could restore an appropriate geriatric UVB response.

Fractionated Laser Resurfacing

FLR has been used over the past two decades for photoaging, acne scarring, and dyschromia (83, 84). The fractionation allows for deeper tissue penetration, and results in tissue remodeling and collagen production (83). FLR delivers infrared light to tissue where it is absorbed by water in the dermis (8). This causes skin heating at non ablative wavelengths such as 1470 nm, 1540 nm, 1550 nm, and 1927 nm and vaporization of tissue layers at ablative wavelengths including 2940 nm and 10,600 nm, which induces skin wounds (8, 85). By thermally altering a distinct area of the skin, the adjacent and untouched skin is able to quickly repopulate the ablated columns of tissue through increased fibroblast and epidermal stem cell activity (85). In addition to requiring less technical skill than dermabrasion, FLR results in more favorable cosmetic outcomes and rapid wound healing (79, 80, 84).

Our group explored whether a FLR-induced wounding response would correct the inappropriate UVB response in geriatric skin (21). Geriatric volunteers (age > 65) received FLR on either sun-protected skin or chronically sun-exposed skin (21). After three months, the FLR-treated skin was irradiated with UVB, and biopsies were taken from irradiated and unirradiated adjacent skin (21). Independent of skin sun exposure, we found increases in collagen expression, amplified numbers of fibroblasts, upregulation of dermal IGF-1 expression, and restoration of the normal UVB response (21). In addition, there was a reduction of photodamaged keratinocytes in chronically sun-exposed skin (21). These results were similar to that of dermabrasion, but with much more desirable cosmetic effects and procedural ease (79, 80). This suggests that FLR could also be used to help protect against future actinic neoplasia (77). Therefore, our group explored the use of single ablative FLR as a modality to treat AK (23). Subjects (age > 60) with at least five AKs on the forearm or wrist received FLR treatment (23). At three and six months, the treated sites were photographed and had the AK lesions counted and mapped in a blinded fashion (23). When compared to pre-treatment, we found that the numbers of AKs on treated locations were significantly lower at both three months and six months (23). Additionally, the average total numbers of AKs on the untreated arm at six months increased by 167%, while the average percentage decrease of AKs on the treated arm was 60% (23).

The results demonstrate the utility of a single FLR treatment as a field therapy to treat precancerous AKs on sun-exposed skin, given its upregulation of dermal IGF-1 and removal of senescent fibroblasts (21, 23). However, these studies only examined responses within a short time frame post-wounding. In addition, the safety, efficacy, and durability of single ablative FLR in high-risk geriatric patients is unknown. Thus, our group assessed the long-term effects of FLR on geriatric skin through a randomized prospective clinical trial. We recruited 48 patients (age > 60) who had at least five AKs that were 3 mm or smaller. Patients underwent a single treatment of FLR on the upper extremity of aged skin. They were examined at three month post-wounding and every six months thereafter for a current 36-month follow-up period (20). To determine the effectiveness of FLR in reducing the occurrence of AKs, the ratio of the number of AKs on FLR-treated arms to untreated arms was tracked. At three months post-FLR treatment, the ratio of AKs on treated versus untreated arms was reduced four-fold. This ratio was maintained throughout the current 36-month period, demonstrating a lack of significant difference in the ratios at 3, 6, 12, 18, 24, 30, or 36 months. Moreover, additional analyses were conducted to model the initiation of new AK lesions. We found that untreated arms continue to accumulate increasing numbers of AKs, while treated arms demonstrated a reduction in the occurrence of new AK lesions with time. In fact, the number of AKs on untreated arms accumulated at a much faster rate than that found on treated arms. The results not only indicate that FLR is an effective treatment for existing AKs, but also prevent the development of new AK lesions. Importantly, the numbers of NMSC on the untreated arms of this population (26 NMSC) was much greater than the arm that underwent FLR (2 NMSC). Moreover, with efficacy lasting for at least two years following treatment, we validate that FLR is a durable treatment for rectifying the inappropriate UVB response in elderly skin. This data suggests that a single treatment of FLR can provide lasting prevention of NMSC in high-risk geriatric patients (20).

Microneedling

Microneedling is a reasonably new treatment modality within the field of dermatology, largely being used for aesthetic purposes (86, 87). It has a broad range of uses including acne and surgical scarring, melasma, rhytides, dyschromia, transdermal drug delivery, and skin rejuvenation (86, 88). Microneedles are reported to be both effective and versatile devices due to its relatively painless penetration, affordability, and ability to deliver transdermal medicinal applications (88). The basic theory behind its mechanism of action is percutaneous collagen induction (78, 87). Histological studies exhibit increased

collagen and elastin after use of a microneedling device, which introduces small zones of dermal injury and subsequent wound healing processes (87). Previous studies by our group have exhibited photorejuvenation through wounding therapies such as dermabrasion and FLR (19, 21, 23). Given its rising popularity for skin rejuvenation, our group tested if controlled microneedling could achieve a similar protective wounding response as exhibited by upregulation of dermal IGF-1 levels (22).

Nine geriatric volunteers (age > 65) with Fitzpatrick Types I and II underwent wounding on the upper buttocks using a commercially available microneedling device (22). After 90 days, a localized area of either microneedle-treated skin or untreated skin was irradiated with a dose of UVB (22). Photographs and punch biopsies of the skin were acquired twenty-four hours post-UVB irradiation (22). At three months after microneedling application, mRNA levels of both collagen 1 and IGF-1 were increased in previously wounded skin (22). These results were similar to that found after application of dermabrasion (19, 22). When comparing UVB irradiated wounded skin versus UVB irradiated normal control skin, we found a statically significant decrease in the numbers of Ki67 +/TD+ basal keratinocytes in wounded skin (22). This paralleled the responses exhibited following dermabrasion and FLR wounding of elderly skin (12, 19, 21). Furthermore, this response to UVB irradiation was similar to the "normal" responses documented in young (age < 30) skin (12, 19, 21, 22). This study indicates that wounding of geriatric skin by use of a microneedling device results in increased dermal collagen 1 and IGF-1 levels as well as normalizes the protective response to UVB irradiation. These findings are promising, but are limited to a short time-frame and small sample size.

Chemical Peels

Chemical Peeling, also known as chemexfoliation, has been used for centuries to attenuate photoaging and holds promise as another skin resurfacing option (89, 90). This modality utilizes a chemical application to the skin that causes controlled wounding of the epidermis and dermis, resulting in skin regeneration (89). The extent of wounding depends on the depth of skin penetration, thus it is characterized as superficial, medium-depth, or deep chemical peels (91). Superficial peels produce wounding limited only to the epidermis, while medium-depth peels penetrate into the papillary dermis. Moreover, deep peels generate injury into the reticular dermis (89, 91). These peels are indicated for a number of skin conditions, including acne, melasma, actinic keratosis, lentigines, photodamaging, and scarring. Additionally, a number of chemicals are used for peeling, such as tretinoin, salicylic acid, trichloroacetic acid (TCA), Jessner's solution (JS), glycolic acid (GA), pyruvic acid and phenol (89, 91). The use of superficial and medium-depth chemical peels has increased in recent years due to its relative procedural ease, minimal side effects, and cost efficiency (92). Thus, an investigation into its potential as a wounding therapy for prevention of photocarcinogenesis is warranted.

There are a number of human studies that suggest chemical resurfacing may be a viable skin cancer prophylaxis (93–98). Using a human keratinocyte cell line, Ahn et al. demonstrated the ability of GA to inhibit UV-induced cytotoxicity and apoptosis, which suggests GA may exert a repressive effect on skin cancer development (93). Kaminaka et al. investigated the efficacy of phenol peels in patients with AK and Bowen disease. They found that 100% pure phenol resulted in a 84.8% complete response after one to eight treatment sessions, with only 4.3% recurrence over a period of one year (94). Lawrence et al. found that a medium-depth peel using JS and 35% TCA reduced the number of visible AK by 75% (95). Similarly, Hantash et al. found that 30% TCA resulted in a 89% clearance of AKs when measured at three months post therapy. Furthermore, this application demonstrated a reduced incidence of NMSC compared to the control as well as a longer timespan until the development of new skin cancer (96). Lastly, two recent studies compared TCA peeling (35% and 50%) and photodynamic therapy with topical 5-aminolevulinic acid (PDT-ALA) for the treatment of AK (97, 98). Although TCA was less painful and less expensive, both studies found that PDT-ALA performed better than TCA. Yet, Di Nuzzo et al. found that 50% TCA had an AK clearance rate of 66.1% at three and six months (97). In addition, Holzer et al. demonstrated that 35% TCA had a 78.6% and 48.8% AK clearance at three and twelve months, respectively (98). This suggests TCA peels have clinical utility in treating AKs. Our group is currently exploring TCA peels in this regard, and our preliminary studies indicate that a 10% TCA peel on geriatric skin upregulates IGF-1 mRNA levels approximately two-fold at 90 days (*unpublished data*). As presented, chemical peeling holds promise as a therapeutic and preventative modality for skin carcinogenesis. More research is needed with this area to elucidate the precise mechanize of skin rejuvenation. Chemical peeling offers a safe, cost-effective and flexible alternative wounding therapy for the prevention of photocarcinogenesis.

CONCLUSION

The IGF-1/IGF-1R signaling pathway stands as a major factor in the development of photocarcinogenesis. Over a lifetime, advanced age and UVB exposure result in diminished dermal IGF-1 and increased keratinocyte mutagenesis. This results in defective DNA repair, checkpoint signaling, and appropriate keratinocyte senescence, which increases the likelihood of neoplastic transformation. NMSC remains a significant driver of increased healthcare costs and morbidity annually, necessitating the identification of effective treatments. With this new model outlined in **Figure 2**, wounding therapies hold promise as evidenced by their ability to restore appropriate IGF-1/IGF-1R signaling to levels found in younger skin. These studies are exciting as they exhibit desirable cosmetic outcomes, efficacious photorejuvation, and protection against skin carcinogenesis. As a commercially available device, microneedling holds promise as a less expensive and more widely available wounding therapy. Chemical peeling offers a beneficial alternative treatment, yet more research is needed to explicate its exact mechanism. Importantly, FLR exhibits both

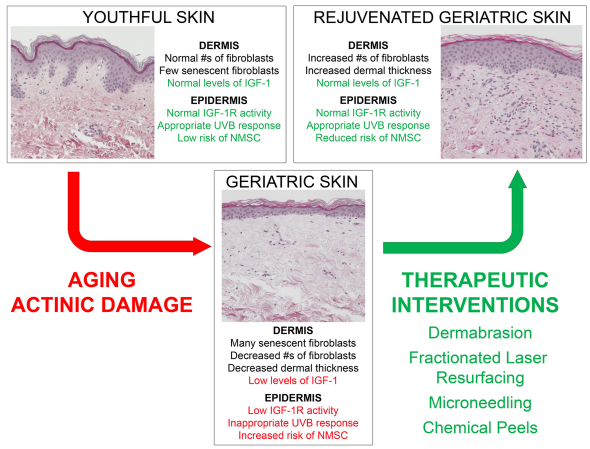

FIGURE 2 | Model demonstrating young versus aged skin and the impact of wounding therapies on the response of geriatric skin to UVB-irradiation.

regenerative and long-term protective effects against pre-cancerous lesions. The concept of restoring youth and combating malignancy through wounding therapies holds potential as a major dermatological treatment modality.

The insights leading to this new paradigm of actinic neoplasia began as pioneering *in vitro* studies in which Dr. Dan Spandau discovered that keratinocyte responses to UVB were dependent upon the presence/absence of IGF-1 (99). Subsequently, Drs. Spandau and Travers devised a strategy to ascertain the importance of IGF-1R activation in the response of geriatric skin to UVB irradiation. These studies led to further collaborations with clinicians (e.g., Drs. Rohan, Tanzi, Wanner) to define the role of IGF-1 and fibroblast senescence in humans. Basic scientist Dr. Kemp has further characterized the exact mechanisms by which IGF-1R activation of the keratinocyte are protective. This new paradigm is clearly an example of a "bench-to-bedside" highly collaborative project with tremendous clinical implications.

AUTHOR CONTRIBUTIONS

TF wrote the first draft. CR, DS, MK, MW, ET, and JT edited and provided further input. The conceptualization of the work was from DS, JT, CR, MK, MW, ET. All authors contributed to the article and approved the submitted version.

FUNDING

This work was supported by grants from the National Institutes of Health (R01 HL062996 to JT; R01 AG048946 to JT and DFS; and R01 GM130583 to MGK) and VA Merit Awards (5I01CX000809 to JT, 1I01CX002242 to MK, and 5I01CX001956 to DS).

REFERENCES

1. Thiele JJ, Podda M, Packer L. Tropospheric Ozone: An Emerging Environmental Stress to Skin. *Biol Chem* (1997) 378(11):1299–305. doi: 10.1515/bchm.1997.378.11.1299
2. Dyer JM, Miller RA. Chronic Skin Fragility of Aging: Current Concepts in the Pathogenesis, Recognition, and Management of Dermatoporosis. *J Clin Aesthet Dermatol* (2018) 11(1):13–8.
3. Ibuki A, Kuriyama S, Toyosaki Y, Aiba M, Hidaka M, Horie Y, et al. Aging-Like Physiological Changes in the Skin of Japanese Obese Diabetic Patients. *SAGE Open Med* (2018) 6:2050312118756662. doi: 10.1177/2050312118756662
4. Lephart ED. A Review of the Role of Estrogen in Dermal Aging and Facial Attractiveness in Women. *J Cosmet Dermatol* (2018) 17(3):282–8. doi: 10.1111/jocd.12508
5. Society AC. *Cancer Facts & Figures 2021*. Atlanta: American Cancer Society (2021).
6. Guy GPJr., Thomas CC, Thompson T, Watson M, Massetti GM, Richardson LC, et al. Vital Signs: Melanoma Incidence and Mortality Trends and Projections - United States, 1982-2030. *MMWR Morb Mortal Wkly Rep* (2015) 64(21):591–6.
7. Rogers HW, Weinstock MA, Feldman SR, Coldiron BM. Incidence Estimate of Nonmelanoma Skin Cancer (Keratinocyte Carcinomas) in the U.S. Population, 2012. *JAMA Dermatol* (2015) 151(10):1081–6. doi: 10.1001/jamadermatol.2015.1187
8. Krbanjevic A, Travers JB, Spandau DF. How Wounding *via* Lasers Has Potential Photocarcinogenic Preventative Effects *via* Dermal Remodeling. *Curr Dermatol Rep* (2016) 5(3):222–7. doi: 10.1007/s13671-016-0143-8
9. Stern RS. Prevalence of a History of Skin Cancer in 2007: Results of an Incidence-Based Model. *Arch Dermatol* (2010) 146(3):279–82. doi: 10.1001/archdermatol.2010.4
10. Godar DE, Urbach F, Gasparro FP, van der Leun JC. UV Doses of Young Adults. *Photochem Photobiol* (2003) 77(4):453–7. doi: 10.1562/0031-8655(2003)077<0453:UDOYA>2.0.CO;2
11. Lewis DA, Travers JB, Spandau DF. A New Paradigm for the Role of Aging in the Development of Skin Cancer. *J Invest Dermatol* (2009) 129(3):787–91. doi: 10.1038/jid.2008.293
12. Lewis DA, Travers JB, Somani A-K, Spandau DF. The IGF-1/IGF-1R Signaling Axis in the Skin: A New Role for the Dermis in Aging-Associated Skin Cancer. *Oncogene* (2010) 29(10):1475–85. doi: 10.1038/onc.2009.440
13. Lewis DA, Krbanjevic A, Travers JB, Spandau DF. "Aging-Associated Nonmelanoma Skin Cancer: A Role for the Dermis". In: MK Farage M, H Maibach, editors. *Textbook of Aging Skin*. Berlin, Heidelberg: Springer (2017).
14. Tyrrell RM. The Molecular and Cellular Pathology of Solar Ultraviolet Radiation. *Mol Aspects Med* (1994) 15(1):1–77.
15. Clingen PH, Arlett CF, Roza L, Mori T, Nikaido O, Green MH. Induction of Cyclobutane Pyrimidine Dimers, Pyrimidine(6-4)Pyrimidone Photoproducts, and Dewar Valence Isomers by Natural Sunlight in Normal Human Mononuclear Cells. *Cancer Res* (1995) 55(11):2245–8.
16. Wikonkal NM, Brash DE. Ultraviolet Radiation Induced Signature Mutations in Photocarcinogenesis. *J Investig Dermatol Symp Proc* (1999) 4(1):6–10. doi: 10.1038/sj.jidsp.5640173
17. Ikehata H, Ono T. The Mechanisms of UV Mutagenesis. *J Radiat Res* (2011) 52(2):115–25. doi: 10.1269/jrr.10175
18. Lewis DA, Yi Q, Travers JB, Spandau DF. UVB-Induced Senescence in Human Keratinocytes Requires a Functional Insulin-Like Growth Factor-1 Receptor and P53. *Mol Biol Cell* (2008) 19(4):1346–53. doi: 10.1091/mbc.e07-10-1041
19. Lewis DA, Travers JB, Machado C, Somani AK, Spandau DF. Reversing the Aging Stromal Phenotype Prevents Carcinoma Initiation. *Aging (Albany NY)* (2011) 3(4):407–16. doi: 10.18632/aging.100318

20. Spandau DF, Chen R, Wargo JJ, Rohan CA, Southern D, Zhang A, et al. Randomized Controlled Trial of Fractionated Laser Resurfacing on Aged Skin as Prophylaxis Against Actinic Neoplasia. *J Clin Invest* (2021) 131(19): e150972. doi: 10.1172/JCI150972
21. Spandau DF, Lewis DA, Somani A-K, Travers JB. Fractionated Laser Resurfacing Corrects the Inappropriate UVB Response in Geriatric Skin. *J Invest Dermatol* (2012) 132(6):1591–6. doi: 10.1038/jid.2012.29
22. Travers JB, Kemp MG, Weir NM, Cates E, Alkawar AM, Mahajan AS, et al. Wounding With a Microneedling Device Corrects the Inappropriate Ultraviolet B Radiation Response in Geriatric Skin. *Arch Dermatol Res* (2020) 312(1):1–4. doi: 10.1007/s00403-019-02001-z
23. Chen R, Wargo JJ, Williams A, Cates E, Spandau DF, Knisely C, et al. Single Ablative Fractional Resurfacing Laser Treatment For Forearm Actinic Keratoses: 6-Month Follow-Up Data From An Intrapatient Comparison Between Treated and Untreated Sites. *Lasers Surg Med* (2020) 52(1):84–7. doi: 10.1002/lsm.23175
24. Muzic JG, Schmitt AR, Wright AC, Alniemi DT, Zubair AS, Lourido JMO, et al. Incidence and Trends of Basal Cell Carcinoma and Cutaneous Squamous Cell Carcinoma: A Population-Based Study in Olmsted County, Minnesota, 2000 to 2010. *Mayo Clin Proc* (2017) 92(6):890–8. doi: 10.1016/j.mayocp.2017.02.015
25. Guy GPJr., Machlin SR, Ekwueme DU, Yabroff KR. Prevalence and Costs of Skin Cancer Treatment in the U.S., 2002-2006 and 2007-2011. *Am J Prev Med* (2015) 48(2):183–7. doi: 10.1016/j.amepre.2014.08.036
26. Samarasinghe V, Madan V. Nonmelanoma Skin Cancer. *J Cutan Aesthet Surg* (2012) 5(1):3–10. doi: 10.4103/0974-2077.94323
27. Gordon R. Skin Cancer: An Overview of Epidemiology and Risk Factors. *Semin Oncol Nurs* (2013) 29(3):160–9. doi: 10.1016/j.soncn.2013.06.002
28. Kraemer KH. Sunlight and Skin Cancer: Another Link Revealed. *Proc Natl Acad Sci USA* (1997) 94(1):11–4. doi: 10.1073/pnas.94.1.11
29. Barysch MJ, Hofbauer GF, Dummer R. Vitamin D, Ultraviolet Exposure, and Skin Cancer in the Elderly. *Gerontology* (2010) 56(4):410–3. doi: 10.1159/000315119
30. Brash DE NP. "Carcinogenesis: Ultraviolet Radiation". In: Wolff, editor. *Fitzpatrick's Dermatology in General Medicine* (2003). New York: McGraw-Hill Professional.
31. Zak-Prelich M, Narbutt J, Sysa-Jedrzejowska A. Environmental Risk Factors Predisposing to the Development of Basal Cell Carcinoma. *Dermatol Surg* (2004) 30(2 Pt 2):248–52. doi: 10.1111/j.1524-4725.2004.30089.x
32. Rosso S, Zanetti R, Martinez C, Tormo MJ, Schruab S, Sancho-Garnier H, et al. The Multicentre South European Study 'Helios'. II: Different Sun Exposure Patterns in the Aetiology of Basal Cell and Squamous Cell Carcinomas of the Skin. *Br J Cancer* (1996) 73(11):1447–54. doi: 10.1038/bjc.1996.275
33. Kricker A, Armstrong BK, English DR, Heenan PJ. Does Intermittent Sun Exposure Cause Basal Cell Carcinoma? A Case-Control Study in Western Australia. *Int J Cancer* (1995) 60(4):489–94. doi: 10.1002/ijc.2910600411
34. Roewert-Huber J, Lange-Asschenfeldt B, Stockfleth E, Kerl H. Epidemiology and Aetiology of Basal Cell Carcinoma. *Br J Dermatol* (2007) 157 Suppl 2:47–51. doi: 10.1111/j.1365-2133.2007.08273.x
35. Whiteman DC, Whiteman CA, Green AC. Childhood Sun Exposure as a Risk Factor for Melanoma: A Systematic Review of Epidemiologic Studies. *Cancer Causes Control* (2001) 12(1):69–82. doi: 10.1023/A:1008980919928
36. Kricker A, Armstrong BK, English DR. Sun Exposure and Non-Melanocytic Skin Cancer. *Cancer Causes Control* (1994) 5(4):367–92. doi: 10.1007/BF01804988
37. Westerdahl J, Olsson H, Ingvar C. At What Age do Sunburn Episodes Play a Crucial Role for the Development of Malignant Melanoma. *Eur J Cancer* (1994) 30A(11):1647–54. doi: 10.1016/0959-8049(94)00337-5
38. Narayanan DL, Saladi RN, Fox JL. Ultraviolet Radiation and Skin Cancer. *Int J Dermatol* (2010) 49(9):978–86. doi: 10.1111/j.1365-4632.2010.04474.x
39. Thompson SC, Jolley D, Marks R. Reduction of Solar Keratoses by Regular Sunscreen Use. *N Engl J Med* (1993) 329(16):1147–51. doi: 10.1056/NEJM199310143291602
40. Naylor MF, Boyd A, Smith DW, Cameron GS, Hubbard D, Neldner KH. High Sun Protection Factor Sunscreens in the Suppression of Actinic Neoplasia. *Arch Dermatol* (1995) 131(2):170–5. doi: 10.1001/archderm.1995.01690140054008
41. Ulrich C, Jurgensen JS, Degen A, Hackethal M, Ulrich M, Patel MJ, et al. Prevention of Non-Melanoma Skin Cancer in Organ Transplant Patients by Regular Use of a Sunscreen: A 24 Months, Prospective, Case-Control Study. *Br J Dermatol* (2009) 161 Suppl 3:78–84. doi: 10.1111/j.1365-2133.2009.09453.x
42. Freitas AA, de Magalhaes JP. A Review and Appraisal of the DNA Damage Theory of Ageing. *Mutat Res* (2011) 728(1-2):12–22. doi: 10.1016/j.mrrev.2011.05.001
43. Hoeijmakers JH. DNA Damage, Aging, and Cancer. *N Engl J Med* (2009) 361(15):1475–85. doi: 10.1056/NEJMra0804615
44. Gruber F, Kremslehner C, Eckhart L, Tschachler E. Cell Aging and Cellular Senescence in Skin Aging - Recent Advances in Fibroblast and Keratinocyte Biology. *Exp Gerontol* (2020) 130:110780. doi: 10.1016/j.exger.2019.110780
45. Eckhart L, Zeeuwen P. The Skin Barrier: Epidermis vs Environment. *Exp Dermatol* (2018) 27(8):805–6. doi: 10.1111/exd.13731
46. Tigges J, Krutmann J, Fritsche E, Haendeler J, Schaal H, Fischer JW, et al. The Hallmarks of Fibroblast Ageing. *Mech Ageing Dev* (2014) 138:26–44. doi: 10.1016/j.mad.2014.03.004
47. Goubran HA, Kotb RR, Stakiw J, Emara ME, Burnouf T. Regulation of Tumor Growth and Metastasis: The Role of Tumor Microenvironment. *Cancer Growth Metastasis* (2014) 7:9–18. doi: 10.4137/CGM.S11285
48. Moriwaki S, Takahashi Y. Photoaging and DNA Repair. *J Dermatol Sci* (2008) 50(3):169–76. doi: 10.1016/j.jdermsci.2007.08.011
49. Coppe JP, Desprez PY, Krtolica A, Campisi J. The Senescence-Associated Secretory Phenotype: The Dark Side of Tumor Suppression. *Annu Rev Pathol* (2010) 5:99–118. doi: 10.1146/annurev-pathol-121808-102144
50. Ghosh K, Capell BC. The Senescence-Associated Secretory Phenotype: Critical Effector in Skin Cancer and Aging. *J Invest Dermatol* (2016) 136(11):2133–9. doi: 10.1016/j.jid.2016.06.621
51. Waldera Lupa DM, Kalfalah F, Safferling K, Boukamp P, Poschmann G, Volpi E, et al. Characterization of Skin Aging-Associated Secreted Proteins (SAASP) Produced by Dermal Fibroblasts Isolated From Intrinsically Aged Human Skin. *J Invest Dermatol* (2015) 135(8):1954–68. doi: 10.1038/jid.2015.120
52. Loesch MM, Collier AE, Southern DH, Ward RE, Tholpady SS, Lewis DA, et al. Insulin-Like Growth Factor-1 Receptor Regulates Repair of Ultraviolet B-Induced DNA Damage in Human Keratinocytes *In Vivo*. *Mol Oncol* (2016) 10(8):1245–54. doi: 10.1016/j.molonc.2016.06.002
53. Melnikova VO, Ananthaswamy HN. Cellular and Molecular Events Leading to the Development of Skin Cancer. *Mutat Res* (2005) 571(1-2):91–106. doi: 10.1016/j.mrfmmm.2004.11.015
54. Madan V, Lear JT, Szeimies RM. Non-Melanoma Skin Cancer. *Lancet* (2010) 375(9715):673–85. doi: 10.1016/S0140-6736(09)61196-X
55. Drouin R, Therrien JP. UVB-Induced Cyclobutane Pyrimidine Dimer Frequency Correlates With Skin Cancer Mutational Hotspots in P53. *Photochem Photobiol* (1997) 66(5):719–26. doi: 10.1111/j.1751-1097.1997.tb03213.x
56. Ichihashi M, Ueda M, Budiyanto A, Bito T, Oka M, Fukunga M, et al. UV-Induced Skin Damage. *Toxicology* (2003) 189(1-2):21–39. doi: 10.1016/S0300-483X(03)00150-1
57. Nishigori C. Cellular Aspects of Photocarcinogenesis. *Photochem Photobiol Sci* (2006) 5(2):208–14. doi: 10.1039/B507471A
58. Krtolica A, Campisi J. Cancer and Aging: A Model for the Cancer Promoting Effects of the Aging Stroma. *Int J Biochem Cell Biol* (2002) 34(11):1401–14. doi: 10.1016/S1357-2725(02)00053-5
59. Mathon NF, Lloyd AC. Cell Senescence and Cancer. *Nat Rev Cancer* (2001) 1(3):203–13. doi: 10.1038/35106045
60. Campisi J. Cancer and Ageing: Rival Demons? *Nat Rev Cancer* (2003) 3(5):339–49. doi: 10.1038/nrc1073
61. Ramos J, Villa J, Ruiz A, Armstrong R, Matta J. UV Dose Determines Key Characteristics of Nonmelanoma Skin Cancer. *Cancer Epidemiol Biomarkers Prev* (2004) 13(12):2006–11.
62. Brash DE. Roles of the Transcription Factor P53 in Keratinocyte Carcinomas. *Br J Dermatol* (2006) 154 Suppl 1:8–10. doi: 10.1111/j.1365-2133.2006.07230.x
63. Kemp MG, Spandau DF, Travers JB. Impact of Age and Insulin-Like Growth Factor-1 on DNA Damage Responses in UV-Irradiated Human Skin. *Molecules* (2017) 22(3):356–76. doi: 10.3390/molecules22030356
64. Tavakkol A, Elder JT, Griffiths CE, Cooper KD, Talwar H, Fisher GJ, et al. Expression of Growth Hormone Receptor, Insulin-Like Growth Factor 1

(IGF-1) and IGF-1 Receptor mRNA and Proteins in Human Skin. *J Invest Dermatol* (1992) 99(3):343–9. doi: 10.1111/1523-1747.ep12616668
65. Kemp MG, Spandau DF, Simman R, Travers JB. Insulin-Like Growth Factor 1 Receptor Signaling Is Required for Optimal ATR-CHK1 Kinase Signaling in Ultraviolet B (UVB)-Irradiated Human Keratinocytes. *J Biol Chem* (2017) 292 (4):1231–9. doi: 10.1074/jbc.M116.765883
66. Hutcherson RJ, Gabbard RD, Castellanos AJ, Travers JB, Kemp MG. Age and Insulin-Like Growth Factor-1 Impact PCNA Monoubiquitination in UVB-Irradiated Human Skin. *J Biol Chem* (2021) 296:100570. doi: 10.1016/j.jbc.2021.100570
67. Fernandez TL, Van Lonkhuyzen D, Dawson R, Kimlin M, Upton Z. Insulin-Like Growth Factor-I and UVB Photoprotection in Human Keratinocytes. *Exp Dermatol* (2015) 24(3):235–8. doi: 10.1111/exd.12637
68. Alkawar AMM, Castellanos AJ, Carpenter MA, Hutcherson RJ, Madkhali MAO, Johnson RM, et al. Insulin-Like Growth Factor-1 Impacts P53 Target Gene Induction in UVB-Irradiated Keratinocytes and Human Skin. *Photochem Photobiol* (2020) 96(6):1332–41. doi: 10.1111/php.13279
69. Lazareth V. Management of Non-Melanoma Skin Cancer. *Semin Oncol Nurs* (2013) 29(3):182–94. doi: 10.1016/j.soncn.2013.06.004
70. Amaral T, Garbe C. Non-Melanoma Skin Cancer: New and Future Synthetic Drug Treatments. *Expert Opin Pharmacother* (2017) 18(7):689–99. doi: 10.1080/14656566.2017.1316372
71. Griffin LL, Ali FR, Lear JT. Non-Melanoma Skin Cancer. *Clin Med (Lond)* (2016) 16(1):62–5. doi: 10.7861/clinmedicine.16-1-62
72. Ceovic R, Petkovic M, Mokos ZB, Kostovic K. Nonsurgical Treatment of Nonmelanoma Skin Cancer in the Mature Patient. *Clin Dermatol* (2018) 36 (2):177–87. doi: 10.1016/j.clindermatol.2017.10.009
73. Malvehy J. A New Vision of Actinic Keratosis Beyond Visible Clinical Lesions. *J Eur Acad Dermatol Venereol* (2015) 29 Suppl 1:3–8. doi: 10.1111/jdv.12833
74. Schmitt AR, Bordeaux JS. Solar Keratoses: Photodynamic Therapy, Cryotherapy, 5-Fluorouracil, Imiquimod, Diclofenac, or What? Facts and Controversies. *Clin Dermatol* (2013) 31(6):712–7. doi: 10.1016/j.clindermatol.2013.05.007
75. Gupta AK, Paquet M, Villanueva E, Brintnell WL. Interventions for Actinic Keratoses. *Cochrane Database Syst Rev* (2012) 12:CD004415. doi: 10.1002/14651858.CD004415.pub2
76. Rosenberg AR, Tabacchi M, Ngo KH, Wallendorf M, Rosman IS, Cornelius LA, et al. Skin Cancer Precursor Immunotherapy for Squamous Cell Carcinoma Prevention. *JCI Insight* (2019) 4(6):e125476. doi: 10.1172/jci.insight.125476
77. Travers JB, Spandau DF, Lewis DA, Machado C, Kingsley M, Mousdicas N, et al. Fibroblast Senescence and Squamous Cell Carcinoma: How Wounding Therapies Could be Protective. *Dermatol Surg* (2013) 39(7):967–73. doi: 10.1111/dsu.12138
78. Loesch MM, Somani AK, Kingsley MM, Travers JB, Spandau DF. Skin Resurfacing Procedures: New and Emerging Options. *Clin Cosmet Investig Dermatol* (2014) 7:231–41. doi: 10.2147/CCID.S50367
79. Alkhawam L, Alam M. Dermabrasion and Microdermabrasion. *Facial Plast Surg* (2009) 25(5):301–10. doi: 10.1055/s-0029-1243078
80. Gold MH. Dermabrasion in Dermatology. *Am J Clin Dermatol* (2003) 4 (7):467–71. doi: 10.2165/00128071-200304070-00003
81. Roenigk HH. Dermabrasion: State of the Art 2002. *J Cosmet Dermatol* (2002) 1(2):72–87. doi: 10.1046/j.1473-2165.2002.00041.x
82. Hamilton MM, Kao R. Recognizing and Managing Complications in Laser Resurfacing, Chemical Peels, and Dermabrasion. *Facial Plast Surg Clin North Am* (2020) 28(4):493–501. doi: 10.1016/j.fsc.2020.06.008
83. Carniol PJ, Hamilton MM, Carniol ET. Current Status of Fractional Laser Resurfacing. *JAMA Facial Plast Surg* (2015) 17(5):360–6. doi: 10.1001/jamafacial.2015.0693
84. Aslam A, Alster TS. Evolution of Laser Skin Resurfacing: From Scanning to Fractional Technology. *Dermatol Surg* (2014) 40(11):1163–72. doi: 10.1097/01.DSS.0000452648.22012.a0
85. Alexiades-Armenakas MR, Dover JS, Arndt KA. The Spectrum of Laser Skin Resurfacing: Nonablative, Fractional, and Ablative Laser Resurfacing. *J Am Acad Dermatol* (2008) 58(5):719–37; quiz 738-40. doi: 10.1016/j.jaad.2008.01.003
86. Alster TS, Graham PM. Microneedling: A Review and Practical Guide. *Dermatol Surg* (2018) 44(3):397–404. doi: 10.1097/DSS.0000000000001248
87. Alessa D, Bloom JD. Microneedling Options for Skin Rejuvenation, Including Non-Temperature-Controlled Fractional Microneedle Radiofrequency Treatments. *Facial Plast Surg Clin North Am* (2020) 28(1):1–7. doi: 10.1016/j.fsc.2019.09.001
88. Mdanda S, Ubanako P, Kondiah PPD, Kumar P, Choonara YE. Recent Advances in Microneedle Platforms for Transdermal Drug Delivery Technologies. *Polymers (Basel)* (2021) 13(15):2405–29. doi: 10.3390/polym13152405
89. Lee KC, Wambier CG, Soon SL, Sterling JB, Landau M, Rullan P, et al. Basic Chemical Peeling: Superficial and Medium-Depth Peels. *J Am Acad Dermatol* (2019) 81(2):313–24. doi: 10.1016/j.jaad.2018.10.079
90. Sidiropoulou P, Gregoriou S, Rigopoulos D, Kontochristopoulos G. Chemical Peels in Skin Cancer: A Review. *J Clin Aesthet Dermatol* (2020) 13(2):53–7.
91. Starkman SJ, Mangat DS. Chemical Peels: Deep, Medium, and Light. *Facial Plast Surg* (2019) 35(3):239–47. doi: 10.1055/s-0039-1688944
92. Soleymani T, Lanoue J, Rahman Z. A Practical Approach to Chemical Peels: A Review of Fundamentals and Step-By-Step Algorithmic Protocol for Treatment. *J Clin Aesthet Dermatol* (2018) 11(8):21–8.
93. Ahn KS, Park KS, Jung KM, Jung HK, Lee SH, Chung SY, et al. Inhibitory Effect of Glycolic Acid on Ultraviolet B-Induced C-Fos Expression, AP-1 Activation and P53-P21 Response in a Human Keratinocyte Cell Line. *Cancer Lett* (2002) 186(2):125–35. doi: 10.1016/S0304-3835(02)00283-5
94. Kaminaka C, Yamamoto Y, Yonei N, Kishioka A, Kondo T, Furukawa F. Phenol Peels as a Novel Therapeutic Approach for Actinic Keratosis and Bowen Disease: Prospective Pilot Trial With Assessment of Clinical, Histologic, and Immunohistochemical Correlations. *J Am Acad Dermatol* (2009) 60(4):615–25. doi: 10.1016/j.jaad.2008.11.907
95. Lawrence N, Cox SE, Cockerell CJ, Freeman RG, Cruz PDJr. A Comparison of the Efficacy and Safety of Jessner's Solution and 35% Trichloroacetic Acid vs 5% Fluorouracil in the Treatment of Widespread Facial Actinic Keratoses. *Arch Dermatol* (1995) 131(2):176–81. doi: 10.1001/archderm.1995.01690140060009
96. Hantash BM, Stewart DB, Cooper ZA, Rehmus WE, Koch RJ, Swetter SM. Facial Resurfacing for Nonmelanoma Skin Cancer Prophylaxis. *Arch Dermatol* (2006) 142(8):976–82. doi: 10.1001/archderm.142.8.976
97. Di Nuzzo S, Cortelazzi C, Boccaletti V, Zucchi A, Conti ML, Montanari P, et al. Comparative Study of Trichloroacetic Acid vs. Photodynamic Therapy With Topical 5-Aminolevulinic Acid for Actinic Keratosis of the Scalp. *Photodermatol Photoimmunol Photomed* (2015) 31(5):233–8. doi: 10.1111/phpp.12164
98. Holzer G, Pinkowicz A, Radakovic S, Schmidt JB, Tanew A. Randomized Controlled Trial Comparing 35% Trichloroacetic Acid Peel and 5-Aminolaevulinic Acid Photodynamic Therapy for Treating Multiple Actinic Keratosis. *Br J Dermatol* (2017) 176(5):1155–61. doi: 10.1111/bjd.15272
99. Kuhn C, Hurwitz SA, Kumar MG, Spandau DF. Activation of the Insulin-Like Growth Factor-1 Receptor Promotes the Survival of Human Keratinocytes Following Ultraviolet B Radiation. *Int J Cancer* (1999) 80(3):431–8. doi: 10.1002/(SICI)1097-0215(19990129)80:3<431::AID-IJC16>3.0.CO;2-5

Author Disclaimer: The content is solely the responsibility of the authors and does not necessarily represent the official views of the National Institutes of Health nor the US Veterans Administration.

Conflict of Interest: MW has a grant and equipment from Solta.

The remaining authors declare that the research was conducted in the absence of any commercial or financial relationships that could be construed as a potential conflict of interest.

Publisher's Note: All claims expressed in this article are solely those of the authors and do not necessarily represent those of their affiliated organizations, or those of the publisher, the editors and the reviewers. Any product that may be evaluated in this article, or claim that may be made by its manufacturer, is not guaranteed or endorsed by the publisher.

frontiers in Oncology

ORIGINAL RESEARCH
published: 31 January 2022
doi: 10.3389/fonc.2022.827985

Adverse Effects of Vemurafenib on Skin Integrity: Hyperkeratosis and Skin Cancer Initiation Due to Altered MEK/ERK-Signaling and MMP Activity

Marius Tham[1†], *Hans-Jürgen Stark*[2†], *Anna Jauch*[3], *Catherine Harwood*[4,5], *Elizabeth Pavez Lorie*[6] *and Petra Boukamp*[1,6*]

[1] Department of Genetics of Skin Carcinogenesis, German Cancer Research Center (DKFZ), Heidelberg, Germany, [2] Department of Applied Tumor Biology, Institute of Pathology, University of Heidelberg, Heidelberg, Germany, [3] Institute of Human Genetics, University Heidelberg, Heidelberg, Germany, [4] Department of Dermatology, Royal London Hospital, Barts Health NHS Trust, London, United Kingdom, [5] Centre for Cell Biology and Cutaneous Research, Blizard Institute, Barts and the London School of Medicine and Dentistry, Queen Mary University of London, London, United Kingdom, [6] IUF–Leibniz Research Institute for Environmental Medicine, Düsseldorf, Germany

OPEN ACCESS

Edited by:
Nabiha Yusuf,
University of Alabama at Birmingham,
United States

Reviewed by:
Keith Pui-Kei Wu,
Medical College of Wisconsin,
United States
Pamela Bond Cassidy,
Oregon Health and Science University,
United States

***Correspondence:**
Petra Boukamp
p.boukamp@dkfz-heidelberg.de

[†]These authors have contributed equally to this work

Specialty section:
This article was submitted to Skin Cancer, a section of the journal Frontiers in Oncology

Received: 02 December 2021
Accepted: 03 January 2022
Published: 31 January 2022

Citation:
Tham M, Stark H-J, Jauch A, Harwood C, Pavez Lorie E and Boukamp P (2022) Adverse Effects of Vemurafenib on Skin Integrity: Hyperkeratosis and Skin Cancer Initiation Due to Altered MEK/ERK-Signaling and MMP Activity. Front. Oncol. 12:827985. doi: 10.3389/fonc.2022.827985

The BRAF inhibitor vemurafenib, approved for treating patients with BRAF V600E-mutant and unresectable or metastatic melanomas, rapidly induces cutaneous adverse events, including hyperkeratotic skin lesions and cutaneous squamous cell carcinomas (cSCC). To determine, how vemurafenib would provoke these adverse events, we utilized long-term *in vitro* skin equivalents (SEs) comprising epidermal keratinocytes and dermal fibroblasts in their physiological environment. We inserted keratinocytes with different genetic background [normal keratinocytes: NHEK, HaCaT (p53/mut), and HrasA5 (p53/mut+Hras/mut)] to analyze effects depending on the stage of carcinogenesis. We now show that vemurafenib activates MEK-ERK signaling in both, keratinocytes, and fibroblasts *in vitro* and in the *in vivo*-like SEs. As a consequence, vemurafenib does not provide a growth advantage but leads to a differentiation phenotype, causing accelerated differentiation and hyperkeratosis in the NHEK and normalized stratification and cornification in the transformed keratinocytes. Although all keratinocytes responded very similarly to vemurafenib in their expression profile, particularly with a significant induction of MMP1 and MMP3, only the HrasA5 cells revealed a vemurafenib-dependent pathophysiological shift to tumor progression, i.e., the initiation of invasive growth. This was shown by increased proteolytic activity allowing for penetration of the basement membrane and invasion into the disrupted underlying matrix. Blocking MMP activity, by the addition of ilomastat, prevented invasion with all corresponding degradative activities, thus substantiating that the RAS-RAF-MEK-ERK/MMP axis is the most important molecular basis for the rapid switch towards tumorigenic conversion of the HrasA5 keratinocytes upon vemurafenib treatment. Finally, cotreatment with vemurafenib and the MEK inhibitor cobimetinib prevented MEK-ERK hyperactivation and with that abolished

both, the epidermal differentiation and the tumor invasion phenotype. This suggests that both cutaneous adverse events are under direct control of vemurafenib-dependent MEK-ERK hyperactivation and confirms the dependence on preexisting genetic alterations of the skin keratinocytes that determine the basis towards induction of tumorigenic progression.

Keywords: skin cancer, organotypic skin cancer model, vemurafenib, cutaneous adverse effects, tumor invasion, matrix metalloproteinase, degradome, MEK inhibition

INTRODUCTION

Targeted therapy has revolutionized the field of medical oncology. Despite being highly successful in treating the specific malignancy, dermatologic toxicities (DT) are among adverse reactions of a variety of targeted therapies. Besides inflammatory dermatoses, i.e., papulopustular eruption, dermal hypersensitivity reaction (DHR), and photoreactivity, also hyperkeratosis and squamoproliferative lesions including actinic keratosis (AK), keratoacanthoma (KA), and cutaneous squamous cell carcinoma (cSCC) were described (for review, see 1 and references therein). Noteworthy, cutaneous epithelial proliferation, i.e., tumor formation, was particularly frequent with the BRAF inhibitors sorafenib and vemurafenib while substantially less frequent with EGFRi, MEKi, PI3Ki, or AKTi.

The oncogenic mutation V600E in BRAF protein accounts for 50%–60% of the somatic mutations in melanoma leading to constitutive activation of the protein kinase BRAF and downstream induction of the MAP kinase/ERK-signaling pathway with correlated melanomagenesis. Vemurafenib, a second-generation selective small molecule inhibitor of RAF, is highly potent in inhibiting the activation of this pathway in BRAF V600E-mutant melanoma cells and thereby is highly effective in combating the growth of metastases in the melanoma patients (for review, see 2). Unfortunately, acquired resistance and a high frequency of cutaneous adverse events, including the rapid development of cSCCs, impeded this treatment strategy. Accordingly, treatment was combined with a MEK inhibitor, with cobimetinib in case of clinical trials with vemurafenib. Concurrent administration of BRAFi and MEKi is now an established therapeutic protocol for the treatment of BRAF V600E-mutant metastatic melanoma and an adjuvant treatment in routine clinical practice. It is noteworthy, that cutaneous adverse events, including "keratinocytic proliferations" such as keratosis pilaris, i.e., small hyperkeratotic follicular papules (in up to 7% of patients), as well as actinic keratoses (AK), keratoacanthomas (KA), skin papillomas, and cSCCs emerged in 1%–2% of the patients (3). Thus, keratinocyte proliferation is still observed as a cutaneous adverse event even when treated with BRAFi+MEKi combination therapy, though at a much lower rate than in vemurafenib monotherapy which causes 6% hyperkeratosis, 8% KA, and 12% cSCC (4).

Generally, the development of cSCC is a multistep process with a latency period of several decades and therefore, cSCCs are frequent in elderly patients. cSCC are among the most common malignancies and characterized by a high load of UV-indicative mutations (5), as well as a high frequency of chromosomal aberrations with only few recurrent chromosomal aberrations (6, 7). Together, this makes these tumors genetically highly heterogeneous. The most frequent recurrent mutations and thus, implicated as driver genes in cSCCs, include NOTCH1/2, TP53, and CDKN2A while oncogenic ras, i.e., mutations in HRAS, Kras, or Nras are infrequent [3%–20% or less; (8) and references therein].

Sequencing of normal human eyelid skin (9) demonstrated a high frequency of mutations with a predominance of UV-indicative mutations (C>T mutations and high rates of CC>TT dinucleotide substitutions). We and others recently showed that normal sun-exposed skin contains numerous epidermal patches that stain positive for p53 protein and contain critically short, dysfunctional telomeres and which may be potential early precursors of skin cancer (7, 10). Cells of these patches contain mutations in multiple genes that are mutated also in cSCC with many of the mutations being subclonal in those lesions. Thus, various genetically altered cells exist in normal human skin, and it is tempting to propose that preexisting subpopulations contribute to the rapid development of skin cancer upon vemurafenib treatment.

Since vemurafenib is still an important component of targeted therapy for melanoma (11), there is a medical need for more extensive analysis of the pathogenesis of vemurafenib-dependent cutaneous adverse events. Considering their rapid appearance in the vemurafenib-treated melanoma patients, we expected to recapitulate the vemurafenib-specific phenotypes in long-term *in vivo*-like skin equivalents and to investigate the underlying regulatory switch responsible for the cutaneous adverse events. By utilizing keratinocytes representing different stages in the multistep process of skin carcinogenesis, we report that vemurafenib-associated MEK-ERK hyperactivation accelerates epidermal differentiation in different keratinocytes correlating with the vemurafenib-dependent adverse event of hyperkeratosis. In addition, we show a vemurafenib-dependent regulation of the degradome that is responsible for immediate initiation of invasive growth by the preneoplastic HrasA5 cells. This substantiates the hypothesis of a causal relationship of the tumorigenic shift observed *in vitro* and the rapid SCC development in Vemurafenib-treated melanoma patients.

RESULTS

Vemurafenib Causes MEK-ERK Pathway Activation in Normal and Transformed Human Skin Keratinocytes

Vemurafenib abrogates RAF-MEK-ERK signaling in melanoma cells that harbor *BRAF V600E* mutations while causing pathway hyperactivation in wildtype melanoma cells (12, 13). MEK-ERK hyperactivation is also seen in epithelial *BRAF* wildtype cells, e.g., the human HaCaT keratinocytes and different human cSCC cells (14).

Thus, we asked how different human keratinocytes would respond to vemurafenib. For this, we investigated normal human epidermal keratinocytes (NHEK) as well as keratinocytes from our isogenic human skin cancer model (15); the HaCaT cells as well as their Hras-containing tumorigenic variants, the benign tumorigenic HrasA5 cells and the malignant tumorigenic HrasII4 cells. Using a phosphorylation-specific Western blot analysis, we investigated the time-dependent pathway activation upon treatment with 1 μM vemurafenib.

In *BRAF V600E*-positive A375 melanoma cells, which we included as control, vemurafenib rapidly (within 30 min) abolished the high basic levels of phosphorylated MEK1/2 and ERK1/2 (**Figure 1A**). In contrast, two different strains of the *BRAF* wildtype NHEKs showed similar results to the different HaCaT variants, HrasA5 and HrasII4 cells, as vemurafenib caused activation of the MEK-ERK pathway, indicated by an increase in P-MEK1/2 and even more so in P-ERK1/2 (**Figures 1B–E**). Interestingly, activation appeared transient in the NHEK, while being long lasting in the HaCaT cells (p53 mut) and the Hras oncogene-containing variants (p53mut/Hras+).

To confirm whether vemurafenib would activate also additional signaling cascades, we analyzed for coactivation of the MAPK-p38 as well as PI3K-PTEN-Akt pathway. In the melanoma cells, Pp38 and P-Akt were temporarily reduced (30 min to 3 h post treatment) (see **Figure 1A**). As reduction was seen in the untreated and vemurafenib-treated cultures, a vemurafenib-specific regulation was unlikely. In the keratinocytes, the level of Pp38 remained largely unaffected except for HrasA5 where P-p38 was temporarily lowered (first 30 min). Likewise, P-Akt showed no major regulation; if at all, there was a slight increased over control.

Together, this shows that vemurafenib causes rapid activation of the MEK-ERK pathway while having little effect on the p38 and Pi3K-PTEN-Akt pathways, thereby making MEK-ERK hyperactivation the major vemurafenib-dependent regulatory consequence in the human skin keratinocytes irrespective of their state of transformation.

Vemurafenib Does Not Increase Proliferation in Cultivated Human Skin Keratinocytes

Commonly, MEK-ERK activation is linked to growth (16) and hyperactivation of the MEK-ERK cascade was supposed to be a major signaling pathway triggering proliferation (17). Increased proliferation was suggested also for HaCaT cells treated with a "low" vemurafenib concentration (2 μM) (18). To address how vemurafenib would affect growth of our different keratinocyte variants, we exposed NHEK, HaCaT, and HrasA5 cells to 0.1 up to 5 μM vemurafenib and determined their growth kinetics over the following 3 days (**Figures 1F–H**). Instead of increased proliferation, vemurafenib-treated NHEK showed the same growth rate as the nontreated control cells at low concentrations (0.1 and 0.01 μM). At higher concentrations (1 and 5 μM), vemurafenib induced significant growth inhibition. HaCaT and HaCaT-rasA5 (HrasA5) cells appeared less sensitive. Even the highest concentration of vemurafenib (5 μM) did not affect short-term growth in conventional cultures. Only upon long-term treatment (>1 week) with 5 μM of vemurafenib, a 50% growth reduction was seen for the HaCaT cells while the HrasA5 cells were not affected at all (data not shown).

Taken together, vemurafenib-induced MEK-ERK hyperactivation did not improve growth in any of the keratinocytes. Instead, we found acute growth inhibition for 1 and 5 μM vemurafenib for the NHEK and delayed growth restraints for the HaCaT keratinocytes. The premalignant HrasA5 cells remained unperturbed, indicating a transformation stage-specific loss of sensitivity for vemurafenib-induced growth restraints in the human keratinocytes.

Vemurafenib Does Not Confer Chromosomal Instability But Rather Promotes a Genetic Drift

The rapid development of cSCC in vemurafenib-treated melanoma patients and the evidence that BRAF inactivation drives aneuploidy (19) may suggest vemurafenib-dependent genomic instability. Alternatively, vemurafenib may select for and promote preexisting subpopulations. To address the role of vemurafenib in genomic instability, we utilized the nontumorigenic HaCaT cells. Like numerous cells present in sun-exposed skin, they carry UV-type-specific p53 mutations, thus suffering from lack of the property of p53 to induce DNA repair and cell cycle arrest. Nevertheless, they are stably nontumorigenic and remain as a superficial epidermis-like epithelium upon long-term propagation as skin equivalents in 3D organotypic cultures or xenotransplants in mice (20, 21).

To determine whether and how vemurafenib would contribute to chromosomal instability, we performed multiplex fluorescence *in situ* hybridization (M-FISH) of HaCaT cells treated with 1 or 5 μM vemurafenib for 5 weeks. We show that neither dose resulted in gross chromosomal changes. Comparison of numerical aberrations for individual chromosomes demonstrated a very similar profile with only few changes (**Supplementary Figure S1A**). However, when comparing the aberration profile of control and vemurafenib-treated HaCaT cells for the distribution of subpopulations, vemurafenib provoked a shift in the dominance of preexisting subpopulations (**Supplementary Figure S1B**). In particular, we detected dominance for a dose-dependent gain of i(1q), carrying genes such as *S100* genes, *RASSF5*, *MAPKAPK2*, *TP53BP*, *WNT3A*, and *WNT9A*, and dose-dependent loss of i(17p), containing genes such as *TP53*, *MAP2K4*, *MAPK7*, or *RASD1*. We also found a selection for an unbalanced translocation

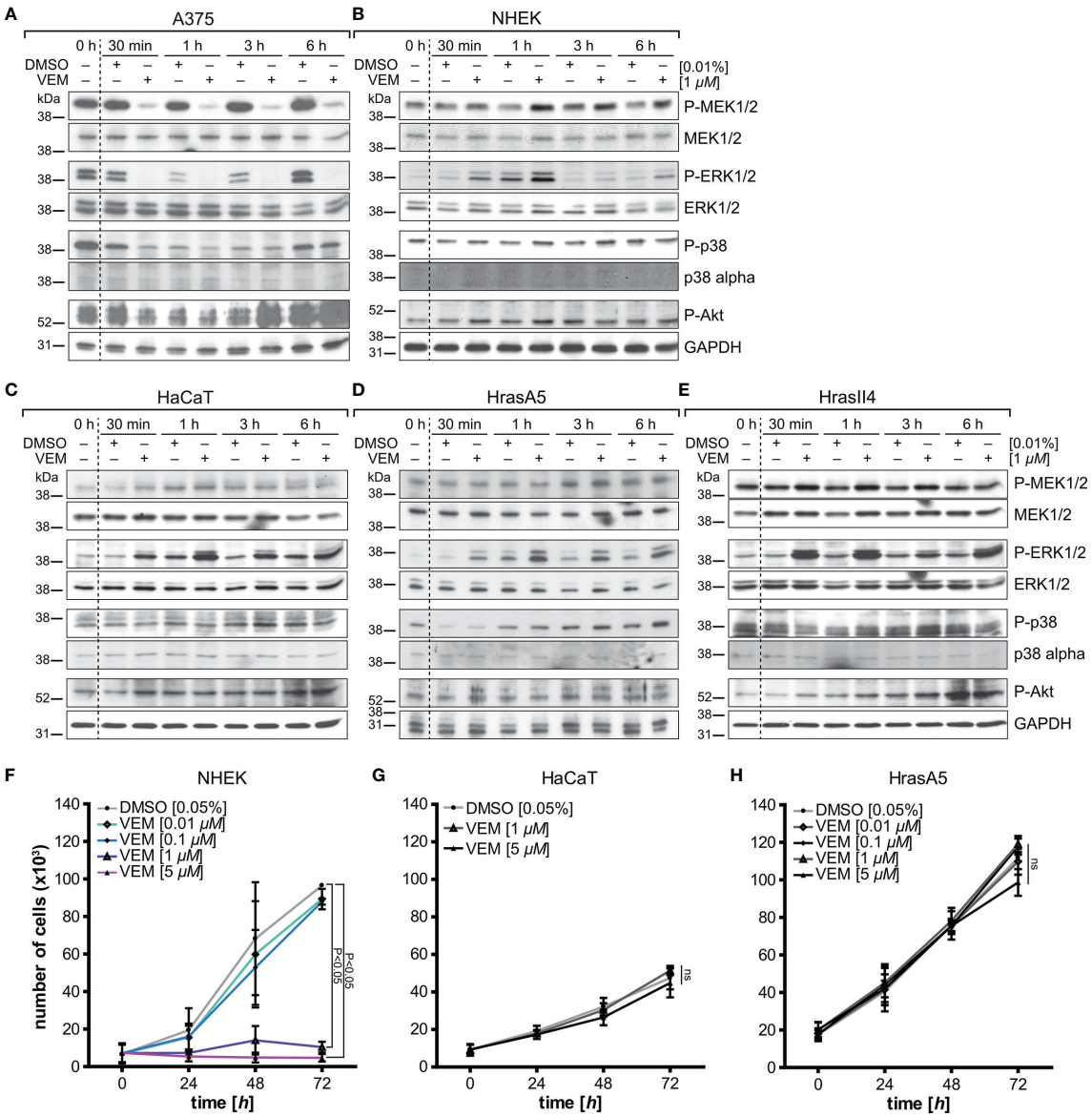

FIGURE 1 | Vemurafenib-dependent pathway regulation and proliferation. A375 (BRAF mutant) melanoma cells **(A)** and BRAF wildtype keratinocytes, represented by normal human keratinocytes (NHEK) **(B)**, HaCaT **(C)**, the premalignant HrasA5 **(D)**, and the malignant HrasII4 cells **(E)**, were incubated with either DMSO (solvent control) or vemurafenib (1 μM) for a period of up to 6 h, and protein expression of MEK/P-MEK, ERK/P-ERK, p38/P-p38, and Akt/PAkt was examined. Opposing effects were seen for P-MEK and P-ERK when comparing the A375 melanoma cells (*BRAF-V600E* mut) and the human keratinocytes. P-p38 and P-Akt were inhibited transiently in the A375 cells, both in control and vemurafenib-treated cells, but did not seem to be regulated in the human keratinocytes. GAPDH was used as loading control in all immunoblots. To study the effects on proliferation, NHEK **(F)**, HaCaT **(G)**, and HrasA5 cells **(H)** were treated with different concentrations of vemurafenib (0.01–5 μM) for a period of up to 72 h, and proliferation was determined at 24, 48, and 72 h by measuring fluorescence intensity (SyBr green proliferation assay). Statistical significance was calculated by two-way ANOVA and Bonferroni posttest (n = 2, mean ± SD, two-way ANOVA + Bonferroni posttest; ns, not significant).

chromosome der(2)t(2;8), leading to copy number gain of 8q harboring the *cMYC* gene—a cytogenetic aberration frequently associated with cSCCs (6, 22).

Together, this genetic analysis suggests that vemurafenib is not a potent inducer of genetic alterations. Instead, vemurafenib may provide a selective advantage for specific subpopulations and those with, e.g., excessive cMyc that are also able to respond with tumorigenic/invasive growth.

Vemurafenib Alters Gene Expression of Keratinocytes

To determine whether vemurafenib would also affect the expression profile of the skin keratinocytes, we performed RNA expression analyses for NHEK, HaCaT, and HrasA5 cells by selecting a panel of genes, including epidermal differentiation markers, pathway-indicative, and invasion-related genes. For this, the different keratinocytes were treated with 1 and 5 μM

vemurafenib and expression was analyzed by qRT-PCR after 8 and 24 h.

Concerning epidermal differentiation, a minor induction of involucrin was seen in NHEK after 8 h, which increased considerably after 24 h. Likewise, keratin 10 (*KRT10*) and filaggrin (*FLG*) were upregulated after 24 h and the degree of regulation appeared dose-dependent (**Figure 2A**). None of those genes were regulated in HaCaT or HrasA5 cells during the first 24 h (**Figures 2B, C**). Only upon long-term treatment of the HaCaT cells with 5 μM vemurafenib for 4 and 8 weeks we saw an increase in the transcription of *KRT10* and *FLG* (data not shown). This suggests that induction of differentiation is rapid and direct in NHEK while delayed and potentially indirect in the transformed keratinocytes.

In addition, we found a 2- to 3-fold induction of the interleukins *IL-1α* and *IL-1β* (**Figure 2A**), factors known to act on the dermal fibroblasts in a paracrine stimulatory loop by inducing, e.g., keratinocyte growth factor (KGF alias *FGF7*) and granulocyte macrophage colony-stimulatory factor (GM-CSF alias *CSF2*). These in turn support epidermal growth and

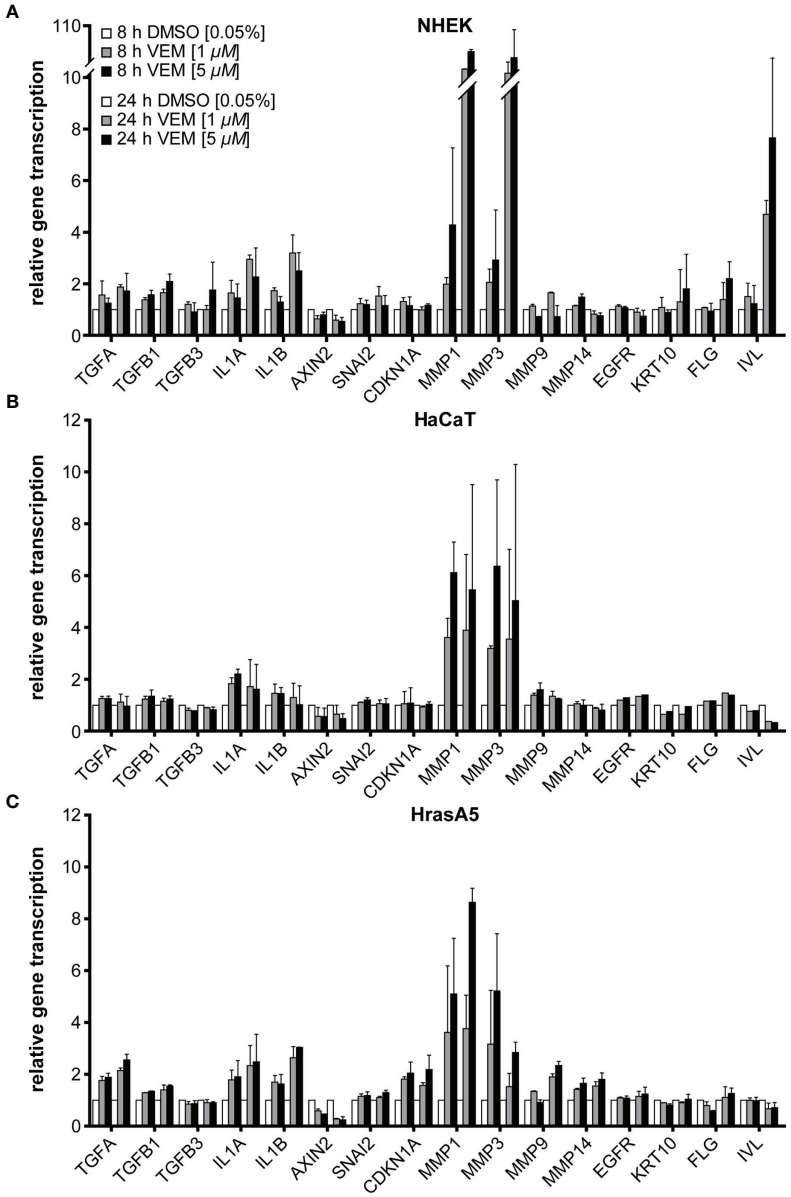

FIGURE 2 | Vemurafenib preferentially targets the degradome. Vemurafenib-altered expression profile of NHEK **(A)**, HaCaT **(B)**, and HrasA5 cells **(C)** after 8 and 24 h of vemurafenib treatment. All human keratinocytes show upregulation of *IL1A* and *IL1B*, with HaCaT cells being the least regulated, as well as a strong induction of *MMP1* and *MMP3* while *MMP9* and *MMP14* remain largely unaffected. In addition, epidermal differentiation markers become upregulated in NHEK only. Normalization was performed using GAPDH as house-keeping gene and foldchanges were expressed by comparing 1 or 5 μM vemurafenib treatment of NHDF to DMSO stimulation, respectively. $n = 2$, mean ± SD.

differentiation (23, 24). Transforming growth factor alpha (*TGF-α*) reached a 2-fold increase in NHEK and HrasA5 cells while transforming growth factors *TGF-β1* and *TGF-ß3* remained largely unaffected. Likewise, *AXIN2* (Wnt/ß-catenin pathway), *CDKN1A* (p21 pathway), *EGFR*, or *SNAI2* (EMT marker) did not appear to be regulated by vemurafenib.

Invasion of the epidermal cells requires proteolytic activity for degradation of, e.g., the basement membrane and dermal collagen. We, therefore, investigated also for the expression of the matrix metalloproteases *MMP1*, *MMP3*, *MMP9*, and *MMP14*, all associated with cSCCs (reviewed in 25). As shown in **Figure 2** and particularly striking, *MMP1* and *MMP3* were induced immediately and strongly in all three keratinocyte variants, suggestive of being direct targets of the MEK-ERK hyperactivation. Interestingly, induction was most prominent in NHEK (>10-fold), again pointing to their high sensitivity to vemurafenib treatment (**Figure 2A**). *MMP9* expression (~2-fold after 24 h) was restricted to the HrasA5 cells (**Figure 2C**). *MMP14* did not seem to be regulated by vemurafenib treatment in any of the keratinocytes (**Figures 2A–C**).

Together, vemurafenib contributes to keratinocyte regulation by directly inducing epidermal differentiation in NHEK and strongly upregulating the expression of components of the degradome, *MMP1* and *MMP3*, in all keratinocytes irrespective of their transformation state and genetic composition.

Vemurafenib Improves Tissue Organization

To determine the role of vemurafenib on tissue regulation, we established skin equivalents (SEs) with NHEK, HaCaT, and HrasA5 cells. For this, dermal equivalents (DEs) were prepared by allowing the fibroblasts to establish their own dermal matrix which after 4 weeks of maturation were supplemented with the keratinocytes. By propagating the cocultures at the air-liquid interphase for 2 weeks, skin equivalents (SEs) develop that are composed of a stratified and differentiated epidermis connected to the dermal matrix through a basement membrane. Such 2-week-old SEs were then treated with vemurafenib or solvent control and histological comparison was performed after 1, 3, or 5 weeks of treatment.

NHEKs start with a wound-like hyperplastic epidermis (first 4 to 5 weeks), which is reduced by reaching tissue homeostasis and long-term regeneration is maintained by an equilibrium of proliferation and differentiation (>week 5). As it is not shed, the stratum corneum continuously expands (**Figure 3A**; 20). Exposure to 1 μM vemurafenib interfered little with tissue morphology, though the epidermis appeared more compact with a slightly reduced number of cell layers and a tendency for an increased stratum corneum. Exposure to 5 μM vemurafenib, however, caused accelerated differentiation leading to significant reduction in living cell layers and hyperkeratosis after only 1 week of treatment (**Figure 3A**).

HaCaT cells form a multilayered parakeratotic epithelium that, in contrast to NHEKs, becomes atrophic upon long-term regeneration (7 weeks) with only few remaining basal cells that are unable to properly connect the epidermis with the underlying dermal equivalent (**Supplementary Figure S2A**). Upon vemurafenib treatment, the epithelium reorganized with a tendency for improved epidermal morphogenesis and differentiation as indicated by the formation of a *stratum granulosum* and an extended and regularly structured parakeratotic *stratum corneum*. Importantly, upon long-term treatment a vital epithelium was maintained, suggesting that Vemurafenib induced a differentiation-dependent tissue normalization being connected with longevity of the HaCaT cells in the *in vivo*-like environment.

Likewise, the premalignant HrasA5 cells form a hyperplastic, moderately differentiated surface epithelium with an undulated BM zone. Of note, also these epithelia become atrophic during long-term propagation (see control of **Figure 3A**). Upon vemurafenib treatment, differentiation was strongly increased, indicated by a steadily growing parakeratotic stratum corneum and occasional horn-pearls within the epithelium (**Figure 3A**). With the shift to increased differentiation, also these epithelia gained longevity. In addition, and unique for the HrasA5 cells, vemurafenib induced rapid and extended invasion. Already after 1 week of treatment with 5 μM vemurafenib, the HrasA5 cells had broken through the BM and invaded the underlying dermal matrix. With 1 μM vemurafenib, invasion was only seen after 3 weeks, arguing for a dose-dependent regulation (**Figure 3A**).

To confirm and extend the histological findings, we next analyzed the expression and distribution of the early (KRT10) and terminal epidermal differentiation markers keratin 2 (KRT2) and FLG. In NHEK SEs, KRT10 was expressed in all suprabasal layers. KRT2 and FLG, on the other hand, were increased with vemurafenib and in addition, KRT2 expression became more restricted and thus, more similar to the distribution in normal human skin (**Figure 3B**). Also, HaCaT (**Supplementary Figure S2B**) and HrasA5 epithelia (**Figure 3B**) were characterized by increased expression and more regular localization of the differentiation markers (for HrasA5 for 5 μM vemurafenib). Together, this confirms the vemurafenib-dependent advancement in epidermal differentiation and shows that an epidermal normalization also occurs to the transformed keratinocytes.

Vemurafenib Induces Invasion in HrasA5 Cells

In addition to the induction of differentiation, vemurafenib promoted invasive growth exclusively for the HrasA5 cells. While NHEK (**Figure 3A**) and HaCaT cells (**Supplementary Figure S2A**) remained as surface epithelia throughout the 5-week treatment period with vemurafenib, HrasA5 cells invaded the underlying dermal matrix within 3 weeks when treated with 1 μM vemurafenib and even more rapidly (within the first week) when 5 μM vemurafenib was applied (**Figure 3A**).

Vemurafenib Does Not Accelerate *In Vivo* Proliferation

In general, tumor growth correlates with increased proliferation. Although in our *in vitro* analyses vemurafenib was rather growth restrictive for NHEKs and did not seem to confer a growth advantage to the HrasA5 cells, we nevertheless determined

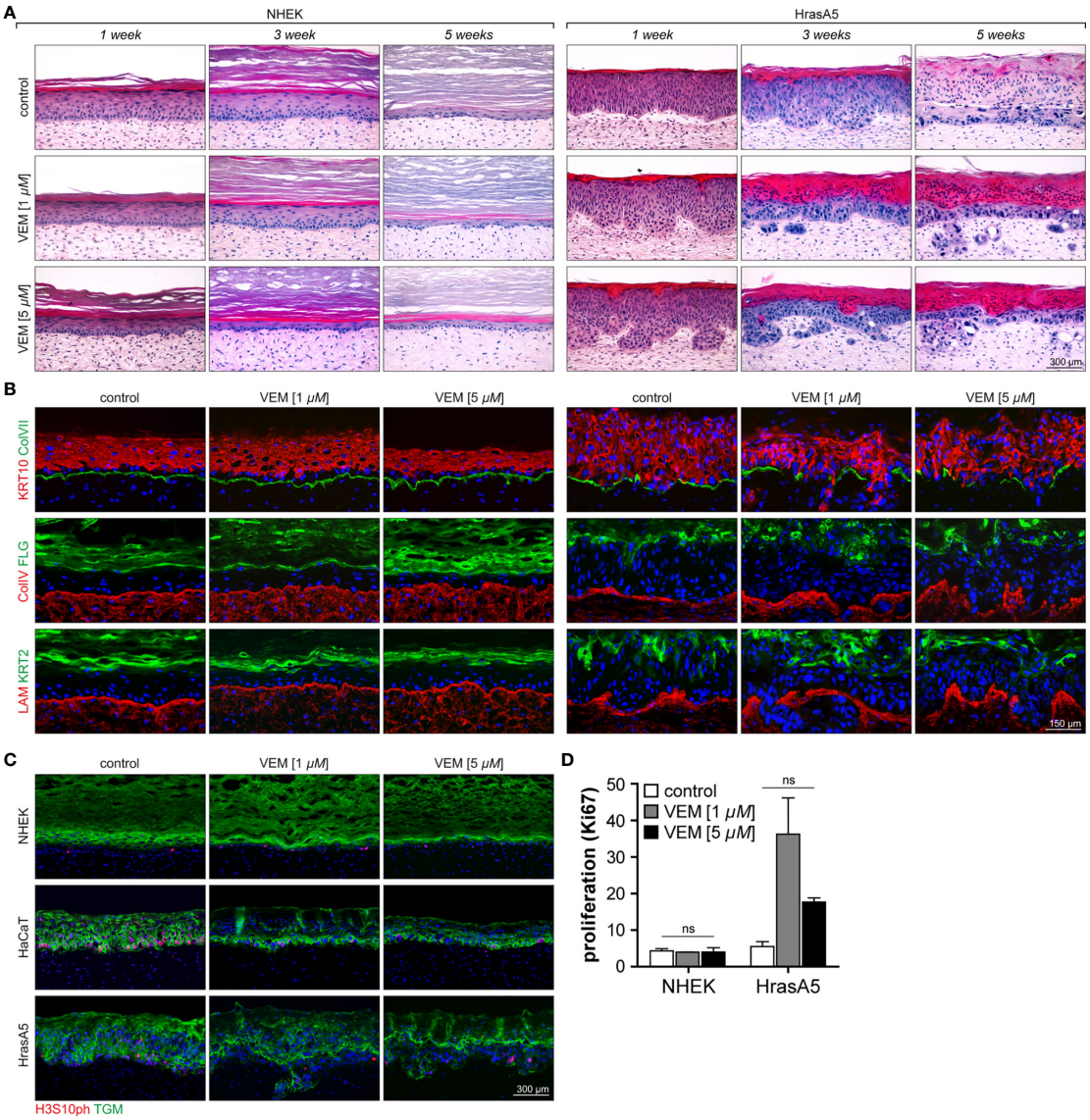

FIGURE 3 | Characterization of the effects of vemurafenib on epithelial differentiation and proliferation in SEs. SEs from NHEK and HrasA5 cells were treated with vemurafenib (VEM) (1 and 5 μM) for up to 5 weeks and histology and immunostaining were performed at the indicated time points. **(A)** H&E staining of SEs from NHEK demonstrates accelerated cornification, particularly evident upon 5 μM VEM (left). Also, HrasA5 epithelia showed a time-dependent increase in cornification. In addition, invasion was seen after 3 (1 μM VEM) and 1 week (5 μM VEM), respectively (right). **(B)** Improved differentiation is confirmed by immunostaining for the early, KRT10, and the late differentiation markers FLG and KRT2 in the epithelium of the NHEKs (left) and the HrasA5 cells (right). The BM components COLVII (green), COLIV (red), and LAM (red) are expressed as contiguous lines in NHEK SEs at all time points and all conditions. Note that COLIV is expressed continuously and present throughout the DE; though enriched in the BM zone (left). In HrasA5 SEs, COLVII is generally reduced and lost at the invasive front. COLIV and LAM rather appear "bloated" with the tumor cells pushing through small gaps (right). **(C)** Same SEs stained for the proliferation marker H3S10ph (red), demonstrating very similar proliferation for all NHEK SEs (left). In HrasA5 SEs, proliferation is present throughout the epithelium (control). Under VEM, proliferation gets restricted to the basal compartment (right). All SEs are counterstained for the early differentiation marker transglutaminase 1 (TGM). **(D)** For quantification of proliferation SEs from NHEK and HrasA5 cells were costained with COLVII and KI67 and the number of proliferating cells (KI67+) correlated with BM (COLVII) length. Neither NHEKs nor HrasA5 cells showed a significant regulation in proliferation (n = 2, mean + SEM, one-way ANOVA + Dunnett's multiple comparison test; ns, not significant). For all conditions, nuclei were counterstained with DAPI (blue). Treatment with the DMSO was used as control. Time specifications relate to time after starting the scale bar = 300 μm [for **(A, C)**]; scale bar = 150 μm [for **(B)**].

whether in the context of invasion, vemurafenib might trigger proliferation. First, we performed staining for the proliferation marker PHH3 [phosphorylated Histone H3-H3s10ph (serine 10 phosphorylated)] on SEs treated with 1 or 5 μM vemurafenib for 3 weeks (**Figure 3C**) and found similar low proliferation for control and vemurafenib-treated NHEKs. In HaCaT SEs, vemurafenib rather reduced proliferation and mediated improved tissue organization by restricting the proliferating

cells to the basal compartment. The same result was observed for the HrasA5 SEs. We additionally quantified proliferation by performing staining with the commonly established proliferation marker Ki67 (**Figure 3D**). Thereby, we found the same low proliferation rate in untreated and vemurafenib-treated NHEK SEs, suggesting that different from conventional cultures, vemurafenib does not constrain keratinocyte growth in the tissue context (see **Figure 1**). For HrasA5 cells, we find an increasing variance between different SEs, with a trend (not statistically significant) towards enhanced proliferation upon vemurafenib treatment (**Figure 3D**). Together, this suggests that the role of vemurafenib on keratinocyte growth is dependent on the respective environment, and we conclude that proliferation is not a major driving force for the invasive growth of the HrasA5 cells.

Vemurafenib Mediates Sustained pERK Activation in SEs

To obtain more insight into the mechanism of vemurafenib-induced invasion, we first investigated vemurafenib-dependent MEK-ERK hyperactivation in the SEs. Using pERK1/2 as a marker for active ERK signaling, we show that pERK1/2 is absent in untreated epidermis but expressed in the suprabasal layers of the epidermis of vemurafenib-treated NHEK (**Supplementary Figure S3**). In HaCaT epithelia, the MEK-ERK kinase pathway appeared constitutively active as indicated by some minor pERK1/2 staining within the epithelium. Upon vemurafenib (5 μM) treatment, however, staining for pERK1/2 strongly increased throughout the living part of the epithelium (**Supplementary Figure S2C**). Similarly, in HrasA5 epithelia, pERK1/2 was already increased upon treatment with 1 μM vemurafenib, and expression became strongly upregulated with 5 μM vemurafenib where it was particularly prominent at the invasive front and in the invasive nodules (**Supplementary Figure S3**). As proof for the presence of ERK, nonphosphorylated ERK1/2 was shown to be expressed rather evenly throughout the epithelium. Thus, corresponding to the expression in conventional (2D) cultures (see **Figure 1**), vemurafenib induced and sustained hyperactivation of the MEK-ERK pathway also in the epithelia of the SEs.

Vemurafenib Does Not Regulate Basement Membrane Integrity

To determine the conditions for invasive growth, we asked whether the basement membrane (BM) structure may be modulated by vemurafenib in order to precondition the environment for rapid tumor cell invasion. We, therefore, analyzed expression and deposition of three different BM components, i.e., collagen type IV (Col IV), collagen type VII (Col VII), and laminin 332 (LAM). This study demonstrated regular expression and continuous linear deposition between epithelium and dermal equivalent for all three BM components at all time points and both vemurafenib concentrations in the NHEK-SEs (**Figure 3B**). Similarly, HaCaT SEs showed a regular distribution of the BM components also under vemurafenib treatment (**Supplementary Figure S2B**). This was, different for HrasA5 cells (**Figure 3B**). While HrasA5 control SEs exhibited a regular distribution of the BM components, treatment with vemurafenib caused changes that were however, strictly linked to invasion of the keratinocytes. Accordingly, Col VII became degraded at the invasive front and remained discontinuous further on. Col IV and LAM were rather pushed aside by the invasive front. Thus, our data suggest that the BM is not a general target of vemurafenib, instead, it gets altered/degraded only in concert with the invasive process initiated by activating the HrasA5 keratinocytes.

Invasion Is Regulated by Vemurafenib-Dependent Induction of Epidermal MMP1 and MMP3

The *in vitro* expression analyses have shown that MMP1 and MMP3 represented the genes with the strongest upregulation upon vemurafenib treatment and irrespective of the transformation state of the keratinocytes. Nevertheless, only HrasA5 cells showed BM degradation and active invasion into the underlying dermal matrix when grown in SEs. To address this discrepancy, we first investigated MMP expression in the SEs (**Figures 4A, B**). Staining of the different SEs for MMP1 and MMP3 showed that both MMPs were expressed upon vemurafenib treatment (5 μM) in all epithelia of NHEK, HaCaT, and HrasA5 cells (**Figures 4A, B**). However, and as compared with NHEK SEs, there appeared to be increased expression of MMP1 in the HaCaT and HrasA5 epithelia (**Figure 4A**) and a particular increase in the HrasA5 epithelia for MMP3 (**Figure 4B**). It is noteworthy that MMP1 and MMP3 were expressed also by the dermal fibroblasts (**Figures 4A, B**).

To determine whether the differences in staining intensity may point to quantitative differences in the expression of MMP1 and MMP3 in HrasA5 versus HaCaT SEs, we next performed ELISA for secreted MMP1 and MMP3. As MMP9 mRNA has shown a slight upregulation in the cultured cells, particularly in HrasA5 cells (see **Figure 2A**), we also included MMP9 in this analysis. While HaCaT SEs only secreted significantly increased levels of pro-MMP1, HrasA5 SEs demonstrated significant levels of both MMP1 and MMP3 upon vemurafenib treatment (5 μM) for 3 weeks (**Figure 4C**). MMP9 was present at similar levels with and without vemurafenib, suggesting that MMP9 is not induced by MEK-ERK hyperactivation and thus, not of major relevance for HrasA5 invasion in this scenario.

In line with the increased MMP secretion, proteolytic activity, as assessed by the gelatinase assay, was only seen in HrasA5 SEs (**Figure 4D**), suggesting that MMP3 either alone or in combination with MMP1 is mainly responsible for invasion of HrasA5.

Inhibition of MMP Causes Reversion of the Invasive Phenotype

To substantiate the role of the MMPs for vemurafenib-dependent invasion, we established SEs with HrasA5 cells and selectively interfered with MMP activity by cotreatment with vemurafenib (5 μM) and the broad band MMP inhibitor ilomastat (10 μM). SEs treated with vemurafenib only, revealed

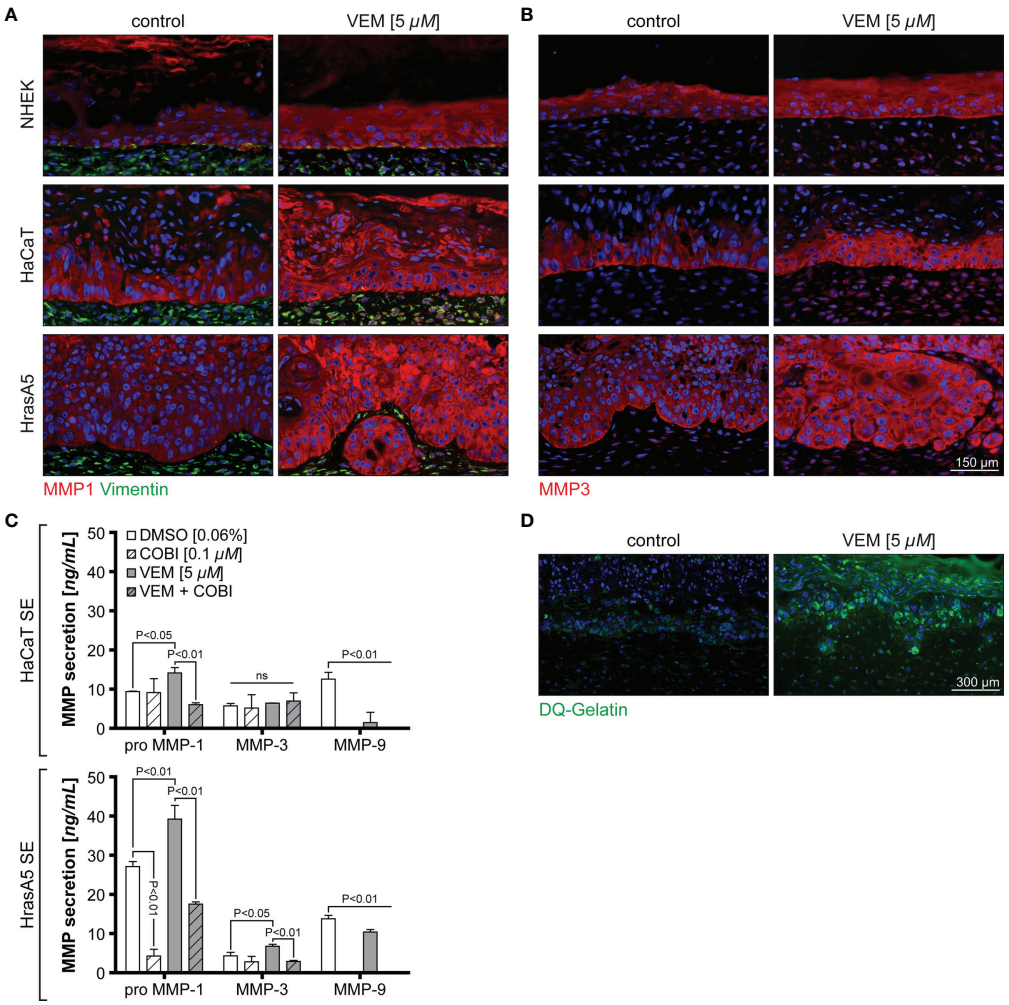

FIGURE 4 | Vemurafenib-dependent degradome. SEs from NHEK, HaCaT cells, and HrasA5 cells were treated with vemurafenib (VEM) (5 μM) for 3 weeks and sections of control (DMSO) and VEM-treated SEs were stained for MMP1 and vimentin **(A)** and MMP3 **(B)**. Nuclei were counterstained with DAPI. All VEM-treated samples show a clear upregulation of both MMPs scale bar = 150 μm. **(C)** ELISA for HaCaT and HrasA5 SEs treated with DMSO (control), cobimetinib (COBI), VEM, and the combination of COBI and VEM with the indicated concentrations. Secretion of MMP1, MMP3, and MMP9 were quantified (n = 3, mean ± SD, one-way ANOVA + Dunnett's multiple comparison test; ns, not significant). **(D)** Gelatinase assay confirms a strong proteolytic activity (green) in the VEM-treated (5 μM) HrasA5 SEs compared with the untreated controls. Scale bar = 300 μm.

the typical induction of differentiation and invasion (**Figure 5A**). Upon cotreatment with ilomastat, the vemurafenib-specific differentiation phenotype was maintained, i.e., the cells continued to build a surface epithelium with a massive stratum corneum. However, the invasive phenotype was clearly suppressed. The early phase of vemurafenib-induced invasion is characterized by a smooth borderline of the invasive front extending into the stroma (**Figure 5A**) and degradation of the BM components LAM and most extensively Col VII (**Figure 5B**). In addition, dermal collagen fibers were affected. By picrosirius red staining, that allows a quantitative morphometric evaluation of the collagen bundles under polarized light, we could confirm the degradation of collagen fibers below the epithelium and at the invasive front of vemurafenib-treated SEs (**Figure 5C**). The entire process was halted upon the addition of ilomastat as shown by a sharp demarcation zone (**Figure 5A**) with a continuous linear deposition of LAM and Col VII (**Figure 5B**) as well as preservation of the collagen fiber network (**Figure 5C**). A confirmative quantification of fibrillar collagen was performed by means of image analysis of those picrosirius red-stained sections and normalized to the level of control SEs (100%, standard deviation (SD) 18.80%). Vemurafenib-treated SEs showed a reduction to 48.80% (SD 13.18%) that was fully outweighed to 100.85% (SD 17.04%) by cotreatment with ilomastat. Together, these data support our hypothesis that vemurafenib-dependent induction of MMP1 and MMP3 is in charge of the rapid tumor cell invasion seen in SEs with the HrasA5 cells.

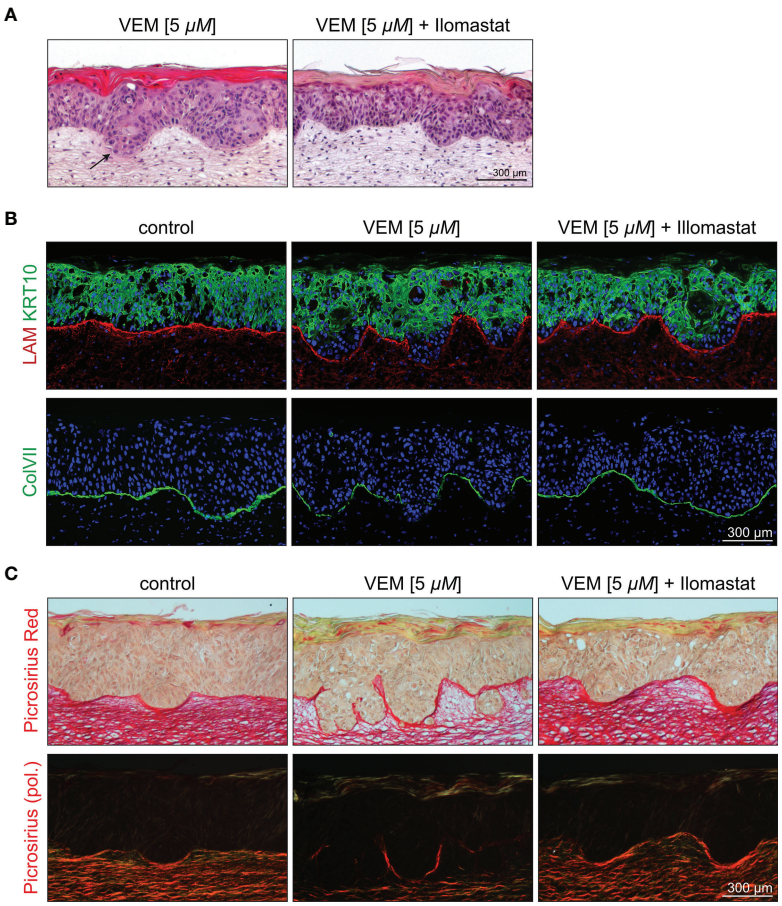

FIGURE 5 | Inhibition of the vemurafenib-dependent degradome in HrasA5 SEs by suppressing MMP activity. **(A)** H&E-stained HrasA5-SEs under vemurafenib (5 μM) exhibit an invasive phenotype with signs of subepithelial disintegration under the invading pegs (left, arrow), a physiological state not seen in SEs treated in addition with the MMP inhibitor ilomastat (10 μM) (right). **(B)** Staining for the BM-components LAM (red, above) and ColVII (green, bottom) points to a pronounced degradation upon vemurafenib (middle) when compared with untreated control SEs (left). Additional application of ilomastat prevents proteolysis and allows for an uninterrupted BM (right). Likewise, delayed onset of KRT10 expression (green, middle, above) is widely renormalized by ilomastat (right, above). **(C)** Beyond the BM, also the subepithelial extracellular matrix is affected by the increased proteolytic activity. Picrosirius red staining visualizes semiquantitatively the amount of stromal collagen in bright field microscopy (above) and even more clearly in circular polarization microscopy that specifically highlights organized collagen bundles (bottom). Whereas under vemurafenib the density of collagen fibers is drastically reduced to 48.80% (middle), cotreatment with ilomastat completely preserves the control state (100.85% vs. 100%, right vs. left). Scale bar = 300 μM.

MEK Inhibitor Cobimetinib Abrogates the MEK-ERK Hyperactivation of Vemurafenib

It is suggested that combination therapy of vemurafenib with the MEK inhibitor cobimetinib is not only more effective in combating resistance of melanoma cells but also in preventing cutaneous adverse events, including the formation of cSCCs [for review, see, e.g., (26)]. Cobimetinib is inhibiting MEK1 (and partially also MEK2) and thereby hinders ERK1/2 phosphorylation and abrogates vemurafenib-dependent MEK-ERK hyperactivation (27). Therefore, we asked how cobimetinib would affect epithelial tissue regulation and whether it would be able to counteract the vemurafenib-induced cutaneous adverse events.

As the RAS-MEK-ERK pathway is involved in many important cellular functions, we were concerned about possible toxicity when completely blocking MEK function in cells or tissues. We therefore first applied 0.1 and 1 μM cobimetinib alone for 3 weeks to HrasA5 SEs. While 0.1 μM cobimetinib already caused some tissue atrophy, strong toxicity was seen with 1 μM, as only remnants of epithelial islands remained, and the number of dermal fibroblasts was reduced as well (**Supplementary Figure S4A**).

We next sought for the cobimetinib concentration which would be sufficient to counteract vemurafenib-induced MEK-ERK hyperactivation by establishing a dose-response profile for the HrasA5 cells. Cultures of HrasA5 cells were treated with either 1 or 5 μM vemuarafenib in combination with increasing doses of cobimetinib (0.01, 0.1, and 1 μM). We found a concentration-dependent increase in P-MEK—due to inhibition of active, phosphorylated MEK [e.g., (12)]—and a blockade of ERK1/2 phosphorylation because of inhibited MEK activity (**Supplementary Figure S4B**). As little as 0.01 μM cobimetinib

was sufficient to block ERK1/2 phosphorylation in combination with 1 μM vemurafenib, while 0.1 μM was required to block ERK1/2 phosphorylation induced by 5 μM vemurafenib. Thus, by combining the data from the toxicity assay with the inhibitory capacity of the vemurafenib-induced hyperactivation by cobimetinib, 0.1 μM was chosen as concentration for further assays.

To determine the molecular consequence accompanying abrogation of ERK signaling, we treated HrasA5 cells with vemurafenib (5 μM) alone or in combination with cobimetinib (0.1 μM) and analyzed transcription of those genes that were regulated by vemurafenib (**Supplementary Figure S4C**; see **Figure 2A**). Accordingly, expression of *TGF-α*, *IL-1A*, *IL-1B*, *IL-8*, *MMP1*, *MMP3*, and *MMP9*, was inhibited upon cotreatment with cobimetinib. *MMP-14* remained unaffected and unexpectedly, the differentiation-specific genes, *KRT10* and *FLG*, were stimulated upon cotreatment, corroborating that the epidermal differentiation markers are not regulated directly by MEK-ERK signaling in the transformed HrasA5 cells.

Cobimetinib Cotreatment Impedes Vemurafenib-Induced Differentiation and Invasive Growth

To determine the physiological relevance of vemurafenib-cobimetinib cotreatment, we next performed SEs with HrasA5 cells treated with vemurafenib (5 μM) or cobimetinib (0.1 μM) applied for 3 weeks either individually or in combination and investigated for their functional consequences.

As demonstrated in **Figure 6**, the treatment of HrasA5 SEs with cobimetinib (0.1 μM) largely abolished pERK1/2 expression, and as expected from the previous experiments (see **Supplementary Figure S4**), this correlated with signs of epithelial atrophy. Vemurafenib (5 μM), on the other hand, caused the characteristic MEK-ERK hyperactivation, as indicated by strong and extended pERK1/2 staining, particularly also at the invading front. This increased ERK activation correlated with pronounced differentiation, recognized by a distinct parakeratotic stratum corneum, and with rapid and ongoing tumor cell invasion. Importantly, cotreatment with cobimetinib strongly reduced the level of pERK1/2, and this was sufficient to hinder atrophy but also to impede both, induction of accelerated differentiation and tumor cell invasion. It is also important to note, that pERK1/2 was not completely abolished but reduced to a similar level as in controls, likely owing to the active Hras oncogene, what might be the reason that epithelial atrophy was counteracted (**Figure 6A**). Repeating a similar set of experiments with the HaCaT cells demonstrated an even more pronounced inhibition of pERK 1/2 upon treatment with cobimetinib alone or in combination with vemurafenib, with the consequence of increased epithelial atrophy (data not shown).

With the halted expression of the MMP RNAs upon cotreatment of vemurafenib and cobimetinib (see **Supplementary Figure S4**) also secretion of the MMPs was inhibited as quantified by enzyme-linked immunosorbent assay (ELISA) (see **Figure 4C**). As a consequence of this, proteolytic activity was strongly reduced in the epithelia of the HrasA5 SEs (**Figure 6C**) and BM integrity was maintained, as demonstrated for the most critical BM component, COL VII, in both the HaCaT and HrasA5 SEs (**Figure 6D**).

Finally, we labeled untreated, vemurafenib-treated, and vemurafenib+cobimetinib cotreated SEs of HaCaT and HrasA5 cells with BrdU to detect S-phase cells in epidermal whole mounts (28). As epidermal proliferation is generally focal, we used this third and most unbiased approach for ensuring precise enumeration (**Figure 6E**). Also, the analysis of large tissue areas demonstrated that vemurafenib did not induce proliferation, particularly not in HrasA5 epithelia, and that the combination treatment did not affect proliferation as well.

Together, this indicates that cobimetinib efficiently blocks the vemurafenib-dependent MEK-ERK hyperactivation. It thereby clearly demonstrates that both, the vemurafenib-specific differentiation and the invasion phenotype, are under direct control of MEK-ERK hyperactivation. Furthermore, our multistep skin carcinogenesis model revealed the ras-oncogene as decisive element provoking immediate tumor cell invasion.

Vemurafenib Also Modulates the Microenvironment: Vemurafenib Causes a Differential Expression Profile in Dermal Fibroblasts in Conventional Cultures Versus Dermal Equivalents

As tissue regulation is controlled by an extensive communication and interaction between epidermis and dermis, we hypothesized that vemurafenib may similarly affect the microenvironment, i.e., the dermal fibroblasts. To address this, we first determined whether normal human dermal fibroblasts (NHDFs) are activated by vemurafenib in a similar manner as the human skin keratinocytes. Two fibroblast strains derived from adult trunk skin were treated with 1 and 5 μM vemurafenib in conventional culture (**Figure 7A**). This caused sustained activation of pMEK and pERK and temporary activation of p38 (at 30 min), demonstrating that vemurafenib-dependent MEK-ERK hyperactivation also arises in the BRAF wildtype dermal fibroblasts.

We next established an expression profile for different growth factors, cytokines, MMPs, indicators for the Wnt (*AXIN2*) and p21 (*CDKN1A*) pathway, and myofibroblast transformation [alpha smooth muscle actin (*αSMA*)] (**Figure 7B**). Different from the distinct regulatory activity seen in the keratinocytes, only little gene regulation occurred in the fibroblasts and none of the selected genes reached 2-fold regulation. *CXCL12*, *CXCL10*, *FGF7 (KGF)*, *FGF10*, and *CSF2* (GM-CSF) as well as *MMP3* and *MMP9* were upregulated approximately 1.5-fold.

In conventional cultures, fibroblasts are permanently activated and highly proliferative while *in situ*, i.e., in intact skin or in DEs, they are largely growth arrested. To determine how this physiological difference would influence the expression response to vemurafenib, we investigated the expression of the same genes in fibroblasts from DEs. To exclude any epidermal impact, "naked" DEs without keratinocytes were treated with vemurafenib (1 and 5 μM) for 3 weeks and further analyzed.

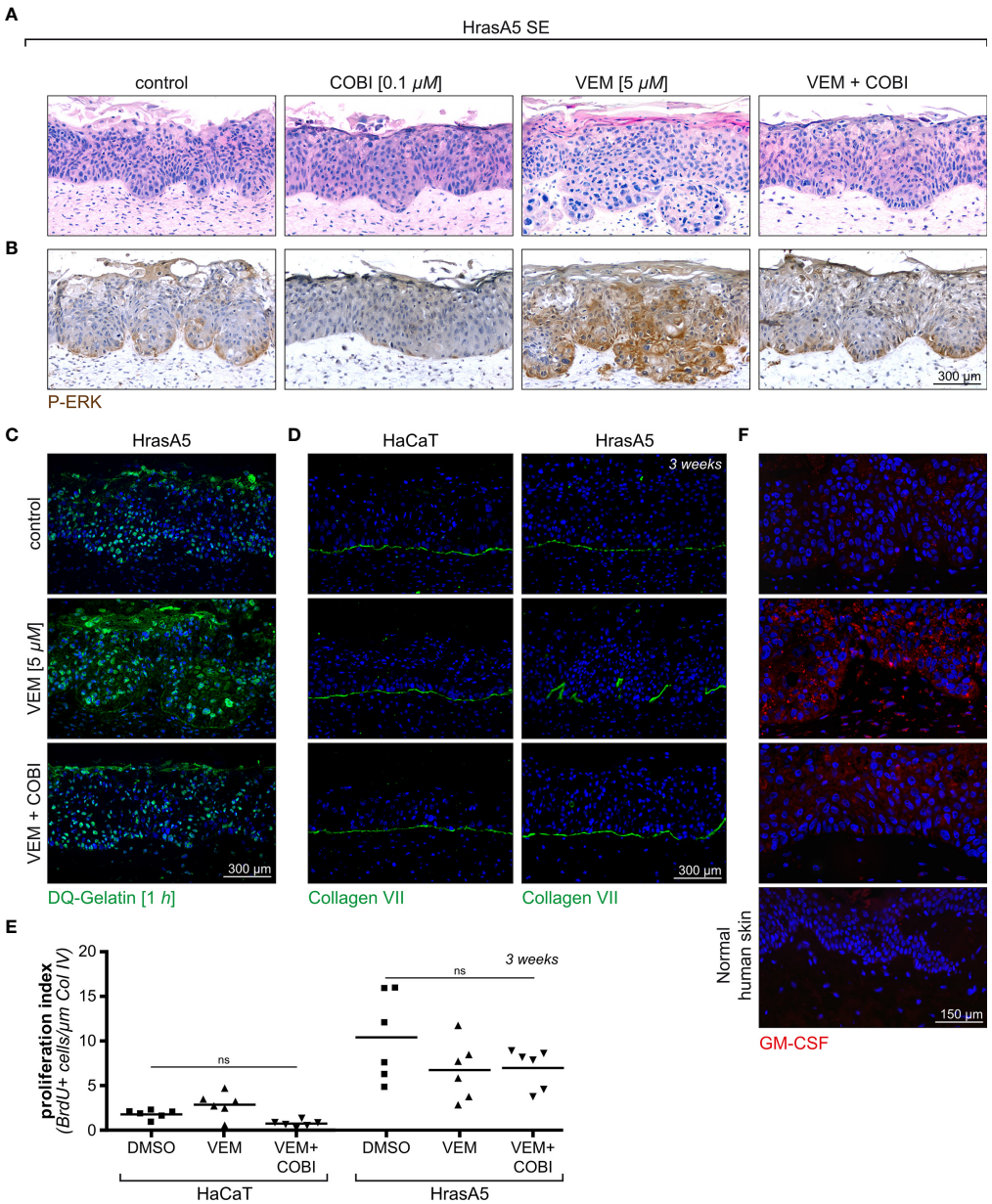

FIGURE 6 | Cotreatment of HrasA5-SEs with vemurafenib and cobimetinib. **(A)** HrasA5 SEs were treated with vemurafenib (VEM) alone (5 μM), cobimetinib (COBI) (0.1 μM) alone, or the combination of both inhibitors for 3 weeks. The histologic H&E stainings demonstrate the respective phenotypes. **(B)** Immunohistochemistry for pERK1/2 of corresponding sections confirms the vemurafenib-dependent increase in pERK and its suppression down to control level by cobimetinib. **(C)** Proteolytic activity *in situ*, visualized by the fluorescent gelatinase assay, results in an intense labeling in vemurafenib-treated SEs (middle) as opposed to a weak labeling in vemurafenib + cobimetinib-treated SEs (bottom), thus providing functional proof for the drop in MMP-expression caused by cobimetinib. **(D)** Immunostaining for COLVII (green) as indicator for BM integrity demonstrates the effectivity of cobimetinib in blocking degradation and invasion in HrasA5-SEs (right column). The noninvasive HaCaT-SEs have an undisturbed BM under all conditions tested (left column). **(E)** Quantification of proliferating cells in whole mounts of HaCaT- and HrasA5-SEs (BrDU positive cells/μm of Col IV) does not show significantly diverse proliferation rates under the different conditions (n = 3, mean, one-way ANOVA + Dunnett's multiple comparison test; ns, not significant). **(F)** GM-CSF is only faintly detectable by immunofluorescence analysis (red) in normal skin (4th from top) and in HrasA5-SE controls (top) while clearly visible in the epithelium and dermal fibroblasts of vemurafenib-treated SEs (2nd from top). Cotreatment with cobimetinib largely abrogates the GM-CSF signals (3rd from top). Scale bar = 300 μm [for **(A–D)**] Scale bar = 150 μm [for **(F)**].

Interestingly, we saw an increase in the number and intensity of genes regulated by vemurafenib. Specifically, we found a >1.5-fold induction of *IL-1A* and *IL-1B* (both also regulated in the keratinocytes), *IL-6*, *IL-8*, and *CXCL10*. *CSF2* (GM-CSF), an important regulator of epidermal growth and differentiation (29, 30) even reached a 2-fold increase. *MMP3* and *MMP9* were upregulated (1.75-fold) and to a very minor degree also *MMP1*. *MMP14* remained unaffected also in the fibroblasts, pointing

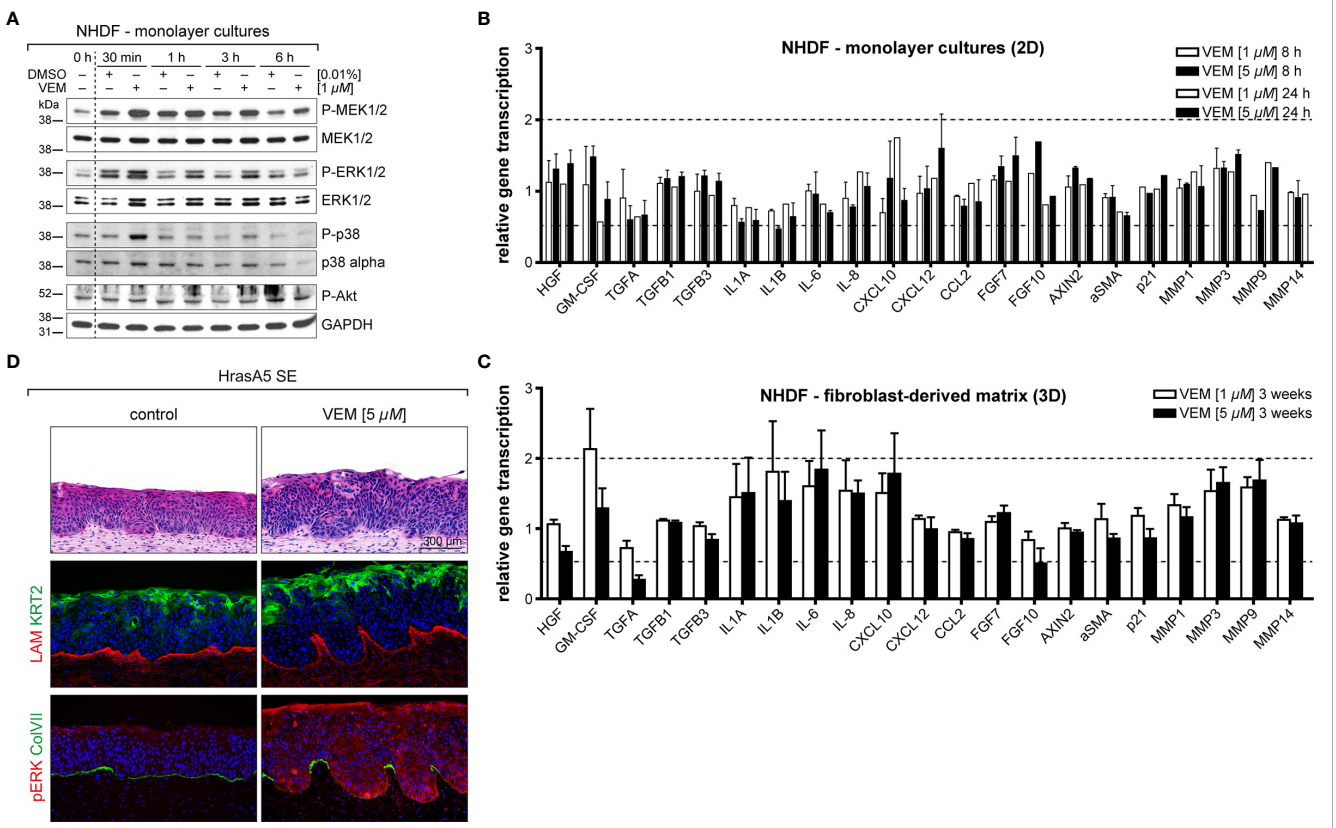

FIGURE 7 | The impact on vemurafenib (VEM) the dermal microenvironment. **(A)** Western blot analysis of vemurafenib-treated fibroblasts (1 μM in monolayer cultures) demonstrates a quick rise in pMEK, pERK, and pp38 alluding to a pathway activation. **(B)** RNA expression analysis of fibroblast monolayer cultures for genes that are relevant for epidermal-stromal interaction demonstrates only little gene regulation upon vemurafenib. **(C)** RNA expression analysis for the same genes in 3D-cultivated fibroblasts (DEs), treated for 3 weeks with vemurafenib, shows enhanced expression of GM-CSF, interleukins, and MMPs. For **(B, C)**, normalization was performed using GAPDH as a house-keeping gene and foldchanges were expressed by comparing 1 or 5 μM vemurafenib treatment of NHDF to DMSO stimulation. $n = 2$, mean ± SD. **(D)** Vemurafenib-pretreated DEs are able to convey the vemurafenib effect when combined with HrasA5 keratinocytes: H&E stainings of HrasA5-SEs demonstrate invasion and differentiation of HrasA5 cells (top, right) as compared with untreated controls (top, left). Immunofluorescence staining for COL IV (red) presents a regular continuous BM in controls (middle left) while being reduced under the invading epithelial pegs on pretreated DEs (middle right). In the latter, boosted differentiation is indicated by enhanced KRT2 (green). In control SEs, pERK is not detectable (red, bottom left), instead a continuous BM is demarcated by COL VII (green). On pretreated DEs, HrasA5 epithelia show intense pERK staining, being particularly enriched in the invading epithelial pegs. COL VII is degraded, leaving only small patches between the invading fronts (bottom, right). Scale bar = 300 μm.

again to a specific set of MMPs as being direct targets of MEK-ERK hyperactivation (**Figure 7C**).

Vemurafenib-Pretreated DEs Contribute to the Vemurafenib-Specific Epidermal Phenotype

To determine whether and how this regulation might contribute to the vemurafenib-dependent skin phenotype, we added HrasA5 cells onto vemurafenib-pretreated DEs and maintained them as cocultures (SEs) for 3 weeks without further addition of vemurafenib. Most excitingly, histology of these SEs indicated that an epidermal phenotype was established (**Figure 7D**). Vemurafenib-dependent preconditioning of the DEs contributed to epidermal differentiation, as demonstrated by an increase in KRT2-positive cells and the appearance of horn-pearls within the epithelium. In addition, the keratinocytes formed large protrusions advancing into the dermal equivalent. While LAM was still present as a contiguous line, though strongly diminished at the invasive sites, Col VII was largely absent at the basal pole of the protrusions (**Figure 7D**), suggesting an incipient BM degradation. Staining for pERK1/2 clearly demonstrated ERK activation in the dermal fibroblasts (**Figure 7D**). Interestingly, pERK1/2 was also evident in the epidermal protrusions. Although some pretreatment-dependent storage of vemurafenib cannot be excluded, it is tempting to suggest this is the result of a paracrine ERK activation through the vemurafenib-stimulated microenvironment.

Based on the fact that *CSF2* (GM-CSF) was the most upregulated gene in the vemurafenib-treated DEs, we hypothesized that the increase in GM-CSF would contribute to the epidermal phenotype, i.e., would support accelerated epidermal differentiation upon vemurafenib treatment. Accordingly, we show a strong increase in GM-CSF in vemurafenib-treated SEs (**Figure 6F**) and demonstrate

that cotreatment with cobimetinib abolished the overexpression of GM-CSF (**Figure 6F**) as it prevented increased differentiation.

Together, these data demonstrate that dermal fibroblasts are also activated by vemurafenib and contribute with their specific expression profile to the epidermal phenotype. This highlights the importance of the interplay of epidermal and dermal regulation on the skin phenotype upon vemurafenib treatment.

Perilesional Skin and cSCCs of Vemurafenib-Treated Melanoma Patients Exhibit a Similar Expression Profile as SEs

Finally, to establish the connection of our experimental findings to clinical cases, we investigated biopsies from vemurafenib-treated melanoma patients. Samples of perilesional skin and different skin tumors (viral warts and different stages of cSCC) were analyzed for hyperactivation of the MEK-ERK pathway by staining for pERK1/2, activation of epidermal MMP1 and MMP3 expression, as well as stromal upregulation of GM-CSF.

Comparing normal skin from healthy donors to perilesional skin from the melanoma patients, we found a slight increase of pERK1/2 as well as an even more extensive increase in pERK1/2 expression in warts and tumor samples (**Figure 8A**), thereby confirming vemurafenib-dependent MEK-ERK activation also in skin keratinocytes *in situ*. Similarly, we found expression of MMP1 and MMP3 with a rise in staining intensity from perilesional skin to cSCC (**Figures 8B, C**). As staining for both MMPs was particularly prominent in the epithelium, it is tempting to suggested that the keratinocytes are the primary target for the vemurafenib-stimulus inducing MMP expression. In addition, staining for the tissue inhibitor of metalloproteinases, TIMP-1, as one of the endogenous MMP inhibitors, showed reduction in perilesional skin as well as tumor samples as compared with normal healthy skin (**Figure 8D**), which may support an increasing imbalance in favor of the degradative phenotype with vemurafenib treatment. GM-CSF was hardly detected in normal human skin but expressed by fibroblasts of perilesional skin and strongly enhanced in the fibroblasts of the tumor microenvironment (**Figure 8E**), suggestive of a role for GM-CSF in the paracrine regulation of epidermal growth and differentiation also *in situ*.

Activated fibroblasts, such as cancer-associated fibroblasts (CAFs), are believed to have a strong tumor-modulating potential also for cSCC (31, 32). In agreement with our experimental analysis which did not provide evidence for a vemurafenib-dependent regulation of *TGF-β* or *αSMA* in fibroblasts (see **Figure 7C**), we found αSMA-positive blood vessels for all tissue samples but rarely identified αSMA-positive fibroblasts suggesting that myofibroblasts/CAFs may not be a major player in vemurafenib-induced cSCC development (**Figure 8C**).

In recent years, the role of immune cells in controlling tumor growth and progression has also gained considerable interest. Accordingly, immunosuppressive regulatory T cells (Tregs) were shown to be present in the immune infiltrate of cSCCs, and it was suggested that they may contribute to an ineffective antitumor immune response and promote SCC development, aggressiveness, and metastasis (33, 34). Utilizing a CD3ζ antibody, we stained all tumor samples for the T-cell receptor. Being aware of the fact that CD3ζ is not all-embracing for immunoregulatory T cells, our stainings indicate that with the exception of one tumor, showing some accumulation of T cells in the stroma and within the tumor, all others only showed few T cells scattered throughout the stroma (**Figure 8D**).

Taken together, we find a similar regulation in perilesional skin and cSCCs of the vemurafenib-treated melanoma patients as we did in our skin and skin cancer models. This directly links vemurafenib-induced MEK-ERK hyperactivation to increased differentiation and hyperkeratotic lesions, as well as to MMP-dependent tumor cell invasion, which culminates in rapid onset of cSCCs. In addition, we demonstrate a role for a tight interaction of the epidermal keratinocytes and the stromal fibroblasts in the development of the vemurafenib-specific phenotype while carcinoma-associated fibroblasts (CAFs) and/or regulatory T cells may not be of major relevance for this process.

DISCUSSION

In this study, we demonstrate that vemurafenib hyperactivates MEK-ERK signaling in two major cell types of the skin, the epidermal keratinocytes and the dermal fibroblasts, and highlight the importance of this activation for the underlying pathogenesis. We utilized long-term skin equivalents to allow for the investigation of both cell types in their physiological environment. In addition, we used keratinocytes of different genetic background (NHEK, HaCaT [p53 mut], and HrasA5 [p53 mut + Hras mut]. Thereby, we confirm vemurafenib-dependent hyperactivation of the MEK-ERK pathway in the epithelia of all keratinocyte variants and confirmed a similar regulation as seen in monolayer cultures of dermal fibroblasts and keratinocytes. These findings are in line with the observed hyperactivation in several BRAF wildtype cell lines that can be explained by dimerization and downstream activation of RAF proteins due to sterical properties of vemurafenib (12, 13, 35). Accordingly, Poulikakos et al. (35) had shown that binding of vemurafenib to the ATP-binding site of one kinase of the RAF dimers (either as CRAF homodimers or CRAF-BRAF heterodimers) causes transactivation of the drug-free protomer and that this transactivation was required for hyperactivating ERK signaling. Thereby, they demonstrated that inhibitor-dependent sterical transactivation was the reason for the paradoxical activation of the CRAF enzyme (35).

Alternatively, MAP3K8, the gene encoding COT/Tpl2, was identified as a MAPK pathway agonist that activates ERK primarily through MEK-dependent mechanisms that do not require RAF signaling (36). Furthermore, TPL2 downstream signaling mediated cell transformation in immortalized human keratinocytes and tumorigenesis in mice and was shown to be overexpressed in metastatic cSCC and KAs (37), Vemurafenib-dependent ERK activation *via* release and activation of COT/TPL2 may also be considered for the human keratinocytes.

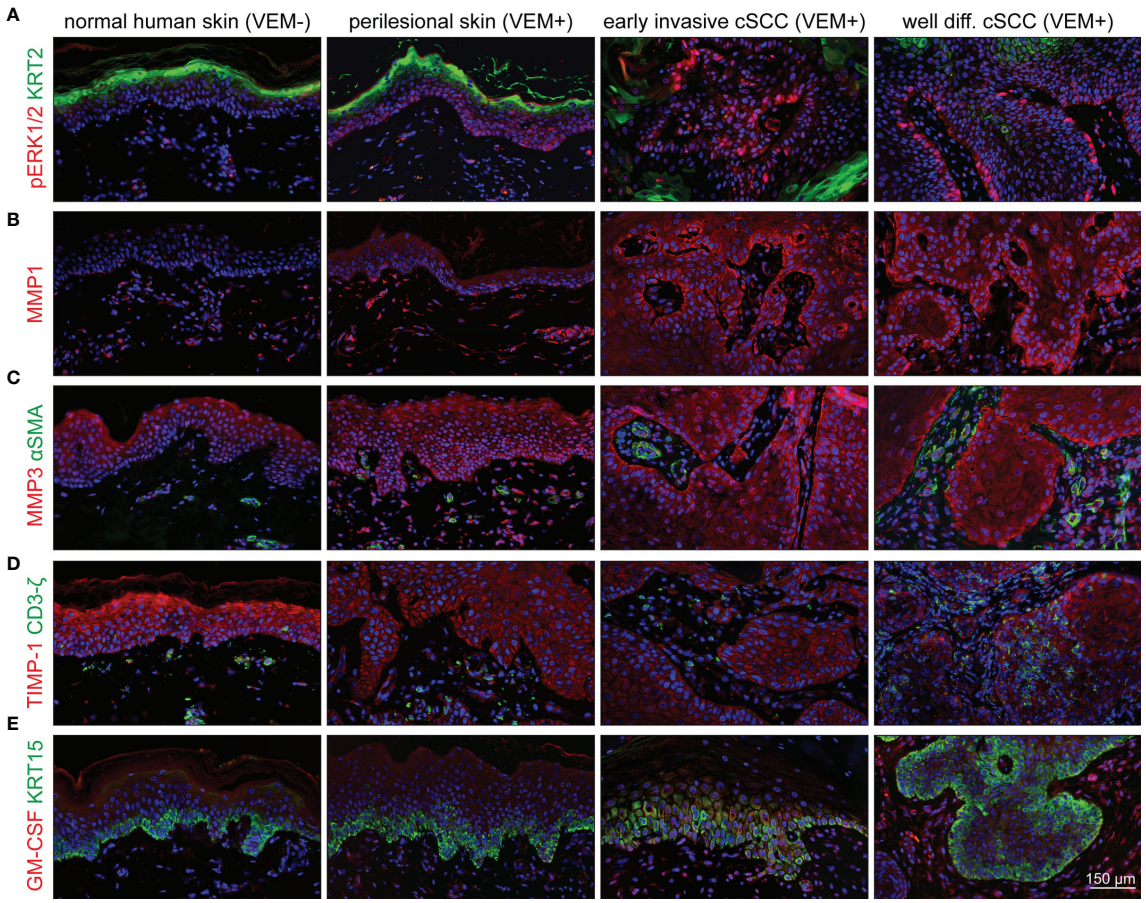

FIGURE 8 | Activation of the MEK-ERK pathway in cutaneous lesions of patients under vemurafenib treatment. Components and targets of the pathway are detected by immunofluorescence microscopy in normal skin (first column) compared with perilesional skin (second column), early invasive SCCs (third column), and well-differentiated SCCs (fourth column). **(A)** Under vemurafenib, pERK (red) is upregulated in the nuclei of basal epidermal cells; KRT2 (green) demarcates terminally differentiated upper epidermal cells. **(B)** The intensity of MMP1 staining (red) significantly increases under vemurafenib treatment and shows enrichment in the invading epithelia. **(C)** MMP3 displays a moderate epithelial staining (red) in normal skin that gains intensity under treatment and progression towards SCC. Also dermal cells stain positive for MMP3. No signs of myofibroblast differentiation; αSMA (green) staining is restricted to vascular structures. **(D)** Decreased intensity of TIMP-1 (red) correlates with an acquired invasive phenotype under vemurafenib; CD3ζ-positive T-cells (green) do not show any significant accumulation. **(E)** Faint epithelial GM-CSF signals (red) are accompanied by a well-detectable staining of stromal cells under vemurafenib, particularly in SCCs. The epidermal basal layer is defined by staining for KRT15 (green). Scale bar = 150 µm.

Regardless of pathway initiation, we show that vemurafenib-dependent MEK-ERK hyperactivation is associated with accelerated differentiation and hyperkeratosis in the normal keratinocytes and normalized stratification and cornification in the transformed keratinocytes. Vemurafenib-dependent pathophysiological changes, i.e., the initiation of invasive growth, as part of tumorigenic conversion, is exclusive for the ras oncogene-expressing keratinocytes, suggesting a combined mechanism of MEK-ERK activation and the intersecting ras oncogenic network. This is also in line with investigations on the mode of action by vemurafenib in BRAF wildtype cells, suggesting the requirement for an upstream Ras activity for the induction of pathway hyperactivation (12).

This interpretation is based on the fact that neither HaCaT cells with vemurafenib-induced hyperactivation of MEK-ERK signaling nor Hras oncogene expressing cells with intrinsic RAS-MEK-ERK activation gain a tumorigenic phenotype. Only the combination of vemurafenib-induced MEK-ERK hyperativation with Hras oncogene expression in the HrasA5 cells, leads to the rapid onset of a proteolytic phenotype with secretion and activation of MMP1 and MMP3. This prepares the path for the keratinocytes to degrade and penetrate the BM and to invade into the degraded underlying collagen matrix. Thus, the MEK-ERK/MMP axis represents the most important molecular basis for the switch towards tumorigenic conversion upon vemurafenib treatment.

The MEK-ERK-signaling pathway as an integral part of the cellular regulatory network is classically induced through epidermal growth factor receptor (EGFR) or constitutively active in ras oncogene-containing cells and is involved in cell proliferation, migration, and inhibition of apoptosis (16). In agreement with previous studies, we show that the BRAF

inhibitor vemurafenib causes MEK-ERK hyperactivation in human skin keratinocytes and dermal fibroblasts, and thereby induces a variety of physiological consequences. Accordingly, it was shown earlier, that vemurafenib stimulated growth in HaCaT cells (18) and mouse skin (14). Interestingly, for two different normal keratinocyte strains (NHEK) as well as the p53-mutant HaCaT cells and its ras-containing variant HrasA5, we could not confirm vemurafenib-dependent growth stimulation. On the contrary, NHEK (2D cultures) were growth inhibited when exposed to 1 and 5 μM vemurafenib and HaCaT cells showed delayed growth reduction upon 5 μM vemurafenib. However, this *in vitro* growth response is not maintained under *in vivo*-like conditions in the skin equivalents. When we analyzed cellular proliferation by three different methods, we realized that vemurafenib neither exerts a reduction nor a distinct increase in cell growth, and so, did not provide a significant growth advantage for any of the keratinocytes. Thus, we must conclude, that control of proliferation is not a major factor driving vemurafenib-dependent pathogenesis in our culture models.

Instead, we show that the most obvious and reproducible physiological consequence of vemurafenib is the induction of epidermal differentiation, correlating well with the clinical picture of hyperkeratotic lesions frequently encountered as adverse events in vemurafenib-treated patients with melanoma (38). It is noteworthy that the sensitivity for induction of differentiation appears reduced in the transformed keratinocytes. While NHEK show vemurafenib-dependent expression of several epidermal differentiation markers (*KRT10*, *INV*, *FLG*), increased expression of these genes was not seen by short-term stimulation of HaCaT or HrasA5 cells, but rather upon continuous treatment of HaCaT cells with 5 μm vemurafenib for 4–8 weeks (*KRT10* and *FLG*). Whether this points to an indirect regulation, remains to be seen.

Induction of differentiation was most obvious in NHEK when grown as SEs. At the expense of a hyperplastic epidermis (as in controls), accelerated cornification resulted in the formation of a massive stratum corneum and reduction of the number of vital cell layers especially within the stratum spinosum. Induction of differentiation was also conspicuous for the transformed keratinocytes (HaCaT and HrasA5) in the *in vivo*-like SEs, with a similar consequence of a reduced vital epithelium with increased and more normally distributed epidermal differentiation markers and an expanded parakeratotic stratum corneum. Together, this suggests that induction of epidermal differentiation is an unequivocal part of the action profile of vemurafenib in the human skin keratinocyte. In good agreement with this is the high frequency of hyperkeratoticlesions in vemurafenib-treated melanoma patients, as well as the well-differentiated and keratoacanthoma-type cSCC as the most prevalent skin carcinoma type in these patients (3, 39).

In addition to the activation of the keratinocytes, we also identified vemurafenib-dependent activation in the dermal fibroblasts and propose a distinct role for the microenvironment in the vemurafenib-dependent scenario. As previously described as a double paracrine loop (23, 24), epidermal IL-1A and IL-1B act on the dermal fibroblasts by inducing the expression of KGF (FGF7) and GM-CSF (CSF2), which in turn act on the keratinocytes to stimulate growth, and in the case of GM-CSF, support epidermal differentiation. First, we not only find a vemurafenib-dependent increase in the expression of *IL-1A* and *IL-1B* in monolayer-cultured keratinocytes but we also find a vemurafenib-specific increase in the expression of GM-CSF in dermal equivalents, i.e., without keratinocyte interaction. In agreement with that, we find expression of GM-CSF also in the stromal fibroblasts of perilesional skin and in the microenvironment of cSCC from vemurafenib-treated melanoma patients, suggesting that the fibroblast-derived GM-CSF supports keratinocyte differentiation also *in situ*. Therefore, we hypothesize that vemurafenib-dependent upregulation of GM-CSF is a further activity contributing to the formation of hyperkeratotic lesions and well-differentiated KAs and cSCCs in the melanoma patients (40–42).

Another relevant pathophysiological consequence of vemurafenib-treatment is the rapid transition from a surface epithelium to an invasively growing tumor epithelium. To determine the genetic requirements for the vemurafenib-dependent tumorigenic switch, we utilized keratinocytes with different genetic make-up, i.e., wildtype cells (NHEK), cells with UV-indicative p53 mutations, and cSCC-characteristic chromosomal aberrations (HaCaT), as well as variants of the HaCaT cells with an additional Hras oncogene (HrasA5). Despite the induction of similar MEK-ERK hyperactivation and gene expression of a similar degradome, only the Hras oncogene-carrying variant became invasive upon vemurafenib treatment. Hras by itself is not a dominant tumor driver in the keratinocyte model. We had shown previously that introduction of Hras oncogene into HaCaT cells resulted in a variety of clones with different pathogenic phenotype from nontumorigenic to malignant tumorigenic clones (15). As the level of ras oncogene was similar in benign and malignant tumorigenic clones this is unlikely to be a determinant of the pathogenic phenotype on its own. However, in combination with vemurafenib-induced MEK-ERK hyperactivation, invasion was induced almost immediately. Besides activating the MAPK pathway, Hras can also boost signaling pathways such as the PIK3CA-AKT-mTOR axis (for review, see 43). However, our Western blot analyses have not pointed to a differential regulation in the Hras-containing versus non-ras oncogene-containing cells.

Instead, we see very similar transcriptional regulation of a selected gene panel in NHEK, HaCaT, and HrasA5 cells with vemurafenib. Particularly striking is the strong and almost identical regulation of members of the degradome. In all three keratinocyte types, *MMP1* and *MMP3* were rapidly induced, while *MMP9* and *MMP14* remained largely unaffected. Immunostaining further verified expression of MMP1 and MMP3 in all types of epithelia in the *in vivo*-like SEs. Appreciable levels of secreted pro-MMP1 and MMP3 were however only detected in HrasA5 SEs while in HaCaT SEs only the secreted pro-MMP1 level was increased. In agreement with that, proteolytic activity was restricted to HrasA5 SEs as was degradation of the BM components Col IV, Col VII, laminin, and the underlying dermal collagens. It was suggested that vemurafenib increased

MMP-2 and MMP-9 in HaCaT cells (18). Our expression analysis did not confirm this but identified MMP-1 and MMP-3 as major targets of MEK-ERK activation. While MMP1 can digest Col I and III, as well as Col VII, MMP3 is supposed to digest laminin and Col IV, as well as Col III. In addition, MMP3 is essential for the activation of pro-MMP1 (for review, see 44, 45). This prompts us to hypothesize that MMP1 and MMP3 together pave the way for HrasA5 keratinocytes permitting them to invade. Accordingly, when inhibiting MMP activity by cotreatment of HrasA5 SEs with vemurafenib and the MMP inhibitor ilomastat, proteolytic activity was prohibited, BM components and dermal collagen remained intact, and invasion was prevented, thus, revealing the causal relationship of the rapid tumorigenic conversion to vemurafenib-dependent epidermal MMP1 and MMP3 expression.

Acquired resistance to vemurafenib monotherapy due to reactivation of the MAPK pathway occurs in about two-thirds of the melanoma patients (27, 46 and references therein), opening the way for new treatment modalities. Combined inhibition of MEK and BRAF V600E turned out as a successful strategy for melanoma patients and in addition, reduce the cutaneous adverse events of developing cSCCs very efficiently (47). Cotreatment of HaCaT and HrasA5 SEs with vemurafenib (5 μM) and cobimetinib (0.1 μM) prevented P-ERK1/2 expression in HaCaT epithelia, resulting in increasing atrophy. In HrasA5 SEs, P-ERK1/2 level was reduced to that of untreated controls, and this was sufficient to hinder the vemurafenib-induced accelerated differentiation, activation of the degradome, and accordingly induction of the tumorigenic switch. In particular, secretion of MMP1, MMP3, and MMP9 levels was significantly reduced by HrasA5 keratinocytes and the invasive phenotype was prevented upon addition of cobimetinib to vemurafenib treatment, thus, once more highlighting that the invasion of HrasA5 is a direct effect of MEK-ERK hyperactivation.

In essence, we here show that the primarily unexpected side effect of Vemurafenib, namely the induction of MEK-ERK, is a strong molecular driver for those phenotypic changes leading to adverse events such as hyperkeratotic lesions, KAs, and cSCC. However, for rapid tumor conversion cofactors are required such as the ras oncogene that prime the keratinocytes to become susceptible for the accelerated tumorigenesis that is fueled by vemurafenib. While the ras oncogene seems to account for not more than 30% to 60% of the cSCCs in melanoma patients (41, 48–50) also other genetic factors should be involved in keratinocyte susceptibility to vemurafenib-dependent tumorigenic conversion. Accordingly, a role for the human papilloma virus or polyomavirus is discussed (51, 52), as is the inactivation of the TGF-β pathway by TGFβR mutations (53). In addition, our genetic analysis with the HaCaT cells treated with vemurafenib for several weeks provokes the idea that the cMYC oncogene may be involved in the vemurafenib-triggered events. Of note, we hardly found new chromosomal aberrations, making vemurafenib-dependent genomic toxicity largely neglectable. Instead, the data point to a selective shift in the cell population that is promoted by vemurafenib and provides an advantage for preexisting subpopulations that, in the case of HaCaT cells, contain increased copy numbers of cMYC. Thus, further analysis is required to establish this connection and leaving the field open for the search for additional factors, other than the ras oncogene, that contribute in the establishment of vemurafenib-induced KAs and cSCCs.

MATERIAL AND METHODS

Tissue Samples

Formalin-fixed tissue sections from 13 biopsies from 9 different patients were contributed by Catherine Harwood, Centre for Cell Biology and Cutaneous Research, Blizard Institute, Barts and the London School of Medicine and Dentistry, Queen Mary University of London, London, UK. These included 1 perilesional skin, 2 viral warts, 2 benign acanthomas, and 8 cSCC. The patient material was part of a study described by Purdie et al. (52). This study was carried out in accordance with the recommendations of East London and City Health Authority local ethics committee. The protocol was approved by the East London and City Health Authority local ethics committee. All subjects gave written informed consent in accordance with the Declaration of Helsinki.

For each of the proteins of interest, up to 6 different specimens were analyzed by immunofluorescence.

Cell Culture

NHEK and NHDF were isolated as described previously (54). NHEK, NHDF, HaCaT, HrasA5, and HaCat-rasII4 (HrasII4) were propagated as previously described (20). NHEK were grown in DermaLife K medium, complete; HaCaT HrasA5, HrasII4, and A375 were cultivated in DMEM plus 10% FCS and 1% (v/v) Penicillin/ Streptomycin at 37°C, 5% CO_2, and 20% O_2. Human dermal fibroblasts were cultivated in DMEM plus 10% FCS and 1% (v/v) Penicillin/ Streptomycin at 37°C, 5% CO_2, and 5% O_2. Mycoplasma and virus contamination was excluded for all cell types by the Multiplex Cell Contamination Test (Multiplexion, Heidelberg, Germany), and HaCaT cells and its variants were authenticated by short tandem repeat (STR) profiling (CLS, Heidelberg, Germany).

Generation of Fibroblast-Derived Matrix-Based Skin Equivalents

Skin equivalents (SEs) were established as described in detail previously (20). In brief, NHDF cells were seeded onto a filter insert at 2-day intervals in three successive steps. During submerged cultivation for 4 weeks, the fibroblasts develop an ECM-rich dermal equivalent (DE). Keratinocytes were seeded onto the DE and after 1 day of submersed growth were cultivated at the air-liquid interface. During a cultivation period of 2 weeks, the keratinocytes develop a stratified and differentiated epithelium and thereafter, the SEs were treated with vemurafenib, vemurafenib plus ilomastat, cobimetinib, or vemurafenib plus cobimetinib, with concentrations indicated in the different

experiments. In all experiments, the control cultures were treated with DMSO in a concentration used as solvent for vemurafenib and cobimetinib.

Proliferation Assay

SYBR Green Proliferation Assay

Cells were seeded in 24-well plates at a density of 10^4 cells in 500 µl medium (NHEK: DermaLife K medium complete/HaCaT and HrasA5 cells: DMEM plus 10% FCS) and incubated for 24 h before treatment. To determine the total cell number per well, plates were incubated with SYBR Green (1:2,500, Life Technologies, Carlsbad, CA, USA) in 0.1% (*v*/*v*) Triton X-100 diluted in PBS for 1 h. Fluorescence was measured at 485 nm with Fluoroskan Ascent (Thermo Fischer Scientific, Waltham, MA, USA) and fluorescence intensity correlated to a defined cell number by using the standard plate as a reference. Each experiment was repeated at least twice, and the mean was plotted. The two-way ANOVA + Bonferroni posttest, comparing each condition to the control-treated cells over time, was used to determine statistically significant differences.

BrdU Incorporation and Whole Mount Analysis

To assay for proliferation in whole mounts, SE were incubated with BrdU for 6 h, a quarter of the SE was transferred into PBS and fixed in 3.7% formadehyde/PBS for 2 h at room temperature (RT). After 3 washing steps in PBS, the tissue was stored at 4°C in PBS containing 0.02% sodium azide until further use. To quantify proliferation, samples were treated with 2 M HCl for 25 min followed by washing and further treatment as described (55). The whole mounts were embedded in fluorescent mounting medium and analyzed using a Cell Observer fluorescence microscope equipped with an AxioCam MRm and ZEN software (Zeiss, Jena, Germany). Each whole mount was entirely imaged, and the number of all cells (Hoechst positive) and BrdU-positive cells was determined with Fiji software to calculate the percentage of proliferation. The mean proliferation of 5,000 cells per data point and SE was plotted. Statistical significance was calculated by one-way ANOVA + Dunnett's multiple comparison test.

Histological Processing

Specimens were fixed in 3.7% buffered formaldehyde for at least 24 h before dehydrating in graded alcohol and embedding in paraffin. A total of 4 µm sections were mounted to glass slides, dried o/n at 45°C and deparaffinized by two washes in xylene (8 min) followed by stepwise incubation in ethanol [96%, 80%, 70% (4 min each)] and finally in demineralized water. Routinely, they underwent a standard staining procedure with hematoxylin and eosin afterwards.

Immunofluorescence and Immunohistochemistry

Immunofluorescence detection of antigens on cryosections. In total, 6-µm sections of the frozen specimens were fixed in 80% methanol at 4°C for 5 min followed by absolute acetone at −20°C for 2 min. The air-dried sections were incubated in 12% BSA in PBS at RT for 30 min, before primary antibodies diluted in PBS with 3% BSA were applied for an overnight incubation at 4°C. The mono- and polyclonal antibodies utilized are listed in **Supplementary Tables S1** and **S2**. After intermediate washing, appropriate combinations of fluorochrome-conjugated secondary antibodies were added together with 0.2 µg 4′,6-diamidino-2-phenylindole (DAPI) per ml for nuclear staining. After 1 h incubation at RT, the sections were washed and mounted in fluorescent mounting medium (Dako, Glostrup, Denmark). Fluorescent images were recorded at an Olympus AX-70 microscope equipped with epifluorescence illumination, an OSIS F-View CCD camera and the accompanying cell^R software (Olympus, Shinjuku, Japan).

Immunohistochemical analyses on histological sections and whole mount specimens of fdmSE. For staining of whole mount specimens, the tissue was fixed in 2% formaldehyde for 2 h, permeabilized in 0.2% Triton-X in phosphate-buffered saline (PBS) for 15 min, and blocked in blocking buffer (5% donkey serum (Dianova, Hamburg, Germany), 5% goat serum (Dianova), 5% BSA in PBS) for 1 h. Primary antibodies were incubated overnight at 4°C in blocking buffer followed by fluorophore-conjugated secondary donkey antibodies and 2 µg/ml DAPI (Sigma-Aldrich, Taufkirchen, Germany) incubation for 2 h at RT. The whole mounts were mounted in fluorescent mounting medium (Dako). Images were taken with the confocal Leica TCS SP5 II (Leica, Wetzlar, Germany). Samples were analyzed at ×40 magnification and images of 1,024 × 1,024 pixels with a pixel size of 0.4 µm generated. Z-stacks were imaged at intervals of 0.7 µm.

Immunohistochemistry histological sections were processed as described for cryosections. For detection of color substrate in transmitting light microscopy, however, the secondary antibodies were conjugated to peroxidase (EnVision HRP Rabbit/Mouse, Dako) and an incubation step with DAB was included. Thereafter, the sections were counterstained with hematoxylin and dehydrated and mounted in Eukitt mounting medium (Sigma-Aldrich, St. Louis, MO, USA). Images were taken using an Olympus-AX-51 microscope equipped with OSIS-Color-View CCD camera and cell^D software (Olympus).

Picrosirius Red Staining for Collagen

For the presentation of collagen fibers, histological sections were stained with Picrosirius red according to the protocol of the manufacturer (MORPHISTO, Frankfurt, Germany) and as described in detail previously (20). Sections were examined at a Zeiss-Axiophot-microscope equipped with modules generating circular polarized light. Images were taken using a Zeiss-AxioCam MRc camera and Zeiss AxioVision 4.8.2 software. In order to quantify the amount of fibrillar collagen micrographs of the different specimens (n = 3 for the different treatment modalities) were recorded with identical settings during polarization microscopy. The resulting image files were evaluated using NIH ImageJ for integrated signal density in the entire stromal area of the sections. Correction was performed by subtraction of integral background intensity in each individual section. Data are presented as means with standard deviation.

Gelatinase Assay (*In Situ* Zymography)

MMP-activity *in situ* was visualized in unfixed cryosections using DQ-gelatin (EnzCheck Gelatinase/Collagenase Assay Kit, Live Technologies) as substrate. By proteolytic cleavage, quenched fluorescence is released and becomes detectable. After 1 h incubation at RT with 50 µg/ml DQ-gelatin together with 5 µg/ml Hoechst 33258, the sections were washed and methanol/acetone fixed before mounting in Dako fluorescent mounting medium. The sections were immediately examined using an Olympus AX-70 fluorescence microscope equipped with a OSIS F View CCD camera and the accompanying cell^R software (Olympus). Fluorescence was documented using equal exposure times for all sections.

Enzyme-Linked Immunosorbent Assay

Matrix metalloproteinase (MMP) secretion was quantified by R&D Quantikine ELISA according to the manufacturer's protocol. The Pro-MMP-1 ELISA is specific for the Pro-MMP-1 only, whereas the MMP-3 and MMP-9 ELISA detect both the pro- and active forms. All assays were performed with a 48-h conditioned culture medium from 2- or 4-week-old SEs. Duplicate cultures were analyzed with technical replica.

Western Blot

Cells were lysed with RIPA buffer for 30 min on ice. After centrifugation for 30 min at 14,000 rpm, the protein content of the supernatant was determined using the Pierce BCA Protein assay (Thermo Fischer Scientific). Proteins were separated on a 10% SDS gel and blotted onto a nitrocellulose membrane. After blocking with 5% skim milk in 0.1% PBS-T (blocking buffer) for 1 h, proteins were detected with the respective primary antibody (diluted in PBS-T) overnight at 4°C, the respective HRP-coupled secondary antibody (in blocking buffer) for 1 h at RT and subsequently identified by luminometric detection with ECL (GE, Buckinghamshire, UK).

Real-Time/Quantitative RT-PCR

For quantitative RT-PCR (qRT-PCR), the Universal Probe Library (UPL) system (Roche, Basel, Switzerland) was used and qRT-PCR was performed in a 96-well plate-based LightCycler 480 Instrument II (Roche) according to the manufacturer's instructions. The UPL tool (www.universalprobelibrary.com) was used for primer design. For each reaction, a 15-µl mix in nuclease-free water containing 10 µl LightCycler master (2×), 0.4 µM forward and reverse primers (stock: 10 µM), and 0.1 µM UPL probe (stock: 10 µM) were used and 50 ng cDNA in 5 µl RNase-free water was added per well. A negative control (water) was run with each primer pair. Each qRT-PCR was carried out in technical duplicates. The reaction was performed in PCR 96-well TW-MT Plate white (Biozym, Hessisch Oldendorf, Germany) and sealed with Adhesive Clear qPCR Seals (Biozym) with the following protocol: preincubation for 10 min at 95°C, 45 cycles of 10 s at 95°C (ramp rate 4.4°C/s), 30 s at 60°C (ramp rate 2.2°C/s), and 1 s at 72°C (ramp rate 4.4°C/s). Fluorescence was measured after each cycle. Standard curves were performed for each primer pair using a dilution series of 100, 20, 4, 0.80, and 0.16 ng pooled cDNA for each target cell type.

For relative quantification, the gene of interest (target) and the housekeeping gene GAPDH (reference) were compared for each control and stimulated sample. For this calculation, the crossing point value (CP) of each gene in a given sample, identifying the cycle number when fluorescence signals rise above threshold fluorescence, was obtained using the Second Derivative Maximum method of the LightCycler 480 Software (Roche). With these CP values, the ratio of relative gene expression of control vs. treated sample, normalized to GAPDH, was calculated as described (56). Data were displayed using linear or logarithmic scales, whereas the corresponding control was always set to one.

For primers and probes, see **Supplementary Table S3**.

Multiplex Fluorescence *In Situ* Hybridization

M-FISH was performed as described by Geigl etal. (57). Briefly, seven pools of flow-sorted human chromosome painting probes were amplified and directly labeled using seven different fluorochromes (DEAC, FITC, Cy3, Cy3.5, Cy5, Cy5.5, and Cy7) by degenerative oligonucleotide-primed PCR (DOP-PCR). Metaphase spreads immobilized on glass slides were denatured in 70% formamide/2xSSC pH 7.0 at 72°C for 2 min followed by dehydration in a degraded ethanol series. Hybridization mixture containing combinatorically labeled painting probes, an excess of unlabeled cot1 DNA, 50% formamide, 2xSSC, and 15% dextran sulfate were denatured for 7 min at 75°C, preannealed at 37°C for 20 min, and hybridized at 37°C to the denaturated metaphase preparations. After 48 h, the slides were washed in 2xSSC at room temperature for 3 × 5 min followed by two washes in 0.2xSSC/0.2% Tween-20 at 56°C for 7 min, each. Metaphase spreads were counterstained with DAPI and covered with antifade solution. Metaphase spreads were recorded using a DM RXA epifluorescence microscope (Leica Microsystems, Bensheim, Germany) equipped with a Sensys CCD camera (Photometrics, Tucson, AZ, USA). Camera and microscope were controlled by the Leica Q-FISH software, and images were processed based on the Leica MCK software and presented as multicolor karyograms (Leica Microsystems Imaging solutions, Cambridge, UK).

Statistical Analysis

Statistical significance was calculated by performing a one-way ANOVA + Dunnett's multiple comparison test or two-way ANOVA + Bonferroni posttest, which both compare each treatment modality to the corresponding controls. The *p*-values as well as the used test are indicated within the figure or legend, respectively. The analyses were performed by GraphPad Prism 4 software.

DATA AVAILABILITY STATEMENT

The original contributions presented in the study are included in the article/**Supplementary Material**, further inquiries can be directed to the corresponding author.

ETHICS STATEMENT

The studies involving human participants were reviewed and approved by the East London and City Health Authority local ethics committee. The protocol was approved by the East London and City Health Authority local ethics committee. The patients/participants provided their written informed consent to participate in this study.

AUTHOR CONTRIBUTIONS

MT and H-JS contributed equally in all aspects of the work. AJ contributed to the genetic analyses. CH contributed to the patients' tumor material. EPL contributed to the writing and submission. PB has contributed to all aspects of the work and led the team effort. All authors contributed to the article and approved the submitted version.

FUNDING

This work was supported by contract research "Adulte epidermale Stammzellen" of the Baden-Württemberg Stiftung (P-BWS-ASII/35) and a grant from the Federal Ministry for Research and Education/BMBF (KAUVIR, 02NUK036A) (all to PB).

ACKNOWLEDGMENTS

We highly acknowledge the excellent technical assistance by Iris Martin, Elke Laport, and Angelika Krischke (DKFZ Heidelberg), as well as Brigitte Schoell and Martin Granzow (Institute of Human genetics, University Heidelberg) for their help with the M-FISH experiments. Moreover, we thank Damir Krunic (DKFZ, Core Facility Microscopy) and Lisa Oettl for their support.

SUPPLEMENTARY MATERIAL

The Supplementary Material for this article can be found online at: https://www.frontiersin.org/articles/10.3389/fonc.2022.827985/full#supplementary-material

Supplementary Figure S1 | Vemurafenib does not cause major chromosomal instability. HaCaT cells were treated with either DMSO or Vemurafenib (1μM or 5μM) for 5 weeks and analyzed by M-FISH for their chromosomal status. **(A)** examples of M-FISH karyograms of control HaCaT cells and HaCaT cells treated with 5 μM Vemurafenib for 5 weeks. **(B)** The comparison of subpopulation distribution showed a shift in superiority of pre-existing populations. Graph indicates pre-existing subpopulations and their shifts in low (1μM, yellow) or high (5μM, green) concentration of Vemurafenib.

Supplementary Figure S2 | Characterization of Vemurafenib's effects on epithelial differentiation in HaCaT SEs. SEs from HaCaT cells were treated with Vemurafenib (1 μM and 5 μM) for up to 5 weeks and histology and immunostaining was performed at the indicated time points. **(A)** H&E staining of SEs demonstrate improved tissue organization with an epidermis-like stratification and improved parakeratotic str. corneum, particularly evident upon 5μM Vemurafenib. In addition, Vemurafenib-treated HaCaT SEs show extended vitality, as evidenced by an increased number of vital basal cells and improved attachment of the epithelium to the DE. **(B)** Improved and more normal differentiation in HaCaT SEs treated with Vemurafenib for 3 weeks. Immunostaining for the early KRT10 and particularly the late differentiation markers FLG and KRT2, point to improved differentiation including a more structured str. granulosum. The BM components COLVII (green), COLIV (red), and LAM (red) are concentrated in the continuous BMs. Note that COLIV is continuously expressed by the fibroblasts and present throughout the DE, though enriched in the BM zone (left panel). LAM, that appears "bloated" in the control SEs, becomes more concentrated upon Vemurafenib treatment. **(C)** Immunohistochemical analysis of the SEs demonstrate a strong increase of pERK1/2 in the vital cell layers of the Vemurafenib-treated (5 μM for 3 weeks, right) SEs, as compared to the control SEs (left). Scale bar = 300 μm in **(A, C)** and 150 μm in **(B)**.

Supplementary Figure S3 | pERK1/2 expression in Vemurafenib (5 μM)-treated SEs. In NHEK SEs pERK1/2 is expressed in the epidermis and prominently also in the dermal fibroblasts. COLVII is expressed all along the BM (upper panel). In HrasA5 SEs, expression of pERK1/2 is increased in the entire epithelium and particularly dominant in the invasive strands. COLVII is lost at the invasive sites (middle panel). Unphosphorylated ERK1/2 (control) is expressed throughout the epithelium in control and Vemurafenib-treated SEs. The dermal fibroblasts are depicted by counterstaining for Vimentin. (lower panel). Scale bar = 300 μm.

Supplementary Figure S4 | Action profile of Cobimetinib in HrasA5-SEs. **(A)** H&E staining of HrasA5-SEs treated for 3 weeks with the MEK-inhibitor Cobimetinib illustrates a toxic effect with dose-dependent tissue atrophy. 0.1 μM Cobimetinib causes an only mild structural impairment (middle) while 1.0 μM leads to strong atrophy (lower). Scale bar = 300 μm. **(B)** Western Blot analysis of a competition experiment with cultured HrasA5-cells treated with Vemurafenib in combination with Cobimetinib reveals a dose-dependent pMEK 1/2 accumulation and complete pERK 1/2 inhibition. **(C)** Vemurafenib- and Vemurafenib + Cobimetinib-treated HrasA5-monolayer cultures were subjected to mRNA expression analysis of a panel of genes that had been identified as Vemurafenib-responsive. All genes, including the main players in the degradome, MMP1 and MMP3, were strongly repressed in the presence of Cobimetinib. Normalization was performed using GAPDH and fold-changes were expressed by comparing each treatment to the DMSO control set to one.; n=2, mean ± SD, log 2-scale.

REFERENCES

1. Curry JL, Torres-Cabala CA, Kim KB, Tetzlaff MT, Duvic M, Tsai KY, et al. Dermatologic Toxicities to Targeted Cancer Therapy: Shared Clinical and Histologic Adverse Skin Reactions. *Int J Dermatol* (2014) 53(3):376–84. doi: 10.1111/ijd.12205
2. Kim A, Cohen MS. The Discovery of Vemurafenib for the Treatment of BRAF-Mutated Metastatic Melanoma. *Expert Opin Drug Discov* (2016) 11 (9):907–16. doi: 10.1080/17460441.2016.1201057
3. Heinzerling L, Eigentler TK, Fluck M, Hassel JC, Heller-Schenck D, Leipe J, et al. Tolerability of BRAF/MEK Inhibitor Combinations: Adverse Event Evaluation and Management. *ESMO Open* (2019) 4(3):e000491. doi: 10.1136/esmoopen-2019-000491
4. Chapman PB, Hauschild A, Robert C, Haanen JB, Ascierto P, Larkin J, et al. Improved Survival With Vemurafenib in Melanoma With BRAF V600E Mutation. *N Engl J Med* (2011) 364(26):2507–16. doi: 10.1056/NEJMoa1103782

5. Durinck S, Ho C, Wang NJ, Liao W, Jakkula LR, Collisson EA, et al. Temporal Dissection of Tumorigenesis in Primary Cancers. *Cancer Discov* (2011) 1 (2):137-43. doi: 10.1158/2159-8290.CD-11-0028
6. Carless MA, Griffiths LR. Cytogenetics of Melanoma and Nonmelanoma Skin Cancer. *Adv Exp Med Biol* (2014) 810:160–81. doi: 10.1007/978-1-4939-0437-2_9
7. Leufke C, Leykauf J, Krunic D, Jauch A, Holtgreve-Grez H, Bohm-Steuer B, et al. The Telomere Profile Distinguishes Two Classes of Genetically Distinct Cutaneous Squamous Cell Carcinomas. *Oncogene* (2014) 33(27):3506–18. doi: 10.1038/onc.2013.323
8. Inman GJ, Wang J, Nagano A, Alexandrov LB, Purdie KJ, Taylor RG, et al. The Genomic Landscape of Cutaneous SCC Reveals Drivers and a Novel Azathioprine Associated Mutational Signature. *Nat Commun* (2018) 9 (1):3667. doi: 10.1038/s41467-018-06027-1
9. Martincorena I, Roshan A, Gerstung M, Ellis P, Van Loo P, McLaren S, et al. Tumor Evolution. High Burden and Pervasive Positive Selection of Somatic Mutations in Normal Human Skin. *Science* (2015) 348(6237):880–6. doi: 10.1126/science.aaa6806
10. Albibas AA, Rose-Zerilli MJJ, Lai C, Pengelly RJ, Lockett GA, Theaker J, et al. Subclonal Evolution of Cancer-Related Gene Mutations in P53 Immunopositive Patches in Human Skin. *J Invest Dermatol* (2018) 138 (1):189–98. doi: 10.1016/j.jid.2017.07.844
11. Daud A, Tsai K. Management of Treatment-Related Adverse Events With Agents Targeting the MAPK Pathway in Patients With Metastatic Melanoma. *Oncologist* (2017) 22(7):823–33. doi: 10.1634/theoncologist.2016-0456
12. Hatzivassiliou G, Song K, Yen I, Brandhuber BJ, Anderson DJ, Alvarado R, et al. RAF Inhibitors Prime Wild-Type RAF to Activate the MAPK Pathway and Enhance Growth. *Nature* (2010) 464(7287):431–5. doi: 10.1038/nature08833
13. Heidorn SJ, Milagre C, Whittaker S, Nourry A, Niculescu-Duvas I, Dhomen N, et al. Kinase-Dead BRAF and Oncogenic RAS Cooperate to Drive Tumor Progression Through CRAF. *Cell* (2010) 140(2):209–21. doi: 10.1016/j.cell.2009.12.040
14. Doma E, Rupp C, Varga A, Kern F, Riegler B, Baccarini M. Skin Tumorigenesis Stimulated by Raf Inhibitors Relies Upon Raf Functions That are Dependent and Independent of ERK. *Cancer Res* (2013) 73 (23):6926–37. doi: 10.1158/0008-5472.CAN-13-0748
15. Boukamp P, Stanbridge EJ, Foo DY, Cerutti PA, Fusenig NE. C-Ha-Ras Oncogene Expression in Immortalized Human Keratinocytes (HaCaT) Alters Growth Potential *In Vivo* But Lacks Correlation With Malignancy. *Cancer Res* (1990) 50(9):2840–7.
16. Dhillon AS, Hagan S, Rath O, Kolch W. MAP Kinase Signalling Pathways in Cancer. *Oncogene* (2007) 26(22):3279–90. doi: 10.1038/sj.onc.1210421
17. Ullah R, Yin Q, Snell AH, Wan L. RAF-MEK-ERK Pathway in Cancer Evolution and Treatment. *Semin Cancer Biol* (2021). doi: 10.1016/j.semcancer.2021.05.010
18. Roh MR, Kim JM, Lee SH, Jang HS, Park KH, Chung KY, et al. Low-Concentration Vemurafenib Induces the Proliferation and Invasion of Human HaCaT Keratinocytes Through Mitogen-Activated Protein Kinase Pathway Activation. *J Dermatol* (2015) 42(9):881–8. doi: 10.1111/1346-8138.12950
19. Kamata T, Hussain J, Giblett S, Hayward R, Marais R, Pritchard C. BRAF Inactivation Drives Aneuploidy by Deregulating CRAF. *Cancer Res* (2010) 70 (21):8475–86. doi: 10.1158/0008-5472.CAN-10-0603
20. Berning M, Pratzel-Wunder S, Bickenbach JR, Boukamp P. Three-Dimensional *In Vitro* Skin and Skin Cancer Models Based on Human Fibroblast-Derived Matrix. *Tissue Eng Part C Methods* (2015) 21(9):958–70. doi: 10.1089/ten.TEC.2014.0698
21. Boukamp P, Petrussevska RT, Breitkreutz D, Hornung J, Markham A, Fusenig NE. Normal Keratinization in a Spontaneously Immortalized Aneuploid Human Keratinocyte Cell Line. *J Cell Biol* (1988) 106(3):761–71. doi: 10.1083/jcb.106.3.761
22. Toll A, Salgado R, Yebenes M, Martin-Ezquerra G, Gilaberte M, Baro T, et al. MYC Gene Numerical Aberrations in Actinic Keratosis and Cutaneous Squamous Cell Carcinoma. *Br J Dermatol* (2009) 161(5):1112–8. doi: 10.1111/j.1365-2133.2009.09351.x
23. Maas-Szabowski N, Stark HJ, Fusenig NE. Keratinocyte Growth Regulation in Defined Organotypic Cultures Through IL-1-Induced Keratinocyte Growth Factor Expression in Resting Fibroblasts. *J Invest Dermatol* (2000) 114 (6):1075–84. doi: 10.1046/j.1523-1747.2000.00987.x
24. Smola H, Thiekotter G, Fusenig NE. Mutual Induction of Growth Factor Gene Expression by Epidermal-Dermal Cell Interaction. *J Cell Biol* (1993) 122 (2):417–29. doi: 10.1083/jcb.122.2.417
25. Nissinen L, Farshchian M, Riihila P, Kahari VM. New Perspectives on Role of Tumor Microenvironment in Progression of Cutaneous Squamous Cell Carcinoma. *Cell Tissue Res* (2016) 365(3):691–702. doi: 10.1007/s00441-016-2457-z
26. Grimaldi AM, Simeone E, Festino L, Vanella V, Strudel M, Ascierto PA. MEK Inhibitors in the Treatment of Metastatic Melanoma and Solid Tumors. *Am J Clin Dermatol* (2017) 18(6):745-54. doi: 10.1007/s40257-017-0292-y
27. Larkin J, Ascierto PA, Dreno B, Atkinson V, Liszkay G, Maio M, et al. Combined Vemurafenib and Cobimetinib in BRAF-Mutated Melanoma. *N Engl J Med* (2014) 371(20):1867–76. doi: 10.1056/NEJMoa1408868
28. Muffler S, Stark HJ, Amoros M, Falkowska-Hansen B, Boehnke K, Buhring HJ, et al. A Stable Niche Supports Long-Term Maintenance of Human Epidermal Stem Cells in Organotypic Cultures. *Stem Cells* (2008) 26 (10):2506-15. doi: 10.1634/stemcells.2007-0991
29. Barrientos S, Stojadinovic O, Golinko MS, Brem H, Tomic-Canic M. Growth Factors and Cytokines in Wound Healing. *Wound Repair Regener* (2008) 16 (5):585–601. doi: 10.1111/j.1524-475X.2008.00410.x
30. Maas-Szabowski N, Shimotoyodome A, Fusenig NE. Keratinocyte Growth Regulation in Fibroblast Cocultures *via* a Double Paracrine Mechanism. *J Cell Sci* (1999) 112(Pt 12):1843–53. doi: 10.1242/jcs.112.12.1843
31. Kim HS, Shin MS, Cheon MS, Kim JW, Lee C, Kim WH, et al. GREM1 is Expressed in the Cancer-Associated Myofibroblasts of Basal Cell Carcinomas. *PloS One* (2017) 12(3):e0174565. doi: 10.1371/journal.pone.0174565
32. Nurmik M, Ullmann P, Rodriguez F, Haan S, Letellier E. In Search of Definitions: Cancer-Associated Fibroblasts and Their Markers. *Int J Cancer* (2020) 146(4):895–905. doi: 10.1002/ijc.32193
33. Azzimonti B, Zavattaro E, Provasi M, Vidali M, Conca A, Catalano E, et al. Intense Foxp3+ CD25+ Regulatory T-Cell Infiltration is Associated With High-Grade Cutaneous Squamous Cell Carcinoma and Counterbalanced by CD8+/Foxp3+ CD25+ Ratio. *Br J Dermatol* (2015) 172(1):64–73. doi: 10.1111/bjd.13172
34. Lai C, August S, Behar R, Polak M, Ardern-Jones M, Theaker J, et al. Characteristics of Immunosuppressive Regulatory T Cells in Cutaneous Squamous Cell Carcinomas and Role in Metastasis. *Lancet* (2015). doi: 10.1016/S0140-6736(15)60374-9
35. Poulikakos PI, Zhang C, Bollag G, Shokat KM, Rosen N. RAF Inhibitors Transactivate RAF Dimers and ERK Signalling in Cells With Wild-Type BRAF. *Nature* (2010) 464(7287):427–30. doi: 10.1038/nature08902
36. Johannessen CM, Boehm JS, Kim SY, Thomas SR, Wardwell L, Johnson LA, et al. COT Drives Resistance to RAF Inhibition Through MAP Kinase Pathway Reactivation. *Nature* (2010) 468(7326):968–72. doi: 10.1038/nature09627
37. Lee JH, Lee JH, Lee SH, Do SI, Cho SD, Forslund O, et al. TPL2 Is an Oncogenic Driver in Keratocanthoma and Squamous Cell Carcinoma. *Cancer Res* (2016) 76(22):6712–22. doi: 10.1158/0008-5472.CAN-15-3274
38. Gnanendran SS, Turner LM, Miller JA, Hwang SJE, Miller AC. Cutaneous Adverse Events of Anti-PD-1 Therapy and BRAF Inhibitors. *Curr Treat Options Oncol* (2020) 21(4):29. doi: 10.1007/s11864-020-0721-7
39. Anforth R, Blumetti TC, Mohd Affandi A, Fernandez-Penas P. Systemic Retinoid Therapy for Chemoprevention of Nonmelanoma Skin Cancer in a Patient Treated With Vemurafenib. *J Clin Oncol* (2012) 30(19):e165–167. doi: 10.1200/JCO.2011.39.8594
40. Anforth R, Menzies A, Byth K, Carlos G, Chou S, Sharma R, et al. Factors Influencing the Development of Cutaneous Squamous Cell Carcinoma in Patients on BRAF Inhibitor Therapy. *J Am Acad Dermatol* (2015) 72(5):809–815 e801. doi: 10.1016/j.jaad.2015.01.018
41. Anforth R, Tembe V, Blumetti T, Fernandez-Penas P. Mutational Analysis of Cutaneous Squamous Cell Carcinomas and Verrucal Keratosis in Patients Taking BRAF Inhibitors. *Pigment Cell Melanoma Res* (2012) 25(5):569–72. doi: 10.1111/j.1755-148X.2012.01031.x
42. Manousaridis I, Mavridou S, Goerdt S, Leverkus M, Utikal J. Cutaneous Side Effects of Inhibitors of the RAS/RAF/MEK/ERK Signalling Pathway and Their Management. *J Eur Acad Dermatol Venereol* (2013) 27(1):11–8. doi: 10.1111/j.1468-3083.2012.04546.x

43. Morkel M, Riemer P, Blaker H, Sers C. Similar But Different: Distinct Roles for KRAS and BRAF Oncogenes in Colorectal Cancer Development and Therapy Resistance. *Oncotarget* (2015) 6(25):20785–800. doi: 10.18632/oncotarget.4750
44. Craig VJ, Zhang L, Hagood JS, Owen CA. Matrix Metalloproteinases as Therapeutic Targets for Idiopathic Pulmonary Fibrosis. *Am J Respir Cell Mol Biol* (2015) 53(5):585–600. doi: 10.1165/rcmb.2015-0020TR
45. Pittayapruek P, Meephansan J, Prapapan O, Komine M, Ohtsuki M. Role of Matrix Metalloproteinases in Photoaging and Photocarcinogenesis. *Int J Mol Sci* (2016) 17(6):868. doi: 10.3390/ijms17060868
46. Long GV, Stroyakovskiy D, Gogas H, Levchenko E, de Braud F, Larkin J, et al. Combined BRAF and MEK Inhibition Versus BRAF Inhibition Alone in Melanoma. *N Engl J Med* (2014) 371(20):1877–88. doi: 10.1056/NEJMoa1406037
47. Luke JJ, Flaherty KT, Ribas A, Long GV. Targeted Agents and Immunotherapies: Optimizing Outcomes in Melanoma. *Nat Rev Clin Oncol* (2017) 14(8):463–82. doi: 10.1038/nrclinonc.2017.43
48. Lacouture ME, Duvic M, Hauschild A, Prieto VG, Robert C, Schadendorf D, et al. Analysis of Dermatologic Events in Vemurafenib-Treated Patients With Melanoma. *Oncologist* (2013) 18(3):314–22. doi: 10.1634/theoncologist.2012-0333
49. Oberholzer PA, Kee D, Dziunycz P, Sucker A, Kamsukom N, Jones R, et al. RAS Mutations are Associated With the Development of Cutaneous Squamous Cell Tumors in Patients Treated With RAF Inhibitors. *J Clin Oncol* (2012) 30(3):316–21. doi: 10.1200/JCO.2011.36.7680
50. Su F, Viros A, Milagre C, Trunzer K, Bollag G, Spleiss O, et al. RAS Mutations in Cutaneous Squamous-Cell Carcinomas in Patients Treated With BRAF Inhibitors. *N Engl J Med* (2012) 366(3):207–15. doi: 10.1056/NEJMoa1105358
51. Holderfield M, Lorenzana E, Weisburd B, Lomovasky L, Boussemart L, Lacroix L, et al. Vemurafenib Cooperates With HPV to Promote Initiation of Cutaneous Tumors. *Cancer Res* (2014) 74(8):2238–45. doi: 10.1158/0008-5472.CAN-13-1065-T
52. Purdie KJ, Proby CM, Rizvi H, Griffin H, Doorbar J, Sommerlad M, et al. The Role of Human Papillomaviruses and Polyomaviruses in BRAF-Inhibitor Induced Cutaneous Squamous Cell Carcinoma and Benign Squamoproliferative Lesions. *Front Microbiol* (2018) 9:1806. doi: 10.3389/fmicb.2018.01806
53. Cammareri P, Rose AM, Vincent DF, Wang J, Nagano A, Libertini S, et al. Inactivation of TGFbeta Receptors in Stem Cells Drives Cutaneous Squamous Cell Carcinoma. *Nat Commun* (2016) 7:12493. doi: 10.1038/ncomms12493
54. Stark HJ, Willhauck MJ, Mirancea N, Boehnke K, Nord I, Breitkreutz D, et al. Authentic Fibroblast Matrix in Dermal Equivalents Normalises Epidermal Histogenesis and Dermoepidermal Junction in Organotypic Co-Culture. *Eur J Cell Biol* (2004) 83(11-12):631–45. doi: 10.1078/0171-9335-00435
55. Noske K, Stark HJ, Nevaril L, Berning M, Langbein L, Goyal A, et al. Mitotic Diversity in Homeostatic Human Interfollicular Epidermis. *Int J Mol Sci* (2016) 17(2):167. doi: 10.3390/ijms17020167
56. Pfaffl MW. A New Mathematical Model for Relative Quantification in Real-Time RT-PCR. *Nucleic Acids Res* (2001) 29(9):e45. doi: 10.1093/nar/29.9.e45
57. Geigl JB, Uhrig S, Speicher MR. Multiplex-Fluorescence *in Situ* Hybridization for Chromosome Karyotyping. *Nat Protoc* (2006) 1(3):1172–84. doi: 10.1038/nprot.2006.160

Conflict of Interest: The authors declare that the research was conducted in the absence of any commercial or financial relationships that could be construed as a potential conflict of interest.

frontiers in Oncology

ORIGINAL RESEARCH
published: 10 February 2022
doi: 10.3389/fonc.2022.811586

Tertiary Lymphoid Structures and Chemokine Landscape in Virus-Positive and Virus-Negative Merkel Cell Carcinoma

Motoki Nakamura[*†], *Tetsuya Magara*, *Shinji Kano*, *Akihiro Matsubara*, *Hiroshi Kato* and *Akimichi Morita*[†]

Department of Geriatric and Environmental Dermatology, Nagoya City University Graduate School of Medical Sciences, Nagoya, Japan

OPEN ACCESS

Edited by:
Giuseppe Palmieri, University of Sassari, Italy

Reviewed by:
Andrea Anichini, National Cancer Institute Foundation (IRCCS), Italy
Luis Del Valle, Louisiana State University, United States

***Correspondence:**
Motoki Nakamura
motoki1@med.nagoya-cu.ac.jp

†ORCID:
Motoki Nakamura
orcid.org/0000-0003-4431-7782
Akimichi Morita
orcid.org/0000-0001-8372-3754

Specialty section:
This article was submitted to Skin Cancer, a section of the journal Frontiers in Oncology

Received: *09 November 2021*
Accepted: *17 January 2022*
Published: *10 February 2022*

Citation:
Nakamura M, Magara T, Kano S, Matsubara A, Kato H and Morita A (2022) Tertiary Lymphoid Structures and Chemokine Landscape in Virus-Positive and Virus-Negative Merkel Cell Carcinoma. Front. Oncol. 12:811586. doi: 10.3389/fonc.2022.811586

Tertiary lymphoid structures (TLSs) are used as biomarkers in many cancers for predicting the prognosis and assessing the response to immunotherapy. In Merkel cell carcinoma (MCC), TLSs have only been examined in MCPyV-positive cases. Here, we examined the prognostic value of the presence or absence of TLSs in 61 patients with MCC, including MCPyV-positive and MCPyV-negative cases. TLS-positive samples had a significantly better prognosis than TLS-negative samples. MCPyV-positive samples had a good prognosis with or without TLSs, and MCPyV-negative/TLS-positive samples had a similarly good prognosis as MCPyV-positive samples. Only MCPyV-negative/TLS-negative samples had a significantly poor prognosis. All cases with spontaneous regression were MCPyV-positive/TLS-positive. We also performed a comprehensive analysis of the chemokines associated with TLS formation using next-generation sequencing (NGS). The RNA sequencing results revealed 5 chemokine genes, *CCL5*, *CCR2*, *CCR7*, *CXCL9*, and *CXCL13*, with significantly high expression in TLS-positive samples compared with TLS-negative samples in both MCPyV-positive and MCPyV-negative samples. Only 2 chemokine genes, *CXCL10* and *CX3CR1*, had significantly different expression levels in the presence or absence of MCPyV infection in TLS-negative samples. Patients with high CXCL13 or CCL5 expression have a significantly better prognosis than those with low expression. In conclusion, the presence of TLSs can be a potential prognostic marker even in cohorts that include MCPyV-negative cases. Chemokine profiles may help us understand the tumor microenvironment in patients with MCPyV-positive or MCPyV-negative MCC and may be a useful prognostic marker in their own right.

Keywords: biomarker, Merkel cell carcinoma (MCC), tertiary lymphoid structure (TLS), tumor microenvironment (TME), chemokine, cohort study

INTRODUCTION

Merkel cell carcinoma (MCC) is a rare malignant skin cancer with potentially high immune activity (1).MCC is treated with immune checkpoint inhibitors (ICIs), but the response rate is only about 30% (2), and many patients exhibit no benefit. Useful biomarkers with practical application are waiting to be discovered. The presence or absence of Merkel cell polyoma virus (MCPyV) infection is reported to be closely related to the tumor mutation burden and amount of neoantigens (3, 4). MCPyV-negative, i.e., ultraviolet-induced, MCCs have a higher tumor mutation burden and more neoantigens than MCPyV-positive MCC. Ultraviolet-induced MCCs, however, are not more responsive to ICIs than virus-induced MCCs (5). The presence of tertiary lymphoid structures (TLSs) in the tumor tissue of many cancers is considered to indicate a better prognosis and a good response to ICIs (6, 7). TLSs are ectopic lymphoid tissues found in inflamed, infected, or tumor tissues. TLSs in solid tumors often activate anti-tumor immunity and contribute to the formation of a favorable immune microenvironment against the tumor (8). A previous study reported that the presence of TLSs correlates with a good prognosis in MCC, but the 21 cases examined in that study were all MCPyV-positive cases (9). Here we examined the correlation between the presence or absence of TLSs and prognosis in 61 MCC cases, including both MCPyV-positive and MCPyV-negative cases. In addition, we performed a comprehensive analysis of immunologic factors, including chemokines, associated with TLS formation using next-generation sequencing (NGS). The involvement of TLSs and chemokines in the cancer microenvironment was investigated in patients with MCPyV-positive or MCPyV-negative MCC.

MATERIALS AND METHODS

Cohort Profile

To examine the relationship between TLSs and prognosis in both MCPyV-positive and MCPyV-negative MCC, we examined 71 samples from 61 Japanese patients with MCC diagnosed histologically on the basis of biopsy or surgical resection samples obtained in 9 facilities (see **Supplementary Table 1**). Among the 71 samples, 61 were primary lesions and 10 were metastatic skin lesions. Metastatic lymph nodes and specimens from other organs were excluded. The patients were predominantly female (63.9%) with a mean age of 77.3 years. Primary tumor sites were the head and neck (67.6%), followed by the limbs (27.9%) and trunk (1.6%). Spontaneous regression occurred after biopsy in 5 cases (8.2%). Primary lesions of other cases were surgically removed, treated with radiation therapy, or both. Chemotherapy, e.g., combined treatment with carboplatin and etoposide, was administered in a few cases with distant metastasis. Two cases were treated with the ICI avelumab. Patient characteristics and treatments are summarized in **Table 1**. This cohort mostly overlaps with the cohort in our previous reports (10, 11), and the 41 cases for which RNA sequencing was performed are the same.

Immunohistochemistry

The presence of MCPyV infection was determined by immunostaining formalin-fixed paraffin-embedded tissue samples obtained by biopsy or surgical resection using the large T-antigen antibody (CM2B4, Santa Cruz Biotechnology, Dallas, TX, USA). For visualization of tumor-infiltrating cells and measurement of PD-L1 expression, indirect immunofluorescence staining was performed using primary antibodies: anti-PD-1 antibody (ab137132, Abcam, Cambridge, UK), anti-PD-L1 antibody (ab205921, Abcam), anti-CD3 antibody (ab17143, Abcam), anti-CD8 antibody (ab17147, Abcam), anti-CD20 antibody (ab78237, Abcam), and anti-CD21 antibody (ab75985, Abcam). Alexa Fluor 488, Alexa Fluor 546, Alexa Fluor 594, and Alexa Fluor 647 (Invitrogen, Waltham, MA, USA) were used as secondary antibodies. The nuclei were stained with 4',6-diamidino-2-phenylindole (Vector Laboratories, Burlingame, CA, USA). Fluorescence was observed and captured using a fluorescence microscope BZ-X800 (Keyence, Osaka, Japan). TLSs were typically identified as clusters of CD20-positive cells surrounded by CD3-positive cells. Including immature TLSs, in which only a few CD3-positive cells surround a CD20-positive cell cluster, if a lesion had at least one TLS, it was counted as TLS-positive, as previously described (12). The fluorescence intensities of PD-L1 were calculated from 10 randomly selected fields using ImageJ Software (NIH, Bethesda, MD, USA) as previously described (11). After evaluating entire specimens, CD8-positive cells and PD-1-positive cells were counted in several locations having a high density of infiltrating cells, and the mean value was calculated.

RNA Extraction and Sequencing

RNA extraction and sequencing were performed for 41 randomly selected samples as previously described (11). Tumor tissue was carefully dissected from 3 to 5 undyed formalin-fixed paraffin-embedded tissue sections (4-μm thick) using a scalpel blade and deparaffinized in 640 μl deparaffinization solution (Qiagen, Hilden, Germany). Total RNA was extracted using an AllPrep DNA/RNA FFPE Kit (Qiagen) according to the supplier's instructions. The RNA integrity number and DV_{200} values were measured using a Bioanalyzer (Agilent Technologies, Santa Clara, CA, USA) to evaluate the quality of the extracted RNA. RNA samples confirmed to be of sufficient quality were reverse-transcribed to cDNA using a SuperScript VILO cDNA Synthesis Kit (Thermo Fisher Scientific, Waltham, MA, USA) after assessing the density using a Qubit 4 Fluorometer (Thermo Fisher Scientific). cDNA samples were amplified and applied to the NGS using a PTC-100 thermal cycler (MJ Research, Watertown, MA, USA) and Ampliseq for the Illumina Immune Response Panel (Illumina, San Diego, CA, USA). After quantifying the library using a Bioanalyzer, NGS analysis was performed using the MiniSeq System (Illumina). Data were uploaded and analyzed on the cloud-based software application BaseSpace Sequence Hub (Illumina). All data were uploaded to the National Center for Biotechnology Information Gene Expression Omnibus database (GSE154938).

TABLE 1 | Patient characteristics.

Characteristics		Value
cases		61
samples		71
Age(range)		77.30 (40-98)
Sex		
	Male	22 (36.1%)
	Female	39 (63.9%)
Race		
	Asian(Japanese)	61 (100%)
MCPyV		Cases (n=61)
	Positive	38 (62.3%)
	Negative	23 (37.7%)
Primary Site		Cases (n=61)
	Head&Neck	43 (67.6%)
	Trunk	1 (1.6%)
	Limbs	17 (27.9%)
Lesion		Samples (n=71)
	Primary	60 (84.5%)
	Skin Meta	11 (15.5%)
Stage at collection		Samples (n=71)
	I	24 (33.8%)
	II	23 (32.4%)
	III	16 (22.5%)
	IV	8 (11.3%)
Treatment		Cases (n=61)
	Surgery	15 (24.6%)
	RT	3 (4.9%)
	Surgery+RT	30 (49.2%)
	Surgery+Chemo	2 (3.3%)
	Surgery+RT+Chemo	4 (6.6%)
	Surgery+RT+ICI	2 (3.3%)
	Spontaneous Regression	5 (8.2%)

RT, radiation therapy; Chemo, chemotherapy; ICI, immune checkpoint inhibitor.

Data Analysis

NGS data were analyzed on the cloud-based software BaseSpace Sequence Hub (Illumina) using the RNA Amplicon application. A clustered heatmap of all samples was generated using the online tool iDEP.91 (http://bioinformatics.sdstate.edu/idep/). Disease-specific survival was calculated as the time that elapsed from sample collection to death from MCC and analyzed using the Kaplan-Meier method. Statistical analyses were performed using Graph Pad Prism 9 (Graph Pad Software, San Diego, CA, USA) and Pharmaco Analyst Software (Humanlife, Tokyo, Japan). Probability values of less than 0.05 were considered statistically significant.

RESULTS

Virus-Negative MCC Without TLSs Has a Poor Prognosis

The positive rate of MCPyV infection was 62.3% in our Japanese cohort. 48 samples were TLS-positive and 23 samples were TLS-negative. A weak magnification image of a typical tumor is shown in **Figures 1A, B** shows the MCPyV large T antigen staining of the same tumor. This tumor was MCPyV positive. Like this tumor, in many samples, TLSs were observed in the stroma inside the tumor, but not in the surrounding area. Most of the TLSs were immature; mature TLSs with CD3-positive cells circumferentially surrounding a cluster of CD20-positive cells were observed only in a few samples (**Figure 1C**). Only in mature TLSs, CD21-positive follicular dendritic cells (FDCs) were observed within a cluster of CD20-positive cells (**Figure 1D**). TLS-positive samples had a significantly better prognosis than TLS-negative samples (Gehan-Breslow-Wilcoxon test, p=0.0468; **Figure 2A**). When further divided by the presence of MCPyV infection, MCPyV-positive samples had a good prognosis with or without TLSs, and the MCPyV-negative/TLS-positive samples had a similarly good prognosis as MCPyV-positive samples. Only MCPyV-negative/TLS-negative samples had a significantly poor prognosis (Logrank test for trend, p=0.0497; **Figure 2B**). Notably, all samples that showed spontaneous regression were MCPyV-positive/TLS-positive. There was no significant difference between samples with 1 or 2 TLSs and TLS-negative samples (Gehan-Breslow-Wilcoxon test, p=0.249), but samples with more than 3 TLSs showed a significantly better prognosis than TLS-negative samples (Gehan-Breslow-Wilcoxon test, p=0.0413, **Figure 2C**). There was no correlation between the presence of TLS and MCPyV infection (p=0.60, Fisher's exact test, 2-tailed), and there was no correlation between the number of TLSs and MCPyV infection (student T test, **Figure 2D**).

The number6 of infiltrating CD8-positive cells and PD-1-positive cells did not differ significantly between samples with and without TLS or MCPyV infection (one-way ANOVA, **Figures 2E, F**). The intensity of PD-L1 expression in the tumors also did not differ significantly between samples with and without TLS or MCPyV infection (one-way ANOVA, **Figure 2G**).

Comprehensive RNA Sequencing

Comprehensive RNA sequencing of 395 immune-related genes revealed high expression of some genes, such as *PTPRC*, *IDO1*, and *CD52*, and some chemokine genes, including *CXCL13, CCL5*, and *CXCR3*, in the TLS-positive samples (**Figure 3A**). Comparison of MCPyV-negative/TLS-negative samples with others revealed that several genes, such as *MYC, PTGS2, KREMEN1, G6PD, DEACAM1*, and *BAGE*, were highly expressed in the MCPyV-negative/TLS-negative samples. In other samples with a good prognosis, including TLS-positive samples and TLS-negative/MCPyV-positive samples, we observed upregulated expression of *IDO1, IDO2*, and *CD27*, and some chemokine genes, including *CCR2*, *CXCR3*, and *CX3CR1*, as well as *PTPRC* (encoding CD45) and *MS4A1* (encoding CD20), which encode cell surface proteins of tumor-infiltrating lymphocytes (**Figure 3B**).

Chemokine Landscape in TLS Formation in Virus-Positive or Virus-Negative MCC

A total of 27 chemokine and chemokine receptor genes included in the Illumina Immune Response Panel were analyzed. Hierarchical cluster analysis revealed that 11 chemokine genes (5 ligands and 6 receptors), including *CXCL13* and *CCR7*, were highly expressed in TLS-positive samples (**Figure 3C**). The

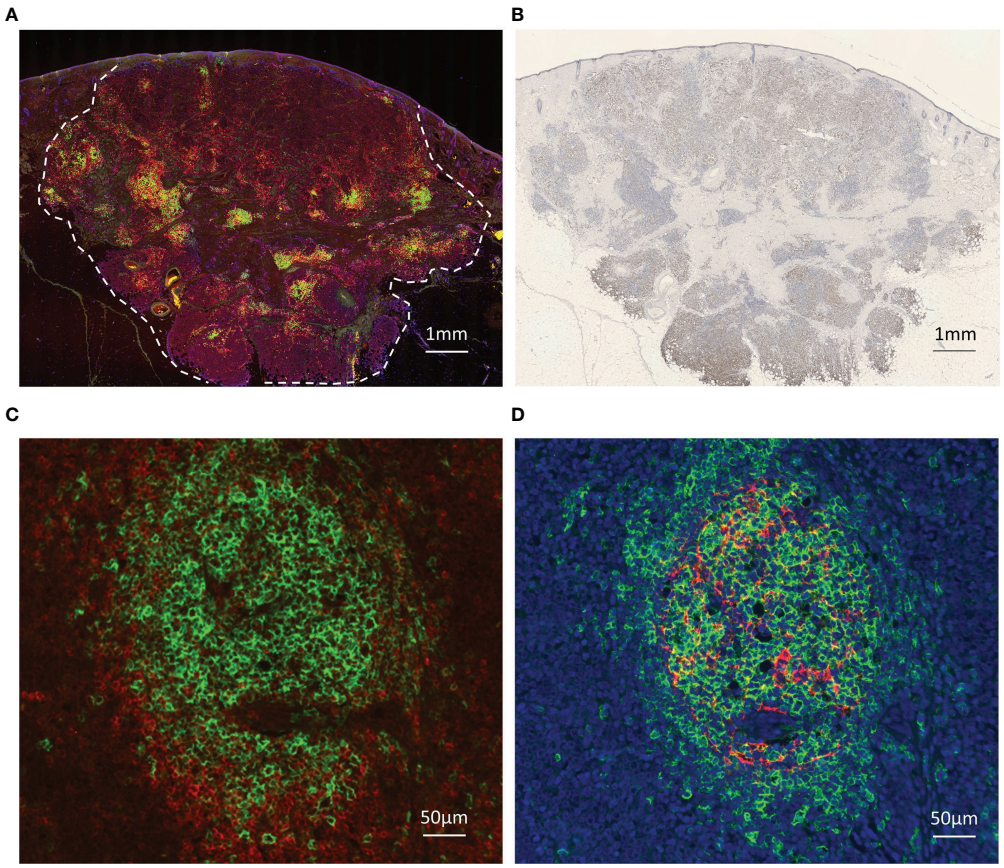

FIGURE 1 | Images of immunohistochemical and immunofluorescent analysis. **(A)** TLSs in Merkel cell carcinoma. Triple immunofluorescence staining for CD20 (green), CD3 (red), and DAPI (blue). Broken line indicates tumor border. Scale bar, 1 mm. **(B)** Immunohistochemical staining for MCPyV large T antigen (CM2B4, brown). Scale bar, 1 mm. TLSs were observed in the stroma inside the tumor, but not in the surrounding area. **(C)** Representative high magnification image of the mature TLS. CD20 (green), CD3 (red), Scale bar, 100 μm. A cluster of CD20-positive cells is surrounded by CD3-positive cells. **(D)** Representative high magnification image of the same mature TLS. CD20 (green), CD21 (red), DAPI (blue). Scale bar, 100 μm. CD21-positive follicular dendritic cells (FDCs) were observed within a cluster of CD20-positive cells.

details of each as violin plots and results of statistical analyses are shown in **Figure 4**. The details of 16 other chemokine genes are shown in **Supplementary Figure 1**. In the TLS-positive samples, 5 chemokine genes, *CCL5*, *CCR2*, *CCR7*, *CXCL9*, and *CXCL13*, were significantly upregulated compared with TLS-negative samples in both MCPyV-positive and MCPyV-negative samples. Only two of them, CXCL13 and CCL5, were barely affected by the presence or absence of MCPyV, but only by the presence or absence of TLSs. On the other hand, 2 chemokine genes, *CXCL10* and *CX3CR1*, had significantly different levels of expression in the presence or absence of MCPyV infection in TLS-negative samples.

Chemokines May Be a Useful Prognostic Marker in Their Own Right

The expression values of *CXCL13* and *CCL5* were separated by the presence or absence of TLSs, and the receiver operating characteristic (ROC) curves were drawn and the cutoff values were set at 142 count per million (CPM) for *CXCL13* and 547.5 CPM for *CCL5*. CXCL13-high samples showed significantly better prognosis than CXCL13-low samples (Gehan-Breslow-Wilcoxon test, p=0.0116, **Figure 5A**). CCL5-high samples also showed significantly better prognosis than CCL5-low samples (Gehan-Breslow-Wilcoxon test, p=0.0202, **Figure 5B**). These analyses were performed on 40 samples, excluding one case of unknown prognosis, from the 41 samples that underwent RNA extraction.

DISCUSSION

Our findings indicate that the presence of TLSs is a potential prognostic marker, even for MCPyV-negative cases. To our knowledge, this study is the first to analyze the relationship between the presence of TLSs, MCPyV infection, and prognosis in MCC. A previous study indicated that MCPyV-positive MCC has a better prognosis than MCPyV-negative MCC (13). In the present study, MCPyV-positive patients had a good prognosis with

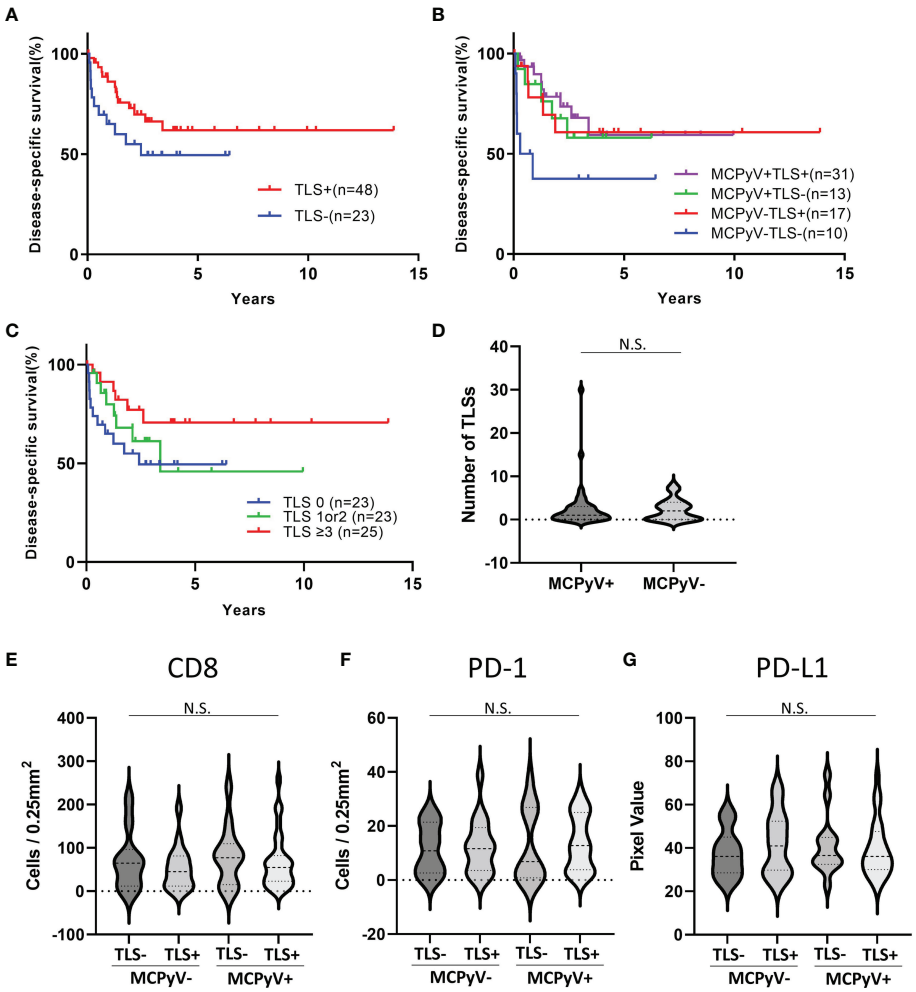

FIGURE 2 | Statistical analyses of immunohistochemical and immunofluorescent analysis. **(A)** Kaplan-Meier curves for the samples with or without TLSs. Gehan-Breslow-Wilcoxon test, p=0.0468. **(B)** Kaplan-Meier curves for the samples with or without TLSs and MCPyV infection. Logrank test for trend, p=0.0497. **(C)** Kaplan-Meier curves for the samples with 0 TLS, 1 or 2 TLSs, and 3 or more TLSs. Logrank test for trend, p=0.0663. **(D)** Violin plots of the number of TLSs with or without MCPyV. There was no significant difference (student T test). **(E–G)** Violin plots of infiltrating lymphocytes and PD-L1 expression. There was no significant difference (one-way ANOVA). N.S., not significant.

or without TLSs. On the other hand, MCPyV-negative cases had a similar prognosis to MCPyV-positive cases if TLSs were present, but a significantly worse prognosis if TLSs were not present.

TLSs are small lymphoid follicle-like structures that appear around various types of inflammation and cancer, apart from the primary lymph nodes of the thymus and bone marrow, and secondary lymph nodes such as lymph nodes, tonsils, and Peyer's plate. It serves as a front base for antigen presentation and lymphocyte activation, reflecting an active immune response in the local microenvironment. When TLSs form inside or around tumors, they activate anti-tumor immunity, and make immunotherapy more effective (6). According to a report by Hiraoka et al. in pancreatic cancer, TLS formed within the tumor has a more favorable prognosis than those formed around it (14). The presence or absence of TLS in MCC is important not only as a prognostic marker, but also as a predictive marker of response to ICIs. The relationship between TLSs and the presence or absence of MCPyV infection, which is a unique and immunologically interesting factor in MCC, has not been studied before. MCPyV-positive MCC shows active tumor immunity and comparable responsiveness to immunotherapy, despite having lower TMB and fewer neoantigens than UV-induced MCCs (3–5). The present study also revealed that the prognosis of MCPyV-positive MCC is not affected by the presence or absence of TLSs. It deserves further investigation and a prospective study should be conducted to investigate the correlation with the actual effect of ICIs.

The present study also suggested associations between many immunological factors and TLSs or MCPyV. For example, based on the RNA sequencing results, *G6PD* was significantly upregulated in MCPyV-negative/TLS-negative samples. Glucose-6-phosphate dehydrogenase (G6PD) is a factor that

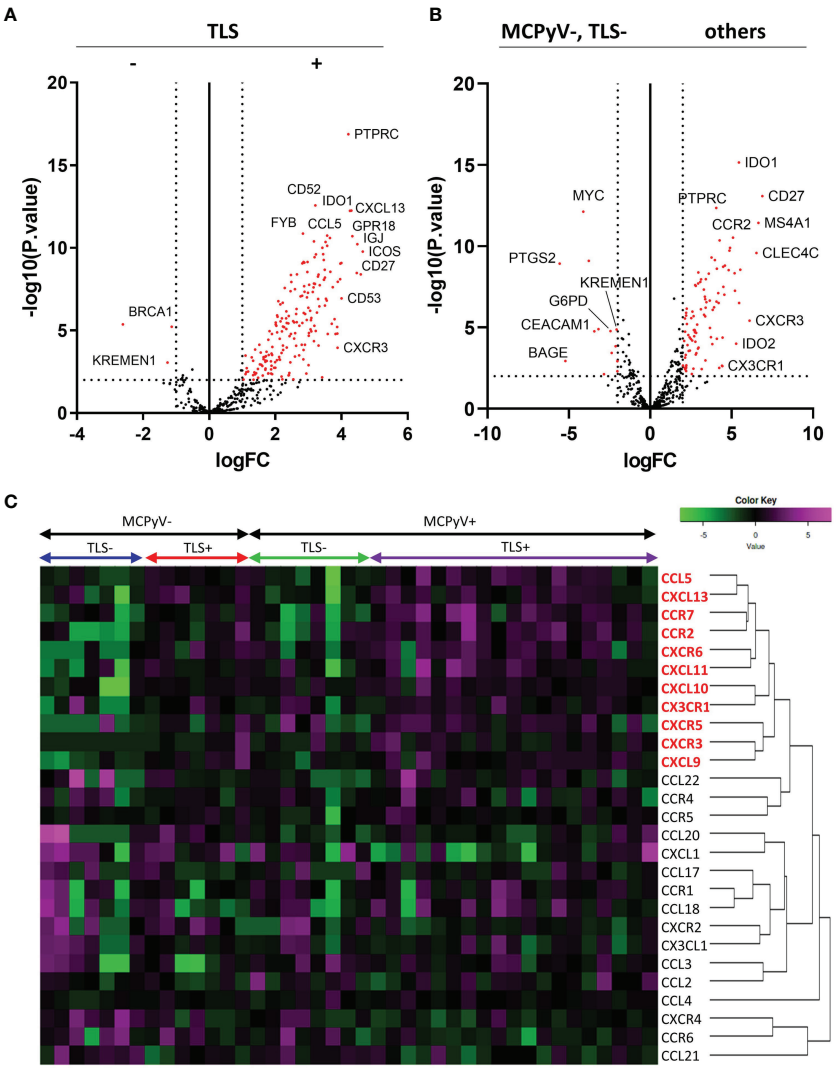

FIGURE 3 | Results of the RNA sequencing. **(A)** Volcano plots comparing TLS-positive and TLS-negative cases. Vertical dotted lines indicate logFC=+/-1. Horizontal dotted line indicates -log10 (p.value)=2. **(B)** Volcano plots comparing MCPyV-negative, TLS=negative cases and others. **(C)** RNA expression heatmap of 27 chemokine and chemokine receptor genes. The chemokines shown in red are elevated in the TLS-positive samples.

we previously reported as a promising prognostic and immune activity biomarker in MCC (15). Thus, in the present study using the same cohort, *G6PD* was highly expressed, indicating a poor prognosis as well as low immune activity in this group. On the other hand, expression of *IDO1*, *IDO2*, and *CD27* is significantly upregulated in TLS-positive samples. Indoleamine 2,3-dioxygenase (IDO) is an immune checkpoint that induces regulatory T cells and suppresses tumor immunity (16, 17), and its high expression correlates with a poor prognosis in several cancers (18, 19). This paradoxical upregulation of IDO in the group with a good prognosis may be a response to increased tumor immune activity as well as PD-L1 expression in MCC (10). CD27 is a member of the tumor necrosis factor receptor superfamily that plays an important role in T cell activation. Its agonistic antibody in combination with ICI therapy is expected to be effective against MCC (20).

A variety of chemokines are involved in the formation of TLSs (21, 22). In particular, CXCL13 is expressed on PD-1–positive lymphocytes and FDCs present in B-cell follicles plays a key role in the formation of TLSs by inducing the migration of B cells having CXCR5 as a receptor (23–25). CXCR5 is also expressed on T cells and CXCL13 mediates T cell recruitment to TLSs (26). Our results revealed that *CXCL13* was expressed with high specificity in TLS-positive samples. Although there was no significant difference in the expression of *CXCR5*, clustering analysis showed a similar trend. The significant difference observed only in *CXCL13* expression and not in *CXCR5* may be due to the immaturity of many of the TLSs observed in MCCs. On the other hand, in the

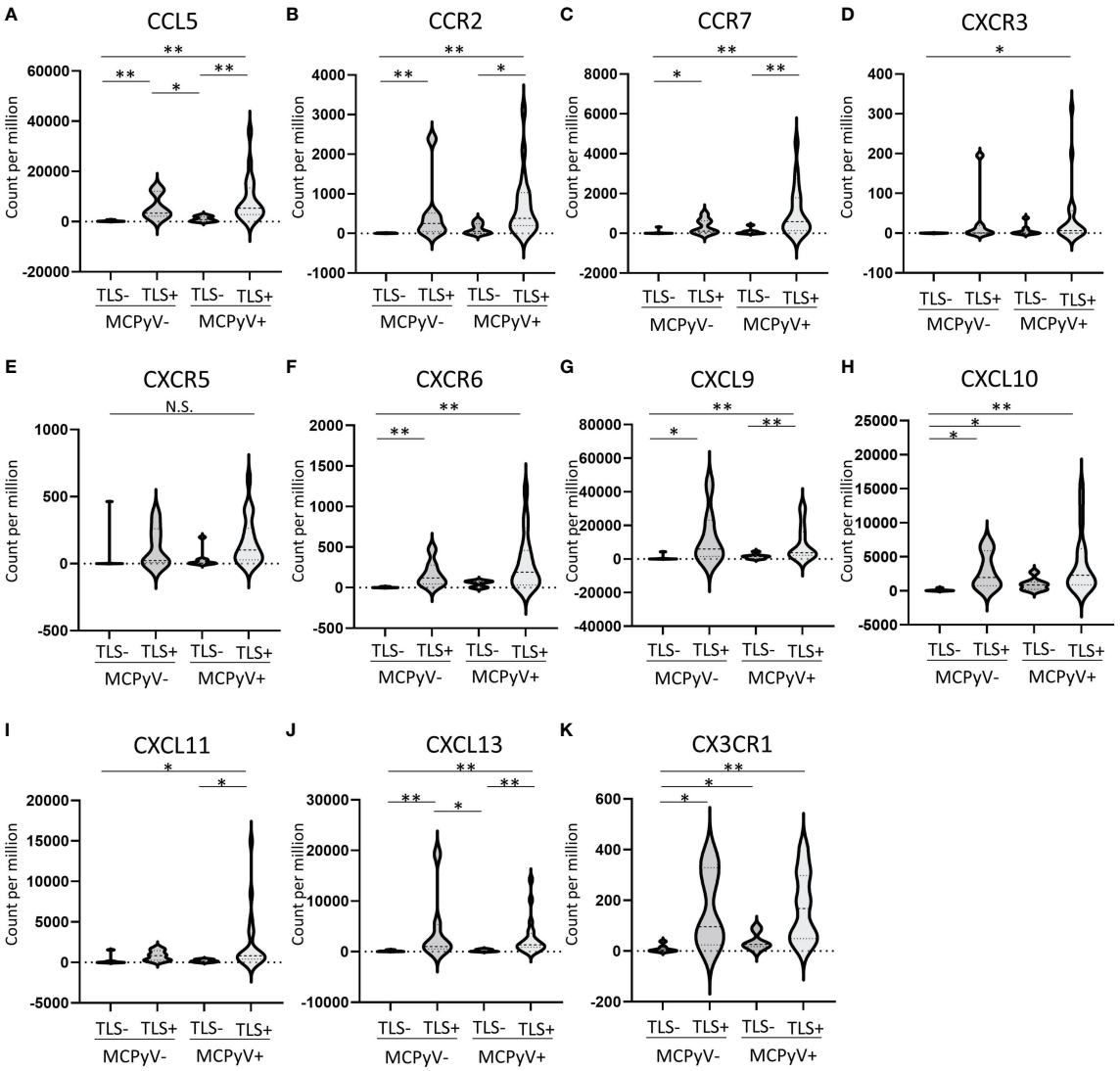

FIGURE 4 | **(A–K)** Violin plots of 11 chemokine genes that were highly expressed in TLS-positive samples. *p ≤ 0.05, **p ≤ 0.01, N.S., not significant; Steel-Dwass test.

CCL21/CCL19-CCR7 axis, which is considered to be as important for the formation of TLSs as the CXCL13-CXCR5 axis, high expression of CCR7 was only observed in TLS-positive cases, and no increase in expression of CCL21 was observed (CCL19 was not measured because it was not included in the panel used). These findings support previous reports that CCL21 expression is restricted to lymphatic vessels and does not contribute to TLS formation in the skin (27, 28).

Contrary to the sharply enhanced chemokine expression in TLS-positive samples, the numbers of infiltrating CD8-positive cells and PD-1-positive cells, and PD-L1 expression in tumors did not differ significantly between patients with and without TLSs. In addition, as mentioned above, the presence or absence of TLSs was not associated with the prognosis in MCPyV-positive cases. This finding suggests that MCPyV-positive MCC has a mechanism to activate tumor immunity that does not require TLSs. The chemokines having significantly upregulated expression in the presence or absence of MCPyV may provide a clue. In this study, *CX3CR1* and *CXCL10* were significantly upregulated in MCPyV-positive/TLS-negative samples compared with MCPyV-negative/TLS-negative samples. CX3CR1 and its ligand CX3CL1 play both a role in activating anti-tumor immunity and in promoting tumor formation and progression (29). High expression of CX3CL1-CX3CR1 enhances the recruitment of CD8+ cytotoxic T cells, natural killer cells, and dendritic cells, and results in a better prognosis (30, 31). On the other hand, the CX3CL1-CX3CR1 axis induces angiogenesis and assists in cancer growth (32). In skin cancer (basal cell carcinoma, squamous cell carcinoma), it is expressed in tumor-associated macrophages and is deeply involved in carcinogenesis (33). CXCL10 binds to CXCR3 (it is also upregulated in TLS-positive samples), which is abundantly expressed on cytotoxic T cells and natural killer cells (34).

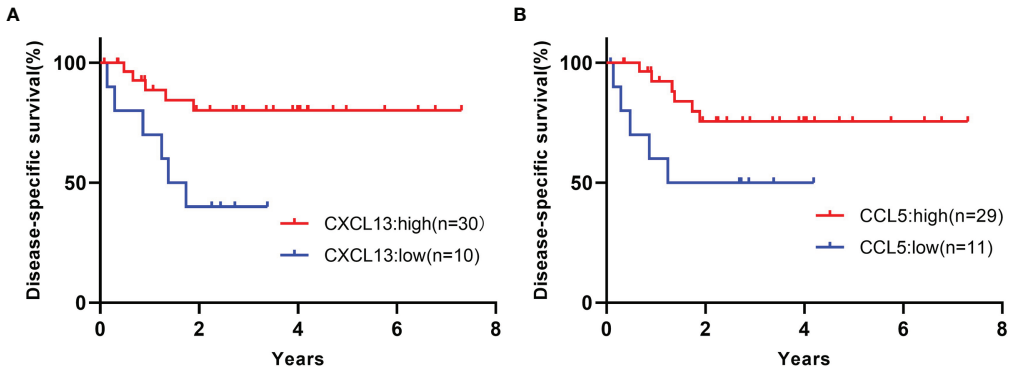

FIGURE 5 | **(A)** Kaplan-Meier curves for the samples of high or low *CXCL13* expression. Gehan-Breslow-Wilcoxon test, p=0.0116. **(B)** Kaplan-Meier curves for the samples of high or low *CCL5* expression. Gehan-Breslow-Wilcoxon test, p=0.0202. These analyses were performed on 40 samples, excluding one case of unknown prognosis, from the 41 samples that underwent RNA extraction.

CXCL10 activates anti-tumor immunity by inducing interferon gamma (35), and inhibits angiogenesis and prevents tumor growth (36). Tumor cell lines with high expression of CXCL10 exhibit suppressed growth (37). Although the roles of these chemokines in MCPyV-positive MCC remain unclear, they may contribute to improve the anti-tumor immune environment and a favorable prognosis even without the formation of TLSs.

In MCPyV-negative MCC, which is ultraviolet-induced and has many genetic mutations and neoantigens, the presence or absence of TLS formation is directly related to patient prognosis. On the other hand, MCPyV-positive MCCs seem to have a different mechanism of tumor immune activation. Elucidation of this mechanism will help us understand tumor immunity in MCC, which is strange compared to other tumors.

DATA AVAILABILITY STATEMENT

The datasets presented in this study can be found in online repositories. The names of the repository/repositories and accession number(s) can be found below: https://www.ncbi.nlm.nih.gov/, GSE154938.

ETHICS STATEMENT

The studies involving human participants were reviewed and approved by Clinical Research Management Center, Nagoya City University Hospital. Written informed consent for participation was not required for this study in accordance with the national legislation and the institutional requirements.

AUTHOR CONTRIBUTIONS

MN contributed to conception and design of the study, performed experiments and statistical analysis, wrote the first draft of the manuscript. TM performed experiments and statistical analysis. SK and AMa performed experiments. HK and AMo contributed to manuscript revision. All authors read and approved the submitted version of the manuscript.

FUNDING

This work was supported by a Grant-in-Aid for Scientific Research (C) from the Ministry of Education, Culture, Sports, Science, and Technology, Japan (No.20K08676) and the Japan Agency for Medical Research and Development (AMED) under grant (No. JP20cm0106301h0005, presented to: Hiroyoshi Nishikawa, National Cancer Center).

ACKNOWLEDGMENTS

We thank Dr. Kobayashi (Kanazawa University), Dr. Teramoto (Saitama Medical University International Medical Center), Dr. Yasuda (Gunma University), Dr. Wada (Yokohama City University), Dr. Ozawa (Osaka City University), Dr. Umemori (Nagaoka Red Cross Hospital), Dr. Ogata (Saitama Medical University), and Dr. Hata (Gifu Prefectural General Medical Center) for providing the tumor samples. We are grateful to Ms. Kasuya and Ms. Nishioka for their technical assistance.

SUPPLEMENTARY MATERIAL

The Supplementary Material for this article can be found online at: https://www.frontiersin.org/articles/10.3389/fonc.2022.811586/full#supplementary-material

Supplementary Table 1 | The 9 facilities where the samples were collected.

Supplementary Figure 1 | **(A–P)** Violin plots of 16 other chemokine genes that were not highly expressed in TLS-positive samples. *p ≤ 0.05, **p ≤ 0.01, N.S., not significant; Steel-Dwass test.

REFERENCES

1. Nakamura M, Morita A. Immune Activity in Merkel Cell Carcinoma. *J Dermatol* (2022) 49(1):68–74. doi: 10.1111/1346-8138.16232
2. Kaufman HL, Russell J, Hamid O, Bhatia S, Terheyden P, D'Angelo SP, et al. Avelumab in Patients With Chemotherapy-Refractory Metastatic Merkel Cell Carcinoma: A Multicentre, Single-Group, Open-Label, Phase 2 Trial. *Lancet Oncol* (2016) 17(10):1374–85. doi: 10.1016/S1470-2045(16)30364-3
3. Knepper TC, Montesion M, Russell JS, Sokol ES, Frampton GM, Miller VA, et al. The Genomic Landscape of Merkel Cell Carcinoma and Clinicogenomic Biomarkers of Response to Immune Checkpoint Inhibitor Therapy. *Clin Cancer Res* (2019) 25(19):5961–71. doi: 10.1158/1078-0432.CCR-18-4159
4. Goh G, Walradt T, Markarov V, Blom A, Riaz N, Doumani R, et al. Mutational Landscape of Mcpyv-Positive and Mcpyv-Negative Merkel Cell Carcinomas With Implications for Immunotherapy. *Oncotarget* (2016) 7 (3):3403–15. doi: 10.18632/oncotarget.6494
5. Topalian SL, Bhatia S, Amin A, Kudchadkar RR, Sharfman WH, Lebbé C, et al. Neoadjuvant Nivolumab for Patients With Resectable Merkel Cell Carcinoma in the Checkmate 358 Trial. *J Clin Oncol* (2020) 38(22):2476–87. doi: 10.1200/JCO.20.00201
6. Cabrita R, Lauss M, Sanna A, Donia M, Skaarup Larsen M, et al. Tertiary Lymphoid Structures Improve Immunotherapy and Survival in Melanoma. *Nature* (2020) 577(7791):561–5. doi: 10.1038/s41586-019-1914-8
7. Helmink BA, Reddy SM, Gao J, Zhang S, Basar R, Thakur R, et al. B Cells and Tertiary Lymphoid Structures Promote Immunotherapy Response. *Nature* (2020) 577(7791):549–55. doi: 10.1038/s41586-019-1922-8
8. Teillaud JL, Dieu-Nosjean MC. Tertiary Lymphoid Structures: An Anti-Tumor School for Adaptive Immune Cells and an Antibody Factory to Fight Cancer? *Front Immunol* (2017) 21:830. doi: 10.3389/fimmu.2017.00830
9. Behr DS, Peitsch WK, Hametner C, Lasitschka F, Houben R, Schönhaar K, et al. Prognostic Value of Immune Cell Infiltration, Tertiary Lymphoid Structures and PD-L1 Expression in Merkel Cell Carcinomas. *Int J Clin Exp Pathol* (2014) 7(11):7610–21.
10. Nakamura M, Magara T, Nojiri Y, Nishihara H, Kato H, Teramoto Y, et al. Increased Programmed Death Ligand-1 Expression in Metastatic Merkel Cell Carcinoma Associates With Better Prognosis. *J Dermatol Sci* (2020) 97 (2):165–7. doi: 10.1016/j.jdermsci.2019.12.012
11. Nakamura M, Magara T, Kobayashi Y, Kato H, Watanabe S, Morita A. Heterogeneity of Programmed Death-Ligand Expression in a Case of Merkel Cell Carcinoma Exhibiting Complete Regression After Multiple Metastases. *Br J Dermatol* (2019) 180(5):1228–9. doi: 10.1111/bjd.17430
12. Magara T, Nakamura M, Nojiri Y, Yoshimitsu M, Kano S, Matsubara A, et al. Tertiary Lymphoid Structures Correlate With Better Prognosis in Cutaneous Angiosarcoma. *J Dermatol Sci* (2021) 103(1):57–9. doi: 10.1016/j.jdermsci.2021.05.006
13. Moshiri AS, Doumani R, Yelistratova L, Blom A, Lachance K, Shinohara MM, et al. Polyomavirus-Negative Merkel Cell Carcinoma: A More Aggressive Subtype Based on Analysis of 282 Cases Using Multimodal Tumor Virus Detection. *J Invest Dermatol* (2017) 137(4):819–27. doi: 10.1016/j.jid.2016.10.028
14. Hiraoka N, Ino Y, Yamazaki-Itoh R, Kanai Y, Kosuge T, Shimada K. Intratumoral Tertiary Lymphoid Organ Is a Favourable Prognosticator in Patients With Pancreatic Cancer. *Br J Cancer* (2015) 112(11):1782–90. doi: 10.1038/bjc.2015.145
15. Nakamura M, Nagase K, Yoshimitsu M, Magara T, Nojiri Y, Kato H, et al. Glucose-6-Phosphate Dehydrogenase Correlates With Tumor Immune Activity and Programmed Death Ligand-1 Expression in Merkel Cell Carcinoma. *J Immunother Cancer* (2020) 8(2):e001679. doi: 10.1136/jitc-2020-001679
16. Munn DH, Mellor AL. IDO in the Tumor Microenvironment: Inflammation, Counter-Regulation, and Tolerance. *Trends Immunol* (2016) 37(3):193–207. doi: 10.1016/j.it.2016.01.002
17. Zhai L, Ladomersky E, Lenzen A, Nguyen B, Patel R, Lauing KL, et al. IDO1 in Cancer: A Gemini of Immune Checkpoints. *Cell Mol Immunol* (2018) 15 (5):447–57. doi: 10.1038/cmi.2017.143
18. Astigiano S, Morandi B, Costa R, Mastracci L, D'Agostino A, Ratto GB, et al. Eosinophil Granulocytes Account for Indoleamine 2,3-Dioxygenase-Mediated Immune Escape in Human Non-Small Cell Lung Cancer. *Neoplasia* (2005) 7(4):390–6. doi: 10.1593/neo.04658
19. Brandacher G, Perathoner A, Ladurner R, Schneeberger S, Obrist P, Winkler C, et al. Prognostic Value of Indoleamine 2,3-Dioxygenase Expression in Colorectal Cancer: Effect on Tumor-Infiltrating T Cells. *Clin Cancer Res* (2006) 12(4):1144–51. doi: 10.1158/1078-0432
20. Starzer AM, Berghoff AS. New Emerging Targets in Cancer Immunotherapy: CD27 (TNFRSF7). *ESMO Open* (2020) 4(Suppl 3):e000629. doi: 10.1136/esmoopen-2019-000629
21. Sautès-Fridman C, Petitprez F, Calderaro J, Fridman WH. Tertiary Lymphoid Structures in the Era of Cancer Immunotherapy. *Nat Rev Cancer* (2019) 19 (6):307–25. doi: 10.1038/s41568-019-0144-6
22. Kang W, Feng Z, Luo J, He Z, Liu J, Wu J, et al. Tertiary Lymphoid Structures in Cancer: The Double-Edged Sword Role in Antitumor Immunity and Potential Therapeutic Induction Strategies. *Front Immunol* (2021) 12:689270:689270. doi: 10.3389/fimmu.2021.689270
23. Vissers JL, Hartgers FC, Lindhout E, Figdor CG, Adema GJ. BLC (CXCL13) Is Expressed by Different Dendritic Cell Subsets *In Vitro* and *In Vivo*. *Eur J Immunol* (2001) 31(5):1544–9. doi: 10.1002/1521-4141(200105)31:5<1544::AID-IMMU1544>3.0.CO;2-I
24. Denton AE, Innocentin S, Carr EJ, Bradford BM, Lafouresse F, Mabbott NA, et al. Type I Interferon Induces CXCL13 to Support Ectopic Germinal Center Formation. *J Exp Med* (2019) 216(3):621–37. doi: 10.1084/jem.20181216
25. Thommen DS, Koelzer VH, Herzig P, Roller A, Trefny M, Dimeloe S, et al. A Transcriptionally and Functionally Distinct PD-1^+ $CD8^+$ T Cell Pool With Predictive Potential in Non-Small-Cell Lung Cancer Treated With PD-1 Blockade. *Nat Med* (2018) 24(7):994–1004. doi: 10.1038/s41591-018-0057-z
26. Kazanietz MG, Durando M, Cooke M. CXCL13 and Its Receptor CXCR5 in Cancer: Inflammation, Immune Response, and Beyond. *Front Endocrinol (Lausanne)* (2019) 10:471. doi: 10.3389/fendo.2019.00471
27. Colbeck EJ, Ager A, Gallimore A, Jones GW. Tertiary Lymphoid Structures in Cancer: Drivers of Antitumor Immunity, Immunosuppression, or Bystander Sentinels in Disease? *Front Immunol* (2017) 8:1830. doi: 10.3389/fimmu.2017.01830
28. Chen SC, Vassileva G, Kinsley D, Holzmann S, Manfra D, Wiekowski MT, et al. Ectopic Expression of the Murine Chemokines CCL21a and CCL21b Induces the Formation of Lymph Node-Like Structures in Pancreas, But Not Skin, of Transgenic Mice. *J Immunol* (2002) 168(3):1001–8. doi: 10.4049/jimmunol.168.3.1001
29. Rivas-Fuentes S, Salgado-Aguayo A, Arratia-Quijada J, Gorocica-Rosete P. Regulation and Biological Functions of the CX3CL1-CX3CR1 Axis and Its Relevance in Solid Cancer: A Mini-Review. *J Cancer* (2021) 12(2):571–83. doi: 10.7150/jca.47022
30. Park MH, Lee JS, Yoon JH. High Expression of CX3CL1 by Tumor Cells Correlates With a Good Prognosis and Increased Tumor-Infiltrating CD8+ T Cells, Natural Killer Cells, and Dendritic Cells in Breast Carcinoma. *J Surg Oncol* (2012) 106(4):386–92. doi: 10.1002/jso.23095
31. Liu J, Li Y, Zhu X, Li Q, Liang X, Xie J, et al. Increased CX3CL1 Mrna Expression Level Is a Positive Prognostic Factor in Patients With Lung Adenocarcinoma. *Oncol Lett* (2019) 17(6):4877–90. doi: 10.3892/ol.2019.10211
32. Ren T, Chen Q, Tian Z, Wei H. Down-Regulation of Surface Fractalkine by RNA Interference in B16 Melanoma Reduced Tumor Growth in Mice. *Biochem Biophys Res Commun* (2007) 364(4):978–84. doi: 10.1016/j.bbrc.2007.10.124
33. Ishida Y, Kuninaka Y, Yamamoto Y, Nosaka M, Kimura A, Furukawa F, et al. Pivotal Involvement of the CX3CL1-CX3CR1 Axis for the Recruitment of M2 Tumor-Associated Macrophages in Skin Carcinogenesis. *J Invest Dermatol* (2020) 140(10):1951–61.e6. doi: 10.1016/j.jid.2020.02.023
34. Tokunaga R, Zhang W, Naseem M, Puccini A, Berger MD, Soni S, et al. CXCL9, CXCL10, CXCL11/CXCR3 Axis for Immune Activation - A Target for Novel Cancer Therapy. *Cancer Treat Rev* (2018) 63:40–7. doi: 10.1016/j.ctrv.2017.11.007
35. Tannenbaum CS, Tubbs R, Armstrong D, Finke JH, Bukowski RM, Hamilton TA. The CXC Chemokines IP-10 and Mig Are Necessary for IL-12-Mediated Regression of the Mouse RENCA Tumor. *J Immunol* (1998) 161(2):927–32.
36. Luster AD, Greenberg SM, Leder P. The IP-10 Chemokine Binds to a Specific Cell Surface Heparan Sulfate Site Shared With Platelet Factor 4 and Inhibits

Endothelial Cell Proliferation. *J Exp Med* (1995) 182(1):219–31. doi: 10.1084/jem.182.1.219

37. Feldman AL, Friedl J, Lans TE, Libutti SK, Lorang D, Miller MS, et al. Retroviral Gene Transfer of Interferon-Inducible Protein 10 Inhibits Growth of Human Melanoma Xenografts. *Int J Cancer* (2002) 99(1):149–53. doi: 10.1002/ijc.10292

Conflict of Interest: MN received honorarium for lecturing at seminars held by companies such as Merck Biopharma Co., Ltd.

The remaining authors declare that the research was conducted in the absence of any commercial or financial relationships that could be construed as a potential conflict of interest.

Publisher's Note: All claims expressed in this article are solely those of the authors and do not necessarily represent those of their affiliated organizations, or those of the publisher, the editors and the reviewers. Any product that may be evaluated in this article, or claim that may be made by its manufacturer, is not guaranteed or endorsed by the publisher.

frontiers in Oncology

REVIEW
published: 03 March 2022
doi: 10.3389/fonc.2022.841721

The Aryl Hydrocarbon Receptor in the Pathogenesis of Environmentally-Induced Squamous Cell Carcinomas of the Skin

Christian Vogeley[†], *Katharina M. Rolfes*[†], *Jean Krutmann and Thomas Haarmann-Stemmann*[*]

IUF - Leibniz-Research Institute for Environmental Medicine, Düsseldorf, Germany

OPEN ACCESS

Edited by:
Suzie Chen, Rutgers, The State University of New Jersey, United States

Reviewed by:
Sheikh Umar Ahmad, Indian Institute of Integrative Medicine (CSIR), India
Shobhan Gaddameedhi, North Carolina State University, United States

***Correspondence:**
Thomas Haarmann-Stemmann Thomas.haarmann-stemmann@iuf-duesseldorf.de

[†]*These authors have contributed equally to this work*

Specialty section:
This article was submitted to Skin Cancer, a section of the journal Frontiers in Oncology

Received: *22 December 2021*
Accepted: *09 February 2022*
Published: *03 March 2022*

Citation:
Vogeley C, Rolfes KM, Krutmann J and Haarmann-Stemmann T (2022) The Aryl Hydrocarbon Receptor in the Pathogenesis of Environmentally-Induced Squamous Cell Carcinomas of the Skin. Front. Oncol. 12:841721. doi: 10.3389/fonc.2022.841721

Cutaneous squamous cell carcinoma (SCC) is one of the most frequent malignancies in humans and academia as well as public authorities expect a further increase of its incidence in the next years. The major risk factor for the development of SCC of the general population is the repeated and unprotected exposure to ultraviolet (UV) radiation. Another important risk factor, in particular with regards to occupational settings, is the chronic exposure to polycyclic aromatic hydrocarbons (PAH) which are formed during incomplete combustion of organic material and thus can be found in coal tar, creosote, bitumen and related working materials. Importantly, both exposomal factors unleash their carcinogenic potential, at least to some extent, by activating the aryl hydrocarbon receptor (AHR). The AHR is a ligand-dependent transcription factor and key regulator in xenobiotic metabolism and immunity. The AHR is expressed in all cutaneous cell-types investigated so far and maintains skin integrity. We and others have reported that in response to a chronic exposure to environmental stressors, in particular UV radiation and PAHs, an activation of AHR and downstream signaling pathways critically contributes to the development of SCC. Here, we summarize the current knowledge about AHR's role in skin carcinogenesis and focus on its impact on defense mechanisms, such as DNA repair, apoptosis and anti-tumor immune responses. In addition, we discuss the possible consequences of a simultaneous exposure to different AHR-stimulating environmental factors for the development of cutaneous SCC.

Keywords: aryl hydrocarbon receptor (AHR), apoptosis, DNA repair, immunosuppression, ultraviolet radiation, skin cancer, polycyclic aromatic hydrocarbons

INTRODUCTION

Non-melanoma skin cancers, in particular basal cell carcinoma and SCC, are among the most frequent malignancies in humans (1–3). Cutaneous SCC primarily develop on sun-exposed areas of the body. Accordingly, a chronic exposure to artificial (tanning beds) or solar UVB radiation and the associated accumulation of damaged keratinocytes is the most important risk factor for SCC (1–3).

Due to the continuously growing number of elderly individuals in the general population as well as the unbroken popularity of tanned skin among younger generations, the incidence of SCC is predicted to further increase (1–3). This trend might be exacerbated by environmental, occupational and life style-related exposure to carcinogenic chemicals, especially combustion-derived PAHs, alone or in combination with UV exposure (3). In addition, the climate change and associated global weather shifts may have an impact on human health and will probably increase the incidence of skin cancers and other malignancies (4, 5). Because SCC is not only a growing medical problem but also a substantial economic burden to health care systems (3, 6), there is an urgent need for the development of novel preventive and therapeutic measures. In this context, the AHR, a ligand-activated transcription factor and key regulator in xenobiotic metabolism and immunity, seems to be a promising molecular target. This notion is strengthened by the outcome of a two-stage genome-wide association study identifying the AHR as a novel susceptibility locus for cutaneous SCC in humans (7).

In this review article, we focus on the critical functions of AHR for DNA damage-dependent processes and immune responses which may contribute to the development of SCC in chronically UV- and/or PAH-exposed skin. Please note that while we are focusing on the mentioned aspects other functions of the AHR system might fall short, which may be also relevant for the process of skin cancer development.

AHR IN XENOBIOTIC METABOLISM AND CHEMICAL CARCINOGENESIS

The multistage model of carcinogenesis, defining the process of tumor development as a strict sequence of initiation, promotion and progression, was established more than 70 years ago (8, 9). In these studies, the researchers induced skin tumorigenesis in mice by applying 7,12-dimethylbenz[*a*]anthracene (DMBA) as tumor-initiator and phorbol ester-containing croton oil as tumor-promoting agent. Sequencing of the tumor DNA as well as further mechanistic studies provided evidence that PAHs initiate carcinogenesis by inducing mutations primarily in the *Ha-Ras* oncogene and that this process requires a metabolic conversion of the *per se* non-toxic chemicals to highly reactive metabolites, a process which is primarily carried out by AHR-regulated cytochrome P450 (CYP) monooxygenases (10–12).

AHR Ligands and Signaling Pathways

The AHR belongs to the basic helix-loop-helix Per-ARNT-Sim superfamily of transcription factors whose members translate developmental, physiological and environmental signals into biochemical processes and cell biological responses (13). Within this protein superfamily, the AHR is the only member which is activated by binding of small molecular weight compounds (ligands). AHR ligands can be divided into exogenous and endogenous compounds (14–17). The list of exogenous AHR ligands encompasses environmental pollutants, such as PAHs and dioxins, plant- and microbiota-derived indoles and polyphenols, and pharmaceutical drugs. Indole derivatives, such as indolo[3,2-*b*]carbazole, 6-formylindolo[3,2-*b*]carbazole (FICZ) and 2-(1'H-Indole-3'-carbonyl)-thiazole-4-carboxylic acid methyl ester as well as tryptophan metabolites, such as kynurenic acid and xanthurenic acid, are considered as relevant endogenous agonists of AHR (14–17).

In its inactive state, the AHR is trapped in a cytosolic multiprotein complex, composed of two heat-shock protein 90 (HSP90) molecules, the AHR-interacting protein, the co-chaperone p23 and the soluble tyrosine kinase c-Src (18) (**Figure 1**). Upon ligand binding, the cytosolic multiprotein complex dissociates, the AHR translocates into the nucleus, and dimerizes with its binding partner AHR nuclear translocator (ARNT). This heterodimer binds to xenobiotic-responsive elements (XRE) in the enhancer region of target genes to induce their expression (14–16). Typical AHR target genes encode for xenobiotic-metabolizing enzymes, such as CYP1A1, CYP1A2 and CYP1B1 (14–16). Another XRE-regulated gene codes for the AHR repressor, an AHR-related protein that lacks a transactivation domain and represses AHR signaling by competing for ARNT- and XRE-binding (19). Next to this so-called canonical AHR signaling pathway, the dissociation of the multiprotein complex leads to the release of c-Src, which subsequently may activate the epidermal growth factor receptor (EGFR) and downstream mitogen-activated protein kinase signal transduction (20–22) (**Figure 1**). Furthermore, AHR interacts with other transcription factors, including nuclear factor-κB (NF-κB) (23, 24), hypoxia-inducible factor-1α (25, 26), estrogen receptor-α (27, 28), and nuclear factor erythroid 2-related factor 2 (29, 30). These non-canonical functions may explain the frequently observed tissue- and cell-specific effects of AHR signaling and probably contribute to the pathogenesis of inflammatory and malignant diseases.

AHR and Metabolic Activation of Polycyclic Aromatic Hydrocarbons

Exposure to environmental, occupational and life-style related organic pollutants is considered to be involved in the onset of cutaneous SCC (3). Especially a long-lasting occupational exposure to PAHs present in soot and various working materials, such as coal tar, bitumen and petroleum, may facilitate skin carcinogenesis (3, 31). In addition, the elevated risk of smokers to develop cutaneous SCC is largely attributed to the PAH fraction present in tobacco smoke (32–34). The genotoxic potential of PAHs is primarily unleashed by their activation through AHR-dependent CYP1 isoforms (10–12) (**Figure 2**). For instance, CYP1A1 and microsomal epoxide hydrolase 1 (EPHX1) sequentially metabolize benzo[*a*]pyrene (B[a]P) to B[a]P-7,8-dihydrodiol-9,10-epoxide (BPDE), a highly carcinogenic compound which forms bulky DNA adducts by binding to guanine at the N2 position (10–12). Since CYP1A1 expression is regulated by the AHR, AHR-deficient mice as well as mice bearing an epidermis-specific ARNT-deletion were resistant towards B[a]P induced skin carcinogenesis (35, 36). In contrast to B[a]P, DMBA is metabolized by CYP1A1, CYP1B1

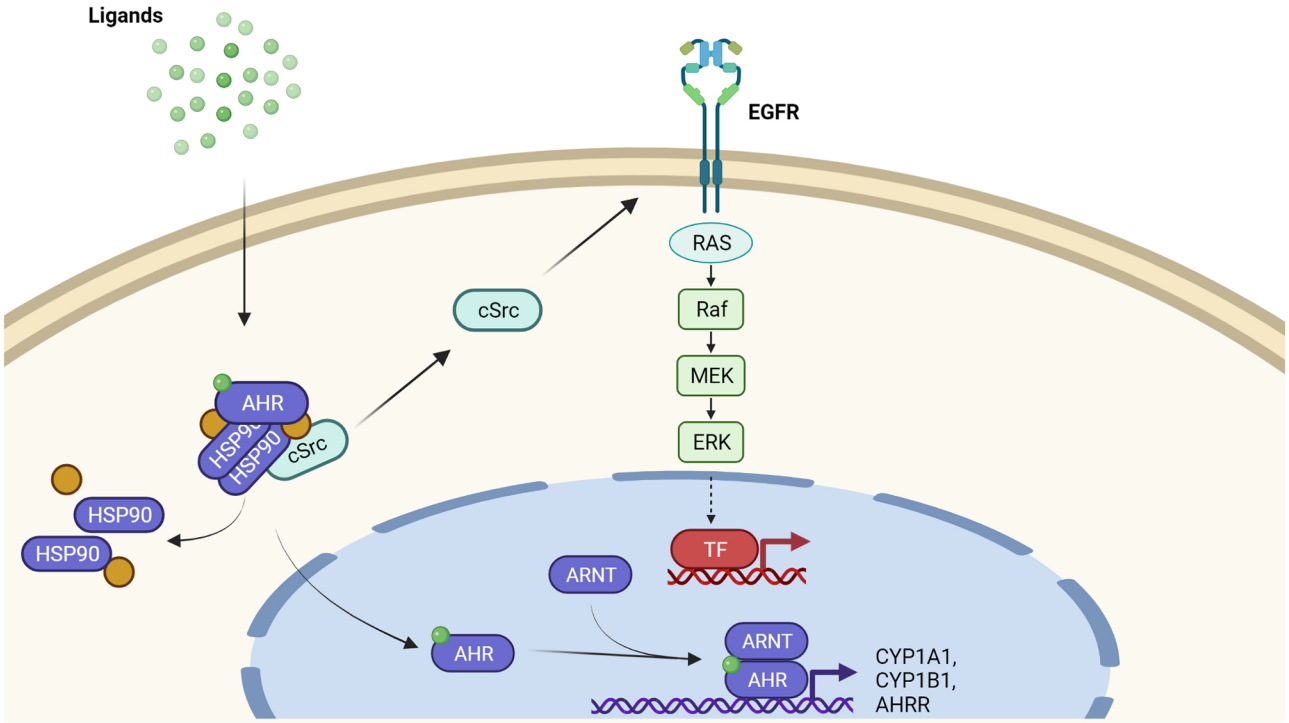

FIGURE 1 | AHR-dependent signaling pathways. Inactive AHR is part of a cytosolic multiprotein. complex consisting of a HSP90 dimer, other chaperone molecules and tyrosine kinase c-Src. Upon ligand binding, the multiprotein complex dissociates and AHR translocates into the nucleus. Nuclear AHR heterodimerizes with ARNT and binds to the enhancer region of target genes, for instance encoding CYP1A1, CYP1B1, and AHRR, to enhance their expression. In addition to this canonical pathway, the AHR ligand-driven release of c-Src from the cytosolic multiportion complex may stimulate EGFR and downstream mitogen-activated protein kinases, resulting in the transcriptional induction of another set of genes.

and EPHX1. Whereas CYP1A1 leads to the detoxification of DMBA, the CYP1B1-mediated oxidation results in an accumulation of highly carcinogenic DMBA-3,4-diol-1,2-epoxide (37, 38). CYP1-specific alterations in the detoxification and metabolic activation was also reported for other PAHs, such as dibenzo[*a,l*]pyrene (39) and dibenzo[*def,p*]chrysene (40). Thus, the carcinogenic potential of PAHs is determined by the CYP1 isoform predominantly expressed in the exposed cell population. Interestingly, the expression of CYP1B1 is not exclusively regulated by AHR (41–43) and, accordingly, AHR-deficient mice still express sufficient amounts of CYP1B1 to toxify DMBA and initiate skin carcinogenesis (44). Another carcinogenesis study revealed that AHR-deficiency protects mice against the skin carcinogenicity of PAH-rich airborne particulate matter (PM) (45).

At this point, we should mention that the CYP1-derived reactive PAH metabolites are efficiently detoxified through conjugation to glutathione, glucuronic acid or other hydrophilic molecules by phase 2 enzymes (11). However, in case the capacity of the conjugating enzyme system is exhausted, relevant amounts of reactive phase 1 metabolites may react with the DNA. Depending on the efficacy of other defense mechanisms, such as DNA repair and apoptosis, these DNA lesions may give rise to mutations (11, 46, 47).

The same is true for oxidative DNA damage that may occur during PAH metabolism. Specifically, CYP1-derived PAH dihydrodiols may serve as substrate for aldo-keto reductases (AKR), a family of cytosolic NADPH-dependent oxidoreductases (48). Several AKR1 isoforms, including AKR1C3, are capable of converting PAH dihydrodiols to the respective catechols which in the presence of oxygen can undergo redox-cycling. This results in the generation of reactive oxygen species (ROS), such as hydrogen peroxide and superoxide, which may contribute to skin carcinogenesis by oxidatively damaging DNA and other macromolecules (49, 50). In addition, AKR1C3 reduces prostaglandin (PG) D_2 to 9α,11β-PGF_2, a process which may fuel type 2 T helper (Th2) cell-related inflammatory responses in the skin (51, 52). Noteworthy, this AKR1C3-catalyzed reaction reduces the spontaneous dehydration of PGD_2 to 15Δ-PGJ_2, an eicosanoid that acts anti-inflammatory by inducing peroxisome proliferator-activated receptor-γ signaling and inhibiting pro-inflammatory NF-κB signaling pathways (51). Importantly, AKR1C3 is highly expressed in human SCC (53) and, moreover, we found that a PAH exposure of human keratinocytes results in an AHR-dependent upregulation of this enzyme (22). Taken together, these findings suggest that an AHR/AKR1C3-dependent modulation of PGD_2 metabolism may foster the growth and apoptosis-resistance of initiated keratinocytes and SCC cells.

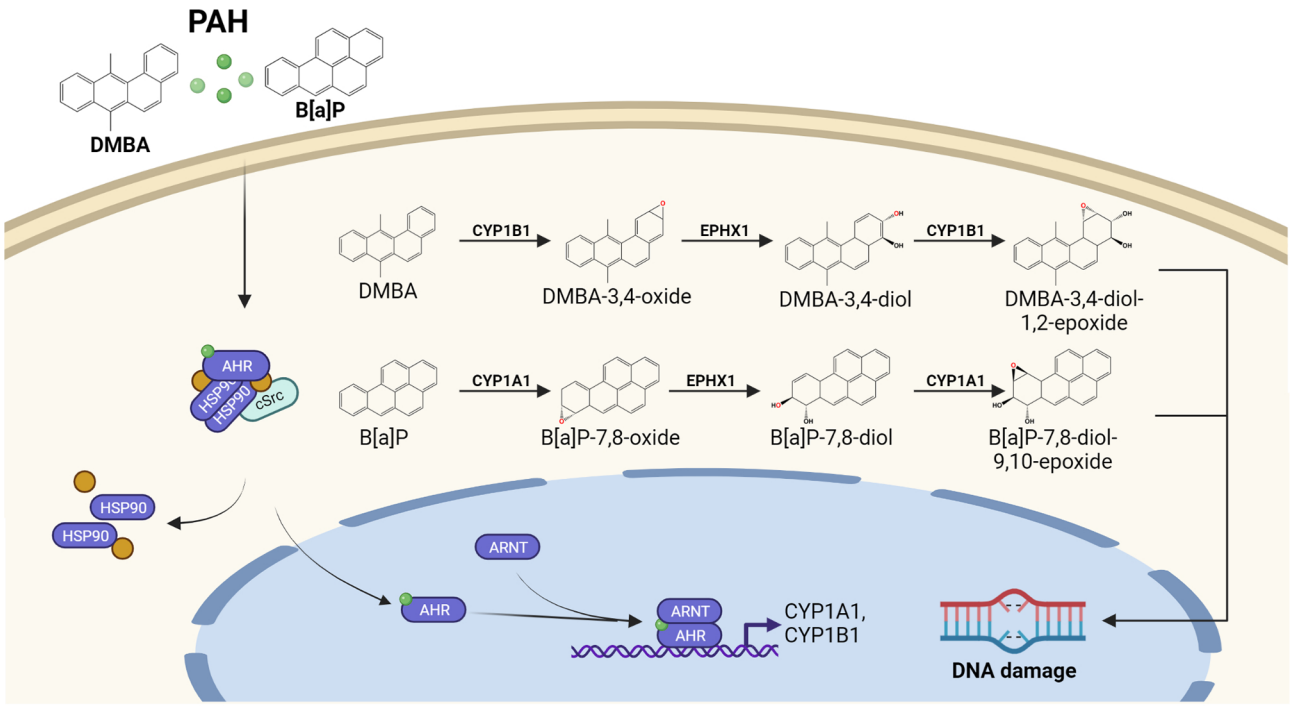

FIGURE 2 | AHR-dependent metabolic activation of PAHs by CYP1 isoforms. Lipophilic PAHs can easily pass the plasma membrane and activate the canonical AHR signaling pathway. The resulting induction of CYP1 isoform expression and enzyme activity accelerates the oxidative metabolism of the invading chemicals. In case a proper detoxification of the resulting reactive PAH metabolites by the conjugating enzyme system (not shown) fails, reactive PAH-diol epoxides may covalently bind to the DNA and form highly mutagenic bulky DNA adducts.

AHR and PAH-Induced Immune Reactions

An epicutaneous sensitization with PAHs, more precisely AHR/CYP1-derived reactive PAH metabolites, results in the development of an early inflammatory response which is responsible for contact hypersensitivity of the skin (54–56). This acute inflammation is triggered by antigen-specific $CD8^+$ cytotoxic T cells and $CD4^+$ type 1 T helper (Th1) cells which may prevent skin tumor development by secreting respective cytokines, such as interleukin (IL)-2 and interferon-γ (54–56). In its extent, this response is controlled by Th2 cells and immunosuppressive $FoxP3^+$ regulatory T cells (Tregs). The induction of keratinocyte apoptosis by cytotoxic T cells leads to the release of further mediators which may stimulate other immune cells to infiltrate the inflamed skin. In case the damage is not resolved, chronic inflammatory condition facilitates the growth and progression of skin tumors (57). In experimental carcinogenesis studies, the application of phorbol ester fosters the expansion of IL-17-producing T cells which further promote tumor growth (58). Recently, various studies reported that by inhibiting the function of immunosuppressive Tregs (59–61) and promoting the polarization of Th2 and Th17 cells (**Figure 3**), an exposure to PAHs or PAH-rich particulate matter facilitates the worsening of chronic inflammatory diseases, including asthma and atopic dermatitis, in an AHR-dependent manner (61–67). Given that Th2 as well as Th17 responses are well recognized for their tumor-promoting capabilities (57), it is tempting to speculate that a chronic exposure of the skin to genotoxic PAH or PAH-rich materials may not only initiate the development of tumors but also promote their growth by creating an inflammatory micromilieu.

ULTRAVIOLET RADIATION AND SKIN PHOTOCARCINOGENESIS

Ultraviolet (UV) radiation is part of the electromagnetic spectrum of sunlight and can be subdivided into UVA, UVB and UVC radiation (68, 69). The latter (100 nm – 280 nm) is almost completely absorbed by the stratospheric ozone layer and thus does not reach our skin in sufficient amounts to cause biological effects. High-energy UVB photons (280 nm – 315 nm) are nearly completely absorbed by the DNA and other macromolecules of epidermal cells, i.e. keratinocytes and melanocytes. In contrast, UVA radiation (315 nm – 400 nm) can penetrate deep into our skin and even reach dermal fibroblasts (68, 69). UVA radiation induces oxidative stress and associated macromolecular damage by excitation of endogenous chromophores, such riboflavin and protoporphyrin IX (70). Importantly, the vast majority of skin cancers, i.e. basal cell carcinoma, SCC and malignant melanoma, originate from epidermal cells. Hence, in the context of skin photocarcinogenesis, UVB radiation can be considered as the most dangerous part of the UV spectrum.

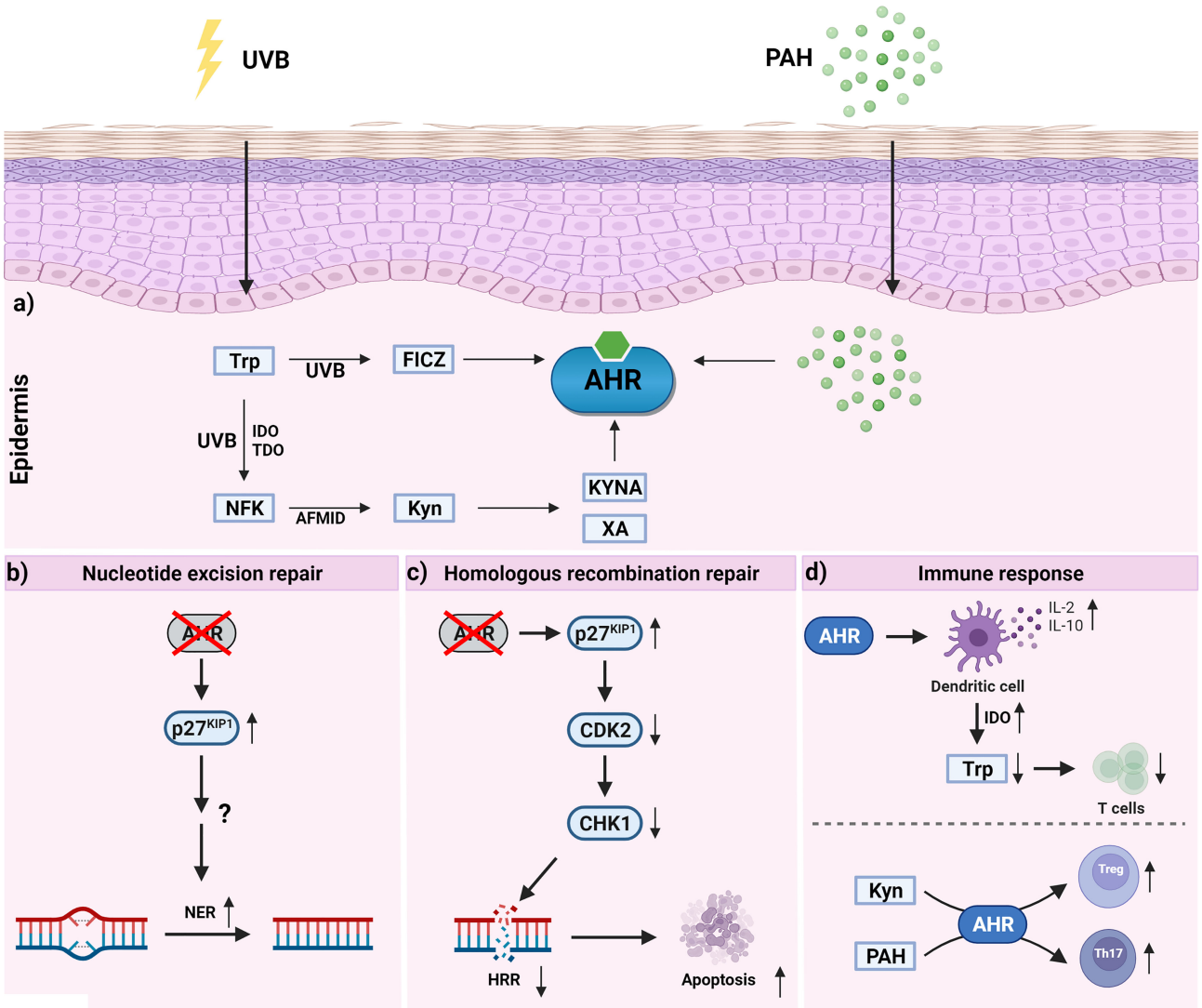

FIGURE 3 | Activation of epidermal AHR signaling and AHR-dependent effects which may contribute to skin carcinogenesis. a) UVB irradiation of epidermal cells results in the formation of tryptophan photoproducts, such as FICZ and NFK. While FICZ is a high-affinity ligand for AHR, NFK is considered as a pro-ligand. Specifically, aryl formamidase converts NFK to kynurenine (kyn) which in subsequent metabolic reactions is metabolized to the AHR agonists kynurenic acid (KYNA) and xanthurenic acid (XA). b) Inhibition of AHR was shown to increase $p27^{KIP1}$ protein content which improves NER of UVB radiation-induced DNA photoproducts by a yet enigmatic mechanism. c) Inhibition of AHR was shown to increase $p27^{KIP1}$ protein content resulting in an inhibition of CDK2 and a time-dependent decline of the CHK1 level. The reduction of CHK1 is associated with a reduced performance of the HRR system and an elevated rate of keratinocyte apoptosis. d) AHR activation affects T cell polarization in a ligand-dependent manner. The upregulation of IL-2, IL-10 and IDO in DC may lead to an expansion of Tregs and inhibit the proliferation of effector T cells *via* tryptophan depletion. In contrast to the pro-ligand KYN, PAHs seem to interfere with differentiation and function of immunosuppressive Tregs.

DNA Damage, DNA Repair, and Apoptosis

Skin photocarcinogenesis is a multistep process, involving initiating and promoting events (71, 72). These include DNA damage and failure of appropriate cell rescue (DNA repair) or cell death (apoptosis) responses, the suppression of anti-tumor immune responses, and the clonal expansion of malignant cells (71–74). To provoke effects at a cellular level, UVB radiation needs to be absorbed by chromophores to convert its physical into chemical energy. The most important chromophore for UVB radiation is the DNA (75). In addition, other cellular components, in particular aromatic amino acids, such as tryptophan (76), can absorb UVB photons and contribute to the generation of the UVB stress response in the epidermal compartment (21, 77). The DNA damage-dependent part of this response is initiated by the UVB radiation-induced formation of two photoproducts between adjacent pyrimidine bases: cyclobutene pyrimidine dimers (CPD) and pyrimidine (6–4) pyrimidone photoproducts (75, 78, 79). Although both DNA

photoproducts are highly mutagenic, CPDs and the resulting signature mutations, in particular C>T and CC>TT transitions, are considered as being mainly responsible for skin photocarcinogenesis (78, 80, 81). Numerous of these signature mutations are present in the p53 gene, a tumor suppressor gene that is inactivated or compromised by respective mutations in nearly 100% of UV radiation-associated skin cancers (78, 79). In placental mammals, UVB radiation-induced DNA photoproducts (as well as bulky PAH-DNA adducts) are removed by nucleotide excision repair (NER) which consists of four steps: Damage recognition, incision, gap filling and ligation (46, 82). NER is divided into two distinct sub-pathways that differ in their way of damage recognition: Transcription-coupled repair (TCR), which quickly removes DNA adducts in actively transcribed genes, and global genome repair (GGR), which removes DNA lesions in the entire genome. In case of TCR, a stalled RNA polymerase II which then is recognized by Cockayne Syndrome (CS) A and CSB proteins serves as damage sensor. In GGR, a complex of xeroderma pigmentosum (XP) C, centrin-2, RAD23B and DNA damage-binding proteins recognizes the DNA damage. DNA unwinding is performed by the DNA helicases XPB and XPD, which are part of the general transcription factor IIH (TFIIH). Excision of the DNA damage is performed by the endonucleases XPG and XPF-ERCC1 and, subsequently, the gap of 25 to 30 nucleotides is filled and sealed by DNA polymerases and DNA ligases, respectively (46, 82).

In case NER fails, the remaining DNA photoproducts will cause DNA double-strand breaks (DSB), which have been denominated as lethal DNA lesions (83). In fact, DSBs are not a direct consequence of UVB irradiation but occur when CPD-positive cells enter mitosis. During S phase, these helix-distorting DNA lesions cause a collapse of the replication fork leading to breakage (enzymatic cleavage) of both DNA strands (84–86). Subsequently, the DNA damage response, amongst others encompassing the activation of ataxia telangiectasia mutated (ATM) kinase and downstream checkpoint kinase 1 (CHK1), is induced to halt the cell-cycle and initiate homologous recombination repair (HRR) (87, 88), which is primarily in charge of fixing replication fork-associated DSBs (89). When HRR fails, apoptosis is initiated by ATM (or related ATR) kinase in both p53-dependent and p53–independent manners (47). Importantly, an elevation of keratinocyte apoptosis may effectively restrain UVB radiation-induced skin carcinogenesis (90–93).

UV Radiation-Induced Immunosuppression

As indicated above, UV radiation suppresses the immune system in an antigen-specific manner by inducing Tregs thereby promoting skin carcinogenesis (73, 74). Using mouse models of contact hypersensitivity, the induction of DNA photoproducts, especially CPDs, has been identified to be the major molecular trigger for the UV radiation-induced suppression of the immune system (94, 95). This result has been confirmed in human volunteers treated with UVB light alone or in combination with photolyase-containing liposomes and photo-reactivating light exposure (96). The Tregs induced by UVB irradiation are $CD4^+$ and $CD25^+$, express FoxP3 and secrete IL-10. Although bearing lymph node-homing receptors, Tregs may switch to skin-homing receptors upon contact with epidermal Langerhans cells, migrate into the skin and suppress cancer cell-killing effector T cells (74, 97). Given that an enforced removal of UVB radiation-induced DNA photoproducts does not completely abrogate immunosuppression (94), other chromophores might also be involved. Besides trans-urocanic acid which upon UVB irradiation may isomerize to immunosuppressive *cis*-urocanic acid in the *stratum corneum* (74), tryptophan is another candidate compound. Indeed, as discussed below in more detail (see *AHR and Immunosuppression*), AHR has been identified to contribute to the suppression of immune responses in UVB-irradiated mice (97) suggesting an involvement of tryptophan photoproducts. FICZ, however, has been reported to enforce the generation of Th17 cells and thereby exacerbate experimental autoimmunity in mice (98, 99).

ROLE OF AHR IN SKIN PHOTOCARCINOGENESIS

AHR Activation by UVB Irradiation

In the epidermis, UVB rays are absorbed by the aromatic amino acid tryptophan, resulting in the formation of photoproducts, such as FICZ and 1-(1H-indol-3-yl)-9H-pyrido(3,4-*b*)indole, which serve as high-affinity AHR ligands (21, 76, 100–102). FICZ is detectable in human skin *in vivo* (103), and FICZ metabolites, i.e. sulfoconjugates of hydroxylated FICZ molecules, are present in human urine samples. Accordingly, an exposure to UVB radiation enhances cutaneous and hepatic CYP1 enzyme activities in rodents (104, 105), and induces the expression of AHR target genes in the skin of human volunteers (106, 107). FICZ is a very good substrate for CYP1 isoforms and their induction by FICZ-stimulated AHR signaling thus ensures a transient activation of the AHR system in response to acute UVB exposure (108, 109). Even though experimental evidence is lacking, it is tempting to speculate that epidermal AHR activity is also fueled by *N*-formylkynurenine (NFK), another tryptophan photoproduct formed in UVB-irradiated cells (110–112). Subsequently, arylformamidase (kynurenine formamidase) may convert NFK to kynurenine which is further metabolized to endogenous AHR ligands, such as kynurenic acid and xanthurenic acid (113, 114). As discussed later on, this process bypasses the first and rate limiting step of tryptophan catabolism, i.e. the tryptophan 2,3-dioxygenase (TDO)- or indoleamine 2,3-dioxygenase (IDO)-mediated oxidation of tryptophan to NFK, and thus may be relevant for a modulation of UVB radiation-induced immunosuppressive effects by the AHR system. Other genes whose expression is upregulated *via* non-canonical AHR signaling pathways in UVB-irradiated keratinocytes and human skin *ex vivo* and which might be relevant concerning skin carcinogenesis encode for cyclooxygenase-2 and matrix metalloproeinase-1 (21, 106).

Under chronic UVB irradiation, overactivation of AHR signaling pathways may have detrimental consequences (**Figure 3**). In fact, in a photocarcinogenesis study AHR-deficient SKH-1 hairless mice developed approximately 50% less cutaneous SCC than their AHR-proficient littermates, providing evidence that AHR signaling critically contributes to UVB radiation-induced skin carcinogenesis (115). Further analyses of the skin lesions did not reveal any obvious genotype-specific differences in tumor histology/biochemistry (115), indicating that, in the context of

photocarcinogenesis, AHR activity mainly affects the tumor initiation phase. However, given that UVB irradiation enhances the expression of inflammatory mediators (e.g. chemokine (C-X-C motif) ligand 5, cyclooxygenase-2) in murine and human skin in an AHR-dependent manner (106, 116), and that a transgenic overexpression of a constitutively active AHR in mice is associated with inflammatory skin lesions (117), it seems to be likely that cutaneous AHR signaling also exhibits tumor-promoting effects.

AHR and Nucleotide Excision Repair

Given that skin photocarcinogenesis depends on the formation and repair of UVB-induced DNA photoproducts, in particular CPDs, our group has elucidated whether AHR activation affects CPD removal *via* NER. In fact, chemical inhibition and genetic targeting of AHR in human epidermal keratinocytes accelerates CPD removal at early time points (4 hrs) after UVB exposure (115). Treatment of keratinocytes with a pan-caspase inhibitor and subsequent CPD quantification excluded an early clearance of CPD-positive cells through apoptosis. Transient RNAi experiments in which the expression of either XPC, the damage recognition factor of GGR, or CSB, an initiator of TCR, was silenced, revealed that AHR attenuated CPD repair by specifically repressing the GGR sub-pathway (115) (**Figure 3**). The clinical relevance of GGR is illustrated by the fact that patients with GGR-inactivating mutations, but not patients suffering from TCR-deficiency, have a 1,000-fold increased risk to develop cutaneous SCC (118, 119). Further RNAi-based mechanistic studies revealed that AHR inhibits GGR by activating EGFR and downstream PI3K/AKT signal transduction, resulting in the phosphorylation and subsequent proteasomal degradation of the cyclin-dependent kinase (CDK) inhibitor and tumor suppressor protein $p27^{KIP1}$ (115, 120). Accordingly, AHR inhibition results in a stabilization of the $p27^{KIP1}$ protein level in keratinocytes *in vitro* and mouse skin *in vivo* (115, 121, 122). This stabilizing effect of AHR inhibition on $p27^{KIP1}$ is not restricted to epidermal keratinocytes but also present in DAYO medulloblastoma (123) and A549 lung adenocarcinoma cells (124). Ectopic overexpression of $p27^{KIP1}$ accelerates CPD repair in UVB radiation-exposed keratinocytes, whereas chemical inhibitors targeting CDK7, mimicked high levels of $p27^{KIP1}$, i.e. inhibited CPD repair. CDK7 is the catalytically active subunit of the CDK-activating kinase, a component of the general transcription factor and NER complex TFIIH (125). In fact, a chemical inhibition of CDK7 has been previously shown to specifically stimulate GGR activity (126). Elevated $p27^{KIP1}$ protein levels were present in the skin of AHR-deficient mice and associated with a faster removal of UVB radiation-induced CPDs (115). These data indicate that by repressing the repair of UVB radiation-induced DNA photoproducts, AHR may critically contribute to skin photocarcinogenesis. Recently, this concept was challenged by a study reporting that an activation of AHR signaling by keratinocyte growth factor-2 (KGF2) stimulates CPD clearance as early as one hour after UVB exposure (127). However, it is not clear whether this effect depended on alterations in NER activity or apoptosis. Given that peptide growth factors do probably not bind to the ligand-binding site of the AHR protein, the mode of AHR activation by KGF2 remains quite enigmatic. KGF2 serves as a ligand for the fibroblast growth factor receptor-2, which acts mitogenic and thereby may reduce apoptotic cell death (128). Hence, it is tempting to speculate that a cross-talk between the receptor tyrosine kinase and AHR signaling may be causative for the described discrepancy in UVB radiation-induced keratinocyte apoptosis.

AHR, Homologues Recombination Repair and Apoptosis

As outlined above, an abrogation of AHR signaling accelerates the removal of mutagenic CPDs through the NER sub-pathway GGR and thus should decrease UVB radiation-induced keratinocyte apoptosis (129). However, it has been previously shown that AHR serves an anti-apoptotic function in UVB-irradiated keratinocytes and mouse skin (115, 121). Interestingly, this anti-apoptotic effect also seems to depend on the AHR-mediated reduction of the $p27^{KIP1}$ protein level. Accordingly, an inhibition of AHR enhances the apoptosis susceptibility of UVB-irradiated keratinocytes by upregulating $p27^{KIP1}$ levels (121). Subsequently, $p27^{KIP1}$ inhibits the activity of its substrate CDK2 and thereby abolishes the downstream phosphorylation of the retinoblastoma protein (RB). RB phosphorylation is necessary to activate E2F1, which controls the expression of CHK1 (121), a stress kinase critically involved in initiating cell-cycle arrest upon DNA damage (88). In UVB-irradiated keratinocytes, DNA double-strand breaks (DSBs) mainly occur when CPD-positive cells start to divide (84–86). Results from Comet assays and γH2AX quantification indicated that the enhanced apoptosis susceptibility of AHR-compromised keratinocytes is indeed due to an elevated formation of DSBs (115). Accordingly, at later time points after UVB exposure (18 h), AHR-compromised keratinocytes exhibited an elevated amount of DSBs as compared to respective control cells. Given that CHK1 is also essential for the initiation of HRR (87), AHR-compromised keratinocytes, exhibiting reduced CHK1 levels, are prone to DSB-induced apoptosis (115). These data indicate that AHR is a positive regulator of the HRR (**Figure 3**) and the associated fixation of DSBs and confirm previously published observations in 2,3,7,8-tetrachlorodibenzo-*p*-dioxin (TCDD)-treated Chinese hamster ovary cells (130, 131). However, in contrast to the described anti-apoptotic role of cutaneous AHR in the context of UVB irradiation, it has been reported that in the absence of DNA damage AHR activation may sensitize keratinocytes to cytokine-/death receptor-induced apoptosis (132).

AHR and Immunosuppression

UVB radiation-induced immunosuppression largely depends on the occurrence of DNA photoproducts (see *UV Radiation-Induced Immunosuppression*). An inhibition of both GGR and apoptotic clearance probably results in an accumulation of CPDs and thus may represent one mechanism through which active AHR maintains the UVB radiation-induced suppression of the immune system. Studies on a mouse model of contact hypersensitivity confirmed this hypothesis by demonstrating that a chemical or genetic inhibition of AHR attenuates the UV radiation-induced expansion of Tregs and associated immunosuppressive effects (97). Further mechanistic studies using

4-n-nonylphenol to induce AHR-dependent immunosuppression, however, showed that AHR activation switches antigen-presenting dendritic cells (DC) from a stimulatory into a regulatory phenotype thereby leading to an induction of Tregs independently from DNA damage (97, 133). The underlying mechanism involves an AHR-dependent induction of IL-2 (133, 134) which subsequently induces IL-10 while repressing the expression of the negative regulatory protein B7-H4, a co-inhibitory molecule of the B7 family (133). In addition, AHR activation by 4-n-nonylphenol induced the expression of IDO in bone marrow-derived DC, thus confirming a previous study reporting that AHR is required for proper IDO induction (135). The enforced degradation of tryptophan and the associated formation of tryptophan metabolites may inhibit T cell proliferation and thereby suppresses antitumor immune responses (114, 136, 137). In fact, the derived tryptophan metabolites may activate AHR to generate regulatory DC which foster the expansion of Tregs while inhibiting T cell polarization towards Th17 cells (114). Noteworthy, kynurenine was found to induce the generation of immunosuppressive Tregs in mice and certain tumor entities in patients in an AHR-dependent manner (136, 138–141). Along the same line, activation of AHR by its prototypic ligand TCDD promotes the expansion of $CD4^+$ $CD25^+$ and $FoxP3^+$ Tregs to suppress experimental autoimmune disease (encephalomyelitis, uveoretinitis) (99, 142, 143). This, however, stands in stark contrast to an activation of AHR signaling by either FICZ (see *UV Radiation-Induced Immunosuppression*) or airborne PAHs and PAH-rich PM (see *AHR and PAH-Induced Immune Reactions*) which stimulate the generation of Th17 cells and exacerbate autoimmune disorders. This discrepancy clearly points to a ligand-specific effect of the AHR system on fate and function of T lymphocytes. Interestingly, results from a study conducted by the Kerkvliet laboratory suggest that this ligand-specific effect is due to differences in the metabolic half-life of the respective AHR ligand and associated dose-dependent effects (144). However, in the context of UVB irradiation, a very interesting facet is that an absorption of UVB rays by tryptophan results in the formation of NFK (110–112), a photochemical reaction which bypasses the first and so-called rate-limiting IDO/TDO-catalyzed step of tryptophan degradation. At biologically relevant doses of UVB radiation and simulated sunlight, approximately 20% of the free tryptophan contained in cell culture medium is converted into the AHR pro-ligand NFK (112). In general, tryptophan is highly susceptible to many oxidizing agents and NFK is one of its major oxidation products (145). Although probably less relevant for the therapy of cutaneous SCC, this observation provides a potential mechanism through which other epidermal cancers, in particular advanced melanomas, may overcome a pharmacological inhibition of IDO/TDO. In fact, a phase III trial (ECHO-301) testing pembrolizumab, an antibody targeting the immune checkpoint protein PD-L1, in combination with the IDO blocker epacadostat revealed that the co-treatment has no benefit for patients suffering from advanced melanoma as compared to the patients treated with pembrolizumab alone (114, 146). The failure of IDO1 inhibitors for melanoma therapy might be related to an enhanced TDO activity or an elevated expression of IL-4-induced gene 1, another tryptophan-metabolizing enzyme that induces immunosuppression by producing AHR ligands (147, 148). Nevertheless, it is tempting to speculate that the UV radiation-induced formation of NFK in the skin and its further catabolism to kynurenic acid and other AHR-agonistic metabolites may, at least partially, contribute to the expansion of Tregs and the suppression of appropriate anti-tumor immune responses. As indicated by studies on patients with lung cancer or oral SCC, the activated AHR may not only enhance the expression of IDO but also attenuate the response to immune checkpoint inhibition by inducing PD-L1 (141, 149). In addition, tumor repopulating melanoma cells may produce kynurenine and associated AHR ligands to activate AHR and induce the expression of the PD-L1 receptor PD-1 in $CD8^+$ T cells (150). Hence, a combination of small molecules inhibiting AHR activity with PD-1 checkpoint inhibitors might be a suitable approach to combat immunotherapy-resistant tumors (151).

Although experimental evidence is yet lacking, it is conceivable that at least in advanced stages of cutaneous SCC, the AHR may play a comparable role in modulating tumor immunity.

CO-CARCINOGENICITY OF UV RADIATION AND PAHS?

Given that environmentally ubiquitous PAHs as well as UV radiation are capable of modulating AHR activity in keratinocytes and other epidermal cell populations, a simultaneous exposure to these factors may cause co-carcinogenic effects. However, as specified below, the data published so far on this topic produce a heterogenous and sometimes even contradictory picture. For instance, some early carcinogenesis studies reported an increased skin tumor formation upon UV irradiation of coal tar-treated mice (152, 153), whereas in another study on albino mice alternately exposed to UV radiation and PAHs, namely 3-methylcholanthrene, DMBA and B[a]P, no additive skin cancer formation was observed (154). A major factor that may contribute to this discrepancy is the pronounced sensitizing property of various PAHs toward UVA radiation. The resulting generation of ROS may on the one hand facilitate carcinogenesis by inducing oxidative DNA damage and inhibiting the function of DNA repair enzymes and other proteins (155–162). On the other hand, strong or longer lasting phototoxic stress may cause ROS-mediated cytotoxicity and necrotic cell death not only in normal epidermal cells but also in initiated keratinocytes and malignant cells. Interestingly, several UVB radiation-induced photoproducts of tryptophan, including NFK and FICZ, have been identified as potent UVA photosensitizers (110, 163, 164), and a combinatorial treatment with FICZ and UVA radiation was proposed as a novel therapeutic approach for skin cancer (165). Notably, other investigators regard the oxidative stress resulting from the FICZ/UVA exposure and the associated inhibition of DNA repair enzymes as a pro-carcinogenic event (166). In general, this process, i.e. the application of a photosensitizing agent and its subsequent irradiation with light of a certain wavelength, has been successfully implemented into the clinical routine for the treatment of certain solid tumors (167), including melanoma and non-melanoma skin cancers (168), and is known as photodynamic

therapy. Other studies have shown that UV irradiation enhances the skin permeation rates of simultaneously applied PAHs (161, 169, 170) and may affect their metabolic activation (105, 155, 171, 172). UVB radiation was proven to sensitize epidermal keratinocytes to PAH-DNA adduct formation and subsequent mutagenesis (105, 171). The laboratory of David Bickers applied the Goeckerman regimen, i.e. a sequential treatment of the skin with PAH-rich crude coal tar and UVB radiation, to neonatal rats and observed an enhanced metabolic activation of B[a]P and associated DNA adduct formation in subsequent *ex vivo* experiments (105). An enhanced amount of PAH metabolites and markers for DNA damage were also observed in the blood and urine of psoriasis patients that underwent the Goeckerman regimen (161). Interestingly, Bickers and co-workers were able to show that the opposite application sequence, i.e. UVB exposure first followed by coal tar treatment, did not cause any significant differences in metabolic activation and BPDE-DNA adduct formation as compared to the samples of the coal tar-only treated animals (105). In contrast, Nair and colleagues reported that a treatment of HaCaT keratinocytes with either UVB radiation, photooxidized tryptophan or FICZ prior to B[a]P application significantly enhanced the expression of CYP1 isoforms and the associated formation of bulky DNA adducts (171). As expected a co-treatment with either α-naphthoflavone, an AHR antagonist, or the HSP90 blocker 17-AAG attenuated CYP1 induction and DNA adduct formation, thus confirming AHR dependency (171). Thierry Douki and co-workers, however, reported that a sequential treatment of keratinocytes and human skin explants with B[a]P or a mixture of PAHs and stimulated sunlight, reduced the expression of CYP1 isoforms, the generation of PAH metabolites and BPDE-DNA adduct formation (155, 170, 172). Given that the applied irradiation device emits UVB and UVA light (wavelengths from 290 nm - 400 nm), it is possible that the resulting generation of ROS is responsible for the observed downregulation of the expression of the CYP1 monooxygenases (173, 174). In addition, the spectrum of cytokines released by the irradiated epidermal cells may depend on the UV wavelength (175, 176). Tumor necrosis factor-α, for instance, is rather produced upon irradiation with UVA than with UVB light, and this cytokine is capable to suppress CYP1 gene expression *via* NF-κB-mediated trans-repression, i.e. a competition for common transcriptional co-activators (24, 177). However, as outlined in this article, PAHs and UV radiation may differently affect the expansion and function of immunosuppressive Tregs, which may be also an important factor that has to be considered in the context of a simultaneous exposure.

In summary, the current data concerning the simultaneous exposure of the skin to UV radiation and PAHs are not coherent and illustrate the need for further studies to ensure a proper risk assessment, in particular for roofers, roadmen, and other occupational groups that are frequently exposed to high doses of both, PAHs and sunlight. Chronic exposure studies on rodents, for instance, using the same irradiation device for single and simultaneous exposure to UVA and UVB light in combination with a pre- and post-treatment with environmentally-relevant PAH mixtures may shed light on a potential interaction of both risk factors in skin carcinogenesis.

CONCLUSION

Proper AHR signaling is indispensable for the development and physiology of the skin (178, 179). However, as outlined in this article, an overactivation of this signaling pathway in skin chronically exposed to one or more environmental stressors may have detrimental consequences (**Figure 3**). By modulating xenobiotic metabolism, different DNA repair systems, apoptosis, various functions of the immune system, and other processes, AHR-dependent signaling pathways may significantly contribute to the development of PAH- and UV radiation-induced skin carcinogenesis. Interestingly, both environmental factors seem to interact on the level of enzyme activity and DNA damage and repair, thus illustrating the critical role of the AHR in either restraining or facilitating the development of skin cancer. Even though, the published data on the potential co-carcinogenic action of UV radiation and PAHs do not produce a clear picture, a transient inhibition of cutaneous AHR signaling probably protects the skin of individuals exposed to UV radiation and PAHs alone or in combination. In the context of a co-exposure, it is tempting to speculate that the application of sunscreen does not only prevent the UV radiation-induced activation of AHR signaling but also the photoactivation of PAHs potentially present on the skin. Given that sun blockers do not protect against the genotoxicity of PAHs, the integration of transient AHR antagonists in sunscreens might be beneficial in order to protect the skin against both environmental/occupational stressors. Notably, it is widely accepted that the integration of antioxidants into sunscreens provides additional skin protection by neutralizing radiation- and pollution-induced ROS (180, 181) and, interestingly, several plant-derived polyphenols combine both properties, i.e. antagonizing AHR signaling and exhibiting antioxidative effects (182, 183). However, further research on the potential interaction of PAHs and UV radiation in the pathogenesis of SCCs is urgently needed in order to improve the risk assessment as well as the preventive strategies depending thereon.

AUTHOR CONTRIBUTIONS

TH-S contributed to the conception and design of the review article. CV, KR, and TH-S wrote the manuscript. JK provided critical feedback during the preparation of the article and contributed to the revision of the manuscript. CV generated the figures. All authors contributed to the article and approved the submitted version.

ACKNOWLEDGMENTS

We thank Charlotte Esser for critical reading of the manuscript and helpful suggestions. The figures were created with BioRender software (www.biorender.com; agreement number JY23CK86BZ, SC23CK8D4Q and PB23CK8HNH). Research in the THS laboratory in supported by the Deutsche Forschungsgemeinschaft (HA 7346/2–2).

REFERENCES

1. Rogers HW, Weinstock MA, Feldman SR, Coldiron BM. Incidence Estimate of Nonmelanoma Skin Cancer (Keratinocyte Carcinomas) in the U.S. Population, 2012. *JAMA Dermatol* (2015) 151:1081–6. doi: 10.1001/jamadermatol.2015.1187
2. Leiter U, Keim U, Eigentler T, Katalinic A, Holleczek B, Martus P, et al. Incidence, Mortality, and Trends of Nonmelanoma Skin Cancer in Germany. *J Invest Dermatol* (2017) 137:1860–7. doi: 10.1016/j.jid.2017.04.020
3. Green AC, Olsen CM. Cutaneous Squamous Cell Carcinoma: An Epidemiological Review. *Br J Dermatol* (2017) 177:373–81. doi: 10.1111/bjd.15324
4. Hiatt RA, Beyeler N. Cancer and Climate Change. *Lancet Oncol* (2020) 21: e519–27. doi: 10.1016/S1470-2045(20)30448-4
5. Lin MJ, Torbeck RL, Dubin DP, Lin CE, Khorasani H. Climate Change and Skin Cancer. *J Eur Acad Dermatol Venereol* (2019) 33:e324–5. doi: 10.1111/jdv.15622
6. Guy GP Jr, Machlin SR, Ekwueme DU, Yabroff KR. Prevalence and Costs of Skin Cancer Treatment in the U.S., 2002-2006 and 2007-2011. *Am J Prev Med* (2015) 48:183–7. doi: 10.1016/j.amepre.2014.08.036
7. Chahal HS, Lin Y, Ransohoff KJ, Hinds DA, Wu W, Dai HJ, et al. Genome-Wide Association Study Identifies Novel Susceptibility Loci for Cutaneous Squamous Cell Carcinoma. *Nat Commun* (2016) 7:12048. doi: 10.1038/ncomms12048
8. Berenblum I, Shubik P. The Role of Croton Oil Applications, Associated With a Single Painting of a Carcinogen, in Tumour Induction of the Mouse's Skin. *Br J Cancer* (1947) 1:379–82. doi: 10.1038/bjc.1947.35
9. Berenblum I, Shubik P. A New, Quantitative, Approach to the Study of the Stages of Chemical Cartinogenesis in the Mouse's Skin. *Br J Cancer* (1947) 1:383–91. doi: 10.1038/bjc.1947.36
10. Gelboin HV. Benzo[alpha]pyrene Metabolism, Activation and Carcinogenesis: Role and Regulation of Mixed-Function Oxidases and Related Enzymes. *Physiol Rev* (1980) 60:1107–66. doi: 10.1152/physrev.1980.60.4.1107
11. Luch A. Nature and Nurture - Lessons From Chemical Carcinogenesis. *Nat Rev Cancer* (2005) 5:113–25. doi: 10.1038/nrc1546
12. McCreery MQ, Balmain A. Chemical Carcinogenesis Models of Cancer: Back to the Future. *Annu Rev Cancer Biol* (2017) 1:295–312. doi: 10.1146/annurev-cancerbio-050216-122002
13. Bersten DC, Sullivan AE, Peet DJ, Whitelaw ML. bHLH-PAS Proteins in Cancer. *Nat Rev Cancer* (2013) 13:827–41. doi: 10.1038/nrc3621
14. Murray IA, Patterson AD, Perdew GH. Aryl Hydrocarbon Receptor Ligands in Cancer: Friend and Foe. *Nat Rev Cancer* (2014) 14:801–14. doi: 10.1038/nrc3846
15. Rothhammer V, Quintana FJ. The Aryl Hydrocarbon Receptor: An Environmental Sensor Integrating Immune Responses in Health and Disease. *Nat Rev Immunol* (2019) 19:184–97. doi: 10.1038/s41577-019-0125-8
16. Avilla MN, Malecki KMC, Hahn ME, Wilson RH, Bradfield CA. The Ah Receptor: Adaptive Metabolism, Ligand Diversity, and the Xenokine Model. *Chem Res Toxicol* (2020) 33:860–79. doi: 10.1021/acs.chemrestox.9b00476
17. Dvorak Z, Poulikova K, Mani S. Indole Scaffolds as a Promising Class of the Aryl Hydrocarbon Receptor Ligands. *Eur J Med Chem* (2021) 215:113231. doi: 10.1016/j.ejmech.2021.113231
18. Enan E, Matsumura F. Identification of C-Src as the Integral Component of the Cytosolic Ah Receptor Complex, Transducing the Signal of 2,3,7,8-Tetrachlorodibenzo-P-Dioxin (TCDD) Through the Protein Phosphorylation Pathway. *Biochem Pharmacol* (1996) 52:1599–612. doi: 10.1016/S0006-2952(96)00566-7
19. Mimura J, Ema M, Sogawa K, Fujii-Kuriyama Y. Identification of a Novel Mechanism of Regulation of Ah (Dioxin) Receptor Function. *Genes Dev* (1999) 13:20–5. doi: 10.1101/gad.13.1.20
20. Dong B, Cheng W, Li W, Zheng J, Wu D, Matsumura F, et al. FRET Analysis of Protein Tyrosine Kinase C-Src Activation Mediated *via* Aryl Hydrocarbon Receptor. *Biochim Biophys Acta* (2011) 1810:427–31. doi: 10.1016/j.bbagen.2010.11.007
21. Fritsche E, Schafer C, Calles C, Bernsmann T, Bernshausen T, Wurm M, et al. Lightening Up the UV Response by Identification of the Arylhydrocarbon Receptor as a Cytoplasmatic Target for Ultraviolet B Radiation. *PNAS* (2007) 104:8851–6. doi: 10.1073/pnas.0701764104
22. Vogeley C, Sondermann NC, Woeste S, Momin AA, Gilardino V, Hartung F, et al. Unraveling the Differential Impact of PAHs and Dioxin-Like Compounds on AKR1C3 Reveals the EGFR Extracellular Domain as a Critical Determinant of the AHR Response. *Environ Int* (2022) 158:106989. doi: 10.1016/j.envint.2021.106989
23. Vogel CF, Sciullo E, Li W, Wong P, Lazennec G, Matsumura F. RelB, a New Partner of Aryl Hydrocarbon Receptor-Mediated Transcription. *Mol Endocrinol* (2007) 21:2941–55. doi: 10.1210/me.2007-0211
24. Tian Y, Rabson AB, Gallo MA. Ah Receptor and NF-kappaB Interactions: Mechanisms and Physiological Implications. *Chem Biol Interact* (2002) 141:97–115. doi: 10.1016/S0009-2797(02)00068-6
25. Gradin K, McGuire J, Wenger RH, Kvietikova I, fhitelaw ML, Toftgard R, et al. Functional Interference Between Hypoxia and Dioxin Signal Transduction Pathways: Competition for Recruitment of the Arnt Transcription Factor. *Mol Cell Biol* (1996) 16:5221–31. doi: 10.1128/MCB.16.10.5221
26. Chan WK, Yao G, Gu YZ, Bradfield CA. Cross-Talk Between the Aryl Hydrocarbon Receptor and Hypoxia Inducible Factor Signaling Pathways. Demonstration of Competition and Compensation. *J Biol Chem* (1999) 274:12115–23. doi: 10.1074/jbc.274.17.12115
27. Wormke M, Stoner M, Saville B, Walker K, Abdelrahim M, Burghardt R, et al. The Aryl Hydrocarbon Receptor Mediates Degradation of Estrogen Receptor Alpha Through Activation of Proteasomes. *Mol Cell Biol* (2003) 23:1843–55. doi: 10.1128/MCB.23.6.1843-1855.2003
28. Ohtake F, Takeyama K, Matsumoto T, Kitagawa H, Yamamoto Y, Nohara K, et al. Modulation of Oestrogen Receptor Signalling by Association With the Activated Dioxin Receptor. *Nature* (2003) 423:545–50. doi: 10.1038/nature01606
29. Kalthoff S, Ehmer U, Freiberg N, Manns MP, Strassburg CP. Interaction Between Oxidative Stress Sensor Nrf2 and Xenobiotic-Activated Aryl Hydrocarbon Receptor in the Regulation of the Human Phase II Detoxifying UDP-Glucuronosyltransferase 1A10. *J Biol Chem* (2010) 285:5993–6002. doi: 10.1074/jbc.M109.075770
30. Tsuji G, Takahara M, Uchi H, Matsuda T, Chiba T, Takeuchi S, et al. Identification of Ketoconazole as an AhR-Nrf2 Activator in Cultured Human Keratinocytes: The Basis of Its Anti-Inflammatory Effect. *J Invest Dermatol* (2012) 132:59–68. doi: 10.1038/jid.2011.194
31. Boffetta P, Jourenkova N, Gustavsson P. Cancer Risk From Occupational and Environmental Exposure to Polycyclic Aromatic Hydrocarbons. *Cancer Causes Control* (1997) 8:444–72. doi: 10.1023/A:1018465507029
32. De Hertog SA, Wensveen CA, Bastiaens MT, Kielich CJ, Berkhout MJ, Westendorp RG, et al. Relation Between Smoking and Skin Cancer. *J Clin Oncol* (2001) 19:231–8. doi: 10.1200/JCO.2001.19.1.231
33. Dusingize JC, Olsen CM, Pandeya NP, Subramaniam P, Thompson BS, Neale RE, et al. Cigarette Smoking and the Risks of Basal Cell Carcinoma and Squamous Cell Carcinoma. *J Invest Dermatol* (2017) 137:1700–8. doi: 10.1016/j.jid.2017.03.027
34. Leonardi-Bee J, Ellison T, Bath-Hextall F. Smoking and the Risk of Nonmelanoma Skin Cancer: Systematic Review and Meta-Analysis. *Arch Dermatol* (2012) 148:939–46. doi: 10.1001/archdermatol.2012.1374
35. Shi S, Yoon DY, Hodge-Bell KC, Bebenek IG, Whitekus MJ, Zhang R, et al. The Aryl Hydrocarbon Receptor Nuclear Translocator (Arnt) Is Required for Tumor Initiation by Benzo[a]Pyrene. *Carcinogenesis* (2009) 30:1957–61. doi: 10.1093/carcin/bgp201
36. Shimizu Y, Nakatsuru Y, Ichinose M, Takahashi Y, Kume H, Mimura J, et al. Benzo[a]pyrene Carcinogenicity Is Lost in Mice Lacking the Aryl Hydrocarbon Receptor. *PNAS* (2000) 97:779–82. doi: 10.1073/pnas.97.2.779
37. Kleiner HE, Vulimiri SV, Reed MJ, Uberecken A, DiGiovanni J. Role of Cytochrome P450 1a1 and 1b1 in the Metabolic Activation of 7,12-Dimethylbenz[a]Anthracene and the Effects of Naturally Occurring Furanocoumarins on Skin Tumor Initiation. *Chem Res Toxicol* (2002) 15:226–35. doi: 10.1021/tx010151v
38. Modi BG, Neustadter J, Binda E, Lewis J, Filler RB, Roberts SJ, et al. Langerhans Cells Facilitate Epithelial DNA Damage and Squamous Cell Carcinoma. *Science* (2012) 335:104–8. doi: 10.1126/science.1211600
39. Buters JT, Mahadevan B, Quintanilla-Martinez L, Gonzalez FJ, Greim H, Baird WM, et al. Cytochrome P450 1B1 Determines Susceptibility to

Dibenzo[a,L]Pyrene-Induced Tumor Formation. *Chem Res Toxicol* (2002) 15:1127–35. doi: 10.1021/tx020017q
40. Siddens LK, Bunde KL, Harper TAJr., McQuistan TJ, Lohr CV, Bramer LM, et al. Cytochrome P450 1b1 in Polycyclic Aromatic Hydrocarbon (PAH)-Induced Skin Carcinogenesis: Tumorigenicity of Individual PAHs and Coal-Tar Extract, DNA Adduction and Expression of Select Genes in the Cyp1b1 Knockout Mouse. *Toxicol Appl Pharmacol* (2015) 287:149–60. doi: 10.1016/j.taap.2015.05.019
41. Zheng W, Jefcoate CR. Steroidogenic Factor-1 Interacts With cAMP Response Element-Binding Protein to Mediate cAMP Stimulation of CYP1B1 *via* a Far Upstream Enhancer. *Mol Pharmacol* (2005) 67:499–512. doi: 10.1124/mol.104.005504
42. Zheng W, Tong T, Lee J, Liu X, Marcus C, Jefcoate CR. Stimulation of Mouse Cyp1b1 During Adipogenesis: Characterization of Promoter Activation by the Transcription Factor Pax6. *Arch Biochem Biophys* (2013) 532:1–14. doi: 10.1016/j.abb.2013.01.007
43. Tsuchiya Y, Nakajima M, Kyo S, Kanaya T, Inoue M, Yokoi T. Human CYP1B1 Is Regulated by Estradiol *via* Estrogen Receptor. *Cancer Res* (2004) 64:3119–25. doi: 10.1158/0008-5472.CAN-04-0166
44. Ide F, Suka N, Kitada M, Sakashita H, Kusama K, Ishikawa T. Skin and Salivary Gland Carcinogenicity of 7,12-Dimethylbenz[a]Anthracene Is Equivalent in the Presence or Absence of Aryl Hydrocarbon Receptor. *Cancer Lett* (2004) 214:35–41. doi: 10.1016/j.canlet.2004.04.014
45. Matsumoto Y, Ide F, Kishi R, Akutagawa T, Sakai S, Nakamura M, et al. Aryl Hydrocarbon Receptor Plays a Significant Role in Mediating Airborne Particulate-Induced Carcinogenesis in Mice. *Environ Sci Technol* (2007) 41:3775–80. doi: 10.1021/es062793g
46. Marteijn JA, Lans H, Vermeulen W, Hoeijmakers JH. Understanding Nucleotide Excision Repair and Its Roles in Cancer and Ageing. *Nat Rev Mol Cell Biol* (2014) 15:465–81. doi: 10.1038/nrm3822
47. Roos WP, Thomas AD, Kaina B. DNA Damage and the Balance Between Survival and Death in Cancer Biology. *Nat Rev Cancer* (2016) 16:20–33. doi: 10.1038/nrc.2015.2
48. Penning TM. Human Aldo-Keto Reductases and the Metabolic Activation of Polycyclic Aromatic Hydrocarbons. *Chem Res Toxicol* (2014) 27:1901–17. doi: 10.1021/tx500298n
49. Birtwistle J, Hayden RE, Khanim FL, Green RM, Pearce C, Davies NJ, et al. The Aldo-Keto Reductase AKR1C3 Contributes to 7,12-Dimethylbenz(a) Anthracene-3,4-Dihydrodiol Mediated Oxidative DNA Damage in Myeloid Cells: Implications for Leukemogenesis. *Mutat Res* (2009) 662:67–74. doi: 10.1016/j.mrfmmm.2008.12.010
50. Park JH, Mangal D, Tacka KA, Quinn AM, Harvey RG, Blair IA, et al. Evidence for the Aldo-Keto Reductase Pathway of Polycyclic Aromatic Trans-Dihydrodiol Activation in Human Lung A549 Cells. *Proc Natl Acad Sci USA* (2008) 105:6846–51. doi: 10.1073/pnas.0802776105
51. Pettipher R, Hansel TT, Armer R. Antagonism of the Prostaglandin D2 Receptors DP1 and CRTH2 as an Approach to Treat Allergic Diseases. *Nat Rev Drug Discov* (2007) 6:313–25. doi: 10.1038/nrd2266
52. Massey WA, Hubbard WC, Liu MC, Kagey-Sobotka A, Cooper P, Lichtenstein LM. Profile of Prostanoid Release Following Antigen Challenge *In Vivo* in the Skin of Man. *Br J Dermatol* (1991) 125:529–34. doi: 10.1111/j.1365-2133.1991.tb14789.x
53. Mantel A, Carpenter-Mendini A, VanBuskirk J, Pentland AP. Aldo-Keto Reductase 1C3 Is Overexpressed in Skin Squamous Cell Carcinoma (SCC) and Affects SCC Growth *via* Prostaglandin Metabolism. *Exp Dermatol* (2014) 23:573–8. doi: 10.1111/exd.12468
54. Yusuf N, Nasti TH, Katiyar SK, Jacobs MK, Seibert MD, Ginsburg AC, et al. Antagonistic Roles of CD4+ and CD8+ T-Cells in 7,12-Dimethylbenz(a) Anthracene Cutaneous Carcinogenesis. *Cancer Res* (2008) 68:3924–30. doi: 10.1158/0008-5472.CAN-07-3059
55. Akiba H, Kehren J, Ducluzeau MT, Krasteva M, Horand F, Kaiserlian D, et al. Skin Inflammation During Contact Hypersensitivity Is Mediated by Early Recruitment of CD8+ T Cytotoxic 1 Cells Inducing Keratinocyte Apoptosis. *J Immunol* (2002) 168:3079–87. doi: 10.4049/jimmunol.168.6.3079
56. Anderson C, Hehr A, Robbins R, Hasan R, Athar M, Mukhtar H, et al. Metabolic Requirements for Induction of Contact Hypersensitivity to Immunotoxic Polyaromatic Hydrocarbons. *J Immunol* (1995) 155:3530–7.
57. Coussens LM, Zitvogel L, Palucka AK. Neutralizing Tumor-Promoting Chronic Inflammation: A Magic Bullet? *Science* (2013) 339:286–91. doi: 10.1126/science.1232227
58. He D, Li H, Yusuf N, Elmets CA, Athar M, Katiyar SK, et al. IL-17 Mediated Inflammation Promotes Tumor Growth and Progression in the Skin. *PloS One* (2012) 7:e32126. doi: 10.1371/journal.pone.0032126
59. Sun L, Fu J, Lin SH, Sun JL, Xia L, Lin CH, et al. Particulate Matter of 2.5 Mum or Less in Diameter Disturbs the Balance of TH17/regulatory T Cells by Targeting Glutamate Oxaloacetate Transaminase 1 and Hypoxia-Inducible Factor 1alpha in an Asthma Model. *J Allergy Clin Immunol* (2020) 145:402–14. doi: 10.1016/j.jaci.2019.10.008
60. Nadeau K, McDonald-Hyman C, Noth EM, Pratt B, Hammond SK, Balmes J, et al. Ambient Air Pollution Impairs Regulatory T-Cell Function in Asthma. *J Allergy Clin Immunol* (2010) 126:845–852 e810. doi: 10.1016/j.jaci.2010.08.008
61. O'Driscoll CA, Owens LA, Gallo ME, Hoffmann EJ, Afrazi A, Han M, et al. Differential Effects of Diesel Exhaust Particles on T Cell Differentiation and Autoimmune Disease. *Part Fibre Toxicol* (2018) 15:35. doi: 10.1186/s12989-018-0271-3
62. Castaneda AR, Vogel CFA, Bein KJ, Hughes HK, Smiley-Jewell S, Pinkerton KE. Ambient Particulate Matter Enhances the Pulmonary Allergic Immune Response to House Dust Mite in a BALB/c Mouse Model by Augmenting Th2- and Th17-Immune Responses. *Physiol Rep* (2018) 6:e13827. doi: 10.14814/phy2.13827
63. Wong TH, Lee CL, Su HH, Lee CL, Wu CC, Wang CC, et al. A Prominent Air Pollutant, Indeno[1,2,3-Cd]Pyrene, Enhances Allergic Lung Inflammation *via* Aryl Hydrocarbon Receptor. *Sci Rep* (2018) 8:5198. doi: 10.1038/s41598-018-23542-9
64. Weng CM, Wang CH, Lee MJ, He JR, Huang HY, Chao MW, et al. Aryl Hydrocarbon Receptor Activation by Diesel Exhaust Particles Mediates Epithelium-Derived Cytokines Expression in Severe Allergic Asthma. *Allergy* (2018) 73:2192–204. doi: 10.1111/all.13462
65. Hong CH, Lee CH, Yu HS, Huang SK. Benzopyrene, a Major Polyaromatic Hydrocarbon in Smoke Fume, Mobilizes Langerhans Cells and Polarizes Th2/17 Responses in Epicutaneous Protein Sensitization Through the Aryl Hydrocarbon Receptor. *Int Immunopharmacol* (2016) 36:111–7. doi: 10.1016/j.intimp.2016.04.017
66. Xia M, Viera-Hutchins L, Garcia-Lloret M, Noval Rivas M, Wise P, McGhee SA, et al. Vehicular Exhaust Particles Promote Allergic Airway Inflammation Through an Aryl Hydrocarbon Receptor-Notch Signaling Cascade. *J Allergy Clin Immunol* (2015) 136:441–53. doi: 10.1016/j.jaci.2015.02.014
67. Hidaka T, Ogawa E, Kobayashi EH, Suzuki T, Funayama R, Nagashima T, et al. The Aryl Hydrocarbon Receptor AhR Links Atopic Dermatitis and Air Pollution *via* Induction of the Neurotrophic Factor Artemin. *Nat Immunol* (2017) 18:64–73. doi: 10.1038/ni.3614
68. Krutmann J, Bouloc A, Sore G, Bernard BA, Passeron T. The Skin Aging Exposome. *J Dermatol Sci* (2017) 85:152–61. doi: 10.1016/j.jdermsci.2016.09.015
69. Young AR, Claveau J, Rossi AB. Ultraviolet Radiation and the Skin: Photobiology and Sunscreen Photoprotection. *J Am Acad Dermatol* (2017) 76:S100–9. doi: 10.1016/j.jaad.2016.09.038
70. Wondrak GT, Jacobson MK, Jacobson EL. Endogenous UVA-Photosensitizers: Mediators of Skin Photodamage and Novel Targets for Skin Photoprotection. *Photochem Photobiol Sci* (2006) 5:215–37. doi: 10.1039/B504573H
71. Ratushny V, Gober MD, Hick R, Ridky TW, Seykora JT. From Keratinocyte to Cancer: The Pathogenesis and Modeling of Cutaneous Squamous Cell Carcinoma. *J Clin Invest* (2012) 122:464–72. doi: 10.1172/JCI57415
72. Elmets CA, Athar M. Milestones in Photocarcinogenesis. *J Invest Dermatol* (2013) 133:E13–7. doi: 10.1038/skinbio.2013.179
73. Bernard JJ, Gallo RL, Krutmann J. Photoimmunology: How Ultraviolet Radiation Affects the Immune System. *Nat Rev Immunol* (2019) 19:688–701. doi: 10.1038/s41577-019-0185-9
74. Schwarz T, Beissert S. Milestones in Photoimmunology. *J Invest Dermatol* (2013) 133:E7–E10. doi: 10.1038/skinbio.2013.177
75. Cadet J, Grand A, Douki T. Solar UV Radiation-Induced DNA Bipyrimidine Photoproducts: Formation and Mechanistic Insights. *Top Curr Chem* (2015) 356:249–75. doi: 10.1007/128_2014_553

76. Rannug A, Rannug U, Rosenkranz HS, Winqvist L, Westerholm R, Agurell E, et al. Certain Photooxidized Derivatives of Tryptophan Bind With Very High Affinity to the Ah Receptor and Are Likely to be Endogenous Signal Substances. *J Biol Chem* (1987) 262:15422–7. doi: 10.1016/S0021-9258(18)47743-5
77. Herrlich P, Karin M, Weiss C. Supreme EnLIGHTenment: Damage Recognition and Signaling in the Mammalian UV Response. *Mol Cell* (2008) 29:279–90. doi: 10.1016/j.molcel.2008.01.001
78. Brash DE, Rudolph JA, Simon JA, Lin A, McKenna GJ, Baden HP, et al. A Role for Sunlight in Skin Cancer: UV-Induced P53 Mutations in Squamous Cell Carcinoma. *Proc Natl Acad Sci USA* (1991) 88:10124–8. doi: 10.1073/pnas.88.22.10124
79. Ziegler A, Jonason AS, Leffell DJ, Simon JA, Sharma HW, Kimmelman J, et al. Sunburn and P53 in the Onset of Skin Cancer. *Nature* (1994) 372:773–6. doi: 10.1038/372773a0
80. Jans J, Schul W, Sert YG, Rijksen Y, Rebel H, Eker AP, et al. Powerful Skin Cancer Protection by a CPD-Photolyase Transgene. *Curr Biol* (2005) 15:105–15. doi: 10.1016/j.cub.2005.01.001
81. Yarosh D, Alas LG, Yee V, Oberyszyn A, Kibitel JT, Mitchell D, et al. Pyrimidine Dimer Removal Enhanced by DNA Repair Liposomes Reduces the Incidence of UV Skin Cancer in Mice. *Cancer Res* (1992) 52:4227–31.
82. DiGiovanna JJ, Kraemer KH. Shining a Light on Xeroderma Pigmentosum. *J Invest Dermatol* (2012) 132:785–96. doi: 10.1038/jid.2011.426
83. Roos WP, Kaina B. DNA Damage-Induced Cell Death by Apoptosis. *Trends Mol Med* (2006) 12:440–50. doi: 10.1016/j.molmed.2006.07.007
84. Batista LF, Kaina B, Meneghini R, Menck CF. How DNA Lesions Are Turned Into Powerful Killing Structures: Insights From UV-Induced Apoptosis. *Mutat Res* (2009) 681:197–208. doi: 10.1016/j.mrrev.2008.09.001
85. Dunkern TR, Kaina B. Cell Proliferation and DNA Breaks Are Involved in Ultraviolet Light-Induced Apoptosis in Nucleotide Excision Repair-Deficient Chinese Hamster Cells. *Mol Biol Cell* (2002) 13:348–61. doi: 10.1091/mbc.01-05-0225
86. Garinis GA, Mitchell JR, Moorhouse MJ, Hanada K, de WH, Vandeputte D, et al. Transcriptome Analysis Reveals Cyclobutane Pyrimidine Dimers as a Major Source of UV-Induced DNA Breaks. *EMBO J* (2005) 24:3952–62. doi: 10.1038/sj.emboj.7600849
87. Sorensen CS, Hansen LT, Dziegielewski J, Syljuasen RG, Lundin C, Bartek J, et al. The Cell-Cycle Checkpoint Kinase Chk1 Is Required for Mammalian Homologous Recombination Repair. *Nat Cell Biol* (2005) 7:195–201. doi: 10.1038/ncb1212
88. Sanchez Y, Wong C, Thoma RS, Richman R, Wu Z, Piwnica-Worms H, et al. Conservation of the Chk1 Checkpoint Pathway in Mammals: Linkage of DNA Damage to Cdk Regulation Through Cdc25. *Science* (1997) 277:1497–501. doi: 10.1126/science.277.5331.1497
89. Helleday T. Homologous Recombination in Cancer Development, Treatment and Development of Drug Resistance. *Carcinogenesis* (2010) 31:955–60. doi: 10.1093/carcin/bgq064
90. Aziz MH, Reagan-Shaw S, Wu J, Longley BJ, Ahmad N. Chemoprevention of Skin Cancer by Grape Constituent Resveratrol: Relevance to Human Disease? *FASEB J* (2005) 19:1193–5. doi: 10.1096/fj.04-3582fje
91. Kawasumi M, Lemos B, Bradner JE, Thibodeau R, Kim YS, Schmidt M, et al. Protection From UV-Induced Skin Carcinogenesis by Genetic Inhibition of the Ataxia Telangiectasia and Rad3-Related (ATR) Kinase. *PNAS* (2011) 108:13716–21. doi: 10.1073/pnas.1111378108
92. Lu YP, Lou YR, Xie JG, Peng QY, Zhou S, Lin Y, et al. Caffeine and Caffeine Sodium Benzoate Have a Sunscreen Effect, Enhance UVB-Induced Apoptosis, and Inhibit UVB-Induced Skin Carcinogenesis in SKH-1 Mice. *Carcinogenesis* (2006) 28:199–206. doi: 10.1093/carcin/bgl112
93. Kim DJ, Kataoka K, Sano S, Connolly K, Kiguchi K, DiGiovanni J. Targeted Disruption of Bcl-xL in Mouse Keratinocytes Inhibits Both UVB- and Chemically Induced Skin Carcinogenesis. *Mol Carcinog* (2009) 48:873–85. doi: 10.1002/mc.20527
94. Applegate LA, Ley RD, Alcalay J, Kripke ML. Identification of the Molecular Target for the Suppression of Contact Hypersensitivity by Ultraviolet Radiation. *J Exp Med* (1989) 170:1117–31. doi: 10.1084/jem.170.4.1117
95. Kripke ML, Cox PA, Alas LG, Yarosh DB. Pyrimidine Dimers in DNA Initiate Systemic Immunosuppression in UV-Irradiated Mice. *PNAS* (1992) 89:7516–20. doi: 10.1073/pnas.89.16.7516
96. Stege H, Roza L, Vink AA, Grewe M, Ruzicka T, Grether-Beck S, et al. Enzyme Plus Light Therapy to Repair DNA Damage in Ultraviolet-B-Irradiated Human Skin. *Proc Natl Acad Sci USA* (2000) 97:1790–5. doi: 10.1073/pnas.030528897
97. Navid F, Bruhs A, Schuller W, Fritsche E, Krutmann J, Schwarz T, et al. The Aryl Hydrocarbon Receptor is Involved in UVR-Induced Immunosuppression. *J Invest Dermatol* (2013) 133:2763–70. doi: 10.1038/jid.2013.221
98. Veldhoen M, Hirota K, Westendorf AM, Buer J, Dumoutier L, Renauld JC, et al. The Aryl Hydrocarbon Receptor Links TH17-Cell-Mediated Autoimmunity to Environmental Toxins. *Nature* (2008) 453:106–9. doi: 10.1038/nature06881
99. Quintana FJ, Basso AS, Iglesias AH, Korn T, Farez MF, Bettelli E, et al. Control of T(reg) and T(H)17 Cell Differentiation by the Aryl Hydrocarbon Receptor. *Nature* (2008) 453:65–71. doi: 10.1038/nature06880
100. Rannug U, Rannug A, Sjoberg U, Li H, Westerholm R, Bergman J. Structure Elucidation of Two Tryptophan-Derived, High Affinity Ah Receptor Ligands. *Chem Biol* (1995) 2:841–5. doi: 10.1016/1074-5521(95)90090-X
101. Diani-Moore S, Ma Y, Labitzke E, Tao H, David Warren J, Anderson J, et al. Discovery and Biological Characterization of 1-(1H-Indol-3-Yl)-9H-Pyrido [3,4-B]Indole as an Aryl Hydrocarbon Receptor Activator Generated by Photoactivation of Tryptophan by Sunlight. *Chem Biol Interact* (2011) 193:119–28. doi: 10.1016/j.cbi.2011.05.010
102. Helferich WG, Denison MS. Ultraviolet Photoproducts of Tryptophan can Act as Dioxin Agonists. *Mol Pharmacol* (1991) 40:674–8.
103. Schallreuter KU, Salem MA, Gibbons NC, Maitland DJ, Marsch E, Elwary SM, et al. Blunted Epidermal L-Tryptophan Metabolism in Vitiligo Affects Immune Response and ROS Scavenging by Fenton Chemistry, Part 2: Epidermal H2O2/ONOO(-)-Mediated Stress in Vitiligo Hampers Indoleamine 2,3-Dioxygenase and Aryl Hydrocarbon Receptor-Mediated Immune Response Signaling. *FASEB J* (2012) 26:2471–85. doi: 10.1096/fj.11-201897
104. Goerz G, Barnstorf W, Winnekendonk G, Bolsen K, Fritsch C, Kalka K, et al. Influence of UVA and UVB Irradiation on Hepatic and Cutaneous P450 Isoenzymes. *Arch Dermatol Res* (1996) 289:46–51. doi: 10.1007/s004030050151
105. Mukhtar H, DelTito BJJr., Matgouranis PM, Das M, Asokan P, Bickers DR. Additive Effects of Ultraviolet B and Crude Coal Tar on Cutaneous Carcinogen Metabolism: Possible Relevance to the Tumorigenicity of the Goeckerman Regimen. *J Invest Dermatol* (1986) 87:348–53. doi: 10.1111/1523-1747.ep12524446
106. Tigges J, Haarmann-Stemmann T, Vogel CF, Grindel A, Hubenthal U, Brenden H, et al. The New Aryl Hydrocarbon Receptor Antagonist E/Z-2-Benzylindene-5,6-Dimethoxy-3,3-Dimethylindan-1-One Protects Against UVB-Induced Signal Transduction. *J Invest Dermatol* (2014) 134:556–9. doi: 10.1038/jid.2013.362
107. Katiyar SK, Matsui MS, Mukhtar H. Ultraviolet-B Exposure of Human Skin Induces Cytochromes P450 1A1 and 1B1. *J Invest Dermatol* (2000) 114:328–33. doi: 10.1046/j.1523-1747.2000.00876.x
108. Bergander L, Wincent E, Rannug A, Foroozesh M, Alworth W, Rannug U. Metabolic Fate of the Ah Receptor Ligand 6-Formylindolo[3,2-B]Carbazole. *Chem Biol Interact* (2004) 149:151–64. doi: 10.1016/j.cbi.2004.08.005
109. Wincent E, Bengtsson J, Mohammadi BA, Alsberg T, Luecke S, Rannug U, et al. Inhibition of Cytochrome P4501-Dependent Clearance of the Endogenous Agonist FICZ as a Mechanism for Activation of the Aryl Hydrocarbon Receptor. *PNAS* (2012) 109:4479–84. doi: 10.1073/pnas.1118467109
110. Walrant P, Santus R, Grossweiner LI. Photosensitizing Properties of N-Formylkynurenine. *Photochem Photobiol* (1975) 22:63–5. doi: 10.1111/j.1751-1097.1975.tb06723.x
111. Asquith RS, Rivett DE. Studies on the Photooxidation of Tryptophan. *Biochim Biophys Acta* (1971) 252:111–6. doi: 10.1016/0304-4165(71)90098-5
112. Youssef A, von Koschembahr A, Caillat S, Corre S, Galibert MD, Douki T. 6-Formylindolo[3,2-B]Carbazole (FICZ) Is a Very Minor Photoproduct of Tryptophan at Biologically Relevant Doses of UVB and Simulated Sunlight. *Photochem Photobiol* (2019) 95:237–43. doi: 10.1111/php.12950

113. DiNatale BC, Murray IA, Schroeder JC, Flaveny CA, Lahoti TS, Laurenzana EM, et al. Kynurenic Acid Is a Potent Endogenous Aryl Hydrocarbon Receptor Ligand That Synergistically Induces Interleukin-6 in the Presence of Inflammatory Signaling. *Toxicol Sci* (2010) 115:89–97. doi: 10.1093/toxsci/kfq024
114. Platten M, Nollen EAA, Rohrig UF, Fallarino F, Opitz CA. Tryptophan Metabolism as a Common Therapeutic Target in Cancer, Neurodegeneration and Beyond. *Nat Rev Drug Discov* (2019) 18:379–401. doi: 10.1038/s41573-019-0016-5
115. Pollet M, Shaik S, Mescher M, Frauenstein K, Tigges J, Braun SA, et al. The AHR Represses Nucleotide Excision Repair and Apoptosis and Contributes to UV-Induced Skin Carcinogenesis. *Cell Death Differ* (2018) 25:1823–36. doi: 10.1038/s41418-018-0160-1
116. Smith KJ, Murray IA, Boyer JA, Perdew GH. Allelic Variants of the Aryl Hydrocarbon Receptor Differentially Influence UVB-Mediated Skin Inflammatory Responses in SKH1 Mice. *Toxicology* (2018) 394:27–34. doi: 10.1016/j.tox.2017.11.020
117. Tauchi M, Hida A, Negishi T, Katsuoka F, Noda S, Mimura J, et al. Constitutive Expression of Aryl Hydrocarbon Receptor in Keratinocytes Causes Inflammatory Skin Lesions. *Mol Cell Biol* (2005) 25:9360–8. doi: 10.1128/MCB.25.21.9360-9368.2005
118. Bradford PT, Goldstein AM, Tamura D, Khan SG, Ueda T, Boyle J, et al. Cancer and Neurologic Degeneration in Xeroderma Pigmentosum: Long Term Follow-Up Characterises the Role of DNA Repair. *J Med Genet* (2011) 48:168–76. doi: 10.1136/jmg.2010.083022
119. Reid-Bayliss KS, Arron ST, Loeb LA, Bezrookove V, Cleaver JE. Why Cockayne Syndrome Patients do Not Get Cancer Despite Their DNA Repair Deficiency. *Proc Natl Acad Sci USA* (2016) 113:10151–6. doi: 10.1073/pnas.1610020113
120. Chu IM, Hengst L, Slingerland JM. The Cdk Inhibitor P27 in Human Cancer: Prognostic Potential and Relevance to Anticancer Therapy. *Nat Rev Cancer* (2008) 8:253–67. doi: 10.1038/nrc2347
121. Frauenstein K, Sydlik U, Tigges J, Majora M, Wiek C, Hanenberg H, et al. Evidence for a Novel Anti-Apoptotic Pathway in Human Keratinocytes Involving the Aryl Hydrocarbon Receptor, E2F1, and Checkpoint Kinase 1. *Cell Death Differ* (2013) 20:1425–34. doi: 10.1038/cdd.2013.102
122. Kalmes M, Hennen J, Clemens J, Blomeke B. Impact of Aryl Hydrocarbon Receptor (AhR) Knockdown on Cell Cycle Progression in Human HaCaT Keratinocytes. *Biol Chem* (2011) 392:643–51. doi: 10.1515/bc.2011.067
123. Dever DP, Opanashuk LA. The Aryl Hydrocarbon Receptor Contributes to the Proliferation of Human Medulloblastoma Cells. *Mol Pharmacol* (2012) 81:669–78. doi: 10.1124/mol.111.077305
124. Hsu HL, Chen HK, Tsai CH, Liao PL, Chan YJ, Lee YC, et al. Aryl Hydrocarbon Receptor Defect Attenuates Mitogen-Activated Signaling Through Leucine-Rich Repeats and Immunoglobulin-Like Domains 1 (LRIG1)-Dependent EGFR Degradation. *Int J Mol Sci* (2021) 22:9988. doi: 10.3390/ijms22189988
125. Compe E, Egly JM. TFIIH: When Transcription Met DNA Repair. *Nat Rev Mol Cell Biol* (2012) 13:343–54. doi: 10.1038/nrm3350
126. Coin F, Oksenych V, Mocquet V, Groh S, Blattner C, Egly JM. Nucleotide Excision Repair Driven by the Dissociation of CAK From TFIIH. *Mol Cell* (2008) 31:9–20. doi: 10.1016/j.molcel.2008.04.024
127. Gao S, Guo K, Chen Y, Zhao J, Jing R, Wang L, et al. Keratinocyte Growth Factor 2 Ameliorates UVB-Induced Skin Damage *via* Activating the AhR/Nrf2 Signaling Pathway. *Front Pharmacol* (2021) 12:655281. doi: 10.3389/fphar.2021.655281
128. Xie Y, Su N, Yang J, Tan Q, Huang S, Jin M, et al. FGF/FGFR Signaling in Health and Disease. *Signal Transduct Target Ther* (2020) 5:181. doi: 10.1038/s41392-020-00222-7
129. Schwarz A, Stander S, Berneburg M, Bohm M, Kulms D, van Steeg H, et al. Interleukin-12 Suppresses Ultraviolet Radiation-Induced Apoptosis by Inducing DNA Repair. *Nat Cell Biol* (2002) 4:26–31. doi: 10.1038/ncb717
130. Chan CY, Kim PM, Winn LM. TCDD-Induced Homologous Recombination: The Role of the Ah Receptor Versus Oxidative DNA Damage. *Mutat Res* (2004) 563:71–9. doi: 10.1016/j.mrgentox.2004.05.015
131. Chan CY, Kim PM, Winn LM. TCDD Affects DNA Double Strand-Break Repair. *Toxicol Sci* (2004) 81:133–8. doi: 10.1093/toxsci/kfh200
132. Stolpmann K, Brinkmann J, Salzmann S, Genkinger D, Fritsche E, Hutzler C, et al. Activation of the Aryl Hydrocarbon Receptor Sensitises Human Keratinocytes for CD95L- and TRAIL-Induced Apoptosis. *Cell Death Dis* (2012) 3:e388. doi: 10.1038/cddis.2012.127
133. Bruhs A, Haarmann-Stemmann T, Frauenstein K, Krutmann J, Schwarz T, Schwarz A. Activation of the Arylhydrocarbon Receptor Causes Immunosuppression Primarily by Modulating Dendritic Cells. *J Invest Dermatol* (2015) 135:435–44. doi: 10.1038/jid.2014.419
134. Jeon MS, Esser C. The Murine IL-2 Promoter Contains Distal Regulatory Elements Responsive to the Ah Receptor, a Member of the Evolutionarily Conserved bHLH-PAS Transcription Factor Family. *J Immunol* (2000) 165:6975–83. doi: 10.4049/jimmunol.165.12.6975
135. Nguyen NT, Kimura A, Nakahama T, Chinen I, Masuda K, Nohara K, et al. Aryl Hydrocarbon Receptor Negatively Regulates Dendritic Cell Immunogenicity *via* a Kynurenine-Dependent Mechanism. *Proc Natl Acad Sci USA* (2010) 107:19961–6. doi: 10.1073/pnas.1014465107
136. Opitz CA, Litzenburger UM, Sahm F, Ott M, Tritschler I, Trump S, et al. An Endogenous Tumour-Promoting Ligand of the Human Aryl Hydrocarbon Receptor. *Nature* (2011) 478:197–203. doi: 10.1038/nature10491
137. Munn DH, Mellor AL. Indoleamine 2,3 Dioxygenase and Metabolic Control of Immune Responses. *Trends Immunol* (2013) 34:137–43. doi: 10.1016/j.it.2012.10.001
138. Mezrich JD, Fechner JH, Zhang X, Johnson BP, Burlingham WJ, Bradfield CA. An Interaction Between Kynurenine and the Aryl Hydrocarbon Receptor Can Generate Regulatory T Cells. *J Immunol* (2010) 185:3190–8. doi: 10.4049/jimmunol.0903670
139. Litzenburger UM, Opitz CA, Sahm F, Rauschenbach KJ, Trump S, Winter M, et al. Constitutive IDO Expression in Human Cancer Is Sustained by an Autocrine Signaling Loop Involving IL-6, STAT3 and the AHR. *Oncotarget* (2014) 5:1038–51. doi: 10.18632/oncotarget.1637
140. D'Amato NC, Rogers TJ, Gordon MA, Greene LI, Cochrane DR, Spoelstra NS, et al. A TDO2-AhR Signaling Axis Facilitates Anoikis Resistance and Metastasis in Triple-Negative Breast Cancer. *Cancer Res* (2015) 75:4651–64. doi: 10.1158/0008-5472.CAN-15-2011
141. Kenison JE, Wang Z, Yang K, Snyder M, Quintana FJ, Sherr DH. The Aryl Hydrocarbon Receptor Suppresses Immunity to Oral Squamous Cell Carcinoma Through Immune Checkpoint Regulation. *PNAS* (2021) 118:e2012692118. doi: 10.1073/pnas.2012692118
142. Funatake CJ, Marshall NB, Steppan LB, Mourich DV, Kerkvliet NI. Cutting Edge: Activation of the Aryl Hydrocarbon Receptor by 2,3,7,8-Tetrachlorodibenzo-P-Dioxin Generates a Population of CD4+ CD25+ Cells With Characteristics of Regulatory T Cells. *J Immunol* (2005) 175:4184–8. doi: 10.4049/jimmunol.175.7.4184
143. Zhang L, Ma J, Takeuchi M, Usui Y, Hattori T, Okunuki Y, et al. Suppression of Experimental Autoimmune Uveoretinitis by Inducing Differentiation of Regulatory T Cells *via* Activation of Aryl Hydrocarbon Receptor. *Invest Ophthalmol Vis Sci* (2010) 51:2109–17. doi: 10.1167/iovs.09-3993
144. Ehrlich AK, Pennington JM, Bisson WH, Kolluri SK, Kerkvliet NI. TCDD, FICZ, and Other High Affinity AhR Ligands Dose-Dependently Determine the Fate of CD4+ T Cell Differentiation. *Toxicol Sci* (2018) 161:310–20. doi: 10.1093/toxsci/kfx215
145. Ronsein GE, Oliveira MCB, Miyamoto S, Medeiros MHG, Di Mascio P. Tryptophan Oxidation by Singlet Molecular Oxygen [O2(1Deltag)]: Mechanistic Studies Using 18O-Labeled Hydroperoxides, Mass Spectrometry, and Light Emission Measurements. *Chem Res Toxicol* (2008) 21:1271–83. doi: 10.1021/tx800026g
146. Van den Eynde BJ, Van Baren N, Baurain JF. Is There a Clinical Future for IDO1 Inhibitors After the Failure of Epacadostat in Melanoma? *Annu Rev Cancer Biol* (2020) 4:241–56. doi: 10.1146/annurev-cancerbio-030419-033635
147. Sadik A, Somarribas Patterson LF, Ozturk S, Mohapatra SR, Panitz V, Secker PF, et al. IL4I1 Is a Metabolic Immune Checkpoint That Activates the AHR and Promotes Tumor Progression. *Cell* (2020) 182:1252–1270 e1234. doi: 10.1016/j.cell.2020.07.038
148. Ramspott JP, Bekkat F, Bod L, Favier M, Terris B, Salomon A, et al. Emerging Role of IL-4-Induced Gene 1 as a Prognostic Biomarker Affecting the Local T-Cell Response in Human Cutaneous Melanoma. *J Invest Dermatol* (2018) 138:2625–34. doi: 10.1016/j.jid.2018.06.178

149. Wang GZ, Zhang L, Zhao XC, Gao SH, Qu LW, Yu H, et al. The Aryl Hydrocarbon Receptor Mediates Tobacco-Induced PD-L1 Expression and Is Associated With Response to Immunotherapy. *Nat Commun* (2019) 10:1125. doi: 10.1038/s41467-019-08887-7
150. Liu Y, Liang X, Dong W, Fang Y, Lv J, Zhang T, et al. Tumor-Repopulating Cells Induce PD-1 Expression in CD8(+) T Cells by Transferring Kynurenine and AhR Activation. *Cancer Cell* (2018) 33:480–94.e487. doi: 10.1016/j.ccell.2018.02.005
151. Labadie BW, Bao R, Luke JJ. Reimagining IDO Pathway Inhibition in Cancer Immunotherapy *via* Downstream Focus on the Tryptophan-Kynurenine-Aryl Hydrocarbon Axis. *Clin Cancer Res* (2019) 25:1462–71. doi: 10.1158/1078-0432.CCR-18-2882
152. Urbach F. Modification of Ultraviolet Carcinogenesis by Photoactive Agents; Preliminary Report. *J Invest Dermatol* (1959) 32:373–8. doi: 10.1038/jid.1959.63
153. Findlay GM. Ultra-Violet Light and Skin Cancer. *Lancet* (1928) 2:1070 – 1073. doi: 10.1016/S0140-6736(00)84845-X
154. Rusch HP, Kline BE, Baumann CA. The Nonadditive Effect of Ultraviolet Light and Other Carcinogenic Procedures. *Cancer Res* (1942) 2:183 – 188.
155. von Koschembahr A, Youssef A, Beal D, Gudimard L, Giot JP, Douki T. Toxicity and DNA Repair in Normal Human Keratinocytes Co-Exposed to Benzo[a]Pyrene and Sunlight. *Toxicol In Vitro* (2020) 63:104744. doi: 10.1016/j.tiv.2019.104744
156. Botta C, Di Giorgio C, Sabatier AS, De Meo M. Effects of UVA and Visible Light on the Photogenotoxicity of Benzo[a]Pyrene and Pyrene. *Environ Toxicol* (2009) 24:492–505. doi: 10.1002/tox.20455
157. Mauthe RJ, Cook VM, Coffing SL, Baird WM. Exposure of Mammalian Cell Cultures to Benzo[a]Pyrene and Light Results in Oxidative DNA Damage as Measured by 8-Hydroxydeoxyguanosine Formation. *Carcinogenesis* (1995) 16:133–7. doi: 10.1093/carcin/16.1.133
158. Wang S, Sheng Y, Feng M, Leszczynski J, Wang L, Tachikawa H, et al. Light-Induced Cytotoxicity of 16 Polycyclic Aromatic Hydrocarbons on the US EPA Priority Pollutant List in Human Skin HaCaT Keratinocytes: Relationship Between Phototoxicity and Excited State Properties. *Environ Toxicol* (2007) 22:318–27. doi: 10.1002/tox.20241
159. Shyong EQ, Lu Y, Goldstein A, Lebwohl M, Wei H. Synergistic Enhancement of H2O2 Production in Human Epidermoid Carcinoma Cells by Benzo[a] pyrene and Ultraviolet A Radiation. *Toxicol Appl Pharmacol* (2003) 188:104–9. doi: 10.1016/S0041-008X(03)00018-8
160. Soeur J, Belaidi JP, Chollet C, Denat L, Dimitrov A, Jones C, et al. Photo-Pollution Stress in Skin: Traces of Pollutants (PAH and Particulate Matter) Impair Redox Homeostasis in Keratinocytes Exposed to UVA1. *J Dermatol Sci* (2017) 86:162–9. doi: 10.1016/j.jdermsci.2017.01.007
161. Borska L, Andrys C, Krejsek J, Palicka V, Vorisek V, Hamakova K, et al. Influence of Dermal Exposure to Ultraviolet Radiation and Coal Tar (Polycyclic Aromatic Hydrocarbons) on the Skin Aging Process. *J Dermatol Sci* (2016) 81:192–202. doi: 10.1016/j.jdermsci.2015.12.010
162. Fu PP, Xia Q, Sun X, Yu H. Phototoxicity and Environmental Transformation of Polycyclic Aromatic Hydrocarbons (PAHs)-Light-Induced Reactive Oxygen Species, Lipid Peroxidation, and DNA Damage. *J Environ Sci Health C Environ Carcinog Ecotoxicol Rev* (2012) 30:1–41. doi: 10.1080/10590501.2012.653887
163. Park SL, Justiniano R, Williams JD, Cabello CM, Qiao S, Wondrak GT. The Tryptophan-Derived Endogenous Aryl Hydrocarbon Receptor Ligand 6-Formylindolo[3,2-B]Carbazole Is a Nanomolar UVA Photosensitizer in Epidermal Keratinocytes. *J Invest Dermatol* (2015) 135:1649–58. doi: 10.1038/jid.2014.503
164. Rolfes KM, Sondermann NC, Vogeley C, Dairou J, Gilardino V, Wirth R, et al. Inhibition of 6-Formylindolo[3,2-B]Carbazole Metabolism Sensitizes Keratinocytes to UVA-Induced Apoptosis: Implications for Vemurafenib-Induced Phototoxicity. *Redox Biol* (2021) 46:102110. doi: 10.1016/j.redox.2021.102110
165. Justiniano R, de Faria Lopes L, Perer J, Hua A, Park SL, Jandova J, et al. The Endogenous Tryptophan-Derived Photoproduct 6-Formylindolo[3,2-B] Carbazole (FICZ) Is a Nanomolar Photosensitizer That Can be Harnessed for the Photodynamic Elimination of Skin Cancer Cells in Vitro and in Vivo. *Photochem Photobiol* (2021) 97:180–91. doi: 10.1111/php.13321
166. Brem R, Macpherson P, Guven M, Karran P. Oxidative Stress Induced by UVA Photoactivation of the Tryptophan UVB Photoproduct 6-Formylindolo[3,2-B]Carbazole (FICZ) Inhibits Nucleotide Excision Repair in Human Cells. *Sci Rep* (2017) 7:4310. doi: 10.1038/s41598-017-04614-8
167. Dolmans DE, Fukumura D, Jain RK. Photodynamic Therapy for Cancer. *Nat Rev Cancer* (2003) 3:380–7. doi: 10.1038/nrc1071
168. Allegra A, Pioggia G, Tonacci A, Musolino C, Gangemi S. Oxidative Stress and Photodynamic Therapy of Skin Cancers: Mechanisms, Challenges and Promising Developments. *Antioxid (Basel)* (2020) 9:448. doi: 10.3390/antiox9050448
169. Hopf NB, Spring P, Hirt-Burri N, Jimenez S, Sutter B, Vernez D, et al. Polycyclic Aromatic Hydrocarbons (PAHs) Skin Permeation Rates Change With Simultaneous Exposures to Solar Ultraviolet Radiation (UV-S). *Toxicol Lett* (2018) 287:122–30. doi: 10.1016/j.toxlet.2018.01.024
170. Bourgart E, Persoons R, Marques M, Rivier A, Balducci F, von Koschembahr A, et al. Influence of Exposure Dose, Complex Mixture, and Ultraviolet Radiation on Skin Absorption and Bioactivation of Polycyclic Aromatic Hydrocarbons Ex Vivo. *Arch Toxicol* (2019) 93:2165–84. doi: 10.1007/s00204-019-02504-8
171. Nair S, Kekatpure VD, Judson BL, Rifkind AB, Granstein RD, Boyle JO, et al. UVR Exposure Sensitizes Keratinocytes to DNA Adduct Formation. *Cancer Prev Res (Phila)* (2009) 2:895–902. doi: 10.1158/1940-6207.CAPR-09-0125
172. von Koschembahr A, Youssef A, Beal D, Calissi C, Bourgart E, Marques M, et al. Solar Simulated Light Exposure Alters Metabolization and Genotoxicity Induced by Benzo[a]Pyrene in Human Skin. *Sci Rep* (2018) 8:14692. doi: 10.1038/s41598-018-33031-8
173. Barker CW, Fagan JB, Pasco DS. Down-Regulation of P4501A1 and P4501A2 mRNA Expression in Isolated Hepatocytes by Oxidative Stress. *J Biol Chem* (1994) 269:3985–90. doi: 10.1016/S0021-9258(17)41731-5
174. Morel Y, Barouki R. Down-Regulation of Cytochrome P450 1A1 Gene Promoter by Oxidative Stress. Critical Contribution of Nuclear Factor 1. *J Biol Chem* (1998) 273:26969–76. doi: 10.1074/jbc.273.41.26969
175. Vostalova J, Rajnochova Svobodova A, Galandakova A, Sianska J, Dolezal D, Ulrichova J. Differential Modulation of Inflammatory Markers in Plasma and Skin After Single Exposures to UVA or UVB Radiation *In Vivo*. *BioMed Pap Med Fac Univ Palacky Olomouc Czech Repub* (2013) 157:137–45. doi: 10.5507/bp.2013.036
176. Kim TY, Kripke ML, Ullrich SE. Immunosuppression by Factors Released From UV-Irradiated Epidermal Cells: Selective Effects on the Generation of Contact and Delayed Hypersensitivity After Exposure to UVA or UVB Radiation. *J Invest Dermatol* (1990) 94:26–32. doi: 10.1111/1523-1747.ep12873322
177. Ke S, Rabson AB, Germino JF, Gallo MA, Tian Y. Mechanism of Suppression of Cytochrome P-450 1A1 Expression by Tumor Necrosis Factor-Alpha and Lipopolysaccharide. *J Biol Chem* (2001) 276:39638–44. doi: 10.1074/jbc.M106286200
178. Vogeley C, Esser C, Tuting T, Krutmann J, Haarmann-Stemmann T. Role of the Aryl Hydrocarbon Receptor in Environmentally Induced Skin Aging and Skin Carcinogenesis. *Int J Mol Sci* (2019) 20:6005. doi: 10.3390/ijms20236005
179. Fernandez-Gallego N, Sanchez-Madrid F, Cibrian D. Role of AHR Ligands in Skin Homeostasis and Cutaneous Inflammation. *Cells* (2021) 10:3176. doi: 10.3390/cells10113176
180. Krutmann J, Schalka S, Watson REB, Wei L, Morita A. Daily Photoprotection to Prevent Photoaging. *Photodermatol Photoimmunol Photomed* (2021) 37:482–9. doi: 10.1111/phpp.12688
181. Burke KE. Mechanisms of Aging and Development-A New Understanding of Environmental Damage to the Skin and Prevention With Topical Antioxidants. *Mech Ageing Dev* (2018) 172:123–30. doi: 10.1016/j.mad.2017.12.003
182. Safe S, Jayaraman A, Chapkin RS, Howard M, Mohankumar K, Shrestha R. Flavonoids: Structure-Function and Mechanisms of Action and Opportunities for Drug Development. *Toxicol Res* (2021) 37:147–62. doi: 10.1007/s43188-020-00080-z
183. Goya-Jorge E, Jorge Rodriguez ME, Veitia MS, Giner RM. Plant Occurring Flavonoids as Modulators of the Aryl Hydrocarbon Receptor. *Molecules* (2021) 26:2315. doi: 10.3390/molecules26082315

Conflict of Interest: The authors declare that the research was conducted in the absence of any commercial or financial relationships that could be construed as a potential conflict of interest.

this article, or claim that may be made by its manufacturer, is not guaranteed or endorsed by the publisher.

frontiers in Oncology

ORIGINAL RESEARCH
published: 03 March 2022
doi: 10.3389/fonc.2022.846760

A Cohort Study: Comorbidity and Stage Affected the Prognosis of Melanoma Patients in Taiwan

*Chin-Kuo Chang[1], Yih-Shou Hsieh[1,2], Pei-Ni Chen[1,2], Shu-Chen Chu[3], Jing-Yang Huang[4], Yu-Hsun Wang[5] and James Cheng-Chung Wei[1,6,7]**

[1] Institute of Medicine, Chung Shan Medical University, Taichung, Taiwan, [2] Department of Biochemistry, School of Medicine, Chung Shan Medical University, Taichung, Taiwan, [3] Institute and Department of Food Science, Central Taiwan University of Science and Technology, Taichung, Taiwan, [4] Center for Health Data Science, Chung Shan Medical University Hospital, Taichung, Taiwan, [5] Department of Medical Research, Chung Shan Medical University Hospital, Taichung, Taiwan, [6] Division of Allergy, Immunology and Rheumatology, Chung Shan Medical University Hospital, Taichung, Taiwan, [7] Graduate Institute of Integrated Medicine, China Medical University, Taichung, Taiwan

OPEN ACCESS

Edited by:
Nabiha Yusuf,
University of Alabama at Birmingham,
United States

Reviewed by:
Yu-Fang Shen,
Asia University, Taiwan
Yao Min Hung,
Kaohsiung Municipal United Hospital,
Taiwan
Wen-Yih Jeng,
National Cheng Kung University,
Taiwan

***Correspondence:**
James Cheng-Chung Wei
jccwei@gmail.com

Specialty section:
This article was submitted to Skin Cancer, a section of the journal Frontiers in Oncology

Received: 31 December 2021
Accepted: 03 February 2022
Published: 03 March 2022

Citation:
Chang C-K, Hsieh Y-S, Chen P-N, Chu S-C, Huang J-Y, Wang Y-H and Wei JC-C (2022) A Cohort Study: Comorbidity and Stage Affected the Prognosis of Melanoma Patients in Taiwan. Front. Oncol. 12:846760. doi: 10.3389/fonc.2022.846760

Background: Comorbidities and stages may influence the prognosis of melanoma patients in Taiwan and need to be determined.

Methods: We performed a retrospective cohort study by using the national health insurance research database in Taiwan. Patients with a primary diagnosis of melanoma by the Taiwan Cancer Registry from 2009 to 2017 were recruited as the study population. The comparison group was never diagnosed with melanoma from 2000 to 2018. The Charlson comorbidity index was conducted to calculate the subjects' disease severity. The Cox proportional hazards model analysis was used to estimate the hazard ratio of death.

Results: We selected 476 patients, 55.5% of whom had comorbidity. A higher prevalence of comorbidity was associated with a more advanced cancer stage. The mortality rate increased with an increasing level of comorbidity in both cohorts and was higher among melanoma patients. The interaction between melanoma and comorbidity resulted in an increased mortality rate.

Conclusion: An association between poorer survival and comorbidity was verified in this study. We found that the level of comorbidity was strongly associated with mortality. A higher risk of mortality was found in patients who had localized tumors, regional metastases, or distant metastases with more comorbidity scores. Advanced stage of melanoma patients with more comorbidities was significantly associated with the higher risk of mortality rate.

Keywords: melanoma, comorbidity, stage, mortality rate, survival, prognosis

INTRODUCTION

Cutaneous melanoma is now regarded as the fifth most common cancer in the United States. It was estimated that there were approximately 96,480 new cases, and 7,230 deaths due to melanoma of the skin will be newly diagnosed in 2019 (1). Despite being the deadliest form of skin cancer with a high mortality rate, many melanoma patients are cured after surgical excision of their primary tumor at

an early stage; however, some still relapse after surgical excision. It is locally invasive and frequently spread out to regional lymph nodes and remote organs, including lung, liver, bone, and brain (2). The most common risk factors for malignant melanoma include family history, multiple moles, ultraviolet radiation, fair skin, and immunosuppression (3, 4). The incidence rate of melanoma has been increasing by between 3% and 7% per year globally for Caucasians (5). The incidence rate (less than 1/100,000) was lower in residents of Asia, including China, India, Singapore, and Japan (6). In Taiwan, the age-adjusted rate in 2006 for aggressive melanoma was 0.65/100,000 (0.71/100,000 for men, and 0.58/100,000 for women). The age distribution plot showed a peak among melanoma patients aged 70–79 years. According to the investigation of the incidence of melanoma from 1997 to 2008 by year and sex, the yearly incidence ranged from 0.66 to 1.24 (mean: 0.9) cases per 100,000 people in Taiwan (7). Excessive exposure to ultraviolet radiation is not the risk factor for most Taiwanese melanoma cases. In addition, 58% of cutaneous melanoma belongs to acral lentiginous melanoma. Advanced disease is found in 50% of cases (8).

Studies on various prognostic factors affecting melanoma survival have been reported frequently. Age has been proven to be a very strong and independent predictor of survival outcome after accounting for all the dominant prognostic factors (9). Sentinel node biopsy is an important prognostic factor in melanoma (10). Lower socioeconomic status (SES) was associated with a decreased median survival time in a statistically significant amount for all stages of melanoma (11). Men have a greater risk of having advanced disease with a poorer outcome (12). Studies have shown that the presence of a melanoma on an axial site conferred a worse prognosis than an extremity site (9). Older age and advanced stage have significant negative effects on the survival of mucosal melanoma (13). The mitotic rate is a continuous prognostic variable. It is a strong independent predictor of outcome and should be assessed and recorded in all primary melanomas including in both initial and excision biopsies (14). Level of invasion has prognostic significance in univariate analysis and remains an independent predictor of outcome in more contemporary analyses. Clinical parameters such as age, sex, skin color, pigmentation status of the tumor, and site of the primary tumor play an important role for the outcome of patients. Ulceration is an adverse prognostic factor of melanoma (15). Stage and anatomic site, but not thickness (i.e., Breslow depth), race, or ethnicity, determine prognosis of mucosal melanomas (16). Stage, male gender, and age are associated with overall survival, along with SES and the presence of multiple comorbidities (17–19). Taken together, various prognostic factors affecting melanoma survival interact mostly synergistically. The prognostic influence of comorbidity and stage on melanoma has also caused many scientists to make many valuable reports. The prevalence of chronic disease in patients with melanoma varies from 19% to 80% (20). The presence of chronic conditions prevents physicians from aggressive treatment for melanoma patients, thereby increasing the mortality rate (20). The prevalence of multiple chronic conditions increased with age (21). The majority of studies from a systematic review reported decreased chemotherapy use (75%) and inferior survival (69%) for patients with comorbidities compared to those without comorbidities (22). Patient comorbidity has a substantial effect on the cancer stage at diagnosis (23). In a cohort study conducted using Danish registry data of 23,476 melanoma patients, Grann et al. (20) reported a higher prevalence of comorbidity associated with more advanced cancer stages. Similar results were acquired by Gonzalez et al. (24) using data from the Florida State Tumor Registry (N = 32,074) in 1994 on colorectal, melanoma, breast, and prostate cancers. Comorbidity was associated with late-stage diagnosis in all four cancers, with the odds of 62% for late-stage melanoma (24). In Taiwan, just a few reports paid attention to malignant melanoma (25–27). Our current study aims at clarifying how comorbidity and stage may affect the prognosis of Taiwan melanoma patients from 2009 to 2017.

MATERIALS AND METHODS

Data Source

This study used the data from the National Health Insurance Research Database (NHIRD) and Taiwan Cancer Registry (TCR) that was constructed by the Health and Welfare Data Science Center (HWDSC). The NHIRD covered more than 99.99% of Taiwan's population of 23 million people in Taiwan. Two million beneficiaries were randomly sampled from the NHIRD in 2000. To protect patients' privacy, according to the "Personal Information Protection Act" and "Non-disclosure agreement of NHIRD," the original identification numbers were not disclosed. Data benefits include disease diagnosis of outpatient, inpatient, emergency medical claims, and cancer staging. The longitudinal characteristic of NHIRD allows researchers to identify a cohort based upon diagnoses and drug utilization, to trace the medical history, and to disclose clinical outcomes and related complications (28). TCR (29) is a nationwide population-based cancer registry system that provides detailed information on all cancer patients in Taiwan. Hospitals with more than 50-bed capacity that could supply outpatient and hospitalized cancer care are required to join in informing all newly diagnosed malignant neoplasms to the registry. In order to measure cancer care methods and treatment outcomes in Taiwan, the TCR constructed a long-form database with cancer staging and detailed treatment and recurrence information. Moreover, the long-form database included detailed information regarding cancer site-specific factors, such as laboratory values, tumor markers, and other clinical data related to patient care (30). The study had been approved by the ethical review board of the Chung Shan Medical University Hospital (CS1-20201) in Taiwan.

Study Design and Outcome

This study used a retrospective cohort study design. The study population was the primary site of melanoma (ICD-O-3=C44) from 2009 to 2017 in the TCR. The index date was admitted with

the first diagnosis date of melanoma. The comparison group was defined as never diagnosis of melanoma (ICD-9-CM=172, ICD-10-CM=C439) from 2000 to 2018 (**Figure 1**). Due to the consistent index date between the melanoma group and the non-melanoma group, a 1:10 age and sex matching was conducted. The outcome variable was all-cause mortality. Both groups were followed up until the onset of death, or December 31, 2018, whichever occurred first.

The demographic variables included age, sex, monthly income, and residential region. We classified diagnoses of chronic diseases into 17 categories based on a modified version of the Charlson comorbidity index (CCI) (31). The 1 score of weight included myocardial infarction, congestive heart failure, peripheral vascular disease, cerebrovascular disease, dementia, chronic pulmonary disease, connective tissue disease, peptic ulcer disease, mild liver disease, and diabetes without chronic complication. The 2 scores of weight included diabetes with chronic complication, hemiplegia or paraplegia, and renal disease. The 3 scores of weight included any malignancy, including lymphoma and leukemia, except malignant neoplasm of skin, and severe liver disease. The 6 scores of weight included metastatic solid tumor and AIDS/HIV (**Supplementary Table 1**). The higher CCI-weighted total score represented the higher severity of the disease. The baseline characteristics also included age, sex, hypertension (ICD-9-CM=401-405, ICD-10-CM=I10-I15), and hyperlipidemia (ICD-9-CM=272, ICD-10-CM=E78). Those comorbidities were defined 1 year before the index date and at least two outpatient visits or once hospitalization.

Statistical Analyses

The comparison of continuous and categorical variables was done using Student's t-test, chi-square test, or Fisher's exact test as appropriate between melanoma and non-melanoma groups. Kaplan–Meier analysis was conducted to calculate the all-cause mortality among the two groups. The log-rank test was used to test the significance. The multivariate Cox proportional hazards model was used to estimate the hazard ratios (HRs) of death. We used a time-dependent variable to assess the proportional hazards assumption. The p value was 0.2805 that it did not violate the proportional hazards assumption. For the unmeasured confounding factor, we performed E-value to define the minimum strength of the association for an unmeasured confounding effect between melanoma and non-melanoma groups (32, 33). The statistical software was SAS version 9.4 (SAS Institute Inc., NC, USA).

RESULTS

Study Population

We identified 476 melanoma patients and 4,760 members of the matched comparison cohort. The majority were men (56.7%), and more than half (85%) were older than 55 years. According to tumor stage, 52 (10.9%) *in situ*, 398 (83.6%) had a localized tumor, 8 (1.7%) had regional metastases, and 18 (3.8%) had distant metastases (**Table 1**).

Prevalence of Comorbidities

Measurement of comorbidity resulted in 212 (44.5%) melanoma patients with comorbidity score 0, 126 patients (26.5%) with comorbidity score 1, and 54 (11.3%) with comorbidity score 2. In the more severe comorbidity categories, 45 (9.5%) had a comorbidity score 3, and 39 (8.2%) had a comorbidity score ≥4. Diabetes without chronic complication was the most prevalent comorbidity, diagnosed in 83 patients (17.4%) (**Table 1**). Chronic pulmonary disease was diagnosed in 63 patients (13.2%), followed by peptic ulcer disease (58 patients, 12.2%). The majority of melanoma patients were diagnosed with the localized stage (**Table 1**).

All-Cause Mortality

The mortality rate of the melanoma group in the Kaplan–Meier plot was significantly higher than that in the non-melanoma group (**Figure 2**). The mortality rate increased with increasing

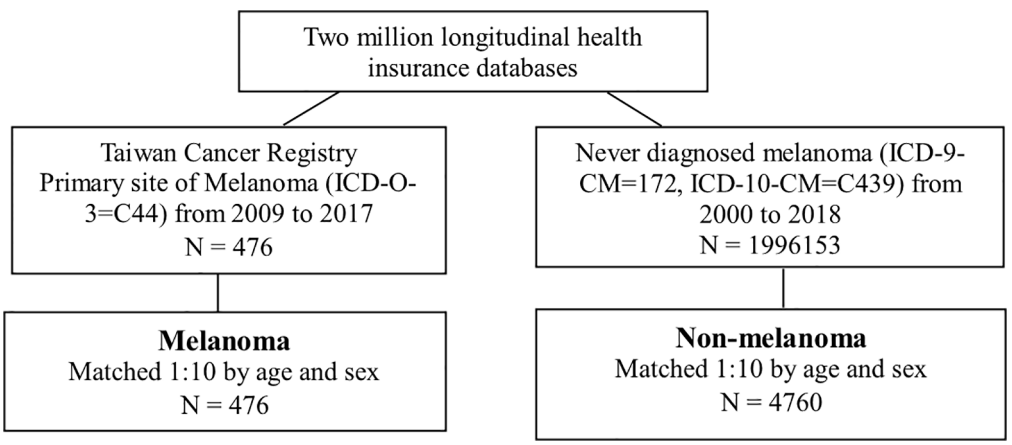

FIGURE 1 | Identified Melanoma and Non-melanoma groups.

TABLE 1 | Demographic characteristics of melanoma and non-melanoma.

	Non-melanoma (N = 4,760)		Melanoma (N = 476)		p value
	n	%	n	%	
Age					1
≤54	710	14.9	71	14.9	
55–69	1,430	30.0	143	30.0	
≥70	2,620	55.1	262	55.1	
Mean ± SD	69.91 ± 15.66		69.91 ± 15.67		1
Sex					1
Female	2,060	43.3	206	43.3	
Male	2,700	56.7	270	56.7	
Monthly income (NT$)					0.5469
<20,000	1,527	32.1	144	30.3	
20,001–40,000	2,349	49.3	235	49.4	
>40,000	884	18.6	97	20.4	
Residential region					0.0014
Northern	1,989	41.8	242	50.8	
Central	1,116	23.4	87	18.3	
Southern	1,212	25.5	111	23.3	
Others	443	9.3	36	7.6	
Stage of melanoma					
0			52	10.9	
I			292	61.3	
II			106	22.3	
III			8	1.7	
IV			18	3.8	
Hypertension	1,997	42.0	242	50.8	0.0002
Hyperlipidemia	986	20.7	108	22.7	0.3123
Categories of Charlson comorbidity index score					
Myocardial infarction	44	0.9	5	1.1	0.7854
Congestive heart failure	197	4.1	14	2.9	0.205
Peripheral vascular disease	56	1.2	8	1.7	0.3398
Cerebrovascular	444	9.3	56	11.8	0.0845
Dementia	175	3.7	18	3.8	0.9077
Chronic pulmonary disease	484	10.2	63	13.2	0.0370
Connective tissue disease	26	0.5	4	0.8	0.4176
Peptic ulcer disease	473	9.9	58	12.2	0.1214
Mild liver disease	187	3.9	33	6.9	0.0018
Diabetes without chronic complication	820	17.2	83	17.4	0.9079
Diabetes with chronic complication	244	5.1	26	5.5	0.7519
Hemiplegia or paraplegia	19	0.4	3	0.6	0.4454¶
Renal disease	310	6.5	41	8.6	0.0806
Any malignancy	50	1.1	21	4.4	<0.0001
Charlson comorbidity index score					<0.0001
0	2,663	55.95	212	44.5	
1	1,024	21.51	126	26.5	
2	478	10.04	54	11.3	
3	280	5.88	45	9.5	
≥4	315	6.62	39	8.2	

¶*Fisher's exact test.*

comorbidity in both cohorts and was higher among melanoma patients (**Figure 3**). The mortality rate for melanoma patients with comorbid score 1 was 57.42 per 1,000 person-years after diagnosis compared with 50.50 in the comparison cohort. In the most severe comorbidity group (≥4), the mortality rate was 147.21 per 1,000 person-years in the melanoma cohort compared with 149.43 in the comparison cohort. The mortality rate ratio (MRR) was 1.59 (95% CI: 1.28–1.98). The number of melanoma patients at stages 0, I, II, III, and IV was 52 (10.9%), 292 (61.3%), 106 (22.3%), 8 (1.7%), and 18 (3.8%), respectively (**Table 1**). In the univariate analysis, old age was associated with a significantly increased risk of death ($p < 0.0001$). Patients greater than and equal to 70 years of age (HR = 18.64, 95% CI: 10.96–31.72) had a worse prognosis than patients less than and equal to 54 years of age. The risk of death for people with comorbidity scores 1, 2, 3, and ≥4 was 2.65, 4.88, 5.48, and 7.77, respectively (**Table 2**). **Table 3** demonstrated the subgroup analysis of the risk of death between melanoma and non-melanoma groups. The risk of death for patients aged ≤54 between melanoma and non-melanoma group was the highest (HR = 13.08, 95% CI = 4.41–38.77, $p < 0.0001$) among the three age groups. For patients between melanoma and non-melanoma

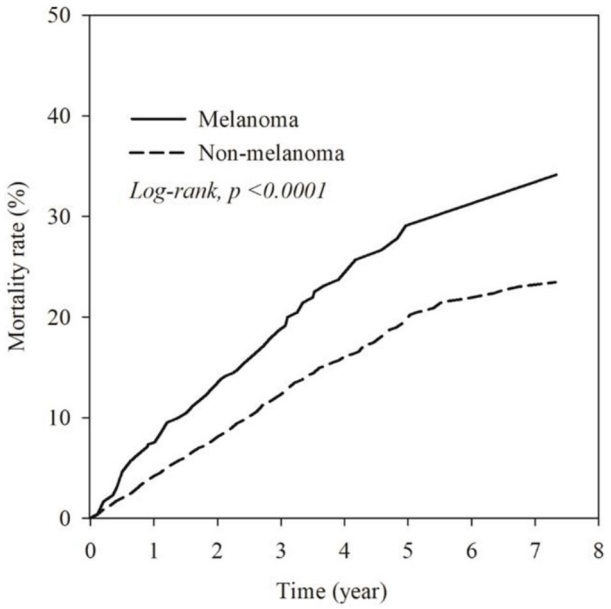

FIGURE 2 | Kaplan-Meier plot for the mortality rate in melanoma group and non-melanoma group.

groups with comorbidity score 0, the HR risk of death was 2.40 (95% CI: 1.56–3.68, p < 0.0001). **Table 4** demonstrated the higher risk of mortality for people with comorbidity score 3 (HR = 2.79, 95% CI: 1.46–5.30, p = 0.002) and score ≥4 (HR = 2.75, 95% CI: 1.39–5.44, p = 0.004). Increased comorbidity was related to the advanced cancer stage at diagnosis. The HR risk of mortality in melanoma patients with comorbidity scores 1, ≥2 at stages 0 and I was 2.61 (95% CI: 1.01–6.78) and 2.62 (95% CI: 1.12–6.13), respectively. For patients with comorbidity scores 1, ≥2 at stage II, the HR of risk of mortality was 3.26 (95% CI: 1.20–8.84). The E-values for patients with comorbidity scores 1, ≥2 at stages 0 and I and comorbidity score ≥2 at stage II were 4.66, 4.68, and 5.97, respectively. We found in this study that the advanced stage of melanoma patients with more comorbidities was significantly associated with the higher risk of mortality rate.

DISCUSSION

In this nationwide registry-based cohort study, we included 476 men and women diagnosed with melanoma. According to tumor stage, 52 (10.9%) *in situ*, 398 (83.6%) had a localized tumor, 8 (1.7%) had regional metastases, 18 (3.8%) had distant metastases, and 364 (55.5%) suffered from one or more comorbidities (**Table 1**). Our study unraveled an association between a higher prevalence of comorbidities and a higher risk of death. The more comorbidity, the higher the risk of mortality. Comorbidity commonly is associated with poorer survival. Old age was associated with a significantly increased risk of death. In our study, patients greater than and equal to 70 years of age (HR = 18.64, 95% CI: 10.96–31.72) had a worse risk of death than patients 55–69 years of age (**Table 2**). There was an association between older age and more advanced tumors at diagnosis, leading to higher mortality among elderly people (34, 35). In Taiwan, malignant melanoma is an uncommon but fatal disease. One possible reason for low survival was that farmers delayed the diagnosis to old age. The comorbidities, or neglecting consciousness of melanoma, adverse effects of their treatment, or disguising the symptoms of the disease by the patient or doctor could be another possibility for late detection in people with comorbid conditions (36).

Gonzalez et al. (24) demonstrated that having comorbidity and cancer (colorectal, melanoma, breast, prostate) has resulted in late diagnosis of cancer. A previous study from Grann et al. (20) showed that comorbidity initiated a higher risk of complications and worse functional status, decreased quality of life, and poorer survival—especially in older patients. Houterman et al. (37) reported that increased levels of severe comorbidity led to less aggressive treatment that negatively influenced the survival of elderly patients aged 60–79 years. Comorbidities could worsen comorbid diseases and lower the functional status of metastatic melanoma patients receiving curative treatment (20). Research from Taiwan reported that a worse prognosis with great differences was mostly found in histologic subtypes, advanced stages, and acral lentiginous melanoma. Melanoma patients had a poorer prognosis when they were diagnosed with more advanced stage (26). Some studies suggested that coexistent disease was associated with

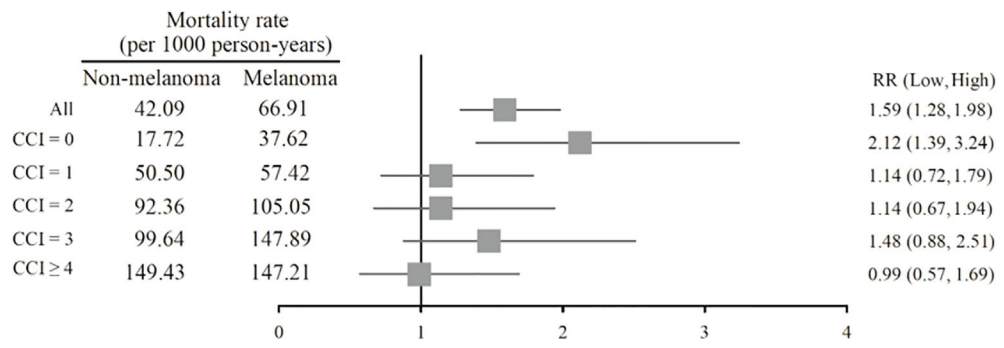

FIGURE 3 | Forest plot of mortality rate according to CCI subgroups.

TABLE 2 | Cox proportional hazards model analysis for risk of death.

	Univariate		Multivariate†	
	HR (95% CI)	**p value**	**HR (95% CI)**	**p value**
Group				
Non-melanoma	Reference		Reference	
Melanoma	1.58 (1.27–1.97)	<0.0001	1.46 (1.17–1.82)	<0.001
Age				
≤54	Reference		Reference	
55–69	2.67 (1.49–4.77)	0.001	2.21 (1.23–3.96)	0.008
≥70	18.64 (10.96–31.72)	<0.0001	11.76 (6.84–20.24)	<0.0001
Sex				
Female	Reference		Reference	
Male	1.15 (0.99–1.33)	0.078	1.10 (0.94–1.28)	0.246
Monthly income (NT$)				
<20,000	Reference		Reference	
20,001–40,000	0.90 (0.77–1.05)	0.186	1.09 (0.86–1.39)	0.473
>40,000	0.58 (0.46–0.74)	<0.0001	1.11 (0.88–1.42)	0.380
Residential region				
Northern	Reference		Reference	
Central	1.26 (1.04–1.51)	0.016	1.07 (0.88–1.30)	0.503
Southern	1.19 (0.99–1.43)	0.061	1.07 (0.89–1.29)	0.487
Others	0.90 (0.67–1.20)	0.471	0.81 (0.60–1.09)	0.158
Hypertension	2.22 (1.91–2.58)	<0.0001	1.09 (0.93–1.28)	0.304
Hyperlipidemia	0.66 (0.54–0.82)	<0.001	0.43 (0.35–0.54)	<0.0001
Charlson comorbidity index score				
0	Reference		Reference	
1	2.65 (2.15–3.26)	<0.0001	1.99 (1.61–2.47)	<0.0001
2	4.88 (3.92–6.09)	<0.0001	3.13 (2.49–3.93)	<0.0001
3	5.48 (4.26–7.04)	<0.0001	3.36 (2.59–4.35)	<0.0001
≥4	7.77 (6.19–9.75)	<0.0001	4.77 (3.75–6.06)	<0.0001

†*Adjusted for age, sex, hypertension, hyperlipidemia, monthly income, residential region, and Charlson comorbidity index score.*

worse survival and increased the possibility of being diagnosed with distant metastasis (8, 23, 38–43). Our study revealed the association between comorbidity and stage that may influence the prognosis of melanoma patients in Taiwan. **Table 4** showed that for people with comorbidity scores 3 and ≥4, HR of the risk of mortality was relatively higher than scores 1 and 2. The risk of mortality for patients with comorbidity score ≥2 at stages 0, I was a little higher than those with comorbidity score 1. The risk of mortality for patients with comorbidity score ≥2 at stage II was significantly higher than those with comorbidity score 1. Though the risk of mortality for patients with comorbidity score ≥2 at stages III, IV was lower than those with comorbidity score 1, no major differences were found because of too small a patient population.

Comorbidity might reduce survival because curative treatment is used less frequently in older patients. Consequently, survival of patients older than 70 years was not significantly influenced by comorbidity (44). Bradley et al. (45) reported that men with more comorbid conditions were less likely to receive treatment than those without comorbidities. The decision to receive treatment was determined mainly by the patient's age, disease stage, tumor characteristics, and experience of the urologist (44, 46). Fowler et al. (47) revealed that associations between age and comorbidity were highly significant ($p < 0.0001$), as the age-adjusted risk of comorbid death was 5.7 times greater in men with severe compared to those without comorbidities. Two previous studies showed that less aggressive treatment for melanoma among patients with comorbidity may affect the mortality rate because of some of the interactions between melanoma and comorbidity. Decreased function of the immune system in older patients with more comorbidities may result in higher mortality because of the interaction between comorbidity and melanoma (48, 49). Koppie et al. (50) also reported that the conditions required for treatment, such as a history of comorbidities, age, performance status, and other related factors, are important for melanoma patients when they plan to receive necessary treatment. Generally, elderly patients with more comorbidities are less likely to receive the most aggressive chemotherapy combinations for avoiding a high risk of significant morbidity (50).

The minority of melanoma patients (44.5%) had none of the selected comorbidities since their melanoma was diagnosed. In the remaining 55.5% of the melanoma cohort with some prevalent comorbidity, the most common comorbid diseases were diabetes without chronic complication, chronic pulmonary disease, peptic ulcer disease, and cerebrovascular (**Table 1**). Among melanoma and non-melanoma groups, the proportion diagnosed with severe comorbidity increased with an increasing mortality rate, and the level of comorbidity was strongly associated with mortality (**Figure 3**).

However, the weight of the association differs by specific comorbid disease, patient age, cancer characteristics, and overall comorbidity burden (23, 34, 35). Comorbidity can be measured by counting the number of coexisting illnesses diagnosed in a cancer patient or by using a comorbidity index that integrates the

TABLE 3 | Subgroup analysis of risk of death between melanoma and non-melanoma group.

	Non-melanoma		Melanoma		HR† (95% CI)	p value
	N	No. of death	N	No. of death		
Age						
≤54	710	7	71	7	13.08 (4.41–38.77)	<0.0001
55–69	1,430	47	143	14	2.85 (1.55–5.23)	<0.001
≥70	2,620	571	262	72	1.33 (1.04–1.70)	0.024
					p for interaction	<0.0001
Sex						
Female	2,060	235	206	39	1.63 (1.16–2.29)	0.005
Male	2,700	390	270	54	1.50 (1.13–2.00)	0.006
					p for interaction =	0.6331
Monthly income (NT$)						
<20,000	1,527	231	144	34	1.76 (1.22–2.54)	0.003
20,001–40,000	2,349	320	235	44	1.33 (0.97–1.83)	0.078
>40,000	884	74	97	15	1.93 (1.09–3.42)	0.024
					p for interaction =	0.3457
Residential region						
Northern	1,989	236	242	42	1.55 (1.12–2.16)	0.009
Central	1,116	172	87	17	1.29 (0.78–2.13)	0.322
Southern	1,212	171	111	27	1.82 (1.20–2.74)	0.005
Others	443	46	36	7	1.37 (0.61–3.09)	0.447
					p for interaction =	0.775
Charlson comorbidity index score						
0	2,663	158	212	25	2.40 (1.56–3.68)	<0.0001
1	1,024	156	126	21	1.22 (0.77–1.93)	0.394
2	478	124	54	15	1.01 (0.58–1.76)	0.977
3	280	75	45	17	1.67 (0.98–2.86)	0.060
≥4	315	112	39	15	1.20 (0.70–2.08)	0.509
					p for interaction =	0.0799
Charlson comorbidity index score						
0	2,663	158	212	25	2.40 (1.56–3.68)	<0.0001
1	1,024	156	126	21	1.22 (0.77–1.93)	0.394
≥2	1,073	311	138	47	1.25 (0.92–1.71)	0.152
					p for interaction =	0.029

†*Adjusted for age, sex, monthly income, residential region, hypertension, and hyperlipidemia.*

TABLE 4 | Cox proportional hazards model analysis for risk of mortality in melanoma patients.

	N	Numbers of death	HR† (95% CI)	p value
Charlson comorbidity index score				
0	212	25	Reference	
1	126	21	1.24 (0.69–2.23)	0.475
2	54	15	1.58 (0.81–3.11)	0.184
3	45	17	2.79 (1.46–5.30)	0.002
≥4	39	15	2.75 (1.39–5.44)	0.004
Stage 0, I				
Charlson comorbidity index score				
0	155	8	Reference	
1	88	11	2.61 (1.01–6.78)	0.048
≥2	101	23	2.62 (1.12–6.13)	0.026
Stage II				
Charlson comorbidity index score				
0	45	12	Reference	
1	NA	NA	0.44 (0.14–1.33)	0.144
≥2	NA	NA	3.26 (1.20–8.84)	0.020
Stage III, IV				
Charlson comorbidity index score				
0	12	5	Reference	
1	NA	NA	3.86 (0.59–25.22)	0.158
≥2	NA	NA	5.17 (0.69–38.92)	0.110

†*Adjusted for age, sex, monthly income, residential region, hypertension, and hyperlipidemia.*
NA, not available.

number and severity of the comorbidity (51). Nowadays, the CCI is the most commonly applied index for comorbidities in cancer patients. The CCI score is the sum of weights of a patient's coexisting conditions based on 19 disease categories. The weights originated from relative risk assessment acquired from a regression model. They are usually assigned from 1 to 6 points and then collapsed into categories of 0 point, 1 to 2 points, 3 to 4 points, and 5 or more points, respectively. The CCI has been previously verified as a prognostic method of comorbidity for some index cancers (31).

A study previously showed that both the survival and treatment of patients were affected by age and the extent of comorbidity. Racial differences in survival were greatest for patients without comorbidities and less pronounced at higher levels of comorbidity. Comorbidity elicited differential impact for prognosis, treatment, and survival (52). However, the outcomes of this study by using the CCI score were similar with many reports in Western countries (24, 39). Comorbidities that influence prognosis seriously may differ between Eastern and Western countries. We expect that future research can focus on which of these comorbidities may most seriously affect the prognosis of melanoma patients.

There is a limitation in this study. From Taiwan's NHIRD, we selected random samples of 2 million from 23 million beneficiaries. Because melanoma is an unusual illness in Taiwan, the sample size of melanoma patients was relatively small in our research. However, NHIRD is a randomly selected representative sample of Taiwan's general population. This may avoid sampling deviation or selection bias and provide more nationwide information in this study.

In conclusion, melanoma patients in Taiwan with comorbidity were associated with poorer survival. The level of comorbidity was robustly associated with the mortality rate. The presence of severe comorbidity was associated with an advanced stage of melanoma. The mortality rate was higher among patients with more comorbidities, and the influence of comorbidity varied by stage. Old age was associated with a significantly increased risk of death. A higher risk of mortality was found in patients who had localized tumors, regional metastases, or distant metastases with more comorbidity scores. Our study demonstrated that comorbidity and stage had an impact on the prognosis of Taiwan melanoma patients.

DATA AVAILABILITY STATEMENT

The data in this study we used were from the National Health Insurance Research Database and Taiwan Cancer Registry.

AUTHOR CONTRIBUTIONS

All authors listed have contributed to the work and approved its publication. Contributors: All other authors (YSH, PNC, SCC, JYH, YHW and JCCW) provided their input by contributing to the conceptualization. CKC contributed to the editing of the article.

ACKNOWLEDGMENTS

I would like to express my thanks to Professor James Cheng-Chung Wei, Professor Yih-Shou Hsieh, Professor Pei-Ni Chen, Professor Shu-Chen Chu, and Dr. Jing-Yang Huang, who all served as scientific advisers, and Yu-Hsun Wang, who collected data for this study. The authors also wish to thank all colleagues from the Department of Medical Research, Chung Shan Medical University Hospital, Taichung, Taiwan.

SUPPLEMENTARY MATERIAL

The Supplementary Material for this article can be found online at: https://www.frontiersin.org/articles/10.3389/fonc.2022.846760/full#supplementary-material

REFERENCES

1. Siegel RL, Miller KD, Jemal A. Cancer Statistics, 2019. *CA Cancer J Clin* (2019) 69:7–34. doi: 10.3322/caac.21551
2. Damsky WE, Theodosakis N, Bosenberg M. Melanoma Metastasis: New Concepts and Evolving Paradigms. *Oncogene* (2014) 33:2413–22. doi: 10.1038/onc.2013.194
3. Lo JA, Fisher DE. The Melanoma Revolution: From UV Carcinogenesis to a New Era in Therapeutics. *Science* (2014) 346:945–9. doi: 10.1126/science.1253735
4. Eggermont AM, Spatz A, Robert C. Cutaneous Melanoma. *Lancet* (2014) 383:816–27. doi: 10.1016/S0140-6736(13)60802-8
5. Erdei E, Torres SM. A New Understanding in the Epidemiology of Melanoma. *Expert Rev Anticancer Ther* (2010) 10:1811–23. doi: 10.1586/era.10.170
6. Shoo BA, Kashani-Sabet M. Melanoma Arising in African-, Asian-, Latino- and Native-American Populations. *Semin Cutan Med Surg* (2009) 28:96–102. doi: 10.1016/j.sder.2009.04.005
7. Hwang CY, Chen YJ, Lin MW, Chen TJ, Chu SY, Chen CC, et al. Elevated Risk of Second Primary Cancer in Patients With Cutaneous Malignant Melanoma: A Nationwide Cohort Study in Taiwan. *J Dermatol Sci* (2010) 60:167–72. doi: 10.1016/j.jdermsci.2010.10.004
8. Chang JW. Cutaneous Melanoma: Taiwan Experience and Literature Review. *Chang Gung Med J* (2010) 33:602–12.
9. Balch CM, Soong SJ, Gershenwald JE, Thompson JF, Coit DG, Atkins MB et al. Age as a Prognostic Factor in Patients With Localized Melanoma and Regional Metastases. *Ann Surg Oncol* (2013) 20:3961–8. doi: 10.1245/s10434-013-3100-9
10. Wu PC, Chen YC, Chen HM, Chen LW. Prognostic Factors and Population-Based Analysis of Melanoma With Sentinel Lymph Node Biopsy. *Sci Rep* (2021) 11:20524. doi: 10.1038/s41598-021-99950-1
11. Salvaggio C, Han SW, Martires K, Robinson E, Madankumar R, Gumaste P, et al. Impact of Socioeconomic Status and Ethnicity on Melanoma Presentation and Recurrence in Caucasian Patients. *Oncology* (2016) 90:79–87. doi: 10.1159/000441524
12. Clark WH Jr, Elder DE, Guerry DT, Braitman LE, Trock BJ, Schultz D, et al. Model Predicting Survival in Stage I Melanoma Based on Tumor Progression. *J Natl Cancer Inst* (1989) 81:1893–904. doi: 10.1093/jnci/81.24.1893
13. Sarac E, Amaral T, Keim U, Leiter U, Forschner A, Eigentler TK, et al. Prognostic Factors in 161 Patients With Mucosal Melanoma: A Study of

German Central Malignant Melanoma Registry. *J Eur Acad Dermatol Venereol* (2020) 34:2021–5. doi: 10.1111/jdv.16306
14. Amin MB, Greene FL, Edge SB, Compton CC, Gershenwald JE, Brookland RK, et al. The Eighth Edition AJCC Cancer Staging Manual: Continuing to Build a Bridge From a Population-Based to a More "Personalized" Approach to Cancer Staging. *CA Cancer J Clin* (2017) 67:93–9. doi: 10.3322/caac.21388
15. Bobos M. Histopathologic Classification and Prognostic Factors of Melanoma: A 2021 Update. *Ital J Dermatol Venerol* (2021) 156:300–21. doi: 10.23736/S2784-8671.21.06958-3
16. Altieri L, Eguchi M, Peng DH, Cockburn M. Predictors of Mucosal Melanoma Survival in a Population-Based Setting. *J Am Acad Dermatol* (2019) 81:136–142 e2. doi: 10.1016/j.jaad.2018.09.054
17. Feigelson HS, Powers JD, Kumar M, Carroll NM, Pathy A, Ritzwoller DP. Melanoma Incidence, Recurrence, and Mortality in an Integrated Healthcare System: A Retrospective Cohort Study. *Cancer Med* (2019) 8:4508–16. doi: 10.1002/cam4.2252
18. Cheng E, Soulos PR, Irwin ML, Cespedes Feliciano EM, Presley CJ, Fuchs CS, et al. Neighborhood and Individual Socioeconomic Disadvantage and Survival Among Patients With Nonmetastatic Common Cancers. *JAMA Netw Open* (2021) 4:e2139593. doi: 10.1001/jamanetworkopen.2021.39593
19. Syriopoulou E, Morris E, Finan PJ, Lambert PC, Rutherford MJ. Understanding the Impact of Socioeconomic Differences in Colorectal Cancer Survival: Potential Gain in Life-Years. *Br J Cancer* (2019) 120:1052–8. doi: 10.1038/s41416-019-0455-0
20. Grann AF, Froslev T, Olesen AB, Schmidt H, Lash TL. The Impact of Comorbidity and Stage on Prognosis of Danish Melanoma Patients, 1987-2009: A Registry-Based Cohort Study. *Br J Cancer* (2013) 109:265–71. doi: 10.1038/bjc.2013.246
21. Salive ME. Multimorbidity in Older Adults. *Epidemiol Rev* (2013) 35:75–83. doi: 10.1093/epirev/mxs009
22. Lee L, Cheung WY, Atkinson E, Krzyzanowska MK. Impact of Comorbidity on Chemotherapy Use and Outcomes in Solid Tumors: A Systematic Review. *J Clin Oncol* (2011) 29:106–17. doi: 10.1200/JCO.2010.31.3049
23. Gurney J, Sarfati D, Stanley J. The Impact of Patient Comorbidity on Cancer Stage at Diagnosis. *Br J Cancer* (2015) 113:1375–80. doi: 10.1038/bjc.2015.355
24. Gonzalez EC, Ferrante JM, Van Durme DJ, Pal N, Roetzheim RG. Comorbid Illness and the Early Detection of Cancer. *South Med J* (2001) 94:913–20. doi: 10.1097/00007611-200109000-00020
25. Chang WS, Yang KC, Chen BF. Malignant Melanoma Metastatic to the Stomach: Upper G-I Endoscopic Finding–Report of a Case. *Zhonghua Yi Xue Za Zhi (Taipei)* (1990) 45:280–3.
26. Chen YJ, Wu CY, Chen JT, Shen JL, Chen CC, Wang HC. Clinicopathologic Analysis of Malignant Melanoma in Taiwan. *J Am Acad Dermatol* (1999) 41:945–9. doi: 10.1016/S0190-9622(99)70251-3
27. Soong CY, Liu HN, Ger LP, Chu TL, Syu HL, Tseng HH. Malignant Melanoma: A Clinicopathologic Study of 22 Cases. *J Formos Med Assoc* (1991) 90:365–70.
28. Tai CS, Wu JF, Chen HL, Hsu HY, Chang MH, Ni YH. Modality of Treatment and Potential Outcome of Wilson Disease in Taiwan: A Population-Based Longitudinal Study. *J Formos Med Assoc* (2018) 117:421–6. doi: 10.1016/j.jfma.2017.05.008
29. Chiang CJ, Wang YW, Lee WC. Taiwan's Nationwide Cancer Registry System of 40 Years: Past, Present, and Future. *J Formos Med Assoc* (2019) 118:856–8. doi: 10.1016/j.jfma.2019.01.012
30. Chiang CJ, You SL, Chen CJ, Yang YW, Lo WC, Lai MS. Quality Assessment and Improvement of Nationwide Cancer Registration System in Taiwan: A Review. *Jpn J Clin Oncol* (2015) 45:291–6. doi: 10.1093/jjco/hyu211
31. Sundararajan V, Henderson T, Perry C, Muggivan A, Quan H, Ghali WA. New ICD-10 Version of the Charlson Comorbidity Index Predicted in-Hospital Mortality. *J Clin Epidemiol* (2004) 57:1288–94. doi: 10.1016/j.jclinepi.2004.03.012
32. Haneuse S, VanderWeele TJ, Arterburn D. Using the E-Value to Assess the Potential Effect of Unmeasured Confounding in Observational Studies. *JAMA* (2019) 321:602–3. doi: 10.1001/jama.2018.21554
33. VanderWeele TJ, Ding P. Sensitivity Analysis in Observational Research: Introducing the E-Value. *Ann Intern Med* (2017) 167:268–74. doi: 10.7326/M16-2607
34. Lasithiotakis KG, Petrakis IE, Garbe C. Cutaneous Melanoma in the Elderly: Epidemiology, Prognosis and Treatment. *Melanoma Res* (2010) 20:163–70. doi: 10.1097/CMR.0b013e328335a8dd
35. Norgaard C, Glud M, Gniadecki R. Are All Melanomas Dangerous? *Acta Derm Venereol* (2011) 91:499–503. doi: 10.2340/00015555-1177
36. Chang HY, Feng HL, Wang L, Chou P, Wang PF, Incidence T. Prevalence, and Survival of Malignant Melanoma in Taiwan. *Value Health* (2014) 17:A740. doi: 10.1016/j.jval.2014.08.135
37. Houterman S, Janssen-Heijnen ML, Hendrikx AJ, van den Berg HA, Coebergh JW. Impact of Comorbidity on Treatment and Prognosis of Prostate Cancer Patients: A Population-Based Study. *Crit Rev Oncol Hematol* (2006) 58:60–7. doi: 10.1016/j.critrevonc.2005.08.003
38. Louwman WJ, Janssen-Heijnen ML, Houterman S, Voogd AC, van der Sangen MJ, Nieuwenhuijzen GA, et al. Less Extensive Treatment and Inferior Prognosis for Breast Cancer Patient With Comorbidity: A Population-Based Study. *Eur J Cancer* (2005) 41:779–85. doi: 10.1016/j.ejca.2004.12.025
39. Cronin-Fenton DP, Norgaard M, Jacobsen J, Garne JP, Ewertz M, Lash TL, et al. Comorbidity and Survival of Danish Breast Cancer Patients From 1995 to 2005. *Br J Cancer* (2007) 96:1462–8. doi: 10.1038/sj.bjc.6603717
40. Land LH, Dalton SO, Jorgensen TL, Ewertz M. Comorbidity and Survival After Early Breast Cancer. A Review. *Crit Rev Oncol Hematol* (2012) 81:196–205. doi: 10.1016/j.critrevonc.2011.03.001
41. Land LH, Dalton SO, Jensen MB, Ewertz M. Impact of Comorbidity on Mortality: A Cohort Study of 62,591 Danish Women Diagnosed With Early Breast Cancer, 1990-2008. *Breast Cancer Res Treat* (2012) 131:1013–20. doi: 10.1007/s10549-011-1819-1
42. Tetsche MS, Dethlefsen C, Pedersen L, Sorensen HT, Norgaard M. The Impact of Comorbidity and Stage on Ovarian Cancer Mortality: A Nationwide Danish Cohort Study. *BMC Cancer* (2008) 8:31. doi: 10.1186/1471-2407-8-31
43. Jiao YS, Gong TT, Wang YL, Wu QJ. Comorbidity and Survival Among Women With Ovarian Cancer: Evidence From Prospective Studies. *Sci Rep* (2015) 5:11720. doi: 10.1038/srep11720
44. Post PN, Hansen BE, Kil PJ, Janssen-Heijnen ML, Coebergh JW. The Independent Prognostic Value of Comorbidity Among Men Aged < 75 Years With Localized Prostate Cancer: A Population-Based Study. *BJU Int* (2001) 87:821–6. doi: 10.1046/j.1464-410x.2001.02189.x
45. Bradley CJ, Dahman B, Anscher M. Prostate Cancer Treatment and Survival: Evidence for Men With Prevalent Comorbid Conditions. *Med Care* (2014) 52:482–9. doi: 10.1097/MLR.0000000000000113
46. Post PN, Kil PJ, Hendrikx AJ, Janssen-Heijnen ML, Crommelin MA, Coebergh JW. Comorbidity in Patients With Prostate Cancer and Its Relevance to Treatment Choice. *BJU Int* (1999) 84:652–6. doi: 10.1046/j.1464-410x.1999.00279.x
47. Fowler JE Jr, Terrell FL, Renfroe DL. Co-Morbidities and Survival of Men With Localized Prostate Cancer Treated With Surgery or Radiation Therapy. *J Urol* (1996) 156:1714–8. doi: 10.1016/S0022-5347(01)65489-2
48. Weinberger B, Herndler-Brandstetter D, Schwanninger A, Weiskopf D, Grubeck-Loebenstein B. Biology of Immune Responses to Vaccines in Elderly Persons. *Clin Infect Dis* (2008) 46:1078–84. doi: 10.1086/529197
49. Mazzola P, Radhi S, Mirandola L, Annoni G, Jenkins M, Cobos E, et al. Aging, Cancer, and Cancer Vaccines. *Immun Ageing* (2012) 9:4. doi: 10.1186/1742-4933-9-4
50. Koppie TM, Serio AM, Vickers AJ, Vora K, Dalbagni G, Donat SM, et al. Age-Adjusted Charlson Comorbidity Score Is Associated With Treatment Decisions and Clinical Outcomes for Patients Undergoing Radical Cystectomy for Bladder Cancer. *Cancer* (2008) 112:2384–92. doi: 10.1002/cncr.23462
51. Sogaard M, Thomsen RW, Bossen KS, Sorensen HT, Norgaard M. The Impact of Comorbidity on Cancer Survival: A Review. *Clin Epidemiol* (2013) 5:3–29. doi: 10.2147/CLEP.S47150
52. Bebe FN, Hu S, Brown TL, Tulp OL. Role, Extent, and Impact of Comorbidity on Prognosis and Survival in Advanced Metastatic Melanoma: A Review. *J Clin Aesthet Dermatol* (2019) 12:16–23.

Conflict of Interest: The authors declare that the research was conducted in the absence of any commercial or financial relationships that could be construed as a potential conflict of interest.

this article, or claim that may be made by its manufacturer, is not guaranteed or endorsed by the publisher.

frontiers in Oncology

MINI REVIEW
published: 10 March 2022
doi: 10.3389/fonc.2022.866733

Ozone Layer Depletion and Emerging Public Health Concerns - An Update on Epidemiological Perspective of the Ambivalent Effects of Ultraviolet Radiation Exposure

Sheikh Ahmad Umar[1,2] *and Sheikh Abdullah Tasduq*[1,2]*

[1] Department of Biological Sciences, Academy of Scientific and Innovative Research (AcSIR), Ghaziabad, India,
[2] Pharmacokinetics-Pharmacodynamics (PK-PD) and Toxicology Division, Council of Scientific and Industrial Research-Indian (CSIR) Institute of Integrative Medicine, Jammu, India

OPEN ACCESS

Edited by:
Nabiha Yusuf,
University of Alabama at Birmingham,
United States

Reviewed by:
Mohammad Asif Sherwani,
University of Alabama at Birmingham,
United States
Hamidullah Khan,
University of Wisconsin-Madison,
United States

***Correspondence:**
Sheikh Abdullah Tasduq
stabdullah@iiim.res.in;
tasduq11@gmail.com

Specialty section:
This article was submitted to Skin Cancer, a section of the journal Frontiers in Oncology

Received: 31 January 2022
Accepted: 17 February 2022
Published: 10 March 2022

Citation:
Umar SA and Tasduq SA (2022) Ozone Layer Depletion and Emerging Public Health Concerns - An Update on Epidemiological Perspective of the Ambivalent Effects of Ultraviolet Radiation Exposure. Front. Oncol. 12:866733. doi: 10.3389/fonc.2022.866733

Solar ultraviolet (UV) radiation exposure is the primary etiological agent responsible for developing cutaneous malignancies. Avoiding excessive radiation exposure, especially by high-risk groups, is recommended to prevent UV-induced photo-pathologies. However, optimal sun exposure is essential for the healthy synthesis of about 90% of vitamin D levels in the body. Insufficient exposure to UV-B is linked to vitamin D deficiency in humans. Therefore, optimal sun exposure is necessary for maintaining a normal state of homeostasis in the skin. Humans worldwide face a major existential threat because of climate change which has already shown its effects in several ways. Over the last 4 to 5 decades, increased incidences in skin cancer cases have led international health organizations to develop strong sun protection measures. However, at the same time, a growing concern about vitamin D deficiency is creating a kind of exposure dilemma. Current knowledge of UV exposure to skin outweighs the adverse effects than the beneficial roles it offers to the body, necessitating a correct public health recommendation on optimal sun exposure. Following an appropriate recommendation on optimal sun exposure will lead to positive outcomes in protecting humans against the adverse effects of strict recommendations on sun protection measures. In this short review, we spotlight the ambivalent health effects of UV exposure and how ozone layer depletion has influenced these effects of UVR. Further, our aim remains to explore how to lead towards a balanced recommendation on sun protection measures to prevent the spurt of diseases due to inadequate exposure to UV-B.

Keywords: ultraviolet radiation (UV), skin photodamage, ozone layer depletion, vitamin D deficiency, sun protection measures, food fortification

INTRODUCTION

Ultraviolet radiation, the main component of sunlight, is divided into three categories, UV-A, UV-B and UV-C based on the wavelength and energy status (1, 2). UV-B has high energy and potential than UV-A to cause the biological damage (3). In contrast, UV-C is retained by the ozone layer and never reaches the lower atmosphere (4). The average UV dose across the globe varies with geographical location and on daily to seasonal timescales. The total ozone is generally lowest at the equator and highest in mid-latitude and Polar regions. This way, the global distributional pattern of UV index varies with the latitude, altitude, cloud cover and haze and is further complicated amid the ozone layer depletion scenario. Therefore, no definite UV dose can be attributed to a particular region across the globe (3). However, substantial UV index changes have happened over the last few decades due to ozone layer depletion that has significantly increased the global burden of skin cancer incidences. The recovery of the ozone layer will depend on how countries abide by the Montreal Protocol treaty terms by the participating countries in times to come and if they take the treaty terms very seriously (5). The impact of future climate change on the ozone layer will vary between the tropics, mid-latitudes and Polar regions and strongly depends on future emissions of ozone-depleting substances. During the long recovery period, volcanic eruptions could temporarily reduce the global ozone levels for several years. Together, these all things will be playing pivotal roles in controlling the global UV changes and the after-effects that ozone layer depletion can have on the different life forms across the globe (6–10).

Likely, fair-skinned individuals are at the highest risk of developing the UV mediated photodamage responses differentially varying with different skin types (11). Yet, most skin types are prone to sun damage with ever-increasing exposure to UV radiation (12). UV radiation not only affects humans but the animal, plant and marine life is also significantly impacted (13). There is a growing concern that ozone layer depletion may lead to the loss of many threatened plant species and disrupt the global food security (14). However, plants have built the ability to respond and adapt to high UV levels; they can be affected directly due to high UV radiations (15), affecting most plant species' survival (16). The adverse effects of ozone depletion on marine ecosystems can be many, including reducing the population of tiny marine organisms due to small increases in UV, significantly disrupting the marine ecosystem (17). An increase in UV-B radiations reaching the earth's surface may also disrupt and change the natural pattern of biogeochemical cycles and contribute to biosphere-atmosphere feedback, which could have even more deleterious effects on different life forms (18). Although the risks of UV radiation overexposure are known and many **(Table 1),** the general public have been made to think about the ill effects of UV and not to weigh the merits of UV radiation exposure being essentially crucial for Vitamin D synthesis. The production of 10μg (400 IU) of vitamin D per day takes approximately 1/3 of the time needed to reach the Minimal Erythemal Dose (MED) for an effective skin area of 600cm^2 for skin phototype III. It indicates that UV exposure has strict bodily requirements to synthesize these required amounts of Vitamin D for proper bone formation and function (19). The optimal UV dose for vitamin D production varies significantly depending on the physiological and pathological condition of every individual. The best assessment of these personal attributes can allow people to find their unique "Goldilock" zones of exposure time. This mini-review highlights the ambivalent biological effects of UVR and how these effects can further modulate if the overhead ozone cover continues to change negatively in the future. It further highlights how to lead towards a suitable public health recommendation on optimal sun exposure amid the climate change triggered ozone layer depletion.

HEALTH PROMOTING EFFECTS OF ULTRAVIOLET RADIATION EXPOSURE TO SKIN

Despite the numerous health concerns that UV radiation exposure comes with. It has several health promoting advantages that make sun exposure a kind of necessary evil having ambivalent effects to human body. Some of the prominent health promoting effects of UV exposure is summarized below.

UV Induced Melanogenesis Acts as a Natural Sunscreen

Melanin is a coloring pigment that is synthesized by the melanocytes in skin and its synthesis is promoted during sunlight exposure due to its UV portion. This is the same pigment that is responsible for giving colour to skin. It is also involved in primary natural defenses against UV-induced DNA damage (20). Special cells synthesize melanosomes under the skin, which produce, store and transport melanin and are absorbed by skin keratinocytes forming a protective, UV-blocking shell around the cells' nuclei. In the cytosol of keratinocytes, melanosomes form a critical shield of DNA by forming perinuclear caps exhibiting photoprotection (21). These responses against UV depend on different parameters including the production, distribution, quantity and type of melanin synthesized in melanocytes and the content transferred to keratinocytes (22). The photoprotective effect of melanin is achieved in part by acting as a physical barrier and as an absorbent filter that reduces the penetration of UV through the epidermis (23). Some persons however, suffering from diseases albinism and vitiligo have a faulty melanin production and are highly susceptible to the effects of UV exposure (24). Epidemiological data strongly suggest and support the protective role of melanin in skin against the UV exposure induced cellular damage as there exists an inverse correlation between skin pigmentation and the incidence of sun-induced skin cancers. Research has suggested that subjects with White skin including albino's, are more likely to develop skin cancer by about 70 times than subjects with Black skin (25). Other important properties of melanin, especially eumelanin are its

TABLE 1 | Classification of skin types/skin color types and burns/tans in the skin after sun exposure.

S.No	Exposure category	UVI range	Skin Type classification	Burns/Tans after sun exposure	Diseases due to inadequate UVR exposure/ vitamin D levels in body	Diseases due to excessive UVR exposure
01	Low	<2	VI • Naturally black skin • High Eumelanin and low Phaeomelanin • Melano- protected	• No • No	**Cancers:** • Prostate • Breast cancer • Colorectal cancer • Ovary cancer • Non-Hodgkin lymphoma **Autoimmune diseases:** • Multiple sclerosis • Type 1 diabetes • Rheumatoid arthritis **Psychiatric disorders:** • Seasonal affective disorder • Mood disorders • Schizophrenia • **Insufficient vitamin D levels** • Rickets • Osteomalacia • Osteoporosis	**Effects on the skin** **Acute** • Sunburn • Photodermatoses **Chronic** • Cutaneous malignant melanoma • Cancer of the lip • Basal cell carcinoma • Squamous cell carcinoma • Chronic sun damage/solar keratoses **Effects on the Eyes** **Acute** • Acute photokeratitis and conjunctivitis • Acute solar retinopathy **Chronic** • Climatic droplet keratopathy • Pterygium • Pinguecula • Squamous cell carcinoma of the cornea • conjunctiva • Cataract • Ocular melanoma • Macular degeneration **Other effects** • Suppression of cell-mediated immunity • Increased susceptibility to infection • Impairment of prophylactic immunization **Indirect effects** • Effect on climate, food supply, disease vectors, atmospheric chemistry
02	Moderate	2-5	V • Naturally brown skin • High Eumelanin and low Phaeomelanin) • Melano- protected	• Negligible • Negligible		
03	High	6-7	IV • Light skin • High phaeomelanin and low eumelanin • Melano- competent	• Sometimes seldom • Always usually		
04	Very High	8-10	III • Light skin and Freckles • High phaeomelanin and low eumelanin) • Melano- competent	• Sometimes seldom • Always usually		
05	Extreme	11+	II I • Pale • None or very little eumelanin or phaeomelanin (albinism) • Melano-compromised	• Always usually • Sometimes seldom		

UV radiation exposure categories, UV index range and diseases due to inadequate/excessive exposure to UVR.

functions acting as a free radical scavenger and superoxide dismutase that reduce oxidative stress in skin cells (26).

UV Phototherapy in Treatment of Numerous Cutaneous Disorders

UV light-based phototherapy is the most frequently used method and has a long, successful history in the management of numerous cutaneous disorders. UV-based phototherapy works by regulating the inflammatory component and inducing apoptosis of pathogenic cells, quickly transforming the microenvironment of UV-exposed skin (27). Phototherapy effects include proapoptotic, anti-fibrotic, pro-pigmentary, immunomodulatory, anti-pruritic and pro-prebiotic that promotes clinical prognosis and outcomes in various skin diseases such as psoriasis, atopic dermatitis, vitiligo, scleroderma, and cutaneous T-cell lymphoma (CTCL) (28). This therapy works by reacting with many elements essentially, chromospheres, metabolic byproducts, innate immune receptors, neurotransmitters and mediators such as chemokines, antimicrobial peptides, and platelet activating factor (PAF) that simultaneously shape the immunomodulatory effects of UV and their interplay with the microbiota of the skin. Most of the positive effects of solar radiation are mediated *via* ultraviolet-B (UVB) induced production of vitamin D in skin.

Psoriasis

UVB phototherapy is used in the treatment of psoriasis, which is an inflammatory skin disease, characterized by keratinocyte hyper proliferation. Even though UVB phototherapy is a standard treatment for psoriasis, however, the underlying molecular mechanisms of its efficacy are not completely understood. It is speculated that the therapeutic effectiveness of phototherapy is mainly due to its antiproliferative properties (29).

Vitiligo

Vitiligo is a de-pigmentation skin disorder and appears to be a combination of genetic effects in both the immune system and in the melanocytes, resulting in melanocyte destruction (30). Multiple treatments are recommended in the treatment of vitiligo, especially phototherapy with narrowband UVB radiation

and excimer laser (308 nm) with/without the topical application of calcineurin antagonists (31). Role of phototherapy in treating vitiligo is supported by the fact that sun-exposed lesions tend to show follicular repigmentation during the summer months in many patients and the effect is transient but repeatable (32). The protective effect of phototherapy in patients with vitiligo is not completely elucidated. It is thought that re-pigmentation after phototherapy may be due to activation, proliferation, and migration of these affected melanocytes to the epidermis, where they form perifollicular pigmentation islands. Furthermore, UV light works as an immunosuppressant in skin that may also be playing a role in initiating re-pigmentation in melanocytes (33).

Atopic Dermatitis

UV light-based phototherapy is also used in the treatment of Atopic dermatitis which is a chronic inflammatory skin disease. Narrowband UVB und UVA-1 is the frequently used treatment setting in atopic dermatitis and in other T cell mediated inflammatory skin diseases. UV light exposure has direct phototoxic effects on T-lymphocytes causing gradual reduction of the inflammatory infiltrate and a concomitant improvement of patients' skin affected with Atopic dermatitis (34).

Multiple Sclerosis

UV-B phototherapy is also used in the treatment of Multiple Sclerosis and has been found to prevent multiple sclerosis like symptoms in a mouse model regardless of the presence of vitamin D or the vitamin D receptor (35). People who are exposed to medium-to-high levels of ultraviolet-B radiation have a lower risk of developing Multiple Sclerosis. Given that UV-B exposure triggers the synthesis of vitamin D in the skin, many researchers have linked MS to a lack of vitamin D due to low sunlight exposure. However, researchers using a mouse model for MS have showed that exposure to UV-B prevent MS-like symptoms without increasing the vitamin D levels challenging a direct link between vitamin D and MS (36).

UV Exposure Induced Nitric Oxide (NO) Reduces Blood Pressure and Mitigates Cardiovascular Disorders

Nitric oxide (NO) is a gaseous lipophilic free radical cellular messenger and plays an important role in the protection against cardiovascular diseases. Research has suggested that reduced bioavailability of NO is one of the central and critical factors common to cardiovascular diseases, although it is unclear whether this is a cause or results due to endothelial dysfunction (37). Low concentrations of $NO^{\bullet}$ has been found to protect cultured keratinocytes from oxidative stress and apoptosis. However, the underlying mechanisms are still unknown. A study demonstrated that UVA –irradiation to healthy individuals lead to a sustained reduction in blood pressure and these effects may be mediated by mechanisms that are independent of vitamin D and exposure to UV alone, but through UVA-induced $NO^{\bullet}$ and nitrite (32). NO_2^- is not only known dilating the blood vessels, but also protect organs against ischemia/reperfusion damage and can be externally delivered to the systemic circulation to exert coronary vasodilator, cardio protective as well as antihypertensive effects. It is also proposed that UVA-induced $NO^{\bullet}$ have antimicrobial effects and is involved in cutaneous wound healing and has antitumor activity as well (38). However, despite its numerous health benefits, $NO^{\bullet}$ has with it toxic effects and that is why it is also known as a Janus molecule. UV exposure-produced $NO^{\bullet}$ can promote many local and systemic UV-induced responses including erythema, edema, inflammation, premature aging and immunosuppression. However, its role in the development and progression of skin cancer remains unclear.

UV Exposure Improves Mood

Sun exposure in non-erythemic doses is considered as a pleasant one. Exposure to sunlight has been linked to improved energy and elevates the mood (39). People feeling better and relaxed after tanning partly support this phenomenon. UV radiation leads to production of an opioid β-endorphin *via* stimulation of the POMC promoter (Pro-opiomelanocortin) in keratinocytes and when released into the bloodstream may reach the brain in sufficient concentrations to elevate mood (32). However, only few studies have demonstrated the mood improving roles of increased β-endorphin levels in blood in healthy volunteers. Furthermore, both sunlight and darkness are involved in triggering the release of hormones in brain. Exposure to sunlight increases the release of serotonin from the brain, associated with boosting mood and helps a person feel calm. However, at night, dark light triggers the synthesis of melatonin in brain, responsible for sleep. Inadequate exposure to sun light can cause dip in the levels of serotonin associated with a risk of major depression with seasonal pattern (formerly seasonal affective disorder). This is a form of depression triggered by the changing seasons (40). Additionally, sunbathing or tanning beds have a potential to reduce pain in patients with fibromyalgia. A study has reported that patients experienced a greater short-term decrease in chronic pain after exposure to UV compared with non-UV radiation exposure (32).

IMPACT OF OZONE LAYER DEPLETION ON THE EFFECTS OF UV EXPOSURE

Disruption in the Evolutionarily Mediated Adaptation of Life Forms to Atmospheric UVR Changes

Living organisms have significantly evolved with time as the atmosphere they habituate changes continuously. The development of skin pigmentation responses in humans are likely due to selection pressures related to ambient ultraviolet radiation exposure. It has significantly influenced the migration of people from areas of high UVR index to regions of low UVR (41). Variation in the global distributional pattern of ultraviolet radiation poses diverse and differential effects based on latitude and altitude. There is always a debate going on among the researchers weighing out the adverse effects of UV exposure, despite the several benefits to different life forms, including

humans, animals and vegetation. Ultraviolet radiation exposure requirements promoting healthy vitamin D synthesis in skin meant that people developed darker skin pigmentation at places of low latitude with high ambient UVR intensity, offering them protection from the effects of UVR. In contrast, those at higher latitudes have fairer skin as an evolutionarily developed trait to potentiate the vitamin D production from low ambient exposure (42). This contrasting requirement of latitudinal orientation set by humans throughout evolution for the healthy synthesis of vitamin D levels have changed as people adopted multiple sun protection measures and avoided sunlight exposure in pursuit of escaping the sun damage. These factors challenged the natural setup system and have adversely manifested into the development of various related skin and skeleton pathologies that requires regular ambient doses of radiation to function normally (43). In the last several decades, intensive human migration has interfered with the natural skin pigmentation patterns suited to the environment humans are born, grow, and evolve. The migration of people who are dark-skinned to areas of high latitude increases their chances of developing rickets and osteomalacia later in their life due to unhealthy/sub-optimal vitamin D synthesis (44). Fair-skinned populations at the other end are experiencing a steep rise in the number of melanoma and non-melanoma skin cancers migrating to low latitude areas from their natural habitats. Additionally, lifestyle changes combined with behavioural and cultural changes meant that humans were exposed to UV radiation than ever before, further compounding the problems the body responds to these changes (45). Increased incidences in skin cancer-related cases, cataracts, particularly in high-risk cataract belts of the world, improper vitamin D levels, skeletal and other cardiovascular diseases in the last 4-5 decades have gained considerable attention of the world scientific community on how to curb this sharp rise associated with the inappropriate exposure to sunlight. It has also led to a search for a viable solution based on one health approach, in addition to strict sun protection measures and vitamin D complementation from external sources (46).

OZONE LAYER DEPLETION AND GLOBAL BURDEN OF INCREASE IN THE UV EXPOSURE MEDIATED DISEASE INCIDENCES

The ozone layer acts as a natural filter, absorbing most of the sun's ultraviolet rays coming towards the earth's atmosphere. Changes to the ozone layer starting in the latter part of the 20th century led to an increase in the proportion of UV-B radiations reaching the earth's surface. It potentially disrupts the biological life and processes, including damaging several non-life entities, including polymer-based materials, such as thermoplastics, thermosets and composites used as replacements for traditional building materials, through a phenomenon known as chalking (10, 47). Ozone layer depletion resulted from rapid industrialization, high consumption of chlorofluorocarbons (CFCs) and halons, and global warming have further worsened the problem towards more destruction (48). This loss of ozone is associated with increased levels of radiation reaching the earth's surface. Still, lower atmospheric pollution makes it difficult to assess changes in UVR patterns using ground-based measurements. Further, there are mainly three ways climate changes and their after-effects have shown their adverse effects on different life forms; stratospheric ozone depletion, increase in surface temperature due to global warming, and air pollution. Research suggests that globally and especially among the fair-skinned populations, melanoma rates are increasing by 4% to 5% annually. Further, increased temperatures/heat also has an impact on carcinogenesis. Past research has shown that non-melanoma skin cancer risk increases for every one-degree rise of temperature, suggesting that as the planet continues to warm, there's the possibility that rising temperatures could further drive and amplify the induction of skin cancer cases due to UV radiation over exposure (49). Although this temporal trend in the increased incidence of non-melanoma skin cancers is difficult to determine, the increase is not simply a result of increased epidemiological surveillance and detection. Specific studies carried out in Australia, Canada and the US indicate that between the 1960-1980s, the prevalence of non-melanoma skin cancers increased by a factor of more than two when examined concerning personal UV exposure. It indicates a positive correlation between climate change mediated high UV exposure to increased skin cancer cases. The increase in skin cancers is most frequent in some parts of the body commonly exposed to the sun, such as the face and hands, implying that long-term, repeated UV radiation exposure is a major causal factor. Also, there exist a clear relationship between increased incidence of non-melanoma skin cancers with decreasing latitude within some countries, i.e. where there are high UV radiation levels (50). It also suggests that this increase in skin cancer incidences is not simply a result of increased epidemiological surveillance and detection (51). Further, studies in the Antarctic have shown that UV-B can double during the yearly ozone hole process measured at the earth's surface (52). Other research studies found that in areas with little or no atmospheric pollution, UVR levels reaching the earth can be even more than observed before the ozone layer depletion started. Similarly, lower ambient levels of UV radiation are detected in areas with intense atmospheric pollution, and highly dense smog remaining through most part of the year (53). Also, studies in experimental animals have shown that elevated temperatures enhance the UV-induced skin cancer compared to that at room temperature. In an intriguing analysis, assuming that ambient temperature would have a similar effect in humans, speculates that long-term elevation of temperature by two °C as a consequence of global warming coupled climate change would increase the carcinogenic effects of solar UV by 10% (54). Further, experimental mouse models have shown that the carcinogenic effects of UV radiation increase by 5% per °C rise in temperature (55). However, research is still going on, and there is no clear evidence of how the increase in surface temperature can increase the carcinogenic effects of UV radiation. Increased incidences in the diseases associated with insufficient vitamin D levels have also been noticed in the past many decades, probably due to avoiding UV-B exposure or using sun protection gears at occupational places despite

the increase in UVR index. These ambivalent and emerging health effects of UVR on net loss or gain will thus depend on various parameters, including the migratory pattern of people influencing their exposure leading to an imbalance in optimal exposure to what is required naturally (56) **(Figure 1).** The social cost of these diseases due to indecent exposure to UVR and the financial burden it entails is overwhelming as human sufferings continue to increase. Further, ozone depletion has come with a dichotomous nature for humans to avoid sun exposure to prevent skin-related pathological conditions or keep taking sunbaths for healthy vitamin D synthesis (57). To further clarify this ambiguity, a comprehensive report by United Nations Environment Programme estimated an additional burden of 4500 melanoma cases and 300,000 non-melanoma cases if there is a 10% decrease in the ozone layer, and these figures are in addition to those cases that happen under normal circumstances. WHO has also made it clear that among the total cataract cases that occur annually the world over, an estimated 3 million cases per year, accounting for 20% of total cases, could be due to UV exposure. Also, for each 1% sustained decrease in ozone, a 0.5% increase in the number of cataracts could be due to UV exposure alone (9, 58–60). These statistics ask for a strategic global action plan as total avoidance of UV exposure is already ruled out due to other problems manifested in the absence of sun exposure. Further, human evolution at low latitudes where sunlight is more intense and their migration towards high latitude areas have been driven by competing for folate deficiency and vitamin D, both of which are phenomena driven by UV exposure (61). In addition to the concerns due to ozone layer depletion, anthropogenic impacts that are more intense than ever can magnify the effects of UV on both humans and the rest of the environment (62). The Montreal Protocol, though, resulted in a considerate reduction in the emissions of CFCs and halons responsible for damaging the ozone layer that has already started to replete itself. There is still an estimated additional burden of 33,000 melanoma/non-melanoma cancer cases attributed to ozone layer depletion (63, 64). Climate change due to global warming is another factor that could play a role in potentiating or magnifying the cancer-causing potential of UV. Although, significant improvements were made by countries in reducing the global consumption of ozone-depleting substance by some 98% under the Montreal Protocol treaty, the full recovery of ozone is not possible for some decades as the depleting substances continue to stay in the atmosphere for years together. Future outcomes will therefore depend on how countries abide by the treaty terms and conditions, thereby preventing the further loss (65).

VITAMIN D DEFICIENCY AND OPTIMIZATION OF APPROPRIATE PUBLIC HEALTH RECOMMENDATION ON UVR EXPOSURE

Although the ambivalent effects of UV radiation exposure are known, we are yet to understand which particular dose of UV is adequate and the one that is excessive to different life forms (66). This standardization of dose is further complicated amid the ozone layer depletion scenario combined with global warming that has significantly impacted the optimization of optimal, suboptimal and above optimal exposure levels of UVR and its post-effects (7). These factors necessitate a suitable public health policy in the wake of these distribution pattern changes of global UV exposure to life on earth. There are specific solutions to these problems, but the outcome is subjective. If we can maintain sufficient vitamin D levels from outside sources, UVR exposure can be optimized, and excessive exposure can be avoided accordingly. Before doing that, we have to rule out any other important function of UV exposure-related biological role in humans and requires further research to deconstruct the hidden facts (67, 68). For this, research has to define what vitamin D sufficiency to the body means and how much vitamin we have to take from the outside sources. This requirement will further depend on age, type of skin, area of location and typical dietary patterns. Only then a counterfactual exposure be defined, which can be a kind of minimum theoretical risk. This way, we can determine the limit of radiation exposure without significantly altering or impacting the vitamin D status in the body (69–71).

Further new structural model-based studies can be used to calculate the burden of diseases due to excessive UVR exposure. Inclusions on human skin pigmentation, physical inactivity, diet patterns, quality of healthcare system, behavioural sun exposure and latitude need to be considered to figure out a near accurate correlation of UVR exposure and its diverse effects. Earlier assessments on quantification of the global burden of diseases due to UVR have pointed out gaps in our current knowledge and understanding of UVR and warrant further research across the interdisciplinary fields to improve precision and broaden the scope of assessment for enduring results. More research is required to clarify the other beneficial effects of sun exposure and if total exposure avoidance with vitamin D supplementation from outside sources could be feasible. Further, strict sun protection measures are being followed, especially by skin types I-IV to prevent the UV–B–induced skin damage by avoiding excessive sun exposure (72). The use of sunscreens is also recommended, especially for fair-skinned individuals, but not a general rule. However, clinical dermatologists and researchers must understand the balancing effects of UV exposure and provide a shred of convincing evidence by weighing the mutagenic effect of less intense UV than its protective effects on different life forms (73, 74). This information also needs to be translated into public-friendly outcomes and could prolong many lives through positive recommendations on strict sun protection measures which require further moderation. Also, researchers need to deconstruct what it means by adequate vitamin D status when sun exposure is seriously curtailed and recommended, taking into account the associated ill effects of low sun exposure.

VITAMIN D FORTIFICATION OF FOODS: A NOVEL BIOTECHNOLOGICAL STRATEGY TO CURB VITAMIN D DEFICIENCY IN HUMANS

Optimum Vitamin D in body is essential for healthy bone and organ function (75). Exposure to sunlight (ultraviolet-B) is the primary natural source of vitamin D in the skin. At the same

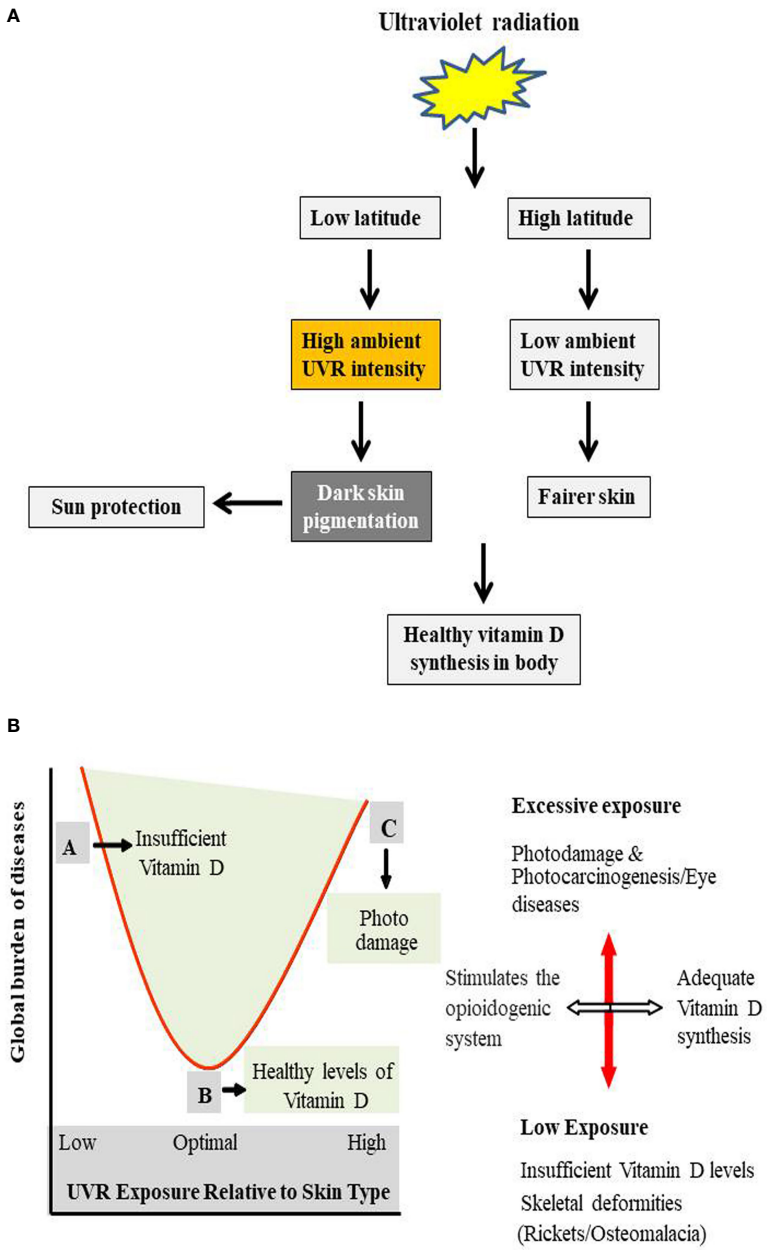

FIGURE 1 | **(A)** Evolutionarily mediated adaptation of life forms to differential atmospheric UVR levels. UV radiation exposure requirements promoting healthy vitamin D synthesis in skin meant that people developed darker skin pigmentation at places of low latitude with high ambient UVR intensity, offering them protection from the effects of UVR. While, those at higher latitude have fairer skin as an evolutionarily developed trait to potentiate the insufficient vitamin D production from low ambient exposure of UV to skin. **(B)** Ambivalent effects of UVR exposure to skin. Schematic diagram showing relationship between benefits of optimum UVR exposure, ill effects of inadequate exposure and the global burden of diseases due to inappropriate UV exposure. A represents insufficient UVR exposure responsible for the improper vitamin D levels in the body leading to skeletal abnormalities and other indirect effects of low ambient UV exposure. B represents optimal UVR exposure required for the essential and healthy synthesis of vitamin D in the body and also stimulates the opioidogenic system in the brain. C shows high UVR exposure leading to skin and ocular malignancies especially, in fair-skinned individuals. Both A & C are related to inappropriate exposure of UVR to the skin.

time, only a tiny portion of the necessary amount can be acquired through diet (76). There are six factors to be considered on the optimal amount of UV exposure depending on the latitude for healthy vitamin D levels, i.e., location, time of day, outdoor weather, skin colour, total sun exposure and age. Based on these factors, every individual has their sunlight exposure requirements based on specific elements that are both intrinsic and extrinsic to the body. However, to maintain healthy blood levels of vitamin D, one should aim to get 10–30 minutes of midday sunlight several times per week, and people with darker

skin may require a little more. Exposure of face and arms to the sunlight for 15–30 minutes, between 11 am–3 pm daily, should be enough to maintain adequate vitamin D status. However, geographical location remains the most important determinant of vitamin D status in the body (77). Although Vitamin D has many health benefits, it might even help lower the risk of some cancers (78). However, researchers aren't sure what the optimal level of vitamin D is, and a lot of research is already going on to understand the intricate relationship clearly.

Further, the optimal level of UV exposure for healthy vitamin D production may increase the cancer risk. As such, the risk-benefit may vary widely due to individual susceptibility, genetic and lifestyle factors (79, 80). The fact is that it doesn't take so much sun exposure for the body to produce required amounts of vitamin D and exposure time less than 10 to 15 minutes, two to three times a week, followed by good sun protection can make all the vitamin D on which a body can muster (81). After the required levels are achieved, the body automatically starts disposing of the excess vitamin D to avoid vitamin overload. At this point, persistent sun exposure gives nothing but sun damage without any of the presumed benefits. Research has shown that this 10-15 minute exposure to the body is enough to cause DNA damage, and every bit of it adds up throughout one's life, producing genetic mutations that keep increasing the lifetime risk of skin cancer (82). The exact UVB wavelength that makes the body synthesize vitamin D also produces sunburn and genetic mutations that can lead to skin cancer. A study has recently found that UVA damage can start in less than a minute. This damage to the skin's pigment cells keeps developing hours after the sun exposure ends, increasing the chances of melanoma (83). This rapid onset of DNA damage is also why researchers recommend more sun protection, not less. That is why this complex set of risks and benefits vary widely, and that guidance that addresses all of these factors is difficult to articulate.

Vitamin D deficiency has emerged as a new public health concern in recent years due to lifestyle changes and strict recommendations on avoiding excessive sun exposure. It has thus received increased attention due to its association with the increased risk of severe acute and chronic illnesses, including rickets, childhood caries, osteoporosis, infections, autoimmune diseases, cardiovascular diseases, cancer, type 2 diabetes and neurological disorders (84). On the other hand, a healthy and balanced diet is not enough to prevent vitamin D insufficiency in the body if it is not accompanied by UV exposure. However, specific approaches such as increased dietary and supplemental intakes and encouraging outdoor activities could guarantee vitamin D sufficiency. However, more recently, biotechnological processes were used to produce novel vitamin D rich or vitamin D fortified foods, which can improve vitamin D status and prevent vitamin D deficiency in high-risk individuals. Various foods were fortified during the early 20th century, including milk, other dairy products, margarine, and even beer. Initially, and since the 1940s, cow's milk became the primary delivery vehicle for vitamin D fortification in the United States and Canada, and a carefully planned fortification policy was introduced to eliminate vitamin D deficiency and as a public health issue (85). Voluntary and mandatory fortification approaches are applied in USA and Canada, respectively. Both are entrusted to provide fortified foods with proven efficacy. Current estimates suggest that ~60% of vitamin D intake from foods in the US and Canada are attributed to fortified foods (85). Further, research has shown higher 25(OH)D serum levels in Canadians ingesting fortified milk than those not consuming it (86). In another prospective controlled trial study, 713 healthy school children aged 10-14 years were randomized to receive unfortified or milk fortified with 600 IU (15ug) and 1000 IU (25ug) of vitamin D per day for 12 weeks. The percentage of subjects having serum 25(OH) D levels >20 ng/ml (50 nmol/L) following supplementation was found 5.9%, 69.95% and 81.11% in comparison to 6.32%, 4.9% and 12%, respectively, at baseline (87), suggesting the success of the fortification policy. Some population groups do not consume fortified milk due to lactose intolerance. Prospective studies have shown that foods of plant origin such as orange juice and bread can also be used as suitable vehicles for vitamin D fortification. Although traditional fortification practices serve as an essential strategy, the introduction of novel biotechnology-based vitamin D fortification approaches will continue to attract attention. Also, fortification approaches need to be tailored to the nutritional habits of each country. In India, it is proposed that the fortification of widely consumed foods such as maida, wheat flour and rice could serve the purpose locally with fewer costs (88).

CONCLUSION

UVR exposure has both positive as well as negative health effects on humans. An increase in skin cancer cases over the last 4 to 5 decades has raised various public health concerns among the scientific community and led international health organizations to develop strong sun protection measures to curb this sharp increase. However, at the same time, a growing concern about vitamin D deficiency, mostly in high-risk groups, is creating a kind of exposure dilemma. Current knowledge and understanding of the ambivalent effects of UV exposure necessitates a correct public health recommendation on optimal sun exposure based on the scientific facts and reasoning. Also, Vitamin D deficiency that has emerged as a significant public health issue can be overcome with biotechnology-based approaches like food fortification. Vitamin D fortification of foods is technically a feasible method that can address the vitamin deficiency in large population segments without modifications in lifestyle and consumption patterns. Further, biotechnology can offer viable solutions in producing new and novel vitamin D fortified foods. This can somehow lead to positive outcomes in protecting humans against the adverse effects of strict recommendations on sun protection measures.

AUTHOR CONTRIBUTIONS

Conceptualization and Formal analysis: SU and ST. Funding acquisition: ST. Writing - original draft: SU. Writing - review and editing: ST and SU. All authors contributed to the article and approved the submitted version.

ACKNOWLEDGMENTS

Senior Research Fellowship (SRF) to author SU by Department of Science and Technology (DST), Ministry of Science and Technology, New Delhi, India Vide No: *IF-160982* is acknowledged. Authors acknowledge financial assistance by the Department of Biotechnology (DBT), Ministry of Science and Technology, New Delhi, India vide project No: *GAP-2166*. This manuscript represents the IIIM communication number (CSIR-IIIM/IPR/00293).

REFERENCES

1. D'Orazio J, Jarrett S, Amaro-Ortiz A, Scott T. UV Radiation and the Skin. *Int J Mol Sci* (2013) 14(6):12222–48. doi: 10.3390/ijms140612222
2. Mohania D, Chandel S, Kumar P, Verma V, Digvijay K, Tripathi D, et al. Ultraviolet Radiations: Skin Defense-Damage Mechanism. In: Ahmad S. (eds). *Ultraviolet Light in Human Health, Diseases and Environment. Advances in Experimental Medicine and Biology*, vol 996. Cham: Springer (2017) 996:71–87. doi: 10.1007/978-3-319-56017-5_7
3. Roy S. Impact of UV Radiation on Genome Stability and Human Health. In: Ahmad S. (eds). *Ultraviolet Light in Human Health, Diseases and Environment. Advances in Experimental Medicine and Biology*, vol 996. Cham: Springer (2017), p. 207–19. doi: 10.1007/978-3-319-56017-5_17
4. Nicholson WL, Schuerger AC, Setlow P. The Solar UV Environment and Bacterial Spore UV Resistance: Considerations for Earth-To-Mars Transport by Natural Processes and Human Spaceflight. *Mutat Research/Fundam Mol Mech Mutagen* (2005) 571(1-2):249–64. doi: 10.1016/j.mrfmmm.2004.10.012
5. McKenzie RL, Aucamp PJ, Bais AF, Björn LO, Ilyas M, Madronich S. Ozone Depletion and Climate Change: Impacts on UV Radiation. *Photochem Photobiol Sci* (2011) 10(2):182–98. doi: 10.1039/c0pp90034f
6. Bais AF, McKenzie RL, Bernhard G, Aucamp PJ, Ilyas M, Madronich S, et al. Ozone Depletion and Climate Change: Impacts on UV Radiation. *Photochem Photobiol Sci* (2015) 14(1):19–52. doi: 10.1039/C4PP90032D
7. Bais AF, Lucas RM, Bornman JF, Williamson CE, Sulzberger B, Austin AT, et al. Environmental Effects of Ozone Depletion, UV Radiation and Interactions With Climate Change: UNEP Environmental Effects Assessment Panel, Update 2017. *Photochem Photobiol Sci* (2018) 17(2):127–79. doi: 10.1039/C7PP90043K
8. Bais AF, Bernhard G, McKenzie RL, Aucamp PJ, Young PJ, Ilyas M, et al. Ozone–climate Interactions and Effects on Solar Ultraviolet Radiation. *Photochem Photobiol Sci* (2019) 18(3):602–40. doi: 10.1039/C8PP90059K
9. Barnes PW, Williamson CE, Lucas RM, Robinson SA, Madronich S, Paul ND, et al. Ozone Depletion, Ultraviolet Radiation, Climate Change and Prospects for a Sustainable Future. *Nat Sustainability* (2019) 2(7):569–79. doi: 10.1038/s41893-019-0314-2
10. McKenzie RL, Björn LO, Bais A, Ilyasd M. Changes in Biologically Active Ultraviolet Radiation Reaching the Earth's Surface. *Photochem Photobiol Sci* (2003) 2(1):5–15. doi: 10.1039/B211155C
11. Kammeyer A, Luiten R. Oxidation Events and Skin Aging. *Ageing Res Rev* (2015) 21:16–29. doi: 10.1016/j.arr.2015.01.001
12. Voss W, Bürger C. Natural Skin Barrier and Immunological Mechanisms against Sunlight. In: *Euro Cosmetics*. München: Inter-Euro Medien GmbH (2004) 12(6):12–25
13. Paul ND, Gwynn-Jones D. Ecological Roles of Solar UV Radiation: Towards an Integrated Approach. *Trends Ecol Evol* (2003) 18(1):48–55. doi: 10.1016/S0169-5347(02)00014-9
14. Muluneh MG. Impact of Climate Change on Biodiversity and Food Security: A Global Perspective—a Review Article. *Agric Food Secur* (2021) 10(1):1–25. doi: 10.1186/s40066-021-00318-5
15. Fiscus EL, Booker FL. Is Increased UV-B a Threat to Crop Photosynthesis and Productivity? *Photosynth Res* (1995) 43(2):81–92. doi: 10.1007/BF00042965
16. Rozema J, van de Staaij J, Björn LO, Caldwell M. UV-B as an Environmental Factor in Plant Life: Stress and Regulation. *Trends Ecol Evol* (1997) 12(1):22–8. doi: 10.1016/S0169-5347(96)10062-8
17. Williamson CE, Neale PJ, Hylander S, Rose KC, Figueroa FL, Robinson SA, et al. The Interactive Effects of Stratospheric Ozone Depletion, UV Radiation, and Climate Change on Aquatic Ecosystems. *Photochem Photobiol Sci* (2019) 18(3):717–46. doi: 10.1039/C8PP90062K
18. Whitehead RF, de Mora SJ, Demers S. Enhanced UV Radiation–a New Problem for the Marine Environment. *Effects UV Radiat Marine Environ* (2000) 10:1–34. doi: 10.1017/CBO9780511535444.002
19. Miyauchi M, Nakajima H. Determining an Effective UV Radiation Exposure Time for Vitamin D Synthesis in the Skin Without Risk to Health: Simplified Estimations From UV Observations. *Photochem photobiol* (2016) 92(6):863–9. doi: 10.1111/php.12651
20. Costin G-E, Hearing VJ. Human Skin Pigmentation: Melanocytes Modulate Skin Color in Response to Stress. *FASEB J* (2007) 21(4):976–94. doi: 10.1096/fj.06-6649rev
21. D'Alba L, Shawkey MD. Melanosomes: Biogenesis, Properties, and Evolution of an Ancient Organelle. *Physiol Rev* (2019) 99(1):1–19. doi: 10.1152/physrev.00059.2017
22. Miyamura Y, Coelho SG, Wolber R, Miller SA, Wakamatsu K, Zmudzka BZ, et al. Regulation of Human Skin Pigmentation and Responses to Ultraviolet Radiation. *Pigment Cell Res* (2007) 20(1):2–13. doi: 10.1111/j.1600-0749.2006.00358.x
23. Christensen L, Suggs A, Baron E. Ultraviolet Photobiology in Dermatology. In: Ahmad S. (eds). *Ultraviolet Light in Human Health, Diseases and Environment. Advances in Experimental Medicine and Biology*, vol 996. Cham: Springer (2017) 996:89–104. doi: 10.1007/978-3-319-56017-5_8
24. Rees JL. The Genetics of Sun Sensitivity in Humans. *Am J Hum Genet* (2004) 75(5):739–51. doi: 10.1086/425285
25. Bhattacharya B, Chauhan D, Singh AK, Chatterjee M. Melanin Based Classification of Skin Types and Their Susceptibility to UV-Induced Cancer. In: *Skin Cancer: Pathogenesis and Diagnosis*. Singapore: Springer (2021). p. 41–67.
26. Brenner M, Hearing VJ. The Protective Role of Melanin Against UV Damage in Human Skin. *Photochem Photobiol* (2008) 84(3):539–49. doi: 10.1111/j.1751-1097.2007.00226.x
27. Vieyra-Garcia PA, Wolf P. A Deep Dive Into UV-Based Phototherapy: Mechanisms of Action and Emerging Molecular Targets in Inflammation and Cancer. *Pharmacol Ther* (2021) 222:107784. doi: 10.1016/j.pharmthera.2020.107784
28. Vangipuram R, Feldman S. Ultraviolet Phototherapy for Cutaneous Diseases: A Concise Review. *Oral Dis* (2016) 22(4):253–9. doi: 10.1111/odi.12366
29. Stern RS. Psoralen and Ultraviolet a Light Therapy for Psoriasis. *N Engl J Med* (2007) 357(7):682–90. doi: 10.1056/NEJMct072317
30. Patel MSS, Shazmeen I. A Comprehensive Review On Current Treatments Of Vitiligo. *World J Pharm Res* (2020) 9(10):434–45. doi: 10.20959/wjpr202010-18512
31. Nordin UU, Ahmad N, Salim N, Yusof NS. Lipid-Based Nanoparticles for Psoriasis Treatment: A Review on Conventional Treatments, Recent Works, and Future Prospects. *RSC Adv* (2021) 11(46):29080–101. doi: 10.1039/D1RA06087B
32. Juzeniene A, Moan J. Beneficial Effects of UV Radiation Other Than via Vitamin D Production. *Dermato-endocrinology* (2012) 4(2):109–17. doi: 10.4161/derm.20013
33. Birlea SA, Costin GE, Norris DA. New Insights on Therapy With Vitamin D Analogs Targeting the Intracellular Pathways That Control Repigmentation in Human Vitiligo. *Med Res Rev* (2009) 29(3):514–46. doi: 10.1002/med.20146
34. Kemény L, Varga E, Novak Z. Advances in Phototherapy for Psoriasis and Atopic Dermatitis. *Expert Rev Clin Immunol* (2019) 15(11):1205–14. doi: 10.1080/1744666X.2020.1672537
35. Irving AA, Marling SJ, Seeman J, Plum LA, DeLuca HF. UV Light Suppression of EAE (a Mouse Model of Multiple Sclerosis) is Independent of Vitamin D and Its Receptor. *Proc Natl Acad Sci* (2019) 116(45):22552–5. doi: 10.1073/pnas.1913294116
36. Amram O, Schuurman N, Randall E, Zhu F, Saeedi J, Rieckmann P. The Use of Satellite Data to Measure Ultraviolet-B Penetrance and Its Potential Association With Age of Multiple Sclerosis Onset. *Multiple Sclerosis Relat Disord* (2018) 21:30–4. doi: 10.1016/j.msard.2018.02.005
37. Naseem KM. The Role of Nitric Oxide in Cardiovascular Diseases. *Mol Aspects Med* (2005) 26(1-2):33–65. doi: 10.1016/j.mam.2004.09.003
38. Pelegrino MT, Weller RB, Chen X, Bernardes JS, Seabra AB. Chitosan Nanoparticles for Nitric Oxide Delivery in Human Skin. *MedChemComm* (2017) 8(4):713–9. doi: 10.1039/C6MD00502K

39. Mohiuddin A. Sunscreen and Suntan Preparations. *ARC J Pharm Sci (AJPS)* (2019) 5(2):8–44. doi: 10.20431/2455-1538.0502002
40. Miller AL. Epidemiology, Etiology, and Natural Treatment of Seasonal Affective Disorder. *Altern Med Rev* (2005) 10(1):5–13.
41. Jablonski NG, Chaplin G. The Evolution of Human Skin Coloration. *J Hum Evol* (2000) 39(1):57–106. doi: 10.1006/jhev.2000.0403
42. Chaplin G, Jablonski NG. Vitamin D and the Evolution of Human Depigmentation. *Am J Phys Anthropol: Off Publ Am Assoc Phys Anthropologists* (2009) 139(4):451–61. doi: 10.1002/ajpa.21079
43. Kechichian E, Ezzedine K. Vitamin D and the Skin: An Update for Dermatologists. *Am J Clin Dermatol* (2018) 19(2):223–35. doi: 10.1007/s40257-017-0323-8
44. Shaw N, Pal B. Vitamin D Deficiency in UK Asian Families: Activating a New Concern. *Arch Dis Childhood* (2002) 86(3):147–9. doi: 10.1136/adc.86.3.147
45. Geller AC, Annas GD. Epidemiology of Melanoma and Nonmelanoma Skin Cancer. *Semin Oncol Nurs* Philadelphia, Pennsylvania, United States:WB Saunders (2003) 19(1):2–11. doi: 10.1053/sonu.2003.50000
46. Lucas RM, Yazar S, Young AR, Norval M, De Gruijl FR, Takizawa Y, et al. Human Health in Relation to Exposure to Solar Ultraviolet Radiation Under Changing Stratospheric Ozone and Climate. *Photochem Photobiol Sci* (2019) 18(3):641–80. doi: 10.1039/C8PP90060D
47. Jones M. Effects of UV Radiation on Building Materials. In. *UV workshop, Christchurch (published in current proceedings)* Judgeford: Building Research Association of New Zealand (BRANZ) (2002) .
48. Andersen SO, Sarma KM. *Protecting the Ozone Layer: The United Nations History*. Routledge, Milton Park, England, UK: Earthscan (2012).
49. Parker ER. The Influence of Climate Change on Skin Cancer Incidence–A Review of the Evidence. *Int J Women's Dermatol* (2021) 7(1):17–27. doi: 10.1016/j.ijwd.2020.07.003
50. Papadopoulos O, Karantonis F-F, Papadopulos NA. Non-Melanoma Skin Cancer and Cutaneous Melanoma for the Plastic and Reconstructive Surgeon. In: *Non-Melanoma Skin Cancer and Cutaneous Melanoma*. Cham: Springer (2020). p. 153–239.
51. Apalla Z, Lallas A, Sotiriou E, Lazaridou E, Ioannides D. Epidemiological Trends in Skin Cancer. *Dermatol Pract conceptual* (2017) 7(2):1. doi: 10.5826/dpc.0702a01
52. Abbasi S, Abbasi T. Impacts of Ozone Hole. In: *Ozone Hole*. New York, NY: Springer (2017). p. 51–99.
53. Diffey B. Stratospheric Ozone Depletion and the Risk of Non-Melanoma Skin Cancer in a British Population. *Phys Med Biol* (1992) 37(12):2267. doi: 10.1088/0031-9155/37/12/008
54. Diffey B. Climate Change, Ozone Depletion and the Impact on Ultraviolet Exposure of Human Skin. *Phys Med Biol* (2003) 49(1):R1. doi: 10.1088/0031-9155/49/1/R01
55. Van der Leun JC, de Gruijl FR. Climate Change and Skin Cancer. *Photochem Photobiol Sci* (2002) 1(5):324–6. doi: 10.1039/b201025a
56. Carlberg C. Molecular Approaches for Optimizing Vitamin D Supplementation. *Vitamins Hormones* (2016) 100:255–71. doi: 10.1016/bs.vh.2015.10.001
57. Mandelcorn-Monson R. *Sun Exposure, Vitamin D Receptor*. Toronto: University of Toronto (2007).
58. El-Kholy O. *The World Environment 1972–1992: Two Decades of Challenge*. Berlin/Heidelberg, Germany: Springer Science & Business Media (2012).
59. Lucas R, McMichael T, Smith W, Armstrong BK, Prüss–Üstün A and World Health Organization. *Solar Ultraviolet Radiation: Global Burden of Disease From Solar Ultraviolet Radiation*. Geneva Switzerland: World Health Organization (2006).
60. World Health Organization and I.C.o.N.-I.R. *Protection, Global Solar UV Index: A Practical Guide*. Geneva Switzerland: World Health Organization (2002).
61. Jablonski NG, Chaplin G. Human Skin Pigmentation as an Adaptation to UV Radiation. *Proc Natl Acad Sci* (2010) 107(Supplement 2):8962–8. doi: 10.1073/pnas.0914628107
62. Bargagli R. *Antarctic Ecosystems: Environmental Contamination, Climate Change, and Human Impact* Vol. 175. Berlin/Heidelberg, Germany: Springer Science & Business Media (2006).
63. Montreal Protocol. *Montreal Protocol on Substances That Deplete the Ozone Layer* Vol. 26. . Washington, DC: US Government Printing Office (1987) p. 128–36.
64. Fathy R, Rosenbach M. Climate Change and Inpatient Dermatology. *Curr Dermatol Rep* (2020) 9(4):201–9. doi: 10.1007/s13671-020-00310-5
65. Chipperfield MP, Hossaini R, Montzka SA, Reimann S, Sherry D, Tegtmeier S. Renewed and Emerging Concerns Over the Production and Emission of Ozone-Depleting Substances. *Nat Rev Earth Environ* (2020) 1(5):251–63. doi: 10.1038/s43017-020-0048-8
66. Turner J. *Ultraviolet Radiation Reflection From Building Materials: Characterisation, Quantification and the Resulting Effects*. Australia: University of Southern Queensland (2011).
67. Misra M, Pacaud D, Petryk A, Collett-Solberg PF, Kappy M. Vitamin D Deficiency in Children and Its Management: Review of Current Knowledge and Recommendations. *Pediatrics* (2008) 122(2):398–417. doi: 10.1542/peds.2007-1894
68. McKenzie RL, Liley JB, Björn LO. UV Radiation: Balancing Risks and Benefits. *Photochem Photobiol* (2009) 85(1):88–98. doi: 10.1111/j.1751-1097.2008.00400.x
69. Hollis BW. Circulating 25-Hydroxyvitamin D Levels Indicative of Vitamin D Sufficiency: Implications for Establishing a New Effective Dietary Intake Recommendation for Vitamin D. *J Nutr* (2005) 135(2):317–22. doi: 10.1093/jn/135.2.317
70. Cashman KD. Vitamin D: Dietary Requirements and Food Fortification as a Means of Helping Achieve Adequate Vitamin D Status. *J Steroid Biochem Mol Biol* (2015) 148:19–26. doi: 10.1016/j.jsbmb.2015.01.023
71. Grant WB, Holick MF. Benefits and Requirements of Vitamin D for Optimal Health: A Review. *Altern Med Rev* (2005) 10(2):94–111.
72. Wacker M, Holick MF. Vitamin D—effects on Skeletal and Extraskeletal Health and the Need for Supplementation. *Nutrients* (2013) 5(1):111–48. doi: 10.3390/nu5010111
73. Nahar VK, Wilkerson AH, Ghafari G, Martin B, Black WH, Boyas JF, et al. Skin Cancer Knowledge, Attitudes, Beliefs, and Prevention Practices Among Medical Students: A Systematic Search and Literature Review. *Int J Women's Dermatol* (2018) 4(3):139–49. doi: 10.1016/j.ijwd.2017.10.002
74. Robinson JK. Sun Exposure, Sun Protection, and Vitamin D. *Jama* (2005) 294 (12):1541–3. doi: 10.1001/jama.294.12.1541
75. Erem S, Atfi A, Razzaque MS. Anabolic Effects of Vitamin D and Magnesium in Aging Bone. *J Steroid Biochem Mol Biol* (2019) 193:105400. doi: 10.1016/j.jsbmb.2019.105400
76. Mohr SB, Garland CF, Gorham ED, Garland FC. The Association Between Ultraviolet B Irradiance, Vitamin D Status and Incidence Rates of Type 1 Diabetes in 51 Regions Worldwide. *Diabetologia* (2008) 51(8):1391–8. doi: 10.1007/s00125-008-1061-5
77. Holick MF. Vitamin D Deficiency. *N Engl J Of Med* (2007) 357(3):266–81. doi: 10.1056/NEJMra070553
78. Manson JE, Rosen CJ. Vitamin D Supplements and Prevention of Cancer and Cardiovascular Disease. *N Engl J Med* (2019) 380(1):33–44. doi: 10.1056/NEJMoa1809944
79. Reichrath J, Nürnberg B. Cutaneous Vitamin D Synthesis Versus Skin Cancer Development: The Janus-Faces of Solar UV-Radiation. *Dermato-Endocrinology* (2009) 1(5):253–61. doi: 10.4161/derm.1.5.9707
80. Reichrath J, Vogt T, Friedrich M, Holick MF, Heyne K, Saternus R, et al. SYMPOSIA "VITAMIN D IN PREVENTION AND THERAPY" AND "BIOLOGIC EFFECTS OF LIGHT. *Anticancer Res* (2019) 39:3273–94. doi: 10.21873/anticanres.12330
81. Holick MF. *The Vitamin D Solution: A 3-Step Strategy to Cure Our Most Common Health Problems*. Westminster, London: Penguin (2010).
82. Wolpowitz D, Gilchrest BA. The Vitamin D Questions: How Much do You Need and How Should You Get it? *J Am Acad Dermatol* (2006) 54(2):301–17. doi: 10.1016/j.jaad.2005.11.1057
83. Martens MC, Seebode C, Lehmann J, Emmert S. Photocarcinogenesis and Skin Cancer Prevention Strategies: An Update. *Anticancer Res* (2018) 38 (2):1153–8. doi: 10.21873/anticanres.12334
84. Wimalawansa SJ. Non-Musculoskeletal Benefits of Vitamin D. *J Steroid Biochem Mol Biol* (2018) 175:60–81. doi: 10.1016/j.jsbmb.2016.09.016
85. Moulas AN, Vaiou M. Vitamin D Fortification of Foods and Prospective Health Outcomes. *J Biotechnol* (2018) 285:91–101. doi: 10.1016/j.jbiotec.2018.08.010
86. Calvo MS, Whiting SJ. Survey of Current Vitamin D Food Fortification Practices in the United States and Canada. *J Steroid Biochem Mol Biol* (2013) 136:211–3. doi: 10.1016/j.jsbmb.2012.09.034
87. Khadgawat R, Marwaha RK, Garg MK, Ramot R, Oberoi AK, Sreenivas V, et al. Impact of Vitamin D Fortified Milk Supplementation on Vitamin D

Status of Healthy School Children Aged 10–14 Years. *Osteoporosis Int* (2013) 24(8):2335–43. doi: 10.1007/s00198-013-2306-9
88. Gupta A. Vitamin D Deficiency in India: Prevalence, Causalities and Interventions. *Nutrients* (2014) 6(2):729–75. doi: 10.3390/nu6020729

Conflict of Interest: The authors declare that the research was conducted in the absence of any commercial or financial relationships that could be construed as a potential conflict of interest.

Publisher's Note: All claims expressed in this article are solely those of the authors and do not necessarily represent those of their affiliated organizations, or those of the publisher, the editors and the reviewers. Any product that may be evaluated in this article, or claim that may be made by its manufacturer, is not guaranteed or endorsed by the publisher.

frontiers in Oncology

SYSTEMATIC REVIEW
published: 22 March 2022
doi: 10.3389/fonc.2022.868781

Prevalence of Merkel Cell Polyomavirus in Normal and Lesional Skin: A Systematic Review and Meta-Analysis

Wilson A. Wijaya, Yu Liu, Yong Qing and Zhengyong Li**

Department of Burn and Plastic Surgery, West China Hospital, Sichuan University, Chengdu, China

The prevalence of Merkel cell polyomavirus(MCPyV) in Merkel cell carcinoma(MCC) and non-MCC skin lesions and its possible role in the etiology of other skin diseases remain controversial. To systematically assess the association between MCPyV infection and MCC, non-MCC skin lesions, and normal skin. For this systematic review and meta-analysis, a comprehensive search for eligible studies was conducted using Medline Ovid, Pubmed, Web of Science, and the Cochrane CENTRAL databases until August 2021; references were searched to identify additional studies. Observational studies that investigated the association between MCPyV infection and MCC, non-MCC skin lesions, and normal skin using polymerase chain reaction(PCR) as a detection method and provided sufficient data to calculate the prevalence of MCPyV positivity. A total of 50 articles were included in the study after exclusion criteria were applied. Two reviewers independently reviewed and assessed the eligibility of the studies, and all disagreements were resolved by consensus. To determine the association between MCPyV and MCC, overall odds ratio (OR) were calculated with 95% CI using a random-effects model. Single-arm meta-analyses were performed to examine the prevalence rate of MCPyV+ in MCC, non-MCC skin lesions, and normal skin. The primary analysis was the prevalence rate of MCPyV+ in MCC. Secondary outcomes included the prevalence rate of MCPyV+ in non-MCC skin lesions and normal skin. A total of 50 studies involving 5428 patients were reviewed based on our inclusion and exclusion criteria. Compared with the control group, MCPyV infection was significantly associated with MCC (OR = 3.51, 95% CI = 2.96 - 4.05). The global prevalence of MCPyV+ in MCC, melanoma, squamous cell carcinoma, basal cell carcinoma, Bowen's disease, actinic keratosis, keratoacanthoma, seborrheic keratosis, and normal skin was 80%, 4%, 15%, 15%, 21%, 6%, 20%, 10%, and 11%, respectively. The current results suggest that MCPyV infection is significantly associated with an increased risk of MCC. However, the low prevalence rate of MCPyV+ in non-MCC skin lesions does not exclude a pathogenic association of this virus with the development of non-MCC skin lesions.

Keywords: merkel cell carcinoma, merkel cell polyomavirus, prevalence, infectivity, pathogenesis, skin cancer

OPEN ACCESS

Edited by:
Motoki Nakamura,
Nagoya City University, Japan

Reviewed by:
Tetsuya Magara,
Nagoya City University, Japan
Kotaro Nagase,
Saga University, Japan

****Correspondence:***
Zhengyong Li
302992694@qq.com
Yong Qing
hxqingyong@163.com

Specialty section:
This article was submitted to Skin Cancer, a section of the journal Frontiers in Oncology

Received: *03 February 2022*
Accepted: *28 February 2022*
Published: *22 March 2022*

Citation:
Wijaya WA, Liu Y, Qing Y and Li Z (2022) Prevalence of Merkel Cell Polyomavirus in Normal and Lesional Skin: A Systematic Review and Meta-Analysis. Front. Oncol. 12:868781. doi: 10.3389/fonc.2022.868781

INTRODUCTION

Merkel cell carcinoma(MCC) is a rare, high-grade, aggressive cutaneous neuroendocrine tumor originally discovered in 1972 (1–3). MCC is prone to recurrence, regional metastases that frequently recur in lymph nodes, and distant metastases. Advanced age(> 50 years), demographic characteristics (predominantly European) and sun-exposed skin(ultraviolet radiation) are established risk factors for MCC (4, 5). In recent decades, the incidence of MCC has increased, as has the mortality rate (6).

Polyomaviruses(PyVs) are small, double-stranded DNA-based viruses that are usually non- oncogenic for their hosts but may be oncogenic to some species under certain circumstances (7). PyVs have three major genomic regions: an early region encoding large T antigen (LTA) and small T antigen (STA), both viral oncoproteins with replicative functions; a late region encoding viral structural proteins such as VP1, VP2, and VP3; and a noncoding control region(NCCR) that controls viral replication (8, 9). The identification of Merkel cell polyomavirus (MCPyV) by digital transcriptome analysis was a significant leap in the knowledge of the pathogenesis of MCC (8). According to molecular epidemiological studies, MCPyV has a wide range of prevalences in MCC. The prevalence of MCPyV varies widely worldwide, ranging from approximately 25% in Australian MCC patients to 100% in a French study (10, 11). In addition, MCPyV DNA has also been detected in non-MCC skin lesions and normal skin (12, 13). However, the mechanism of MCPyV infection and the prevalence of MCPyV in non-MCC skin lesions and its potential role in the pathogenesis of other malignant skin diseases are still unknown. To better understand this problem, we performed a systematic review and meta-analysis to examine the relationship between MCPyV and MCC, non-MCC skin lesions, and normal skin.

METHODS

Literature Search

This article complies with the Declaration of Helsinki. Preferred Reporting Items for Systematic Reviews and Meta-analyses (PRISMA) guideline was used to conduct the study. Two of us (WAW and LY) comprehensively searched Medline Ovid, Pubmed, Web of Science, and the Cochrane CENTRAL databases from inception to August 1, 2021. Search terms were "merkel cell polyomavirus" and "skin neoplasms," "skin malignancy," "skin cancer," "merkel cell carcinoma," "squamous cell carcinoma," "basal cell carcinoma," "melanoma," "bowen disease," "actinic keratosis," "keratoacanthoma," "seborrheic keratosis" "non-lesional skin" or "normal skin." Searches were limited to human participants and English-language publications. We also conducted manual searches of the reference lists of the extracted articles to identify additional relevant publications. Only studies meeting the eligibility criteria outlined below were included in the meta-analysis.

Eligibility Criteria

The extracted data were required to meet the following criteria: (1) designed as a cohort, case-control study, or cross-sectional study; (2) confirmed the presence of MCPyV by polymerase chain reaction(PCR); (3) reported the detection of MCPyV in MCC, squamous cell carcinoma(SCC), basal cell carcinoma (BCC), melanoma, Bowen's disease, actinic keratosis, keratoacanthoma, seborrheic keratosis or normal skin; (4) full text available.

Studies that met more than one of the following criteria were excluded: (1) insufficient raw data to estimate the outcome; (2) animal study, *in vitro* study, case report, review, editorial, or commentary; (2) the available data could not be extracted from the article by calculation or by contacting the authors; and (3) multiple studies with overlapping samples. The studies with a more significant number of patients were selected when overlapping study samples were identified. Two reviewers (WAW and LY) independently performed the study selection process, and consensus resolved disagreements.

Data Extraction and Quality Assessment

Data were extracted by the two independent reviewers (WAW and LY) using a structured Excel(Microsoft Corp., Redmond, Washington) data collection spreadsheet as a priori. Discrepancies were discussed and resolved within the research team. The following data were retrieved for the included studies: first author, publication year, country, study design, number of patients in each group (MCC, SCC, BCC, melanoma, Bowen's disease, actinic keratosis, keratoacanthoma, seborrheic keratosis, and normal skin), number of patients in each group above with MCPyV+, sample types [frozen section(FR) or formalin-fixed paraffin-embedded (FFPE)], PCR primers, and immune status. Eligible studies were further divided into two different analyses: primary and secondary. The primary analysis was the prevalence rate of MCPyV in MCC. Secondary outcomes included the prevalence rate of MCPyV in non-MCC skin lesions (melanoma, SCC, BCC, Bowen's disease, actinic keratosis, keratoacanthoma, and seborrheic keratosis) and normal skin.

Quality assessment of included studies was performed using the Newcastle-Ottawa scale for cohort and case-control studies (14). The Newcastle-Ottawa scale consists of selection, comparability, and outcome(or exposure for case-control studies). A study can receive one score in each of the domains of selection and outcome and two scores in the domain of comparability. Studies with a low risk of bias had a score of less than 4, those with a score of 4 to 6 had an intermediate risk of bias, and those with a score of 7 or higher had a low risk of bias.

Statistical Analysis

Stata 15.1(StataCorp, College Station, TX USA, 2018) was used to analyze the data after it had been checked for consistency. The "metaprop" command was used to generate pooled effect size(ES) for noncomparative binary outcomes. The 95% confidence interval (CI) was generated using the DerSimonian-Laird random-effects model with FreemanTukey double arcsine transformation and evaluated using the Wilson score technique.

The Cochran Q and I^2 statistics were used to test for heterogeneity among the chosen studies. Mild, moderate, and severe heterogeneity were defined as I^2 statistics of 25% - 50%, 50% - 75%, and >75%, respectively. A random-effects model was used to produce the pooled estimate and 95% CI if heterogeneity was more than 50%. The Mantel-Haenszel method was used to evaluate dichotomous variables, and the results are presented as ORs. Subgroup analysis and meta-regression were employed when heterogeneity was evident based on important variables (country, continent, sample type). Sensitivity analysis was performed to estimate the influence of a single study on the pooled ORs. Statistical significance is defined as a two-tailed P-value of less than 0.05. The visual estimation of a funnel pot, Egger's test, Begg's test, and the trim & fill method were used to determine and correct publication bias (P =0.05 was considered significant).

RESULTS

Search Results and Included Trials

A total of 1308 studies were identified through the literature search. After adjustment for duplicates, 623 articles remained. Of these, 421 articles were removed after reviewing the titles and abstracts. After a full-text review of the remaining 108 articles, 58 articles were further excluded based on the following criteria: 3 studies were not in the field of interest, 21 studies were review articles, 14 studies were duplicates, 12 were conference abstracts, and eight studies had insufficient data. Finally, 50 studies consisting of 31 case-control studies (1812 participants) and 19 cross-sectional studies (3616 participants) were included in the meta-analysis. The flowchart for the selection process and detailed identification is shown in **Figure 1**. The 50 included studies were published between 2008 and 2021 in 15 different countries. Thirty five studies reported the prevalence of MCPyV+ in MCC patients, 13 studies in normal skin, 11 studies in cutaneous melanoma patients, 23 studies in SCC patients, 17 studies in BCC patients, seven studies in keratoacanthoma patients, six studies in Bowen's disease and actinic keratosis patients, and five studies in patients with seborrheic keratosis. Thirty studies (8, 10, 11, 13, 15–40) received a score of 7 on the NOS score, while 1 study (41) received a score of 6. All were classified as low risk of bias after quality assessment. However, 19 studies (42–60) had a intermediate risk of bias. **Table 1** summarizes the characteristics of the included articles, and the quality of the papers is assessed in **Table S1**.

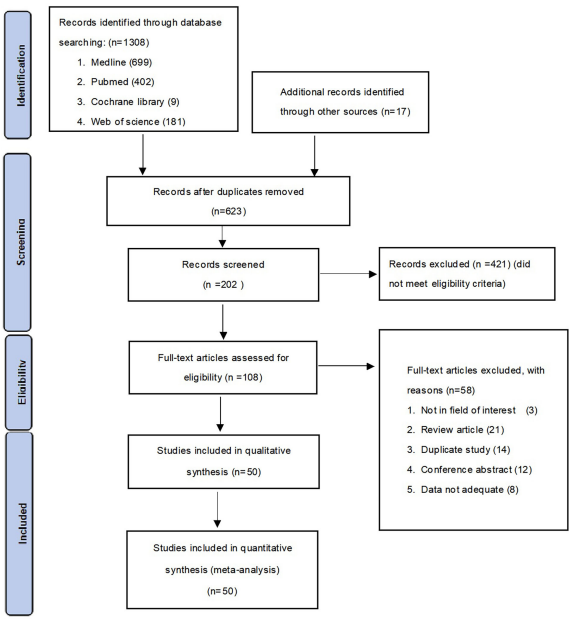

FIGURE 1 | Flow diagram of studies selection.

Primary Meta-Analysis: Merkel Cell Polyomavirus Prevalence in MCC

In the pooled analysis, the association between MCPyV and MCC was significant with an adjusted pooled OR of 3.51 (95% CI = 2.96 - 4.05, $P<0.05$) in the random-effects model due to significant heterogeneity between studies (I^2 = 58.02%) (**Figure 2**). The meta-regression analysis revealed that country (P=0.474), continent (P=0.220) and sample type (P=0.675) did not influence the heterogeneity between studies. The sensitivity analysis showed that no single study influenced the recalculated pooled ORs (**Figure S1**). Visual inspection of the funnel plot showed evidence of publication bias (**Figure S2**), which was confirmed by Egger's test(P= 0.0006) and Begg's test(P= 0.0037). We then applied the trim and fill method to correct the asymmetry of the funnel plot (**Figure S3**). Pooled analysis included the imputed studies continued to indicate a statistically significant association between MCPyV and MCC. The result showed that the effect of publication bias was not significant and the conclusion was relatively stable.

The overall pooled prevalence rate of MCPyV+ in MCC was 80% (95% CI = 71% - 88%, I^2 = 89.93%, $P<0.05$)(**Figure 3**). We then performed a subgroup analysis based on country, continent, and sample type (frozen section or formalin-fixed paraffin-embedded material). This pooled rate remained consistent in the subgroup analysis, with statistically significant heterogeneity between subgroups (**Table 2** and **Figures S4–6**). There was no obvious source of heterogeneity in the meta-regression analysis (P=0.587). The funnel plot, Egger's test (P = 0.284) and Begg's test (P = 0.173) did not indicate publication bias.

Secondary Meta-Analyses: Non-MCC Skin Lesions and Normal Skin

Melanoma

Eleven studies (11, 18, 19, 21, 22, 26, 39, 41, 46, 51, 60) investigated the prevalence rate of MCPyV+ in melanoma, the overall prevalence rate was 4% (95% CI = 1% - 9%, I^2 = 0%, P = 0.473)(**Figure 4A**). In addition, subgroup analysis by country, continent, and sample type still showed significant heterogeneity (**Table 2** and **Figures S10–12**). The funnel plot, Egger's test (P = 0.150), and Begg's test (P = 0.080) detected no publication bias.

TABLE 1 | Main characteristics of included studies.

Study	Country	Study type	Sample types	MCC	Control	Normal skin	Melanoma	SCC	BCC	Bowen	Actinic keratosis	Keratoacanthoma	Seborrheic keratoses	PCR primers	Immune status
Feng et al. 2008 (8)	USA	case control	Fr	10	84	NR	NR	NR	NR	NR	NR	NR	NR	LT1, LT3, VP1	control group: skin and skin tumor from 25 immunocompetent and immunosuppressed without MCC; MCC: NR
Kassem et al. 2008 (15)	Germany	case control	FFPE	39	45	NR	NR	NR	NR	NR	NR	NR	NR	LT1, LT3, VP1, M1/2	NR
Becker et al. 2009 (16)	Germany	case control	FFPE	53	24	NR	NR	NR	24	NR	NR	NR	NR	LT1, LT3	NR
Garneski et al. 2009 (10)	USA / Australia	case control	NR	37	30	15	NR	15	NR	NR	NR	NR	NR	LT1	NR
Helmbold et al. 2009 (17)	Germany	case control	FFPE	98	44	NR	NR	NR	NR	NR	NR	NR	NR	MCPyV	NR
Kassem et al. 2009 (42)	Germany	cross-sectional	FFPE	NR	NMSC immunosuppresed: 56; immunocompetent.: 147	NR	NR	SCC immunosuppresed: /25; immunocompetent:28	BCC immunosuppresed:18; immunocompetent:96	Bowen immunosuppresed:13; immunocompetent :24	NR	NR	NR	LT3, VP1	56 NMSC immunosuppressed ; 147 NMSC immunocompetent
Sihto et al. 2009 (18)	Finland	case control	FFPE	114	22	NR	7	NR	NR	NR	NR	NR	NR	LTA	Eight MCC subjects were considered to be immunocompromised, of which five of them were positive for MCPyV
Varga et al. 2009 (19)	Hungary	case control	FFPE	7	29	NR	3	13	10	NR	NR	NR	NR	LT1, LT3, VP1	NR
Touze et al. 2009 (20)	France	case control	FFPE/Fr	32	9	NR	NR	NR	NR	NR	NR	NR	NR	LT1, VP1	NR
Wieland et al. 2009 (21)	Germany	case control	NR	34	95	34	12	6	21	4	7	7	NR	LT1, LT3	immunocompetent
Andres et al. 2009 (22)	Germany	case control	FFPE	33	33	NR	10	NR	11	NR	NR	NR	12	LTA (MCV 138), STA (MCV 191)	NR
Bhatia et al. 2009 (23)	USA	case control	FFPE	23	52	NR	NR	NR	NR	NR	NR	NR	NR	MCPyV (EU375804)	NR
Dworkin et al. 2009 (43)	USA	cross-sectional	FFPE	NR	NR	63	NR	177	NR	NR	NR	NR	NR	LT3, VP1	immunocompetent and immunosuppressed
Foulongne et al. 2009 (24)	France	case control	FFPE/Fr	11	24	6	NR	NR	NR	NR	NR	NR	NR	LT1, LT3, VP1	NR
Sastre-Garau et al. 2009 (11)	France	case control	FFPE/Fr	10	1241	4	13	NR	13	NR	NR	NR	NR	MCV350 (MCV_ST_A, MCV_ST_B, MCV_LT_C, MCV_LT_D,MCV_VP1_A,MCV_VP1_B)	
Mertz et al. 2010 (44)	Switzerland	cross-sectional	FFPE	NR	NR	NR	NR	6	3	8	4	3	3	LT1, LT3, VP1	immunocompromised
Loyo et al. 2010 (13)	USA	case control	FFPE/Fr	7	286	9	NR	12	NR	NR	NR	NR	NR	LT3, VP1	NR
Mangana et al. 2010 (25)	Switzerland	case control	FFPE	30	19	11	NR	8	NR	NR	NR	NR	NR	LT1, LT3, VP1	NR
Jung et al. 2011 (26)	Korea	case control	FFPE	11	24	NR	12	NR	NR	NR	NR	NR	NR	LT1, LT3, VP1 LT1-1, LT1-1a, LT3a	NR
Kuwamoto et al. 2011 (41)	Japan	case control	FFPE	22	3	NR	1	1	NR	NR	NR	NR	NR	LT3, MCVPS1, MCVKW3	NR
Murakami et al. 2011 (45)	Japan	cross-sectional	FFPE	NR	NR	NR	NR	30	10	NR	NR	NR	NR	LT3, VP1	immunocompetent
Martel-Jantin et al. 2012 (27)	France	case control	FFPE/Fr	36	31	NR	NR	NR	NR	NR	NR	NR	NR	LT3, MerkT	NR
Ota et al. 2012 (46)	Japan	cross-sectional	FFPE	9	142	NR	5	NR	46	34	52	NR	5	ST, LT1, LT2, VP1, VP2, VP3	1 case in which primary MCC had developed within 2 months after a living donor liver transplantation for fulminant hepatitis of unknown etiology

(Continued)

TABLE 1 | Continued

Study	Country	Study type	Sample types	MCC	Control	Normal skin	Melanoma	SCC	BCC	Bowen	Actinic keratosis	Keratoacanthoma	Seborrheic keratoses	PCR primers	Immune status
Rodig et al. 2012 (28)	USA	case control	FFPE	51	6	NR	NR	NR	NR	NR	NR	NR	NR	LT2, Set 6, 7, 9 LT3	14 MCC patients had a prior history, comorbidity, or medication consistent with an immunocompromised state from malignancy, autoimmune disease, or solid organ transplantation.
Rollison et al. 2012 (67)	USA	cross-sectional	Fr	NR	NR	NR	NR	145	NR	NR	NR	NR	NR	LTA, VP1F	9 SCC cases reported a history of organ transplantation.
Scola et al. 2012 (68)	Germany	cross-sectional	FFPE	NR	NR	NR	NR	52	41	8	31	42	NR	LTA	immunocompetent
Wieland et al. 2012 (69)	Germany	cross-sectional	FFPE	43	NR	NR	NR	52	NR	NR	NR	42	NR	LTA	immunocompetent
Iwasaki et al. 2013 (60)	Japan	cross-sectional	FFPE	39	NR	NR	NR	NR	NR	NR	NR	NR	NR	ST, LT3, VP1	NR
Chun et al. 2013 (29)	Korea	case control	FFPE	7	32	NR	NR	8	8	NR	8	NR	8	LTA (MCV 138), STA (MCV 191)	immunocompetent
Hattori et al. 2013 (30)	Japan	case control	FFPE/Fr	26	21	NR	NR	11	10	NR	NR	NR	NR	LT1, LT3, VP1	NR
Fukumoto et al. 2013 (31)	Japan	case control	FFPE/Fr	30	183	NR	NR	NR	NR	NR	NR	NR	NR	STA, LT1,LT3, VP1, VP2, VP3	immunocompetent and immunosuppressed
Imajoh et al. 2013 (51)	Japan	cross-sectional	FFPE	NR	NR	NR	47	63	50	NR	NR	NR	NR	MCPyV (EU375804)	NR
Mertz et al. 2013 (52)	Switzerland	cross-sectional	FFPE	NR	NR	47	NR	immunocompetent:60; immunosuppressed: 15	immunocompetent : 71 ; immunosuppressed:17	NR	NR	NR	NR	LTA (DTS1, DTS2)	immunocompetent and immunosuppressed
Leroux-Kozal et al. 2015 (32)	France	case control	FFPE/Fr	36	3	NR	NR	NR	NR	NR	NR	NR	NR	LTA	immunocompetent
Falchook et al. 2015 (53)	USA	cross-sectional	FFPE	NR	NR	9	NR	12	NR	NR	NR	NR	NR	STA	NR
Bellot et al. 2016 (54)	Brazil	cross-sectional	Fr	immunosuppressed : 1	immunosuppressed: 5; immunocompetent: 86	NR	NR	11	65 ; immunosuppressed : 5	4	5	1	NR	LT3	A total of five tumours were extracted from two immuno suppressed patients (two BCCs from a kidney trans plant patient, and two BCCs and one MCC from a patient infected with human immunodeficiency virus (HIV)
Haeggblom et al. 2016 (55)	Sweden	cross-sectional	FFPE	NR	NR	NR	NR	NR	NR	NR	NR	22	NR	LTA, VP1	NR
Alvarez-Arguelles et al. 2017 (33)	Spain	case control	FFPE	34	6	NR	NR	NR	NR	NR	NR	NR	NR	VP1	Five MCC patients were immunocompromised
Avia et al. 2017 (56)	Italy	cross-sectional	FFPE	12	64	10	NR	34	NR	NR	NR	NR	NR	MCPyV	NR
Wang et al. 2017 (34)	USA	case control	FFPE	52	19	18	NR	NR	NR	NR	NR	NR	NR	MCPyV LTAg (LT2) and sTAg (SET9)	NR
Mohebbi et al. 2017 (35)	Iran	case control	FFPE	NR	NR	50	NR	50	NR	NR	NR	NR	NR	LT3, VP1	NR
Kervarrec et al. 2018 (36)	France	case control	FFPE	99	12	NR	NR	NR	NR	NR	NR	NR	NR	MCPyV VP1, LTA	immunocompetent and immunosuppressed
Hillen et al. 2018 (37)	Germany	case control	FFPE	NR	NR	16	NR	NR	NR	NR	NR	NR	23	VP1, M1M2	NR
Kim et al. 2019 (57)	Korea	cross-sectional	FFPE	NR	NR	NR	NR	NR	NR	NR	NR	10	NR	STA, LTA (MCP138, MCP191)	immunocompetent
Rekhi et al. 2019 (58)	India	cross-sectional	FFPE	12	NR	NR	NR	NR	NR	NR	NR	NR	NR	STA, LTA	NR
Neto et al. 2019 (38)	Brazil	case control	FFPE	13	20	NR	NR	NR	NR	NR	NR	NR	NR	LT1	NR

(Continued)

TABLE 1 | Continued

Study	Country	Study type	Sample types	MCC	Control	Normal skin	Melanoma	SCC	BCC	Bowen	Actinic keratosis	Keratoacanthoma	Seborrheic keratoses	PCR primers	Immune status
Goncalves et al. 2020 (59)	Brazil	cross-sectional	Fr	NR	NR	NR	NR	NR	35	NR	NR	NR	NR	L73	immunocompetent and immunosuppressed
Costa et al. 2020 (61)	Brazil	cross-sectional	FFPE	20	89	NR	14	20	20	NR	NR	NR	NR	LT1	18 patients were immunosuppressed
Mokanszki et al. 2021 (33)	Hungary	case control	FFPE	9	60	NR	60	NR	NR	NR	NR	NR	NR	LT1, LT3, VP1	NR
Motaveli et al. 2021 (60)	Iran	case control	NR	NR	NR	NR	NR	20	60	NR	NR	NR	NR	LT3, VP1	immunocompetent

Fr, Frozen section; FFPE, formalin-fixed paraffin-embedded material; NR, Not Reported; MCC, Merkel Cell Carcinoma; SCC, Squamous Cell Carcinoma; BCC, Basal Cell Carcinoma; NMSC, Non-Melanoma Skin Cancer; LTA, Large T antigen; STA, Small T antigen; PCR, Polymerase Chain Reaction.

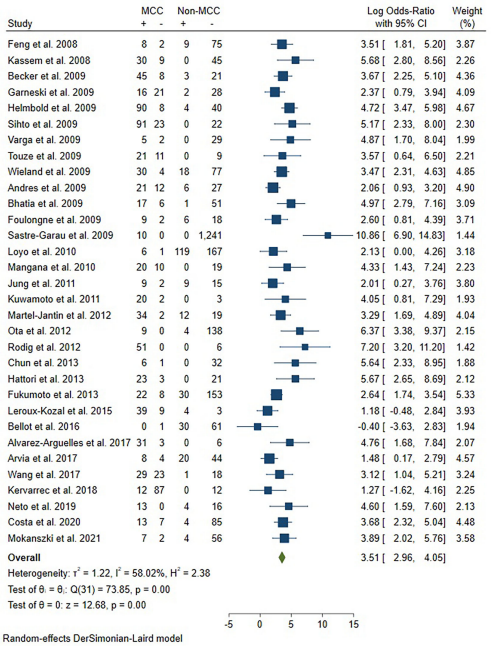

FIGURE 2 | Forest plot illustrating the odd ratio for the association between MCPyV and MCC.

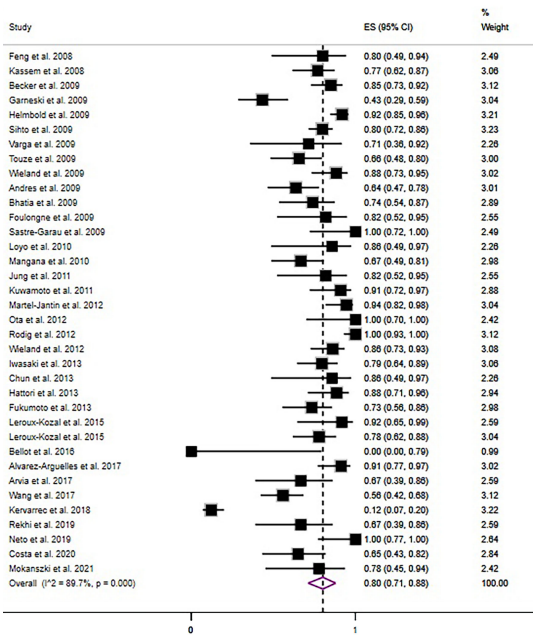

FIGURE 3 | Forest plot illustrating the pooled prevalence rate of the MCPyV positivity in MCC.

TABLE 2 | Subgroup results for MCC.

	Stratification criterion	Number of studies	Pooled results (95% CI)	I^2	P-value for difference
Merkel cell carcinoma	**Overall**	35	80% (71% - 88%)	89.93%	<0.05
	Country				
	- USA	5	83% (53% - 100%)	91.5%	<0.05
	- Germany	6	83% (75% - 90%)	65.9%	<0.05
	- USA/Australia	1	43% (29% - 59%)	-	-
	- Finland	1	80% (72% - 86%)	-	-
	- Hungary	2	75% (49% - 95%)	-	-
	- France	6	75% (36% - 99%)	96.8%	<0.05
	- Switzerland	1	67% (49% - 81%)	-	-
	- Korea	2	84% (61% - 98%)	-	-
	- Japan	5	86% (76% - 93%)	34.8%	0.19
	- Brazil	3	80% (21% - 100%)	-	-
	- Spain	1	91% (77% - 97%)	-	-
	- Italy	1	67% (39% - 86%)	-	-
	- India	1	67% (39% - 86%)	-	-
	Continent				
	- America	9	78% (54% - 96%)	89.9%	<0.05
	- Europe	18	78% (65% - 89%)	93.1%	<0.05
	- Asia	8	84% (76% - 90%)	13.3%	0.33
	Sample types				
	- Frozen section (Fr)	3	85% (46% - 100%)	-	-
	- Formalin-fixed paraffin-embedded (FFPE)	24	79% (67% - 89%)	92.2%	<0.05
	- Formalin-fixed paraffin-embedded / Frozen section (FFPE/Fr)	7	85% (74% - 94%)	59.8%	0.02
	- Not reported (NR)	2	67% (55% - 77%)	-	-
Normal skin	**Overall**	13	11% (4% - 20%)	71.2%	<0.05
	Country				
	- USA	4	19% (1%- 48%)	84.2%	<0.05
	- Germany	2	22% (11% - 35%)	-	-
	- USA/Australia	1	0% (0-20%)	-	-
	- France	2	7% (0%-37%)	-	-
	- Switzerland	2	15% (6% - 26%)	-	-
	- Italy	1	10% (2% - 40%)	-	-
	- Iran	1	2% (0% - 10%)	-	-
	Continent				
	- America	5	13% (0% - 36%)	83.5%	<0.05
	- Europe	7	15% (9% - 23%)	3.3%	0.40
	- Asia	1	2% (0% - 10%)	-	-
	Sample type				
	- Formalin-fixed paraffin-embedded (FFPE)	8	8% (3% - 16%)	57.9%	0.02
	- Formalin-fixed paraffin-embedded / Frozen section (FFPE/Fr)	3	30% (0% - 84%)	-	-
	- Not reported (NR)	2	13% (5% - 25%)	-	-
Melanoma	**Overall**	11	4% (1% - 9%)	0%	0.478
	Country				
	- Finland	1	0%(0% - 35%)	-	-
	- Hungary	2	2% (0% - 10%)	-	-
	- Germany	2	13% (1% - 32%)	-	-
	- France	1	0% (0% - 23%)	-	-
	- Korea	1	0% (0% - 24%)	-	-
	- Japan	3	8% (0% - 22%)	-	-
	- Brazil	1	7% (1% - 31%)	-	-
	Continent				
	- America	1	7% (1% - 31%)	-	-
	- Europe	6	3% (0% - 9%)	0%	0.66
	- Asia	4	2% (0% - 18%)	36.8%	0.19
	Sample type				
	- Formalin-fixed paraffin-embedded (FFPE)	9	4% (0% - 9%)	0%	0.55
	- Formalin-fixed paraffin-embedded / Frozen section (FFPE/Fr)	1	0% (0% - 23%)	-	-
	- Not reported (NR)	1	17% (5% - 45%)	-	-
Squamous cell carcinoma	**Overall**	23	15% (9% - 22%)	77.3%	<0.05
	Country				
	- USA	4	35% (15% - 57%)	91.5%	<0.05
	- Germany	4	29% (22% - 37%)	0%	0.54

(Continued)

TABLE 2 | Continued

	Stratification criterion	Number of studies	Pooled results (95% CI)	I^2	P-value for difference
	- USA/Australia	1	13% (4% - 38%)	-	-
	- Hungary	1	0% (0% - 23%)	-	-
	- Switzerland	3	8% (0% - 35%)	-	-
	- Italy	1	12% (5% - 27%)	-	-
	- Iran	2	9% (3% - 18%)	-	-
	- Korea	1	0%(0% - 32%)	-	-
	- Japan	4	10% (1% - 25%)	42.7%	0.16
	- Brazil	2	3%(0% -14%)	-	-
	Continent				
	- America	7	22% (9% - 39%)	88.1%	<0.05
	- Europe	9	18% (9% - 27%)	66%	<0.05
	- Asia	7	6% (0% - 17%)	61.7%	0.02
	Sample type				
	- Frozen section (Fr)	2	36%(28% - 44%)	-	-
	- Formalin-fixed paraffin-embedded (FFPE)	16	16% (9% - 23%)	74.9%	<0.05
	- Formalin-fixed paraffin-embedded / Frozen section (FFPE/Fr)	2	9% (0% - 26%)	-	-
	- Not reported (NR)	3	5% (0% - 24%)	-	-
Basal cell carcinoma	**Overall**	18	14% (7% - 22%)	82.6%	<0.05
	Country				
	- Germany	5	26% (14% - 40%)	71.2%	0.01
	- Hungary	1	0% (0% -28%)	-	-
	- France	1	0% (0% - 23%)	-	-
	- Switzerland	2	38% (27% - 49%)	-	-
	- Japan	4	4% (0% - 15%)	66.2%	0.03
	- Korea	1	0% (0% - 32%)	-	-
	- Brazil	3	24% (13% - 38%)	-	-
	- Iran	1	10% (5% - 20%)	-	-
	Continent				
	- America	3	24% (13% - 38%)	-	-
	- Europe	9	19% (8% - 32%)	79.4%	<0.05
	- Asia	6	5% (1% - 12%)	48.8%	0.08
	Sample type				
	- Frozen section (Fr)	2	31% (22% - 40%)	-	-
	- Formalin-fixed paraffin-embedded (FFPE)	12	14% (5% - 26%)	84.8%	<0.05
	- Formalin-fixed paraffin-embedded / Frozen section (FFPE/Fr)	2	0% (0% - 8%)	-	-
	- Not reported (NR)	2	11% (5% - 19%)	-	-
Bowen's disease	**Overall**	6	21% (2% - 48%)	81.5%	-
	Country				
	- Germany	3	32% (18% - 48%)	-	-
	- Switzerland	1	25% (7% - 59%)	-	-
	- Japan	1	0% (0% - 10%)	-	-
	- Brazil	1	50% (15% - 85%)	-	-
	Continent				
	- America	1	50% (15% - 85%)	-	-
	- Europe	4	31% (18% - 45%)	0%	0.93
	- Asia	1	0%(0% - 10%)	-	-
	Sample type				
	- Frozen section (Fr)	1	50%(15% - 85%)	-	-
	- Formalin-fixed paraffin-embedded (FFPE)	4	17% (0% - 49%)	87.6%	<0.05
	- Not reported (NR)	1	25% (5% - 70%)	-	-
Actinic keratosis	**Overall**	6	6% (0% - 17%)	38.7%	0.148
	Country				
	- Germany	2	13% (3% - 27%)	-	-
	- Switzerland	1	0% (0% - 49%)	-	-
	- Japan	1	6% (2% - 16%)	-	-
	- Korea	1	0% (0% -32%)	-	-
	- Brazil	1	40% (12% - 77%)	-	-
	Continent				
	- America	1	40% (12% - 77%)	-	-
	- Europe	3	8% (0% - 25%)	-	-
	- Asia	2	3% (0% - 11%)	-	-
	Sample type				

(Continued)

TABLE 2 | Continued

	Stratification criterion	Number of studies	Pooled results (95% CI)	I^2	P-value for difference
	- Frozen section (Fr)	1	40% (12% - 77%)	-	-
	- Formalin-fixed paraffin-embedded (FFPE)	4	6% (0% - 16%)	32%	0.22
	- Not reported (NR)	1	0% (0% - 35%)	-	-
Keratoacanthoma	**Overall**	7	20% (0% - 51%)	91.6%	<0.05
	Country				
	- Germany	3	29%(20% - 39%)	-	-
	- Switzerland	1	0% (0% - 56%)	-	-
	- Brazil	1	100% (21% - 100%)	-	-
	- Sweden	1	36% (20% - 57%)	-	-
	- Korea	1	0% (0% - 51%)	-	-
	Continent				
	- America	1	100% (21% - 100%)	-	-
	- Europe	5	28%(20% - 38%)	0%	0.64
	- Asia	1	0% (0% - 4%)	-	-
	Sample type				
	- Frozen section (Fr)	1	100% (21% - 100%)	-	-
	- Formalin-fixed paraffin-embedded (FFPE)	5	15% (0% - 44%)	93.6%	<0.05
	- Not reported (NR)	1	43% (16% - 75%)	-	-
Seborrheic keratosis	**Overall**	5	10% (1% - 24%)	20%	0.287
	Country				
	- Germany	2	23% (10% - 39%)	-	-
	- Switzerland	1	0% (0% - 56%)	-	-
	- Japan	1	0% (0% - 43%)	-	-
	- Korea	1	0% (0% - 32%)	-	-
	Continent				
	- Europe	3	18%(6% - 34%)	-	-
	- Asia	2	0%(0% - 14%)	-	-
	Sample type				
	- Formalin-fixed paraffin-embedded (FFPE)	5	10% (1% - 24%)	20%	0.29

Squamous Cell Carcinoma

Twenty three studies (10, 13, 19, 21, 25, 29, 30, 35, 40–45, 47–49, 51–54, 56, 60) reported the prevalence rate of MCPyV+ in squamous cell carcinoma samples, with the overall prevalence rate was 15%(95% CI = 9% - 22%, I^2 = 77.3%, P<0.05) (**Figure 4B**). The pooled prevalence rate remained similar in the stratified analysis, with statistically significant heterogeneity across all subgroups(**Table 2** and **Figures S13-15**). We discovered a significant difference in pooled MCPyV+ prevalence in squamous cell carcinoma in American studies 22%(95% CI = 9% - 39%) when compared to Asian studies 6% (95% CI = 0% - 17%), but not when compared to prevalence in Europe 18%(95% CI = 9% - 27%). The point estimates for the prevalence of MCPyV+ in squamous cell carcinoma in frozen section sample 36%(95% CI = 28% - 44%) was twice of the formalin-fixed paraffin-embedded sample. There was no evidence of publication bias as indicated by funnel plot analysis, Egger's test(P = 0.133), and Begg's test(P = 0.065).

Basal Cell Carcinoma

The 18 included studies (11, 16, 19, 21, 22, 29, 30, 40, 42, 44–46, 48, 51, 52, 54, 59, 60) reported the prevalence rate of the MCPyV+ in basal cell carcinoma, with the overall prevalence rate was 14%(95% CI = 7% - 22%, I^2 = 82.58%, P<0.05) (**Figure 4C**). Stratification analysis showed increasing trends for American studies 24%(95% CI = 13% - 38%) and stable trends for European 19%(95% CI = 8% - 32%) and Asian studies 5%(95% CI = 1% - 12%). Frozen section samples 31%(95% CI = 22% - 40%) showed a higher prevalence rate than FFPE samples 14%(95% CI = 5% - 26%). While stratification analysis still showed significant heterogeneity(**Table 2 and Figures S16-18**). According to the funnel plot, Egger's test(P = 0.059), and Begg's test(P = 0.075), there was no significant publication bias across the studies for either analysis.

Bowen's Disease

Several studies (21, 42, 44, 46, 48, 54) investigated the prevalence rate of MCPyV+ in Bowen's disease, with the pooled prevalence rate was 21%(95% CI = 2% - 48%, I^2 = 81.53%, P<0.05) (**Figure 4D**). All subgroup analysis still showed significant heterogeneity (**Table 2** and **Figures S19-21**). In addition, there was an apparent lower prevalence in Asia than Americas(0% vs 50%). The funnel plot, Egger's test(P = 0.257), and Begg's test(P = 0.388) revealed no substantial publication bias.

Actinic Keratosis

The pooled analysis of six studies (21, 29, 44, 46, 48, 54) reporting the prevalence of MCPyV+ in actinic keratosis showed a prevalence rate of 6%(95% CI = 0% - 17%, I^2 = 38.69%, P = 0.15)(**Figure 4E**). Results of the stratification analysis are shown in **Table 2** and **Figures S22-24**. Visual inspection of the funnel plot, Egger's test(P = 0.899), and Begg's test(P = 0.274), there was no evidence of significant publication bias.

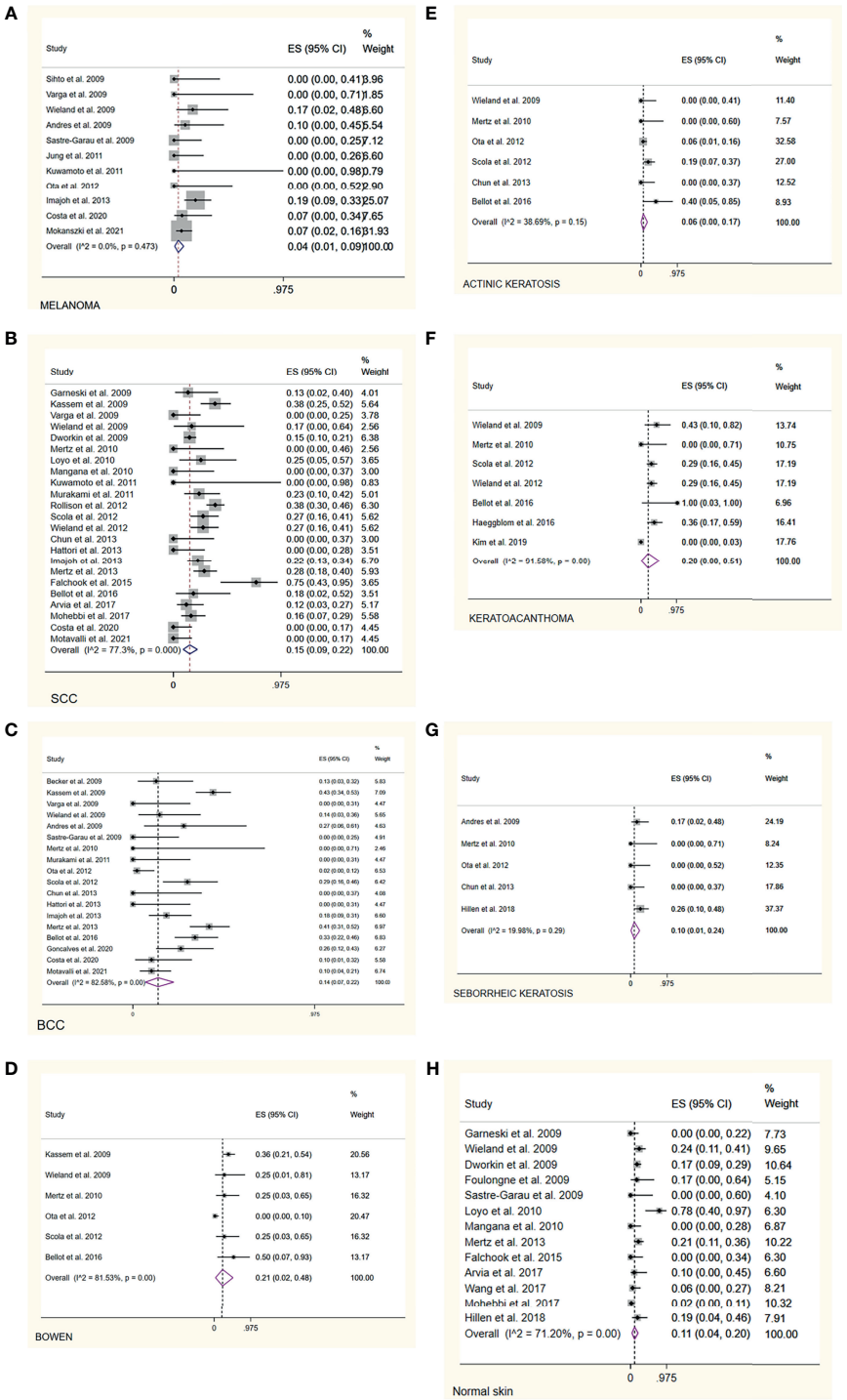

FIGURE 4 | Forest plot illustrating the pooled prevalence rate of the MCPyV positivity in non-MCC skin lesions and normal skin. **(A)** melanoma; **(B)** squamous cell carcinoma; **(C)** basal cell carcinoma; **(D)** Bowen's disease; **(E)** actinic keratosis; **(F)** keratoacanthoma; **(G)** seborrheic keratosis; **(H)** normal skin.

Keratoacanthoma

According to seven publications (21, 44, 48, 49, 54, 55, 57) that examined the prevalence rate of MCPyV+ in keratoacanthoma, the pooled prevalence rate was 20%(95% CI = 0% - 51%), I^2 = 91.58%, P<0.05)(**Figure 4F**). Stratified analysis showed statistically significant heterogeneity in all subgroups, although the pooled prevalence rate remained identical (**Table 2** and **Figures S25–27**). There was no evidence of substantial

publication bias, as determined by visual inspection of the funnel plot, Egger's test(P = 0.126), and Begg's test(P = 0.301).

Seborrheic Keratosis

Five studies (22, 29, 37, 44, 46) were included in the analysis of the prevalence rate of MCPyV+ in seborrheic keratosis, with the overall prevalence rate was 10% (95% CI = 1% - 24%, I^2 = 19.98%, P = 0.29)(**Figure 4G**). This pooled rate remained consistent in subgroup analysis, with statistically significant heterogeneity between subgroups (**Table 2** and **Figures S28-30**). According to the funnel plot analysis, Egger's test(P = 0.105), and Begg's test(P = 0.072) there was no evidence of publication bias.

Normal Skin

Based on data from 13 publications (10, 11, 13, 21, 24, 25, 34, 35, 37, 43, 52, 53, 56) the overall pooled estimate of the prevalence of MCPyV+ in normal skin was 11% (95% CI = 4% - 20%, I^2 = 71.2%, P<0.05)(**Figure 4H**). Further stratification by country, continent, and sample type are shown in **Table 2** and **Figures S7-9**. In the USA, the American continent, and the FFPE study subgroups, heterogeneity remained significant. No publication bias was detected by funnel plot, Egger's test (P = 0.967), or Begg's test (P = 0.802).

DISCUSSION

Numerous factors contribute to the aetiology of non-MCC skin lesions, including UV exposure, immunosuppression, and ageing, which are also risk factors for the development of MCC (45, 53). Feng et al. (8) first discovered MCPyV as a human polyomavirus that reveals clonal integration in MCC. MCPyV showed that the viral genome was integrated into the host genome, disrupting the late region. In addition, a C-terminal truncated LT was expressed. The helicase activity of LT, which is required for viral DNA replication, was removed by this deletion (16). MCPyV infects the majority of people and, according to seroepidemiological studies, causes lifelong harmless chronic infection in healthy people (61–63). MCPyV is also regularly shed from the skin of healthy people, proving that it is a component of the human skin microbiome (64). Dermal fibroblast cells could be the natural host cell for replication of MCPyV in the human body, as the virus could be propagated in human dermal fibroblast cell cultures (65). The role of MCPyV in the development of MCC and the wide distribution of the virus in the body prompted researchers to investigate the prevalence of MCPyV in non-MCC skin lesions. Several studies have shown clonal integration of MCPyV in the non-MCC skin lesions. However, the prevalence of MCPyV in the MCC and non-MCC skin lesions is still controversial. Our study aimed to shed light on this matter.

To the best of our knowledge, this is the first systematic review and meta-analysis to provide comprehensive, up-to-date estimates of the association of MCPyV in MCC and non-MCC skin lesions. We identified a global pooled prevalence of 80% MCPyV+ among 1112 patients with MCC. This finding is consistent with a previous meta-analysis by Santos-Juanes et al. (66) which reported a prevalence of 79%. A geographic and sample type variation of MCPyV+ MCC has well been documented in a previous study. Data from the Americas and Europe show that nearly 80% of MCC cases are MCPyV+ (10, 67), while studies from Australia found that only 24% of cases are MCPyV+ (67). The lower prevalence of MCPyV+ in Australian studies compared to other continents may be due to the increased sun exposure in Australia, making a possible viral contribution less common and the possibility that a different and unknown strain of MCPyV is undetectable (10). In Asia, MCPyV+ is found in 76.9% to 88.5% of Japanese (29, 41, 45, 46, 48), 81.2% to 85.71% of Korean (29, 57), and 25% of Indian MCC patients (58). Several studies have shown that the MCPyV detection rate of DNA was greater in frozen samples than in FFPE tissue samples (12, 27). On the contrary, through subgroup analyses, we found no significant differences in the prevalence rate of MCPyV+ MCC among countries, continents, and different sample types (**Table 2**).

The discovery of MCPyV DNA in non-melanoma skin cancers(NMSCs) from immunocompromised people was the first observation linking MCPyV to non-MCC (15). MCPyV was later found in various non-MCC skin lesions and normal skin (**Table 1**). Recent studies showed that non-MCC skin lesions significantly have lower MCPyV DNA viral loads than in MCC. MCPyV DNA was significantly positive in non-melanoma skin cancer in immunosuppressed patients compared with non-immunosuppressed patients (38, 48, 68). Our meta-analytic study showed that the pooled prevalence rate of MCPyV+ in melanoma, SCC, BCC, Bowen's disease, actinic keratosis, keratoacanthoma, seborrheic keratosis, and normal skin was 4%, 15%, 14%, 21%, 6%, 20%, 10%, and 11%, respectively (**Table 2**). The low prevalence rate of MCPyV in non-MCC skin lesions, which is similar or even lower to that in normal skin, suggests that MCPyV probably plays a minor role in the development of non-MCC skin lesions. Subgroup analysis by continent showed that trends were higher in the Americas for SCC, BCC, Bowen's disease, actinic keratosis, and keratoacanthomas, with the corresponding rates being lower or relatively similar to the overall pooled prevalence in the Asian and European continents, respectively. In addition, we found that the detection rate for DNA extracted from frozen section samples was higher than for DNA extracted from FFPE samples, suggesting that degradation of DNA in FFPE tissues caused by formalin fixation makes PCR less sensitive (12, 20, 24, 27). The presence of MCPyV DNA in the skin and non-MCC skin lesions might not be a surprising phenomenon, as one would expect, because it is due to the ability of HPyVs to infect the skin and remain in a latent form that can be reactivated in states of profound immunosuppression (69, 70). MCPyV is a cutaneous microbe that is generally acquired in early childhood when it has the opportunity to integrate into the host genome of dermal fibroblast cells (65, 71). Regardless of these findings, it is apparent that the presence of MCPyV DNA alone is not sufficient to cause malignancy (38). Therefore, the oncogenic

significance of MCPyV in non-MCC skin lesions is still debatable.

The limitations of our article also warrant considerations. First, because randomized trials are neither currently available nor likely to be conducted in the future, this meta-analysis relies on observational data. As a result, unmeasured biases in individual studies must be taken into consideration. Second, further assessment revealed that there were several sources of heterogeneity among the included studies: (1) heterogeneity of study population(age, gender, immune status, smoking and drinking habits, geographic differences, sun exposure, etc.), (2) the relatively small number of specimens examined may give a wrong view of the prevalence of MCPyV in specific samples, (3) methods performed to detect MCPyV viral load(i.e., primers selection, viral DNA copy number, etc.), and (4) PCR screening method (i.e., the quality of the samples, viral gene target selection, DNA extraction method, primer selection, PCR technique, false-positivity due to PCR contamination, etc.). To overcome these problems and convincingly determine MCPyV positivity, several multimodal approaches have recently been proposed, such as immunohistochemistry and PCR assay (IHC + PCR), fluorescence *in situ* hybridization(FISH) coupled with DNA hybridization chain reaction(HCR-DNA FISH), etc., which have been shown to be a highly sensitive approach to detect the viral genome in tissue samples (72, 73). Third, MCPyV may contribute to cancer onset through a "hit-and-run" mechanism (74, 75). Therefore, tumor samples from different stages should be examined because the virus has only transient effects in cellular transformation, as it can be silenced or its genome lost during cancer progression (76).

CONCLUSION

Our results suggest a ubiquitous distribution of MCPyV in the skin with higher MCPyV positivity in MCC tumors, closely linking MCPyV as a putative etiologic agent to the carcinogenesis of MCC. However, the significantly lower prevalence rate of MCPyV+ in non-MCC skin lesions does not exclude a pathogenic association of this virus with the development of non-MCC skin lesions. Further large-scale studies using uniform viral genome detection methods are needed to determine the precise role of MCPyV in MCC pathogenesis and to define the significance of detecting viral DNA in non-MCC skin lesions.

DATA AVAILABILITY STATEMENT

The original contributions presented in the study are included in the article/**Supplementary Material**. Further inquiries can be directed to the corresponding authors.

AUTHOR CONTRIBUTIONS

WW, conceptualization, methodology, visualization, and writing—original draft preparation, formal analysis, investigation, writing— review and editing, and supervision. ZL, YQ, supervision and funding acquisition. WW, YL methodology and visualization. YL data curationand sample contribution. All authors contributed to the article and approved the submitted version.

FUNDING

This research article was funded by the Science and Technology Support Program of Science and Technology Department of Sichuan Province (2020YFS0267), the Key Project Research and Invention Program of Science and Technology Department of Sichuan Province(2021YFS0245), the National Natural Science Foundation of China (81871574).

SUPPLEMENTARY MATERIAL

The Supplementary Material for this article can be found online at: https://www.frontiersin.org/articles/10.3389/fonc.2022.868781/full#supplementary-material

REFERENCES

1. Harms KL, Healy MA, Nghiem P, Sober AJ, Johnson TM, Bichakjian CK, et al. Analysis of Prognostic Factors From 9387 Merkel Cell Carcinoma Cases Forms the Basis for the New 8th Edition AJCC Staging System. *Ann Surg Oncol* (2016) 23:3564–71. doi: 10.1245/s10434-016-5266-4
2. Harms PW. Update on Merkel Cell Carcinoma. *Clin Lab Med* (2017) 37:485–501. doi: 10.1016/j.cll.2017.05.004
3. Toker C. Trabecular Carcinoma of the Skin. *Arch Dermatol* (1972) 105:107–10. doi: 10.1001/archderm.105.1.107
4. Bichakjian CK, Lowe L, Lao CD, Sandler HM, Bradford CR, Johnson TM, et al. Merkel Cell Carcinoma: Critical Review With Guidelines for Multidisciplinary Management. *Cancer* (2007) 110:1–12. doi: 10.1002/cncr.22765
5. Rockville Merkel Cell Carcinoma Group. Merkel Cell Carcinoma: Recent Progress and Current Priorities on Etiology, Pathogenesis, and Clinical Management. *J Clin Oncol* (2009) 27:4021–6. doi: 10.1200/JCO.2009.22.6605
6. Hodgson NC. Merkel Cell Carcinoma: Changing Incidence Trends. *J Surg Oncol* (2005) 89:1–4. doi: 10.1002/jso.20167
7. zur Hausen H. A Specific Signature of Merkel Cell Polyomavirus Persistence in Human Cancer Cells. *Proc Natl Acad Sci USA* (2008) 105:16063. doi: 10.1073/pnas.0808973105
8. Feng H, Shuda M, Chang Y, Moore PS. Clonal Integration of a Polyomavirus in Human Merkel Cell Carcinoma. *Science* (2008) 319(5866):1096–100. doi: 10.1126/science.1152586
9. Lim ES, Reyes A, Antonio M, Saha D, Ikumapayi UN, Adeyemi M, et al. Discovery of STL Polyomavirus, a Polyomavirus of Ancestral Recombinant Origin That Encodes a Unique T Antigen by Alternative Splicing. *Virology* (2013) 436(2):295–303. doi: 10.1016/j.virol.2012.12.005
10. Garneski KM, Warcola AH, Feng Q, Kiviat NB, Leonard JH, Nghiem P. Merkel Cell Polyomavirus is More Frequently Present in North American Than Australian Merkel Cell Carcinoma Tumors. *J Invest Dermatol* (2009) 129(1):246–8. doi: 10.1038/jid.2008.229
11. Sastre-Garau X, Peter M, Avril MF, Laude H, Couturier J, Rozenberg F, et al. Merkel Cell Carcinoma of the Skin: Pathological and Molecular Evidence for a Causative Role of MCV in Oncogenesis. *J Pathol* (2009) 218(1):48–56. doi: 10.1002/path.2532

12. Laude HC, Jonchere B, Maubec E, Carlotti A, Marinho E, Couturaud B, et al. Distinct Merkel Cell Polyomavirus Molecular Features in Tumour and non Tumour Specimens From Patients With Merkel Cell Carcinoma. *PloS Pathog* (2010) 6(8):e1001076. doi: 10.1371/journal.ppat.1001076
13. Loyo M, Guerrero-Preston R, Brait M, Hoque MO, Chuang A, Kim MS, et al. Quantitative Detection of Merkel Cell Virus in Human Tissues and Possible Mode of Transmission. *Int J Cancer* (2010) 126(12):2991–6. doi: 10.1002/ijc.24737
14. Wells G, Shea B, O'Connell D, Peterson J, Welch V, Losos M, Tugwell P, et al. *The Newcastle–Ottawa Scale (NOS) for Assessing the Quality of Nonrandomised Studies in Metaanalysis*. Available at: http://www.ohri.ca/programs/clinical_epidemiology/oxford.asp.
15. Kassem A, Schopflin A, Diaz C, Weyers W, Stickeler E, Werner M, et al. Frequent Detection of Merkel Cell Polyomavirus in Human Merkel Cell Carcinomas and Identification of a Unique Deletion in the VP1 Gene. *Cancer Res* (2008) 68(13):5009–13. doi: 10.1158/0008-5472.CAN-08-0949
16. Becker JC, Houben R, Ugurel S, Trefzer U, Pfohler C, Schrama D. MC Polyomavirus is Frequently Present in Merkel Cell Carcinoma of European Patients. *J Invest Dermatol* (2009) 129(1):248–50. doi: 10.1038/jid.2008.198
17. Helmbold P, Lahtz C, Enk A, Herrmann-Trost P, Marsch WCH, Kutzner H, et al. Frequent Occurrence of RASSF1A Promoter Hypermethylation and Merkel Cell Polyomavirus in Merkel Cell Carcinoma. Research Support, non-U.S. Gov't. *Mol Carcinog* (2009) 48(10):903–9. doi: 10.1002/mc.20540
18. Sihto H, Kukko H, Koljonen V, Sankila R, Bohling T, Joensuu H. Clinical Factors Associated With Merkel Cell Polyomavirus Infection in Merkel Cell Carcinoma. *J Natl Cancer Instit* (2009) 101(13):938–45. doi: 10.1093/jnci/djp139
19. Varga E, Kiss M, Szabo K, Kemeny L. Detection of the Merkel Cell Polyomavirus (MCV) DNA in Tumor Samples of Merkel Cell Carcinoma Patients. Conference Abstract. *J Invest Dermatol* (2009) 129(2):S74. doi: 10.1111/j.1365-2133.2009.09221
20. Touze A, Gaitan J, Maruani A, Le Bidre E, Doussinaud A, Clavel C, et al. Merkel Cell Polyomavirus Strains in Patients With Merkel Cell Carcinoma. *Emerg Infect Dis* (2009) 15(6):960–2. doi: 10.3201/eid1506.081463
21. Wieland U, Mauch C, Kreuter A, Krieg T, Pfister H. Merkel Cell Polyomavirus Is Prevalent in Normal and Lesional Skin and Mucosa of Individuals Without Merkel Cell Carcinoma. Conference Abstract. *J Invest Dermatol* (2009) 129(2):S101. doi: 10.3201/eid1509.081575
22. Andres C, Belloni B, Puchta U, Sander CA, Flaig MJ. Prevalence of Mcpyv in Merkel Cell Carcinoma and non-MCC Tumors. *J Cutaneous Pathol* (2010) 37(1):28–34. doi: 10.1111/j.1600-0560.2009.01352.x
23. Bhatia K, Goedert JJ, Modali R, Preiss L, Ayers LW. Merkel Cell Carcinoma Subgroups by Merkel Cell Polyomavirus DNA Relative Abundance and Oncogene Expression. *Int J Cancer* (2010) 126(9):2240–6. doi: 10.1002/ijc.24676
24. Foulongne V, Dereure O, Kluger N, Molès J, Guillot B, Segondy M. Merkel Cell Polyomavirus DNA Detection in Lesional and Nonlesional Skin From Patients With Merkel Cell Carcinoma or Other Skin Diseases. *Br J Dermatol* (2010) 162(1):59–63. doi: 10.1111/j.1365-2133.2009.09381.x
25. Mangana J, Dziunycz P, Kerl K, Dummer R, Cozzio A. Prevalence of Merkel Cell Polyomavirus Among Swiss Merkel Cell Carcinoma Patients. *Dermatology* (2010) 221(2):184–8. doi: 10.1159/000315067
26. Jung HS, Choi YL, Choi JS, Roh JH, Pyon JK, Woo KJ, et al. Detection of Merkel Cell Polyomavirus in Merkel Cell Carcinomas and Small Cell Carcinomas by PCR and Immunohistochemistry. *Histol Histopathol* (2011) 26(10):1231–41. doi: 10.14670/HH-26.1231
27. Martel-Jantin C, Filippone C, Cassar O, Peter M, Tomasic G, Vielh P, et al. Genetic Variability and Integration of Merkel Cell Polyomavirus in Merkel Cell Carcinoma. *Virology* (2012) 426(2):134–42. doi: 10.1016/j.virol.2012.01.018
28. Rodig SJ, Cheng JW, Wardzala J, DoRosario A, Scanlon JJ, Laga AC, et al. Improved Detection Suggests All Merkel Cell Carcinomas Harbor Merkel Polyomavirus. *J Clin Invest* (2012) 122(12):4645–53. doi: 10.1172/JCI64116
29. Chun SM, Yun SJ, Lee SC, Won YH, Lee JB. Merkel Cell Polyomavirus is Frequently Detected in Korean Patients With Merkel Cell Carcinoma. *Ann Dermatol* (2013) 25(2):203–7. doi: 10.5021/ad.2013.25.2.203
30. Hattori T, Takeuchi Y, Takenouchi T, Hirofuji A, Tsuchida T, Kabumoto T, et al. The Prevalence of Merkel Cell Polyomavirus in Japanese Patients With Merkel Cell Carcinoma. Multicenter Study. *J Dermatol Sci* (2013) 70(2):99–107. doi: 10.1016/j.jdermsci.2013.02.010
31. Fukumoto H, Sato Y, Hasegawa H, Katano H. Frequent Detection of Merkel Cell Polyomavirus DNA in Sera of HIV-1-Positive Patients. *Virol J* (2013) 10:84. doi: 10.1186/1743-422X-10-84
32. Leroux-Kozal V, Leveque N, Brodard V, Lesage C, Dudez O, Makeieff M, et al. Merkel Cell Carcinoma: Histopathologic and Prognostic Features According to the Immunohistochemical Expression of Merkel Cell Polyomavirus Large T Antigen Correlated With Viral Load. *Hum Pathol* (2015) 46(3):443–53. doi: 10.1016/j.humpath.2014.12.001
33. Alvarez-Arguelles ME, Melon S, Rojo S, Fernandez-Blázquez A, Boga JA, Palacio A, et al. Detection and Quantification of Merkel Cell Polyomavirus. Analysis of Merkel Cell Carcinoma Cases From 1977 to 2015. *J Med Virol* (2017) 89(12):2224–9. doi: 10.1002/jmv.24896
34. Wang L, Harms PW, Palanisamy N, Carskadon S, Cao X, Siddiqui J, et al. Age and Gender Associations of Virus Positivity in Merkel Cell Carcinoma Characterized Using a Novel RNA *in Situ* Hybridization Assay. *Clin Cancer Res* (2017) 23(18):5622–30. doi: 10.1158/1078-0432.CCR-17-0299
35. Mohebbi E, Noormohamadi Z, Sadeghi-Rad H, Sadeghi F, Yahyapour Y, Vaziri F, et al. Low Viral Load of Merkel Cell Polyomavirus in Iranian Patients With Head and Neck Squamous Cell Carcinoma: Is it Clinically Important? *J Med Virol* (2018) 90(2):344–50. doi: 10.1002/jmv.24953
36. Kervarrec T, Samimi M, Gaboriaud P, Gheit T, Beby-Defaux A, Houben R, et al. Detection of the Merkel Cell Polyomavirus in the Neuroendocrine Component of Combined Merkel Cell Carcinoma. *Virchows Archiv* (2018) 472(5):825–37. doi: 10.1007/s00428-018-2342-0
37. Hillen LM, Rennspiess D, Speel EJ, Haugg AM, Winnepenninckx V, Hausen AZ. Detection of Merkel Cell Polyomavirus in Seborrheic Keratosis. *Front Microbiol* (2018) 8:2648. doi: 10.3389/fmicb.2017.02648
38. Neto CF, Oliveira WRP, Costa PVA, Cardoso MK, Barreto PG, Romano CM, et al. The First Observation of the Association of Merkel Cell Polyomavirus and Merkel Cell Carcinoma in Brazil. *Int J Dermatol* (2019) 58(6):703–6. doi: 10.1111/ijd.14325
39. Mokánszki A, Méhes G, Csoma SL, Kollár S, Chang Chien YC. Molecular Profiling of Merkel Cell Polyomavirus-Associated Merkel Cell Carcinoma and Cutaneous Melanoma. *Diagn (Basel)* (2021) 11(2):212. doi: 10.3390/diagnostics11020212
40. Motavalli Khiavi F, Nasimi M, Rahimi H. Merkel Cell Polyomavirus Gene Expression and Mutational Analysis of Large Tumor Antigen in non-Merkel Cell Carcinoma Tumors of Iranian Patients. *Public Health Genomics* (2021) 23(5-6):210–7. doi: 10.1159/000510254
41. Kuwamoto S, Higaki H, Kanai K, Iwasaki T, Sano H, Nagata K, et al. Association of Merkel Cell Polyomavirus Infection With Morphologic Differences in Merkel Cell Carcinoma. *Hum Pathol* (2011) 42(5):632–40. doi: 10.1016/j.humpath.2010.09.011
42. Kassem A, Technau K, Kurz AK, Pantulu D, Löning M, Kayser G, et al. Merkel Cell Polyomavirus Sequences Are Frequently Detected in Nonmelanoma Skin Cancer of Immunosuppressed Patients. *Int J Cancer* (2009) 125(2):356–61. doi: 10.1002/ijc.24323
43. Dworkin AM. Merkel Cell Polyomavirus in Cutaneous Squamous Cell Carcinoma of Immunocompetent Individuals. *J Invest Dermatol* (2011) 131(6):1388–8. doi: 10.1038/jid.2011.97
44. Mertz K, Pfaltz M, Junt T, Schmid M, Fernandez Figueras MT, Pfaltz K, et al. Merkel Cell Polyomavirus Is Present in Common Warts and Carcinoma *in Situ* of the Skin. *Hum Pathol* (2010) 41(10):1369–79. doi: 10.1016/j.humpath.2010.01.023
45. Murakami M, Imajoh M, Ikawa T, Nakajima H, Kamioka M, Nemoto Y, et al. Presence of Merkel Cell Polyomavirus in Japanese Cutaneous Squamous Cell Carcinoma. *J Clin Virol* (2011) 50(1):37–41. doi: 10.1016/j.jcv.2010.09.013
46. Ota S, Ishikawa S, Takazawa Y, Goto A, Fujii T, Ohashi K, et al. Quantitative Analysis of Viral Load Per Haploid Genome Revealed the Different Biological Features of Merkel Cell Polyomavirus Infection in Skin Tumor. *PloS One* (2012) 7(6):e39954. doi: 10.1371/journal.pone.0039954
47. Rollison DE, Giuliano AR, Messina JL, Fenske NA, Cherpelis BS, Sondak VK, et al. Case-Control Study of Merkel Cell Polyomavirus Infection and Cutaneous Squamous Cell Carcinoma. *Cancer Epidemiol Biomark Prev* (2012) 21(1):74–81. doi: 10.1158/1055-9965.EPI-11-0764

48. Scola N, Wieland U, Silling S, Altmeyer P, Stucker M, Kreuter A. Prevalence of Human Polyomaviruses in Common and Rare Types of non-Merkel Cell Carcinoma Skin Cancer. *Br J Dermatol* (2012) 167(6):1315–20. doi: 10.1111/j.1365-2133.2012.11141.x
49. Wieland U, Scola N, Stolte B, Stucker M, Silling S, Kreuter A. No Evidence for a Causal Role of Merkel Cell Polyomavirus in Keratoacanthoma. *J Am Acad Dermatol* (2012) 67(1):41–6. doi: 10.1016/j.jaad.2011.07.026
50. Iwasaki T, Matsushita M, Kuwamoto S, Kato M, Murakami I, Higaki-Mori H, et al. Usefulness of Significant Morphologic Characteristics in Distinguishing Between Merkel Cell Polyomavirus-Positive and Merkel Cell Polyomavirus-Negative Merkel Cell Carcinomas. *Hum Pathol* (2013) 44(9):1912–7. doi: 10.1016/j.humpath.2013.01.026
51. Imajoh M, Hashida Y, Nakajima H, Sano S, Daibata M. Prevalence and Viral DNA Loads of Three Novel Human Polyomaviruses in Skin Cancers From Japanese Patients. *J Dermatol* (2013) 40(8):657–60. doi: 10.1111/1346-8138.12180
52. Mertz KD, Paasinen A, Arnold A, Baumann M, Offner F, Willi N, et al. Merkel Cell Polyomavirus Large T Antigen Is Detected in Rare Cases of Nonmelanoma Skin Cancer. *J Cutaneous Pathol* (2013) 40(6):543–9. doi: 10.1111/cup.12129
53. Falchook GS, Rady P, Konopinski JC, Busaidy N, Hess K, Hymes S, et al. Merkel Cell Polyomavirus and Human Papilloma Virus in Proliferative Skin Lesions Arising in Patients Treated With BRAF Inhibitors. *Arch Dermatol Res* (2016) 308(5):357–65. doi: 10.1007/s00403-016-1650-y
54. Bellott TR, Baez CF, Almeida SG, Venceslau MT, Zalis MG, Guimarães MA, et al. Molecular Prevalence of Merkel Cell Polyomavirus in Nonmelanoma Skin Cancer in a Brazilian Population. *Clin Exp Dermatol* (2017) 42(4):390–394. doi: 10.1111/ced.13069
55. Haeggblom L, Franzen J, Nasman A. Human Polyomavirus DNA Detection in Keratoacanthoma and Spitz Naevus: No Evidence for a Causal Role. *J Clin Pathol* (2017) 70(5):451–3. doi: 10.1136/jclinpath-2016-204197
56. Arvia R, Sollai M, Pierucci F, Urso C, Massi D, Zakrzewska K. Droplet Digital PCR (Ddpcr) vs Quantitative Real-Time PCR (Qpcr) Approach for Detection and Quantification of Merkel Cell Polyomavirus (Mcpyv) DNA in Formalin Fixed Paraffin Embedded (FFPE) Cutaneous Biopsies. *J Virol Methods* (2017) 246:15–20. doi: 10.1016/j.jviromet.2017.04.003
57. Kim DK. No Association Between Merkel Cell Polymavirus Infection and Keratoacanthoma in Korean Patients. *Asian Pacific J Cancer Prevention: APJCP* (2019) 20(5):1299–301. doi: 10.31557/APJCP.2019.20.5.1299
58. Rekhi B, Arora R, Chandrani P, Krishna S, Dutt A. Merkel Cell Polyomavirus is Implicated in a Subset of Cases of Merkel Cell Carcinomas From the Indian Subcontinent. *Conf Abstract Modern Pathol* (2020) 33(3):491–2. doi: 10.1016/j.micpath.2019.103778
59. Goncalves MTV, Varella RB, Almeida NKO, Guimaraes M, Luz FB. Molecular Detection of Merkel Cell Polyomavirus in Basal Cell Carcinoma and Perilesional Tissue: A Cross-Sectional Study. *Anais Brasileiros Dermatol* (2020) 95(4):527–8. doi: 10.1016/j.abd.2019.10.007
60. Costa PVA, Ishiy PS, Urbano PRP, Romano CM, Tyring SK, Oliveira WRP, et al. Identification of Polyomaviruses in Skin Cancers. *Intervirology* (2021) 64 (3):119–25. doi: 10.1159/000513544
61. Kean JM, Rao S, Wang M, Garcea RL. Seroepidemiology of Human Polyomaviruses. *PloS Pathog* (2009) 5:e1000363. doi: 10.1371/journal.ppat.1000363
62. Pastrana DV, Tolstov YL, Becker JC, Moore PS, Chang Y, Buck CB. Quantitation of Human Seroresponsiveness to Merkel Cell Polyomavirus. *PloS Pathog* (2009) 5(9):e1000578. doi: 10.1371/journal.ppat.1000578
63. Kamminga S, van der Meijden E, Feltkamp MCW, Zaaijer HL. Seroprevalence of Fourteen Human Polyomaviruses Determined in Blood Donors. *PloS One* (2018) 13(10):e0206273. doi: 10.1371/journal.pone.0206273
64. Schowalter RM, Pastrana DV, Pumphrey KA, Moyer AL, Buck CB. Merkel Cell Polyomavirus and Two Previously Unknown Polyomaviruses are Chronically Shed From Human Skin. *Cell Host Microbe* (2010) 7:509–15. doi: 10.1016/j.chom.2010.05.006
65. Liu W, Yang R, Payne AS, Schowalter RM, Spurgeon ME, Lambert PF, et al. Identifying the Target Cells and Mechanisms of Merkel Cell Polyomavirus Infection. *Cell Host Microbe* (2016) 19:775–87. doi: 10.1016/j.chom.2016.04.024
66. Santos-Juanes J, Fernandez-Vega I, Fuentes N, Galache C, Coto-Segura P, Vivanco B, et al. Merkel Cell Carcinoma and Merkel Cell Polyomavirus: A Systematic Review and Meta-Analysis. *Rev Br J Dermatol* (2015) 173(1):42–9. doi: 10.1111/bjd.13870
67. Colunga A, Pulliam T, Nghiem P. Merkel Cell Carcinoma in the Age of Immunotherapy: Facts and Hopes. *26 Clin Cancer Res* (2018) 24:2035–43. doi: 10.1158/1078-0432.CCR-17-0439
68. Dalianis T, Hirsch HH. Human Polyomaviruses in Disease and Cancer. *Virology* (2013) 437(2):63–72. doi: 10.1016/j.virol.2012.12.015
69. Moens U, Ludvigsen M, Van Ghelue M. Human Polyomaviruses in Skin Diseases. *Patholog Res Int* (2011) 2011:123491–12. doi: 10.4061/2011/123491
70. Sheu JC, Tran J, Rady PL, Dao H, Tyring SK, Nguyen HP. Polyomaviruses of the Skin: Integrating Molecular and Clinical Advances in an Emerging Class of Viruses. *Br J Dermatol* (2019) 180(6):1–10. doi: 10.1111/bjd.17947
71. Amber K, McLeod MP, Nouri K. The Merkel Cell Polyomavirus and its Involvement in Merkel Cell Carcinoma. *Dermatol Surg* (2013) 39:232–8. doi: 10.1111/dsu.12079
72. Liu W, Krump NA, Buck CB, You J. Merkel Cell Polyomavirus Infection and Detection. *J Vis Exp* (2019) 144:10.3791/58950. doi: 10.3791/58950
73. Moshiri AS, Doumani R, Yelistratova L, Blom A, Lachance K, Shinohara MM, et al. Polyomavirus-Negative 31 Merkel Cell Carcinoma: A More Aggressive Subtype Based on Analysis of 282 Cases Using Multimodal Tumor 32 Virus Detection. *J Invest Dermatol* (2017) 137:819–27. doi: 10.1016/j.jid.2016.10.028
74. Sadeghi F, Salehi-Vaziri M, Alizadeh A, Ghodsi SM, Bokharaei-Salim F, Fateh A, et al. Detection of Merkel Cell Polyomavirus Large T-Antigen Sequences in Human Central Nervous System Tumors. *J Med Virol* (2015) 87(7):1241–1247. doi: 10.1002/jmv.24178
75. Behdarvand A, Zamani MS, Sadeghi F, Yahyapour Y, Vaziri F, Jamnani FR, et al. Evaluation of Merkel Cell Polyomavirus in Non-Small Cell Lung Cancer and Adjacent Normal Cells. *Microb Pathog* (2017) 108:21–6. doi: 10.1016/j.micpath.2017.04.033
76. Jung WT, Li MS, Goel A, Boland CR. JC Virus T-Antigen Expression in Sporadic Adenomatous Polyps of the Colon. *Cancer* (2008) 112(5):1028–36. doi: 10.1002/cncr.23266

Conflict of Interest: The authors declare that the research was conducted in the absence of any commercial or financial relationships that could be construed as a potential conflict of interest.

frontiers | Frontiers in Oncology

REVIEW
published: 29 April 2022
doi: 10.3389/fonc.2022.887220

Hypochlorous Acid: From Innate Immune Factor and Environmental Toxicant to Chemopreventive Agent Targeting Solar UV-Induced Skin Cancer

*Jeremy A. Snell, Jana Jandova and Georg T. Wondrak**

Department of Pharmacology and Toxicology, R.K. Coit College of Pharmacy & UA Cancer Center, University of Arizona, Tucson, AZ, United States

OPEN ACCESS

Edited by:
Nabiha Yusuf, University of Alabama at Birmingham, United States

Reviewed by:
Michael Davies, University of Copenhagen, Denmark
Shiyong Wu, Ohio University, United States

***Correspondence:**
Georg T. Wondrak
wondrak@pharmacy.arizona.edu

Specialty section:
This article was submitted to Skin Cancer, a section of the journal Frontiers in Oncology

Received: *01 March 2022*
Accepted: *31 March 2022*
Published: *29 April 2022*

Citation:
Snell JA, Jandova J and Wondrak GT (2022) Hypochlorous Acid: From Innate Immune Factor and Environmental Toxicant to Chemopreventive Agent Targeting Solar UV-Induced Skin Cancer. Front. Oncol. 12:887220. doi: 10.3389/fonc.2022.887220

A multitude of extrinsic environmental factors (referred to in their entirety as the 'skin exposome') impact structure and function of skin and its corresponding cellular components. The complex (i.e. additive, antagonistic, or synergistic) interactions between multiple extrinsic (exposome) and intrinsic (biological) factors are important determinants of skin health outcomes. Here, we review the role of hypochlorous acid (HOCl) as an emerging component of the skin exposome serving molecular functions as an innate immune factor, environmental toxicant, and topical chemopreventive agent targeting solar UV-induced skin cancer. HOCl [and its corresponding anion (OCl^-; hypochlorite)], a weak halogen-based acid and powerful oxidant, serves two seemingly unrelated molecular roles: (*i*) as an innate immune factor [acting as a myeloperoxidase (MPO)-derived microbicidal factor] and (*ii*) as a chemical disinfectant used in freshwater processing on a global scale, both in the context of drinking water safety and recreational freshwater use. Physicochemical properties (including redox potential and photon absorptivity) determine chemical reactivity of HOCl towards select biochemical targets [i.e. proteins (e.g. IKK, GRP78, HSA, Keap1/NRF2), lipids, and nucleic acids], essential to its role in innate immunity, antimicrobial disinfection, and therapeutic anti-inflammatory use. Recent studies have explored the interaction between solar UV and HOCl-related environmental co-exposures identifying a heretofore unrecognized photo-chemopreventive activity of topical HOCl and chlorination stress that blocks tumorigenic inflammatory progression in UV-induced high-risk SKH-1 mouse skin, a finding with potential implications for the prevention of human nonmelanoma skin photocarcinogenesis.

Keywords: hypochlorous acid, chlorination stress, environmental exposure, skin exposome, solar ultraviolet radiation, inflammation, skin cancer

INTRODUCTION: ENVIRONMENTAL EXPOSURE AND SKIN HEALTH: FOCUS ON SOLAR ULTRAVIOLET RADIATION AND CO-EXPOSURE TO ENVIRONMENTAL TOXICANTS

Skin, the largest part of the human integumentary system constituting about 15% of the total adult body mass, is positioned at the interface between environment and the body's internal organs (1). The skin is a crucial and dynamic barrier against the constantly changing environment, autonomously maintaining organ-level and systemic homeostasis. As one of the key barriers of defense against physical, chemical, and microbial stressors, the skin is a complex organ functioning in tissue regeneration and wound healing, hydro-, osmo-, and thermoregulation, endocrine and sensory functions, biosynthesis, metabolism, innate and adaptive immunity, circadian rhythmicity, and neuro-psychosocial communication (1–8). Among various environmental factors relevant to human health, solar exposure is known to impact tissue homeostasis modulating many of these cutaneous functions. Indeed, skin barrier dysfunction is a hallmark of numerous cutaneous pathologies including allergic reactions, microbial infection, photoaging, and photocarcinogenesis.

As an outer surface organ, human skin is ubiquitously exposed to solar ultraviolet (UV) radiation. UV exposure has both positive and negative effects on human health (9). It is responsible for the biosynthesis of vitamin D_3, can stimulate the production of photoprotective melanin, and is used therapeutically to treat inflammatory skin diseases (such as psoriasis, vitiligo, localized scleroderma, and atopic dermatitis). At the same time, solar UV is a potent environmental human carcinogen (10–12). The mechanisms by which solar UV-radiation causes skin photodamage are wavelength-dependent (11). UVB (290-320 nm) is thought to cause direct structural damage to DNA in the form of epidermal cyclobutane pyrimidine dimers (CPDs) and other photoproducts. Most of the solar UV energy incident on human skin derives from the deeply penetrating UVA region (≥ 95%, 320-400 nm) not directly absorbed by DNA, and UVA-induced photodamage occurs by oxidative mechanisms mediated by reactive oxygen species (ROS). Contributing to the adverse effects of solar UV exposure is its known action as a systemic immunosuppressant, compromising an individual's immune response with mechanistic implications for photocarcinogenesis (13).

UV and other environmental toxicants can be conceptualized as components of the overall skin exposome (**Figure 1**), a term integrating all environmental cutaneous exposures and consequent biological effects including antagonism and potentiation that may result from co-exposures (14): (*i*) physical (such as thermal and mechanical trauma), (*ii*) chemical/xenobiotic [such as industrial pollutants, topical and systemic drugs, disinfectants, pharmaceuticals and personal care products (PPCPs)], (*iii*) microbiomic (originating from commensal and pathogenic microbes), (*iv*) allergenic (either of chemical or biological nature), and (*v*) life style-associated (such as tobacco product use, dietary choices, circadian rhythmicity, sleep pattern etc.) factors. Importantly, the complete skin exposome is subject to cross-talk with intrinsic factors (i.e. an individual's primary biological determinants of skin structure and function) including: (*i*) genetics (as associated with ethnicity, sex as a biological variable (SABV), disease vulnerabilities etc.), (*ii*) pathobiological occurrences [such as infections, metabolic dysregulation (including diabetes), and autoimmune disturbances], and (*iii*) chronological aging (7, 15–20). Certain aspects and subcategories of the skin exposome have been expertly reviewed including the skin microbiome and the skin redoxome (7, 8).

Molecular crosstalk and mechanistic overlap between various components of the extrinsic skin exposome is well substantiated at the molecular level. For example, potentiation of solar UV-induced cutaneous and systemic injury by co-exposure to other environmental toxicants/pollutants has attracted much attention due to its negative impact on public health worldwide. Indeed, common environmental toxicants such as heavy metals (e.g. cadmium), metalloids (e.g. arsenic), and organic xenobiotics (e.g. benzo[a]pyrene, TCDD) are established potentiators of solar UV damage and skin carcinogenesis (21–23). Co-carcinogenicity of various exposome factors potentiating solar UV-induced skin photocarcinogenicity is firmly documented, as applicable to: (*i*) pollutants such as polyaromatic hydrocarbons including benz[a] pyrene (from cigarette smoke and combustion engines), (*ii*) arsenic (from drinking water), (*iii*) hypercaloric dietary intake/metabolic dysregulation, (*iv*) molecular therapeutics [acting as photo sensitizers or immunosuppressants], (*v*) and microbial infection (HPV, Merkel cell polyoma virus, Malassezia spp.) (21–28). To the contrary, dietary intake of specific phytochemicals representing an extrinsic exposome-related factor might enhance skin barrier function and antagonize photo-carcinogenesis, acting through modulation of specific molecular pathways associated with enhancement of antioxidant stress response (with involvement of the Keap1/NRF2 pathway) and suppression of inflammatory signaling (NFκB and AP-1) (9, 29).

Likewise, impairment of skin barrier function and health can result from the overlap of extrinsic (exposome-related) and intrinsic factors that interact and potentially synergize in complex ways. For example, it is well documented that smoking (an external exposomal factor) accelerates skin aging (intrinsic factor) (30). Likewise, human skin photoaging represents the overlap of intrinsic factors (such as cellular senescence as a function of chronological age) and structural/functional alterations due to environmental solar exposure (31). In the context of co-carcinogenicity, it has long been known that intrinsic genetic alterations that impair DNA repair capacity are associated with an increased UV-induced skin cancer incidence as substantiated paradigmatically by xeroderma pigmentosum patients with excision repair deficiencies underlying a pronounced increase in skin cancer risk (32, 33).

Abbreviations: HOCl, Hypochlorous acid; UV, Ultraviolet; CPDs, Cyclobutane pyrimidine dimers; ROS, Reactive oxygen species; SABV, Sex as a biological variable; MPO, Myeloperoxidase; CBPs, Chlorination byproducts; CSAD, Cysteine sulfinic acid decarboxylase; CDO1, Cysteine dioxygenase; FIFRA, Federal Insecticide, Fungicide, and Rodenticide Act; DBP, Disinfection byproducts; PPCPs, Pharmaceuticals and personal care products; AHR, Airway hyperresponsiveness; GI, Gastrointestinal.

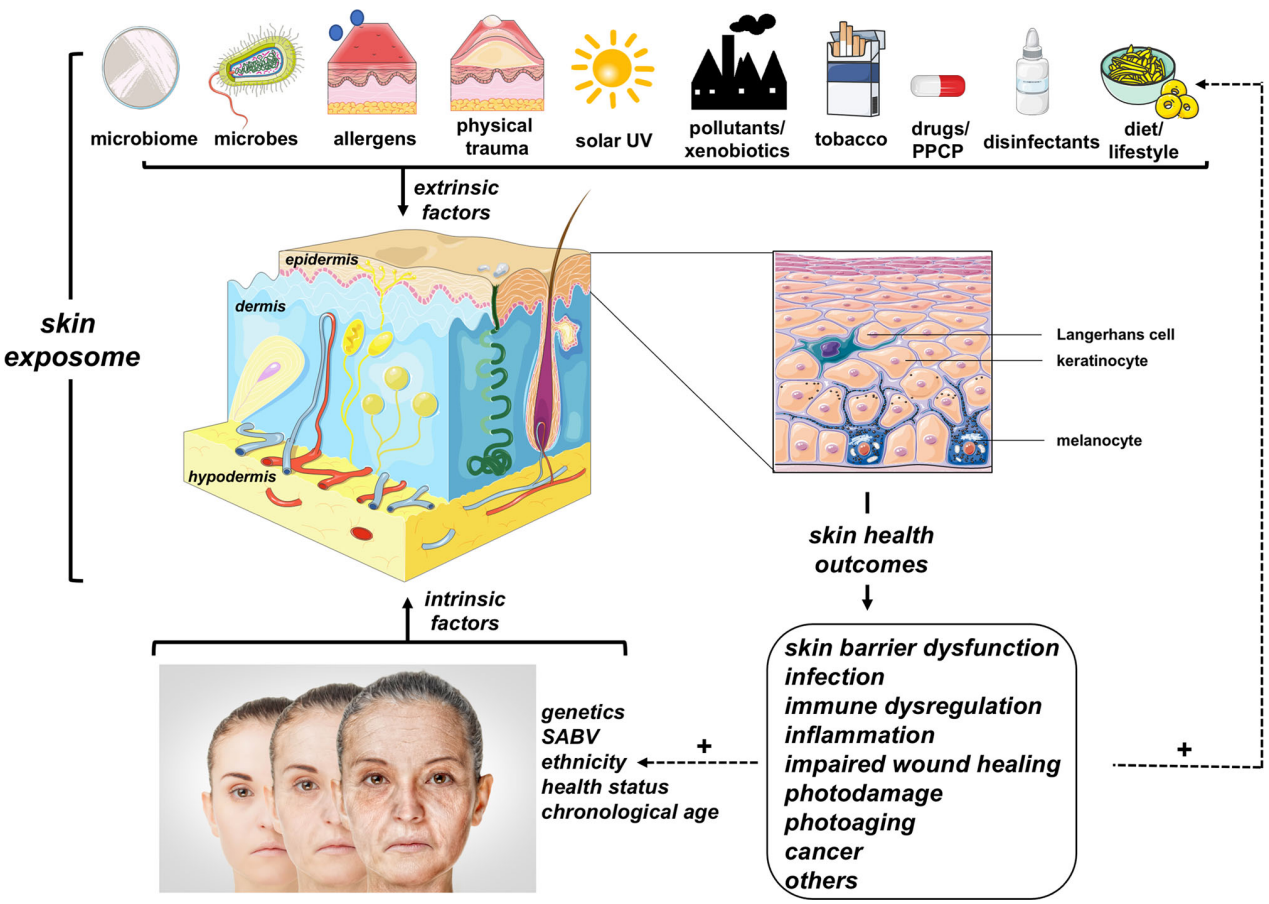

FIGURE 1 | The Skin Exposome. A multitude of extrinsic environmental factors (referred to in their entirety as the 'skin exposome') impact structure and function of skin and its corresponding cellular components. The complex (i.e. additive, antagonistic, or synergistic) interactions between multiple extrinsic (exposome) and intrinsic (biological) factors are important determinants of skin health outcomes. Unfolding skin pathology can potentiate (+) the cutaneous vulnerability to further environmental exposures or intrinsic factors (fueling a positive feedback loop). (PPCP, pharmaceuticals and personal care products; SABV, sex as a biological variable). Image was created using free imaging software: smart.servier.com.

Recently, hypochlorous acid (HOCl) has been identified as an environmental toxicant relevant to cutaneous exposures (34–36). Here, given the ubiquitous use of topical HOCl-based disinfection strategies combined with its established biological role as an essential determinant of neutrophil-related innate immunity, we review the role of this powerful electrophile as an understudied chemical component of the skin exposome with special emphasis on novel data that substantiate HOCl-dependent modulation of solar UV-induced skin carcinogenesis.

HYPOCHLOROUS ACID AND ITS CONJUGATED ANION: INNATE AND ENVIRONMENTAL MEDIATORS OF OXIDANT CHLORINATION STRESS

HOCl in Innate Immunity

Basic physicochemical properties of HOCl are relevant to its endogenous physiological function including its role as an innate immune factor, topical antimicrobial, and environmental toxicant (**Figure 2**) (37, 38).

Importantly, multiple chemical parameters dictate the biological function of HOCl serving as an important component of the skin exposome. In this context it should also be mentioned that HOCl-dependent chlorination stress is dictated by both thermodynamic and kinetic parameters that ultimately determine susceptibility of various biochemical targets (39–43).

First, HOCl is (*i*) a weak acid, (*ii*) a powerful chlorination agent, and (*iii*) direct- or indirect-acting oxidant. HOCl contains one labile proton (pKa = 7.46) dictating the co-existence between acid and conjugated base under physiological conditions at near equimolar ratio (**Figure 2A**). Another important physico-chemical feature of HOCl and its corresponding anion [OCl^- (hypochlorite)], relevant to environmental co-exposure scenarios, is its ability to absorb solar UVB (290-320 nm) photons and, as a consequence, undergo photolysis (**Figure 2B**). HOCl maximally absorbs at 237 nm and 289 nm

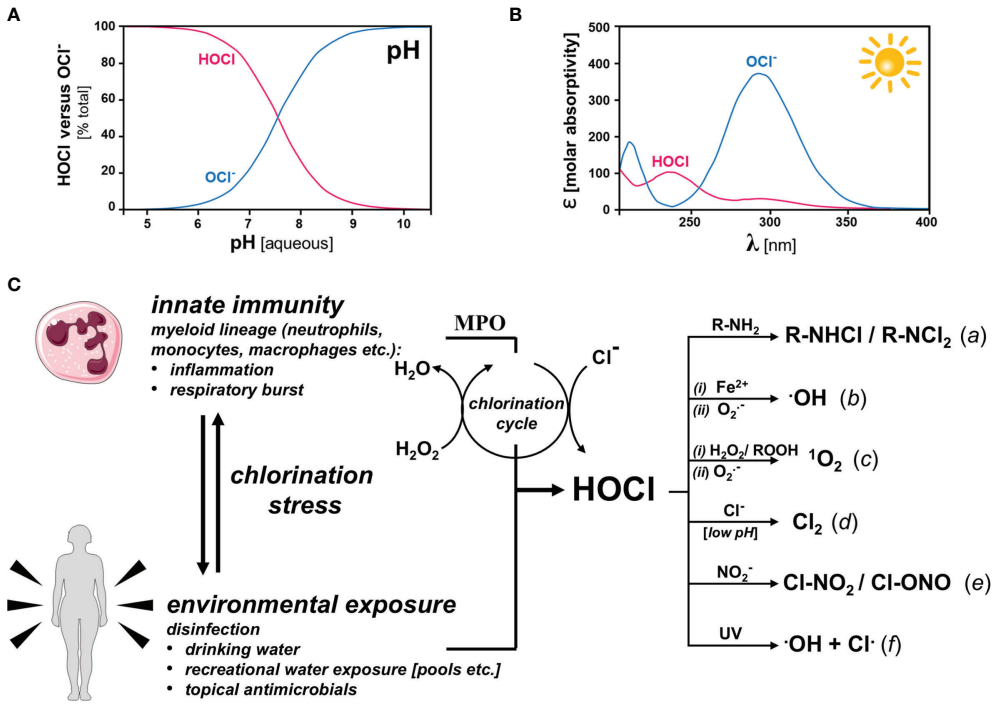

FIGURE 2 | HOCl/OCl-: Physicochemical Properties, Innate and Environmental Origin, and Formation of HOCl-Derived Secondary Oxidants Under Physiological Conditions (**A**) pH-dependent speciation (HOCl versus OCl-). At physiological pH, HOCl and OCl- occur at near equimolar ratios **(B)** Photon Absorptivity. HOCl and its corresponding anion differ with regard to photo-absorptive properties: HOCl (λ_{max} = 235 nm; ϵ = 101); OCl^- (λ_{max} = 292 nm; ϵ = 365). OCl^- absorptivity covers the solar UVB (290-320 nm) and UVA-II (320-340 nm) regions. **(C)** Biological and environmental sources of HOCl formation and HOCl-derived secondary oxidants. Left panel: Innate immune activation causes HOCl production by specific myeloid cells under conditions of inflammation and respiratory burst *via* the myeloperoxidase (MPO)-catalyzed chlorination cycle that consumes H_2O_2 for Cl^- oxidation. Environmental exposure to HOCl occurs in the context of freshwater disinfection (e.g. drinking water, recreational use, etc.) and topical antimicrobial intervention. Right panel: HOCl-derived secondary oxidants. Apart from acting as potent oxidizing species, HOCl/OCl^- may be involved in a number of biochemically relevant reactions producing secondary oxidants including: (*a*) chloramine formation; (*b*) hydroxyl radical formation downstream of (*i*) Fe(II)-dependent Fenton or (*ii*) superoxide chemistry; (*c*) singlet oxygen formation downstream of (*i*) peroxide or (*ii*) superoxide chemistry; (*d*) molecular chlorine formation with involvement of Cl^- at low pH; (*e*) formation of nitryl chloride and chlorine nitrite upon reaction with nitrite; and (*f*) formation of hydroxyl and chlorine radicals as a result of UV-driven photolysis.

with molar extinction coefficients of 102 and 36.1, respectively; OCl^- maximally absorbs at 292 nm with a molar extinction coefficient of 378. Consequently, photolysis of HOCl by environmentally relevant UVB is a function of pH. Indeed, environmental UV exposure might cause photolysis reactions with formation of various reactive species including the hydroxyl and chlorine free radicals, among others. However, the specific role of photolysis in the mediation of biological HOCl-based chlorination stress remains to be explored, given the opposing effects of a short reactivity-limited lifetime and sustained HOCl-release from photostable organic precursors including chloramines (such as the swimming pool disinfectant trichloroisocyanuric acid; see **Figure 5A**, structure 5) (44, 45).

Remarkably, HOCl, a weak halogen-based acid and powerful oxidant, serves two seemingly unrelated molecular roles: (*i*) as an innate immune factor [acting as a myeloperoxidase (MPO)-derived microbicidal factor] and (*ii*) as a chemical disinfectant used in freshwater processing, both in the context of drinking water safety and recreational use (e.g. swimming pool/hot tub disinfection) (37, 38). Importantly, HOCl and its conjugated base represent a potent oxidizing redox system [$E^{0'}$ = +0.9 (OCl^-); $E^{0'}$ = +1.48 V (HOCl)] under physiological conditions. In this context, it is important to notice that the major anti-microbially active species is thought to be HOCl (compared to the hypochlorite anion), consistent with the half-cell oxidation-reduction potentials and an increased ability of the uncharged HOCl species to penetrate cell walls and membranes of pathogens. Involvement of MPO in antimicrobial response and host pathogen interaction have been covered elsewhere and will not be the topic of this review (46). The potent oxidant HOCl/OCl^- serves as an endogenous microbicidal agent, generated by myeloid lineage-derived effector cells (including neutrophils). Indeed, during the respiratory burst, MPO-dependent oxidation of chloride anions (using NADPH oxidase-derived superoxide/hydrogen peroxide) produces HOCl and other hypohalous acids such as HOBr (hypobromous acid), HOI (hypoiodous acid), and HOSCN (hypothiocyanous acid)] as an essential component of antimicrobial innate immunity (**Figure 2C**) (47, 48). The 'chlorination cycle' catalyzed by MPO involves the hydrogen peroxide-dependent oxidation of reactive site ferric iron [Fe

(III)] forming a highly reactive oxy-ferryl [Fe(IV)=O] radical cation capable of oxidizing chloride anions leading to the formation of HOCl and regeneration of the ferric iron MPO. Importantly, endogenous hypohalous acids, even though serving innate host defense functions, may also induce tissue damage at sites of inflammation, an area of active research in the context of neurodegenerative disease (M. Alzheimer; M. Parkinson), metabolic and cardiovascular dysfunction (atherosclerosis; diabetes), autoimmune dysregulation, cancer, and chronological aging, among others (47, 49, 50). Importantly, beyond a role in cutaneous innate immunity, the MPO system has also been involved in various skin pathologies, either serving as a causative factor or biomarker in inflammation, contact hypersensitivity and irritation, psoriasis, UV-damage, photoaging, and carcinogenesis (51–59).

HOCl in Freshwater Disinfection: From Human Consumption to Recreational Use

The disinfection of drinking water supply by HOCl-dependent chlorination may well be regarded as the most important public health milestone in human history. Among the sustainable development goals adopted by members of the United Nations in 2015 is goal 6, which aims to provide all people with equal access to safe and affordable drinking water, sanitation and hygiene as consistent with the 2010 proclamation of the general assembly that such encompasses a human right. Despite substantial progress, it is currently estimated that more than 2 billion people lack access to safely managed drinking water and basic hygiene, while nearly half of the human population lacks sanitation. Indeed, according to global population projections and climate change models, supply problems surrounding safe water will be of utmost importance for this century. Considering these trends, continual optimization of the methods for drinking water sanitation, distribution, safe storage and wastewater treatment will be necessary to reduce water related health disparities on a global scale (60).

HOCl-Based Swimming Pool Disinfectants: Oxidative Potentiators of Cutaneous Solar UV Damage as an Unexplored Environmental Exposure of Global Importance

HOCl is the active microbicidal principle released by standard swimming pool disinfectants employed abundantly worldwide. According to CDC, there are 10.4 million residential and 309,000 public swimming pools and over 7.3 million hot tubs in the United States alone (https://www.cdc.gov/healthywater/swimming/fast-facts.html). Even though HOCl, commonly referred to as 'swimming pool chlorine', is the most frequently used halogen-based oxidizing pool disinfectant, little research has addressed toxicological implications and damage potentiation resulting from combined exposure to HOCl-based swimming pool disinfectants and solar UV as it occurs on a global scale in the context of recreational swimming pool use (34). Pool disinfection is an essential barrier to the spread of germs. To ensure a non-infectious healthy pool environment, operators try to maintain a desired range (1.0-1.5 ppm free HOCl; for outdoor swimming pools and indoor pools smaller than 20 m^2, the recommended maximum level is 5 ppm). In recent years, use of sodium dichloroisocyanurate, an organic HOCl-precursor, has gained frequent use, but HOCl/OCl^- is the predominantly active microbicidal agent (34, 61).

Human skin is extensively exposed to HOCl-based pool disinfectants causing oxidation and chlorination of specific molecular targets; however, little molecular research exploring the potentially adverse cutaneous and systemic effects resulting from exposure to HOCl-disinfectants during recreational swimming pool use has been conducted. Given the important role of photo-oxidative mechanisms underlying adverse cutaneous effects of solar UV exposure and the largely oxidative nature of chlorination-induced damage, it seems reasonable to expect synergistic molecular interactions that drive HOCl-potentiation of sun damage in exposed individuals. Indeed, according to the recent *WHO Guidelines for Safe Recreational Water Environments*, epidemiological evidence indicates that risk of sunburn and cutaneous photodamage is increased in swimming pool environments.

In addition to direct target chlorination and oxidation, HOCl-dependent reactions of biological relevance in inflammation and antimicrobial defense (-also observed in the context of topical disinfectant use-), might be mediated through the formation of numerous HOCl-derived electrophilic species (**Figure 2C**; right portion). Chloramine formation involves the HOCl-dependent derivatization of primary and secondary biological amines as contained in small biochemicals (such as histamine and taurine) and macromolecules (proteins etc.) (62–64). Moreover, hydroxyl radical formation may occur downstream of either Fe(II)-dependent Fenton chemistry, scenarios observable under conditions of MPO-facilitated heme degradation as a consequence of excess HOCl formation or pathological elevation of labile iron (65–67). Likewise, hydroxyl radicals can form upon reaction of HOCl with superoxide free radicals (68). Interestingly, HOCl-dependent formation of highly reactive photoexcited molecular oxygen [$^1O_2$ (singlet oxygen)] has been documented without mechanistic involvement of photons downstream of peroxide (including linoleic acid hydroperoxide), superoxide, or chloramine chemistry involving the chemical formation of photo-excited states (commonly referred to as 'chemiexcitation') (69–71). Molecular chlorine (Cl_2) is another species formed downstream of MPO-dependent transformation of Cl^- anions and hydrogen peroxide at low pH, relevant to cholesterol chlorination in atherosclerotic pathology (72–74). Furthermore, upon reaction with nitrite, formation of nitryl chloride and chlorine nitrite might occur, reactions relevant to inflammatory protein nitration (75). Lastly, as a result of UV-driven photolysis generation of hydroxyl and chlorine radicals has been documented, a reaction of potential relevance to environmental co-exposure scenarios where solar photons in the UVB range might cause HOCl/OCl^- degradation with formation of reactive free radical species consistent with the extensive UVB absorptivity of OCl^- (38).

BIOMOLECULAR TARGETS OF CHLORINATION STRESS: FROM CHEMICAL MODIFICATION TO PATHOPHYSIOLOGICAL CONSEQUENCES

Chlorination stress that occurs under physiological or environmental exposure-relevant conditions impacts structure and function of numerous classes of biomolecules, either through covalent introduction of chlorine (and chlorine-derived substituents) or through indirect oxidative insult. HOCl, in equilibrium at physiological pH with its anionic form [hypochlorite (OCl^-)], may also induce tissue damage at sites of inflammation involving the oxidation and chlorination of biomolecules targeting peptides (e.g. glutathione), proteins, lipids, and nucleic acids (39, 42, 43, 47, 76, 77).

Previous research has identified key molecular modifications downstream of chlorination stress targeting amino acids, peptides, and proteins as dominant targets of biologically-relevant chlorination stress (**Figure 3A**). For illustration, a hypothetical heptapeptide [H_2N-Tyr-Trp-His-Lys-Met-Cys-Arg-COOH] has been envisioned that exemplifies the range of possible amino acid modifications induced by HOCl exposure including dichloro-tyrosine, hydroxy-tryptophan, histidine chloramine, lysine mono- or dichloramine, methionine sulfoxide, cysteine sulfenic/sulfinic/sulfonic acid, and arginine chloramine (78). Protein chlorination has been associated with structural changes of target proteins including fragmentation, crosslinking, aggregation, unfolding, and modulation of specific functions such as immunogenicity, enzymatic activity and ligand-receptor interaction (48, 79). Numerous proteins are subject to chlorination stress-induced modulation through chemical changes under physiological conditions, including plasma proteins [e.g. HSA, alpha2M], histones, heat shock/ER stress response mediators and calcium signaling components (e.g. GRP78, SERCA), inflammatory signaling molecules (e.g. IL-6, IKK) and mediators of tissue remodeling (e.g. MMP7, TIMP-1), causing effects that are mostly consistent with modulation, attenuation, and resolution of inflammatory tissue responses (35, 80–89). Specifically, inactivation of IKK (inhibitor of IκB kinase) through oxidation (Cys114/115) is thought to cause the hypochlorite-dependent attenuation of psoriasis observable upon topical application (35). Similarly, GRP78 (glucose-regulated protein 78, HSPA5) modification through chloramine adduction (Lys 353) has been suggested to modulate autophagy and apoptosis in A549 lung cancer cells, and N-chlorination of HSA (human serum albumin) converts plasma proteins into efficient activators of the phagocytic respiratory burst (46, 86). In addition, biogenic amines, mostly through chloramine formation, have been demonstrated to serve as biomolecular targets of chlorination stress including histamine, serotonin, melatonin, and taurine among others (90, 91).

Consistent with chlorination-associated electrophilic stress, unsaturated lipids serve as major HOCl-targets under physiological conditions (**Figure 3B**) (92–99). Indeed, free fatty acids, triglycerides, phospholipids, as well as cholesterol and its derivatives, have all been validated as being susceptible to chemical modification under conditions of physiological or environmental chlorination stress conditions (**Figure 3B**). For example, HOCl-mediated modification of cholesterol forms a number of cholesterol-chlorohydrin stereoisomers as depicted; in addition, phospholipids may undergo derivatization at nitrogen-containing head groups (forming the respective chloramine) or at sites of unsaturation, followed by further oxidation/decarboxylation and N-centered free radical formation. In addition, other biochemical lipid mediators including plasmalogens, prostaglandins, and leucotrienes, involved in tissue remodeling and inflammatory signaling, have been shown to be subject to HOCl-dependent adduction with consequent alteration of signaling properties (98).

Nucleic acids are important targets of chlorination stress with possible mutagenic, genotoxic, and cytotoxic outcomes downstream of chemical modification (**Figure 3C**) (39, 100–102). Specifically, it is well documented that HOCl exposure causes chemical modification of DNA and RNA (and their respective nucleotides, nucleoside, and free nucleobases, irrespective of ribose- or deoxyribose- substitution). For example, HOCl-modification of deoxyadenosine forms 8-chlorodeoxyadenosine, and HOCl-modification of deoxyguanosine forms 8-chlorodeoxyguanosine. Interestingly, HOCl-modification of deoxycytidine forms a 5-chlorodeoxycytidine-intermediate, followed by spontaneous deamination forming stable 5-chlorodeoxyuridine causing miscoding damage downstream of chlorination stress. Indeed, chloro-derivatives of nucleic acids and their constitutive bases, apart from their functional involvement in mutagenic events, may also play an important yet underappreciated role as biomarkers of chlorination stress characteristic of specific pathological conditions.

ENDOGENOUS, PHYTOCHEMICAL, AND SYNTHETIC HOCL-ANTAGONISTS: ANTIOXIDANTS AND QUENCHERS

Numerous molecular entities of endogenous or phytochemical origin have been shown to antagonize chlorination stress that occurs as a consequence of exposure to HOCl including amino acid derivatives (taurine, glutathione, serotonin, serotonin, carnosine, ovothiol, ergothioneine), phenolics (gallic acid, nordihydroguaiaretic acid, quercetin), and B_6 vitamers (pyridoxal, pyridoxine, and pridoxamine), attributed mostly to chemical reactivity (i.e. sacrificial quenching) (**Figure 4A**). In addition, antagonists of MPO enzymatic activity (such as the synthetic MPO inhibitor verdiperstat or the endogenous metabolite uric acid) blocking HOCl formation have been explored for pharmacological control of pathophysiological chlorination stress (47, 62, 91, 103–109).

Among these biomolecules, B_6-vitamers deserve special recognition since they have been shown to exert protection against chlorination stress as assessed using *in vivo* disease models, an effect attributed to formation of stabilized chloramine derivatives (110). Likewise, imidazole-derivatives

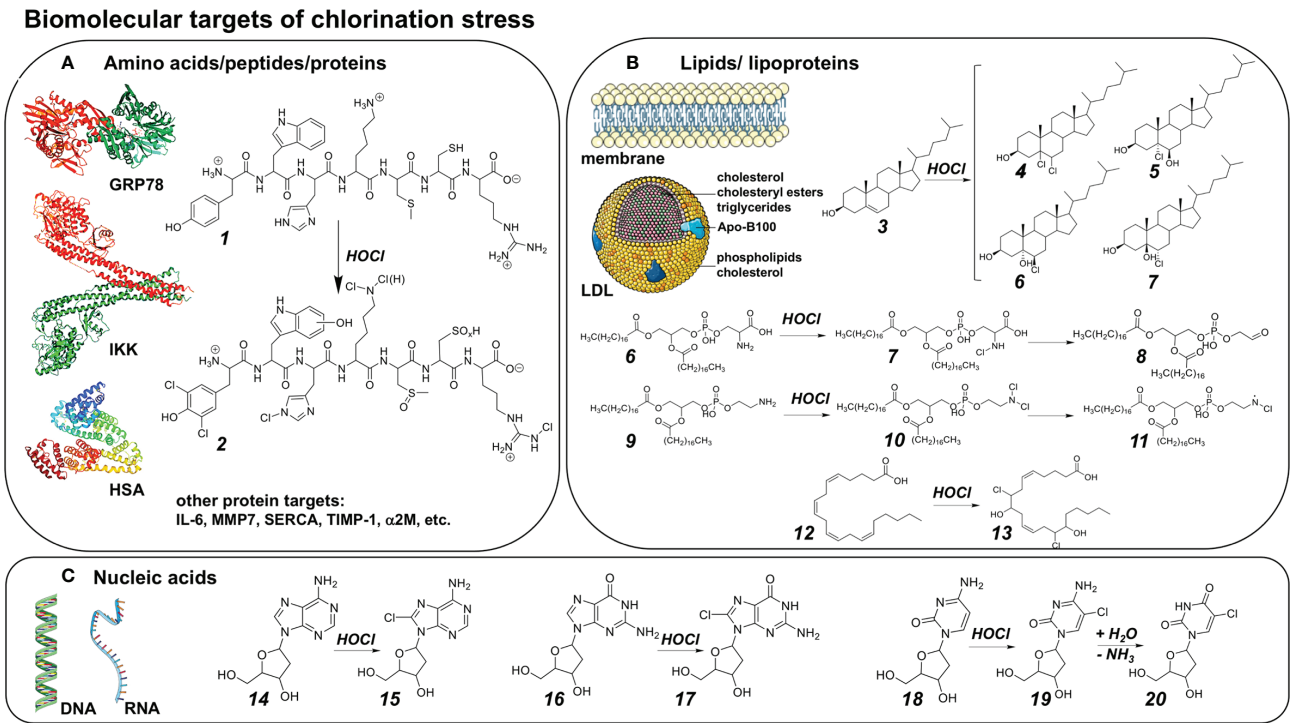

FIGURE 3 | Biomolecular Targets of Chlorination Stress **(A)** Amino acids, peptides, and protein targets of chlorination stress. Theoretical heptapeptide [H_2N-Tyr-Trp-His-Lys-Met-Cys-Arg-COOH (1)] illustrating the range of possible amino acid modifications (2) induced by HOCl (from amino- to carboxyterminus): Dichloro-tyrosine, hydroxy-tryptophan, histidine chloramine, lysine mono- or dichloramine, methionine sulfoxide, cysteine sulfenic/sulfinic/sulfonic acid, arginine chloramine. **(B)** Fatty acids, lipids, and lipoproteins as targets of chlorination stress. HOCl-mediated modification of cholesterol (3) forms a number of cholesterol chlorohydrin stereoisomers: 5,6-dichloro cholesterol (4); (5R,6R)-5-chloro-6-hydroxy cholesterol (5); (5R,6R)-6-chloro-5-hydroxy cholesterol (6); (5S,6S)-6-chloro-5-hydroxy cholesterol (7), among others. For phospholipids, HOCl may either exert its effects near the head group, or at sites of unsaturation: HOCl-mediated modification of phosphatidylserine (6) results in phosphatidylserine chloramine (7), with further oxidation/decarboxylation to phosphatidyl glycoaldehyde (8). HOCl-mediated modification of phosphatidylethanolamine (9) results in the respective dichloramine (10) subsequently forming N-centered radicals acting as long-lived mediators. For simplicity, for both phospholipids each lipid moiety is stearate. Fatty acids possessing greater degrees of unsaturation are more prone to modification by HOCl: HOCl-mediated modification of arachidonic acid (12) results in the formation of arachidonic acid chlorhydrins such as 8,14-dichloro-9,15 dihydroxy arachidonic acid bis-chlorohydrin (13). **(C)** Nucleic acids as targets of chlorination stress. HOCl may modify DNA, RNA, and free nucleobases. (For simplicity, only HOCl-mediated modification of deoxyribosides is shown.) HOCl-modification of deoxyadenosine (14) forms 8-chlorodeoxyadenosine (15). HOCl-modification of deoxyguanosine (16) forms 8-chlorodeoxyguanosine (17). HOCl-modification of deoxycytidine (18) forms 5-chlorodeoxycytidine (19), followed by spontaneous deamination forming 5-chlorodeoxyuridine (20).

(e.g. L-histidine, carnosine, carcinine) and thio-imidazole-derivatives (ergothioneine and sea urchin-derived ovothiol) have been identified as potent chlorination stress inhibitors (111–113).

Moreover, the cysteine-derived metabolite taurine (2-amino-ethane-sulfonic acid) has now been identified as a major endogenous HOCl-directed scavenger and antioxidant, attenuating physiologically relevant chlorination stress (**Figure 4B**). Strikingly, neutrophils represent a large reservoir of free taurine compromising approximately 50% of the cellular amino acid/amino acid-derivative pool thought to be involved in direct chemical protection against cytotoxic consequences of the respiratory burst associated with microbicidal HOCl formation (114). Taurine formation occurs as the result of enzyme-catalyzed cysteine transformation through intermediate generation of L-cysteine sulfinic acid and hypotaurine (**Figure 4B**). The consequent formation of N-chlorotaurine, representing a chlorinated adduct with attenuated reactivity, has also been interpreted as an intermediate step facilitating the extension of the phagocytic activity range, enabling enhanced stability and diffusion, spatially amplifying the range of oxidative antimicrobial effects. Indeed, attenuated chlorination reactivity of N-Chlorotaurine has been attributed to sulfonic acid-dependent electrostatic anionic shielding of the adjacent chloramine function that is amenable to chloro-transfer if attacked by biomolecular nucleophiles (115).

Importantly, N-chlorotaurine formation may cause the negative regulation of inflammatory processes by multiple distinct molecular mechanisms attenuating NF-kB and related cytokine signaling (88, 116). Interestingly, taurine might not only attenuate direct chemical reactivity of HOCl through sacrificial quenching, but chloro-taurine may then act as a redox-directed signaling modulator of major inflammatory targets and pathways. Indeed, it has been shown that N-chlorotaurine modulates inflammatory pathologies attributed to chemical

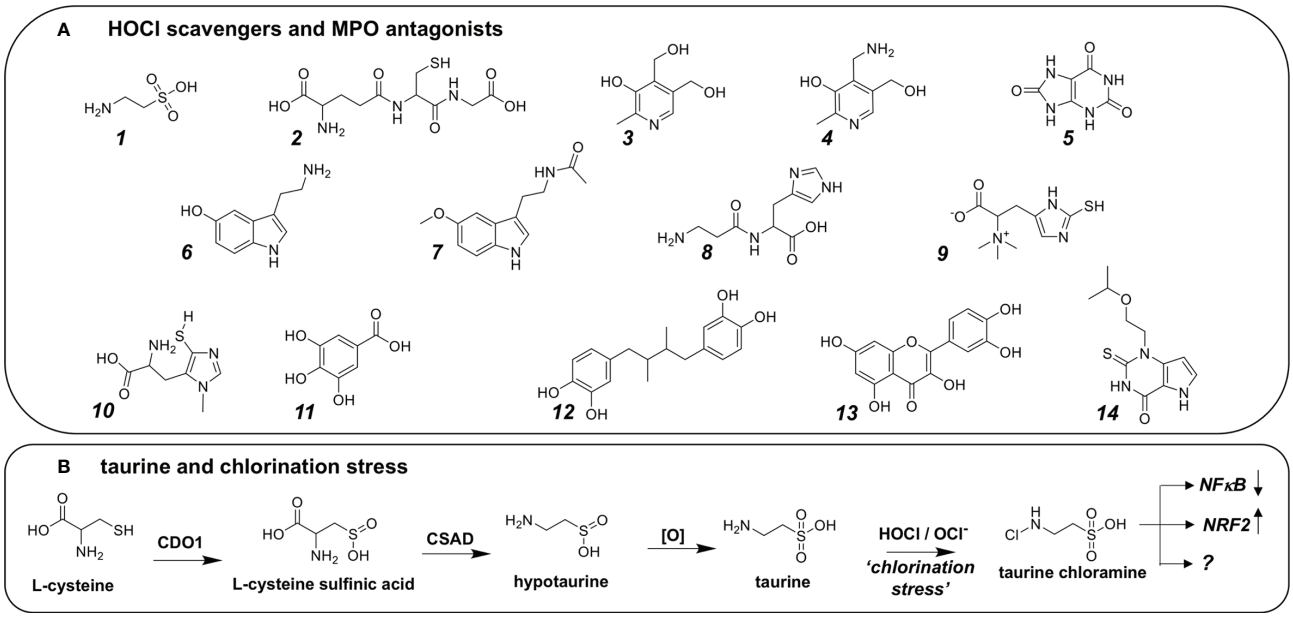

FIGURE 4 | Biochemical, Natural Product, and Synthetic HocI Scavengers and MPO Antagonists. **(A)** Endogenous chemical entities: 1. Taurine, 2. Glutathione, vitamins: 3. Vitamin B_6, 4. Pyridoxamine; neurotransmitters: 6. Serotonin, 7. Melatonin 8. Carnosine; 9. Ergothioneine. Natural products: 10. Ovothiol, 11. Gallic acid, 12. Nordihydroguaiaretic acid, 13. Quercetin. Endogenous and synthetic MPO antagonists: 5. Uric acid, 7. Melatonin, 14. AZD3241 (Verdiperstat). **(B)** Endogenous production of taurine as a possible sink for HOCl. First, L-cysteine is oxidized by cysteine dioxygenase (CDO1) to form L-cysteine sulfinic acid, which in turn is decarboxylated by the enzyme cysteine sulfinic acid decarboxylase (CSAD) forming hypotaurine. Hypotaurine may undergo spontaneous oxidation to form taurine, acting as a sacrificial quencher of HOCl/OCl^- forming taurine chloramine as a moderately active chloramine with attenuated chlorination reactivity. Interestingly, taurine chloramine has been demonstrated to exert control over downstream signaling pathways including downregulation of NFκB, and upregulation of KEAP1-NRF2. As such, it has been hypothesized that taurine chloramine acts through posttranslational modification of distinct amino acid residues on transcription factors, among other effects.

modification of inflammatory factors, such as IL-6 and NFkB. Indeed, N-chlorotaurine exposure of IL-6 causes oxidation of residues relevant to IL6R receptor-binding (Met161 and Trp157) (88). Negative modulation of NF-κB by N-chlorotaurine (and other chloramines such as glycine chloramine) is thought to originate from oxidation of Met45 in IκB (preventing its ubiquitination and proteasomal degradation) (116, 117). Importantly, NRF2, the master transcriptional regulator of cellular antioxidant responses, has also been shown to be responsive to N-chlorotaurine-mediated chlorination stress, an effect attributed to electrophilic adduction and inactivation of Keap-1, the redox-sensitive negative regulator of this transcription factor (118).

MOLECULAR MEDIATORS, SIGNALING PATHWAYS, AND HUMAN TARGET ORGANS OF CHLORINATION STRESS

Molecular chlorination stress relevant to human health originates from HOCl (among other endogenous hypohalous acids including HOI and HOBr, formed mostly in the context of innate immunity) and is complemented by exposure to HOCl (and related derivatives) originating from exogenous sources. Specifically, environmental exposure-relevant chlorination agents include hypochlorous acid (and its corresponding anion) as well as diverse chloramines (e.g. monochloramine, dichloramine, nitrogen trichloride, chlorinated isocyanuric acid-derivatives) formed as a result of freshwater chlorination (**Figure 5A**) (119, 120). Interestingly, trichloroisocyanuric acid as well as its di-chloro-analogue are EPA-approved under FIFRA (Federal Insecticide, Fungicide, and Rodenticide Act) regulations, used globally for drinking water and freshwater disinfection (such as in swimming pools), offering increased photostability and sustained HOCl release (44, 121). Importantly, chlorination byproducts (CBPs) including organohaloacetic acids and trihalomethanes (formed due to the presence of dissolved organic matter) and chlorite are subject to strict EPA regulation due to potential adverse health effects (122, 123). Strikingly, out of more than six hundred halogenation byproducts identified as of to date, only eleven are currently subject to strict EPA regulation (124). For example, mutagen X (3-chloro-4-(dichloromethyl)-5-hydroxy-5*H*-furan-2-one) is a disinfection byproduct derived from humic acids, not regulated by EPA, with suspected involvement in cancer risk elevation associated with consumption of chlorinated drinking water, an effect attributed to genotoxicity surpassing that of currently regulated CBPs

(including chloroform and bromodichloromethane) (125). Additionally, PPCPs introduced into the water supply are subject to HOCl-mediated chlorination and subsequent formation of CBPs. For example, common drugs including metformin, diclofenac, and tamoxifen entering freshwater sources are subject to direct chlorination causing drinking water contamination associated with largely unexplored implications for human health (126–129). Likewise, chlorination of PPCPs including sunscreen ingredients such as the common UVA-sunscreen avobenzone are associated with formation of a dichloro-species, and cosmetics are equally subject to chlorination with unexplored effects on human health (16, 130–135).

Human Target Organs of Environmental Chlorination Stress

Importantly, human organ dysfunction may occur as a result of chlorination stress originating from exogenous (environmental) and endogenous (innate) sources (47, 49). Indeed, these pathophysiological outcomes have been attributed to the molecular consequences of chlorination stress (mediated through HOCl/OCl^- and HOCl-derived organic chloramines) impacting genotoxic, proteotoxic, inflammatory, and redox stress responses involving modulation of crucial transcription factor systems including p53, Keap1/NRF2, HSF1, IKK/NFκB, and AP-1 (**Figure 5B**) (35, 36, 118, 136–138). Likewise, signaling cascades including MAPKs (p38, ERK1/2) are sensitive to HOCl exposure attributed in part to tyrosine phosphatase modulation through cysteine-oxidation (139, 140). Also, in the context of balancing HOCl-related organ toxicity and therapeutic effects, it should be mentioned that the indiscriminate HOCl-dependent induction of chlorination stress might be associated with adverse irritant effects (51, 141–144).

Here, we will briefly focus on organ-specific toxicity of environmental exposure-induced chlorination stress (**Figure 5C**). In the lung, exposure to chlorination stressors has long been associated with a role in chronic inflammatory diseases of the respiratory system (137, 144–148). For example, competitive swimmers have been shown to suffer from high rates of asthma and airway hyperresponsiveness attributed to HOCl and volative DBP exposure (149, 150). In the context of pulmonary exposure, it is noteworthy that inhalational HOCl formulations are now undergoing clinical trials for prophylaxis and treatment of COVID-related respiratory infectious illness (*ClinicalTrials.gov Identifier: NCT04684550*). Moreover, there are concerns that innate or environmental chlorination stress might be related to the occurrence of lung malignancy related to genotoxic effects (86, 151, 152). Likewise, in the gastrointestinal tract, chlorination-associated changes have been substantiated, potentially impacting microbiome and barrier function, occurrence and severity of inflammatory pathology, and malignant progression (153–157). Hepatic toxicity related to chlorination stress, particularly in the context of environmental exposure to chlorination byproducts, has been documented extensively. Hepatic metabolism, biotransformation of drugs and xenobiotics have been investigated, and liver injury as well as malignancy have been substantiated as pathological outcomes resulting from chronic and dysregulated chlorination stress that might be potentiated by synergistic co-exposure involving multiple chlorinated chemical entities (158–161). Nephrotoxity and urogenital tract dysfunction are established pathological outcomes of chlorination stress. Among other pathologies, acute kidney injury, glomerulonephritis, diabetic nephropathy, and bladder cancer have been associated with exposure to pathological chlorination stress (110, 162–166).

Potential Therapeutic and Chemopreventive Opportunities of Topical HOCl With a Focus on Solar UV-Induced Skin Carcinogenesis

Remarkably, in addition to endogenous and environmental sources, skin HOCl exposure also occurs through application of topical disinfectants employed worldwide as clinical and consumer products (167–171). In human skin (as a function of concentration, pH, and exposure time), irritation and disruption of barrier function, alteration of the commensal microbiome, allergy, and contact hypersensitivity are expected outcomes of inappropriate topical HOCl product use not compliant with standard of care (**Figure 5D**) (142, 143). Also, it has been hypothesized that DBPs in drinking water correlate with risk of skin cancer (172). Importantly, HOCl-based therapeutics optimized for topical delivery are now serving as pharmaceutical formulations for wound management, scar prevention, diabetic ulcers, atopic dermatitis, pruritus, psoriasis, and seborrheic dermatitis (84, 168, 173, 174). Suppression of inflammatory gene expression with downregulation of iNOS and COX-2 downstream of HOCl-dependent IKK inactivation represents the crucial mechanistic basis underlying HOCl-dependent therapeutic efficacy targeting psoriasis and radiation dermatitis (35). The same mechanism has also been substantiated attenuating experimental melanoma progression as a result of myeloid cell-derived HOCl (175). In addition, HOCl-hydrogel formulations have shown immunotherapeutic efficacy against experimental murine melanoma (176). Consistent with these observations, a suppressive role of HOCl in the control of cancer cell viability and tumor progression has been envisioned and further substantiated (71, 177, 178).

More recently, we have investigated the molecular consequences of solar simulated ultraviolet (UV) radiation and HOCl combinations, a procedure mimicking co-exposure experienced for example by recreational swimmers exposed to both HOCl (pool disinfectant) and UV (solar radiation). First, we have profiled the HOCl-induced stress response in reconstructed human epidermis and SKH-1 hairless mouse skin (36). In AP-1 transgenic SKH-1 luciferase-reporter mice, topical HOCl suppressed UV-induced inflammatory signaling assessed by bioluminescent imaging and gene expression analysis documenting HOCl-antagonism of solar UV-induced AP-1 activation. Co-exposure studies (combining topical HOCl and UV) performed in SKH-1 hairless mouse skin revealed that the HOCl-induced cutaneous stress response blocks redox and

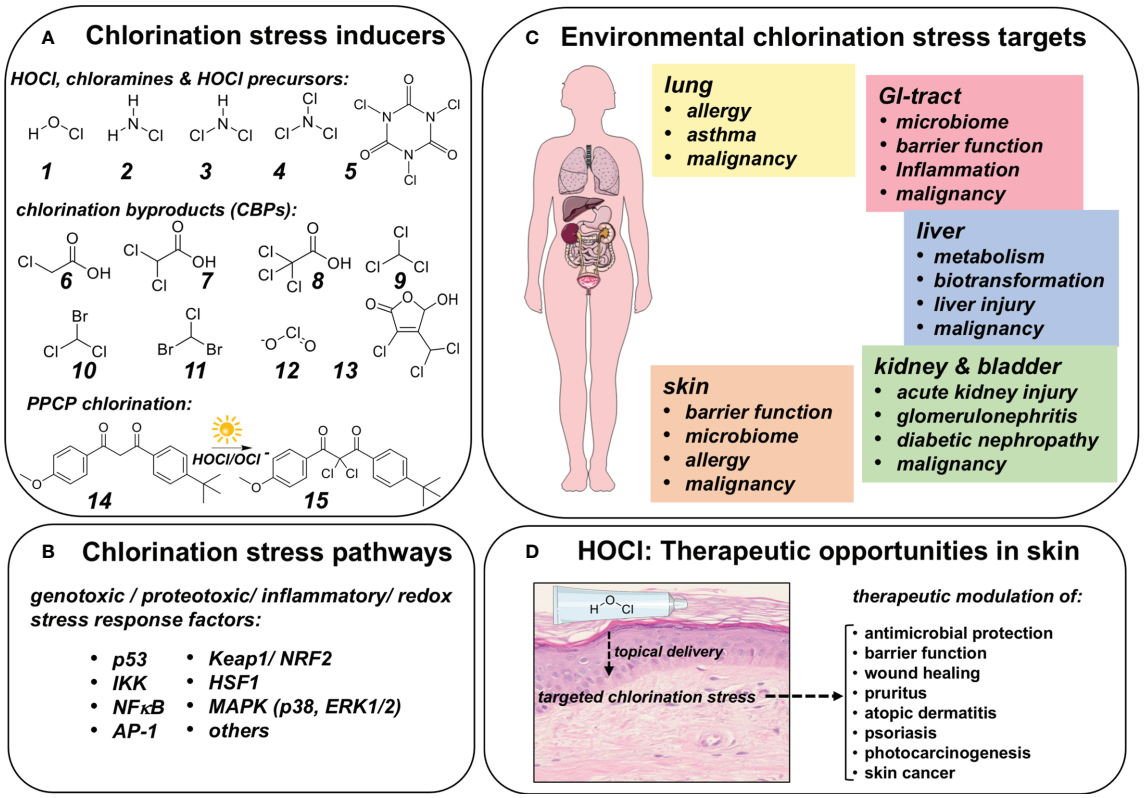

FIGURE 5 | Chlorination Stress: Molecular Inducers, Signaling Pathways, Human Target Organs and Therapeutic Opportunities In Skin. **(A)** Direct and indirect chlorination stress inducers. 1. Hypochlorous acid, 2. Monochloramine, 3. Dichloramine, 4. Nitrogen Trichloride, 5. Trichloroisocyanuric acid. Upon chlorination of fresh water, chlorination byproducts (CBPs) are formed due to the presence of dissolved organic matter: Haloacetic acids: 6. Chloroacetic acid, 7. Dichloroacetic acid, 8. Trichloroacetic acid; Trihalomethanes: 9. Trichloromethane, 10. Bromodichloromethane, 11. Chlorodibromomethane, 12. Chlorite, all of which are subject to governmental regulation. Remarkably, numerous major chlorinated byproducts remain largely unexplored (and unregulated) such 3-chloro-4-(dichloromethyl)-5-hydroxy-5*H*-furan-2-one (13, commonly referred to as 'mutagen X'). Additionally, pharmaceuticals and personal care products (PPCPs) introduced into the water supply are subject to HOCl mediated chlorination. As shown, the common UVA-sunscreen avobenzone (14) is chlorinated to produce a dichloro-species (15). **(B)** Chlorination stress signaling pathways. It has been demonstrated that chlorination stress may impact genotoxic, proteotoxic, inflammation and redox responses including p53, Keap1/NRF2, IKK/NFκB, and AP-1. **(C)** Human target organs of chlorination stress. Chlorination stress impacts multiple organ systems causing specific functional outcomes as discussed. **(D)** HOCl: Therapeutic opportunities in skin. HOCl may be used as a topical agent for therapeutic induction of chlorination stress in the context of antimicrobial intervention, impaired barrier function, wound healing, pruritus, atopic dermatitis, psoriasis, skin cancer, and prevention of photocarcinogenesis.

inflammatory gene expression elicited by subsequent acute solar UV exposure. Remarkably, in the SKH-1 high-risk mouse model of UV-induced human keratinocytic skin cancer, relevant to actinic keratosis and subsequent malignant progression, topical HOCl blocked tumorigenic progression and inflammatory gene expression (*Ptgs2*, *Il19*, *Tlr4*), confirmed by immunohistochemical analysis including 3-chloro-tyrosine-epitopes.

These data illuminate the molecular consequences of HOCl-exposure in cutaneous organotypic and murine models assessing inflammatory gene expression and modulation of UV-induced carcinogenesis. However, the specific mechanistic involvement of NFκB and AP-1 in the HOCl-induced attenuation of UV-induced skin inflammatory gene expression and carcinogenesis remains to be elucidated. With relevance to cancer-directed preventive and potentially therapeutic activity, an HOCl-induced increased immunogenicity of proteins and enhanced uptake by dendritic cells have been observed (179). Likewise, activity as a natural adjuvant (through induction of adaptive immunity by HOCl-dependent oxidation of N-linked carbohydrates in glycoprotein), subsequently enhancing scavenger receptor uptake by antigen presenting cells, has been demonstrated, linking HOCl-potentiation of innate and adaptive immunity (180).

If translatable to photodamaged human skin, these observations provide novel insights on molecular consequences of chlorination stress not only relevant to environmental exposure but indicative of a potential photo-chemopreventive utility for topical intervention targeting early (actinic keratosis) and advanced stages of nonmelanoma skin cancer.

FUTURE DIRECTIONS

Chlorination stress associated with HOCl/OCl^- exposure originating from innate and environmental sources has now been identified as a double-edged molecular sword, mediating essential functions in the context of innate immunity towards microbial attack and exerting effects that are either detrimental or therapeutic to human health, particularly in the context of skin anti-inflammatory and cancer photochemopreventive topical intervention. Harnessing HOCl-dependent preventive and therapeutic effects that might benefit human patients will depend on the development of novel chemical entities and advanced formulations allowing a more controlled and targeted modulation of chlorination stress (70, 181). Indeed, additional research must carefully explore dose regimens and extended release formulations that achieve anti-inflammatory and photo-chemopreventive effects while avoiding potential HOCl-induced tissue damage and irritation. In the same way, availability of specific biocompatible molecular fluorescent probes with diagnostic utility *in vitro* and *in vivo* (allowing imaging and quantitative analysis of physiological and therapeutic chlorination stress conditions) will expand our understanding of these multi-faceted versatile biochemical actors and processes as key determinants of health and disease (182).

AUTHOR CONTRIBUTIONS

Manuscript preparation: JS, JJ, GW. Conceptualization of work: GW. All authors contributed to the article and approved the submitted version.

FUNDING

Supported in part by grants from the National Institutes of Health (1R01CA229418, 1R21ES029579, 1P01CA229112, ES007091, ES006694, and UA Cancer Center Support Grant CA023074).

REFERENCES

1. McLafferty E, Hendry C, Alistair F. The Integumentary System: Anatomy, Physiology and Function of Skin. *Nurs Stand* (2012) 27(3):35–42. doi: 10.7748/ns2012.09.27.3.35.c9299
2. Slominski A. A Nervous Breakdown in the Skin: Stress and the Epidermal Barrier. *J Clin Invest* (2007) 117(11):3166–9. doi: 10.1172/JCI33508
3. Elias PM. Skin Barrier Function. *Curr Allergy Asthma Rep* (2008) 8(4):299–305. doi: 10.1007/s11882-008-0048-0
4. Plikus MV, Van Spyk EN, Pham K, Geyfman M, Kumar V, Takahashi JS, et al. The Circadian Clock in Skin: Implications for Adult Stem Cells, Tissue Regeneration, Cancer, Aging, and Immunity. *J Biol Rhythms* (2015) 30 (3):163–82. doi: 10.1177/0748730414563537
5. Gallo RL. Human Skin Is the Largest Epithelial Surface for Interaction With Microbes. *J Invest Dermatol* (2017) 137(6):1213–4. doi: 10.1016/j.jid.2016.11.045
6. Coates M, Blanchard S, MacLeod AS. Innate Antimicrobial Immunity in the Skin: A Protective Barrier Against Bacteria, Viruses, and Fungi. *PloS Pathog* (2018) 14(12):e1007353. doi: 10.1371/journal.ppat.1007353
7. Byrd AL, Belkaid Y, Segre JA. The Human Skin Microbiome. *Nat Rev Microbiol* (2018) 16(3):143–55. doi: 10.1038/nrmicro.2017.157
8. Schalka S, Silva MS, Lopes LF, de Freitas LM, Baptista MS. The Skin Redoxome. *J Eur Acad Dermatol Venereol* (2022) 36(2):181–95. doi: 10.1111/jdv.17780
9. Wondrak GT. Let the Sun Shine in: Mechanisms and Potential for Therapeutics in Skin Photodamage. *Curr Opin Investig Drugs* (2007) 8 (5):390–400.
10. Brash DE, Ziegler A, Jonason AS, Simon JA, Kunala S, Leffell DJ. Sunlight and Sunburn in Human Skin Cancer: P53, Apoptosis, and Tumor Promotion. *J Investig Dermatol Symp Proc* (1996) 1(2):136–42.
11. Wondrak GT, Jacobson MK, Jacobson EL. Endogenous UVA-Photosensitizers: Mediators of Skin Photodamage and Novel Targets for Skin Photoprotection. *Photochem Photobiol Sci* (2006) 5(2):215–37. doi: 10.1039/B504573H
12. Cadet J, Mouret S, Ravanat JL, Douki T. Photoinduced Damage to Cellular DNA: Direct and Photosensitized Reactions. *Photochem Photobiol* (2012) 88 (5):1048–65. doi: 10.1111/j.1751-1097.2012.01200.x
13. Prasad R, Katiyar SK. Crosstalk Among UV-Induced Inflammatory Mediators, DNA Damage and Epigenetic Regulators Facilitates Suppression of the Immune System. *Photochem Photobiol* (2017) 93 (4):930–6. doi: 10.1111/php.12687
14. Appenzeller BMR, Chadeau-Hyam M, Aguilar L. Skin Exposome Science in Practice : Current Evidence on Hair Biomonitoring and Future Perspectives. *J Eur Acad Dermatol Venereol* (2020) 34 Suppl 4:26–30. doi: 10.1111/jdv.16640
15. Grice EA, Segre JA. The Skin Microbiome. *Nat Rev Microbiol* (2011) 9 (4):244–53. doi: 10.1038/nrmicro2537
16. Juliano C, Magrini GA. Cosmetic Ingredients as Emerging Pollutants of Environmental and Health Concern. *A Mini-Rev Cosmetics* (2017) 4(2):11. doi: 10.3390/cosmetics4020011
17. Krutmann J, Bouloc A, Sore G, Bernard BA, Passeron T. The Skin Aging Exposome. *J Dermatol Sci* (2017) 85(3):152–61. doi: 10.1016/j.jdermsci.2016.09.015
18. Ferrara F, Prieux R, Woodby B, Valacchi G. Inflammasome Activation in Pollution-Induced Skin Conditions. *Plast Reconstr Surg* (2021) 147(1S-2):15S–24S. doi: 10.1097/PRS.0000000000007617
19. Xerfan EMS, Andersen ML, Facina AS, Tufik S, Tomimori J. Sleep Loss and the Skin: Possible Effects of This Stressful State on Cutaneous Regeneration During Nocturnal Dermatological Treatment and Related Pathways. *Dermatol Ther* (2022) 35(2):e15226. doi: 10.1111/dth.15226
20. Celebi Sozener Z, Ozdel Ozturk B, Cerci P, Turk M, Gorgulu Akin B, Akdis M, et al. Epithelial Barrier Hypothesis: Effect of External Exposome on Microbiome and Epithelial Barriers in Allergic Disease. *Allergy* (2022). doi: 10.1111/all.15240
21. Cope RB, Imsilp K, Morrow CK, Hartman J, Schaeffer DJ, Hansen LG. Exposure to Soil Contaminated With an Environmental PCB/PCDD/PCDF Mixture Modulates Ultraviolet Radiation-Induced Non-Melanoma Skin Carcinogenesis in the Crl:SKH1-hrBR Hairless Mouse. *Cancer Lett* (2003) 191(2):145–54. doi: 10.1016/S0304-3835(02)00636-5
22. Burns FJ, Uddin AN, Wu F, Nadas A, Rossman TG. Arsenic-Induced Enhancement of Ultraviolet Radiation Carcinogenesis in Mouse Skin: A Dose-Response Study. *Environ Health Perspect* (2004) 112(5):599–603. doi: 10.1289/ehp.6655
23. Wang Y, Gao D, Atencio DP, Perez E, Saladi R, Moore J, et al. Combined Subcarcinogenic Benzo[a]Pyrene and UVA Synergistically Caused High Tumor Incidence and Mutations in H-Ras Gene, But Not P53, in SKH-1 Hairless Mouse Skin. *Int J Cancer* (2005) 116(2):193–9. doi: 10.1002/ijc.21039
24. Meeran SM, Singh T, Nagy TR, Katiyar SK. High-Fat Diet Exacerbates Inflammation and Cell Survival Signals in the Skin of Ultraviolet B-Irradiated C57BL/6 Mice. *Toxicol Appl Pharmacol* (2009) 241(3):303–10. doi: 10.1016/j.taap.2009.09.003

25. Magiatis P, Pappas P, Gaitanis G, Mexia N, Melliou E, Galanou M, et al. Malassezia Yeasts Produce a Collection of Exceptionally Potent Activators of the Ah (Dioxin) Receptor Detected in Diseased Human Skin. *J Invest Dermatol* (2013) 133(8):2023–30. doi: 10.1038/jid.2013.92
26. O'Gorman SM, Murphy GM. Photosensitizing Medications and Photocarcinogenesis. *Photodermatol Photoimmunol Photomed* (2014) 30 (1):8–14. doi: 10.1111/phpp.12085
27. Hasche D, Stephan S, Braspenning-Wesch I, Mikulec J, Niebler M, Grone HJ, et al. The Interplay of UV and Cutaneous Papillomavirus Infection in Skin Cancer Development. *PloS Pathog* (2017) 13(11):e1006723. doi: 10.1371/journal.ppat.1006723
28. Godar DE. UV and Reactive Oxygen Species Activate Human Papillomaviruses Causing Skin Cancers. *Curr Probl Dermatol* (2021) 55:339–53. doi: 10.1159/000517643
29. Rojo de la Vega M, Zhang DD, Wondrak GT. Topical Bixin Confers NRF2-Dependent Protection Against Photodamage and Hair Graying in Mouse Skin. *Front Pharmacol* (2018) 9:287. doi: 10.3389/fphar.2018.00287
30. Morita A, Torii K, Maeda A, Yamaguchi Y. Molecular Basis of Tobacco Smoke-Induced Premature Skin Aging. *J Investig Dermatol Symp Proc* (2009) 14(1):53–5. doi: 10.1038/jidsymp.2009.13
31. Gromkowska-Kepka KJ, Puscion-Jakubik A, Markiewicz-Zukowska R, Socha K. The Impact of Ultraviolet Radiation on Skin Photoaging - Review of *In Vitro* Studies. *J Cosmet Dermatol* (2021) 20(11):3427–31. doi: 10.1111/jocd.14033
32. Martens MC, Emmert S, Boeckmann L. Sunlight, Vitamin D, and Xeroderma Pigmentosum. *Adv Exp Med Biol* (2020) 1268:319–31. doi: 10.1007/978-3-030-46227-7_16
33. Rizza ERH, DiGiovanna JJ, Khan SG, Tamura D, Jeskey JD, Kraemer KH. Xeroderma Pigmentosum: A Model for Human Premature Aging. *J Invest Dermatol* (2021) 141(4S):976–84. doi: 10.1016/j.jid.2020.11.012
34. Richardson SD, DeMarini DM, Kogevinas M, Fernandez P, Marco E, Lourencetti C, et al. What's in the Pool? A Comprehensive Identification of Disinfection by-Products and Assessment of Mutagenicity of Chlorinated and Brominated Swimming Pool Water. *Environ Health Perspect* (2010) 118(11):1523–30. doi: 10.1289/ehp.1001965
35. Leung TH, Zhang LF, Wang J, Ning S, Knox SJ, Kim SK. Topical Hypochlorite Ameliorates NF-kappaB-Mediated Skin Diseases in Mice. *J Clin Invest* (2013) 123(12):5361–70. doi: 10.1172/JCI70895
36. Jandova J, Snell J, Hua A, Dickinson S, Fimbres J, Wondrak GT. Topical Hypochlorous Acid (HOCl) Blocks Inflammatory Gene Expression and Tumorigenic Progression in UV-Exposed SKH-1 High Risk Mouse Skin. *Redox Biol* (2021) 45:102042. doi: 10.1016/j.redox.2021.102042
37. Kishimoto N, Nishimura H. Effect of pH and Moar Ratio of Pollutant to Oxidant on a Photochemical Advanced Oxidation Process Using Hypochlorite. *Environ Technol* (2015) 36(19):2436–42. doi: 10.1080/09593330.2015.1034187
38. Remucal CK, Manley D. Emerging Investigators Series: The Efficacy of Chlorine Photolysis as an Advanced Oxidation Process for Drinking Water Treatment. *Environ Sci Water Res Technol* (2016) 2:565–79. doi: 10.1039/C6EW00029K
39. Prutz WA. Hypochlorous Acid Interactions With Thiols, Nucleotides, DNA, and Other Biological Substrates. *Arch Biochem Biophys* (1996) 332(1):110–20. doi: 10.1006/abbi.1996.0322
40. Armesto XL, Canle ML, Garcia MV, Santaballa JA. Aqueous Chemistry of N-Halo-Compounds. *Chem Soc Rev* (1998) 27:453–60. doi: 10.1039/a827453z
41. Armesto XL, Canle ML, Fernandez MI, Garcia MV, Santaballa JA. First Steps in the Oxidation of Sulfur-Containing Amino Acids by Hypohalogenation: Very Fast Generation of Intermediate Sulfenyl Halides and Halosulfonium Cations. *Tetrahedron* (2000) 56:1103–9. doi: 10.1016/S0040-4020(99)01066-2
42. Pattison DI, Davies MJ. Absolute Rate Constants for the Reaction of Hypochlorous Acid With Protein Side Chains and Peptide Bonds. *Chem Res Toxicol* (2001) 14(10):1453–64. doi: 10.1021/tx0155451
43. Pattison DI, Hawkins CL, Davies MJ. Hypochlorous Acid-Mediated Oxidation of Lipid Components and Antioxidants Present in Low-Density Lipoproteins: Absolute Rate Constants, Product Analysis, and Computational Modeling. *Chem Res Toxicol* (2003) 16(4):439–49. doi: 10.1021/tx025670s
44. Wahman DG. Chlorinated Cyanurates: Review of Water Chemistry and Associated Drinking Water Implications. *J Am Water Works Assoc* (2018) 110(9):E1–E15. doi: 10.1002/awwa.1086
45. Chuang YH, Shi HJ. UV/Chlorinated Cyanurates as an Emerging Advanced Oxidation Process for Drinking Water and Potable Reuse Treatments. *Water Res* (2022) 211:118075. doi: 10.1016/j.watres.2022.118075
46. Ulfig A, Leichert LI. The Effects of Neutrophil-Generated Hypochlorous Acid and Other Hypohalous Acids on Host and Pathogens. *Cell Mol Life Sci* (2021) 78(2):385–414. doi: 10.1007/s00018-020-03591-y
47. Hawkins CL. Hypochlorous Acid-Mediated Modification of Proteins and its Consequences. *Essays Biochem* (2020) 64(1):75–86. doi: 10.1042/EBC20190045
48. Davies MJ. Myeloperoxidase: Mechanisms, Reactions and Inhibition as a Therapeutic Strategy in Inflammatory Diseases. *Pharmacol Ther* (2021) 218:107685. doi: 10.1016/j.pharmthera.2020.107685
49. Casciaro M, Di Salvo E, Pace E, Ventura-Spagnolo E, Navarra M, Gangemi S. Chlorinative Stress in Age-Related Diseases: A Literature Review. *Immun Ageing* (2017) 14:21. doi: 10.1186/s12979-017-0104-5
50. Samanta S, Govindaraju T. Unambiguous Detection of Elevated Levels of Hypochlorous Acid in Double Transgenic AD Mouse Brain. *ACS Chem Neurosci* (2019) 10(12):4847–53. doi: 10.1021/acschemneuro.9b00554
51. Trush MA, Egner PA, Kensler TW. Myeloperoxidase as a Biomarker of Skin Irritation and Inflammation. *Food Chem Toxicol* (1994) 32(2):143–7. doi: 10.1016/0278-6915(94)90175-9
52. Metz M, Lammel V, Gibbs BF, Maurer M. Inflammatory Murine Skin Responses to UV-B Light are Partially Dependent on Endothelin-1 and Mast Cells. *Am J Pathol* (2006) 169(3):815–22. doi: 10.2353/ajpath.2006.060037
53. Meeran SM, Punathil T, Katiyar SK. IL-12 Deficiency Exacerbates Inflammatory Responses in UV-Irradiated Skin and Skin Tumors. *J Invest Dermatol* (2008) 128(11):2716–27. doi: 10.1038/jid.2008.140
54. Rijken F, Bruijnzeel PL. The Pathogenesis of Photoaging: The Role of Neutrophils and Neutrophil-Derived Enzymes. *J Investig Dermatol Symp Proc* (2009) 14(1):67–72. doi: 10.1038/jidsymp.2009.15
55. Gasparoto TH, de Oliveira CE, de Freitas LT, Pinheiro CR, Ramos RN, da Silva AL, et al. Inflammatory Events During Murine Squamous Cell Carcinoma Development. *J Inflammation (Lond)* (2012) 9(1):46. doi: 10.1186/1476-9255-9-46
56. Zawrotniak M, Bartnicka D, Rapala-Kozik M. UVA and UVB Radiation Induce the Formation of Neutrophil Extracellular Traps by Human Polymorphonuclear Cells. *J Photochem Photobiol B* (2019) 196:111511. doi: 10.1016/j.jphotobiol.2019.111511
57. Haskamp S, Bruns H, Hahn M, Hoffmann M, Gregor A, Lohr S, et al. Myeloperoxidase Modulates Inflammation in Generalized Pustular Psoriasis and Additional Rare Pustular Skin Diseases. *Am J Hum Genet* (2020) 107 (3):527–38. doi: 10.1016/j.ajhg.2020.07.001
58. Strzepa A, Gurski CJ, Dittel LJ, Szczepanik M, Pritchard KAJr., Dittel BN. Neutrophil-Derived Myeloperoxidase Facilitates Both the Induction and Elicitation Phases of Contact Hypersensitivity. *Front Immunol* (2020) 11:608871. doi: 10.3389/fimmu.2020.608871
59. Neu SD, Strzepa A, Martin D, Sorci-Thomas MG, Pritchard KAJr., Dittel BN. Myeloperoxidase Inhibition Ameliorates Plaque Psoriasis in Mice. *Antioxid (Basel)* (2021) 10(9):1338. doi: 10.3390/antiox10091338
60. Moe CL, Rheingans RD. Global Challenges in Water, Sanitation and Health. *J Water Health* (2006) 4 Suppl 1:41–57. doi: 10.2166/wh.2006.0043
61. Rutala WA, Cole EC, Thomann CA, Weber DJ. Stability and Bactericidal Activity of Chlorine Solutions. *Infect Control Hosp Epidemiol* (1998) 19 (5):323–7. doi: 10.1086/647822
62. Daumer KM, Khan AU, Steinbeck MJ. Chlorination of Pyridinium Compounds. Possible Role of Hypochlorite, N-Chloramines, and Chlorine in the Oxidation of Pyridinoline Cross-Links of Articular Cartilage Collagen Type II During Acute Inflammation. *J Biol Chem* (2000) 275(44):34681–92. doi: 10.1074/jbc.M002003200
63. Wastensson G, Eriksson K. Inorganic Chloramines: A Critical Review of the Toxicological and Epidemiological Evidence as a Basis for Occupational Exposure Limit Setting. *Crit Rev Toxicol* (2020) 50(3):219–71. doi: 10.1080/10408444.2020.1744514

64. Gottardi W, Debabov D, Nagl M. N-Chloramines, a Promising Class of Well-Tolerated Topical Anti-Infectives. *Antimicrob Agents Chemother* (2013) 57(3):1107–14. doi: 10.1128/AAC.02132-12
65. Maitra D, Byun J, Andreana PR, Abdulhamid I, Saed GM, Diamond MP, et al. Mechanism of Hypochlorous Acid-Mediated Heme Destruction and Free Iron Release. *Free Radic Biol Med* (2011) 51(2):364–73. doi: 10.1016/j.freeradbiomed.2011.03.040
66. Maitra D, Shaeib F, Abdulhamid I, Abdulridha RM, Saed GM, Diamond MP, et al. Myeloperoxidase Acts as a Source of Free Iron During Steady-State Catalysis by a Feedback Inhibitory Pathway. *Free Radic Biol Med* (2013) 63:90–8. doi: 10.1016/j.freeradbiomed.2013.04.009
67. Candeias LP, Stratford MR, Wardman P. Formation of Hydroxyl Radicals on Reaction of Hypochlorous Acid With Ferrocyanide, a Model Iron(II) Complex. *Free Radic Res* (1994) 20(4):241–9. doi: 10.3109/10715769409147520
68. Candeias LP, Patel KB, Stratford MR, Wardman P. Free Hydroxyl Radicals are Formed on Reaction Between the Neutrophil-Derived Species Superoxide Anion and Hypochlorous Acid. *FEBS Lett* (1993) 333(1-2):151–3. doi: 10.1016/0014-5793(93)80394-A
69. Miyamoto S, Martinez GR, Rettori D, Augusto O, Medeiros MH, Di Mascio P. Linoleic Acid Hydroperoxide Reacts With Hypochlorous Acid, Generating Peroxyl Radical Intermediates and Singlet Molecular Oxygen. *Proc Natl Acad Sci USA* (2006) 103(2):293–8. doi: 10.1073/pnas.0508170103
70. Ximenes VF, Ximenes TP, Morgon NH, de Souza AR. Taurine Chloramine and Hydrogen Peroxide as a Potential Source of Singlet Oxygen for Topical Application. *Photochem Photobiol* (2021) 97(5):963–70. doi: 10.1111/php.13410
71. Bauer G. HOCl-Dependent Singlet Oxygen and Hydroxyl Radical Generation Modulate and Induce Apoptosis of Malignant Cells. *Anticancer Res* (2013) 33(9):3589–602.
72. Hazen SL, Hsu FF, Duffin K, Heinecke JW. Molecular Chlorine Generated by the Myeloperoxidase-Hydrogen Peroxide-Chloride System of Phagocytes Converts Low Density Lipoprotein Cholesterol Into a Family of Chlorinated Sterols. *J Biol Chem* (1996) 271(38):23080–8. doi: 10.1074/jbc.271.38.23080
73. Hazen SL, Hsu FF, Mueller DM, Crowley JR, Heinecke JW. Human Neutrophils Employ Chlorine Gas as an Oxidant During Phagocytosis. *J Clin Invest* (1996) 98(6):1283–9. doi: 10.1172/JCI118914
74. Hazen SL, Hsu FF, Gaut JP, Crowley JR, Heinecke JW. Modification of Proteins and Lipids by Myeloperoxidase. *Methods Enzymol* (1999) 300:88–105. doi: 10.1016/S0076-6879(99)00117-2
75. Eiserich JP, Cross CE, Jones AD, Halliwell B, van der Vliet A. Formation of Nitrating and Chlorinating Species by Reaction of Nitrite With Hypochlorous Acid. A Novel Mechanism for Nitric Oxide-Mediated Protein Modification. *J Biol Chem* (1996) 271(32):19199–208. doi: 10.1074/jbc.271.32.19199
76. Hawkins CL, Pattison DI, Davies MJ. Hypochlorite-Induced Oxidation of Amino Acids, Peptides and Proteins. *Amino Acids* (2003) 25(3-4):259–74. doi: 10.1007/s00726-003-0016-x
77. Villamena FA. Chemistry of Reactive Species. In: *Reactive Species Detection in Biology*. Amsterdam, Netherland: Elsevier (2017). p. 13–64. doi: 10.1016/B978-0-12-420017-3.00005-0
78. Davies MJ, Hawkins CL. The Role of Myeloperoxidase in Biomolecule Modification, Chronic Inflammation, and Disease. *Antioxid Redox Signal* (2020) 32(13):957–81. doi: 10.1089/ars.2020.8030
79. Hazell LJ, van den Berg JJ, Stocker R. Oxidation of Low-Density Lipoprotein by Hypochlorite Causes Aggregation That is Mediated by Modification of Lysine Residues Rather Than Lipid Oxidation. *Biochem J* (1994) 302(Pt 1):297–304. doi: 10.1042/bj3020297
80. Shabani F, McNeil J, Tippett L. The Oxidative Inactivation of Tissue Inhibitor of Metalloproteinase-1 (TIMP-1) by Hypochlorous Acid (HOCI) is Suppressed by Anti-Rheumatic Drugs. *Free Radic Res* (1998) 28(2):115–23. doi: 10.3109/10715769809065797
81. Kang JIJr., Neidigh JW. Hypochlorous Acid Damages Histone Proteins Forming 3-Chlorotyrosine and 3,5-Dichlorotyrosine. *Chem Res Toxicol* (2008) 21(5):1028–38. doi: 10.1021/tx7003486
82. Strosova M, Karlovska J, Spickett CM, Grune T, Orszagova Z, Horakova L. Oxidative Injury Induced by Hypochlorous Acid to Ca-ATPase From Sarcoplasmic Reticulum of Skeletal Muscle and Protective Effect of Trolox. *Gen Physiol Biophys* (2009) 28(2):195–209. doi: 10.4149/gpb_2009_02_195
83. Cook NL, Viola HM, Sharov VS, Hool LC, Schoneich C, Davies MJ. Myeloperoxidase-Derived Oxidants Inhibit Sarco/Endoplasmic Reticulum Ca2+-ATPase Activity and Perturb Ca2+ Homeostasis in Human Coronary Artery Endothelial Cells. *Free Radic Biol Med* (2012) 52(5):951–61. doi: 10.1016/j.freeradbiomed.2011.12.001
84. Pelgrift RY, Friedman AJ. Topical Hypochlorous Acid (HOCl) as a Potential Treatment of Pruritus. *Curr Derm Rep* (2013) 2:181–90. doi: 10.1007/s13671-013-0052-z
85. Gorudko IV, Grigorieva DV, Shamova EV, Kostevich VA, Sokolov AV, Mikhalchik EV, et al. Hypohalous Acid-Modified Human Serum Albumin Induces Neutrophil NADPH Oxidase Activation, Degranulation, and Shape Change. *Free Radic Biol Med* (2014) 68:326–34. doi: 10.1016/j.freeradbiomed.2013.12.023
86. Ning J, Lin Z, Zhao X, Zhao B, Miao J. Inhibiting Lysine 353 Oxidation of GRP78 by a Hypochlorous Probe Targeting Endoplasmic Reticulum Promotes Autophagy in Cancer Cells. *Cell Death Dis* (2019) 10(11):858. doi: 10.1038/s41419-019-2095-y
87. Ulfig A, Schulz AV, Muller A, Lupilov N, Leichert LI. N-Chlorination Mediates Protective and Immunomodulatory Effects of Oxidized Human Plasma Proteins. *Elife* (2019) 8:e47395. doi: 10.7554/eLife.47395
88. Robins LI, Keim EK, Robins DB, Edgar JS, Meschke JS, Gafken PR, et al. Modifications of IL-6 by Hypochlorous Acids: Effects on Receptor Binding. *ACS Omega* (2021) 6(51):35593–9. doi: 10.1021/acsomega.1c05297
89. Ulfig A, Bader V, Varatnitskaya M, Lupilov N, Winklhofer KF, Leichert LI. Hypochlorous Acid-Modified Human Serum Albumin Suppresses MHC Class II - Dependent Antigen Presentation in Pro-Inflammatory Macrophages. *Redox Biol* (2021) 43:101981. doi: 10.1016/j.redox.2021.101981
90. Mainnemare A, Megarbane B, Soueidan A, Daniel A, Chapple IL. Hypochlorous Acid and Taurine-N-Monochloramine in Periodontal Diseases. *J Dent Res* (2004) 83(11):823–31. doi: 10.1177/154405910408301101
91. Kalogiannis M, Delikatny EJ, Jeitner TM. Serotonin as a Putative Scavenger of Hypohalous Acid in the Brain. *Biochim Biophys Acta* (2016) 1862(4):651–61. doi: 10.1016/j.bbadis.2015.12.012
92. Winterbourn CC, van den Berg JJ, Roitman E, Kuypers FA. Chlorohydrin Formation From Unsaturated Fatty Acids Reacted With Hypochlorous Acid. *Arch Biochem Biophys* (1992) 296(2):547–55. doi: 10.1016/0003-9861(92)90609-Z
93. Carr AC, van den Berg JJ, Winterbourn CC. Chlorination of Cholesterol in Cell Membranes by Hypochlorous Acid. *Arch Biochem Biophys* (1996) 332(1):63–9. doi: 10.1006/abbi.1996.0317
94. Carr AC, Vissers MC, Domigan NM, Winterbourn CC. Modification of Red Cell Membrane Lipids by Hypochlorous Acid and Haemolysis by Preformed Lipid Chlorohydrins. *Redox Rep* (1997) 3(5-6):263–71. doi: 10.1080/13510002.1997.11747122
95. Spickett CM, Jerlich A, Panasenko OM, Arnhold J, Pitt AR, Stelmaszynska T, et al. The Reactions of Hypochlorous Acid, the Reactive Oxygen Species Produced by Myeloperoxidase, With Lipids. *Acta Biochim Pol* (2000) 47(4):889–99. doi: 10.18388/abp.2000_3944
96. Thukkani AK, McHowat J, Hsu FF, Brennan ML, Hazen SL, Ford DA. Identification of Alpha-Chloro Fatty Aldehydes and Unsaturated Lysophosphatidylcholine Molecular Species in Human Atherosclerotic Lesions. *Circulation* (2003) 108(25):3128–33. doi: 10.1161/01.CIR.0000104564.01539.6A
97. Kawai Y, Kiyokawa H, Kimura Y, Kato Y, Tsuchiya K, Terao J. Hypochlorous Acid-Derived Modification of Phospholipids: Characterization of Aminophospholipids as Regulatory Molecules for Lipid Peroxidation. *Biochemistry* (2006) 45(47):14201–11. doi: 10.1021/bi0610909
98. Lessig J, Fuchs B. HOCl-Mediated Glycerophosphocholine and Glycerophosphoethanolamine Generation From Plasmalogens in Phospholipid Mixtures. *Lipids* (2010) 45(1):37–51. doi: 10.1007/s11745-009-3365-8
99. Schroter J, Schiller J. Chlorinated Phospholipids and Fatty Acids: (Patho) physiological Relevance, Potential Toxicity, and Analysis of Lipid

Chlorohydrins. *Oxid Med Cell Longev* (2016) 2016:8386362. doi: 10.1155/2016/8386362
100. Masuda M, Suzuki T, Friesen MD, Ravanat JL, Cadet J, Pignatelli B, et al. Chlorination of Guanosine and Other Nucleosides by Hypochlorous Acid and Myeloperoxidase of Activated Human Neutrophils. Catalysis by Nicotine and Trimethylamine. *J Biol Chem* (2001) 276(44):40486–96. doi: 10.1074/jbc.M102700200
101. Hawkins CL, Davies MJ. Hypochlorite-Induced Damage to DNA, RNA, and Polynucleotides: Formation of Chloramines and Nitrogen-Centered Radicals. *Chem Res Toxicol* (2002) 15(1):83–92. doi: 10.1021/tx015548d
102. Macer-Wright JL, Stanley NR, Portman N, Tan JT, Bursill C, Rayner BS, et al. A Role for Chlorinated Nucleosides in the Perturbation of Macrophage Function and Promotion of Inflammation. *Chem Res Toxicol* (2019) 32(6):1223–34. doi: 10.1021/acs.chemrestox.9b00044
103. Winterbourn CC. Comparative Reactivities of Various Biological Compounds With Myeloperoxidase-Hydrogen Peroxide-Chloride, and Similarity of the Oxidant to Hypochlorite. *Biochim Biophys Acta* (1985) 840(2):204–10. doi: 10.1016/0304-4165(85)90120-5
104. Gottardi W, Nagl M. N-Chlorotaurine, a Natural Antiseptic With Outstanding Tolerability. *J Antimicrob Chemother* (2010) 65(3):399–409. doi: 10.1093/jac/dkp466
105. Siwak J, Lewinska A, Wnuk M, Bartosz G. Protection of Flavonoids Against Hypochlorite-Induced Protein Modifications. *Food Chem* (2013) 141(2):1227–41. doi: 10.1016/j.foodchem.2013.04.018
106. Shaeib F, Khan SN, Ali I, Najafi T, Maitra D, Abdulhamid I, et al. Melatonin Prevents Myeloperoxidase Heme Destruction and the Generation of Free Iron Mediated by Self-Generated Hypochlorous Acid. *PloS One* (2015) 10(3):e0120737. doi: 10.1371/journal.pone.0120737
107. Asahi T, Wu X, Shimoda H, Hisaka S, Harada E, Kanno T, et al. A Mushroom-Derived Amino Acid, Ergothioneine, is a Potential Inhibitor of Inflammation-Related DNA Halogenation. *Biosci Biotechnol Biochem* (2016) 80(2):313–7. doi: 10.1080/09168451.2015.1083396
108. Carvalho LAC, Lopes J, Kaihami GH, Silva RP, Bruni-Cardoso A, Baldini RL, et al. Uric Acid Disrupts Hypochlorous Acid Production and the Bactericidal Activity of HL-60 Cells. *Redox Biol* (2018) 16:179–88. doi: 10.1016/j.redox.2018.02.020
109. Nagl M, Arnitz R, Lackner M. N-Chlorotaurine, a Promising Future Candidate for Topical Therapy of Fungal Infections. *Mycopathologia* (2018) 183(1):161–70. doi: 10.1007/s11046-017-0175-z
110. Madu H, Avance J, Chetyrkin S, Darris C, Rose KL, Sanchez OA, et al. Pyridoxamine Protects Proteins From Damage by Hypohalous Acids *In Vitro* and In Vivo. *Free Radic Biol Med* (2015) 89:83–90. doi: 10.1016/j.freeradbiomed.2015.07.001
111. Zoete V, Bailly F, Vezin H, Teissier E, Duriez P, Fruchart JC, et al. 4-Mercaptoimidazoles Derived From the Naturally Occurring Antioxidant Ovothiols 1. Antioxidant Properties. *Free Radic Res* (2000) 32(6):515–24. doi: 10.1080/10715760000300521
112. Carroll L, Karton A, Radom L, Davies MJ, Pattison DI. Carnosine and Carcinine Derivatives Rapidly React With Hypochlorous Acid to Form Chloramines and Dichloramines. *Chem Res Toxicol* (2019) 32(3):513–25. doi: 10.1021/acs.chemrestox.8b00363
113. Choe JK, Hua LC, Komaki Y, Simpson AM, McCurry DL, Mitch WA. Evaluation of Histidine Reactivity and Byproduct Formation During Peptide Chlorination. *Environ Sci Technol* (2021) 55(3):1790–9. doi: 10.1021/acs.est.0c07408
114. Marcinkiewicz J, Kontny E. Taurine and Inflammatory Diseases. *Amino Acids* (2014) 46(1):7–20. doi: 10.1007/s00726-012-1361-4
115. Gottardi W, Nagl M. Chemical Properties of N-Chlorotaurine Sodium, a Key Compound in the Human Defence System. *Arch Pharm (Weinheim)* (2002) 335(9):411–21. doi: 10.1002/1521-4184(200212)335:9<411::AID-ARDP411>3.0.CO;2-D
116. Midwinter RG, Cheah FC, Moskovitz J, Vissers MC, Winterbourn CC. IkappaB is a Sensitive Target for Oxidation by Cell-Permeable Chloramines: Inhibition of NF-kappaB Activity by Glycine Chloramine Through Methionine Oxidation. *Biochem J* (2006) 396(1):71–8. doi: 10.1042/BJ20052026
117. Kanayama A, Inoue J, Sugita-Konishi Y, Shimizu M, Miyamoto Y. Oxidation of Ikappa Balpha at Methionine 45 is One Cause of Taurine Chloramine-Induced Inhibition of NF-Kappa B Activation. *J Biol Chem* (2002) 277(27):24049–56. doi: 10.1074/jbc.M110832200
118. Seidel U, Huebbe P, Rimbach G. Taurine: A Regulator of Cellular Redox Homeostasis and Skeletal Muscle Function. *Mol Nutr Food Res* (2019) 63(16):e1800569. doi: 10.1002/mnfr.201800569
119. van Veldhoven K, Keski-Rahkonen P, Barupal DK, Villanueva CM, Font-Ribera L, Scalbert A, et al. Effects of Exposure to Water Disinfection by-Products in a Swimming Pool: A Metabolome-Wide Association Study. *Environ Int* (2018) 111:60–70. doi: 10.1016/j.envint.2017.11.017
120. Leusch FDL, Neale PA, Busetti F, Card M, Humpage A, Orbell JD, et al. Transformation of Endocrine Disrupting Chemicals, Pharmaceutical and Personal Care Products During Drinking Water Disinfection. *Sci Total Environ* (2019) 657:1480–90. doi: 10.1016/j.scitotenv.2018.12.106
121. Suppes LM, Abrell L, Dufour AP, Reynolds KA. Assessment of Swimmer Behaviors on Pool Water Ingestion. *J Water Health* (2014) 12(2):269–79. doi: 10.2166/wh.2013.123
122. Srivastav AL, Patel N, Chaudhary VK. Disinfection by-Products in Drinking Water: Occurrence, Toxicity and Abatement. *Environ Pollut* (2020) 267:115474. doi: 10.1016/j.envpol.2020.115474
123. Li XF, Mitch WA. Drinking Water Disinfection Byproducts (DBPs) and Human Health Effects: Multidisciplinary Challenges and Opportunities. *Environ Sci Technol* (2018) 52(4):1681–9. doi: 10.1021/acs.est.7b05440
124. Muellner MG, Wagner ED, McCalla K, Richardson SD, Woo YT, Plewa MJ. Haloacetonitriles vs. Regulated Haloacetic Acids: Are Nitrogen-Containing DBPs More Toxic? *Environ Sci Technol* (2007) 41(2):645–51. doi: 10.1021/es0617441
125. Bagheban M, Baghdadi M, Mohammadi A, Roozbehnia P. Investigation of the Effective Factors on the Mutagen X Formation in Drinking Water by Response Surface Methodology. *J Environ Manage* (2019) 251:109515. doi: 10.1016/j.jenvman.2019.109515
126. Soufan M, Deborde M, Legube B. Aqueous Chlorination of Diclofenac: Kinetic Study and Transformation Products Identification. *Water Res* (2012) 46(10):3377–86. doi: 10.1016/j.watres.2012.03.056
127. Zhang R, He Y, Yao L, Chen J, Zhu S, Rao X, et al. Metformin Chlorination Byproducts in Drinking Water Exhibit Marked Toxicities of a Potential Health Concern. *Environ Int* (2021) 146:106244. doi: 10.1016/j.envint.2020.106244
128. He Y, Jin H, Gao H, Zhang G, Ju F. Prevalence, Production, and Ecotoxicity of Chlorination-Derived Metformin Byproducts in Chinese Urban Water Systems. *Sci Total Environ* (2022) 816:151665. doi: 10.1016/j.scitotenv.2021.151665
129. Negreira N, Regueiro J, Lopez de Alda M, Barcelo D. Transformation of Tamoxifen and its Major Metabolites During Water Chlorination: Identification and in Silico Toxicity Assessment of Their Disinfection Byproducts. *Water Res* (2015) 85:199–207. doi: 10.1016/j.watres.2015.08.036
130. Zhuang R, Zabar R, Grbovic G, Dolenc D, Yao J, Tisler T, et al. Stability and Toxicity of Selected Chlorinated Benzophenone-Type UV Filters in Waters. *Acta Chim Slov* (2013) 60(4):826–32.
131. Crista DM, Miranda MS, Esteves da Silva JC. Degradation in Chlorinated Water of the UV Filter 4-Tert-Butyl-4'-Methoxydibenzoylmethane Present in Commercial Sunscreens. *Environ Technol* (2015) 36(9-12):1319–26. doi: 10.1080/09593330.2014.988184
132. Sharifan H, Klein D, Morse AN. UV Filters Interaction in the Chlorinated Swimming Pool, a New Challenge for Urbanization, a Need for Community Scale Investigations. *Environ Res* (2016) 148:273–6. doi: 10.1016/j.envres.2016.04.002
133. Zhang S, Wang X, Yang H, Xie YF. Chlorination of Oxybenzone: Kinetics, Transformation, Disinfection Byproducts Formation, and Genotoxicity Changes. *Chemosphere* (2016) 154:521–7. doi: 10.1016/j.chemosphere.2016.03.116
134. Wang C, Bavcon Kralj M, Kosmrlj B, Yao J, Kosenina S, Polyakova OV, et al. Stability and Removal of Selected Avobenzone's Chlorination Products. *Chemosphere* (2017) 182:238–44. doi: 10.1016/j.chemosphere.2017.04.125
135. Yang P, Kong D, Ji Y, Lu J, Yin X, Zhou Q. Chlorination and Chloramination of Benzophenone-3 and Benzophenone-4 UV Filters. *Ecotoxicol Environ Saf* (2018) 163:528–35. doi: 10.1016/j.ecoenv.2018.07.111
136. Vile GF, Rothwell LA, Kettle AJ. Hypochlorous Acid Activates the Tumor Suppressor Protein P53 in Cultured Human Skin Fibroblasts. *Arch Biochem Biophys* (1998) 359(1):51–6. doi: 10.1006/abbi.1998.0881

137. Zhu L, Pi J, Wachi S, Andersen ME, Wu R, Chen Y. Identification of Nrf2-Dependent Airway Epithelial Adaptive Response to Proinflammatory Oxidant-Hypochlorous Acid Challenge by Transcription Profiling. *Am J Physiol Lung Cell Mol Physiol* (2008) 294(3):L469–77. doi: 10.1152/ajplung.00310.2007
138. West JD, Wang Y, Morano KA. Small Molecule Activators of the Heat Shock Response: Chemical Properties, Molecular Targets, and Therapeutic Promise. *Chem Res Toxicol* (2012) 25(10):2036–53. doi: 10.1021/tx300264x
139. Midwinter RG, Vissers MC, Winterbourn CC. Hypochlorous Acid Stimulation of the Mitogen-Activated Protein Kinase Pathway Enhances Cell Survival. *Arch Biochem Biophys* (2001) 394(1):13–20. doi: 10.1006/abbi.2001.2530
140. Lane AE, Tan JT, Hawkins CL, Heather AK, Davies MJ. The Myeloperoxidase-Derived Oxidant HOSCN Inhibits Protein Tyrosine Phosphatases and Modulates Cell Signalling *via* the Mitogen-Activated Protein Kinase (MAPK) Pathway in Macrophages. *Biochem J* (2010) 430 (1):161–9. doi: 10.1042/BJ20100082
141. Hoyle GW, Svendsen ER. Persistent Effects of Chlorine Inhalation on Respiratory Health. *Ann N Y Acad Sci* (2016) 1378(1):33–40. doi: 10.1111/nyas.13139
142. Chia Shi Zhe G, Green A, Fong YT, Lee HY, Ho SF. Rare Case of Type I Hypersensitivity Reaction to Sodium Hypochlorite Solution in a Healthcare Setting. *BMJ Case Rep* (2016) 2016:bcr2016217228. doi: 10.1136/bcr-2016-217228
143. Goma A, de Lluis R, Roca-Ferrer J, Lafuente J, Picado C. Respiratory, Ocular and Skin Health in Recreational and Competitive Swimmers: Beneficial Effect of a New Method to Reduce Chlorine Oxidant Derivatives. *Environ Res* (2017) 152:315–21. doi: 10.1016/j.envres.2016.10.030
144. Van Den Broucke S, Pollaris L, Vande Velde G, Verbeken E, Nemery B, Vanoirbeek J, et al. Irritant-Induced Asthma to Hypochlorite in Mice Due to Impairment of the Airway Barrier. *Arch Toxicol* (2018) 92(4):1551–61. doi: 10.1007/s00204-018-2161-8
145. Thickett KM, McCoach JS, Gerber JM, Sadhra S, Burge PS. Occupational Asthma Caused by Chloramines in Indoor Swimming-Pool Air. *Eur Respir J* (2002) 19(5):827–32. doi: 10.1183/09031936.02.00232802
146. Venglarik CJ, Giron-Calle J, Wigley AF, Malle E, Watanabe N, Forman HJ. Hypochlorous Acid Alters Bronchial Epithelial Cell Membrane Properties and Prevention by Extracellular Glutathione. *J Appl Physiol (1985)* (2003) 95 (6):2444–52. doi: 10.1152/japplphysiol.00002.2003
147. Bougault V, Turmel J, St-Laurent J, Bertrand M, Boulet LP. Asthma, Airway Inflammation and Epithelial Damage in Swimmers and Cold-Air Athletes. *Eur Respir J* (2009) 33(4):740–6. doi: 10.1183/09031936.00117708
148. Li JH, Wang ZH, Zhu XJ, Deng ZH, Cai CX, Qiu LQ, et al. Health Effects From Swimming Training in Chlorinated Pools and the Corresponding Metabolic Stress Pathways. *PloS One* (2015) 10(3):e0119241. doi: 10.1371/journal.pone.0119241
149. Font-Ribera L, Kogevinas M, Zock JP, Gomez FP, Barreiro E, Nieuwenhuijsen MJ, et al. Short-Term Changes in Respiratory Biomarkers After Swimming in a Chlorinated Pool. *Environ Health Perspect* (2010) 118 (11):1538–44. doi: 10.1289/ehp.1001961
150. Font-Ribera L, Marco E, Grimalt JO, Pastor S, Marcos R, Abramsson-Zetterberg L, et al. Exposure to Disinfection by-Products in Swimming Pools and Biomarkers of Genotoxicity and Respiratory Damage - The PISCINA2 Study. *Environ Int* (2019) 131:104988. doi: 10.1016/j.envint.2019.104988
151. Kogevinas M, Villanueva CM, Font-Ribera L, Liviac D, Bustamante M, Espinoza F, et al. Genotoxic Effects in Swimmers Exposed to Disinfection by-Products in Indoor Swimming Pools. *Environ Health Perspect* (2010) 118 (11):1531–7. doi: 10.1289/ehp.1001959
152. Vizcaya D, Christensen KY, Lavoue J, Siemiatycki J. Risk of Lung Cancer Associated With Six Types of Chlorinated Solvents: Results From Two Case-Control Studies in Montreal, Canada. *Occup Environ Med* (2013) 70(2):81–5. doi: 10.1136/oemed-2012-101155
153. Dias MF, Reis MP, Acurcio LB, Carmo AO, Diamantino CF, Motta AM, et al. Changes in Mouse Gut Bacterial Community in Response to Different Types of Drinking Water. *Water Res* (2018) 132:79–89. doi: 10.1016/j.watres.2017.12.052
154. Fish KE, Reeves-McLaren N, Husband S, Boxall J. Unchartered Waters: The Unintended Impacts of Residual Chlorine on Water Quality and Biofilms. *NPJ Biofilms Microbiomes* (2020) 6(1):34. doi: 10.1038/s41522-020-00144-w
155. Sasada T, Hinoi T, Saito Y, Adachi T, Takakura Y, Kawaguchi Y, et al. Chlorinated Water Modulates the Development of Colorectal Tumors With Chromosomal Instability and Gut Microbiota in Apc-Deficient Mice. *PloS One* (2015) 10(7):e0132435. doi: 10.1371/journal.pone.0132435
156. El-Tawil AM. Colorectal Cancers and Chlorinated Water. *World J Gastrointest Oncol* (2016) 8(4):402–9. doi: 10.4251/wjgo.v8.i4.402
157. Prochazka E, Melvin SD, Escher BI, Plewa MJ, Leusch FDL. Global Transcriptional Analysis of Nontransformed Human Intestinal Epithelial Cells (FHs 74 Int) After Exposure to Selected Drinking Water Disinfection By-Products. *Environ Health Perspect* (2019) 127(11):117006. doi: 10.1289/EHP4945
158. Chang JH, Vogt CR, Sun GY, Sun AY. Effects of Acute Administration of Chlorinated Water on Liver Lipids. *Lipids* (1981) 16(5):336–40. doi: 10.1007/BF02534958
159. Plaa GL. Chlorinated Methanes and Liver Injury: Highlights of the Past 50 Years. *Annu Rev Pharmacol Toxicol* (2000) 40:42–65. doi: 10.1146/annurev.pharmtox.40.1.43
160. Faustino-Rocha AI, Rodrigues D, da Costa RG, Diniz C, Aragao S, Talhada D, et al. Trihalomethanes in Liver Pathology: Mitochondrial Dysfunction and Oxidative Stress in the Mouse. *Environ Toxicol* (2016) 31(8):1009–16. doi: 10.1002/tox.22110
161. Zheng S, Yang Y, Wen C, Liu W, Cao L, Feng X, et al. Effects of Environmental Contaminants in Water Resources on Nonalcoholic Fatty Liver Disease. *Environ Int* (2021) 154:106555. doi: 10.1016/j.envint.2021.106555
162. Peck B, Workeneh B, Kadikoy H, Patel SJ, Abdellatif A. Spectrum of Sodium Hypochlorite Toxicity in Man-Also a Concern for Nephrologists. *NDT Plus* (2011) 4(4):231–5. doi: 10.1093/ndtplus/sfr053
163. Brown KL, Darris C, Rose KL, Sanchez OA, Madu H, Avance J, et al. Hypohalous Acids Contribute to Renal Extracellular Matrix Damage in Experimental Diabetes. *Diabetes* (2015) 64(6):2242–53. doi: 10.2337/db14-1001
164. Afshinnia F, Zeng L, Byun J, Gadegbeku CA, Magnone MC, Whatling C, et al. Myeloperoxidase Levels and Its Product 3-Chlorotyrosine Predict Chronic Kidney Disease Severity and Associated Coronary Artery Disease. *Am J Nephrol* (2017) 46(1):73–81. doi: 10.1159/000477766
165. Parvez S, Ashby JL, Kimura SY, Richardson SD. Exposure Characterization of Haloacetic Acids in Humans for Exposure and Risk Assessment Applications: An Exploratory Study. *Int J Environ Res Public Health* (2019) 16(3):471. doi: 10.3390/ijerph16030471
166. Evlampidou I, Font-Ribera L, Rojas-Rueda D, Gracia-Lavedan E, Costet N, Pearce N, et al. Trihalomethanes in Drinking Water and Bladder Cancer Burden in the European Union. *Environ Health Perspect* (2020) 128 (1):17001. doi: 10.1289/EHP4495
167. Stroman DW, Mintun K, Epstein AB, Brimer CM, Patel CR, Branch JD, et al. Reduction in Bacterial Load Using Hypochlorous Acid Hygiene Solution on Ocular Skin. *Clin Ophthalmol* (2017) 11:707–14. doi: 10.2147/OPTH.S132851
168. Del Rosso JQ, Bhatia N. Status Report on Topical Hypochlorous Acid: Clinical Relevance of Specific Formulations, Potential Modes of Action, and Study Outcomes. *J Clin Aesthet Dermatol* (2018) 11(11):36–9.
169. SanMiguel AJ, Meisel JS, Horwinski J, Zheng Q, Bradley CW, Grice EA. Antiseptic Agents Elicit Short-Term, Personalized, and Body Site-Specific Shifts in Resident Skin Bacterial Communities. *J Invest Dermatol* (2018) 138 (10):2234–43. doi: 10.1016/j.jid.2018.04.022
170. Severing AL, Rembe JD, Koester V, Stuermer EK. Safety and Efficacy Profiles of Different Commercial Sodium Hypochlorite/Hypochlorous Acid Solutions (NaClO/HClO): Antimicrobial Efficacy, Cytotoxic Impact and Physicochemical Parameters In Vitro. *J Antimicrob Chemother* (2019) 74(2):365–72. doi: 10.1093/jac/dky432
171. Tran AQ, Topilow N, Rong A, Persad PJ, Lee MC, Lee JH, et al. Comparison of Skin Antiseptic Agents and the Role of 0.01% Hypochlorous Acid. *Aesthet Surg J* (2021) 41(10):1170–5. doi: 10.1093/asj/sjaa322
172. Karagas MR, Villanueva CM, Nieuwenhuijsen M, Weisel CP, Cantor KP, Kogevinas M. Disinfection Byproducts in Drinking Water and Skin Cancer? A Hypothesis. *Cancer Causes Control* (2008) 19(5):547–8. doi: 10.1007/s10552-008-9116-y

173. Fukuyama T, Ehling S, Wilzopolski J, Baumer W. Comparison of Topical Tofacitinib and 0.1% Hypochlorous Acid in a Murine Atopic Dermatitis Model. *BMC Pharmacol Toxicol* (2018) 19(1):37. doi: 10.1186/s40360-018-0232-3
174. Fukuyama T, Martel BC, Linder KE, Ehling S, Ganchingco JR, Baumer W. Hypochlorous Acid is Antipruritic and Anti-Inflammatory in a Mouse Model of Atopic Dermatitis. *Clin Exp Allergy* (2018) 48(1):78–88. doi: 10.1111/cea.13045
175. Liu TW, Gammon ST, Yang P, Fuentes D, Piwnica-Worms D. Myeloid Cell-Derived HOCl is a Paracrine Effector That Trans-Inhibits IKK/NF-kappaB in Melanoma Cells and Limits Early Tumor Progression. *Sci Signal* (2021) 14 (677):eaax5971. doi: 10.1126/scisignal.aax5971
176. Zhou Y, Ye T, Ye C, Wan C, Yuan S, Liu Y, et al. Secretions From Hypochlorous Acid-Treated Tumor Cells Delivered in a Melittin Hydrogel Potentiate Cancer Immunotherapy. *Bioact Mater* (2022) 9:541–53. doi: 10.1016/j.bioactmat.2021.07.019
177. Bauer G. HOCl and the Control of Oncogenesis. *J Inorg Biochem* (2018) 179:10–23. doi: 10.1016/j.jinorgbio.2017.11.005
178. Freund E, Miebach L, Stope MB, Bekeschus S. Hypochlorous Acid Selectively Promotes Toxicity and the Expression of Danger Signals in Human Abdominal Cancer Cells. *Oncol Rep* (2021) 45(5):71. doi: 10.3892/or.2021.8022
179. Biedron R, Konopinski MK, Marcinkiewicz J, Jozefowski S. Oxidation by Neutrophils-Derived HOCl Increases Immunogenicity of Proteins by Converting Them Into Ligands of Several Endocytic Receptors Involved in Antigen Uptake by Dendritic Cells and Macrophages. *PloS One* (2015) 10(4): e0123293. doi: 10.1371/journal.pone.0123293
180. Prokopowicz ZM, Arce F, Biedron R, Chiang CL, Ciszek M, Katz DR, et al. Hypochlorous Acid: A Natural Adjuvant That Facilitates Antigen Processing, Cross-Priming, and the Induction of Adaptive Immunity. *J Immunol* (2010) 184(2):824–35. doi: 10.4049/jimmunol.0902606
181. Gold MH, Andriessen A, Bhatia AC, Bitter PJr., Chilukuri S, Cohen JL, et al. Topical Stabilized Hypochlorous Acid: The Future Gold Standard for Wound Care and Scar Management in Dermatologic and Plastic Surgery Procedures. *J Cosmet Dermatol* (2020) 19(2):270–7. doi: 10.1111/jocd.13280
182. Han J, Liu X, Xiong H, Wang J, Wang B, Song X, et al. Investigation of the Relationship Between H2O2 and HClO in Living Cells by a Bifunctional, Dual-Ratiometric Responsive Fluorescent Probe. *Anal Chem* (2020) 92 (7):5134–42. doi: 10.1021/acs.analchem.9b05604

Author Disclaimer: The content is solely the responsibility of the authors and does not necessarily represent the official views of the National Cancer Institute or the National Institutes of Health.

Conflict of Interest: The authors declare that the research was conducted in the absence of any commercial or financial relationships that could be construed as a potential conflict of interest.

Publisher's Note: All claims expressed in this article are solely those of the authors and do not necessarily represent those of their affiliated organizations, or those of the publisher, the editors and the reviewers. Any product that may be evaluated in this article, or claim that may be made by its manufacturer, is not guaranteed or endorsed by the publisher.

Advantages of publishing in Frontiers

OPEN ACCESS
Articles are free to read for greatest visibility and readership

FAST PUBLICATION
Around 90 days from submission to decision

HIGH QUALITY PEER-REVIEW
Rigorous, collaborative, and constructive peer-review

TRANSPARENT PEER-REVIEW
Editors and reviewers acknowledged by name on published articles

Frontiers
Avenue du Tribunal-Fédéral 34
1005 Lausanne | Switzerland

Visit us: www.frontiersin.org
Contact us:frontiersin.org/about/contact

REPRODUCIBILITY OF RESEARCH
Support open data and methods to enhance research reproducibility

DIGITAL PUBLISHING
Articles designed for optimal readership across devices

FOLLOW US
@frontiersin

IMPACT METRICS
Advanced article metrics track visibility across digital media

EXTENSIVE PROMOTION
Marketing and promotion of impactful research

LOOP RESEARCH NETWORK
Our network increases your article's readership